

frontiers RESEARCH TOPICS

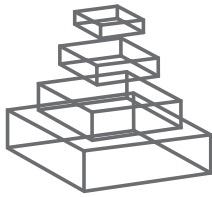
WAYS TO IMPROVE TUMOR UPTAKE
AND PENETRATION OF DRUGS
INTO SOLID TUMORS

Topic Editors

Fabrizio Marcucci, Angelo Corti
and Ronald Berenson



frontiers in
ONCOLOGY



FRONTIERS COPYRIGHT STATEMENT

© Copyright 2007-2014
Frontiers Media SA.
All rights reserved.

All content included on this site, such as text, graphics, logos, button icons, images, video/audio clips, downloads, data compilations and software, is the property of or is licensed to Frontiers Media SA ("Frontiers") or its licensees and/or subcontractors. The copyright in the text of individual articles is the property of their respective authors, subject to a license granted to Frontiers.

The compilation of articles constituting this e-book, wherever published, as well as the compilation of all other content on this site, is the exclusive property of Frontiers. For the conditions for downloading and copying of e-books from Frontiers' website, please see the Terms for Website Use. If purchasing Frontiers e-books from other websites or sources, the conditions of the website concerned apply.

Images and graphics not forming part of user-contributed materials may not be downloaded or copied without permission.

Individual articles may be downloaded and reproduced in accordance with the principles of the CC-BY licence subject to any copyright or other notices. They may not be re-sold as an e-book.

As author or other contributor you grant a CC-BY licence to others to reproduce your articles, including any graphics and third-party materials supplied by you, in accordance with the Conditions for Website Use and subject to any copyright notices which you include in connection with your articles and materials.

All copyright, and all rights therein, are protected by national and international copyright laws.

The above represents a summary only. For the full conditions see the Conditions for Authors and the Conditions for Website Use.

Cover image provided by Iblb sarl,
Lausanne CH

ISSN 1664-8714

ISBN 978-2-88919-350-9

DOI 10.3389/978-2-88919-350-9

ABOUT FRONTIERS

Frontiers is more than just an open-access publisher of scholarly articles: it is a pioneering approach to the world of academia, radically improving the way scholarly research is managed. The grand vision of Frontiers is a world where all people have an equal opportunity to seek, share and generate knowledge. Frontiers provides immediate and permanent online open access to all its publications, but this alone is not enough to realize our grand goals.

FRONTIERS JOURNAL SERIES

The Frontiers Journal Series is a multi-tier and interdisciplinary set of open-access, online journals, promising a paradigm shift from the current review, selection and dissemination processes in academic publishing.

All Frontiers journals are driven by researchers for researchers; therefore, they constitute a service to the scholarly community. At the same time, the Frontiers Journal Series operates on a revolutionary invention, the tiered publishing system, initially addressing specific communities of scholars, and gradually climbing up to broader public understanding, thus serving the interests of the lay society, too.

DEDICATION TO QUALITY

Each Frontiers article is a landmark of the highest quality, thanks to genuinely collaborative interactions between authors and review editors, who include some of the world's best academicians. Research must be certified by peers before entering a stream of knowledge that may eventually reach the public - and shape society; therefore, Frontiers only applies the most rigorous and unbiased reviews.

Frontiers revolutionizes research publishing by freely delivering the most outstanding research, evaluated with no bias from both the academic and social point of view.

By applying the most advanced information technologies, Frontiers is catapulting scholarly publishing into a new generation.

WHAT ARE FRONTIERS RESEARCH TOPICS?

Frontiers Research Topics are very popular trademarks of the Frontiers Journals Series: they are collections of at least ten articles, all centered on a particular subject. With their unique mix of varied contributions from Original Research to Review Articles, Frontiers Research Topics unify the most influential researchers, the latest key findings and historical advances in a hot research area!

Find out more on how to host your own Frontiers Research Topic or contribute to one as an author by contacting the Frontiers Editorial Office: researchtopics@frontiersin.org

WAYS TO IMPROVE TUMOR UPTAKE AND PENETRATION OF DRUGS INTO SOLID TUMORS

Topic Editors:

Fabrizio Marcucci, Regina Elena National Cancer Institute, Italy

Angelo Corti, San Raffaele Scientific Institute, Italy

Ronald Berenson, Compliment Corporation, USA

The main scope of this topic is to give an update on pharmacologic and non-pharmacologic approaches to enhance uptake and penetration of cancer drugs into tumors. Inadequate accumulation of drugs in tumors has emerged over the last decade as one of the main problems underlying therapeutic failure and drug resistance in the treatment of cancer.

Insufficient drug uptake and penetration is causally related to the abnormal tumor architecture. Thus, poor vascularization, increased resistance to blood flow and impaired blood supply represent a first obstacle to the delivery of antitumor drugs to tumor tissue. Decreased or even inverted transvascular pressure gradients compromise convective delivery of drugs. Eventually, an abnormal extracellular matrix offers increased frictional resistance to tumor drug penetration.

Abnormal tumor architecture also changes the biology of tumor cells, which contributes to drug resistance through several different mechanisms. The variability in vessel location and structure can make many areas of the tumor hypoxic, which causes the tumor cells to become quiescent and thereby resistant to many antitumor drugs. In addition, the abnormally long distance of part of the tumor cell population from blood vessels provides a challenge to delivering cancer drugs to these cells. We have recently proposed additional mechanisms of tumor drug resistance, which are also related to abnormal tumor architecture. First, increased interstitial fluid pressure can by itself induce drug resistance through the induction of resistance-promoting paracrine factors. Second, the interaction of drug molecules with vessel-proximal tumor cell layers may also induce the release of these factors, which can spread throughout the cancer, and induce drug resistance in tumor cells distant from blood vessels.

As can be seen, abnormal tumor architecture, inadequate drug accumulation and tumor drug resistance are tightly linked phenomena, suggesting the need to normalize the tumor architecture, including blood vessels, and/or increase the accumulation of cancer drugs in

tumors in order to increase therapeutic effects. Indeed, several classes of drugs (that we refer to as promoter drugs) have been described, that promote tumor uptake and penetration of antitumor drugs, including those that are vasoactive, modify the barrier function of tumor vessels, debulk tumor cells, and overcome intercellular and stromal barriers. In addition, also non-pharmacologic approaches have been described that enhance tumor accumulation of effector drugs (e.g. convection-enhanced delivery, hyperthermia, etc.).

Some drugs that have already received regulatory approval (e.g. the anti-VEGF antibody bevacizumab) exert antitumor effects at least in part through normalization of the tumor vasculature and enhancement of the accumulation of effector drugs. Other drugs, acting through different mechanisms of action, are now in clinical development (e.g. NGR-TNF in phase II/III studies) and others are about to enter clinical investigation (e.g. JO-1).

Table of Contents

- 05 *Improving Drug Uptake and Penetration into Tumors: Current and Forthcoming Opportunities***
Fabrizio Marcucci, Ronald Berenson and Angelo Corti
- 08 *The Tumor Microenvironment and Strategies to Improve Drug Distribution***
Jasdeep K. Saggar, Man Yu, Qian Tan and Ian F. Tannock
- 15 *Influence of the Duration of Intravenous Drug Administration on Tumor Uptake***
Sylvain Fouliard, Marylore Chenel and Fabrizio Marcucci
- 22 *Strategies to Increase Drug Penetration in Solid Tumors***
Il-Kyu Choi, Robert Strauss, Maximilian Richter, Chae-Ok Yun and Andre Lieber
- 40 *Nanocarrier-Mediated Targeting of Tumor and Tumor Vascular Cells Improves Uptake and Penetration of Drugs into Neuroblastoma***
Fabio Pastorino, Chiara Brignole, Monica Loi, Daniela Di Paolo, Annarita Di Fiore, Patrizia Perri, Gabriella Pagnan and Mirco Ponzoni
- 50 *Positron Emission Tomography as a Method for Measuring Drug Delivery to Tumors in Vivo: The Example of [¹¹C]Docetaxel***
Astrid Van Der Veldt, Egbert Smit and Adriaan Anthonius Lammertsma
- 57 *Vascular Permeability and Drug Delivery in Cancers***
Sandy Azzi, Jagoda K. Hebda and Julie Gavard
- 71 *Ultrasonic Enhancement of Drug Penetration in Solid Tumors***
Chun-yen Lai, Brett Z. Fite and Katherine W. Ferrara
- 78 *Tumor-Penetrating Peptides***
Tambet Teesalu, Kazuki N. Sugahara and Erkki Ruoslahti
- 86 *Tumor Targeting Via Integrin Ligands***
Udaya Kiran Marelli, Florian Rechenmacher, Tariq Rashad Ali Sobahi, Carles Mas-Moruno and Horst Kessler
- 98 *Ways to Enhance Lymphocyte Trafficking into Tumors and Fitness of Tumor Infiltrating Lymphocytes***
Matteo Bellone and Arianna Calcinotto
- 113 *Tumor Delivery of Chemotherapy Combined with Inhibitors of Angiogenesis and Vascular Targeting Agents***
Marta Cesca, Francesca Bizzaro, Massimo Zucchetti and Raffaella Giavazzi
- 120 *Current Advances in Mathematical Modeling of Anti-Cancer Drug Penetration into Tumor Tissues***
MunJu Kim, Robert J. Gillies and Katarzyna Anna Rejniak



Improving drug uptake and penetration into tumors: current and forthcoming opportunities

Fabrizio Marcucci^{1,2*}, Ronald Berenson³ and Angelo Corti⁴

¹ Centro Nazionale di Epidemiologia, Sorveglianza e Promozione della Salute, Istituto Superiore di Sanita', Roma, Italy

² Hepatology Association of Calabria, Reggio Calabria, Italy

³ ImmunoMod Consulting, Mercer Island, WA, USA

⁴ Tumor Biology and Vascular Targeting Unit, Division of Molecular Oncology, San Raffaele Scientific Institute, Milano, Italy

*Correspondence: fabmarcu@gmail.com

Edited by:

Olivier Feron, University of Louvain, Belgium

The main scope of this topic is to give an update on approaches being studied and developed to improve tumor drug delivery through active targeting and other methods. Inadequate drug accumulation has emerged as one of the main problems underlying therapeutic failure and drug resistance in the treatment of solid tumors (Trédan et al., 2007; Marcucci and Corti, 2012a). It is causally related to the abnormal tumor architecture. Poor vascularization, increased resistance to blood flow and impaired blood supply represent a first obstacle to the delivery of antitumor drugs to tumor cells. Decreased or even inverted transvascular pressure gradients compromise convective transport of drugs. Eventually, an abnormal extracellular matrix offers increased frictional resistance to tumor drug penetration. The net result is reduced overall drug accumulation in tumors, and the propensity of drugs to accumulate in perivascular spaces without penetrating vessel-distant tumor areas. This promotes passive and active induction of drug resistance (Marcucci and Corti, 2012b).

Abnormal tumor architecture, inadequate drug accumulation and tumor drug resistance are tightly linked phenomena, suggesting that normalization of the tumor architecture, including tumor blood vessels, may result in increased drug delivery to tumors and improve the therapeutic efficacy of anticancer drugs. Indeed, several classes of drugs, that we have referred to as promoter drugs, (Marcucci and Corti, 2012a) have been reported to increase tumor uptake and penetration of antitumor drugs, including drugs that are: (1) vasoactive (Nagamitsu et al., 2009), (2) normalize tumor vessels (Jain, 2005), (3) modify the barrier function of tumor vessels (Corti and Marcucci, 1998; Curnis et al., 2000, 2002), (4) debulk tumor cells (Padera et al., 2004; Moschetta et al., 2012), (5) overcome intercellular (Beyer et al., 2011, 2012; Wang et al., 2011) and stromal barriers (Provenzano et al., 2012). In addition, non-pharmacologic approaches have been described that enhance tumor accumulation of effector drugs (e.g., convection-enhanced delivery, hyperthermia, ultrasound, etc.) (Sen et al., 2011; Watson et al., 2012).

Some drugs that have already received regulatory approval (e.g., the anti-vascular endothelial growth factor antibody bevacizumab) (Hurwitz et al., 2004) exert antitumor effects at least in part by normalizing the tumor vasculature and enhancing tumor accumulation of chemotherapeutic drugs (Willett et al., 2004). Bevacizumab, however, has a problematic side-effect profile, and the effective doses of the drug encompass a very narrow range beyond which it may even lead to a reduction in drug delivery (Van der Veldt

et al., 2012). Additional drugs, acting through other mechanisms of action, are now in clinical development (e.g., vascular targeted NGR-tumor necrosis factor, in phase II/III studies) (Sacchi et al., 2006) and others are about to enter clinical investigation (e.g., Junction Opener-1) (Beyer et al., 2011, 2012).

To date, the focus has been primarily on the identification of novel promoter drugs that improve tumor drug delivery. This has led to a considerable number of promoter drugs and devices that are effective in preclinical studies, and some of which have proceeded into clinical investigation or are about to do so. Regarding the types of drugs to be delivered, chemotherapeutics have been the obvious first choice, because they are the antitumor drugs in most widespread use (Curnis et al., 2002; Beyer et al., 2012). Another area of interest is antitumor monoclonal antibodies or related compounds (e.g., immunocytokines) (Beyer et al., 2011; Moschetta et al., 2012), which have become an important component of the antitumor drug armamentarium over the last 15 years. Preclinical investigations have produced promising results when these therapeutic agents are combined with drugs that enhance their penetration into tumors, and it is reasonable to predict that clinical studies will follow in the forthcoming years. So far, so good, but what next? Have we looked at all possible applications for promoter drugs, or are there further applications that we can envisage? We believe that there is still an important field of application for promoter drugs that has been relatively unexplored so far, i.e., the possibility to improve delivery of anticancer cells, in particular immune cells to the tumor (Marcucci et al., 2013), an area of increasing clinical interest.

Enhancing penetration of immune cells into tumors may have two main therapeutic applications. The first is to improve the efficacy of immune-regulatory antibodies, such as the anti-cytotoxic T-lymphocyte antigen-4 antibody ipilimumab, and the anti-programmed death-1 antibody nivolumab. These antibodies yield impressive, and often long-lasting therapeutic responses in a limited fraction (10–20% depending on the antibody) of heavily pretreated patients with metastatic melanoma and other solid tumors (Hodi et al., 2010; Topalian et al., 2012). There is a relationship between the number of tumor-infiltrating immune cells and responsiveness to ipilimumab (Lynch et al., 2012). In this setting, promoter drugs could be of value at two levels: first, to improve tumor delivery of the antibody itself, and second, improve penetration of immune cells into the tumor. This has the potential to increase the fraction of patients that become responders to these antibodies. A second

possible field of application are antitumor vaccines. Antitumor vaccines are often active only when administered in a prophylactic setting. With growing tumors, vaccination becomes progressively less effective. One reason might be that tumor-specific lymphocytes become sensitized in draining lymph nodes but are then unable to enter tumors and eliminate tumor cells (Ganss and Hanahan, 1998). Promoter drugs that improve infiltration of immune cells into tumors may prove useful in increasing the effectiveness of cancer vaccines. However, infiltration of immune cells into tumors has requirements that go beyond those of antitumor drugs. Physiological pathways of immune cell extravasation depend on a multistep cascade of events involving tethering, rolling, firm adhesion, and migration. These steps are mediated by distinct adhesion molecules and activation pathways (Springer, 1994); however, adhesion molecules are often downregulated on tumor endothelial cells, a phenomenon defined as endothelial cell anergy (Piali et al., 1995). This impairs the entry of immune cells into tumor sites. In order to enhance tumor infiltration of immune cells, promoter

drugs may be required that induce a local inflammatory reaction. This leads to up-regulation of adhesion receptors that are able to attach immune cells to vessel walls and enable their penetration into tumors. Preliminary studies suggest that certain promoter drugs may achieve this goal (Calcinotto et al., 2012).

Promoter drugs that improve tumor delivery of chemotherapeutics and antitumor antibodies are likely to become a clinical reality in forthcoming years. In addition, new possibilities are emerging to enhance the entrance of therapeutic agents into tumors. For example, recent results suggest that promoter drugs may be useful also for improving infiltration of immune cells into tumors. This may increase the antitumor effects of a broad range of immune-based therapeutics, including immune-regulatory antibodies, antibodies that engage cytotoxic immune cells, and cancer vaccines.

ACKNOWLEDGMENT

This work was supported by Associazione Italiana per la Ricerca sul Cancro (AIRC 9965 and 9180) of Italy.

REFERENCES

- Beyer, I., Cao, H., Persson, J., Song, H., Richter, M., Feng, Q., et al. (2012). Co-administration of epithelial junction opener JO-1 improves the efficacy and safety of chemotherapeutic drugs. *Clin. Cancer Res.* 18, 3340–3351. doi: 10.1158/1078-0432.CCR-11-3213
- Beyer, I., van Rensburg, R., Strauss, R., Li, Z. Y., Wang, H., Persson, J., et al. (2011). Epithelial junction opener JO-1 improves monoclonal antibody therapy of cancer. *Cancer Res.* 71, 7080–7090. doi: 10.1158/0008-5472.CAN-11-2009
- Calcinotto, A., Grioni, M., Jachetti, E., Curnis, F., Mondino, A., Parmiani, G., et al. (2012). Targeting TNF- α to neoangiogenic vessels enhances lymphocyte infiltration in tumors and increases the therapeutic potential of immunotherapy. *J. Immunol.* 188, 2687–2694. doi: 10.4049/jimmunol.1101877
- Corti, A., and Marcucci, F. (1998). Tumour necrosis factor: strategies for improving the therapeutic index. *J. Drug Target.* 5, 403–413. doi: 10.3109/10611869808997869
- Curnis, F., Sacchi, A., Borgna, L., Magni, F., Gasparri, A., and Corti, A. (2000). Enhancement of tumor necrosis factor α antitumor immunotherapeutic properties by targeted delivery to aminopeptidase N (CD13). *Nat. Biotechnol.* 18, 1185–1190. doi: 10.1038/81183
- Curnis, F., Sacchi, A., and Corti, A. (2002). Improving chemotherapeutic drug penetration in tumors by vascular targeting and barrier alteration. *J. Clin. Invest.* 110, 475–482. doi: 10.1172/JCI200215223
- Ganss, R., and Hanahan, D. (1998). Tumor microenvironment can restrict the effectiveness of activated antitumor lymphocytes. *Cancer Res.* 58, 4673–4681.
- Hodi, F. S., O'Day, S. J., McDermott, D. F., Weber, R. W., Sosman, J. A., Haanen, J. B., et al. (2010). Improved survival with ipilimumab in patients with metastatic melanoma. *N. Engl. J. Med.* 363, 711–723. doi: 10.1056/NEJMoa1003466
- Hurwitz, H., Fehrenbacher, L., Novotny, W., Cartwright, T., Hainsworth, J., Heim, W., et al. (2004). Bevacizumab plus irinotecan, fluorouracil, and leucovorin for metastatic colorectal cancer. *N. Engl. J. Med.* 350, 2335–2342. doi: 10.1056/NEJMoa032691
- Jain, R. K. (2005). Normalization of tumor vasculature: an emerging concept in antiangiogenic therapy. *Science* 307, 58–62. doi: 10.1126/science.1104819
- Lynch, T. J., Bondarenko, I., Luft, A., Serwatowski, P., Barlesi, F., Chacko, R., et al. (2012). Ipilimumab in combination with paclitaxel and carboplatin as first-line treatment in stage IIIB/IV non-small-cell lung cancer: results from a randomized, double-blind, multicenter phase II study. *J. Clin. Oncol.* 30, 2046–2054. doi: 10.1200/JCO.2011.38.4032
- Marcucci, F., Bellone, M., Rumio, C., and Corti, A. (2013). Approaches to improve tumor accumulation and interactions between monoclonal antibodies and immune cells. *MABS* 5, 36–46. doi: 10.4161/mabs.22775
- Marcucci, F., and Corti, A. (2012a). How to improve exposure of tumor cells to drugs – promoter drugs increase tumor uptake and penetration of effector drugs. *Adv. Drug Deliv. Rev.* 64, 53–68. doi: 10.1016/j.addr.2011.09.007
- Marcucci, F., and Corti, A. (2012b). Improving drug penetration to curb tumor drug resistance. *Drug Discov. Today* 17, 1139–1147. doi: 10.1016/j.drudis.2012.06.004
- Moschetta, M., Pretto, F., Berndt, A., Galler, K., Richter, P., Bassi, A., et al. (2012). Paclitaxel enhances therapeutic efficacy of the F8-JL2 immunocytokine to EDA-fibronectin-positive metastatic human melanoma xenografts. *Cancer Res.* 72, 1814–1824. doi: 10.1158/0008-5472.CAN-11-1919
- Nagamitsu, A., Greish, K., and Maeda, H. (2009). Elevating blood pressure as a strategy to increase tumor-targeted delivery of macromolecular drug SMANCS: cases of advanced solid tumors. *Jpn. J. Clin. Oncol.* 39, 756–766. doi: 10.1093/jjco/hyp074
- Padera, T. P., Stoll, B. R., Tooredman, J. B., Capen, D., di Tomaso, E., and Jain, R. K. (2004). Pathology: cancer cells compress intratumour vessels. *Nature* 427, 695. doi: 10.1038/427695a
- Piali, L., Fichtel, A., Terpe, H.-J., Imhof, B. A., and Gisler, R. H. (1995). Endothelial vascular cell adhesion molecule 1 expression is suppressed by melanoma and carcinoma. *J. Exp. Med.* 181, 811–816. doi: 10.1084/jem.181.2.811
- Provenzano, P. P., Cuevas, C., Chang, A. E., Goel, V. K., Von Hoff, D. D., and Hingorani, S. R. (2012). Enzymatic targeting of the stroma ablates physical barriers to treatment of pancreatic ductal adenocarcinoma. *Cancer Cell* 21, 82–91. doi: 10.1016/j.ccr.2011.11.023
- Wang, H., Li, Z.-Y., Liu, Y., Persson, J., Beyer, I., Möller, T., et al. (2011). Desmoglein 2 is a receptor for adenovirus serotypes 3, 7, 11 and 14. *Nat. Med.* 17, 96–105. doi: 10.1038/nm.2270
- Watson, K. D., Lai, C.-Y., Qin, S., Kruse, D. E., Lin, Y.-C., Seo, J. W., et al. (2012). Ultrasound increases nanoparticle delivery by reducing intratumoral pressure and increasing transport in Sen, A., Capitano, M. L., Spernyak, J. A., Schueckler, J. T., Thomas, S., Singh, A. K., et al. (2011). Mild elevation of body temperature reduces tumor interstitial fluid pressure and hypoxia and enhances efficacy of radiotherapy in murine tumor models. *Cancer Res.* 71, 3872–3880. doi: 10.1158/0008-5472.CAN-10-4482
- Springer, T. A. (1994). Traffic signals for lymphocyte recirculation and leukocyte emigration: the multistep paradigm. *Cell* 76, 301–314. doi: 10.1016/0092-8674(94)90337-9
- Topalian, S. L., Hodi, F. S., Brahmer, J. R., Gettinger, S. N., Smith, D. C., McDermott, D. F., et al. (2012). Safety, activity, and immune correlates of anti-PD-1 antibody in cancer. *N. Engl. J. Med.* 366, 2443–2454. doi: 10.1056/NEJMoa1200690
- Trédan, O., Galmarini, C. M., Patel, K., and Tannock, I. F. (2007). Drug resistance and the solid tumor microenvironment. *J. Natl. Cancer Inst.* 99, 1441–1454. doi: 10.1093/jnci/djm135
- Van der Veldt, A. A. M., Lubberink, M., Bahce, I., Walraven, M., de Boer, M. P., Greuter, H. N. J. M., et al. (2012). Rapid decrease in delivery of chemotherapy to tumors after anti-VEGF therapy: implications for scheduling of antiangiogenic drugs. *Cancer Cell* 21, 82–91. doi: 10.1016/j.ccr.2011.11.023
- Watson, K. D., Lai, C.-Y., Qin, S., Kruse, D. E., Lin, Y.-C., Seo, J. W., et al. (2012). Ultrasound increases nanoparticle delivery by reducing intratumoral pressure and increasing transport in

epithelial and epithelial-mesenchymal transition tumors. *Cancer Res.* 72, 1485–1493. doi: 10.1158/0008-5472.CAN-11-3232

Willett, C. G., Boucher, Y., di Tomaso, E., Duda, D. G., Munn, L. L., Tong, R. T., et al. (2004). Direct evidence that the VEGF-specific antibody bevacizumab

has antivascular effects in human rectal cancer. *Nat. Med.* 10, 145–147. doi: 10.1038/nm988

Received: 22 May 2013; accepted: 05 June 2013; published online: 18 June 2013.

Citation: Marcucci F, Berenson R and Corti A (2013) Improving drug uptake

and penetration into tumors: current and forthcoming opportunities. *Front. Oncol.* 3:161. doi: 10.3389/fonc.2013.00161

This article was submitted to Frontiers in Pharmacology of Anti-Cancer Drugs, a specialty of Frontiers in Oncology.

Copyright © 2013 Marcucci, Berenson and Corti. This is an open-access

article distributed under the terms of the Creative Commons Attribution License, which permits use, distribution and reproduction in other forums, provided the original authors and source are credited and subject to any copyright notices concerning any third-party graphics etc.



The tumor microenvironment and strategies to improve drug distribution

Jasdeep K. Saggar¹, Man Yu¹, Qian Tan¹ and Ian F. Tannock^{1,2*}

¹ Department of Medical Biophysics, University of Toronto, Toronto, ON, Canada

² Division of Medical Oncology and Hematology, Princess Margaret Cancer Centre, Toronto, ON, Canada

Edited by:

Angelo Corti, San Raffaele Scientific Institute, Italy

Reviewed by:

Angelo Corti, San Raffaele Scientific Institute, Italy

Fabrizio Marzocchi, Istituto Superiore di Sanità, Italy

***Correspondence:**

Ian F. Tannock, Princess Margaret Cancer Centre, Suite 5-208, 610 University Avenue, Toronto, ON M5G 2M9, Canada

e-mail: ian.tannock@uhn.ca

The microenvironment within tumors is composed of a heterogeneous mixture of cells with varying levels of nutrients and oxygen. Differences in oxygen content result in survival or compensatory mechanisms within tumors that may favor a more malignant or lethal phenotype. Cells that are rapidly proliferating are richly nourished and preferentially located close to blood vessels. Chemotherapy can target and kill cells that are adjacent to the vasculature, while cells that reside farther away are often not exposed to adequate amounts of drug and may survive and repopulate following treatment. The characteristics of the tumor microenvironment can be manipulated in order to design more effective therapies. In this review, we describe important features of the tumor microenvironment and discuss strategies whereby drug distribution and activity may be improved.

Keywords: drug distribution, pharmacodynamic markers, tumor microenvironment, drug penetration, hypoxia-activated pro-drugs, solid tumor

INTRODUCTION

SOLID TUMORS AND DRUG RESISTANCE

The tumor microenvironment within solid tumors

Solid tumors contain a heterogeneous mixture of tumor cells and non-malignant cells within an extracellular matrix (ECM) supported by an irregular vascular network. Tumor blood vessels are often farther apart than in normal tissues, and have variable blood flow, leading to poor delivery of nutrients and impaired clearance of metabolic breakdown products from the tumor (Minchinton and Tannock, 2006; Tredan et al., 2007). Many solid tumors develop regions of hypoxia, which may lead to up-regulation of genes that predispose to a more malignant phenotype (Wilson and Hay, 2011). Blood vessels are also the route by which anticancer drugs are delivered to the tumor, and our laboratory and others have shown that the limited blood supply may put tumors at a disadvantage in terms of drug delivery as compared to better-vascularized normal tissues (Hirst and Denekamp, 1979; Minchinton and Tannock, 2006; Tredan et al., 2007). Also, poor nutrition of tumor cells may lead to low rates of cell proliferation in some tumor regions (Hirst and Denekamp, 1979; Ljungqvist et al., 2002), and cells in such regions are likely to be resistant to cycle-active drugs as shown in Figure 1A.

Tumor acidity

The poor vascular organization and lack of lymphatic drainage of solid tumors contributes to a build up in metabolic byproducts such as lactic and carbonic acids leading to a reduced extracellular pH. The production of lactate arises from glycolysis – a favored route of energy production in tumors. Glycolysis typically takes place under hypoxic conditions, when oxidative phosphorylation is not possible, but in tumors glycolysis also takes place in oxygenated regions (Song et al., 2006). Tumor acidity influences drug uptake into tumor cells. When the extracellular tumor

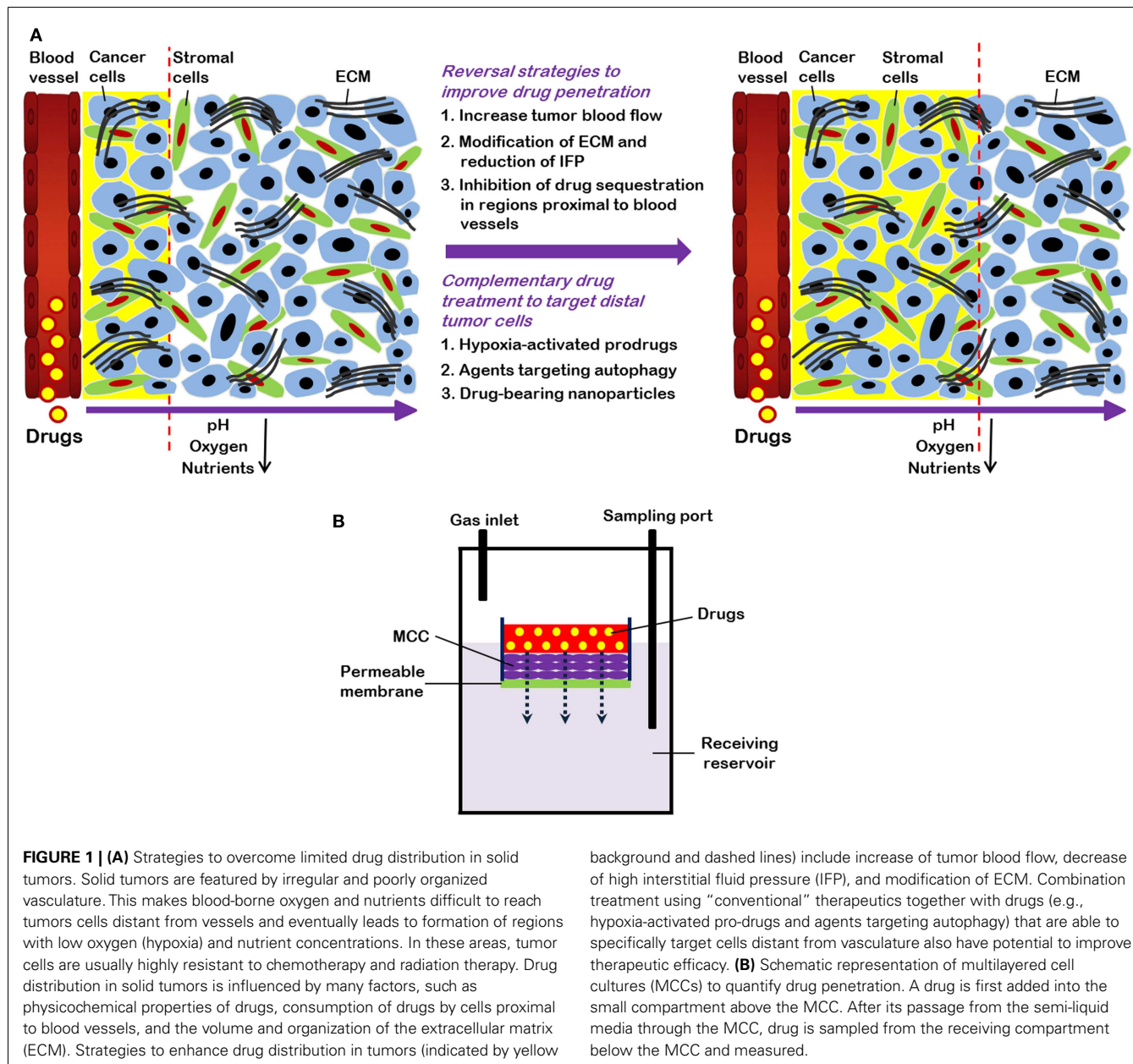
environment is acidic, chemotherapeutic drugs that are basic (such as doxorubicin, mitoxantrone, vincristine, and vinblastine) are protonated; this decreases cellular uptake since charged drugs pass through the cellular membrane less efficiently than those that are uncharged (Manallack, 2008). In contrast, drugs that are acidic (such as chlorambucil and cyclophosphamide) will tend to concentrate within cells. Even if basic drugs pass through the cellular membrane, sequestration within acidic organelles such as endosomes may occur, leaving less drug to attack tumor DNA and produce antitumor effects (Mayer et al., 1986).

Tumor hypoxia

Hypoxia is a hallmark of many different tumor types. The convoluted vasculature of tumors can result in insufficient oxygen supply through blood vessels as seen in Figure 1A. This type of hypoxia is known as chronic or diffusion limited hypoxia. Acute hypoxia may also occur in solid tumors due to intermittent blood flow.

Cells that reside far away from functional blood vessels may become hypoxic due to the limited diffusion of oxygen: the distance from blood vessels to hypoxic regions will depend on the rate of oxygen consumption by the tumor cells, but typically cells residing at a distance greater than 70 μm from functional blood vessels receive inadequate amounts of oxygen (Vaupel and Harrison, 2004). Hypoxic cells can be viable, but usually proliferate slowly, presumably due to their reduced production of ATP; however recent work from our laboratory has shown that as chemotherapy induces the death of cells close to blood vessels, hypoxic cells may reoxygenate and proliferate, presumably because of a better supply of nutrients and oxygen.

Hypoxia in tumors is associated with a poor clinical outcome as compared to patients with tumors lacking hypoxia (Hockel et al., 1996; Fyles et al., 2002; Nordmark et al., 2005; Jubb et al.,



2010). The presence of hypoxia leads to up-regulation of genes that promote a more malignant phenotype and favor cell survival. The transcription factor hypoxia inducible factor 1 (HIF-1) is induced, and causes the synthesis of angiogenesis-relevant proteins, suppression of apoptosis, and enhanced receptor tyrosine kinase signaling (Mizukami et al., 2007). These in turn favor epithelial to mesenchymal transition (EMT) – a process that is associated with tumor invasiveness and metastasis (Wilson and Hay, 2011). HIF-1 also induces the expression of carbonic anhydrase 9 (CA9) which favors the hydration of CO₂ leading to the production of carbonic acid – further contributing to a decrease in extracellular pH (Potter and Harris, 2004).

Tumor hypoxia is linked with loss of the p53 tumor suppressor protein that may result in a loss of apoptotic ability

(Haensgen et al., 2001). Furthermore, hypoxia confers radio-resistance because reactive oxygen radicals that are produced following radiation under well-oxygenated conditions contribute to DNA damage (Rofstad et al., 2000). Hypoxia may also inhibit the effects of chemotherapy via the same mechanism since in the presence of oxygen drugs such as doxorubicin can produce reactive oxygen species such as super-oxides that can damage DNA (Luanpitpong et al., 2012). Hypoxia has also been shown to down-regulate expression of DNA topoisomerase II, so that drugs such as doxorubicin and etoposide that target this protein will be inefficient (Ogiso et al., 2000).

Transient hypoxia can stimulate gene amplification, leading to increased expression of genes that encode proteins that cause drug resistance; these proteins include dihydrofolate reductase, with

associated resistance to methotrexate and the multi-drug resistant transporter P-glycoprotein (Wartenberg et al., 2003). Increased expression of P-glycoprotein results in increased levels of substrate drugs being pumped out of cells thus resulting in inadequate intracellular levels to cause cytotoxicity (Matheny et al., 2001).

Factors influencing drug distribution within solid tumors

Anticancer drugs must reach target tumor cells through the vasculature. The penetration of drugs to tumor cells is reliant upon convection and/or diffusion. Convection depends on pressure gradients and given that the pressure within tumor blood vessels and the tumor interstitium are both quite high, there is probably minimal movement of drugs from the vasculature to the tumor via this mechanism (Kuszyk et al., 2001). Diffusion involves the movement of drugs along a concentration gradient, i.e., from areas where they are concentrated (within the vasculature) to less concentrated regions (the tumor interstitium). Larger molecules tend to move more slowly than smaller molecules via diffusion, and tissue penetration will depend on consumption by the cells (Tredan et al., 2007). Drugs that are water-soluble will diffuse more readily through the extracellular fluid, although the diffusion coefficient will depend on the nature of the ECM. Drugs with higher lipid solubility can penetrate into cells more easily (Undevia et al., 2005). Drug half-life is also an important determinant influencing drug penetration, since drugs with longer half-lives in the circulation have a better opportunity to establish themselves within tumor tissues (Undevia et al., 2005).

Quantifying drug distribution

Quantification of drug distribution is important in order to determine a drug's ability to penetrate tissue within solid tumors. Both *in vitro* and *in vivo* techniques have been used for quantifying drug distribution. A common *in vitro* technique uses tumor spheroids, and adherent tumor cells can grow spheroids to up to 3 mm in diameter (Conger and Ziskin, 1983). Spheroids develop hypoxic areas as well as central necrosis once they have reached $\sim 500 \mu\text{m}$ in diameter (Vinci et al., 2011). Drug distribution in spheroids can be studied for fluorescent drugs, or by using autoradiography to determine the distribution of labeled drugs (Lesser et al., 1995; Kuh et al., 1999). An alternative is to generate multicellular layers (MCL) on collagen-coated micro-porous membranes: the rate of penetration can then be evaluated by adding a drug on one side of the MCL and measuring its concentration on the other as a function of time, as shown in **Figure 1B** (Wilson and Hay, 2011). Spheroids and MCL have been used to study the distribution of a wide range of drugs (Tannock et al., 2002), and most drugs show rather poor distribution in tumor tissue.

Drug distribution can also be studied in tumors grown in animals. Growth of tumors in window and ear chambers allows for direct observation of tumor microcirculation, but a disadvantage is that tumors are relatively small with limited areas of hypoxia and/or necrosis (Hak et al., 2010). Tissue sections can be obtained after drug treatment of animals bearing transplanted tumors or human tumor xenografts and used for immunohistochemical analysis. This analysis will allow the quantification of fluorescent drugs in relation to blood vessels or regions of hypoxia, and the technique can be applied to human biopsies

(Lankelma et al., 1999; Primeau et al., 2005; Fung et al., 2012). These studies have revealed decreasing concentration of fluorescent doxorubicin, mitoxantrone, or topotecan with increasing distance from blood vessels (Hirst and Denekamp, 1979). Distribution of other drugs such as cetuximab, trastuzumab (Lee and Tannock, 2010), and melphalan (Saggar et al., 2013) within tumor sections can be quantified with the use of anti-IgG specific (for the former two) or melphalan DNA adduct specific (for the former) monoclonal antibodies that recognize the drug activity.

Most anticancer drugs are non-fluorescent so their distribution within tumor tissue is difficult to assess. An alternative is to evaluate molecular markers of drug effect, using antibodies that recognize cell proliferation (Ki67, cyclin D1, or bromodeoxyuridine incorporation into DNA), antibodies that mark cell death or apoptosis (e.g., caspase-3 or -6), and markers of DNA damage such as γ H2aX. We recently used antibodies to γ H2aX, caspase-3 or -6, and Ki67, and a computer-based algorithm, to quantify the distribution of (non-fluorescent) docetaxel (Saggar et al., 2013). **Figure 2** depicts the expression of γ H2aX following docetaxel treatment in xenografts; use of this and the other markers show that docetaxel also has limited distribution from tumor blood vessels.

Given the limited penetration of many chemotherapeutic agents, cells that are distal from blood vessels do not receive adequate amounts of drug to cause cell death. Thus, tumor cell repopulation arising from areas where cells are not killed and previously under-nourished (e.g., hypoxic regions) is probable, and indeed we have recently shown that previously hypoxic cells may reoxygenate and repopulate after treatment of human tumor xenografts with doxorubicin or docetaxel (Saggar et al., 2013).

Tumor autophagy

Autophagy is a cellular process of self-consumption characterized by sequestration of bulk cytoplasm, long-lived proteins, and cellular organelles into double-membrane vesicles called autophagosomes which are delivered to, and degraded in lysosomes (Larsen et al., 1985; Funderburk et al., 2010). The autophagosomal membrane requires a kinase complex consisting of class III phosphoinositol 3-kinase (PI3K), p150 myristylated protein kinase and Beclin1 (Atg 6). Subsequently, two further protein complexes are involved, the Atg4-Atg8 [also known as light chain (LC3/MAP1LC3B)] and the Atg12-Atg5/Atg7-Atg16 complex (Levine, 2007). Autophagy is thought to have at least three roles within the cell (Lee and Tannock, 2006; Levine, 2007): (1) it is a major pathway for quality control because it degrades damaged or superfluous cellular components in order to avoid mutational accumulation; (2) it may facilitate cell death as an alternative or complementary pathway to apoptosis; (3) it provides an alternative energy source by recycling cellular constituents during periods of metabolic stress to maintain cellular viability. Such stressors may include nutrient deprivation, hypoxia and cytotoxic agents, and markers of autophagy co-localize with hypoxia in tumor sections (Hoyer-Hansen and Jaattela, 2007). Hypoxic areas are reported to be primary sites of autophagy in 12 head and neck tumor cell lines (Rouschop et al., 2010) and recent data from our laboratory suggest that tumors grown from cells that do not express Atg7 and beclin-1 genes do not contain hypoxic regions.

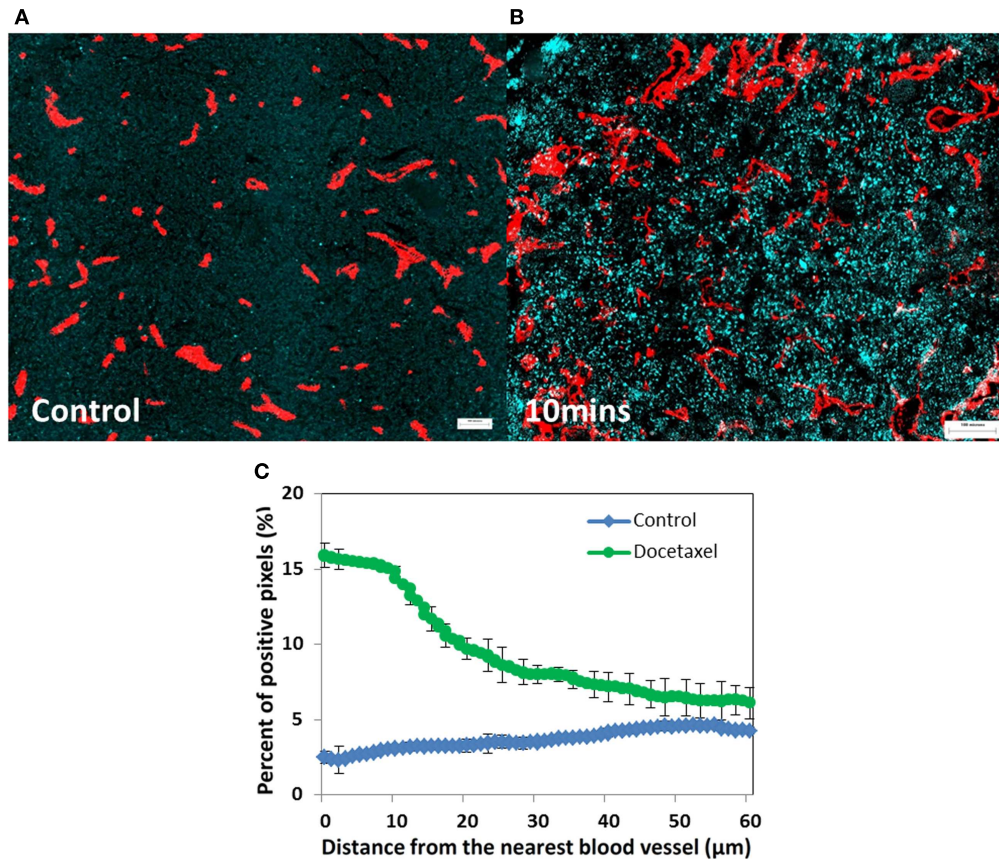


FIGURE 2 | Prostate cancer PC-3 xenografts (A) untreated control or (B) treated with docetaxel (15 mg/kg). (A,B) Show changes in γ H2aX (in cyan), a biomarker of drug effect, in relation to tumor blood vessels (in red) at 10 min after injection. (C) Represents quantitative analysis of the

distribution of γ H2aX-positive cells in relation to the nearest blood vessel in tumors treated with docetaxel for 10 min (green line) and untreated controls (blue line). Points indicate average of six mice per group; bars, SE. ◊: control; ◚: docetaxel.

Autophagy is prognostic of poor outcome in multiple tumor types, including cancers of the breast, lung, and colon (Karpathiou et al., 2011; Sivridis et al., 2011). High levels of autophagy have been associated with resistance to systemic therapy in several preclinical and clinical models presumably because it facilitates survival of stressed or damaged cells through recycling of cellular breakdown products (Yang et al., 2011). Hence targeting of autophagy with pharmacological agents may be a mechanism to improve the effectiveness of anticancer drugs for solid tumors.

STRATEGIES TO IMPROVE THERAPY BY MODULATING THE TUMOR MICROENVIRONMENT

Inhibiting tumor autophagy

The Atg proteins are involved in autophagosome formation – a critical step required for autophagy to occur, therefore the inhibition of autophagy can be achieved by knockdown of *Atg* genes or by pharmacological inhibition. For example, deletion of *Atg7* and *Beclin1* inhibited autophagy induced by nutrient deprivation of cervical cancer cells and induced cell death (Yu et al., 2004) while stable knockdown of *Atg7* in human breast cancer cells inhibited cell growth in soft

agar and tumor formation in nude mice (Kim et al., 2011). These strategies can also enhance tumor cell death induced by diverse anticancer drugs in preclinical models (Yang et al., 2011).

Agents which inhibit endosomal acidification, including (hydroxy)chloroquine and proton pump inhibitors (PPIs), can suppress autophagy and may therefore inhibit survival mechanisms for nutrient deprived cells (Marino et al., 2010). Luciani et al. (2004) reported the use of PPIs to sensitize cancer cells and solid tumors to various chemotherapeutic agents. Multiple mechanisms are probably involved, but appear to relate to changes in acidity in both intra and extracellular compartments of tumor cells. This group also reported that PPIs inhibit autophagy (Marino et al., 2010) probably because fusion of autophagosomes with acidic endosomes is central to the process, and we have confirmed this. Several studies have shown that PPIs such as omeprazole, esomeprazole, and pantoprazole have activity against human hematopoietic and solid tumors; they may revert chemo-resistance in drug-resistant tumors and directly induce killing of tumor cells (Yeo et al., 2004; De Milito et al., 2007, 2010). Growing evidence suggests that the major mechanism may be inhibition of autophagy.

Strategies to reduce interstitial fluid pressure

The interstitial fluid pressure (IFP) within solid tumors is often high (Heldin et al., 2004; Lunt et al., 2008), and this can inhibit the penetration of drugs into tumor tissue. This is particularly true in human pancreatic tumors that are extremely resistant to systemic cancer therapy (Olive et al., 2009; Provenzano et al., 2012). Raised IFP is due, at least in part, to a dense ECM and high cell density that lead to compression of blood vessels, and to inadequate lymphatic drainage (Ferretti et al., 2009). High IFP may have an adverse effect on treatment since it may cause vascular compression and inadequate drug delivery. A recent study by Provenzano et al. (2012) showed that there is an abundance of hyaluronic acid (HA) in the ECM of pancreatic tumors. HA is a large glycosaminoglycan that is associated with elevated IFP, and treatment with a HA-targeting enzyme (PEGPH20) was able to diminish HA levels and result in patent blood vessels and a corresponding increase in doxorubicin penetration (Provenzano et al., 2012). Other methods of improving vascular perfusion have also been investigated: Olive et al. (2009) reported that reduction in levels of tumor-associated stromal fibroblasts through disruption of Hedgehog signaling resulted in increased angiogenesis and greater penetration of gemcitabine into pancreatic tumors. The use of HA-targeting enzymes (PEGPH20) and Hedgehog signaling disruptors (GDC-0449 and LDE225) are being investigated in clinical trials.

Hypoxia-activated pro-drugs

Since hypoxic cells may survive after systemic drug treatment, and since tumor hypoxia confers a particularly metastatic and aggressive tumor phenotype, it is a logical target for new approaches to therapy. Hypoxia-activated pro-drugs (HAPS) have been developed, such that a pro-drug is administered in an inactive form, and is activated via a reduction reaction in hypoxic regions to

damage DNA (Wilson and Hay, 2011). Since the pro-drug does not bind to DNA in oxygenated cells, it should diffuse readily to hypoxic tumor regions. Several HAPs have been investigated including tirapazamine, AQ4N, PR-104, and TH-302. Tirapazamine was investigated in phase III clinical trials, but due to limited clinical benefit (perhaps because of poor distribution in tumor tissue of both the pro-drug, and the activated drug), further clinical investigation was halted (Denny, 2010).

TH-302 is a 2-nitroimidazole whose nitro group undergoes fragmentation releasing the active bromo-isophosphoramide group that binds to DNA and causes cross-linkage to occur (Meng et al., 2012). TH-302 has been shown to decrease the hypoxic fraction and increase necrosis following treatment of many different tumors in animals (Sun et al., 2012). In a randomized phase II clinical trial of gemcitabine and TH-302 in pancreatic cancer, combined therapy increased progression-free survival from 3.6 to 5.6 months (Borad et al., 2012) and a phase III trial is in progress. Thus, TH-302 appears to be a promising addition to traditional chemotherapy, and recent studies in our laboratory suggest that it can inhibit the repopulation and reoxygenation of formerly hypoxic cells following treatment of human tumor xenografts with chemotherapy.

CONCLUSION

Limited drug delivery to tumors is an important cause of treatment failure. The tumor microenvironment exerts effects that can alter the delivery of agents to neoplastic cells. Novel therapies that are able to leverage key characteristics of the tumor microenvironment such as hypoxia-activated pro-drugs and PPIs have potentials to result in improved therapeutic outcome.

ACKNOWLEDGMENTS

Canadian Institutes of Health Research.

REFERENCES

- Borad, M. J., Reddy, S., Bahary, N., Uronis, H., Sigal, D. S., Cohn, A. L., et al. (2012). Randomized Phase II Study of the Efficacy and Safety of Gemcitabine + TH-302 (G+T) vs Gemcitabine (G) Alone in Previously Untreated Patients with Advanced Pancreatic Cancer. Chicago, IL: American Association of Cancer Research.
- Conger, A. D., and Ziskin, M. C. (1983). Growth of mammalian multicellular tumor spheroids. *Cancer Res.* 43, 556–560.
- De Milito, A., Canese, R., Marino, M. L., Borghi, M., Iero, M., Villa, A., et al. (2010). pH-dependent antitumor activity of proton pump inhibitors against human melanoma is mediated by inhibition of tumor acidity. *Int. J. Cancer* 127, 207–219. doi:10.1002/ijc.25009
- De Milito, A., Iessi, E., Logozzi, M., Lozupone, F., Spada, M., Marino, M. L., et al. (2007). Proton pump inhibitors induce apoptosis of human B-cell tumors through a caspase-independent mechanism involving reactive oxygen species. *Cancer Res.* 67, 5408–5417. doi:10.1158/0008-5472.CAN-06-4095
- Denny, W. A. (2010). Hypoxia-activated prodrugs in cancer therapy: progress to the clinic. *Future Oncol.* 6, 419–428. doi:10.2217/fon.10.1
- Ferretti, S., Allegrini, P. R., Becquet, M. M., and McSheehy, P. M. (2009). Tumor interstitial fluid pressure as an early-response marker for anti-cancer therapeutics. *Neoplasia* 11, 874–881.
- Funderburk, S. F., Wang, Q. J., and Yue, Z. (2010). The Beclin 1-VPS34 complex – at the crossroads of autophagy and beyond. *Trends Cell Biol.* 20, 355–362. doi:10.1016/j.tcb.2010.03.002
- Fung, A. S., Jonkman, J., and Tanenock, I. F. (2012). Quantitative immunohistochemistry for evaluating the distribution of Ki67 and other biomarkers in tumor sections and use of the method to study repopulation in xenografts after treatment with paclitaxel. *Neoplasia* 14, 324–334.
- Fyles, A., Milosevic, M., Hedley, D., Pintilie, M., Levin, W., Manchul, L., et al. (2002). Tumor hypoxia has independent predictor impact only in patients with node-negative cervix cancer. *J. Clin. Oncol.* 20, 680–687. doi:10.1200/JCO.20.3.680
- Haensgen, G., Krause, U., Becker, A., Stadler, P., Lautenschlaeger, C., Wohlrab, W., et al. (2001). Tumor hypoxia, p53, and prognosis in cervical cancers. *Int. J. Radiat. Oncol. Biol. Phys.* 50, 865–872. doi:10.1016/S0360-3016(01)01523-1
- Hak, S., Reitan, N. K., Haraldseth, O., and de Lange Davies, C. (2010). Intravital microscopy in window chambers: a unique tool to study tumor angiogenesis and delivery of nanoparticles. *Angiogenesis* 13, 113–130. doi:10.1007/s10456-010-9176-y
- Heldin, C. H., Rubin, K., Pietras, K., and Ostman, A. (2004). High interstitial fluid pressure – an obstacle in cancer therapy. *Nat. Rev. Cancer* 4, 806–813. doi:10.1038/nrc1456
- Hirst, D. G., and Denekamp, J. (1979). Tumor cell proliferation in relation to the vasculature. *Cell Tissue Kinet.* 12, 31–42.
- Hockel, M., Schlenger, K., Aral, B., Mitze, M., Schaffer, U., and Vaupel, P. (1996). Association between tumor hypoxia and malignant progression in advanced cancer of the uterine cervix. *Cancer Res.* 56, 4509–4515.
- Hoyer-Hansen, M., and Jaattela, M. (2007). Connecting endoplasmic reticulum stress to autophagy by unfolded protein response and calcium. *Cell Death Differ.* 14, 1576–1582. doi:10.1038/sj.cdd.4402200
- Jubb, A. M., Buffa, F. M., and Harris, A. L. (2010). Assessment of tumor hypoxia for prediction of response to therapy and cancer prognosis. *J. Cell. Mol. Med.* 14, 18–29. doi:10.1111/j.1582-4934.2009.00944.x

- Karpathiou, G., Sivridis, E., Koukourakis, M. I., Mikroulis, D., Bouros, D., Froudarakis, M. E., et al. (2011). Light-chain 3A autophasic activity and prognostic significance in non-small cell lung carcinomas. *Chest* 140, 127–134. doi:10.1378/chest.10-1831
- Kim, M. J., Woo, S. J., Yoon, C. H., Lee, J. S., An, S., Choi, Y. H., et al. (2011). Involvement of autophagy in oncogenic K-Ras-induced malignant cell transformation. *J. Biol. Chem.* 286, 12924–12932. doi:10.1074/jbc.M110.138958
- Kuh, H. J., Jang, S. H., Wientjes, M. G., Weaver, J. R., and Au, J. L. (1999). Determinants of paclitaxel penetration and accumulation in human solid tumor. *J. Pharmacol. Exp. Ther.* 290, 871–880.
- Kuszyk, B. S., Corl, F. M., Franano, F. N., Bluemke, D. A., Hofmann, L. V., Fortman, B. J., et al. (2001). Tumor transport physiology: implications for imaging and imaging-guided therapy. *AJR Am. J. Roentgenol.* 177, 747–753. doi:10.2214/ajr.177.4.1770747
- Lankelma, J., Dekker, H., Luque, F. R., Luykx, S., Hoekman, K., van der Valk, P., et al. (1999). Doxorubicin gradients in human breast cancer. *Clin. Cancer Res.* 5, 1703–1707.
- Larsson, H., Mattson, H., Sundell, G., and Carlsson, E. (1985). Animal pharmacodynamics of omeprazole. A survey of its pharmacological properties in vivo. *Scand. J. Gastroenterol. Suppl.* 108, 23–35.
- Lee, C. M., and Tannock, I. F. (2006). Inhibition of endosomal sequestration of basic anticancer drugs: influence on cytotoxicity and tissue penetration. *Br. J. Cancer* 94, 863–869. doi:10.1038/sj.bjc.6603010
- Lee, C. M., and Tannock, I. F. (2010). The distribution of the therapeutic monoclonal antibodies cetuximab and trastuzumab within solid tumors. *BMC Cancer* 10:255. doi:10.1186/1471-2407-10-255
- Lesser, G. J., Grossman, S. A., Eller, S., and Rowinsky, E. K. (1995). The distribution of systemically administered [³H]-paclitaxel in rats: a quantitative autoradiographic study. *Cancer Chemother. Pharmacol.* 37, 173–178. doi:10.1007/BF00685646
- Levine, B. (2007). Cell biology: autophagy and cancer. *Nature* 446, 745–747. doi:10.1038/446745a
- Ljungkvist, A. S., Bussink, J., Rijken, P. F., Kaanders, J. H., van der Kogel, A. J., and Denekamp, J. (2002). Vascular architecture, hypoxia, and proliferation in first-generation xenografts of human head-and-neck squamous cell carcinomas. *Int. J. Radiat. Oncol. Biol. Phys.* 54, 215–228. doi:10.1016/S0360-3016(02)02938-3
- Luanpitpong, S., Chanvorachote, P., Nimmanit, U., Leonard, S. S., Stehlík, C., Wang, L., et al. (2012). Mitochondrial superoxide mediates doxorubicin-induced keratinocyte apoptosis through oxidative modification of ERK and Bcl-2 ubiquitination. *Biochem. Pharmacol.* 83, 1643–1654. doi:10.1016/j.bcp.2012.03.010
- Luciani, F., Spada, M., De Milito, A., Molinari, A., Rivoltini, L., Montinaro, A., et al. (2004). Effect of proton pump inhibitor pretreatment on resistance of solid tumors to cytotoxic drugs. *J. Natl. Cancer Inst.* 96, 1702–1713. doi:10.1093/jnci/djh305
- Lunt, S. J., Fyles, A., Hill, R. P., and Milosevic, M. (2008). Interstitial fluid pressure in tumors: therapeutic barrier and biomarker of angiogenesis. *Future Oncol.* 4, 793–802. doi:10.2217/14796694.4.6.793
- Manallack, D. T. (2008). The pK(a) distribution of drugs: application to drug discovery. *Perspect. Medicin. Chem.* 1, 25–38.
- Marino, M. L., Fais, S., Djavaheri-Mergny, M., Villa, A., Meschini, S., Lozupone, F., et al. (2010). Proton pump inhibition induces autophagy as a survival mechanism following oxidative stress in human melanoma cells. *Cell Death Dis.* 1, e87. doi:10.1038/cddis.2010.67
- Matheny, C. J., Lamb, M. W., Brouwer, K. R., and Pollack, G. M. (2001). Pharmacokinetic and pharmacodynamic implications of P-glycoprotein modulation. *Pharmacotherapy* 21, 778–796. doi:10.1592/phco.21.9.778.34558
- Mayer, L. D., Bally, M. B., and Cullis, P. R. (1986). Uptake of adriamycin into large unilamellar vesicles in response to a pH gradient. *Biochim. Biophys. Acta* 857, 123–126. doi:10.1016/0005-2736(86)90105-7
- Meng, F., Evans, J. W., Bhupathi, D., Banica, M., Lan, L., Lorente, G., et al. (2012). Molecular and cellular pharmacology of the hypoxia-activated prodrug TH-302. *Mol. Cancer Ther.* 11, 740–751. doi:10.1158/1535-7163.MCT-11-0634
- Minchinton, A. I., and Tannock, I. F. (2006). Drug penetration in solid tumors. *Nat. Rev. Cancer* 6, 583–592. doi:10.1038/nrc1893
- Mizukami, Y., Kohgo, Y., and Chung, D. C. (2007). Hypoxia inducible factor-1 independent pathways in tumor angiogenesis. *Clin. Cancer Res.* 13, 5670–5674. doi:10.1158/1078-0432.CCR-07-0111
- Nordsmark, M., Bentzen, S. M., Rudat, V., Brizel, D., Lartigau, E., Stadler, P., et al. (2005). Prognostic value of tumor oxygenation in 397 head and neck tumors after primary radiation therapy. An international multi-center study. *Radiat. Oncol.* 77, 18–24. doi:10.1016/j.radonc.2005.06.038
- Ogiso, Y., Tomida, A., Lei, S., Omura, S., and Tsuruo, T. (2000). Proteasome inhibition circumvents solid tumor resistance to topoisomerase II-directed drugs. *Cancer Res.* 60, 2429–2434.
- Olive, K. P., Jacobetz, M. A., Davidson, C. J., Gopinathan, A., McIntyre, D., Honess, D., et al. (2009). Inhibition of Hedgehog signaling enhances delivery of chemotherapy in a mouse model of pancreatic cancer. *Science* 324, 1457–1461. doi:10.1126/science.1171362
- Potter, C., and Harris, A. L. (2004). Hypoxia inducible carbonic anhydrase IX, marker of tumor hypoxia, survival pathway and therapy target. *Cell Cycle* 3, 164–167. doi:10.4161/cc.3.2.618
- Primeau, A. J., Rendon, A., Hedley, D., Lilge, L., and Tannock, I. F. (2005). The distribution of the anticancer drug Doxorubicin in relation to blood vessels in solid tumors. *Clin. Cancer Res.* 11, 8782–8788. doi:10.1158/1078-0432.CCR-05-1664
- Provenzano, P. P., Cuevas, C., Chang, A. E., Goel, V. K., Von Hoff, D. D., and Hingorani, S. R. (2012). Enzymatic targeting of the stroma ablates physical barriers to treatment of pancreatic ductal adenocarcinoma. *Cancer Cell* 21, 418–429. doi:10.1016/j.ccr.2012.01.007
- Rofstad, E. K., Sundfor, K., Lyng, H., and Trope, C. G. (2000). Hypoxia-induced treatment failure in advanced squamous cell carcinoma of the uterine cervix is primarily due to hypoxia-induced radiation resistance rather than hypoxia-induced metastasis. *Br. J. Cancer* 83, 354–359. doi:10.1054/bjoc.2000.1266
- Rouschop, K. M., van den Beucken, T., Dubois, L., Niessen, H., Bussink, J., Savelkouls, K., et al. (2010). The unfolded protein response protects human tumor cells during hypoxia through regulation of the autophagy genes MAP1LC3B and ATG5. *J. Clin. Invest.* 120, 127–141. doi:10.1172/JCI40027
- Saggar, J. K., Fung, A. S., Patel, K. J., and Tannock, I. F. (2013). Use of molecular biomarkers to quantify the spatial distribution of effects of anti-cancer drugs in solid tumors. *Mol. Cancer Ther.* 12, 542–552. doi:10.1158/1535-7163.MCT-12-0967
- Sivridis, E., Koukourakis, M. I., Mendrinos, S. E., Karpouzis, A., Fiska, A., Kouskoukis, C., et al. (2011). Beclin-1 and LC3A expression in cutaneous malignant melanomas: a biphasic survival pattern for beclin-1. *Melanoma Res.* 21, 188–195. doi:10.1097/CMR.0b013e328346612c
- Song, C. W., Griffin, R., and Park, H. J. (2006). “Influence of tumor pH on therapeutic response,” in *Cancer Drug Resistance*, ed. B. A. Teicher (New Jersey: Springer), 617.
- Sun, J. D., Liu, Q., Wang, J., Ahluwalia, D., Ferraro, D., Wang, Y., et al. (2012). Selective tumor hypoxia targeting by hypoxia-activated prodrug TH-302 inhibits tumor growth in preclinical models of cancer. *Clin. Cancer Res.* 18, 758–770. doi:10.1158/1078-0432.CCR-11-1980
- Tannock, I. F., Lee, C. M., Tunggal, J. K., Cowan, D. S., and Egorin, M. J. (2002). Limited penetration of anti-cancer drugs through tumor tissue: a potential cause of resistance of solid tumors to chemotherapy. *Clin. Cancer Res.* 8, 878–884.
- Tredan, O., Galmarini, C. M., Patel, K., and Tannock, I. F. (2007). Drug resistance and the solid tumor microenvironment. *J. Natl. Cancer Inst.* 99, 1441–1454. doi:10.1093/jnci/djm135
- Undeva, S. D., Gomez-Abuin, G., and Ratain, M. J. (2005). Pharmacokinetic variability of anticancer agents. *Nat. Rev. Cancer* 5, 447–458. doi:10.1038/nrc1629
- Vaupel, P., and Harrison, L. (2004). Tumor hypoxia: causative factors, compensatory mechanisms, and cellular response. *Oncologist* 9(Suppl. 5), 4–9. doi:10.1634/theoncologist.9-9005-4
- Vinci, M., Gowan, S., Boxall, F., Patterson, L., Zimmermann, M., Court, W., et al. (2011). Advances in establishment and analysis of three-dimensional tumor spheroid-based functional assays for target validation and drug evaluation. *BMC Biol.* 10:29. doi:10.1186/1741-7007-10-29
- Wartenberg, M., Ling, F. C., Muschen, M., Klein, F., Acker, H., Gassmann, M., et al. (2003). Regulation of the multidrug resistance transporter P-glycoprotein in multicellular tumor

spheroids by hypoxia-inducible factor (HIF-1) and reactive oxygen species. *FASEB J.* 17, 503–505.

Wilson, W. R., and Hay, M. P. (2011). Targeting hypoxia in cancer therapy. *Nat. Rev. Cancer* 11, 393–410. doi:10.1038/nrc3064

Yang, Z. J., Chee, C. E., Huang, S., and Sinicrope, F. A. (2011). The role of autophagy in cancer: therapeutic implications. *Mol. Cancer Ther.* 10, 1533–1541. doi:10.1158/1535-7163.MCT-11-0047

Yeo, M., Kim, D. K., Kim, Y. B., Oh, T. Y., Lee, J. E., Cho, S. W., et al. (2004). Selective induction of apoptosis with proton pump inhibitor in gastric cancer cells. *Clin. Cancer Res.* 10, 8687–8696. doi:10.1158/1078-0432.CCR-04-1065

Yu, L., Alva, A., Su, H., Dutt, P., Freundt, E., Welsh, S., et al. (2004). Regulation of an ATG7-beclin 1 program of autophagic cell death by caspase-8. *Science* 304, 1500–1502. doi:10.1126/science.109645

Conflict of Interest Statement: The authors declare that the research was conducted in the absence of any commercial or financial relationships that could be construed as a potential conflict of interest.

Received: 01 May 2013; *paper pending published:* 20 May 2013; *accepted:* 29 May 2013; *published online:* 10 June 2013.

Citation: Saggar JK, Yu M, Tan Q and Tannock IF (2013) The tumor microenvironment and strategies to

improve drug distribution. *Front. Oncol.* 3:154. doi: 10.3389/fonc.2013.00154
This article was submitted to Frontiers in Pharmacology of Anti-Cancer Drugs, a specialty of Frontiers in Oncology.

Copyright © 2013 Saggar, Yu, Tan and Tannock. This is an open-access article distributed under the terms of the Creative Commons Attribution License, which permits use, distribution and reproduction in other forums, provided the original authors and source are credited and subject to any copyright notices concerning any third-party graphics etc.



Influence of the duration of intravenous drug administration on tumor uptake

Sylvain Fouliard¹, Marylore Chenel¹ and Fabrizio Marcucci^{2,3*}

¹ Clinical Pharmacokinetics Department, Institut de Recherches Internationales Servier, Suresnes, France

² Centro Nazionale di Epidemiologia, Sorveglianza e Promozione della Salute (CNEPS), Istituto Superiore di Sanita' (ISS), Roma, Italy

³ Hepatology Association of Calabria (ACE), Reggio Calabria, Italy

Edited by:

Angelo Corti, San Raffaele Scientific Institute, Italy

Reviewed by:

Vincenzo Russo, San Raffaele Scientific Institute, Italy

Ronald Berenson, Compliment Corporation, USA

***Correspondence:**

Fabrizio Marcucci, Centro Nazionale di Epidemiologia, Sorveglianza e Promozione della Salute (CNEPS), Istituto Superiore di Sanita' (ISS), via Giano della Bella 34, 00162 Rome, Italy

e-mail: fabmarcu@gmail.com

Enhancing tumor uptake of anticancer drugs is an important therapeutic goal, because insufficient drug accumulation is now considered to be an important reason for unresponsiveness or resistance to antitumor therapy. Based on a mechanistic tumor uptake model describing tumor exposure to molecules of different molecular size after bolus administration, we have investigated the influence of the duration of intravenous administration on tumor uptake. The model integrates empirical relationships between molecular size and drug disposition (capillary permeability, interstitial diffusivity, available volume fraction, and plasma clearance), together with a compartmental pharmacokinetics model and a drug/target binding model. Numerical simulations were performed using this model for protracted intravenous drug infusion, a common mode of administration of anticancer drugs. The impact of mode of administration on tumor uptake is described for a large range of molecules of different molecular size. Evaluation was performed not only for the maximal drug concentration achieved in the tumor, but also for the dynamic profile of drug concentration. It is shown that despite a lower maximal uptake for a given dose, infusion allows for a prolonged exposure of tumor tissues to both small- and large-sized molecules. Moreover, infusion may allow higher doses to be administered by reducing Cmax-linked toxicity, thereby achieving a similar maximal uptake compared to bolus administration.

Keywords: tumor, uptake, size, infusion, affinity

INTRODUCTION

Solid tumors are characterized by important abnormalities in tissue architecture and composition (1). These abnormalities represent considerable obstacles for uptake and penetration of antitumor drugs. Thus, tumor blood supply is often inefficient and, consequently, drug delivery to the tumor is impaired. Also the transvascular and interstitial transport of antitumor drugs is impaired because of reduced transvascular pressure gradient, high interstitial fluid pressure (2), high packing density of tumor cells (3), intercellular junctions (4), and altered composition of the extracellular matrix that increases frictional resistance (5). These abnormalities compromise the tumor delivery of antitumor drugs of all molecular sizes, i.e., low molecular weight drugs, macromolecular drugs, and nanoparticulate drug formulations. In fact, transvascular and interstitial transport of molecules is governed by flow (convection) and diffusion from regions of high concentration to regions of lower concentration. For macromolecules diffusion is extremely slow, and they are transported mainly by convection, that is, by streaming of a flowing fluid (6). As regards low molecular weight drugs, many of them show significant binding to plasma proteins, which leads them to behave, functionally, like macromolecules. Convection-driven transport, however, is often compromised in solid tumors because of decrease or loss of the transvascular pressure gradient.

Cytotoxic drugs (chemotherapeutics or antibodies mediating antibody-dependent cellular cytotoxicity or complement-dependent cytotoxicity) can, at least in part, limit the negative consequences of these effects. In fact, it has been proposed that cytotoxic effector drugs that are administered repeatedly at regular intervals cause “peeling” of increasing numbers of tumor cell layers until tumor regression is observed (2, 7, 8). Such a mechanism of action is expected to suffer less from the negative consequences of an impaired interstitial transport and penetration. The tumor cell layers that are eliminated are the most proximal to the tumor vessels from which the drug extravasates. Elimination of vessel-proximal tumor cell layers, however, may stimulate proliferation and repopulation of more vessel-distant tumor cells leading them to replace the cells that have been eliminated as a result of drug-induced cytotoxicity. This can be an important cause of treatment failure (9). Moreover, cytotoxic drugs can also promote active mechanisms of resistance induction. Thus, it has been shown that intermittent treatment of mice bearing ovarian cancer xenografts with docetaxel led to the development of different mechanisms of drug resistance, while continuous drug infusion resulted in superior antitumor efficacy and prevented drug resistance (10). These results suggested that continuous drug infusion may have considerable advantages over the more commonly used, intermittent, bolus administration protocols (11).

On the basis of these considerations it appeared of obvious interest to elaborate mechanistic models that describe the effects of continuous infusion on the tumor uptake of molecules compared to bolus administration. We have performed such a study taking advantage of a mechanistic tumor uptake model that had been described for bolus administration (12). In this report we describe the results of this study and compare them with those obtained for bolus administration.

MATERIALS AND METHODS

Simulations were performed using the equations of the model described by Schmidt and Wittrup (12), implemented in R (13) and modified in its pharmacokinetic components in order to integrate the intravenous administration rate. The model describes the relationships between molecular radius (R_{mol}) and permeability across the tumor capillary wall (P), diffusivity within the tumor interstitium (D), available volume fraction in the tumor (ε), and rate of plasma clearance (k_{clear}), respectively. These relationships are based on previously reported experimental measurements for molecules of various sizes in tumor tissues [supplementary data from Schmidt and Wittrup (12)].

The impact of molecular radius (R_{mol}) on diffusivity and available volume fraction was described by modeling tumor tissue as a series of small and large right circular cylindric pores (14). Diffusivity of molecules in each pore (D_{poretum}) can be estimated from diffusivity in solution (D_{free}) and the ratio (λ) of molecular radius (R_{mol}) to pore radius (R_{pore}) using the equations:

$$D_{\text{poretum}} = D_{\text{free}} \times \frac{1 - 2.105\lambda + 2.0865\lambda^3 - 1.7068\lambda^5 + 0.72603\lambda^6}{1 - 0.78587\lambda^5}$$

$$D_{\text{free}} = \frac{3 \times \frac{10^{-6} \text{ cm}^2}{\text{s}}}{R_{\text{mol}}}$$

for $\lambda < 0.6$. For $\lambda > 1$, $D_{\text{poretum}} = 0$. For other values of λ , the ratio $D_{\text{poretum}}/D_{\text{free}}$ was determined from previously described work (15). R_{mol} is expressed in nanometers. Overall, diffusion within the tumor is:

$$D = A \times D_{\text{poretum,small}} + B \times D_{\text{poretum,large}}$$

where A and B are the relative diffusions occurring in small and large pores, respectively. According to this two-pore tumor model, the available volume fraction is defined as:

$$\varepsilon = V_i \left(A \times \varphi_{\text{poretum,small}} + B \times \varphi_{\text{poretum,large}} \right)$$

where V_i is the interstitial fluid volume fraction [approximated at 0.5 (16)], and partition coefficients for each pore size (φ_{pore}) is $(1 - \lambda^2)$ when $\lambda < 1$, and 0 when $\lambda > 1$ (17). Vascular permeability was also modeled using a two-pore model of the capillary wall, and transport was assumed to be mainly diffusive; therefore, permeability across each pore was:

$$P_{\text{porecap}} = D_{\text{porecap}} \times \varphi_{\text{porecap}}$$

Overall, total permeability was defined as:

$$P = A_{\text{cap}} \times P_{\text{porecap,small}} + B_{\text{cap}} \times P_{\text{porecap,large}}$$

The impact of molecular size was modeled both on the renal plasma clearance (CL_R) and the non-renal plasma clearance (CL_{NR}). For non-renal plasma clearance, an empirical model accounted for loss of molecules above the cutoff size for glomerular filtration with an empirical model:

$$CL_{NR} = CL_{NR,0} - \delta \frac{R_{\text{mol}}}{R_{\text{mol}} + \gamma}$$

where $CL_{NR,0}$ is the non-renal clearance for small molecule tracers (set to 2 mL/h), and δ (mL/h) and γ (nm) are empirical constants fit to the data. Renal plasma clearance is modeled as $CLR = GFR \times \theta$ where GFR is the glomerular filtration rate (10 mL/h) and θ is the macromolecular sieving coefficient, depending on molecular size:

$$\theta = \frac{\Phi K_{\text{conv}}}{1 - e^{-\sigma P_e} + \Phi K_{\text{conv}} e^{-\sigma P_e}}$$

where Φ is the equilibrium partition coefficient, σ is a correction term for the geometry of the glomerular slits approximately equal to 2 for baseline glomeruli, K_{conv} is the solute hindrance factor for convection, and P_e is the Péclet number defined as:

$$P_e = \frac{\Phi K_{\text{conv}} \times v \times L}{\Phi K_{\text{diff}} \times D_{\text{free}}}$$

where v is the fluid velocity vector (0.001 cm/s), L is the membrane thickness [100 nm in mice (18)], and K_{diff} is the diffusive hindrance factor. K_{conv} and K_{diff} , along with the partition coefficient, are empirically modeled as (19) $\Phi K_{\text{diff}} = \exp(-\alpha R_{\text{mol}})$ and $\Phi K_{\text{conv}} = \exp(-\beta R_{\text{mol}})$.

Plasma clearance (CL) was derived from renal and non-renal components $CL = CLR + CL_{NR}$, and along with plasma volume V (2 mL in mice), constituted the pharmacokinetic parameters of the one-compartment pharmacokinetic model.

Eventually, the tumor uptake was computed using a compartmental pharmacokinetic model in equilibrium with the tumor interstitium and a drug/receptor binding model. Considering Ω defined as:

$$\Omega = \left(\frac{2PR_{\text{cap}}}{\varepsilon R_{\text{Krogh}}^2} \right) \left(\frac{K_d}{([A_g]/\varepsilon) - K_d} \right) + K_e \left(\frac{([A_g]/\varepsilon)}{([A_g]/\varepsilon) - K_d} \right)$$

the concentration in tumor after a single bolus administration is:

$$[AB]_{\text{tumor}} = \left(\frac{2PR_{\text{cap}}}{R_{\text{Krogh}}^2} \right) \left(\frac{\text{Dose}/V_{\text{plasma}} (e^{-k_{\text{clear}} t} - e^{-\Omega t})}{(\Omega - k_{\text{clear}})} \right)$$

tumor concentration after intravenous infusion of rate, Rate = Dose/T_{perf}, when t > T_{perf} is:

$$[AB]_{\text{tumor}} = \int_0^t \left(\frac{2PR_{\text{cap}}}{R_{\text{Krogh}}^2} \right) \times \left(\frac{\text{Rate}/V_{\text{plasma}} \left(e^{-k_{\text{clear}}(t-u)} - e^{-\Omega(t-u)} \right)}{(\Omega - k_{\text{clear}})} \right) du$$

which can be rewritten as:

$$[AB]_{\text{tumor}} = \left(\frac{2PR_{\text{cap}}}{R_{\text{Krogh}}^2} \right) \times \left(\frac{\text{Rate}/V_{\text{plasma}}}{(\Omega - k_{\text{clear}})} \right) \left(\frac{1 - e^{-k_{\text{clear}}t}}{k_{\text{clear}}} - \frac{1 - e^{-\Omega t}}{\Omega} \right)$$

and tumor concentration after intravenous infusion of rate, Rate = Dose/T_{perf}, when t < T_{perf} is:

$$[AB]_{\text{tumor}} = \int_0^{T_{\text{perf}}} \left(\frac{2PR_{\text{cap}}}{R_{\text{Krogh}}^2} \right) \times \left(\frac{\text{Rate}/V_{\text{plasma}} \left(e^{-k_{\text{clear}}(t-u)} - e^{-\Omega(t-u)} \right)}{(\Omega - k_{\text{clear}})} \right) du$$

which can be rewritten as:

$$[AB]_{\text{tumor}} = \left(\frac{2PR_{\text{cap}}}{R_{\text{Krogh}}^2} \right) \left(\frac{\text{Rate}/V_{\text{plasma}}}{(\Omega - k_{\text{clear}})} \right) \times \left(\frac{e^{-k_{\text{clear}}t} (e^{k_{\text{clear}}T_{\text{perf}}} - 1)}{k_{\text{clear}}} - \frac{e^{-\Omega t} (e^{\Omega T_{\text{perf}}} - 1)}{\Omega} \right)$$

where Dose is the amount of drug administered, t is the time, [Ag] is the target antigen concentration (mol/L), k_e is the rate of endocytic clearance (s⁻¹), K_d is the affinity of the targeting molecule for the antigen (mol/L), R_{cap} is the capillary radius (μm), and R_{Krogh} is the average radius of tissue surrounding each blood vessel (μm).

Simulations of tumor uptake versus time profiles were performed for both intravenous bolus administration and continuous infusion. Duration of continuous infusion T_{perf} was set to 60 h with no loss of generality. The range of molecular radius (R_{mol}) for simulations was set from 0.1 to 100 nm, and the corresponding molecular weight (MW, expressed in kDa) was approximated as MW = 1.32 × R_{mol}³. The range of affinity for the target (K_d) for simulations was [10⁻¹²; 10⁻⁶] (K_d was set

to 10⁻⁹ when investigating tumor uptake/time relationship). The case of IgG molecules is out of the scope of the present work, as their plasma clearance is smaller than other molecules with the same molecular weight due to their binding to FcRn receptors (20).

Simulations were performed using estimated parameter values described in Table 1, consistently with values used by Schmidt and Wittrup (12). In order to better assess differences in tumor

Table 1 | Definition of the parameters and values used for simulations.

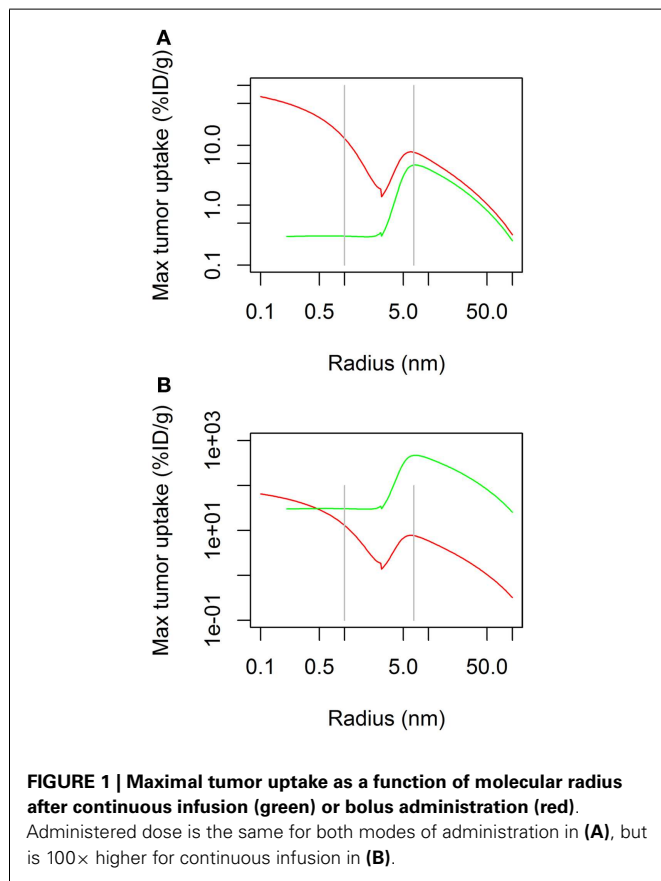
Parameter	Definition	Value
MW	Molecular weight (kDa)	1–1000
R _{tumsmall}	Radius of smaller tumor pore within tumor (nm)	13.8
R _{tumlarge}	Radius of larger tumor pore within tumor (nm)	1000
R _{capsmall}	Radius of smaller tumor pore within capillary wall (nm)	4.5
R _{caplarge}	Radius of larger tumor pore within capillary wall (nm)	500
A _{tum}	Partition coefficient in smaller pores within tumor (–)	0.9
B _{tum}	Partition coefficient in larger pores within tumor (–)	0.1
A _{cap}	Partition coefficient in smaller pores within capillary wall per unit membrane thickness (cm ⁻¹)	17.6
B _{cap}	Partition coefficient in larger pores within capillary wall per unit membrane thickness (cm ⁻¹)	0.65
V _i	Interstitial fluid volume fraction (–)	0.5
GFR	Glomerular filtration rate (mL/h)	10
α	Empirical fitting constant (nm ⁻¹)	1.6
β	Empirical fitting constant (nm ⁻¹)	0.95
γ	Empirical fitting constant (nm)	0.2
δ	Empirical fitting constant (mL/h)	1.94
v	Fluid velocity vector (cm/s)	0.001
L	Membrane thickness (nm)	100
CL _{NR,0}	Non-renal clearance for small molecules tracers (mL/h)	2
V _{plasma}	Plasma volume (mL)	2
σ	Correction term for geometry of glomeruli (–)	2
R _{cap}	Capillary radius	8
R _{Krogh}	Average radius of tissue surrounding blood vessels (μm)	75
K _d	Molecule affinity for antigen (mol/L)	10 ⁻¹² –10 ⁻⁶
K _e	Rate of endocytic clearance (1/s)	0.000016
[A _g]	Target antigen concentration in the tumor (nmol/L)	1.5

uptake between modes of administration, simulations were performed both using the same administered dose (D) for bolus administration and continuous infusion, and using D and $100 \times D$ for bolus administration and continuous infusion, respectively. Tumor uptake was expressed as a fraction of injected dose/gram (% ID/g).

RESULTS

We simulated the influence of the molecular radius, the time-course, and the affinity on the maximal tumor uptake of molecules administered by continuous infusion. Duration of infusion was set to 60 h.

The simulation of the influence of the molecular radius on maximal tumor uptake (ID/g) showed (Figure 1A) that maximal tumor uptake after continuous infusion was similar to that after bolus administration for large molecules ($R_{\text{mol}} > 3 \text{ nm}$), but it was lower for small molecules ($R_{\text{mol}} < 3 \text{ nm}$). The dose administered by continuous infusion was then increased by a factor of 100 in order to achieve a maximal tumor uptake (Figure 1B) for small molecules similar to that after bolus administration. Under these conditions, the reduced maximal tumor uptake of small molecules after continuous infusion was no longer observed. Regarding large molecules, the same pattern was observed after both modes of administration (i.e., bolus and continuous), with an increase to a maximal value of tumor uptake, and a decrease as molecules exceeded a size of $\sim 10 \text{ nm}$.



The time-course of tumor uptake (Figures 2A,B) showed that the increase in concentration was delayed after continuous infusion compared to bolus administration, both for large and small molecules. However, peak tumor uptake of small molecules was more affected by the mode of administration than that of large molecules, i.e., the increase in tumor uptake was higher for small molecules than for large molecules. Regarding large molecules, while maximal tumor uptake was comparable between bolus administration and continuous infusion, tumor exposure was longer after continuous infusion. The benefit of a higher maximal tumor uptake of small molecules observed after bolus administration was balanced by the shorter duration of tumor exposure.

Eventually, we investigated the relationship between affinity and maximal tumor uptake (Figure 3). Increasing the affinity of a molecule increased its maximal tumor uptake up to a plateau value. This was seen for both bolus (Figure 3A) and continuous infusion (Figure 3B). The affinity at which this plateau value was attained depended for both modes of administration on the size of the administered molecule (10^{-9} for larger molecules, and 10^{-11} for smaller molecules). The fact that the affinity required to achieve a similar tumor uptake is much lower for larger than for smaller molecules shows that although the time-course of tumor uptake is strongly dependent on the mode of administration, the relationship between tumor uptake and affinity is unaffected.

DISCUSSION

In this article we have simulated the influence of molecular radius, time-course, and affinity of a molecule (e.g., an antitumor drug) on its maximal tumor uptake after continuous infusion and compared the results with those obtained in a similar model after bolus administration (12). For continuous infusion we set the duration to 60 h, a time period sufficient to attain equilibrium between the different compartments of the body.

We found that administration of a molecule by continuous infusion led to a relatively homogeneous uptake, that was independent of the molecular radius. A further increase of uptake, with a bell-shaped curve, was observed for molecules with a radius of $\sim 5\text{--}20 \text{ nm}$, with a maximal uptake at $\sim 10 \text{ nm}$. This is likely due to increased systemic accumulation of molecules that are larger than the size allowing for elimination through kidney filtration. Not surprisingly, at similar doses, maximal tumor uptake is much higher for bolus administration than continuous infusion, but this can be overcome by increasing the dose administered by continuous infusion (in Figure 1B, the dose administered by infusion is $100\times$ higher than that administered by bolus). It is interesting to note that the shape of the uptake curve upon continuous infusion did not show the uptake minimum at $\sim 3 \text{ nm}$ (25 kDa molecular weight) that is observed after bolus administration. This molecular size corresponds to that, for example, of a bispecific single-chain variable fragment. A compound of this kind (blinatumomab) is now in advanced clinical trials for the treatment of lymphoma acute lymphoblastic leukemia, and it is interesting to note that it is administered to patients by continuous infusion (21, 22). While lymphoma therapy is expected to suffer less

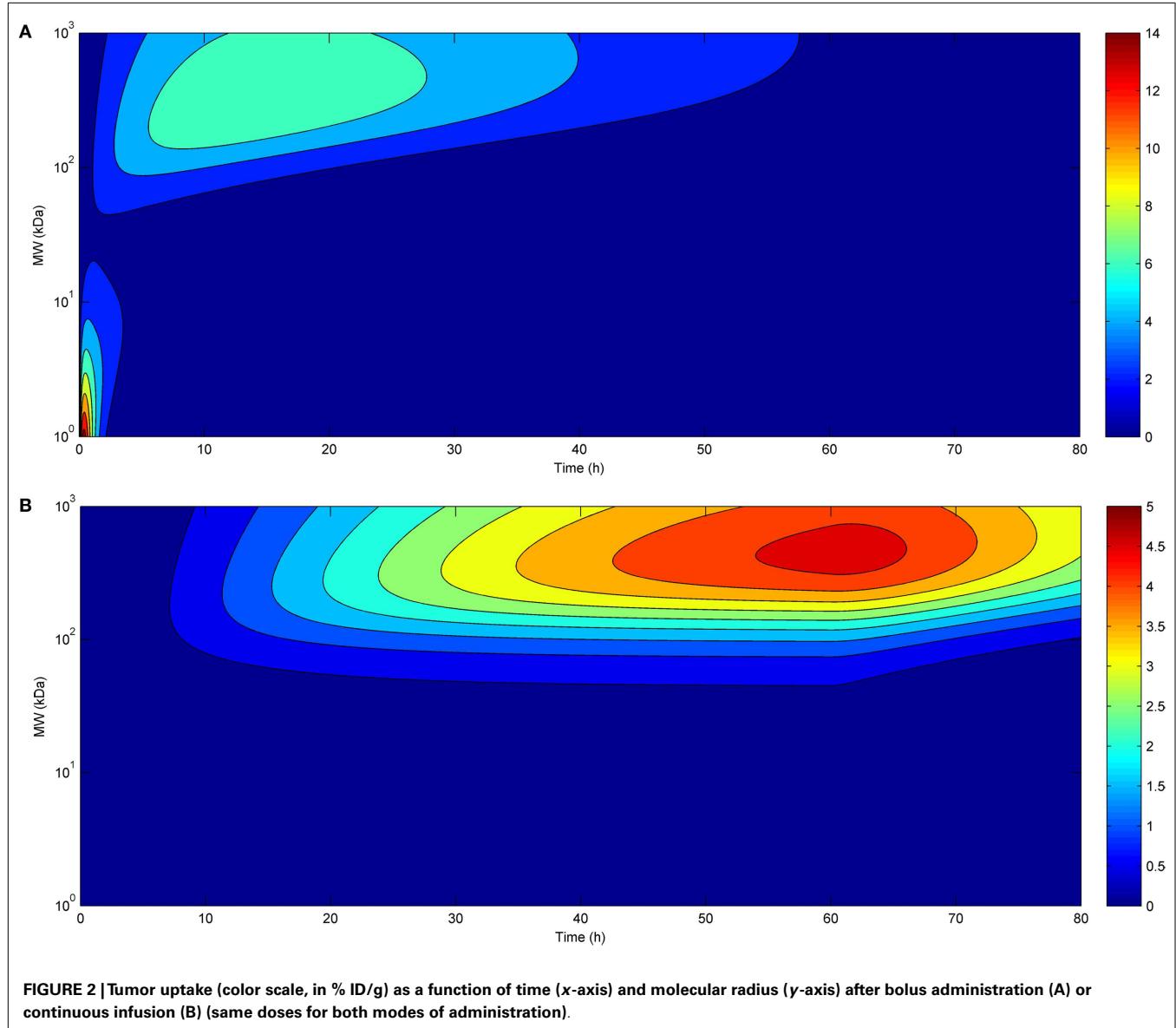


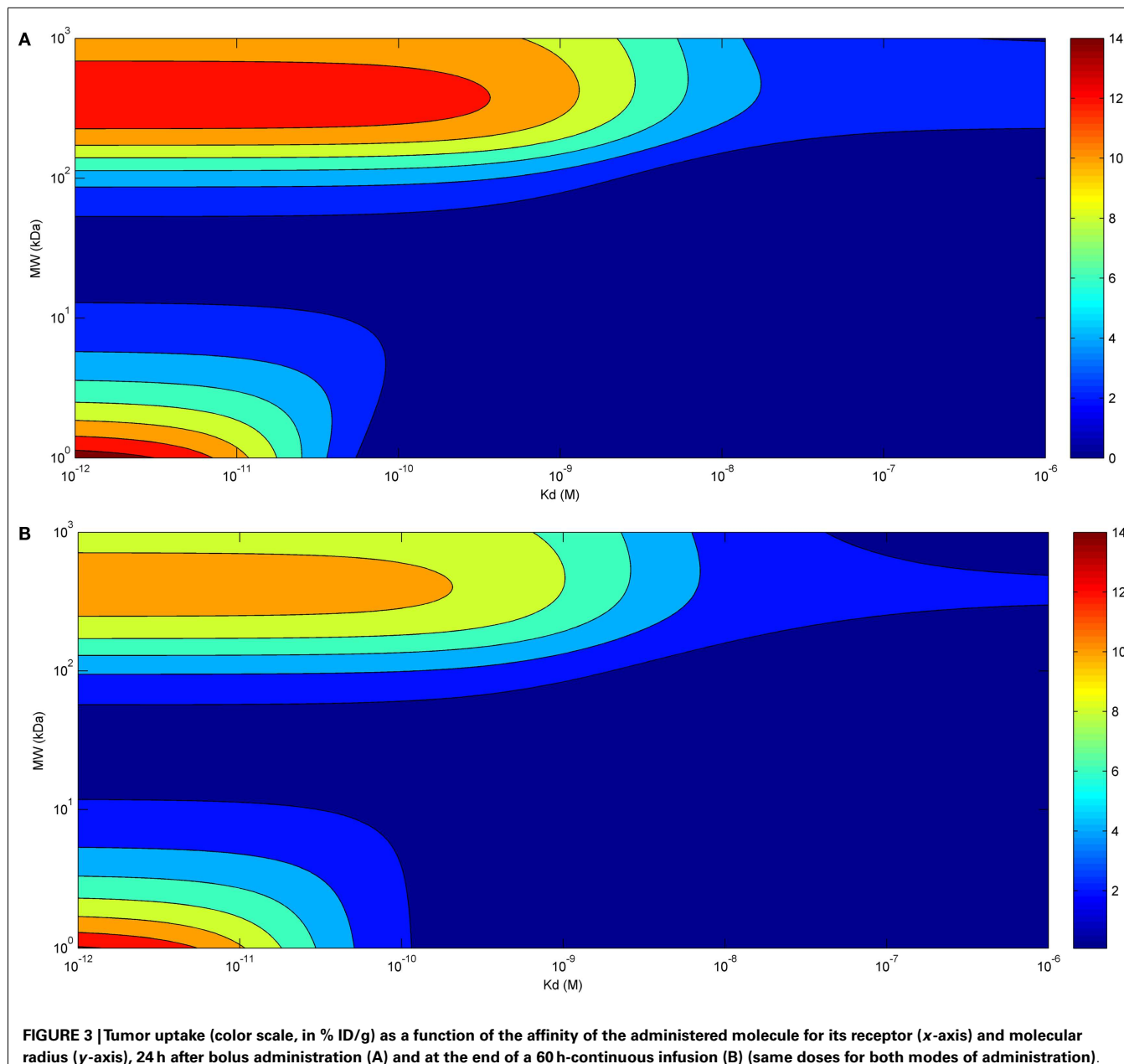
FIGURE 2 |Tumor uptake (color scale, in % ID/g) as a function of time (x-axis) and molecular radius (y-axis) after bolus administration (A) or continuous infusion (B) (same doses for both modes of administration).

from the impediments that characterize solid tumors, it appears, nonetheless, that administration of agents of this molecular size by continuous infusion is optimal to achieve the highest possible tumor uptake and accumulation. Overall, continuous infusion appears to be preferable to bolus administration in view of the possibility of achieving a more predictable tumor uptake of molecules of varying molecular size.

Also regarding the time-course of tumor uptake, continuous infusion appears to present advantages compared to bolus administration, allowing for longer exposure of the tumor. For small molecules, maximal tumor uptake was higher for bolus administration, but, again, this can be easily overcome by increasing the dose administered by infusion. Eventually, the relationship between tumor uptake and affinity of the administered molecules appears to be independent of the mode of administration. Thus, in accordance with previous results obtained with

a similar model (12), the affinity required to achieve a similar tumor uptake is much lower for larger than for smaller molecules, and this is true for both bolus administration and continuous infusion.

Overall, the results from the mechanistic model used in this study suggest that continuous infusion offers some advantages compared with the more commonly used bolus administration. Most importantly, differences in uptake between molecules of different molecular size become less relevant upon continuous infusion than bolus administration. In particular, the nadir in tumor uptake at a ~ 3 nm size disappears. Moreover, infusion allows for a prolonged exposure of tumor tissues to both small- and large-sized molecules. Eventually, this mode of administration may allow higher doses to be administered by reducing Cmax-linked toxicity, thereby allowing a similar maximal uptake compared to bolus administration. These



advantages add to those related to reduced induction of drug resistance as a consequence of more homogeneous distribution of the drug throughout the tumor (10), thereby preventing or

limiting repopulation of the tumor by proliferating tumor cells (9) and inhibiting induction of active mechanisms of resistance induction (7).

REFERENCES

- Marcucci F, Corti A. How to improve exposure of tumor cells to drugs – promoter drugs increase tumor uptake and penetration of effector drugs. *Adv Drug Deliv Rev* (2012) **64**:53–68. doi:10.1016/j.addr.2011.09.007
- Trédan O, Galmarini CM, Patel K, Tannock IF. Drug resistance and the solid tumor microenvironment. *J Natl Cancer Inst* (2007) **99**:1441–54. doi:10.1093/jnci/djm135
- Grantab R, Sivananthan S, Tannock IF. The penetration of anticancer drugs through tumor tissue as a function of cellular adhesion and packing density of tumor cells. *Cancer Res* (2006) **66**:1033–9. doi:10.1158/0008-5472.CAN-05-3077
- Beyer I, Cao H, Persson J, Song H, Richter M, Feng Q, et al. Co-administration of epithelial junction opener JO-1 improves the efficacy and safety of chemotherapeutic drugs. *Clin Cancer Res* (2012) **18**:3340–51. doi:10.1158/1078-0432.CCR-11-3213
- Provenzano PP, Cuevas C, Chang AE, Goel VK, Von Hoff DD, Hingorani SR. Enzymatic targeting of the stroma ablates physical barriers to treatment of pancreatic ductal adenocarcinoma. *Cancer Cell* (2012) **21**:418–29. doi:10.1016/j.ccr.2012.01.007
- Heldin C-H, Rubin K, Pietras K, Östman A. High interstitial fluid pressure – an obstacle in cancer therapy. *Nat Rev Cancer* (2004) **4**:806–13. doi:10.1038/nrc1456

7. Marcucci F, Corti A. Improving drug penetration to curb tumor drug resistance. *Drug Discov Today* (2012) **17**:1139–47. doi:10.1016/j.drudis.2012.06.004
8. Marcucci F, Bellone M, Rumio C, Corti A. Approaches to improve tumor accumulation and interactions between monoclonal antibodies and immune cells. *MAbs* (2013) **5**:36–46. doi:10.4161/mabs.22775
9. Kim JJ, Tannock IF. Repopulation of cancer cells during therapy: an important cause of treatment failure. *Nat Rev Cancer* (2005) **5**:516–25. doi:10.1038/nrc1650
10. De Souza R, Zahedi P, Badame RM, Allen C, Piquette-Miller M. Chemotherapy dosing schedule influences drug resistance development in ovarian cancer. *Mol Cancer Ther* (2011) **10**:1289–99. doi:10.1158/1535-7163.MCT-11-0058
11. O'Dwyer PJ, Manola J, Valone FH, Ryan LM, Hines JD, Wadler S, et al. Fluorouracil modulation in colorectal cancer: lack of improvement with N-phosphonoacetyl-L-aspartic acid or oral leucovorin or interferon, but enhanced therapeutic index with weekly 24-hour infusion schedule—an Eastern Cooperative Oncology Group/Cancer and Leukemia Group B Study. *J Clin Oncol* (2001) **19**:2413–21.
12. Schmidt MM, Wittrup KD. A modeling analysis of the effects of molecular size and binding affinity on tumor targeting. *Mol Cancer Ther* (2009) **8**:2861–71. doi:10.1158/1535-7163.MCT-09-0195
13. R Core Team. (2013). *R: A Language and Environment for Statistical Computing*. R Foundation for Statistical Computing, Vienna. Available from: <http://www.R-project.org/>
14. Nugent LJ, Jain RK. Pore and fiber-matrix models for diffusive transport in normal and neoplastic tissues. *Microvasc Res* (1984) **28**:270–4. doi:10.1016/0026-2862(84)90022-0
15. Paine PL, Scherr P. Drag coefficients for the movement of rigid spheres through liquid-filled cylindrical pores. *Biophys J* (1975) **15**:1087–91. doi:10.1016/S0006-3495(75)85884-X
16. Krol A, Maresca J, Dewhirst MW, Yuan F. Available volume fraction of macromolecules in the extravascular space of a fibrosarcoma: implications for drug delivery. *Cancer Res* (1999) **59**:4136–41.
17. Michel CC, Curry FE. Microvascular permeability. *Physiol Rev* (1999) **79**:703–61.
18. Yamada E. The fine structure of the renal glomerulus of the mouse. *J Biophys Biochem Cytol* (1955) **1**:551–66. doi:10.1083/jcb.1.5.445
19. Lazzara MJ, Deen WM. Effects of plasma proteins on sieving of tracer macromolecules in glomerular basement membrane. *Am J Physiol Renal Physiol* (2001) **281**:F860–8.
20. Ghetie V, Ward ES. Transcytosis and catabolism of antibody. *Immunol Res* (2002) **25**:97–113. doi:10.1385/IR:25:2:097
21. Topp MS, Kufer P, Gökbüget N, Goebeler M, Klinger M, Neumann S, et al. Targeted therapy with the T-cell-engaging antibody blinatumomab of chemotherapy-refractory minimal residual disease in B-lineage acute lymphoblastic leukemia patients results in high response rate and prolonged leukemia-free survival. *J Clin Oncol* (2011) **29**:2493–8. doi:10.1200/JCO.2010.32.7270
22. Bargou R, Leo E, Zugmaier G, Klinger M, Goebeler M, Knop S, et al. Tumor regression in cancer patients by very low doses of a T cell-engaging antibody. *Science* (2008) **321**:974–8. doi:10.1126/science.1158545

Conflict of Interest Statement: The authors declare that the research was conducted in the absence of any commercial or financial relationships that could be construed as a potential conflict of interest.

Received: 04 June 2013; paper pending published: 21 June 2013; accepted: 09 July 2013; published online: 25 July 2013.

*Citation: Fouliard S, Chenel M and Marcucci F (2013) Influence of the duration of intravenous drug administration on tumor uptake. *Front. Oncol.* **3**:192. doi:10.3389/fonc.2013.00192*

This article was submitted to Frontiers in Pharmacology of Anti-Cancer Drugs, a specialty of Frontiers in Oncology.

Copyright © 2013 Fouliard, Chenel and Marcucci. This is an open-access article distributed under the terms of the Creative Commons Attribution License, which permits use, distribution and reproduction in other forums, provided the original authors and source are credited and subject to any copyright notices concerning any third-party graphics etc.



Strategies to increase drug penetration in solid tumors

Il-Kyu Choi¹, Robert Strauss², Maximilian Richter³, Chae-Ok Yun^{1*} and André Lieber^{3*}

¹ Department of Bioengineering, College of Engineering, Hanyang University, Seoul, South Korea

² Genome Integrity Unit, Danish Cancer Society Research Center, Copenhagen, Denmark

³ Department of Medicine, University of Washington, Seattle, WA, USA

Edited by:

Fabrizio Maruccci, Istituto Superiore di Sanità, Italy

Reviewed by:

Fabrizio Maruccci, Istituto Superiore di Sanità, Italy

Julie Gavard, University Paris Descartes, France

***Correspondence:**

Chae-Ok Yun, Department of Bioengineering, College of Engineering, Hanyang University, 17 Haengdang-dong, Seongdong-gu, Seoul 133-791, South Korea
e-mail: chaeok@hanyang.ac.kr;
André Lieber, Department of Medicine, Division of Medical Genetics, University of Washington, Box 357720, Seattle, WA 98195, USA
e-mail: lieber00@u.washington.edu

Despite significant improvement in modalities for treatment of cancer that led to a longer survival period, the death rate of patients with solid tumors has not changed during the last decades. Emerging studies have identified several physical barriers that limit the therapeutic efficacy of cancer therapeutic agents such as monoclonal antibodies, chemotherapeutic agents, anti-tumor immune cells, and gene therapeutics. Most solid tumors are of epithelial origin and, although malignant cells are de-differentiated, they maintain intercellular junctions, a key feature of epithelial cells, both in the primary tumor as well as in metastatic lesions. Furthermore, nests of malignant epithelial tumor cells are shielded by layers of extracellular matrix (ECM) proteins (e.g., collagen, elastin, fibronectin, laminin) whereby tumor vasculature rarely penetrates into the tumor nests. In this chapter, we will review potential strategies to modulate the ECM and epithelial junctions to enhance the intratumoral diffusion and/or to remove physical masking of target receptors on malignant cells. We will focus on peptides that bind to the junction protein desmoglein 2 and trigger intracellular signaling, resulting in the transient opening of intercellular junctions. Intravenous injection of these junction openers increased the efficacy and safety of therapies with monoclonal antibodies, chemotherapeutics, and T cells in mouse tumor models and was safe in non-human primates. Furthermore, we will summarize approaches to transiently degrade ECM proteins or downregulate their expression. Among these approaches is the intratumoral expression of relaxin or decorin after adenovirus- or stem cell-mediated gene transfer. We will provide examples that relaxin-based approaches increase the anti-tumor efficacy of oncolytic viruses, monoclonal antibodies, and T cells.

Keywords: epithelial junctions, tumor stroma, extracellular matrix, relaxin, junction opener, tumor-associated macrophages

TUMOR MICROENVIRONMENT

TUMOR STROMA

Tumors are heterogeneous cellular entities in which progression depends on the crosstalk between the genetically abnormal cells (the epithelial parenchyma of carcinomas) and the tumor stroma (the supportive framework of a tumor tissue). This tumor stroma is basically composed of the non-malignant cells (stromal cells) of the tumor such as cancer-associated fibroblasts (CAFs), immune cells [tumor-associated macrophages (TAMs) and tumor-associated neutrophils (TANs)], and mesenchymal stem cells as well as the extracellular matrix (ECM) consisting of fibrous structural proteins (collagen and elastin), fibrous adhesive proteins (fibronectin and laminin), and proteoglycans (1–3) (**Figure 1A**). In most solid tumors derived from epithelial tissues, nests of malignant tumor cells are linked through junction proteins such as E-cadherin, claudins, and desmoglein 2 (DSG2). Tumor nests are surrounded by tumor stroma (**Figures 1B,C**). The stroma is indispensable for normal tissue development and homeostasis, since it has a vital role in regulating behavior of cells residing in the local milieu (4–7). Likewise, various components of the tumor stroma create a niche favoring seeding of metastatic tumor cells. More importantly, tumor stroma mediates the resistance to cancer

therapeutic agents (8–10). Tumor stroma contributes in at least two critical ways to drug resistance: (i) by creating a physical barrier formed by stroma proteins that prevents intratumoral drug penetration and direct contact between drugs/tumor-infiltrating immune effector cells and their target receptors on malignant cells and (ii) by production of cytokines and chemokines that trigger the synthesis of stroma proteins, block activation of immune cells, or attract/activate immuno-suppressive cells such as regulatory T cells (T_{regs}).

It is well established that stroma that is associated with normal tissue development and homeostasis is strikingly distinct from that associated with carcinomas (1). Specifically, the composition of tumor-derived ECM is different from normal ECM (11). Excess ECM production or reduced ECM turnover are noticeable in the majority of tumors (12, 13). Various collagens (e.g., collagen type I, II, III, V, and IX), fibronectin, tenasin C, and proteoglycans exhibit increased accumulation and generate a dense network in tumor tissues (14–17). Excessive deposition of ECM components decreases the distance between neighboring ECM components and diminishes the pore size of the tumor matrix. This adds diffusional impediment to macromolecules (IgG, IgM, and dextran 2,000,000 MW) in tumors (18). A strong inverse

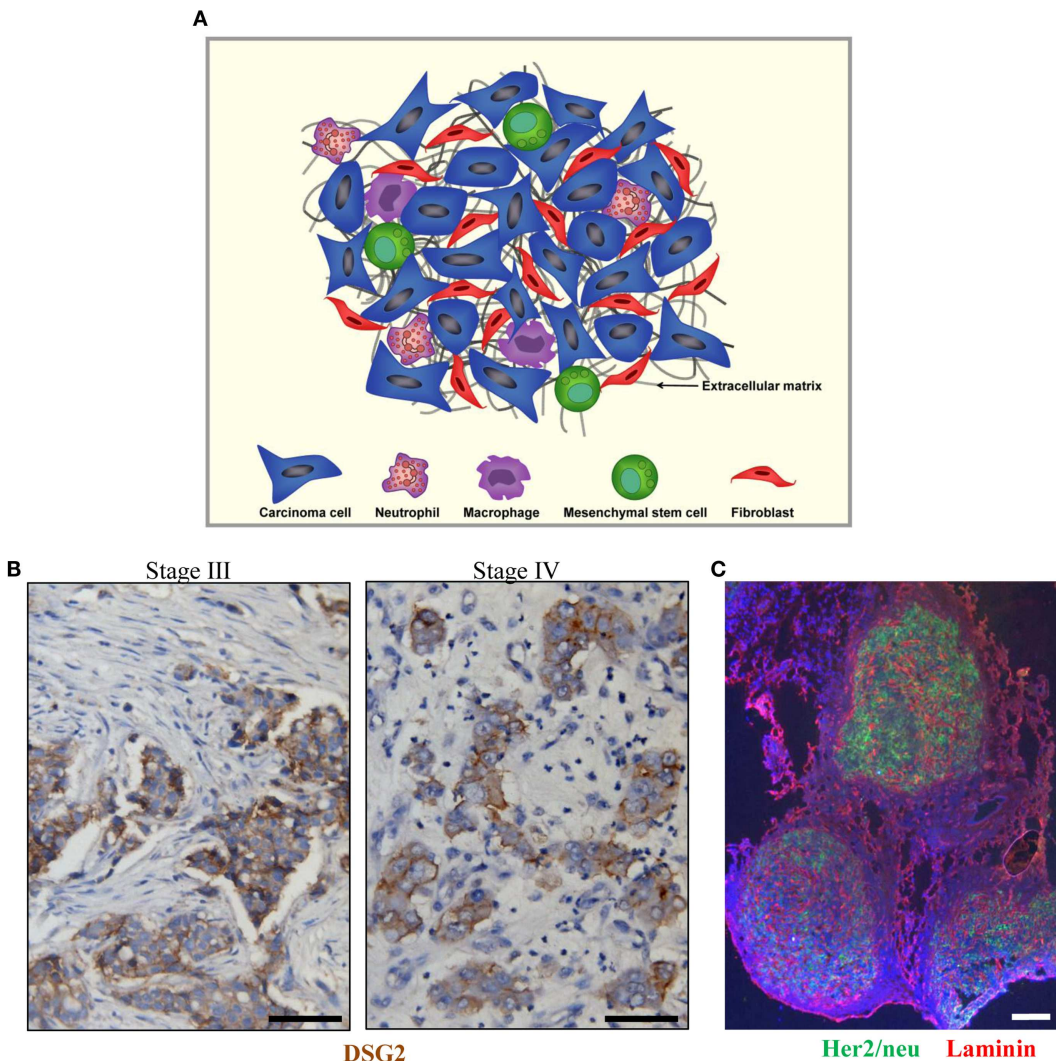


FIGURE 1 | Tumor stroma. **(A)** Schematic representation of tumor stroma components. The tumor stroma is composed of stromal cells (fibroblasts, macrophages, neutrophils, and mesenchymal stem cells) as well as extracellular matrix. **(B)** Sections from breast cancer patient biopsies (stage III and IV). DSG2 staining appears in brown.

Malignant cells are DSG2-positive and form nests that are surrounded by tumor stroma containing DSG2-negative stroma cells such as fibroblasts. **(C)** Immunofluorescence analysis for Her2/neu (green) and the stroma protein laminin (red) on a breast cancer section. The scale bar is 20 μ m.

correlation between tumor ECM content and tumor penetration of cancer drugs has been demonstrated for therapeutic agents such as anti-tumor immune cells, therapeutic viruses, chemotherapeutic agents, monoclonal antibodies, immunotoxins, interferons, and complement (18–24). Due to increased ECM deposition, tumor tissue commonly exhibits increased stiffness compared to normal tissue. For breast cancer, tumor tissue was found to be 10 times stiffer than normal breast tissue (26, 27). The elevated ECM stiffness progressively increases interstitial fluid pressure (IFP) which thereafter interferes with effective spread of anti-cancer therapeutics within the solid tumor (28–30). In summary, the deregulation and disorganization of the tumor stroma alter the composition, structure, and stiffness of the ECM, leading to limited penetration and dissemination of therapeutic agents within solid tumors.

Killing the genetically stable tumor stroma cells has definitive advantages over targeting the malignant cells, i.e., cells that are genetically unstable and heterogeneous and represent a moving target for therapies.

TUMOR STROMAL CELLS

The major contributors of abnormal ECM in solid tumors are stromal cells such as cancer-associated fibroblasts (CAFs), TAMs, and TANs (3, 13, 31). These stromal cells display sustained synthesis and secretion of connective tissue components, growth factors, and cytokines, which promote the ability of malignant cells to proliferate, invade, and metastasize (32, 33). Thus targeting the tumor stromal cells is considered a promising approach to the treatment of cancer.

Cancer-associated fibroblasts

Cancer-associated fibroblasts are the predominant cell type in the tumor-associated stroma. Their numbers are elevated in tumor stroma compared to stroma found in healthy tissue (34, 35). In many carcinomas, the fraction of CAFs is even greater than the fraction of malignant cells (32). In the tumor microenvironment, tumor and stromal cells upregulate various profibrotic growth factors such as transforming growth factor- β (TGF- β), platelet-derived growth factor (PDGF), and basic fibroblast growth factor (bFGF), all of which are main mediators for the transdifferentiation of stromal fibroblasts into CAFs (36, 37). CAFs are phenotypically and functionally distinct from normal stromal fibroblasts (38). CAFs are large spindle-shaped mesenchymal cells that share morphological characteristics of both smooth-muscle cells and fibroblasts (39). Metabolically, CAFs are perpetually activated, proliferate faster, and accumulate greater amounts of ECM constituents than fibroblasts in normal tissues (2, 32, 40). In addition to creating tumor-derived ECM, CAFs have an impact on cancer cell proliferation, invasion, and metastasis through secretion of different growth factors [epidermal growth factor (EGF), FGF, hepatocyte growth factor (HGF), and insulin-like growth factor-1 (IGF-1) (2, 3, 31, 34, 41–44)]. CAFs are also involved in the activation of angiogenic programs as well as the recruitment of inflammatory cells (45). Local expression of vascular endothelial growth factor (VEGF) or monocyte chemoattractant protein-1 (MCP-1) by CAFs stimulates angiogenesis and the recruitment of pro-tumor myeloid cells.

TAMs and TANs

As another major component in the tumor stroma, TAMs have emerged as a significant player in the stromal compartment of virtually all types of carcinoma (46). While type M1 macrophages are antigen-presenting cells that incite T cells to mount immune responses, TAMs are M2-type macrophages and tumor promoting. Tumor cells, among other cytokines, produce MCP-1 and colony stimulating factor-1 (CSF-1) which participates in mobilization of TAM-progenitors from the bone marrow and homing to tumor stroma. Homing of TAMs to tumors is also supported by the specific architecture of tumor blood vessels which promote efficient trafficking of blood cells. There is convincing evidence that the extent of MCP-1 expression in human cancers correlated with both TAM infiltration and tumor malignancy (47–53). TAMs contribute to tumor-associated alteration in the ECM by releasing profibrotic growth factors, which then act in an autocrine and/or paracrine manner to differentiate normal stromal fibroblasts into CAFs (33, 37, 46). TAMs also produce growth factors (EGF, HGF, bFGF, and VEGF), cytokines [IL-1, IL-8, and tumor necrosis factor- α (TNF α)], and enzymes [MMP-2, MMP-7, MMP-9, MMP-12, and cyclooxygenase-2 (COX-2)] (46, 54). Additionally, TAMs can suppress anti-tumor immune responses. For example, TAMs secret a distinctive set of cytokines (IL-10 and TGF- β) as well as chemokines [chemokine (C-C motif) ligand (CCL)17, CCL22, and CCL24] favoring recruitment of T_{regs} and generation of an immune suppressive microenvironment (55–57). As outlined in Section “Epithelial-to-Mesenchymal Transition and Mesenchymal-to-Epithelial Transition in Cancer,” TAMs also promote epithelial-to-mesenchymal transition (EMT) via TGF-

(58) and regulate cancer stem cell (CSC) activities (59) in solid tumors.

Tumor-associated neutrophils comprise another prominent portion of the immune cell infiltrates observed in a wide variety of murine models and human cancers (60–63). Similar to TAMs, products secreted from neutrophils, including reactive oxygen species, cytokine (IL-8), growth factors (VEGF and HGF), and proteinases [arginase (ARG 1), MMP-2, MMP-8, MMP-9, and MMP-13], have defined and specific roles in both regulating tumor cell proliferation, angiogenesis, and metastasis and suppressing the anti-tumor immune response (64).

TUMOR VASCULARIZATION

Transendothelial transport

Once systemically administered drugs reach the tumor sites, they have to exit the tumor vasculature and translocate through the interstitial space in order to reach their target cells. The endothelial cell layer, lining the blood vessels, is thought to present a barrier to macromolecular drugs (20). Transendothelial transport of macromolecular drugs involves a phenomenon known as the enhanced permeability and retention (EPR) effect in solid tumors. The EPR effect is observed for intravenously administered macromolecular anti-cancer drugs that escape renal clearance, due to their large molecular size (10–500 nm). They are mostly unable to pass the tight endothelial junctions of normal blood vessels, but can extravasate and then become trapped in the tumor vicinity (65). Unlike normal tissues that feature an organized vascular network, the blood vessel system in solid tumors is rather chaotic. The endothelial cell layers are poorly aligned (66) and elevated levels of vascular permeability factors generate “leaky” capillaries (65). It is therefore thought that transendothelial transport is not a critical limiting obstacle for large sized drugs.

Intratumoral pressure

Rapid tumor cell proliferation and weakly developed lymphatics cause high IFP (67, 68) and blood vessel remodeling by intussusception (69) or compression (70). Additionally, the increased hydraulic conductivity of “leaky” capillaries can further increase the IFP in tumors (71). Together, this leads to an imbalance in blood flow and nutrient supply within the tumor microenvironment. The uniformly high IFP in the center of solid tumors drops toward the periphery (72), which could negatively affect drug extravasations in the high-pressure regions. Cells that are distant to blood vessels (100–200 μ m) and located in high-pressure regions subsequently constitute large areas of hypoxic, necrotic, or semi-necrotic tissue. This exacerbates the tendency of tumor cells to overproduce and release lactic acids within these regions, which results in acidosis (73). Moreover, the vascular surface area per unit tissue weight is decreasing with tumor growth, which further limits transvascular exchange for large tumors when compared to small tumors (74, 75). In contrast, cells situated in the invasive front benefit from the enhanced vascular permeability that supplies adequate amounts of macromolecules for rapid tumor growth (76). Furthermore, the blood flow rates in non-necrotic regions can be substantially higher than in the surrounding normal tissue (77). It is therefore expected that the uptake of drugs in solid tumors is heterogeneous and the general distribution might

decrease with increasing tumor weight. It is thought that induction of massive cell death by chemo- and radio-therapy can lower the IFP in tumors (78). The application of chemotherapy to lower the IFP is also used in approaches to “normalize” the tumor vasculature. Anti-angiogenic drugs are thought to compensate for the pro-angiogenic factors that are extensively produced in the tumor in order to eliminate “leaky” blood vessels. Ideally, this would lead to a more organized blood vessel system that features more functional and more uniformly perfused capillaries within solid tumors. On the other hand, this would also inhibit the extravasation of large drugs.

Hypoxia

Two major consequences of abnormal microcirculation in solid tumors are hypoxia and low extracellular pH. Hypoxia or oxygen deprivation is a key factor in tumor progression and resistance to therapy. The most important regulatory factor of the hypoxia-signaling pathway activity in cells is hypoxia-inducible transcription factor 1 (HIF-1 α). Under hypoxic condition, tumors produce a number of chemokines that attract and differentiate CAFs, TAMs, and TANs. Approaches that reduced intratumoral hypoxia therefore block pro-tumoral functions of these cells, including the production of stroma proteins. It is therefore thought that hypoxia targeting strategies improve the intratumoral penetration of drugs (79).

EPITHELIAL PHENOTYPE OF SOLID TUMORS

EPITHELIAL JUNCTIONS

About 90% of solid tumors are of epithelial origin, often featuring a stratified epithelium characterized by multilayered cells with three-dimensional intercellular junctions. This is in contrast to monolayered epithelial cells lining epithelial tracts (e.g., airway, gastrointestinal, and urinary tracts), epithelial ducts (e.g., bile and pancreatic ducts), or cavities (e.g., brain ventricles), which possess an apical-basal polarization of their cell membranes and cytoskeleton. The epithelial phenotype is generally defined by tight and adherence junctions that seal the paracellular space between adjacent cells and thereby providing a barrier that restricts passing of ions and macromolecules (Figure 2A) (80).

Tight junctions (*zonula occludens*)

Tight junctions play a key role in the formation of epithelial sheets. Strictly linked to tight junctions is a barrier function within a sheet of cells that restricts ions and small molecules to pass through the paracellular space between two adjacent epithelial cells (80). Additionally, tight junctions function as a “fence” that separates the apical and basal membrane compartments in an individual cell (81). Importantly, the tight junction strands on one cell are associated laterally to tight junction strands of opposing membranes on neighboring cells (82). The permselective barrier function is based on occludins and claudins, two types of transmembrane proteins that have been identified among more than 40 proteins within tight junctions (81, 83). Other tight junction transmembrane proteins comprise the single-span junctional adhesion molecules (JAMs) or coxsackie and adenovirus receptor (CAR) (83–86) and the lately identified tetraspan tricellulin, which is enriched in areas where three cells meet (86).

Adherens junctions (*zonula adherens*)

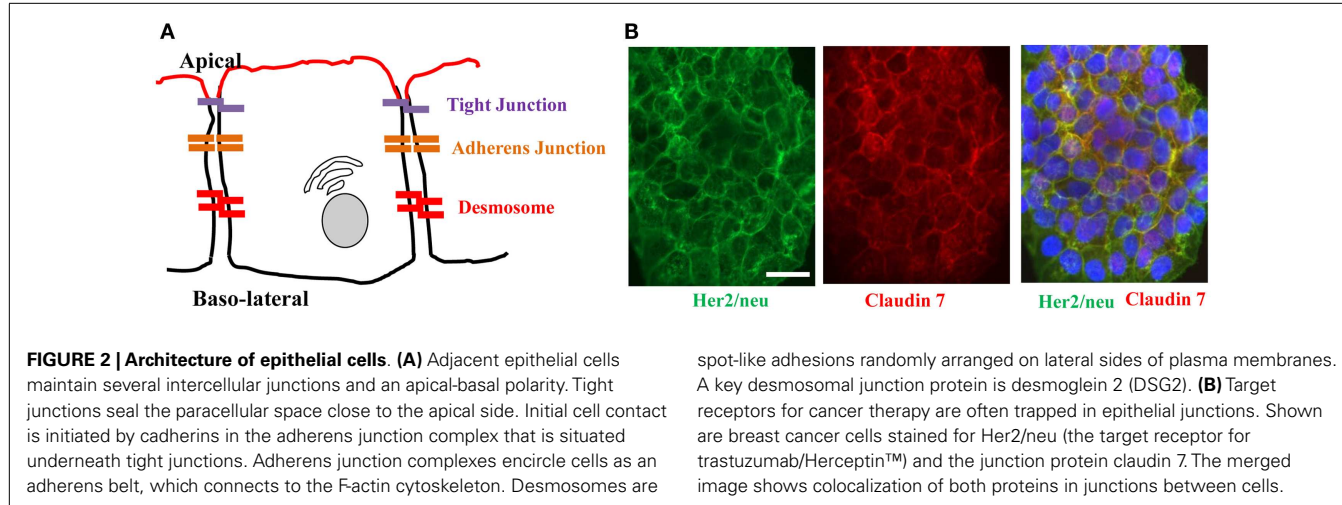
The major transmembrane proteins of adherens junctions are classical cadherins, such as epithelial cadherin (E-cadherin). Members of this protein superfamily promote homophilic intercellular adhesion in a Ca²⁺-dependent manner. Their cytoplasmic domain binds cytosolic catenins that link the cadherin/catenin complex to the actin cytoskeleton. The formation of adherens junctions consequently leads to the assembly of tight junctions, but E-cadherin is dispensable for tight junction maintenance (87). A central role in maintenance and initiation of an epithelial phenotype is attributed to E-cadherin, the core protein of adherens junctions. In addition to its homophilic intercellular adhesive features, the extracellular E-cadherin domain functions as a direct repressor of receptor tyrosine kinase (RTK) signaling via blockage of FGF or EGF ligand binding stimulation (88, 89). The cytoplasmic part of E-cadherin connects to the actin cytoskeleton and also influences a number of signaling pathways via direct binding to p120- and β -catenin. When adjunct to E-cadherin at the membrane, β -catenin inhibits cell growth (90), whereas its translocation to the nucleus activates canonical Wnt signaling (91). Similarly, p120-catenin stabilizes E-cadherin at the membrane, while blocking NF- κ B and Ras-MAPK signaling (92, 93).

Desmosomal junctions/desmosomes (*macula adherens*)

Desmosomes are molecular complexes of cell adhesion proteins and linking proteins that attach the cell surface adhesion proteins to intracellular keratin cytoskeletal filaments. The cell adhesion proteins of the desmosome, desmoglein, and desmocollin, are members of the cadherin family of cell adhesion molecules. They are transmembrane proteins that bridge the space between adjacent epithelial cells by way of homophilic binding of their extracellular domains to other desmosomal cadherins on the adjacent cell. Both have five extracellular domains, and have calcium-binding motifs. One of these junction proteins, DSG2, is upregulated in malignant cells (94, 95). DSG2 contains four extracellular cadherin domains (ECDs; ECD1–ECD4), which link neighboring cells to each other through homodimers. ECDs are linked via an extracellular anchor and membrane-spanning domain to the intracellular anchor and intracellular cadherin-typical sequence (ICS) motifs. The role of the conserved ICS is not known, although consensus sites for protein kinase C phosphorylation and a caspase-3 cleavage site have been identified and could contribute to signaling (96). Desmosomes probably do not directly regulate paracellular permeability, but they seem to do this indirectly by altering the structure and the stability of tight junctions (97).

BLOCK OF INTRATUMORAL DIFFUSION OF MACROMOLECULES

One of the key features of epithelial tumors is the presence of intercellular junctions, which link cells to one another, and act as barriers to the penetration of molecules with a molecular weight of >400 Da (98–100). Most of commonly used chemotherapy drugs are either nanoparticle-based or encapsulated into liposomes with diameter greater than 100 nm. For example, nanoparticle albumin bound paclitaxel/nab-paclitaxel/Abraxane™ has an effective diameter of 130 nm and liposomal doxorubicin/Doxil™ has a size of 90 nm. Even non-encapsulated chemotherapy drugs have a molecular weight of greater 400 Da (for example: paclitaxel/Taxol™: MW



856.9 Da or irinotecan/Camptosar™: MW 586.7 Da). Several studies have shown that upregulation of epithelial junction proteins correlated with increased resistance to therapy, including therapy with the two major classes of cancer drugs – monoclonal antibodies and chemotherapeutics (101–103). It is thought that the epithelial phenotype of cancer cells and their ability to form physical barriers protect the tumor cells from attacks by the host-immune system or from elimination by cancer therapeutics (104).

INACCESSIBILITY OF THERAPY TARGET RECEPTORS

Receptors for therapeutic antibodies are often localized at the baso-lateral membrane of epithelial cells. This includes Her2/neu (105, 106) and EGFR (107, 108). In our studies on epithelial tumors we found that target receptors are trapped in intercellular junctions (109). For example, Her2/neu, the receptor for the widely used monoclonal antibody Herceptin (trastuzumab) co-stained with the tight junction protein claudin 7 (Figure 2B).

EPIHELIAL-TO-MESENCHYMAL TRANSITION AND MESENCHYMAL-TO-EPIHELIAL TRANSITION IN CANCER

Epithelial-to-mesenchymal transition and mesenchymal-to-epithelial transition (MET) are important mechanisms that drive tumor progression and therapy resistance, and indirectly affect intratumoral drug penetration. EMT and MET have been accredited important roles in embryogenic development, tissue regeneration, cancer progression, and recently also the induction and maintenance of stem cell properties (110). Importantly, the phenotypic switches between epithelial and mesenchymal phenotypes are not irreversible, as they occur several times during formation of the complex three-dimensional structure of internal organs. In contrast to epithelial cells, mesenchymal cells exhibit an irregular shape, which is based on unpolarized cytoskeletons and membranes. Further mesenchymal traits include the deposition of ECM components, increased motility, invasiveness, as well as elevated resistance to apoptosis and anoikis (110). EMT engages a series of events involving inter- and intra-cellular changes in affected cells. Importantly, not all of which have to occur during the trans-differentiation process. Often cells remain in stages referred to as an “incomplete” EMT, suggesting a spectrum of intermediate

stages rather than a strict lineage switch (104). Examples of such epithelial/mesenchymal (E/M) hybrid cells have been reported for multiple tissues including the ovarian surface epithelium (111), ovarian cancer (25), cells within the invasive front of colon (112) and breast cancer (113), as well as in normal epidermal tissue during wound healing (114).

EMT and induction of tumor ECM proteins

During progression toward metastatic disease carcinoma cells engage EMT. The EMT program can be activated by a multitude of factors secreted by tumor stroma cells, which triggers a complex signaling network including TGF- β , Wnt, HGF, EGF, and PDGF pathways (115). The morphological changes that occur during EMT are a consequence of diverse molecular mechanisms that contribute to the acquisition of mesenchymal features. A central event during EMT is the functional loss of E-cadherin. Subsequent breakdown of intercellular epithelial junctions plays a major role in cancer progression, where E-cadherin therefore acts as a repressor of invasion (116). Accordingly, the reduced expression of this major regulator of the epithelial phenotype is associated with poor prognosis in several cancers (117). The loss of E-cadherin and several other epithelial genes including multiple members of the claudin family as well as occludin is mainly regulated via transcriptional repression by EMT inducers that include transcription factors Snail, ZEB, Twist, FOXC2, and E47 (118–126). Notably, these EMT inducers also act as positive regulators of gene expression for several mesenchymal genes (127, 128). A consequent event in EMT is the change from E-cadherin to N-cadherin (129). The importance of this cadherin switch is highlighted by the fact that homophilic intercellular junctions formed by N-cadherin are less resistant to rupture under physiological stress conditions, when compared with E-cadherin (130). Additionally, a shift from several keratins (-8, -9, and -18) to vimentin occurs, resulting in a more flexible cytoskeleton (131, 132). Concomitantly with the acquisition of such mesenchymal features, the expression of several ECM proteins is induced. Fibronectin, collagen precursors, laminin, and vitronectin are all reported to be elevated in mesenchymal cells (133). These and other proteins, including Src kinase, integrin-linked kinase, integrin β -5, and MMPs, are upregulated during

EMT, have an impact on cytoskeletal remodeling, and promote cell motility (104).

MET and cancer stem cells

Successful EMT induction ultimately enables cancer cells to leave the primary tumor, enter the bloodstream, and attach to distant organ sites in order to build metastases. The endpoint of this process however, involves the reversed process (MET), where cells that underwent EMT regain epithelial properties and form tumors that histopathologically resemble the primary cancer (110, 134). Although the underlying mechanisms are currently unknown, it is likely that MET events are initiated due to the lack of EMT-inducing signals at attachment sites of metastatic tumor cells. In support, numerous examples of advanced carcinomas exist, showing that mesenchymal cells can regain characteristics of epithelial cells or undergo MET (104). It is now generally accepted that the reverting to an epithelial phenotype through MET represents a protective mechanism against host-immune attacks and creates resistance to anti-cancer drugs. The transdifferentiation into an epithelial phenotype and the formation of tight junctions between malignant cells that prevent penetration of host anti-tumor immune cells, host anti-tumor antibodies, and therapeutics represents one of the most basic cancer resistance mechanisms.

Importantly, changes between EMT and MET occur gradually, which leads to a wide range of intermediate cell stages that consequently possess an E/M hybrid phenotype. The E/M hybrid phenotype is especially prominent in the invasive front of several carcinomas where it has also initially been linked to cells with a stem cell-like phenotype (112, 113). We have recently shown in cancer cells derived from ovarian cancer biopsies that CSCs generate mesenchymal cells via EMT *in vitro* and undergo MET to form tumors containing epithelial cells when injected into immunodeficient mice (135). A marker combination widely used to identify CSCs in multiple cancers including prostate, pancreatic, and colon is EpCAM and CD44 (136, 137). Interestingly, the expression of these proteins can be accredited to epithelial and mesenchymal cells, respectively, suggesting a more general pattern of an E/M hybrid phenotype for tumor-initiating cells (TICs) (25). Very recently, work by Yu et al. demonstrated that cells, which leave the primary tumor, possess an epithelial or E/M hybrid phenotype. In the bloodstream these circulating tumor cells are bound by platelets, which trigger EMT via TGF- β signaling (138). However, cells undergoing EMT that leave the primary tumor experience a proliferation arrest, which is mediated by EMT inducers, like Twist1. In order to reenter a proliferative stage that allows for colonization and macrometastasis, the downregulation of Twist1 and concomitant MET is critically needed, while ongoing EMT signaling leads to dormancy and micrometastases at sites of reattachment (139). Additionally, it was recently reported that two distinct types of EMT exist in carcinomas, depending on the presence or absence of EMT inducer paired-related homeobox transcription factor 1 (Prrx1). When Prrx1 is expressed in cells undergoing Twist1-induced EMT, a CSC pattern is suppressed and cells fail to colonize. After Prrx1 is downregulated and other EMT inducers, such as Twist1 or ZEB1 have vanished, MET occurs and metastatic growth can be initiated (140). Notably, MET has also been reported in non-epithelial cancers, e.g., sarcoma (141, 142).

STRATEGIES TO DEGRADE TUMOR ECM PROTEINS OR DOWNREGULATE THEIR EXPRESSION

Tumor-derived ECM plays an important role in inhibiting penetration and dispersion of cancer therapeutic agents within tumor masses and has been implicated in resistance to therapy of solid tumors (143). This has been shown for therapeutic modalities such as oncolytic Ads (21), antibodies (18, 19), immunotoxins (24), interferons (23), or complement (144). A series of approaches have been tested to partially degrade ECM proteins and improve the penetration of macromolecules and nanoparticle-based drugs. (i) The first type of approaches involves the intratumoral injection of proteases that can target ECM proteins. These proteases include trypsin, collagenase, hyaluronidase, MMPs, relaxin, and decorin. For example, intratumoral injection of collagenase has been shown to remove diffusive hindrance to the penetration of therapeutic molecules in subcutaneous human osteosarcoma and glioblastoma multiforme xenografts (145, 146). Similar approaches have been tested in combination with cancer virotherapy, including Ads (diameter: ~100 nm) and herpes simplex virus (HSV) (diameter: ~190 nm). These viruses represent prototypes of nano-particles and lessons learned from studies with oncolytic viruses are relevant for other large anti-cancer drugs. Direct injection of subcutaneous human glioblastoma multiforme tumor with a proteolytic enzyme (trypsin) or a protease mixture (collagenase/dispsase) before intratumoral injection with reporter gene-expressing Ad vector elicited enhanced virus-mediated gene expression within the solid tumor (147). Intratumoral co-injection of collagenase with an oncolytic HSV vector in a human melanoma xenograft resulted in increased intratumoral viral spread and therapeutic benefit (148). Likewise, co-delivery of hyaluronidase and oncolytic Ads led to improved intratumoral diffusion and virus potency through degradation of hyaluronan-rich ECM in human prostate and melanoma xenograft models (149). (ii) The second approach involves the delivery of a protease-encoding gene expression cassette to tumors. Cheng et al. generated replication-incompetent Ads expressing MMP-8 that breaks down collagen type I, II, and III in subcutaneous human A549 lung cancer and BxPC-3 pancreatic cancer xenograft tumors (150). In studies testing MMP-8-expressing Ads, MMP-8 expression efficiently degraded collagen *in vitro*. Furthermore, co-injection of MMP-8-expressing Ads in combination with wild-type Ads resulted in reduced tumor cell growth and collagen expression within areas of virus-induced necrosis compared with wild-type Ad given together with a control Ad vector. Moreover, Mok et al. showed that intratumoral expression of MMP-1 and MMP-8 in the human HSTS26T soft tissue sarcoma xenograft degraded collagen, reduced the levels of sulfated proteoglycans, and increased spread and effectiveness of an oncolytic HSV (151). While degradation of ECM with enzymes, such as collagenase and MMPs, may improve viral penetration and distribution, there is a concern that this strategy may also increase tumor spread; MMPs and collagenase play an important role in tumor invasion and metastasis, which might limit the use of these proteins in a clinical setting (152, 153). Therefore, further thorough and detailed studies are required to gain an improved understanding of the potential risk associated with combined replicating oncolytic virus and ECM-degrading enzyme or protein therapy.

Our laboratories have tested approaches involving the expression of relaxin (154–157) or decorin (158). We will therefore describe these approaches in more detail.

RELAXIN-BASED APPROACHES TO INCREASE DRUG PENETRATION IN SOLID TUMORS

Relaxin is an insulin-related peptide hormone (159). During pregnancy, relaxin has an integral role in softening the uterine cervix, vagina, and interpubic ligaments in preparation for parturition (160). Relaxin is the ligand for two leucine-rich repeat-containing G protein coupled receptors (LGRs), LGR7, and LGR8, now classified as relaxin family peptide receptors 1 and 2 (RXFP1 and RXFP2), respectively (161). These receptors have been found on relaxin target tissues, particularly on endometrial stromal cells and CAFs (161). Binding of relaxin to these receptors triggers intracellular signaling resulting in downregulation of ECM protein expression and upregulation of MMPs, which degrade stroma proteins. Importantly, relaxin decreases the synthesis of collagens and increases the expression of MMPs when collagen is abnormally upregulated, but it does not significantly alter basal levels of collagen expression, in contrast to other collagen-modulatory cytokines (e.g., interferon- γ) (162). This implies that relaxin acts predominantly on tissues with increased ECM protein expression such as fibrotic tissues and tumors. In agreement with these observations, earlier reports showed that relaxin expression mediated by an Ad vector reversed cardiac fibrosis without adversely affecting normal collagen levels in other organs in a transgenic murine model of cardiac fibrosis (163). Relaxin has been used for degradation of tumor-derived ECM components (164). In immunodeficient mice bearing human HSTS26T soft tissue sarcomas in dorsal skinfold chamber, chronic relaxin treatment via osmotic pumps elicited improved collagen down-regulation and intratumoral dispersion of macromolecules in tumor tissues, whereby the new tumor ECM, that is generated after relaxin treatment, was more porous and had a decreased diffusive resistance (145). *In vitro* studies with human OHS osteosarcoma multicell spheroids, recombinant relaxin increased the diffusion of the 150 kDa FITC-dextran, in part, due to increased production of collagenase (146). Similar results were reported in *in vivo* tumor models after intratumoral injection of recombinant relaxin (145). In cancer virotherapy studies, relaxin was demonstrated to enhance tumor penetration and dispersion of oncolytic Ad, thereby eliciting improved cancer gene therapy (155) (Figure 3). In this study, the growth of both subcutaneous xenograft (human glioma, hepatocellular carcinoma, cervical carcinoma, and lung carcinoma) and orthotopic tumors (human hepatocellular carcinoma) treated with relaxin-expressing oncolytic Ad was markedly inhibited compared to tumors treated with control oncolytic Ad that did not express relaxin. When viral persistence and distribution was confirmed by immunohistochemical studies, more Ad particles were observed across wider areas of tumor tissues treated with relaxin-expressing oncolytic Ad. Moreover, the collagen content of tumor tissues was reduced significantly by relaxin-expressing oncolytic Ad without affecting adjacent normal tissue. A relaxin-expressing oncolytic Ad containing Ad5/35 chimeric fibers in a subcutaneous human A375-mln1 malignant melanoma xenograft model also exhibited increased

viral spread and transduction efficiency through the tumor mass and thereby increased anti-tumor efficacy and overall survival in metastatic tumor models (154).

Access of anti-tumor immune cells and their intratumoral infiltration is limited by tumor stroma (19). More specifically, the tumor stroma contributes to tumor immune escape by creating a physical barrier formed by ECM components that restricts direct physical contact between tumor-infiltrating anti-tumor immune cells and cancer cells. As an approach to overcome this limitation, Li et al. showed that the inducible intratumoral expression of relaxin through the transplantation of mouse hematopoietic stem cells transduced with a relaxin-expressing lentivirus vector led to suppressed tumor growth in an immunocompetent mouse breast cancer model (157). The therapeutic mechanism of the anti-tumor effect is associated with the degradation of tumor stroma mediated by relaxin and enhanced anti-tumor immune responses mediated by better intratumoral infiltration of anti-tumor immune cells. The same investigators also tested whether intratumoral relaxin expression facilitates transplanted anti-tumor T cells to control tumor growth. In a breast cancer model, they demonstrated that relaxin augmented the efficacy of *neu*-targeted adoptively transferred T cells, and improved survival of mice with *neu*-expressing mammary tumors. At day 33, in the T cell transplanted group, 25% of the mice were alive. Combined with relaxin expression, survival increased to 62.5%. Relaxin expression combined with naïve T cell treatment also increased survival (37.5%), compared to naïve T cell treatment alone (0%). Better survival of relaxin-expressing mice was due to a higher number of *neu*-specific T cells inside the tumor.

Tumor ECM as well as tumor cell density can inhibit diffusional transport of monoclonal antibody therapeutics in tumor tissues. In a study of the monoclonal antibody trastuzumab (Herceptin) penetration, Beyer et al. observed extensive tumor ECM and intercellular junctions in breast cancer patients and xenograft models (156). Therefore, the authors hypothesized that this hinders the access to Her2/neu and/or the intratumoral dispersion of trastuzumab. They showed that hematopoietic stem cell-mediated intratumoral relaxin expression in combination with trastuzumab therapy resulted in a decrease of ECM proteins and a significant delay of tumor growth, indicating that a stem cell-based approach for relaxin expression in tumors facilitates tumor ECM degradation and substantially enhances effectiveness of antibody therapy of cancer.

In all of these studies, relaxin expression did not induce metastasis. In fact, it reversed the spread of tumor cells that normally would metastasize. The latter is in conflict with earlier studies by Silvertown et al. reporting that permanent relaxin overexpression increased *in vivo* prostate xenograft tumor growth and angiogenesis (165). These results were recently revised by the same group (166). While short-term exposure of tumor cells to relaxin *in vitro* seems to enhance invasiveness (167), long-term exposure reduces it (168). The general consensus is that relaxin expression alone is not sufficient to induce metastasis, a process that involves dissociation of cells from the primary tumor, enhanced cell motility, and the ability of cells to invade blood vessels and to grow effectively at distant sites (154).

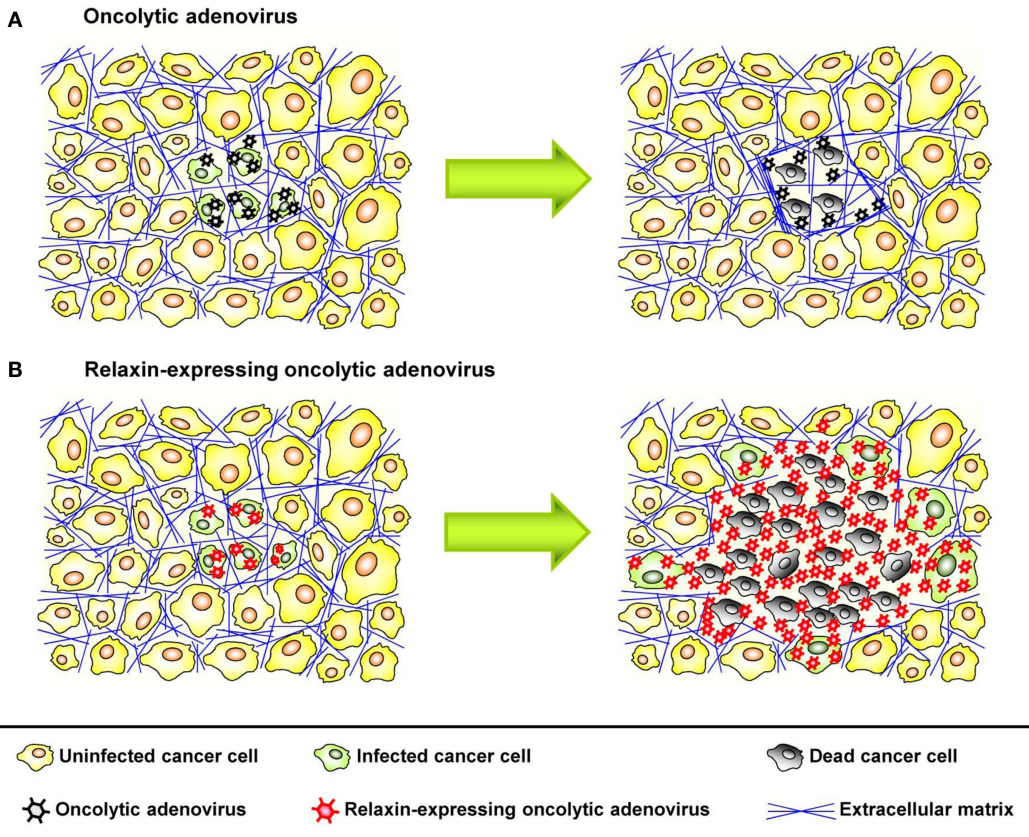


FIGURE 3 | Therapeutic effect of relaxin-expressing oncolytic adenovirus. (A) ECM acts as a physical barrier in solid tumors, so that interstitial viral penetration and cell-to-cell spread of conventional oncolytic adenoviruses is restricted to the site of administration,

leading to limited therapeutic efficacy. **(B)** Relaxin-expressing oncolytic adenovirus decreases ECM components within a tumor mass and increases its tumor penetration and dispersion, thereby eliciting improved antitumor efficacy.

DECORIN-BASED APPROACHES TO INCREASE DRUG PENETRATION IN SOLID TUMORS

Decorin, a small leucine-rich proteoglycan consisting of a core protein and a single glycosaminoglycan chain, is a ubiquitous component of ECM. Decorin has an impact on the production of several ECM components. For example, it regulates collagen fibril formation by interacting with collagen fibrils and delaying the lateral assembly of individual triple helical collagen molecules, leading to the reduced diameter of the fibrils (169). Decorin also influences the production of other ECM components by inhibiting the expression of TGF- β , a key profibrotic growth factor (170). Moreover, decorin has an important role in inducing ECM remodeling through promotion of MMP-1 activity (171). These observations suggest that decorin can modulate tumor ECM production and composition at several levels, and hence has an integral role in degradation and/or downregulation of tumor ECM constituents. Downregulation of TGF- β production by decorin could also facilitate anti-tumor immune responses through inhibition of immuno-suppressive T cells (172). In an oncolytic virotherapy study using decorin, Choi et al. showed that tumor tissue dispersion by decorin-expressing oncolytic Ad was substantially enhanced compared with that of control oncolytic Ad, in tumor

spheroids prepared from glioma or breast cancer patients as well as established subcutaneous human glioma xenograft tumors *in vivo* (158). In this study, decorin-expressing oncolytic Ad significantly reduced ECM components within the tumor tissues while normal tissue adjacent to the tumor was not affected. Decorin-expressing oncolytic Ad therefore led to dramatically increased anti-tumor effect as well as survival benefit in a variety of tumor xenograft models. Importantly, intratumoral administration of decorin-expressing oncolytic Ad to the primary tumor site substantially reduced the formation of B16BL6 melanoma pulmonary metastases in mice, indicating that this approach is capable of inducing a systemic anti-tumor immune response (158).

STRATEGIES TO OPEN EPITHELIAL JUNCTIONS JUNCTION OPENERS

Various pathogens must first breach the epithelial barrier before gaining access to the body in order to initiate infection. Several mechanisms to disrupt junctional integrity developed in these pathogens, e.g., *Clostridium perfringens* enterotoxin removes claudins-3 and -4 from tight junctions to facilitate bacterial invasion (173). Also, *zona occludens* toxin (Zot) is produced by *Vibrio cholerae* strains and possesses the ability to reversibly modify

intestinal epithelial tight junctions, granting the passage of macromolecules through mucosal barriers (174). Notably Cox et al. have shown that Zot increases the transport of drugs with low bioavailability (e.g., paclitaxel, doxorubicin, acyclovir, and cyclosporin A) up to 30-fold (175). Additionally, oncoproteins encoded by human papillomavirus (HPV), human Ad, and human T-lymphotropic virus 1 (HTLV-1) can transiently open tight junctions by the mislocalization of the tight junction protein ZO-1, thereby enhancing paracellular permeability in epithelial cells (176). It is intriguing that several viruses target epithelial junction protein to achieve infection of and dissemination in epithelial tissues. Most species of human adenoviruses (except species B) binds to the CAR. CAR is a tight junction protein. A number of studies have demonstrated that during replication of Ad5, excess production of fiber or fiber/penton base complexes results in the disruption of epithelial junctions either by interfering with CAR dimerization or by triggering intracellular signaling that leads to reorganization of intercellular junctions (177, 178). Measles virus uses the adherence junction protein nectin 4 (179). Finally, we have shown that species B adenoviruses target the desmosomal junction protein DSG2. To date, however, there are no epithelial junction openers that are being used for cancer therapy. A number of chemical detergents, surfactants, calcium-chelating agents, and phospholipids have been used to increase drug absorption through the gastrointestinal (GI) tract epithelium (180). Recently, Kytogenics Pharmaceuticals, Inc., has developed a tight junction opener based on chitosan derivatives. It is thought to act by electronegative forces applied to tight junction proteins. However, all of these agents act indiscriminately to mechanically disrupt junctions and cannot be applied systemically without major toxic side effects.

AD SEROTYPE 3 DERIVED JUNCTION OPENER JO-1

Human Ads have been classified into 7 species (A to G) currently containing 57 serotypes. Wang et al. recently reported that a group of human Ads uses DSG2 as a receptor for infection (181). Among DSG2-targeting viruses is serotype 3 (Ad3). Ad3 is able to efficiently breach the epithelial barrier in the airway tract and infect airway epithelial cells. This is achieved by the binding of Ad3 to DSG2, and subsequent intracellular signaling that results in transient opening of tight junctions between epithelial cells. Wang et al. have capitalized on this mechanism and created a recombinant protein that contains the minimal structural domains from Ad3 that are required for opening of the intercellular junctions in epithelial tumors. This protein is called “junction opener 1” or “JO-1.” JO-1 is a self-dimerizing recombinant protein derived from the Ad3 fiber (182). JO-1 has a molecular weight of approximately 60 kDa (**Figure 4A**). It can be easily produced in *E. coli* and purified by affinity chromatography. JO-1 binding to and clustering of DSG2 triggers EMT that results in transient opening of epithelial junctions, in polarized epithelial cancer cells *in vitro* (**Figures 4B,C**) and *in vivo*, in mouse models with epithelial tumors. Wang et al. have shown in over 25 xenograft tumor models that the intravenous injection of JO-1 increased the efficacy of cancer therapies, including many different monoclonal antibodies and chemotherapy drugs, in a broad range of epithelial tumors. Further studies showed that the effective doses of chemotherapy can be reduced when the chemotherapy drugs are combined with

JO-1. Finally, studies have demonstrated that combining JO-1 with chemotherapy drugs markedly reduced the toxic side effects of chemotherapy. The application of JO-1 was safe and well-tolerated in toxicology studies carried out in human DSG2-transgenic mice and macaques (109, 181).

Mechanism of JO-1-mediated junction opening

Wang et al. suggested that at least two mechanisms are involved in JO-1-mediated opening of tight junctions: DSG2 cleavage/internalization and EMT-like intracellular signaling. Epithelial cells are linked to each other by homodimers of DSG2. Studies *in vitro* and in xenograft models have shown that the DSG2 ECD is cleaved upon binding of JO-1, which results in DSG2 internalization (109). On the other hand, a series of data indicate that Ad3 binding triggers EMT-like signaling, which most likely involves the intracellular domain (ICD) of DSG2. Using mRNA expression arrays and qRT-PCR, Wang et al. found 12 h after incubation of polarized breast cancer epithelial cells with a JO-1-like ligand that 430 genes were upregulated and 352 genes were downregulated compared to incubation with a control protein (181). mRNA expression profiling revealed the activation of pathways involved in EMT (MAPK/ERK, adherens junctions, focal adhesion, and regulation of actin cytoskeleton signaling). Further studies showed an increase in PI3K and MAPK/ERK1/2 phosphorylation within 1 h after incubation with Ad type 3 pento-dodecahedral particles or JO-1 (109, 181). PI3K and MAPK/ERK1/2 activation was significantly decreased in cells in which DSG2 expression was suppressed by siRNA. Beyer et al. also found that subsequently to MAPK and PI3K activation, the protein levels of E-cadherin, a key junction protein, decreased in epithelial cells, indicating a down-regulation of gene expression of junction proteins (109).

JO-1 increases the efficacy of cancer therapy by monoclonal antibodies and chemotherapy drugs

Beyer et al. have also shown in mouse xenograft tumor models that the i.v. administration of JO-1-mediated junction opening in epithelial tumors (183). The changes triggered by JO-1 were detectable within 1 h after its i.v. injection. This, subsequently, enabled the increased intratumoral penetration of the anti-Her2/neu mAb trastuzumab (109). These biological effects of JO-1 translated into an increased therapeutic efficacy of several mAbs, including trastuzumab and cetuximab, in xenograft tumor models, e.g., models of colon, breast, gastric, lung, and ovarian cancer (109). JO-1 co-administration also enhanced the therapeutic efficacy of several chemotherapy drugs, including PEGylated liposomal doxorubicin (PLD or Doxil®), paclitaxel (Taxol®), nanoparticle albumin bound paclitaxel (Abraxane®), and irinotecan (Camptosar®) in tumor xenograft models of breast, lung, and prostate cancer (183). Furthermore, chemotherapy doses could be decreased without compromising the anti-tumor effects due to JO-1 co-therapy. This also provided protective effects to normal tissues (183). For example, we showed that the ability of JO-1 to open intercellular junctions in tumors increased the uptake and amount of therapeutics in the tumor environment (**Figures 5A–C**). This then resulted in reduced drug levels in normal tissues, thereby providing a larger therapeutic window. Immunofluorescence analysis of tissue sections also revealed higher levels of PLD in tumors of JO-1 + PLD treated mice

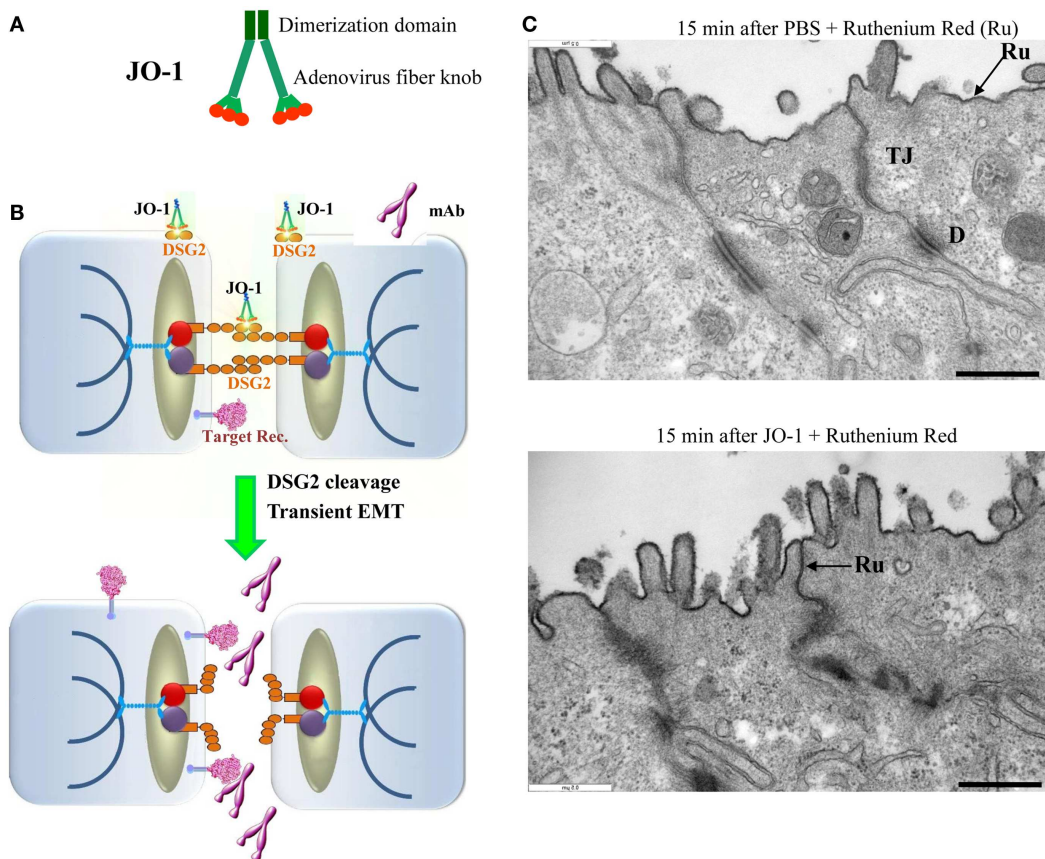


FIGURE 4 | Junction opener 1 (JO-1). **(A)** Schematic structure of JO-1. The Ad serotype 3 fiber knob domain and one fiber shaft motif was fused through a flexible linker to a homodimerizing K-coil domain (182). The protein is self-dimerizing and can be purified by His-Ni-NTA affinity chromatography. **(B)** Mode of action. JO-1 binds with picomolar avidity to DSG2. In epithelial cancer cells, DSG2 is overexpressed and exposed on the cell surface with preferential localization to desmosomes. JO-1 binding to DSG2 triggers cleavage of DSG2 dimers between neighboring cells and the transient activation of EMT pathways. This triggers junction opening and relocalization of target receptors that are often trapped in epithelial

junctions. Junction opening allows for access of drugs (for example mAbs) to their target receptors. **(C)** Transmission electron microscopy of junctional areas of T84 cells. Cells were either treated with PBS (upper panel) or JO-1 (lower panel) for 1 h on ice, washed, and then incubated for 15 min at 37°C. At this time, the electron-dense dye ruthenium red (Ru) (1) was added together with the fixative. If tight junctions (above the desmosomes) are closed, the dye only stains the apical membrane (black line). If tight junctions are open, the dye penetrates between the cells and stains the baso-lateral membrane. JO-1 also mediates the partial dissociation of desmosomes (D). The scale bar is 0.5 μ m.

compared to mice treated with PLD alone. In these animals, PLD is found to be more broadly distributed over a greater distance from blood vessels, suggesting better intratumoral penetration and absorption by tumor tissue (**Figure 5B**). Using an ELISA to measure PEGylated compounds in tissues (184), we found more PLD in tumors and less in normal tissues of mice that received JO-1 prior to i.v. PLD injection (**Figure 5C**). Better intratumoral penetration and accumulation of PLD after JO-1-mediated junction opening, resulted in enhanced therapeutic efficacy of PLD chemotherapy. This was shown in a model with mammary fat pad tumors derived from primary ovarian cancer cells (obtained from a patient biopsy) (135). This cell line was nearly resistant to PLD injected intravenously at a dose that corresponds to PLD doses used in patients. Importantly, JO-1 pre-treatment significantly improved PLD therapy (**Figure 5D**). JO-1 also relieved adverse side effects from PLD treatment, e.g., liver enzymes (AST, ALT, and alkaline phosphatase) were significantly decreased in animals

treated with JO-1 and PLD compared to mice treated with PLD alone. Mice that received JO-1 injections also had less severe tissue damage in the bone marrow and intestine caused by PLD treatment (183).

Relocalization of target receptors

In breast cancer xenograft sections and in cultured breast cancer cells, Beyer et al. found co-staining of Her2/neu and the adherens junction protein claudin 7 (183). Confocal microscopy of breast cancer BT474 cells confirmed the trapping of Her2/neu in lateral junctions. Incubation of the Her2/neu positive breast cancer cell lines BT474 or HCC1954 with JO-1 changed the composition of the lateral epithelial junctions within 1 h. As a result of this, Her2/neu staining at the cells surface became more intense, while it faded in areas distal of the cell surface. This suggests that JO-1-mediated junction opening triggered a translocation of Her2/neu from lateral membranes to the cell surface.

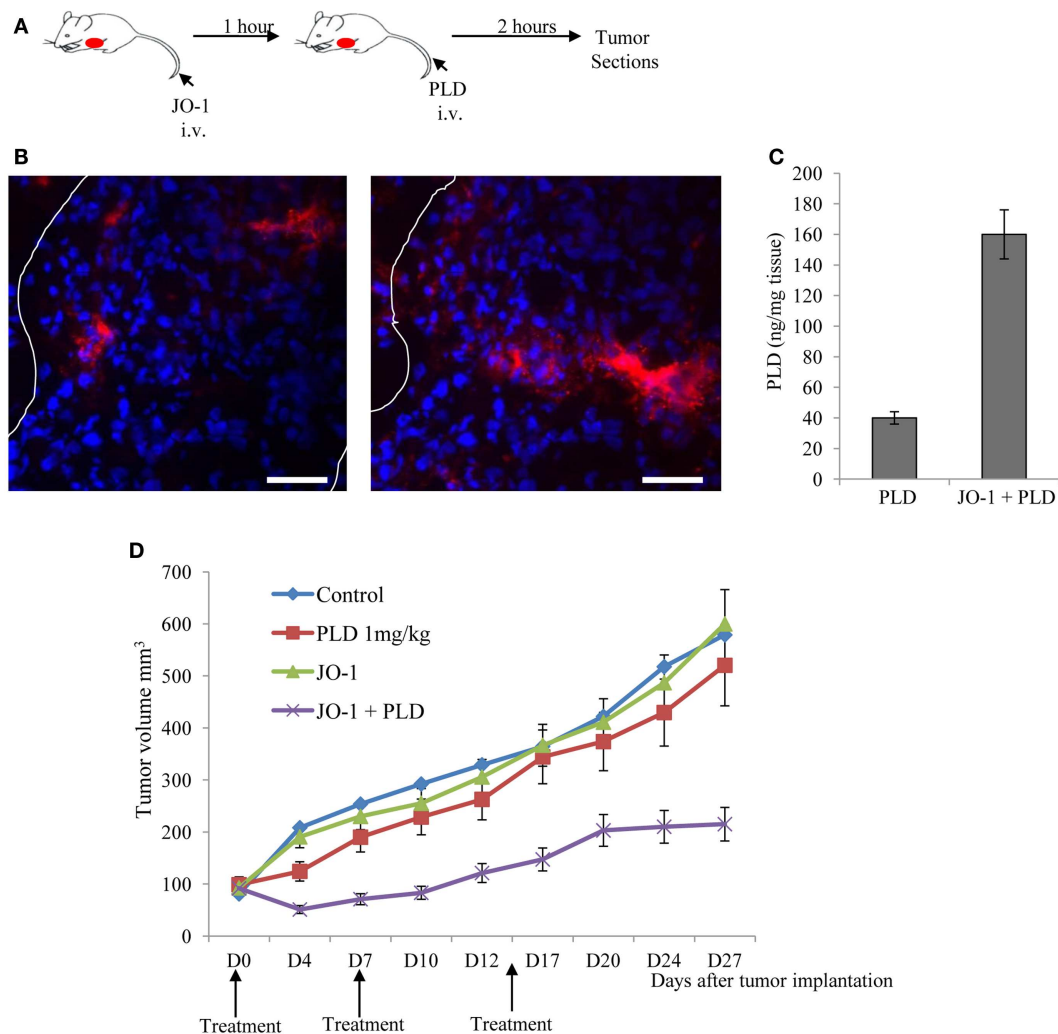


FIGURE 5 | Junction opener 1 increases tumor penetration and efficacy of PEGylated liposomal doxorubicin (PLD)/Doxil™. Studies were performed in mice with mammary fat pad tumors derived from ovc316 cells (135, 206). Ovc316 cells are Her2/neu positive epithelial tumor cells derived from an ovarian cancer biopsy. **(A)** Scheme of experiment on tumor penetration of PLD. Mice were intravenously injected with PBS or JO-1 (2 mg/kg) followed by PLD or PBS 1 h later. Two hours after PBS or PLD injection, mice were sacrificed and tumors harvested. **(B)**

Immunofluorescence analysis for PLD on tumor sections with anti-PEG antibodies. PLT appears in red. The scale bar is 20 μm. Notably, free PEG is poorly detected by ELISA or immunohistochemistry (184). **(C)** PLD concentrations in tumors measured by ELISA ($N=3$). **(D)** Therapy study in mice with ovc316 tumors. Treatment was started when tumors reached a volume of 100 mm³ (D0). Mice were injected intravenously with 2 mg/kg JO-1 or PBS, followed by an intravenous injection of PLD (1 mg/kg) or PBS 1 h later. Treatment was repeated weekly ($N=5$).

Tumor-specificity of JO-1 action

Junction opener 1 does not efficiently bind to mouse (185), hamster, or dog DSG2 (André Lieber, unpublished data). To perform efficacy and safety studies in a small animal model, we generated human DSG2-transgenic mice that expressed human DSG2 at a level and in a pattern similar to humans (185). Using the hDSG2-transgenic mouse model with syngeneic hDSG2^{high} tumors, we demonstrated that JO-1 predominantly accumulates in tumors (183). This could be explained by either one of the following factors: (i) the overexpression of DSG2 by tumor cells, (ii) better accessibility of DSG2 on tumor cells due to a lack of strict cell polarization compared to DSG2-expressing normal epithelial cells, or (iii) a high degree of vascularization and vascular permeability in tumors.

Toxic side effects and immunogenicity

The i.v. injection of JO-1 at a dose of 2 mg/kg into hDSG2-transgenic mice had no observed adverse side effects, except for mild, transient diarrhea. There were also no abnormalities found in laboratory parameters as well as histopathological studies of tissues. We speculate that this is due to the fact that DSG2 in tissues, other than the tumor and a subset of epithelial cells in the intestine/colon, is not accessible to i.v. injected JO-1. The hDSG2-transgenic mouse model was also used to obtain biodistribution and pharmacokinetics data for JO-1 (183).

Recently, we started safety studies with JO-1 in macaques. So far, we injected two animals intravenously with JO-1 at a dose of 0.6 mg/kg and performed a full necropsy 3 days later. Behavior and health was normal in both animals. In blood and tissue

analyses, we did not find hematological or histological abnormalities, except for a mild inflammation in the small intestine. JO-1 binding to DSG2 on tumor cells triggers pathways involved in EMT, a process which, as mentioned above, has been associated with tumor metastasis. Over 20 *in vivo* studies conducted with JO-1 combined with a range of cancer therapeutics in various different cancers with long-term follow-up, have not provided any evidence of metastases (183). Transient activation of the EMT pathway is only one of many steps required for tumor metastasis. Detachment of tumor cells from epithelial cancers and their subsequent migration is only possible after long-term crosstalk between malignant cells and the tumor microenvironment, resulting in changes in the tumor stroma and phenotypic reprogramming of epithelial cells into mesenchymal cells (186).

Junction opener 1 is a protein derived from Ad3 and therefore potentially immunogenic. This might not be a critical issue if JO-1 is used in combination with chemotherapy, which suppresses immune responses (187–189). In addition, Beyer et al. have shown that JO-1 remains active *in vitro* and *in vivo*, even in the presence of anti-JO-1 antibodies generated by the JO-1 vaccination of mice (183). This may be due to the fact that JO-1 binds to DSG2 with a very high avidity, thus potentially disrupting the complexes between JO-1 and antibodies against JO-1. Notably, JO-1 is a dimer of a trimeric fiber knob, which contributes to the picomolar avidity to DSG2 (182). Wang et al. performed repeated injections of JO-1 in an immunocompetent hDSG2 mouse tumor model to test the effect of anti-JO-1 antibodies on the therapeutic efficacy of JO-1 (185). Importantly JO-1 had an enhancing effect on PLD therapy after repeated JO-1 pre-treatment, demonstrating that JO-1 continues to be effective after multiple treatment cycles, even in the presence of detectable antibodies.

STRATEGIES TO REMODEL THE TUMOR STROMA THROUGH TARGETING OF TAMs

As outlined in chapter 1.2, bone marrow-derived cells, including TAMs, have a pro-tumor effect, in part through the stimulation of ECM protein synthesis, which in turn blocks intratumoral penetration of drugs. Therefore, killing of TAMs should, theoretically, increase the intratumoral penetration and accumulation of anti-cancer drugs. TAM depletion results in tumor growth suppression. This has been shown in animal models of cancer by using transgenic mice (190, 191), clodronate liposome-depletion of macrophages (192), DNA vaccination against macrophages (193), and neutralizing antibodies against macrophage chemoattractants (194). For example, Zeisberger et al. showed that combining macrophage depletion with antibody therapy greatly decreased the tumor size (195). Furthermore, a recent study showed that TAM targeting by inhibiting either the myeloid cell receptors colony stimulating factor-1 receptor (CSF1R) or chemokine (C-C motif) receptor 2 (CCR2) decreased the number of TICs in pancreatic tumors, improved chemotherapeutic efficacy, inhibited metastasis, and increased anti-tumor T cell responses (196). Overall these studies showed that decreasing the number of TAMs in the tumor stroma effectively altered the tumor microenvironment and markedly suppressed tumor growth and metastasis. Targeting TAMs did not interfere with the biological functions of M1 macrophages, including cytotoxicity and antigen presentation.

We are currently attempting to deliver a suicide gene to TAMs using TAM targeting Ad vectors or the HSC-based approach described for relaxin gene delivery (157). To restrict suicide gene expression to TAMs we utilized a miRNA-based system that avoids transgene expression in other myeloid cells. As a therapeutic gene for killing TAMs, we are currently focusing on the enzyme cytosine deaminase, which converts the prodrug 5-Fluorocytosine (5-FC) to the active chemotherapeutic agent 5-Fluorouracil (5-FU) (197). Toxic 5-FU and metabolites diffuse out of TAMs to surrounding cells killing TAMs as well as neighboring dividing tumor cells.

STRATEGIES TO INHIBIT EMT TO REMODEL THE TUMOR STROMA

As outlined above, EMT in solid tumors promotes the expression of several ECM proteins and thus blocks penetration of anti-cancer drugs. This give a rationale for inhibiting EMT processes in epithelial tumors. Accumulating knowledge about EMT pathways in solid tumors led to the development of EMT targeted therapies (198). Classically, such treatment strategies concentrate on the blockage of ATP-binding sites in affected kinases using small molecule inhibitors, as the RTK inhibitor Gefitinib for treatment of non-small cell lung cancer with activated EGFR mutation (199). While originally designed for their anti-proliferative effect on cancer cells, it was also shown that such molecules can influence the EMT status. In a cell-based screening of 267 small molecules, several compounds targeting ALK5, MEK, and SRC kinases were identified as potent inhibitors of EMT induced by EGF, HGF, and IGF-1 (200). It was also shown that counteracting TGF- β -induced EMT by treatment with troglitazone or knockdown of Smad3 in tumor cells can significantly inhibit experimental metastasis in mice (201). Furthermore, targeting early specific EMT events, like the degradation of epithelial basement membranes, can be a successful strategy, as shown in renal interstitial fibrosis. Deficiency of plasminogen activator (tPA), which is a potent activator of MMP-9, resulted in stable epithelial basement membranes and inhibition of EMT (202). Furthermore, studies involving the expression of pro-epithelial factors such as BMP-7 and Dkk, have demonstrated the inhibition of EMT and consequent CSC induction as well as metastasis in colon and prostate cancer models (203, 204). In pioneering work to understand the complexity underlying EMT induction, Scheel and colleagues showed recently that canonical and non-canonical Wnt signaling cooperate with TGF- β in order to initiate EMT in breast cancer (205). Consequently, a series of commercial or experimental Wnt-pathway inhibitors counteracted EMT. In summary, similar pathways promote therapy resistance, EMT, CSCs, and metastasis. This gives a rationale to inhibit processes that induce the mesenchymal phenotype of cancer cells. Clearly, inhibition of EMT must target a variety of pathways and should only be considered when combined therapy is applied that targets proliferating cells.

CONCLUSION

Most solid tumors are derived from epithelial cells. Malignant tumor cells actively protect themselves from host-immune responses and anti-cancer therapeutics by creating physical barriers that prevent the intratumoral penetration and contact to malignant cells. This is achieved by the production of cytokines

and chemokines that attract fibroblasts and myeloid cells into the tumor and differentiate them into cells that support tumor growth and produce ECM proteins that shield nests of malignant tumor cells. Furthermore, although malignant cells display a high degree of dedifferentiation, they maintain epithelial junctions that seal the paracellular space between tumor cells and block access to tumor antigens or target receptors. Tumor ECM and epithelial junctions represent the most basic mechanisms that create resistance to cancer treatment. Because of their importance to the tumor, they also represent an "Achilles' heel" that can be used for cancer therapy. Removal of these barriers will either directly negatively affect tumor cells or facilitate anti-tumor immune responses and drug treatment, through better intratumoral penetration and accessibility of target cells. A number of experimental approaches are aimed toward the transient degradation or downregulation of ECM proteins using injection of ECM-degrading enzymes into the tumor or their intratumoral

expression after viral- or stem cell-based gene transfer. We recently finished a phase I clinical trial with a relaxin-expressing oncolytic Ad in patients with recurrent cancer, demonstrating a clinical benefit with a good safety profile. Furthermore, we are focusing on the clinical development of a recombinant epithelial junction opener to be used in combination with Doxil chemotherapy in ovarian cancer patients. Other approaches to overcome physical barriers in tumors are at a less advanced stage. These approaches attempt to indirectly decrease tumor-associated ECM by killing tumor stromal cells that produce ECM proteins (e.g., tumor-associated fibroblasts or macrophages). ECM production and epithelial junctions can also be targeted through influencing signaling pathways in tumor cells, specifically pathways involved in the regulation of EMT/MET and hypoxia. In conclusion, there is an increasing arsenal of approaches that can be used to enhance the efficacy of more classical cancer therapeutics and overcome treatment resistance.

REFERENCES

- Bissell MJ, Radisky D. Putting tumours in context. *Nat Rev Cancer* (2001) **1**(1):46–54. doi:10.1038/35094059
- Mueller MM, Fusenig NE. Friends or foes – bipolar effects of the tumour stroma in cancer. *Nat Rev Cancer* (2004) **4**(11):839–49. doi:10.1038/nrc1477
- Bhowmick NA, Neilson EG, Moses HL. Stromal fibroblasts in cancer initiation and progression. *Nature* (2004) **432**(7015):332–7. doi:10.1038/nature03096
- Wiseman BS, Werb Z. Stromal effects on mammary gland development and breast cancer. *Science* (2002) **296**(5570):1046–9. doi:10.1126/science.1067431
- Stickens D, Behonick DJ, Ortega N, Heyer B, Hartenstein B, Yu Y, et al. Altered endochondral bone development in matrix metalloproteinase 13-deficient mice. *Development* (2004) **131**(23):5883–95. doi:10.1242/dev.01461
- Rebustini IT, Myers C, Lassiter KS, Surmak A, Szabova L, Holmbeck K, et al. MT2-MMP-dependent release of collagen IV NC1 domains regulates submandibular gland branching morphogenesis. *Dev Cell* (2009) **17**(4):482–93. doi:10.1016/j.devcel.2009.07.016
- Puri S, Hebrok M. Cellular plasticity within the pancreas – lessons learned from development. *Dev Cell* (2010) **18**(3):342–56. doi:10.1016/j.devcel.2010.02.005
- Tlsty TD, Coussens LM. Tumor stroma and regulation of cancer development. *Annu Rev Pathol* (2006) **1**:119–50. doi:10.1146/annurev.pathol.1.110304.100224
- Feig C, Gopinathan A, Neesse A, Chan DS, Cook N, Tuveson DA. The pancreas cancer microenvironment. *Clin Cancer Res* (2012) **18**(16):4266–76. doi:10.1158/1078-0432.CCR-11-3114
- Yun CO. Overcoming the extracellular matrix barrier to improve intratumoral spread and therapeutic potential of oncolytic virotherapy. *Curr Opin Mol Ther* (2008) **10**(4):356–61.
- Egeblad M, Nakasone ES, Werb Z. Tumors as organs: complex tissues that interface with the entire organism. *Dev Cell* (2010) **18**(6):884–901. doi:10.1016/j.devcel.2010.05.012
- Cox TR, Erler JT. Remodeling and homeostasis of the extracellular matrix: implications for fibrotic diseases and cancer. *Dis Model Mech* (2011) **4**(2):165–78. doi:10.1242/dmm.004077
- Lu P, Weaver VM, Werb Z. The extracellular matrix: a dynamic niche in cancer progression. *J Cell Biol* (2012) **196**(4):395–406. doi:10.1083/jcb.201102147
- Zhu GG, Risteli L, Makinen M, Risteli J, Kauppila A, Stenback F. Immunohistochemical study of type I collagen and type I pN-collagen in benign and malignant ovarian neoplasms. *Cancer* (1995) **75**(4):1010–7. doi:10.1002/1097-0142(19950215)75:4<1010::AID-CNCR2820750417>3.0.CO;2-O
- Ronnov-Jessen L, Petersen OW, Bissell MJ. Cellular changes involved in conversion of normal to malignant breast: importance of the stromal reaction. *Physiol Rev* (1996) **76**(1):69–125.
- Kauppila S, Stenback F, Risteli J, Jukkola A, Risteli L. Determinants of paclitaxel penetration and accumulation in human solid tumor. *J Pharmacol Exp Ther* (1999) **290**(2):871–80.
- Gorlach A, Herter P, Hentschel H, Frosch PJ, Acker H. Effects of rIFN beta and rIFN gamma on growth and morphology of two human melanoma cell lines: comparison between two- and three-dimensional culture. *Int J Cancer* (1994) **56**(2):249–54. doi:10.1002/ijc.2910560218
- Wenning LA, Murphy RM. Coupled cellular trafficking and diffusional limitations in delivery of immunotoxins to multicell tumor spheroids. *Biotechnol Bioeng* (1999) **62**(5):562–75. doi:10.1002/(SICI)1097-0290(19990305)62:5<562::AID-BIT8>3.0.CO;2-4
- Strauss R, Sova P, Liu Y, Li ZY, Tuve S, Pritchard D, et al. Epithelial phenotype confers resistance of ovarian cancer cells to oncolytic adenoviruses. *Cancer Res* (2009) **69**(12):5115–25. doi:10.1158/0008-5472.CAN-09-0645
- Levental KR, Yu H, Kass L, Lakins JN, Egeblad M, Erler JT, et al. Matrix crosslinking forces tumor progression by enhancing integrin signaling. *Cell* (2009) **139**(5):891–906. doi:10.1016/j.cell.2009.10.027
- Lopez JI, Kang I, You WK, McDonald DM, Weaver VM. In situ force mapping of mammary gland transformation. *Integr Biol (Camb)* (2011) **3**(9):910–21. doi:10.1039/c1ib00043h
- Netti PA, Berk DA, Swartz MA, Grodzinsky AJ, Jain RK. Role of extracellular matrix assembly in interstitial transport in solid tumors. *Cancer Res* (2000) **60**(9):2497–503.

29. Brown EB, Boucher Y, Nasser S, Jain RK. Measurement of macromolecular diffusion coefficients in human tumors. *Microvasc Res* (2004) **67**(3):231–6. doi:10.1016/j.mvr.2004.02.001
30. Hedin CH, Rubin K, Pietras K, Ostman A. High interstitial fluid pressure – an obstacle in cancer therapy. *Nat Rev Cancer* (2004) **4**(10):806–13. doi:10.1038/nrc1456
31. Orimo A, Gupta PB, Sgroi DC, Arenzana-Seisdedos F, Delaunay T, Naeem R, et al. Stromal fibroblasts present in invasive human breast carcinomas promote tumor growth and angiogenesis through elevated SDF-1/CXCL12 secretion. *Cell* (2005) **121**(3):335–48. doi:10.1016/j.cell.2005.02.034
32. Li H, Fan X, Houghton J. Tumor microenvironment: the role of the tumor stroma in cancer. *J Cell Biochem* (2007) **101**(4):805–15. doi:10.1002/jcb.21159
33. Leonardi GC, Candido S, Cervello M, Nicolosi D, Raiti F, Travali S, et al. The tumor microenvironment in hepatocellular carcinoma (review). *Int J Oncol* (2012) **40**(6):1733–47. doi:10.3892/ijo.2012.1408
34. Kalluri R, Zeisberg M. Fibroblasts in cancer. *Nat Rev Cancer* (2006) **6**(5):392–401. doi:10.1038/nrc1877
35. Ostman A, Augsten M. Cancer-associated fibroblasts and tumor growth – bystanders turning into key players. *Curr Opin Genet Dev* (2009) **19**(1):67–73. doi:10.1016/j.gde.2009.01.003
36. Elenbaas B, Weinberg RA. Heterotypic signaling between epithelial tumor cells and fibroblasts in carcinoma formation. *Exp Cell Res* (2001) **264**(1):169–84. doi:10.1006/excr.2000.5133
37. Coussens LM, Werb Z. Inflammation and cancer. *Nature* (2002) **420**(6917):860–7. doi:10.1038/nature01322
38. Dean JP, Nelson PS. Profiling influences of senescent and aged fibroblasts on prostate carcinogenesis. *Br J Cancer* (2008) **98**(2):245–9. doi:10.1038/sj.bjc.6604087
39. Gabbiani G. The myofibroblast in wound healing and fibrocontractive diseases. *J Pathol* (2003) **200**(4):500–3. doi:10.1002/path.1427
40. Barsky SH, Green WR, Grotenhorst GR, Liotta LA. Desmoplastic breast carcinoma as a source of human myofibroblasts. *Am J Pathol* (1984) **115**(3):329–33.
41. Pietras K, Ostman A. Hallmarks of cancer: interactions with the tumor stroma. *Exp Cell Res* (2010) **316**(8):1324–31. doi:10.1016/j.yexcr.2010.02.045
42. De Wever O, Nguyen QD, Van Hoorde L, Bracke M, Bruyneel E, Gespach C, et al. Tenascin-C and SF/HGF produced by myofibroblasts in vitro provide convergent pro-invasive signals to human colon cancer cells through RhoA and Rac. *FASEB J* (2004) **18**(9):1016–8.
43. Li G, Satyamoorthy K, Meier F, Berking C, Bogenrieder T, Herlyn M. Function and regulation of melanoma-stromal fibroblast interactions: when seeds meet soil. *Oncogene* (2003) **22**(20):3162–71. doi:10.1038/sj.onc.1206455
44. Sato T, Sakai T, Noguchi Y, Takita M, Hirakawa S, Ito A. Tumor-stromal cell contact promotes invasion of human uterine cervical carcinoma cells by augmenting the expression and activation of stromal matrix metalloproteinases. *Gynecol Oncol* (2004) **92**(1):47–56. doi:10.1016/j.ygyno.2003.09.012
45. Orimo A, Tomioka Y, Shimizu Y, Sato M, Oigawa S, Kamata K, et al. Cancer-associated myofibroblasts possess various factors to promote endometrial tumor progression. *Clin Cancer Res* (2001) **7**(10):3097–105.
46. Lewis CE, Pollard JW. Distinct role of macrophages in different tumor microenvironments. *Cancer Res* (2006) **66**(2):605–12. doi:10.1158/0008-5472.CAN-05-4005
47. Ueno T, Toi M, Saji H, Muta M, Bando H, Kuroi K, et al. Significance of macrophage chemoattractant protein-1 in macrophage recruitment, angiogenesis, and survival in human breast cancer. *Clin Cancer Res* (2000) **6**(8):3282–9.
48. Lin EY, Pollard JW. Role of infiltrated leucocytes in tumour growth and spread. *Br J Cancer* (2004) **90**(11):2053–8. doi:10.1038/sj.bjc.6601705
49. Balkwill F, Charles KA, Mantovani A. Smoldering and polarized inflammation in the initiation and promotion of malignant disease. *Cancer Cell* (2005) **7**(3):211–7. doi:10.1016/j.ccr.2005.02.013
50. Lin EY, Pollard JW. Tumor-associated macrophages press the angiogenic switch in breast cancer. *Cancer Res* (2007) **67**(11):5064–6. doi:10.1158/0008-5472.CAN-07-0912
51. van der Bij GJ, Oosterling SJ, Meijer S, Beelen RH, van Egmond M. The role of macrophages in tumor development. *Cell Oncol* (2005) **27**(4):203–13.
52. Lewis C, Murdoch C. Macrophage responses to hypoxia: implications for tumor progression and anti-cancer therapies. *Am J Pathol* (2005) **167**(3):627–35. doi:10.1016/S0002-9440(10)62038-X
53. Barbera-Guillem E, Nyhus JK, Wolford CC, Friece CR, Sampsel JW. Vascular endothelial growth factor secretion by tumor-infiltrating macrophages essentially supports tumor angiogenesis, and IgG immune complexes potentiate the process. *Cancer Res* (2002) **62**(23):7042–9.
54. Pollard JW. Tumour-educated macrophages promote tumour progression and metastasis. *Nat Rev Cancer* (2004) **4**(1):71–8. doi:10.1038/nrc1256
55. Biswas SK, Mantovani A. Macrophage plasticity and interaction with lymphocyte subsets: cancer as a paradigm. *Nat Immunol* (2010) **11**(10):889–96. doi:10.1038/ni.1937
56. Gabrilovich DI, Nagaraj S. Myeloid-derived suppressor cells as regulators of the immune system. *Nat Rev Immunol* (2009) **9**(3):162–74. doi:10.1038/nri2506
57. Movahedi K, Laoui D, Gysemans C, Baeten M, Stange G, Van den Bossche J, et al. Different tumor microenvironments contain functionally distinct subsets of macrophages derived from Ly6C(high) monocytes. *Cancer Res* (2010) **70**(14):5728–39. doi:10.1158/0008-5472.CAN-09-4672
58. Bonde AK, Tischler V, Kumar S, Soltermann A, Schwendener RA. Intratumoral macrophages contribute to epithelial-mesenchymal transition in solid tumors. *BMC Cancer* (2012) **12**:35. doi:10.1186/1471-2407-12-35
59. Jinushi M, Baghdadi M, Chiba S, Yoshiyama H. Regulation of cancer stem cell activities by tumor-associated macrophages. *Am J Cancer Res* (2012) **2**(5):529–39.
60. Eck M, Schmausser B, Scheller K, Brandlein S, Muller-Hermelink HK. Pleiotropic effects of CXC chemokines in gastric carcinoma: differences in CXCL8 and CXCL1 expression between diffuse and intestinal types of gastric carcinoma. *Clin Exp Immunol* (2003) **134**(3):508–15. doi:10.10111/j.1365-2249.2003.02305.x
61. Jensen HK, Donskov F, Marcussen N, Nordmark M, Lundbeck F, von der Maase H. Presence of intratumoral neutrophils is an independent prognostic factor in localized renal cell carcinoma. *J Clin Oncol* (2009) **27**(28):4709–17. doi:10.1200/JCO.2008.18.9498
62. Wislez M, Rabbe N, Marchal J, Milleron B, Crestani B, Mayaud C, et al. Hepatocyte growth factor production by neutrophils infiltrating bronchioloalveolar subtype pulmonary adenocarcinoma: role in tumor progression and death. *Cancer Res* (2003) **63**(6):1405–12.
63. Bellocq A, Antoine M, Flahault A, Philippe C, Crestani B, Bernaudin JF, et al. Neutrophil alveolitis in bronchioloalveolar carcinoma: induction by tumor-derived interleukin-8 and relation to clinical outcome. *Am J Pathol* (1998) **152**(1):83–92.
64. Schmielau J, Finn OJ. Activated granulocytes and granulocyte-derived hydrogen peroxide are the underlying mechanism of suppression of t-cell function in advanced cancer patients. *Cancer Res* (2001) **61**(12):4756–60.
65. Maeda H, Wu J, Sawa T, Matsumura Y, Hori K. Tumor vascular permeability and the EPR effect in macromolecular therapeutics: a review. *J Control Release* (2000) **65**(1-2):271–84. doi:10.1016/S0168-3659(99)00248-5
66. Iyer AK, Khaled G, Fang J, Maeda H. Exploiting the enhanced permeability and retention effect for tumor targeting. *Drug Discov Today* (2006) **11**(17–18):812–8. doi:10.1016/j.drudis.2006.07.005
67. Jain RK. Delivery of molecular and cellular medicine to solid tumors. *Adv Drug Deliv Rev* (1997) **26**(2-3):71–90. doi:10.1016/S0169-409X(97)00027-6
68. Milosevic MF, Fyles AW, Wong R, Pintilie M, Kavanagh MC, Levin W, et al. Interstitial fluid pressure in cervical carcinoma: within tumor heterogeneity, and relation to oxygen tension. *Cancer* (1998) **82**(12):2418–26. doi:10.1002/(SICI)1097-0142(19980615)82:12<2418::AID-CNCR16>3.0.CO;2-S
69. Patan S, Munn LL, Jain RK. Intussusceptive microvascular growth in a human colon adenocarcinoma xenograft: a novel mechanism of tumor angiogenesis. *Microvasc Res* (1996) **51**(2):260–72. doi:10.1006/mvre.1996.0025
70. Padera TP, Stoll BR, Tooredman JB, Capen D, di Tomaso

- E, Jain RK. Pathology: cancer cells compress intratumour vessels. *Nature* (2004) **427**(6976):695. doi:10.1038/427695a
71. Jain RK, Tong RT, Munn LL. Effect of vascular normalization by antiangiogenic therapy on interstitial hypertension, peritumor edema, and lymphatic metastasis: insights from a mathematical model. *Cancer Res* (2007) **67**(6):2729–35. doi:10.1158/0008-5472.CAN-06-4102
72. Boucher Y, Baxter LT, Jain RK. Interstitial pressure gradients in tissue-isolated and subcutaneous tumors: implications for therapy. *Cancer Res* (1990) **50**(15):4478–84.
73. Gatenby RA, Gillies RJ. Why do cancers have high aerobic glycolysis? *Nat Rev Cancer* (2004) **4**(11):891–9. doi:10.1038/>{break}nrc1478
74. Baxter LT, Jain RK. Transport of fluid and macromolecules in tumors. I. Role of interstitial pressure and convection. *Microvasc Res* (1989) **37**(1):77–104. doi:10.1016/0026-2862(89)90074-5
75. Baxter LT, Jain RK. Transport of fluid and macromolecules in tumors. II. Role of heterogeneous perfusion and lymphatics. *Microvasc Res* (1990) **40**(2):246–63. doi:10.1016/0026-2862(90)90023-K
76. Jain RK. Delivery of molecular medicine to solid tumors: lessons from in vivo imaging of gene expression and function. *J Control Release* (2001) **74**(1-3):7–25. doi:10.1016/S0168-3659(01)00306-6
77. Sevick EM, Jain RK. Effect of red blood cell rigidity on tumor blood flow: increase in viscous resistance during hyperglycemia. *Cancer Res* (1991) **51**(10):2727–30.
78. Znati CA, Rosenstein M, Boucher Y, Epperly MW, Bloomer WD, Jain RK. Effect of radiation on interstitial fluid pressure and oxygenation in a human tumor xenograft. *Cancer Res* (1996) **56**(5):964–8.
79. Casazza A, Di Conza G, Wenes M, Finisguerra V, Deschoemaeker S, Mazzzone M. Tumor stroma: a complexity dictated by the hypoxic tumor microenvironment. *Oncogene* (2013). doi:10.1038/onc.2013.121. [Epub ahead of print].
80. Madara JL. Regulation of the movement of solutes across tight junctions. *Annu Rev Physiol* (1998) **60**:143–59. doi:10.1146/annurev.physiol.60.1.143
81. Turksen K, Troy TC. Barriers built on claudins. *J Cell Sci* (2004) **117**(Pt 12):2435–47. doi:10.1242/jcs.01235
82. Sasaki H. Freeze-fracture analysis of renal-epithelial tight junctions. *Methods Mol Med* (2003) **86**:155–66.
83. Furuse M, Hirase T, Itoh M, Nagafuchi A, Yonemura S, Tsukita S. Occludin: a novel integral membrane protein localizing at tight junctions. *J Cell Biol* (1993) **123**(6 Pt 2):1777–88. doi:10.1083/jcb.200805113
84. Liu Y, Nusrat A, Schnell FJ, Reaves TA, Walsh S, Pochet M, et al. Human junction adhesion molecule regulates tight junction resealing in epithelia. *J Cell Sci* (2000) **113**(Pt 13):2363–74.
85. Cohen CJ, Shieh JT, Pickles RJ, Okegawa T, Hsieh JT, Bergelson JM. The coxsackievirus and adenovirus receptor is a transmembrane component of the tight junction. *Proc Natl Acad Sci U S A* (2001) **98**(26):15191–6. doi:10.1073/pnas.261452898
86. Ikenouchi J, Furuse M, Furuse K, Sasaki H, Tsukita S. Tricellulin constitutes a novel barrier at tricellular contacts of epithelial cells. *J Cell Biol* (2005) **171**(6):939–45. doi:10.1083/jcb.200510043
87. Capaldo CT, Macara IG. Depletion of E-cadherin disrupts establishment but not maintenance of cell junctions in Madin-Darby canine kidney epithelial cells. *Mol Biol Cell* (2007) **18**(1):189–200. doi:10.1091/mbc.E06-05-0471
88. Bryant DM, Wylie FG, Stow JL. Regulation of endocytosis, nuclear translocation, and signaling of fibroblast growth factor receptor 1 by E-cadherin. *Mol Biol Cell* (2005) **16**(1):14–23. doi:10.1091/mbc.E04-09-0845
89. Qian X, Karpova T, Sheppard AM, McNally J, Lowy DR. E-cadherin-mediated adhesion inhibits ligand-dependent activation of diverse receptor tyrosine kinases. *EMBO J* (2004) **23**(8):1739–48. doi:10.1038/sj.emboj.7600136
90. Perraiz M, Chen X, Perez-Moreno M, Gumbiner BM. E-cadherin homophilic ligation inhibits cell growth and epidermal growth factor receptor signalling independently of other cell interactions. *Mol Biol Cell* (2007) **18**(6):2013–25. doi:10.1091/mbc.E06-04-0348
91. Moon RT, Bowerman B, Boutros M, Perrimon N. The promise and perils of Wnt signaling through beta-catenin. *Science* (2002) **296**(5573):1644–6. doi:10.1126/science.1071549
92. Soto E, Yanagisawa M, Marlow LA, Copland JA, Perez EA, Anastasiadis PZ. p120 Catenin induces opposing effects on tumor cell growth depending on E-cadherin expression. *J Cell Biol* (2008) **183**(4):737–49. doi:10.1083/jcb.200805113
93. Perez-Moreno M, Song W, Pasolli HA, Williams SE, Fuchs E. Loss of p120 catenin and links to mitotic alterations, inflammation, and skin cancer. *Proc Natl Acad Sci U S A* (2008) **105**(40):15399–404. doi:10.1073/pnas.0807301105
94. Biedermann K, Vogelsang H, Becker I, Plaschke S, Siewert JR, Hofler H, et al. Desmoglein 2 is expressed abnormally rather than mutated in familial and sporadic gastric cancer. *J Pathol* (2005) **207**(2):199–206. doi:10.1002/path.1821
95. Harada H, Iwatsuki K, Ohtsuka M, Han GW, Kaneko F. Abnormal desmoglein expression by squamous cell carcinoma cells. *Acta Derm Venereol* (1996) **76**(6):417–20.
96. Chen J, Nekrasova OE, Patel DM, Klessner JL, Godsel LM, Koetsier JL, et al. The C-terminal unique region of desmoglein 2 inhibits its internalization via tail-tail interactions. *J Cell Biol* (2012) **199**(4):699–711. doi:10.1083/jcb.201202105
97. Nava P, Laukoetter MG, Hopkins AM, Laur O, Gerner-Smidt K, Green KJ, et al. Desmoglein-2: a novel regulator of apoptosis in the intestinal epithelium. *Mol Biol Cell* (2007) **18**(11):4565–78. doi:10.1091/mbc.E07-05-0426
98. Lipinski CA, Lombardo F, Dominy BW, Feeney PJ. Experimental and computational approaches to estimate solubility and permeability in drug discovery and development settings. *Adv Drug Deliv Rev* (2001) **46**(1-3):3–26. doi:10.1016/S0169-409X(00)00129-0
99. Lavin SR, McWhorter TJ, Karasov WH. Mechanistic bases for differences in passive absorption. *J Exp Biol* (2007) **210**(Pt 15):2754–64. doi:10.1242/jeb.006114
100. Green SK, Karlsson MC, Ravetch JV, Kerbel RS. Disruption of cell-cell adhesion enhances antibody-dependent cellular cytotoxicity: implications for antibody-based therapeutics of cancer. *Cancer Res* (2011) **71**(22):7080–90. doi:10.1158/0008-5472.CAN-11-2009
101. Fessler SP, Wotkowicz MT, Mahanta SK, Bamdad C. MUC1* is a determinant of trastuzumab (Herceptin) resistance in breast cancer cells. *Breast Cancer Res Treat* (2009) **118**(1):113–24. doi:10.1007/s10549-009-0412-3
102. Oliveras-Ferraro C, Vazquez-Martin A, Cufi S, Queralt B, Baez L, Guardeno R, et al. Stem cell property epithelial-to-mesenchymal transition is a core transcriptional network for predicting cetuximab (Erbitux) efficacy in KRAS wild-type tumor cells. *J Cell Biochem* (2011) **112**(1):10–29. doi:10.1002/jcb.22952
103. Lee CM, Tannock IF. The distribution of the therapeutic monoclonal antibodies cetuximab and trastuzumab within solid tumors. *BMC Cancer* (2010) **10**:255. doi:10.1186/1471-2407-10-255
104. Christiansen JJ, Rajasekaran AK. Reassessing epithelial to mesenchymal transition as a prerequisite for carcinoma invasion and metastasis. *Cancer Res* (2006) **66**(17):8319–26. doi:10.1158/0008-5472.CAN-06-0410
105. Shelly M, Mosesson Y, Citri A, Lavi S, Zwang Y, Melamed-Book N, et al. Polar expression of ErBB-2/HER2 in epithelia. Bimodal regulation by Lin-7. *Dev Cell* (2003) **5**(3):475–86. doi:10.1016/j.devcel.2003.08.001
106. Toledo C, Matus CE, Barraza X, Arroyo P, Ehrenfeld P, Figueira CD, et al. Expression of HER2 and bradykinin B(1) receptors in precursor lesions of gallbladder carcinoma. *World J Gastroenterol* (2012) **18**(11):1208–15. doi:10.3748/wjg.v18.i11.1208
107. Tong WM, Ellinger A, Sheinin Y, Cross HS. Epidermal growth factor receptor expression in primary cultured human colorectal carcinoma cells. *Br J Cancer* (1998) **77**(11):1792–8. doi:10.1038/bjc.1998.298
108. Vermeer PD, Einwalter LA, Moninger TO, Rokhlin T, Kern JA, Zabner J, et al. Segregation of receptor and ligand regulates activation of epithelial growth factor receptor. *Nature* (2003) **422**(6929):322–6. doi:10.1038/nature01440
109. Beyer I, van Rensburg R, Strauss R, Li Z, Wang H, Persson J, et al. Epithelial junction opener JO-1 improves monoclonal antibody therapy of cancer. *Cancer Res* (2011) **71**(22):7080–90. doi:10.1158/0008-5472.CAN-11-2009
110. Thiery JP, Acloude H, Huang RY, Nieto MA. Epithelial-mesenchymal transitions in development and disease. *Cell*

- (2009) **139**(5):871–90. doi: 10.1016/j.cell.2009.11.007
111. Wong AS, Auersperg N. Normal ovarian surface epithelium. *Cancer Treat Res* (2002) **107**:161–83.
112. Brabletz T, Jung A, Spaderna S, Hlubek F, Kirchner T. Opinion: migrating cancer stem cells – an integrated concept of malignant tumour progression. *Nat Rev Cancer* (2005) **5**(9):744–9. doi: 10.1038/nrc1694
113. Come C, Magnino F, Bibeau F, De Santa Barbara P, Becker KF, Theillet C, et al. Snail and slug play distinct roles during breast carcinoma progression. *Clin Cancer Res* (2006) **12**(18):5395–402. doi: 10.1158/1078-0432.CCR-06-0478
114. Arnoux V, Come C, Kusewitt D, Hudson L, Savagner P. Cutaneous wound reepithelialization: a partial and reversible EMT. In: Savagner P, editor. *Rise and Fall of Epithelial Phenotype: Concepts of Epithelial-Mesenchymal Transition*. Berlin: Springer (2005). p. 111–34.
115. Kalluri R, Weinberg RA. The basics of epithelial-mesenchymal transition. *J Clin Invest* (2009) **119**(6):1420–8. doi: 10.1172/JCI39104
116. Birchmeier W, Behrens J. Cadherin expression in carcinomas: role in the formation of cell junctions and the prevention of invasiveness. *Biochim Biophys Acta* (1994) **1198**(1):11–26.
117. Sabbah M, Emami S, Redeuilh G, Julien S, Prevost G, Zimber A, et al. Molecular signature and therapeutic perspective of the epithelial-to-mesenchymal transitions in epithelial cancers. *Drug Resist Updat* (2008) **11**(4–5):123–51. doi: 10.1016/j.drup.2008.07.001
118. Nieto MA. The snail superfamily of zinc-finger transcription factors. *Nat Rev Mol Cell Biol* (2002) **3**(3):155–66. doi: 10.1038/nrm757
119. Leptin M. Twist and snail as positive and negative regulators during *Drosophila* mesoderm development. *Genes Dev* (1991) **5**(9):1568–76. doi: 10.1101/gad.5.9.1568
120. Batlle E, Sancho E, Franci C, Dominguez D, Monfar M, Baulida J, et al. The transcription factor snail is a repressor of E-cadherin gene expression in epithelial tumour cells. *Nat Cell Biol* (2000) **2**(2):84–9. doi: 10.1038/35000034
121. Postigo AA, Depp JL, Taylor JJ, Kroll KL. Regulation of Smad signaling through a differential recruitment of coactivators and corepressors by ZEB proteins. *EMBO J* (2003) **22**(10):2453–62. doi: 10.1093/emboj/cdg226
122. Ellenberger T, Fass D, Arnaud M, Harrison SC. Crystal structure of transcription factor E47: E-box recognition by a basic region helix-loop-helix dimer. *Genes Dev* (1994) **8**(8):970–80. doi: 10.1101/gad.8.8.970
123. Ikenouchi J, Matsuda M, Furuse M, Tsukita S. Regulation of tight junctions during the epithelium-mesenchyme transition: direct repression of the gene expression of claudins/octulin by Snail. *J Cell Sci* (2003) **116**(Pt 10):1959–67. doi: 10.1242/jcs.00389
124. Ohkubo T, Ozawa M. The transcription factor Snail downregulates the tight junction components independently of E-cadherin downregulation. *J Cell Sci* (2004) **117**(Pt 9):1675–85. doi: 10.1242/jcs.01004
125. Vandewalle C, Comijn J, De Craene B, Vermassen P, Bruyneel E, Andersen H, et al. SIP1/ZEB2 induces EMT by repressing genes of different epithelial cell-cell junctions. *Nucleic Acids Res* (2005) **33**(20):6566–78. doi: 10.1093/nar/gki965
126. Martinez-Estrada OM, Culleres A, Soriano FX, Peinado H, Bolos V, Martinez FO, et al. The transcription factors Slug and Snail act as repressors of claudin-1 expression in epithelial cells. *Biochem J* (2006) **394**(Pt 2):449–57. doi: 10.1042/BJ20050591
127. Yang J, Mani SA, Donaher JL, Ramaswamy S, Itzykson RA, Come C, et al. Twist, a master regulator of morphogenesis, plays an essential role in tumor metastasis. *Cell* (2004) **117**(7):927–39. doi: 10.1016/j.cell.2004.06.006
128. Perez-Moreno MA, Locascio A, Rodrigo I, Dhondt G, Portillo F, Nieto MA, et al. A new role for E12/E47 in the repression of E-cadherin expression and epithelial-mesenchymal transitions. *J Biol Chem* (2001) **276**(29):27424–31. doi: 10.1074/jbc.M100827200
129. Thiery JP. Epithelial-mesenchymal transitions in tumour progression. *Nat Rev Cancer* (2002) **2**(6):442–54. doi: 10.1038/nrc822
130. Panorchan P, Thompson MS, Davis KJ, Tseng Y, Konstantopoulos K, Wirtz D. Single-molecule analysis of cadherin-mediated cell-cell adhesion. *J Cell Sci* (2006) **119**(Pt 1):66–74. doi: 10.1242/jcs.02719
131. Janmey PA, Euteneuer U, Traub P, Schliwa M. Viscoelastic properties of vimentin compared with other filamentous biopolymer networks. *J Cell Biol* (1991) **113**(1):155–60. doi: 10.1083/jcb.113.1.155
132. Wagner OI, Rammensee S, Korde N, Wen Q, Leterrier JE, Janmey PA. Softness, strength and self-repair in intermediate filament networks. *Exp Cell Res* (2007) **313**(10):2228–35. doi: 10.1016/j.yexcr.2007.04.025
133. LaGamba D, Nawashad A, Hay ED. Microarray analysis of gene expression during epithelial-mesenchymal transformation. *Dev Dyn* (2005) **234**(1):132–42. doi: 10.1002/dvdy.20489
134. Brabletz T, Jung A, Reu S, Porzner M, Hlubek F, Kunz-Schughart LA, et al. Variable beta-catenin expression in colorectal cancers indicates tumor progression driven by the tumor environment. *Proc Natl Acad Sci U S A* (2001) **98**(18):10356–61. doi: 10.1073/pnas.171610498
135. Strauss R, Li ZY, Liu Y, Beyer I, Persson J, Sova P, et al. Analysis of epithelial and mesenchymal markers in ovarian cancer reveals phenotypic heterogeneity and plasticity. *PLoS ONE* (2011) **6**(1):e16186. doi: 10.1371/journal.pone.0016186
136. Visvader JE, Lindeman GJ. Cancer stem cells in solid tumours: accumulating evidence and unresolved questions. *Nat Rev Cancer* (2008) **8**(10):755–68. doi: 10.1038/nrc2499
137. Marhaba R, Klingbeil P, Nuebel T, Nazarenko I, Buechler MW, Zoeller M. CD44 and EpCAM: cancer-initiating cell markers. *Curr Mol Med* (2008) **8**(8):784–804. doi: 10.2174/156652408786733667
138. Yu M, Bardia A, Wittner BS, Stott SL, Smas ME, Ting DT, et al. Circulating breast tumor cells exhibit dynamic changes in epithelial and mesenchymal composition. *Science* (2013) **339**(6119):580–4. doi: 10.1126/science.1228522
139. Tsai JH, Donaher JL, Murphy DA, Chau S, Yang J. Spatiotemporal regulation of epithelial-mesenchymal transition is essential for squamous cell carcinoma metastasis. *Cancer Cell* (2012) **22**(6):725–36. doi: 10.1016/j.ccr.2012.09.022
140. Ocana OH, Corcoles R, Fabra A, Moreno-Bueno G, Acloque H, Vega S, et al. Metastatic colonization requires the repression of the epithelial-mesenchymal transition inducer Prrx1. *Cancer Cell* (2012) **22**(6):709–24. doi: 10.1016/j.ccr.2012.10.012
141. Saito T, Nagai M, Ladanyi M. SYT-SSX1 and SYT-SSX2 interfere with repression of E-cadherin by snail and slug: a potential mechanism for aberrant mesenchymal to epithelial transition in human synovial sarcoma. *Cancer Res* (2006) **66**(14):6919–27. doi: 10.1158/0008-5472.CAN-05-3697
142. Fitzgerald MP, Gourronc F, Teoh ML, Provenzano MJ, Case AJ, Martin JA, et al. Human chondrosarcoma cells acquire an epithelial-like gene expression pattern via an epigenetic switch: evidence for mesenchymal-epithelial transition during sarcomagenesis. *Sarcoma* (2011) **2011**:598218. doi: 10.1155/2011/598218
143. Egeblad M, Rasch MG, Weaver VM. Dynamic interplay between the collagen scaffold and tumor evolution. *Curr Opin Cell Biol* (2010) **22**(5):697–706. doi: 10.1016/j.ceb.2010.08.015
144. Bjorge L, Junnikkala S, Kristoffersen EK, Hakulinen J, Matre R, Meri S. Resistance of ovarian teratocarcinoma cell spheroids to complement-mediated lysis. *Br J Cancer* (1997) **75**(9):1247–55. doi: 10.1038/bjc.1997.213
145. Brown E, McKee T, diTomaso E, Pluen A, Seed B, Boucher Y, et al. Dynamic imaging of collagen and its modulation in tumors in vivo using second-harmonic generation. *Nat Med* (2003) **9**(6):796–800. doi: 10.1038/nm879
146. Eikenes L, Tufto I, Schnell EA, Bjorkoy A, De Lange Davies C. Effect of collagenase and hyaluronidase on free and anomalous diffusion in multicellular spheroids and xenografts. *Anticancer Res* (2010) **30**(2):359–68.
147. Kuriyama N, Kuriyama H, Julin CM, Lamborn K, Israel MA. Pretreatment with protease is a useful experimental strategy for enhancing adenovirus-mediated cancer gene therapy. *Hum Gene Ther* (2000) **11**(16):2219–30. doi: 10.1089/104303400750035744
148. McKee TD, Grandi P, Mok W, Alexandrakis G, Insin N, Zimmer JP, et al. Degradation of fibrillar collagen in a human melanoma xenograft improves the efficacy of an oncolytic herpes simplex virus vector. *Cancer Res* (2006)

- 66**(5):2509–13. doi:10.1158/0008-5472.CAN-05-2242
149. Ganesh S, Gonzalez-Edick M, Gibbons D, Van Roey M, Jooss K. Intratumoral coadministration of hyaluronidase enzyme and oncolytic adenoviruses enhances virus potency in metastatic tumor models. *Clin Cancer Res* (2008) **14**(12):3933–41. doi:10.1158/1078-0432.CCR-07-4732
150. Cheng J, Sauthoff H, Huang Y, Kutler DI, Bajwa S, Rom WN, et al. Human matrix metalloproteinase-8 gene delivery increases the oncolytic activity of a replicating adenovirus. *Mol Ther* (2007) **15**(11):1982–90. doi:10.1038/sj.mt.6300264
151. Mok W, Boucher Y, Jain RK. Matrix metalloproteinases-1 and -8 improve the distribution and efficacy of an oncolytic virus. *Cancer Res* (2007) **67**(22):10664–8. doi:10.1158/0008-5472.CAN-07-3107
152. Coussens LM, Werb Z. Matrix metalloproteinases and the development of cancer. *Chem Biol* (1996) **3**(11):895–904. doi:10.1016/S1074-5521(96)90178-7
153. Kessenbrock K, Plaks V, Werb Z. Matrix metalloproteinases: regulators of the tumor microenvironment. *Cell* (2010) **141**(1):52–67. doi:10.1016/j.cell.2010.03.015
154. Ganesh S, Gonzalez Edick M, Idamakanti N, Abramova M, Vanroey M, Robinson M, et al. Relaxin-expressing, fiber chimeric oncolytic adenovirus prolongs survival of tumor-bearing mice. *Cancer Res* (2007) **67**(9):4399–407. doi:10.1158/0008-5472.CAN-06-4260
155. Kim JH, Lee YS, Kim H, Huang JH, Yoon AR, Yun CO. Relaxin expression from tumor-targeting adenoviruses and its intratumoral spread, apoptosis induction, and efficacy. *J Natl Cancer Inst* (2006) **98**(20):1482–93. doi:10.1093/jnci/djj397
156. Beyer I, Li Z, Persson J, Liu Y, van Rensburg R, Yumul R, et al. Controlled extracellular matrix degradation in breast cancer tumors improves therapy by trastuzumab. *Mol Ther* (2011) **19**(3):479–89. doi:10.1038/mt.2010.256
157. Li Z, Liu Y, Tuve S, Xun Y, Fan X, Min L, et al. Toward a stem cell gene therapy for breast cancer. *Blood* (2009) **113**(22):5423–33. doi:10.1182/blood-2008-10-187237
158. Choi IK, Lee YS, Yoo JY, Yoon AR, Kim H, Kim DS, et al. Effect of decorin on overcoming the extracellular matrix barrier for oncolytic virotherapy. *Gene Ther* (2010) **17**(2):190–201. doi:10.1038/gt.2009.142
159. Dschietzig T, Bartsch C, Baumann G, Stangl K. Relaxin-a pleiotropic hormone and its emerging role for experimental and clinical therapeutics. *Pharmacol Ther* (2006) **112**(1):38–56. doi:10.1016/j.pharmthera.2006.03.004
160. Sherwood OD. Relaxin's physiological roles and other diverse actions. *Endocr Rev* (2004) **25**(2):205–34. doi:10.1210/er.2003-0013
161. Van Der Westhuizen ET, Summers RJ, Halls ML, Bathgate RA, Sexton PM. Relaxin receptors – new drug targets for multiple disease states. *Curr Drug Targets* (2007) **8**(1):91–104. doi:10.2174/138945007779315650
162. Amento EP, Bhan AK, McCullagh KG, Krane SM. Influences of gamma interferon on synovial fibroblast-like cells. Ia induction and inhibition of collagen synthesis. *J Clin Invest* (1985) **76**(2):837–48. doi:10.1172/JCI112041
163. Bathgate RA, Lekgabé ED, McGuane JT, Su Y, Pham T, Ferraro T, et al. Adenovirus-mediated delivery of relaxin reverses cardiac fibrosis. *Mol Cell Endocrinol* (2008) **280**(1–2):30–8. doi:10.1016/j.mce.2007.09.008
164. Cernaro V, Lacquaniti A, Lupica R, Buemi A, Trimboli D, Giorgianni G, et al. Relaxin: new pathophysiological aspects and pharmacological perspectives for an old protein. *Med Res Rev* (2013). doi:10.1002/med.21277. [Epub ahead of print].
165. Silvertown JD, Ng J, Sato T, Summerlee AJ, Medin JA. H2 relaxin overexpression increases in vivo prostate xenograft tumor growth and angiogenesis. *Int J Cancer* (2006) **118**(1):62–73. doi:10.1002/ijc.21288
166. Silvecrtown JD, Symes JC, Neschadim A, Nonaka T, Kao JC, Summerlee AJ, et al. Analog of H2 relaxin exhibits antagonistic properties and impairs prostate tumor growth. *FASEB J* (2007) **21**(3):754–65. doi:10.1096/fj.06-6847com
167. Binder C, Hagemann T, Husen B, Schulz M, Einspanier A. Relaxin enhances in-vitro invasiveness of breast cancer cell lines by up-regulation of matrix metalloproteases. *Mol Hum Reprod* (2002) **8**(9):789–96. doi:10.1093/molehr/8.9.789
168. Radestock Y, Hoang-Vu C, Hombach-Klonisch S. Relaxin reduces xenograft tumour growth of human MDA-MB-231 breast cancer cells. *Breast Cancer Res* (2008) **10**(4):R71. doi:10.1186/bcr2136
169. Vogel KG, Paulsson M, Heinegard D. Specific inhibition of type I and type II collagen fibrillogenesis by the small proteoglycan of tendon. *Biochem J* (1984) **223**(3):587–97.
170. Yamaguchi Y, Mann DM, Ruoslahti E. Negative regulation of transforming growth factor-beta by the proteoglycan decorin. *Nature* (1990) **346**(6281):281–4. doi:10.1038/346281a0
171. Danielson KG, Baribault H, Holmes DF, Graham H, Kadler KE, Iozzo RV. Targeted disruption of decorin leads to abnormal collagen fibril morphology and skin fragility. *J Cell Biol* (1997) **136**(3):729–43. doi:10.1083/jcb.136.3.729
172. Wei H, Liu P, Swisher E, Yip YY, Tse JH, Agnew K, et al. Silencing of the TGF-beta1 gene increases the immunogenicity of cells from human ovarian carcinoma. *J Immunother* (2012) **35**(3):267–75. doi:10.1097/CJI.0b013e31824d72ee
173. Sonoda N, Furuse M, Sasaki H, Yonemura S, Katahira J, Horiguchi Y, et al. Clostridium perfringens enterotoxin fragment removes specific claudins from tight junction strands: evidence for direct involvement of claudins in tight junction barrier. *J Cell Biol* (1999) **147**(1):195–204. doi:10.1083/jcb.147.1.195
174. Fasano A, Baudry B, Pumplin DW, Wasserman SS, Tall BD, Ketley JM, et al. *Vibrio cholerae* produces a second enterotoxin, which affects intestinal tight junctions. *Proc Natl Acad Sci U S A* (1991) **88**(12):5242–6. doi:10.1073/pnas.88.12.5242
175. Cox DS, Raje S, Gao H, Salama NN, Eddington ND. Enhanced permeability of molecular weight markers and poorly bioavailable compounds across Caco-2 cell monolayers using the absorption enhancer, zonula occludens toxin. *Pharm Res* (2002) **19**(11):1680–8. doi:10.1023/A:1020709513562
176. Latorre IJ, Roh MH, Fress KK, Weiss RS, Margolis B, Javier RT. Viral oncoprotein-induced mislocalization of select PDZ proteins disrupts tight junctions and causes polarity defects in epithelial cells. *J Cell Sci* (2005) **118**(Pt 18):4283–93. doi:10.1242/jcs.02560
177. Walters RW, Freimuth P, Moninger TO, Ganske I, Zabner J, Welsh MJ. Adenovirus fiber disrupts CAR-mediated intercellular adhesion allowing virus escape. *Cell* (2002) **110**(6):789–99. doi:10.1016/S0092-8674(02)00912-1
178. Coyne CB, Shen L, Turner JR, Bergelson JM. Coxsackievirus entry across epithelial tight junctions requires occludin and the small GTPases Rab34 and Rab5. *Cell Host Microbe* (2007) **2**(3):181–92. doi:10.1016/j.chom.2007.07.003
179. Muhlebach MD, Mateo M, Sinn PL, Prüfer S, Uhlig KM, Leonard VH, et al. Adherens junction protein nectin-4 is the epithelial receptor for measles virus. *Nature* (2011) **480**(7378):530–3. doi:10.1038/nature10639
180. Aungst BJ. Intestinal permeation enhancers. *J Pharm Sci* (2000) **89**(4):429–42. doi:10.1002/(SICI)1520-6017(200004)89:4<429::AID-JPS1>3.0.CO;2-J
181. Wang H, Li ZY, Liu Y, Persson J, Beyer I, Moller T, et al. Desmoglein 2 is a receptor for adenovirus serotypes 3, 7, 11 and 14. *Nat Med* (2011) **17**(1):96–104. doi:10.1038/nm.2270
182. Wang H, Li Z, Yumul R, Lara S, Hemminki A, Fender P, et al. Multimerization of adenovirus serotype 3 fiber knob domains is required for efficient binding of virus to desmoglein 2 and subsequent opening of epithelial junctions. *J Virol* (2011) **85**(13):6390–402. doi:10.1128/JVI.00514-11
183. Beyer I, Cao H, Persson J, Song H, Richter M, Feng Q, et al. Coadministration of epithelial junction opener JO-1 improves the efficacy and safety of chemotherapeutic drugs. *Clin Cancer Res* (2012) **18**(12):3340–51. doi:10.1158/1078-0432.CCR-11-3213
184. Su YC, Chen BM, Chuang KH, Cheng TL, Roffler SR. Sensitive quantification of PEGylated compounds by second-generation anti-poly(ethylene glycol) monoclonal antibodies. *Bioconjug Chem* (2010) **21**(7):1264–70. doi:10.1021/bc100067t
185. Wang H, Beyer I, Persson J, Song H, Li Z, Richter M, et al. A new human DSG2-transgenic mouse model for studying the tropism and pathology of human adenoviruses. *J Virol* (2012) **86**(11):6286–302. doi:10.1128/JVI.00205-12

186. Guarino M. Epithelial-mesenchymal transition and tumour invasion. *Int J Biochem Cell Biol* (2007) **39**(12):2153–60. doi:10.1016/j.biocel.2007.07.011
187. Dhar D, Spencer JE, Toth K, Wold WS. Pre-existing immunity and passive immunity to adenovirus 5 prevents toxicity caused by an oncolytic adenovirus vector in the Syrian hamster model. *Mol Ther* (2009) **17**(10):1724–32. doi:10.1038/mt.2009.156
188. Thomas MA, Spencer JE, Toth K, Sagartz JE, Phillips NJ, Wold WS. Immunosuppression enhances oncolytic adenovirus replication and antitumor efficacy in the Syrian hamster model. *Mol Ther* (2008) **16**(10):1665–73. doi:10.1038/mt.2008.162
189. Bouvet M, Fang B, Ekmekcioglu S, Ji L, Bucana CD, Hamada K, et al. Suppression of the immune response to an adenovirus vector and enhancement of intratumoral transgene expression by low-dose etoposide. *Gene Ther* (1998) **5**(2):189–95. doi:10.1038/sj.gt.3300564
190. Sinha P, Clements VK, Ostrand-Rosenberg S. Interleukin-13-regulated M2 macrophages in combination with myeloid suppressor cells block immune surveillance against metastasis. *Cancer Res* (2005) **65**(24):11743–51. doi:10.1158/0008-5472.CAN-05-0045
191. Zou W. Regulatory T cells, tumour immunity and immunotherapy. *Nat Rev Immunol* (2006) **6**(4):295–307. doi:10.1038/nri1806
192. Kimura YN, Watari K, Fotovati A, Hosoi F, Yasumoto K, Izumi H, et al. Inflammatory stimuli from macrophages and cancer cells synergistically promote tumor growth and angiogenesis. *Cancer Sci* (2007) **98**(12):2009–18. doi:10.1111/j.1349-7006.2007.00633.x
193. Luo Y, Zhou H, Krueger J, Kaplan C, Lee SH, Dolman C, et al. Targeting tumor-associated macrophages as a novel strategy against breast cancer. *J Clin Invest* (2006) **116**(8):2132–41. doi:10.1172/JCI27648
194. Fujimoto H, Sangai T, Ishii G, Ichihara A, Nagashima T, Miyazaki M, et al. Stromal MCP-1 in mammary tumors induces tumor-associated macrophage infiltration and contributes to tumor progression. *Int J Cancer* (2009) **125**(6):1276–84. doi:10.1002/ijc.24378
195. Zeisberger SM, Odermatt B, Marty C, Zehnder-Fjallman AH, Ballmer-Hofer K, Schwendener RA. Clodronate-liposome-mediated depletion of tumour-associated macrophages: a new and highly effective antiangiogenic therapy approach. *Br J Cancer* (2006) **95**(3):272–81. doi:10.1038/sj.bjc.6603240
196. Mitchem JB, Brennan DJ, Knolhoff BL, Belt BA, Zhu Y, Sanford DE, et al. Targeting tumor-infiltrating macrophages decreases tumor-initiating cells, relieves immunosuppression, and improves chemotherapeutic responses. *Cancer Res* (2013) **73**(3):1128–41. doi:10.1158/0008-5472.CAN-12-2731
197. Aboody KS, Najbauer J, Metz MZ, D'Apuzzo M, Gutova M, Annala AJ, et al. Neural stem cell-mediated enzyme/prodrug therapy for glioma: preclinical studies. *Sci Transl Med* (2013) **5**(184):184ra59. doi:10.1126/scitranslmed.3005365
198. Arora A, Scholar EM. Role of tyrosine kinase inhibitors in cancer therapy. *J Pharmacol Exp Ther* (2005) **315**(3):971–9. doi:10.1124/jpet.105.084145
199. Mok TS, Wu YL, Thongprasert S, Yang CH, Chu DT, Sajio N, et al. Gefitinib or carboplatin-paclitaxel in pulmonary adenocarcinoma. *N Engl J Med* (2009) **361**(10):947–57. doi:10.1056/NEJMoa0810699
200. Chua KN, Sim WJ, Racine V, Lee SY, Goh BC, Thiery JP. A cell-based small molecule screening method for identifying inhibitors of epithelial-mesenchymal transition in carcinoma. *PLoS ONE* (2012) **7**(3):e33183. doi:10.1371/journal.pone.0033183
201. Reka AK, Kurapati H, Narala VR, Bommer G, Chen J, Standiford TJ, et al. Peroxisome proliferator-activated receptor-gamma activation inhibits tumor metastasis by antagonizing Smad3-mediated epithelial-mesenchymal transition. *Mol Cancer Ther* (2010) **9**(12):3221–32. doi:10.1158/1535-7163.MCT-10-0570
202. Yang J, Shultz RW, Mars WM, Wegner RE, Li Y, Dai C, et al. Disruption of tissue-type plasminogen activator gene in mice reduces renal interstitial fibrosis in obstructive nephropathy. *J Clin Invest* (2002) **110**(10):1525–38. doi:10.1172/JCI200216219
203. Kobayashi A, Okuda H, Xing F, Pandey PR, Watabe M, Hirota S, et al. Bone morphogenetic protein 7 in dormancy and metastasis of prostate cancer stem-like cells in bone. *J Exp Med* (2011) **208**(13):2641–55. doi:10.1084/jem.20110840
204. Qi L, Sun B, Liu Z, Li H, Gao J, Leng X. Dickkopf-1 inhibits epithelial-mesenchymal transition of colon cancer cells and contributes to colon cancer suppression. *Cancer Sci* (2012) **103**(4):828–35. doi:10.1111/j.1349-7006.2012.02222.x
205. Scheel C, Eaton EN, Li SH, Chaffer CL, Reinhardt F, Kah KJ, et al. Paracrine and autocrine signals induce and maintain mesenchymal and stem cell states in the breast. *Cell* (2011) **145**(6):926–40. doi:10.1016/j.cell.2011.04.029

Conflict of Interest Statement: The authors declare that the research was conducted in the absence of any commercial or financial relationships that could be construed as a potential conflict of interest.

Received: 30 May 2013; paper pending published: 13 June 2013; accepted: 11 July 2013; published online: 26 July 2013.

Citation: Choi I-K, Strauss R, Richter M, Yun C-O and Lieber A (2013) Strategies to increase drug penetration in solid tumors. Front. Oncol. 3:193. doi:10.3389/fonc.2013.00193

This article was submitted to Frontiers in Pharmacology of Anti-Cancer Drugs, a specialty of Frontiers in Oncology.

Copyright © 2013 Choi, Strauss, Richter, Yun and Lieber. This is an open-access article distributed under the terms of the Creative Commons Attribution License, which permits use, distribution and reproduction in other forums, provided the original authors and source are credited and subject to any copyright notices concerning any third-party graphics etc.



Nanocarrier-mediated targeting of tumor and tumor vascular cells improves uptake and penetration of drugs into neuroblastoma

Fabio Pastorino*, Chiara Brignole, Monica Loi, Daniela Di Paolo, Annarita Di Fiore, Patrizia Perri, Gabriella Pagnan and Mirco Ponzoni*

Experimental Therapy Unit, Laboratory of Oncology, Istituto Giannina Gaslini, Genoa, Italy

Edited by:

Angelo Corti, San Raffaele Scientific Institute, Italy

Reviewed by:

Marcel Verheij, The Netherlands Cancer Institute – Antoni van Leeuwenhoek Hospital, Netherlands
Fabrizio Marcucci, Istituto Superiore di Sanità, Italy

***Correspondence:**

Fabio Pastorino and Mirco Ponzoni,
Experimental Therapy Unit,
Laboratory of Oncology, Istituto
Giannina Gaslini, Via G. Gaslini 5,
16148 Genoa, Italy
e-mail: fabiopastorino@ospedale-gaslini.ge.it;
mircoponzoni@ospedale-gaslini.ge.it

Neuroblastoma (NB) is the most common extracranial solid tumor in children, accounting for about 8% of childhood cancers. Despite aggressive treatment, patients suffering from high-risk NB have very poor 5-year overall survival rate, due to relapsed and/or treatment-resistant tumors. A further increase in therapeutic dose intensity is not feasible, because it will lead to prohibitive short-term and long-term toxicities. New approaches with targeted therapies may improve efficacy and decrease toxicity. The use of drug delivery systems allows site specific delivery of higher payload of active agents associated with lower systemic toxicity compared to the use of conventional ("free") drugs. The possibility of imparting selectivity to the carriers to the cancer foci through the use of a targeting moiety (e.g., a peptide or an antibody) further enhances drug efficacy and safety. We have recently developed two strategies for increasing local concentration of anti-cancer agents, such as CpG-containing oligonucleotides, small interfering RNAs, and chemotherapeutics in NB. For doing that, we have used the monoclonal antibody anti-disialoganglioside (GD₂), able to specifically recognize the NB tumor and the peptides containing NGR and CPRECES motifs, that selectively bind to the aminopeptidase N-expressing endothelial and the aminopeptidase A-expressing perivascular tumor cells, respectively. The review will focus on the use of tumor- and tumor vasculature-targeted nanocarriers to improve tumor targeting, uptake, and penetration of drugs in preclinical models of human NB.

Keywords: drug delivery, targeting, nanocarriers, tumor vasculature, tumor uptake, tumor penetration, neuroblastoma

INTRODUCTION

Neuroblastoma (NB) is the most common solid tumor in children derived from the sympathetic nervous system and the commonest type of cancer to be diagnosed in the first year of life (1). The effective treatment of NB, either at advanced stages or at minimal residual disease, remains one of the major challenges in pediatric oncology. While Stage I and II tumors are localized and well differentiated, and can be successfully treated by surgical resection, patients with stage III and IV tumors present regional and disseminated disease with poor prognosis and low response to intensive therapeutic intervention and conventional treatments (2). Moreover, despite some advances, these tumors still have unacceptably low cure rates, and, even when treatment is successful, the acute and long-term morbidity of current therapy can be substantial (3, 4).

In vitro preclinical research has identified novel agents with promising therapeutic potential for the treatment of this malignancy, however their *in vivo* efficacy is limited by unfavorable pharmacokinetic properties resulting in either insufficient drug delivery and penetration into the tumor and/or metastatic sites, or high systemic and/or organ-specific toxicities.

Currently, anti-tumor compounds share, indeed, two properties: short half-life and small therapeutic index (the range of concentration between efficacy and toxicity). However, it

has been demonstrated that the encapsulation of these "drugs" into nanocarriers drastically ameliorates their kinetic profiles, increasing tumor targeting and reducing side effects.

NANOCARRIERS FOR DRUG DELIVERY

The medical community has recently sought alternative therapies that improve selective toxicity against cancer cells, while decreasing side effects. Nano-biotechnology, defined as biomedical applications of nano-sized systems, is a rapidly developing area within nanotechnology (5). Nanoparticles, such as liposomes, allow unique interaction with biological systems at the molecular level. They can also facilitate important advances in detection, diagnosis, and treatment of human cancers and have led to a new discipline of nano-biotechnology, called nano-oncology. Nanoparticles are being actively developed for tumor imaging *in vivo*, biomolecular profiling of cancer biomarkers, and targeted drug delivery (6–8).

Growing solid tumors have capillaries with increased permeability as a result of the disease process (e.g., tumor angiogenesis). Pore diameters in these capillaries can range from 100 to 800 nm. Drug-containing liposomes that have diameters in the range of approximately 50–200 nm are small enough to extravasate from the blood into the tumor interstitial space through these pores

(9). Normal tissues contain capillaries with tight junctions that are impermeable to liposomes and other particles of this diameter. This differential accumulation and penetration of liposomal drugs in tumor tissues relative to normal cells is the basis for the increased tumor specificity of liposomal drugs relative to free drugs. In addition, due to impaired and defective lymphatic vessels, tumors lack lymphatic drainage and therefore there is low clearance of the extravasated liposomes from tumors. Thus, this liposome-mediated passive targeting can result in increases in drug concentrations within solid tumors of several-fold relative to those obtained with free drugs. This phenomenon has been termed the enhanced permeability and retention effect (EPR) (10–12). This mechanism of action of the liposomal drugs is thought to be due to sustained release of drug from the liposomes and diffusion of the released drug throughout the tumor interstitial fluid, with subsequent uptake of the released drug by tumor cells.

At present, however, EPR effect has been measured mostly, if not exclusively, in implanted tumors with limited data on EPR in metastatic lesions. Moreover, EPR heterogeneity effect in different tumors (with either differences in vessel structures within a single tumor type, or different pore dimensions in the vasculature and changed pore size with the location for a given type of tumor) as well as limited experimental data from patients on the effectiveness of this mechanism, seems to hamper the progress in developing drugs using this approach (13). Furthermore, EPR effect has been demonstrated to be insufficiently performatory in different animal models of human NB used for testing our pre-clinical nanocarriers-based therapies (14–19), likely because of the above mentioned tumor heterogeneity.

Consequently, in the attempt of globally increasing the specificity of interaction of liposomal drugs with target cells and the penetration of more amount of drug delivered to latter, recent efforts in the nanocarriers field have been addressed to the development of Ligand-Targeted Liposomes (LTLs). These liposomes utilize targeting moieties coupled to the liposome surface, for delivering the drug-liposome package to the desired site of action (active targeting). Targeting moieties may include antibody molecules, or fragments thereof, small molecular weight naturally occurring or synthetic ligands like peptides, carbohydrates, glycoproteins, or receptor ligands, i.e., essentially any molecule that selectively recognizes and binds to target antigens or receptors over-expressed or selectively expressed on cancer cells (20).

The great advantages of LTLs encapsulating cytotoxic drugs over free drugs have been unquestionably demonstrated in a number of experimental models of cancer (15, 20–22). The mechanism whereby LTLs appears to act is related to the specific binding of the drug carrying liposomes to the selective receptor expressed on cell surface of tumor cells and the subsequent internalization of the liposomal drug package.

Interestingly, localized release of the encapsulated drug at the targeted cell surface may occur, contributing to the mechanism of drug penetration and cytotoxicity mainly due as a consequence of binding to the specific receptor(s) (11, 20). Since most tumors are heterogeneous with regard to tumor-associated-antigen expression, another advantage may be the “bystander effect”: specific binding of LTLs to a tumor cell, with release and diffusion of

the drug into tumor parenchyma may result in cytotoxicity of bystander tumor cells lacking the specific epitope. It has been shown that approximately 400-fold more monoclonal antibody was required to achieve similar results with antibody-drug conjugates. Hence, high drug: antibody ratios can be achieved with LTLs, thus decreasing the need for expensive and potentially immunogenic antibodies.

TUMOR CELL TARGETING LEADS TO INCREASED UPTAKE OF ANTI-CANCER AGENTS IN NB

Neuroblastoma tumors express abundant amounts of the disialoganglioside GD₂ at the cell surface and this epitope is only minimally expressed by normal tissues, such as the cerebellum and peripheral nerves (23), thus the use of anti-GD₂ whole antibodies or their corresponding Fab' fragments were used as a selective ligand for targeting liposomal “drug” to human NB cells.

Below are reported our recent results obtained by using “drug”-loaded, nanocarrier-mediated targeting of the GD₂ epitope, via coupled anti-GD₂ whole antibodies, with improved uptake and penetration of drugs into experimental models of human NB.

LIPOSOMAL FENRETINIDE

Due to the success of 13-cis-retinoic acid in NB high-risk patients with elevated frequency of relapse from minimal residual disease (24), an increased scientific interest has been consolidated in developing retinoids, a known class of molecules able to trigger both terminal differentiation and apoptosis/necrosis on NB cells (25, 26). In this scenario, newer chemotherapeutic approaches also count on the addition of more potent retinoids, such as fenretinide (HPR), a synthetic retinoic acid derivative, which has a very low degree of toxicity relative to others and has shown efficacy as a highly active and promising therapeutic and chemopreventive agent in different experimental models and clinical trials (27, 28). However, despite good tolerability in humans, therapeutic efficacy of HPR is limited by its relatively poor bioavailability particularly from ingested tablets (29). Indeed, the phase II study of oral capsular HPR has recently underlined how, this formulation is characterized by intraindividual and interindividual variation in pharmacokinetic features as HPR is too lipophilic to easily pass the intestinal membrane (30). This hindrance has prompted scientists to draw clinical protocols based on more appropriate HPR formulations with improved biodistribution after both oral route and intravenous injection and suitable also for pediatric use. Maurer et al. (31) has proposed a lipid complex to deliver HPR, called 4-HPR/Lym-X-Sorb (LXS), that was able to improve the retinoid solubility and oral bioavailability and to significantly increase plasma and tissue levels in mice (32). On the other hand, an *in vitro* study has proposed, as novel carriers for HPR, specific amphiphilic macromolecules formed by branched polyethylene glycol covalently linked with alkyl hydrocarbon chains: in this formulation, HPR is entrapped onto hydrophobic inner cores and the resultant complexes have dimensions suitable for intravenous administration (33).

In order to improve tumor targeting, drug stability, and drug pharmacokinetics and bioavailability, we designed a formulation of HPR, encapsulated in sterically stabilized, GD₂-targeted immunoliposomes [GD₂-SIL(HPR)]. We demonstrated that HPR

efficiently induced a dramatic inhibition of metastases, leading to almost 100% of curability in NB-bearing mice, only when encapsulated in GD₂-targeted nanocarriers (14). These achievements totally disappeared when HPR was administered either free (free HPR) or loaded in non-targeted liposomes [SL(HPR)], confirming the importance of the tumor targeting as a mandatory tool for enhancing binding, uptake, and anti-tumor effects against NB (**Figure 1A**).

On the other hand, in this NB animal model, anti-GD₂ monoclonal antibody (anti-GD₂ mAb) also led to a considerable anti-tumor effect, indicating that the anti-GD₂ “di per se” was responsible of part of the observed therapeutic effects (**Figure 1B**) (14). Thus, in the subsequent therapeutic, liposomes-based experiments we decided to use nanocarriers decorated with the non-immunogenic Fab' fragments of anti-GD₂, thus avoiding antibody-dependent cell cytotoxicity.

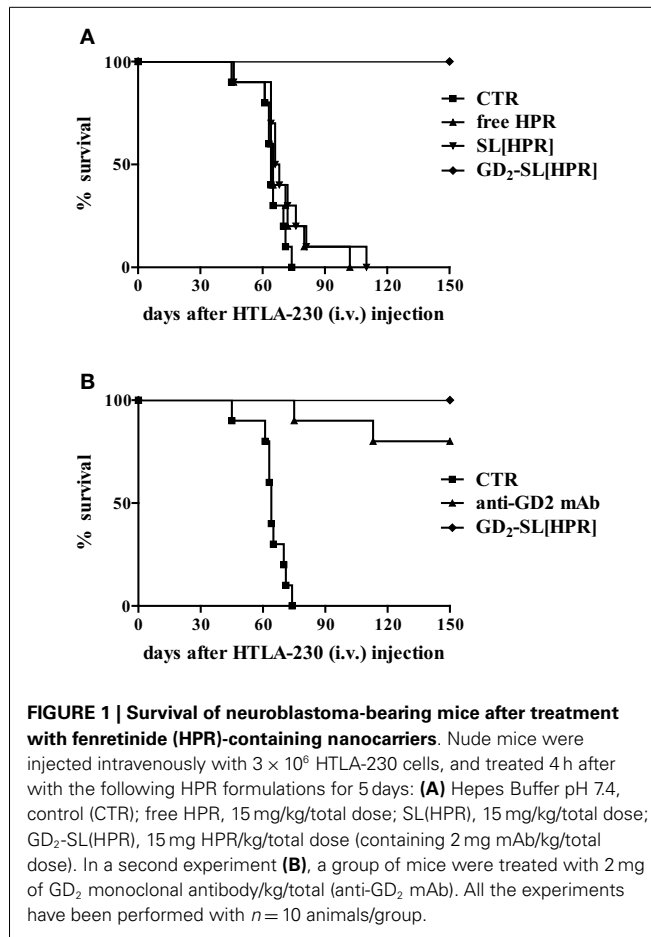
Indeed, the coupling of antibody Fab' fragments instead of whole immunoglobulin molecules abolishes the mononuclear phagocyte system uptake of the anti-GD₂, which takes place via an Fc receptor-mediated mechanism (34). Consequently, small LTLs decorated with Fab' fragments have significantly longer circulation time than comparable formulations containing whole mAbs (20). This can result in an enhanced accumulation of the liposomes in solid tumor (35) and in a significant suppression of tumor growth (36, 37).

Here, we present some results obtained by using Fab' fragments of anti-GD₂ immunoliposomes to increase uptake and anti-tumor activity of CpG-containing antisense oligonucleotides (asODNs), small interfering RNAs (siRNAs), and chemotherapeutics in animal models of human NB.

LIPOSOMAL ANTISENSE OLIGONUCLEOTIDES

The identification of cancer-associated genes hold promise for the development of novel therapeutic strategies that selectively target tumor cells. asODNs can be used to specifically down modulate tumor associated gene expression (resulting in a direct anti-cancer effect) and as immune adjuvant by CpG-containing asODN-driven cytokines production and innate immune stimulation (38). However, since the *in vivo* applicability of ODNs is impaired by their high sensitivity to extracellular and cellular nuclease degradation (39), their encapsulation within liposomes should increase their stability. C-myb gene expression has been reported in several solid tumors of different embryonic origin, including NB, where it is linked to cell proliferation and/or differentiation (40, 41). We performed a new technique to encapsulate CpG-containing c-myb asODNs within lipid particles. Liposomes resulting from this technique were called coated cationic liposomes (CCLs) (41), since they were made up of a central core of a cationic phospholipids bound to myb asODNs and an outer shell of neutral lipids.

Fab'-GD₂-targeted, CpG-containing c-myb asODNs-loaded CCLs reduced in a specific and time-dependent manner the expression of c-Myb protein by NB cells (**Figure 2A**). Importantly, we also demonstrated that their systemic administration in NB-bearing mice, induced anti-tumor effects with increased survival only when encapsulated in nanocarriers targeting the NB surface antigen, GD₂, that internalizes after binding its ligand (**Figure 2B**)



(17). We further demonstrated that increased animals life span was due to a dual mechanism of action. Firstly, a direct inhibition of tumor growth, via tumor cell binding, uptake, and inhibition of c-myb proto-oncogene expression; secondly, an indirect CpG-dependent immune stimulation, whose function was lost as the result of using clodronate-driven macrophage depletion in nude mice (**Figure 2C**) and B and NK cells depletion in SCID-bg mice (**Figure 2D**) (17).

LIPOSOMAL SMALL INTERFERING RNAs

Despite the considerable potential of RNA interference (RNAi) for treating cancers (42, 43), several challenges still need to be overcome for exogenous siRNAs to be widely used as cancer therapeutics. The most significant hurdle is the specific and non-toxic delivery of siRNAs to the site of action. siRNA applications are so far limited almost to targets within the liver, where the delivery systems naturally occur, while delivery of siRNAs to extra-hepatic targets remain a serious challenge.

In order to solve this limitation, we consequently developed a new tumor-targeted delivery system for siRNAs, through their encapsulation into Fab' fragments GD₂-targeted coated CCLs, and validated their ability to silence the oncogene anaplastic lymphoma kinase (ALK) by increasing NB tumor binding and siRNA penetration-driven anti-tumor effect.

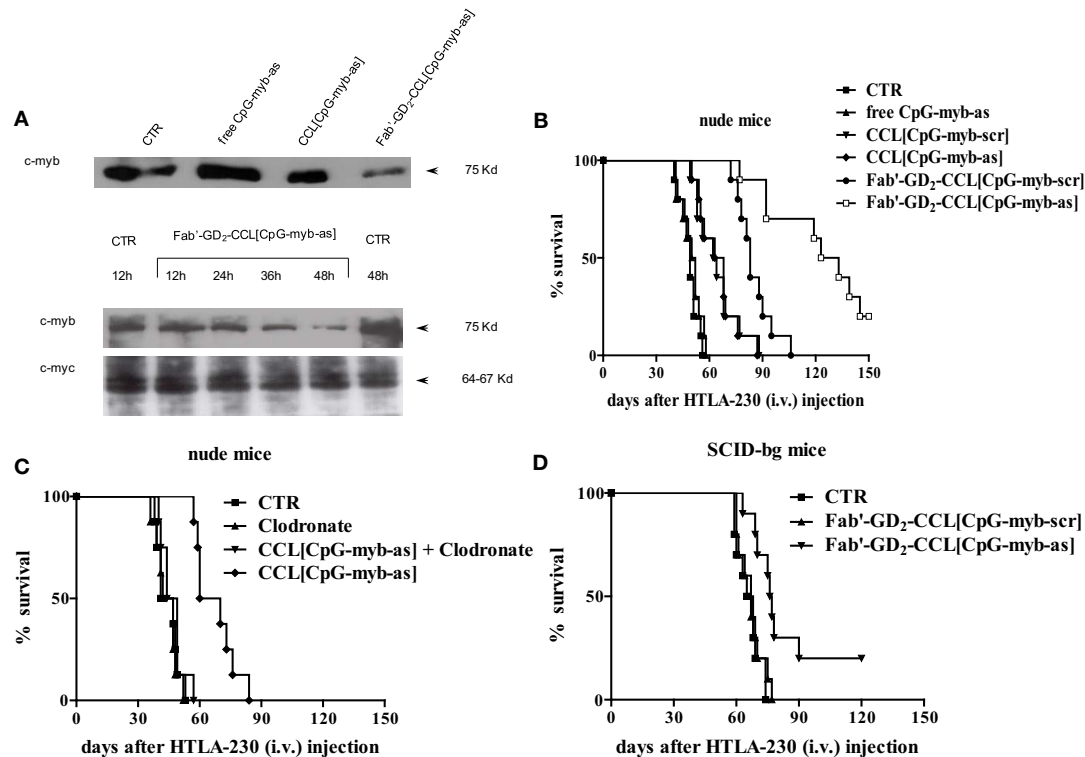


FIGURE 2 | Inhibition of c-Myb protein expression and increase of survival of neuroblastoma-bearing mice after treatment with c-Myb antisense oligonucleotides (asODNs)-containing nanocarriers. **(A)** GI-LI-N neuroblastoma cells were treated with CpG-containing c-Myb asODNs, either free (free CpG-myb-as) or encapsulated in untargeted [CCL(CpG-myb-as)] and targeted [Fab'-GD₂-CCL(CpG-myb-as)] nanocarriers, at a concentration of 100 µg/ml at the beginning of the experiment and 18 and 36 h later. Two hours after each addition, the cells were washed and transferred to CpG-myb-as-free fresh complete medium. The cells were harvested at 48 h (upper panel) or at the indicated time points (lower panels) and analysis of protein expression (c-Myb and c-Myc as control) was performed by immunoblotting. **(B)** Nude mice ($n = 10$ animals/group) were

injected intravenously with 3.5×10^6 HTLA-230 cells. Treatment with either as or scrambled (scr), CpG-containing ODNs, administered free and encapsulated in untargeted (CCL) and targeted (Fab'-GD₂-CCL) liposomes was started at 4 h after cell inoculation. Mice were treated 4 days a week, for 2 weeks, with 3 day rest between treatments. Each mouse received 50 µg ODN. Control mice (CTR) received HEPES-buffered saline. **(C,D)** Effects of either macrophages or natural killer (NK) cells depletion on anti-tumor activity mediated by treatment with liposomal formulations containing ODNs. Mice [nude, $n = 8$ animals/group **(C)** and SCID-bg, $n = 10$ animals/group **(D)**] were inoculated with HTLA-230 cells and then treated as already mentioned in **Figure 1**. In some treatment groups of **(C)**, mice were injected with Clodronate-liposomes to deplete macrophages.

Indeed, over expression of either mutated or wild-type ALK tyrosine kinase receptor proteins induces constitutive kinase activity in NB (44), while ALK expression knockdown leads to a pronounced decreased cell proliferation. Moreover, ALK mutations and amplifications, as well as gene over expression, clearly correlate with poor outcomes in both advanced and metastatic NB disease, when compared with localized tumors (44). Based on these concepts, we tested the therapeutic efficacy of targeting ALK gene in NB, by developing a selective silencing approach (45).

We showed that, while almost no binding and uptake was observed by siRNA-containing, untargeted liposomes [CCL(siRNA)] in NB cells, Fab'-GD₂-targeted CCL(siRNA) were efficiently internalized (**Figure 3A**). Interestingly, in biologically relevant NB animal models, we demonstrated that, compared to free ALK-siRNA, Fab'-GD₂-CCL(ALK-siRNA) increased siRNA stability, and a selective block of NB tumor growth, resulting in partial tumor regression (**Figure 3B**), improved silencing of the specific gene (**Figure 3C**), and increased life span in NB xenografts (**Figure 3D**) (45). This strategy also induced inhibition of

angiogenesis and of metastatic potential in a safe and highly effective manner (46), confirming the pivotal role of targeted therapies to enhance tumor “drug” penetration and cytotoxic effects.

LIPOSOMAL DOXORUBICIN

To eradicate tumors with chemotherapy, anti-cancer drugs must reach lethal concentrations, in theory, in all of the tumor cells. Failure to achieve high local levels of drugs, e.g., due to limited drug delivery and/or penetration within tumors is critical for the effectiveness of solid-tumor chemotherapy (47). Methods for improving drug delivery and penetration in tumor tissues are, therefore, of great experimental and clinical interest. On this direction, one approach to selectively eradicate NB tumor cells is based on the fact that NB is a chemosensitive tumor and cytotoxic agents, such as doxorubicin (DXR), are considered to be effective treatment modalities. However, the therapeutic efficacy of DXR, which is widely used in the treatment of solid tumors, is restricted by dose-limiting toxicity to bone marrow and heart tissue (48). The selective toxicity of DXR would be greatly improved if the

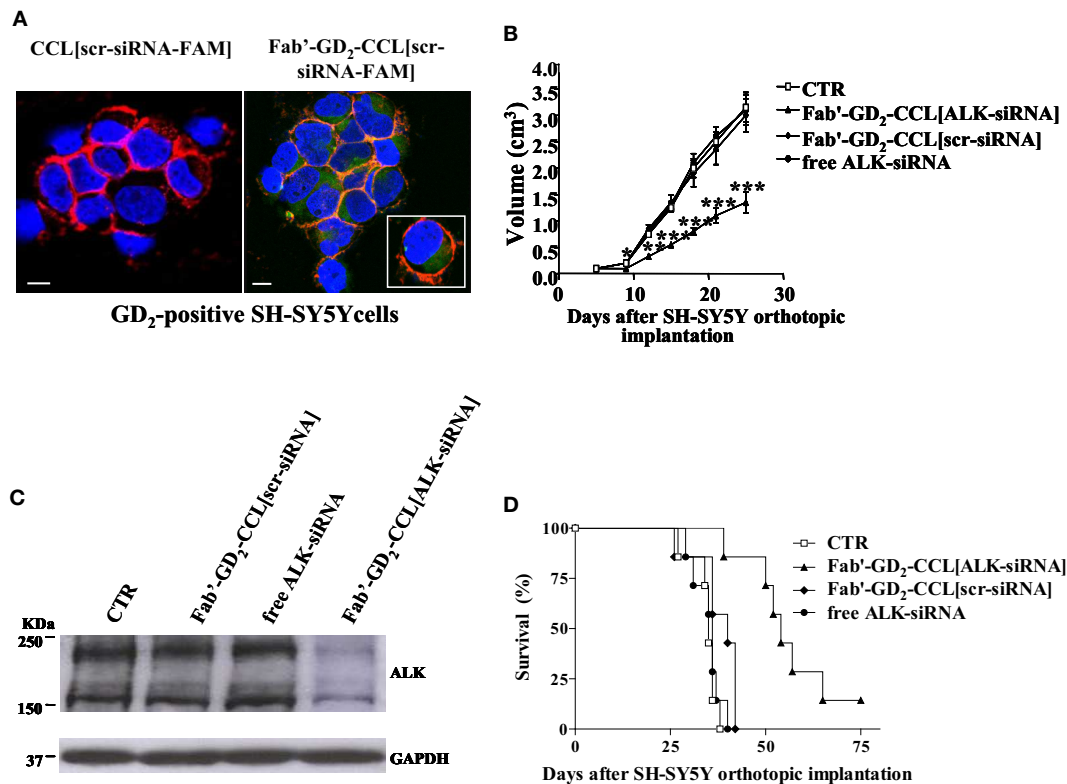


FIGURE 3 | Neuroblastoma-targeted nanoparticles entrapping siRNA specifically knockdown ALK. (A) Uptake and internalization of liposome-encapsulated FAM-labeled scrambled-siRNA (scr-siRNA-FAM) into GD₂-expressing neuroblastoma cells (SH-SY5Y). Cells were incubated at 37°C for 1 h, with either untargeted [CCL(scr-siRNA-FAM)] or Fab' fragments GD₂-targeted coated cationic liposomes [Fab'-GD₂-CCL(scr-siRNA-FAM)]. After washing and cytopsin centrifugation, cells were fixed and stained with a monoclonal antibody specific for the cellular adhesion molecule N-CAM (α-CD56) to reveal plasma membrane localization. Cell nuclei were stained with 4',6-diamidino-2-phenylindole (DAPI). The cellular distribution of scr-siRNA-FAM (green), CD56 (red), nuclear DAPI staining (blue), and merged colors resulting from siRNA-liposome binding to the cell surface (orange) fluorescences was analyzed with a laser scanning spectral confocal microscope. Bars: 50 μm. **(B–D)** Tumor growth inhibition *in vivo* by ALK-siRNA encapsulated in Fab'-GD₂-CCL. SCID-bg mice (*n* = 8) were orthotopically injected with 1.5 × 10⁶ SH-SY5Y cells in the capsule of the left adrenal gland. Seven days after the tumor implantation, mice were treated, two-time a week for 3 weeks with ALK-siRNA, either free or encapsulated in GD₂-targeted nanocarriers [Fab'-GD₂-CCL(ALK-siRNA)]. Another group of mice received a scrambled (scr) siRNA-loaded nanoparticles [Fab'-GD₂-CCL (scr-siRNA)] as control or HEPES-buffered saline (CTR). Tumor expansion over time measured by calipers **(B)** and survival times **(D)** were used for determination of the treatment efficacy. **(C)** The day after the last treatment (25 day), tumors from three mice per group were recovered for western blot analyses and ALK protein expression. **P* < 0.05; ***P* < 0.01; ****P* < 0.001, Fab'-GD₂-CCL(ALK-siRNA) vs. Fab'-GD₂-CCL(scr-siRNA).

concentration of drug in tumors could be increased relative to that in sensitive normal tissues.

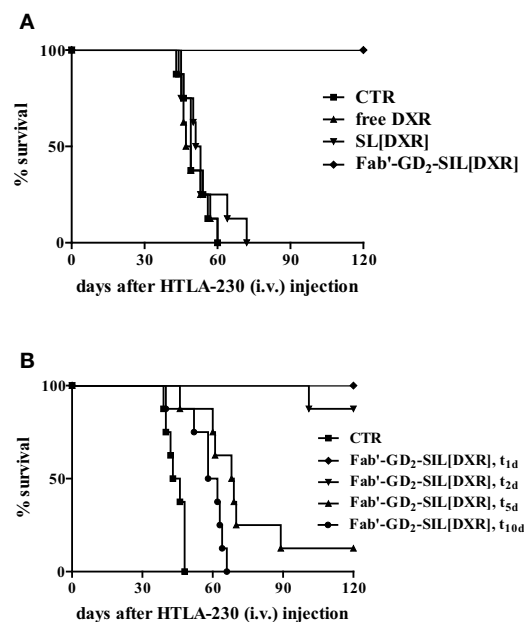
Two strategies, based on tumor and vascular targeting, have been recently described for increasing the local concentration of the chemotherapeutic drug DXR in tumors and its therapeutic index. The first strategy is based on the direct targeting of the tumor cells by the use of Fab' fragments of GD₂-targeted DXR liposomal [Fab'-GD₂-SIL(DXR)] (15). The second approach that will be discussed in the next chapter, is based on direct targeting of the tumor vasculature, using DXR encapsulated into modified liposomes able to bind and home to tumor blood vessels (16, 21, 49).

In the first study Fab'-GD₂-SIL(DXR) has presented increased selectivity and efficacy in inhibiting NB cell proliferation compared to free drug and non-targeted DXR formulation. The *in vivo* anti-tumor activity of Fab'-GD₂-SIL(DXR) was evaluated in terms of metastasis growth inhibition and increased life span

microscope. Bars: 50 μm. **(B–D)** Tumor growth inhibition *in vivo* by ALK-siRNA encapsulated in Fab'-GD₂-CCL. SCID-bg mice (*n* = 8) were orthotopically injected with 1.5 × 10⁶ SH-SY5Y cells in the capsule of the left adrenal gland. Seven days after the tumor implantation, mice were treated, two-time a week for 3 weeks with ALK-siRNA, either free or encapsulated in GD₂-targeted nanocarriers [Fab'-GD₂-CCL(ALK-siRNA)]. Another group of mice received a scrambled (scr) siRNA-loaded nanoparticles [Fab'-GD₂-CCL (scr-siRNA)] as control or HEPES-buffered saline (CTR). Tumor expansion over time measured by calipers **(B)** and survival times **(D)** were used for determination of the treatment efficacy. **(C)** The day after the last treatment (25 day), tumors from three mice per group were recovered for western blot analyses and ALK protein expression. **P* < 0.05; ***P* < 0.01; ****P* < 0.001, Fab'-GD₂-CCL(ALK-siRNA) vs. Fab'-GD₂-CCL(scr-siRNA).

in a pseudometastatic animal model of human NB. In this study, 100% of mice treated with DXR-loaded Fab'-immunoliposomes 1 day after tumor cells injection, were still alive more than 4 months after treatment. DXR administered either free or encapsulated in non-targeted nanocarriers did not show any anti-tumor effect, again confirming the important role of the specific tumor targeting in improving drug uptake and consequent tumor cells killing (Figure 4A) (15).

The next aim was to verify whether these anti-tumor effects were maintained in more established tumors or if the therapeutic efficacy declined when treatment was delayed. Indeed, a longer period of time between inoculation of cells and the administration of treatment would allow the tumor cells to establish metastases that might escape treatment. The metastatic cells would become less accessible from the vasculature and the tumor-targeted liposomes become less effective as their accessibility to the tumor cells becomes compromised. As expected, a delay in the



start of treatment substantially reduced the therapeutic efficacy of Fab'-GD₂-SIL(DXR), demonstrating the time dependence of the anti-tumor activity of the tumor-targeted formulation against advanced NB animal models (Figure 4B). However, with increasing time, the new lesions begin to recruit blood vessels to support their growth and the lesions will have increased sensitivity to anti-vascular therapy with time (21). Thus, our findings suggest the subsequent use of therapies targeting the vascular network of the tumor, as discussed below, to treat more mature solid tumors.

INCREASING LOCAL CONCENTRATION OF ANTI-CANCER AGENTS IN NB BY TUMOR VASCULATURE TARGETING STRATEGY

The alternative strategy we pursued to increase the delivery and the uptake of DXR into NB is based on the use of tumor vasculature-targeted liposomes. The targeting of therapeutics to blood vessels, using probes that bind to specific molecular addresses in the vasculature, has indeed become a major research area (50). The inhibition of tumor growth by attacking the vascular supply of the tumor offers a primary target for therapeutic intervention. Indeed, host endothelial cells are believed to play a central role in tumor growth, progression, and metastasis, acting as the primary building blocks of the tumor microvasculature (51). Because of the “angiogenesis dependence” of solid tumors, predicted by

Folkman nearly 40 years ago, selective inhibition or destruction of the tumor vasculature (using anti-angiogenic or anti-vascular treatments, respectively) could trigger tumor growth inhibition, regression, and/or a state of dormancy and thereby offer a novel approach to cancer treatment.

There are several advantages of targeting chemotherapeutic agents to proliferating endothelial cells in the tumor vasculature rather than directly to tumor cells. First, acquired drug resistance, resulting from genetic and epigenetic mechanisms reduces the effectiveness of available drugs (52). Anti-angiogenic/anti-vascular therapy has the potential to overcome these problems or reduce their impact. The tumor vasculature, composed of non-malignant cells that are genetically more stable than malignant cells, is therefore unlikely to mutate into drug-resistant variants. Second, the fact that a large number of cancer cells depend upon a small number of endothelial cells for their growth and survival might also amplify the therapeutic effect (53). Third, anti-angiogenic therapies may also circumvent what may be a major mechanism of intrinsic drug resistance, namely insufficient drug penetration into the interior of a tumor mass due to high interstitial pressure gradients within tumors (54). A strategy that targets both the tumor vasculature and the tumor cells themselves may be more effective than strategies that target only tumor vasculature, since this strategy can leave a cuff of unaffected tumor cells at the tumor periphery that can subsequently re-grow and kill the animals (55). Fourth, oxygen consumption by neoplastic and endothelial cells, along with poor oxygen perfusion, creates hypoxia within tumors. These pathophysiological characteristics of solid tumors compromise the delivery and effectiveness of conventional cytotoxic therapies as well as molecularly targeted therapies (53, 54). Finally, the therapeutic target is independent of the type of solid tumor; killing of proliferating endothelial cells in the tumor microenvironment can be effective against a variety of malignancies.

Phage display technology has been recently used to discover novel ligands specific to receptors on the surface of tumor epithelial and endothelial cells (56). *In vivo* panning of phage libraries in tumor-bearing mice has selected peptides that interact with proteins expressed on tumor-associated vessels and that home to neoplastic tissues (57). This technology, for instance, was used to isolate peptides homing specifically to the tumor blood vessel-associated addresses, aminopeptidase N (APN) and A (APA) (58, 59). We have firstly demonstrated that liposome-entrapped DXR, and targeted to APN via an NGR-containing peptide, induced tumor regression, pronounced destruction of the tumor vessels, and prolonged survival in NB-bearing mice (16).

Specifically, to determine whether the NGR-targeted liposomes [NGR-SL(DXR)] could deliver DXR to angiogenic tumor-associated blood vessels, we injected them into the tail vein of mice bearing established adrenal tumors. In one set of experiments, liposomes were allowed to circulate from 2 to 24 h, followed by perfusion and immediate tissue recovery. There was a clear time-dependent uptake of DXR in the tumor vasculature. At 24 h, the staining pattern indicated that the DXR had spread outside the blood vessels and into the tumors (16). This spreading was attributable to increased permeability of tumor blood vessels to the intact liposomes (60) and/or uptake of the targeted liposomes

by angiogenic endothelial cells and subsequent penetration and transfer to tumor cells. Likely both mechanisms are working at the same time. In the second set of experiments, tissues were examined 16 h after the injection of DXR-loaded liposomes, decorated with either the specific NGR [NGR-SL(DXR)] or with the miss-matched ARA [ARA-SL(DXR)] peptides. Strong DXR staining in tumor vasculature was seen only in animals treated with NGR-liposomes (**Figure 5A**). Tumor-specific DXR uptake was completely blocked when mice were co-injected with a 50-fold molar excess of the soluble NGR peptide (16), confirming the peptide recognizing tumor vasculature-driven cell drug binding and penetration.

Histopathological analysis of cryosections taken from NGR-SL(DXR) treated mice revealed pronounced destruction of the tumor vasculature. Indeed, double staining of tumors with TUNEL and anti-factor VIII antibody or anti-human NB, demonstrated endothelial cell apoptosis in the vasculature as well as increased tumor cell apoptosis (16). Moreover, mice displayed rapid tumor regression, inhibition of metastases growth, and suppression of blood vessel density, while mice treated with ARA-SL(DXR) formed large well-vascularized tumors (**Figures 5B–D**) (16).

Subsequently, we developed a novel liposomal formulation targeting the perivascular tumor cell marker APA, expressed in the vascular wall of NB primary and metastatic lesions.

The primary goal of this study was to validate the hypothesis that the combined targeting of both the tumor endothelial cells (recognizing APN) and the pericytes (recognizing APA), supporting the vessels wall within the tumor, has improved tumor targeting, uptake, drug penetration, and therapeutic effects relative to each therapy alone.

Neuroblastoma-bearing mice receiving APA-targeted liposomal DXR [CPRECES-SL(DXR)] exhibited an increased life span in comparison to control mice, but to a lesser extent relative to that in mice treated with APN-targeted formulation [NGR-SL(DXR)] (18). However, mice treated with a combination (COMBO) of APA- and APN-targeted, liposomal DXR had an enhanced accumulation of both the carriers and the drug in the tumor mass (**Figures 6A,B**), and a significant increase in life span compared to each treatment administered separately (18). There was a significant increase in the level of apoptosis in the tumors of mice on the combination therapy, and a pronounced destruction of the tumor vasculature with nearly total ablation of endothelial cells and pericytes (**Figure 6C**). Thus, these results clearly demonstrated that the combined targeted strategy, through an increased drug penetration, was more effective for destruction of the tumor vasculature than either monotherapy. Combination therapy led to a statistically significant increase in life span in a murine xenograft model of human NB compared to the formulations given alone (18).

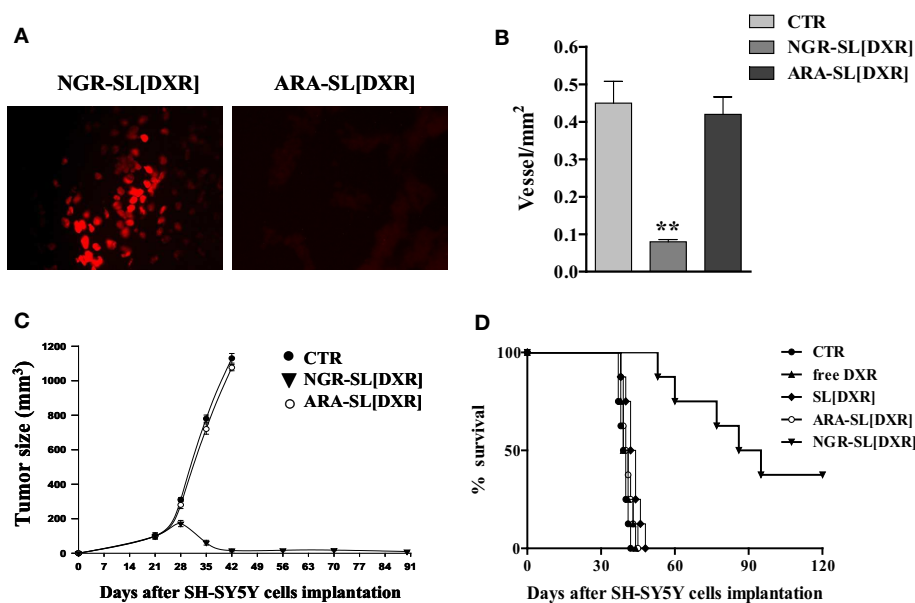


FIGURE 5 | Anti-angiogenic and anti-tumor effects of doxorubicin (DXR)-containing, tumor vascular targeted nanocarriers. **(A)** Tumor homing of NGR-targeted liposomal DXR in SCID mice orthotopically injected in the left adrenal gland with 1.5×10^6 SH-SY5Y neuroblastoma cells. DXR-loaded, either NGR-targeted or miss-matched peptide ARA-targeted nanocarriers, were injected via the tail vein as a single bolus dose. After 16 h, tumors were collected and DXR (red) visualized by fluorescence microscopy of fixed, paraffin embedded, tissue sections. **(B–D)** Delivery of DXR to tumor vessels inhibits angiogenesis, causing regression of established NB tumors. SCID mice orthotopically implanted with SH-SY5Y cells were injected intravenously with 3 mg DXR/kg, 21, 28, and 35 days post tumor inoculation. Treatment groups ($n=8/\text{group}$)

consisted of DXR administered either free (free DXR) or encapsulated in untargeted [SL(DXR)] and either NGR-targeted [NGR-SL(DXR)] or miss-matched peptide ARA-targeted [ARA-SL(DXR)] nanocarriers. Control mice (CTR) received HEPES-buffered saline. **(B)** Tumor vessels density inhibition after NGR-targeted liposomal DXR treatments. Orthotopic tumors, at day 36 from CTR and from both NGR- and ARA-targeted, DXR-treated groups, were sectioned and stained with an antibody to factor VIII to count blood vessels. Each bar represents the mean \pm SD of five replicates. **(C)** Neuroblastoma tumor growth arrest by NGR-targeted liposomal DXR. Each point represents the mean \pm SD of six replicates. **(D)** Increase in animal life span by NGR-targeted liposomal DXR. Partially reproduced from Pastorino et al. (16).

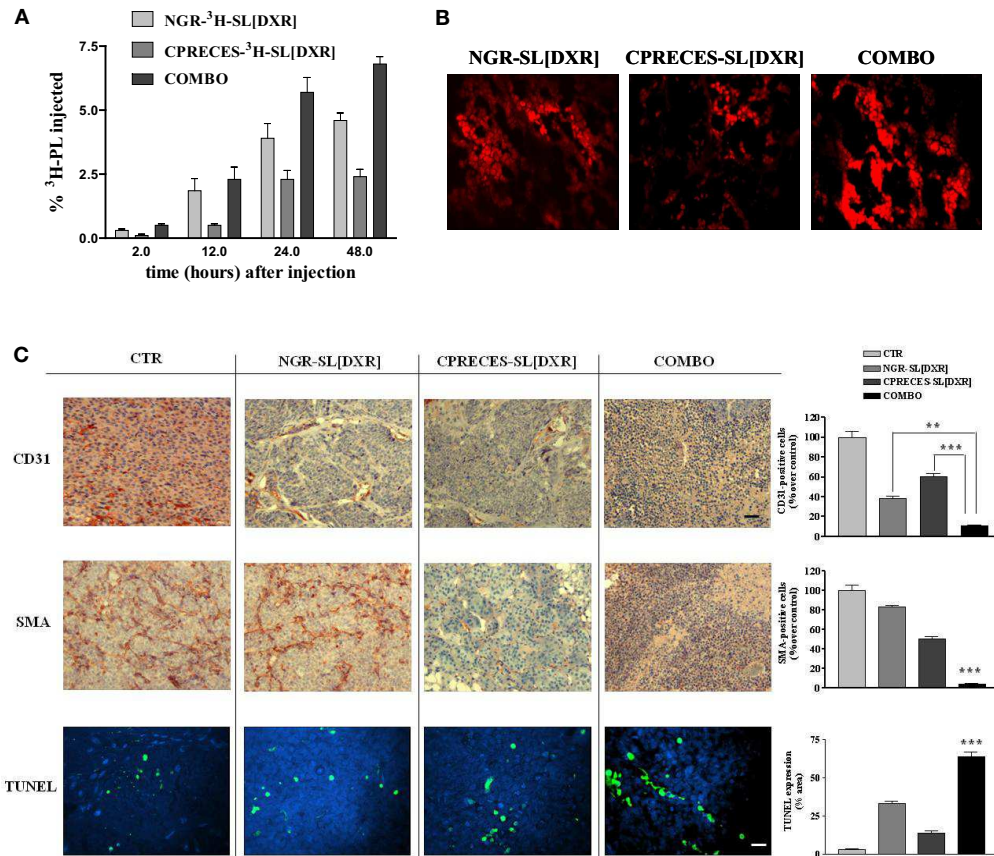


FIGURE 6 | Combined targeting of endothelial and perivascular tumor cells enhances anti-tumor efficacy of liposomal doxorubicin (DXR) in neuroblastoma. **(A,B)** Accumulation of APN- and APA-targeted, DXR-loaded, nanocarriers in nude mice orthotopically implanted with GI-LI-N neuroblastoma cells. **(A)** ³H-labeled, endothelial- (via NGR peptide) and perivascular- (via CPRECES peptide) targeted, DXR-loaded nanocarriers were injected intravenously in a single bolus. Treatment groups consisted of NGR-³H-SL(DXR), CPRECES-³H-SL(DXR), and combination of targeted liposomes (COMBO). At selected time points post-injection, blood was measured for ³H in a beta-counter. Points, average of three mice; bars, \pm 95% C.I. **(B)** Tumor accumulation of DXR visualized by fluorescence microscopy of

NB tissue sections. Magnitude, 40 \times . **(C)** Effects of the combination therapy on endothelial, perivascular, and tumor cells *in vivo*. Immunohistochemistry was performed on established NB tumors removed from untreated mice (CTR) or from mice treated with DXR-loaded, NGR-targeted or CPRECES-targeted nanocarriers, or with a combination of the two liposomal formulations (COMBO). Tumors were removed on day 36 and tissue sections were immunostained for CD31 and SMA to detect tumor vasculature (scale bar, 250 μ m). TUNEL was performed to detect tumor apoptosis (scale bar, 100 μ m). Cell nuclei were stained with DAPI. Columns, mean of CD31, SMA, and TUNEL staining intensities; error bars represent 95% C.I. ** P < 0.01; *** P < 0.001, COMBO vs. single treatments.

CONCLUDING REMARKS

In a tumor mass, neoplastic cells and the vascular endothelium of angiogenic blood vessels that support tumor growth express targetable surface markers that are accessible from the circulation. Thus, targeting therapeutic agents to tumor cells and to tumor vessels made it possible to deliver the anti-cancer agents to the tumor site, and to combine blood vessel destruction with the conventional anti-tumor actions of drugs, leading to more efficacious effects and less systemic toxicity than conventional therapy.

However, despite good results obtained in preclinical experimental models, targeted therapies have also practically met with some drawbacks, restricting their clinical translation. In particular, this approach has only a partial success for the treatment of well-established solid tumors, where tumor vessels are poorly perfused with blood and are dysfunctional, limiting the delivery of blood-borne compounds into the tumor masses (61). Tumors have also

an high interstitial pressure deriving from dysfunctional lymphatics, which causes tissue fluid to flow out of the tumor thus reducing diffusion of drugs from the blood vessels into the tumors (61, 62). Finally, interstitial fibrosis can further retard the diffusion of targeted compounds through the dense tumor parenchyma (63).

Consequently, to further overcome these drawbacks and to increase anti-tumor efficacy of the targeted therapies, in the near future the use of targeting probes with even more enhanced tumor-penetrating properties and receptors that are likely shared between tumor vessels and tumor cells should be envisaged.

ACKNOWLEDGMENTS

Work supported by Associazione Italiana per la Ricerca sul Cancro [My First AIRC Grant (MFAG) to Fabio Pastorino and IG to Mirco Ponzoni]; Fondazione Umberto Veronesi (Grant Fabio Pastorino and Grant Chiara Brignole); Italian Ministry of

Health Finanziamento Ricerca Corrente 2010, Ministero Salute (contributo per la ricerca intramurale), Istituto Giannina Gaslini; European Commission FP7 program Grant “INFLA-CARE” (EC contract number 223151; <http://InflaCare.forth.gr>) to Mirco Ponzi. Monica Loi is a recipient of a Fondazione Italiana per la

Ricerca sul Cancro (FIRC) fellowship; Daniela Di Paolo is a recipient of a Fondazione Umberto Veronesi fellowship. Thanks to P. Becherini, I. Caffa, A. Zorzoli, R. Carosio, M. Zancolli, M. Rossi, D. Marimpietri, L. Raffaghelli, E. Cosimo, G. L. Caridi, P. G. Montaldo, and T. M. Allen for technical assistance.

REFERENCES

- Maris JM. Recent advances in neuroblastoma. *N Engl J Med* (2010) **362**:2202–11. doi:10.1056/NEJMra0804577
- Mueller S, Matthay KK. Neuroblastoma: biology and staging. *Curr Oncol Rep* (2009) **11**:431–8. doi:10.1007/s11912-009-0059-6
- Oeffinger KC, Mertens AC, Sklar CA, Kawashima T, Hudson MM, Meadows AT, et al. Chronic health conditions in adult survivors of childhood cancer. *N Engl J Med* (2006) **355**:1572–82. doi:10.1056/NEJMsa060185
- Norris RE, Adamson PC. Challenges and opportunities in childhood cancer drug development. *Nat Rev Cancer* (2012) **12**:776–82. doi:10.1038/nrc3370
- Davis SS. Biomedical applications of nanotechnology – implications for drug targeting and gene therapy. *Trends Biotechnol* (1997) **15**:217–24. doi:10.1016/S0167-7799(97)01036-6
- Yezhelyev MV, Gao X, Xing Y, Al-Hajj A, Nie S, O'Regan RM. Emerging use of nanoparticles in diagnosis and treatment of breast cancer. *Lancet Oncol* (2006) **7**:657–67. doi:10.1016/S1470-2045(06)70793-8
- Sinha R, Kim GJ, Nie S, Shin DM. Nanotechnology in cancer therapeutics: bioconjugated nanoparticles for drug delivery. *Mol Cancer Ther* (2006) **5**:1909–17. doi:10.1158/1535-7163.MCT-06-0141
- Simberg D, Duza T, Park JH, Essler M, Pilch J, Zhang L, et al. Biomimetic amplification of nanoparticle homing to tumors. *Proc Natl Acad Sci U S A* (2007) **104**:932–6. doi:10.1073/pnas.0610298104
- Maeda H. The enhanced permeability and retention (EPR) effect in tumor vasculature: the key role of tumor-selective macromolecular drug targeting. *Adv Enzyme Regul* (2001) **41**:189–207. doi:10.1016/S0065-2571(00)00013-3
- Torchilin V. Tumor delivery of macromolecular drugs based on the EPR effect. *Adv Drug Deliv Rev* (2011) **63**:131–5. doi:10.1016/j.addr.2010.03.011
- Allen TM, Cullis PR. Drug delivery systems: entering the mainstream. *Science* (2004) **303**:1818–22. doi:10.1126/science.1095833
- Fang J, Nakamura H, Maeda H. The EPR effect: unique features of tumor blood vessels for drug delivery, factors involved, and limitations and augmentation of the effect. *Adv Drug Deliv Rev* (2011) **63**:136–51. doi:10.1016/j.addr.2010.04.009
- Prabhakar U, Maeda H, Jain RK, Sevick-Muraca EM, Zamboni W, Farokhzad OC, et al. Challenges and key considerations of the enhanced permeability and retention effect for nanomedicine drug delivery in oncology. *Cancer Res* (2013) **73**:2412–7. doi:10.1158/0008-5472.CAN-12-4561
- Raffaghelli L, Pagnan G, Pastorino F, Cosimo E, Brignole C, Marimpietri D, et al. In vitro and in vivo anti-tumor activity of liposomal Fenretinide targeted to human neuroblastoma. *Int J Cancer* (2003) **104**:559–67. doi:10.1002/ijc.10991
- Pastorino F, Brignole C, Marimpietri D, Sapra P, Moase EH, Allen TM, et al. Doxorubicin-loaded Fab' fragments of anti-disialoganglioside immunoliposomes selectively inhibit the growth and dissemination of human neuroblastoma in nude mice. *Cancer Res* (2003a) **63**:86–92.
- Pastorino F, Brignole C, Marimpietri D, Cilli M, Gambini C, Ribatti D, et al. Vascular damage and anti-angiogenic effects of tumor vessel-targeted liposomal chemotherapy. *Cancer Res* (2003b) **63**:7400–9.
- Brignole C, Pastorino F, Marimpietri D, Pagnan G, Pistorio A, Allen TM, et al. Immune cell-mediated antitumor activities of GD2-targeted liposomal c-myc antisense oligonucleotides containing CpG motifs. *J Natl Cancer Inst* (2004) **96**:1171–80. doi:10.1093/jnci/djh221
- Loi M, Marchiò S, Becherini P, Di Paolo D, Soster M, Curinis F, et al. Combined targeting of perivascular and endothelial tumor cells enhances anti-tumor efficacy of liposomal chemotherapy in neuroblastoma. *J Control Release* (2010) **145**:66–73. doi:10.1016/j.jconrel.2010.03.015
- Loi M, Di Paolo D, Soster M, Brignole C, Bartolini A, Emionite L, et al. Novel phage display-derived neuroblastoma-targeting peptides potentiate the effect of drug nanocarriers in preclinical settings. *J Control Release* (2013) **170**:233–41. doi:10.1016/j.jconrel.2013.04.029
- Allen TM. Ligand-targeted therapeutics in anticancer therapy. *Nat Rev Cancer* (2002) **2**:750–63. doi:10.1038/nrc903
- Pastorino F, Brignole C, Di Paolo D, Nico B, Pezzolo A, Marimpietri D, et al. Targeting liposomal chemotherapy via both tumor cell-specific and tumor vasculature-specific ligands potentiates therapeutic efficacy. *Cancer Res* (2006) **66**:10073–82. doi:10.1158/0008-5472.CAN-06-2117
- Moura V, Lacerda M, Figueiredo P, Corvo ML, Cruz ME, Soares R, et al. Targeted and intracellular triggered delivery of therapeutics to cancer cells and the tumor microenvironment: impact on the treatment of breast cancer. *Breast Cancer Res Treat* (2012) **133**:61–73. doi:10.1007/s10549-011-1688-7
- Mujoo K, Cheresh DA, Yang HM, Reisfeld RA. Disialoganglioside GD2 on human neuroblastoma cells: target antigen for monoclonal antibody-mediated cytolytic and suppression of tumor growth. *Cancer Res* (1987) **47**:1098–104.
- Matthay KK, Reynolds CP, Seeger RC, Shimada H, Adkins ES, Haas-Kogan D, et al. Long-term results for children with high-risk neuroblastoma treated on a randomized trial of myeloablative therapy followed by 13-cis-retinoic acid: a Children's Oncology Group Study. *J Clin Oncol* (2009) **27**:1007–13. doi:10.1200/JCO.2007.13.8925
- Ponzoni M, Bocca P, Chiesa V, Decensi A, Pistoia V, Raffaghelli L, et al. Differential effects of N-(4-hydroxyphenyl)retinamide and retinoic acid on neuroblastoma cells: apoptosis versus differentiation. *Cancer Res* (1995) **55**:853–61.
- Lovat PE, Ranalli M, Annichiarico-Petruzzelli M, Bernassola F, Piacentini M, Malcolm AJ, et al. Effector mechanisms of fenretinide-induced apoptosis in neuroblastoma. *Exp Cell Res* (2000) **260**:50–60. doi:10.1006/excr.2000.4988
- Modak S, Cheung NK. Neuroblastoma: therapeutic strategies for a clinical enigma. *Cancer Treat Rev* (2010) **36**:307–17. doi:10.1016/j.ctrv.2010.02.006
- Villablanca JG, Kralio MD, Ames MM, Reid JM, Reaman GH, Reynolds CP. Phase I trial of oral fenretinide in children with high-risk solid tumors: a report from the Children's Oncology Group (CCG 09709). *J Clin Oncol* (2006) **24**:3423–30. doi:10.1200/JCO.2005.03.9271
- Garaventa A, Luksch R, Lo Piccolo MS, Cavardini E, Montaldo PG, Pizzitola MR, et al. Phase I trial and pharmacokinetics of fenretinide in children with neuroblastoma. *Clin Cancer Res* (2003) **9**:2032–9.
- Villablanca JG, London WB, Naranjo A, McGrady P, Ames MM, Reid JM, et al. Phase II study of oral capsular 4-hydroxyphenylretinamide (4-HPR/fenretinide) in pediatric patients with refractory or recurrent neuroblastoma: a report from the Children's Oncology Group. *Clin Cancer Res* (2011) **17**:6858–66. doi:10.1158/1078-0432.CCR-11-0995
- Maurer BJ, Kalous O, Yesair DW, Wu X, Janeba J, Maldonado V, et al. Improved oral delivery of N-(4-hydroxyphenyl)retinamide with a novel LYM-X-SORB organized lipid complex. *Clin Cancer Res* (2007) **13**:3079–86. doi:10.1158/1078-0432.CCR-06-1889
- Kang MH, Marachelian A, Villablanca JG, Maris JM, Ames MM, Reid JM, et al. Fenretinide (4-HPR) orally formulated in Lym-X-Sorb(LXS) lipid matrix or as an intravenous emulsion increased 4-HPR systemic exposure in patients with Recurrent or Resistant Neuroblastoma. A New Approaches To Neuroblastoma Therapy (NANT) Consortium Trial [abstract]. *Proc ANR OR57* (2010). 123 p.
- Orienti I, Zuccari G, Falconi M, Teti G, Illingworth NA, Veal GJ. Novel micelles based on amphiphilic branched PEG as carriers for fenretinide. *Nanomedicine* (2012) **8**:880–90. doi:10.1016/j.nano.2011.10.008
- Tardi P, Bally MB, Harasym TO. Clearance properties of liposomes involving conjugated proteins for targeting. *Adv Drug Deliv Rev* (1998) **32**:99–118. doi:10.1016/S0169-409X(97)00134-8

35. Maruyama K, Takahashi N, Tagawa T, Nagaike K, Iwatsuru M. Immunoliposomes bearing polyethyleneglycol-coupled Fab' fragment show prolonged circulation time and high extravasation into targeted solid tumors *in vivo*. *FEBS Lett* (1997) **413**:177–80. doi: 10.1016/S0014-5793(97)00905-8
36. Sapra P, Moase EH, Ma J, Allen TM. Improved therapeutic responses in a xenograft model of human B lymphoma (Namalwa) for liposomal vincristine versus liposomal doxorubicin targeted via anti-CD19 IgG2a or Fab' fragments. *Clin Cancer Res* (2004) **10**:1100–11. doi: 10.1158/1078-0432.CCR-03-0041
37. Sugano M, Egilmez NK, Yokota SJ, Chen FA, Harding J, Huang SK, et al. Antibody targeting of doxorubicin-loaded liposomes suppresses the growth and metastatic spread of established human lung tumor xenografts in severe combined immunodeficient mice. *Cancer Res* (2000) **60**:6942–9.
38. Goodchild J. Therapeutic oligonucleotides. *Methods Mol Biol* (2011) **764**:1–15. doi: 10.1007/978-1-61737-922-0_1
39. Crooke ST. Therapeutic applications of oligonucleotides. *Annu Rev Pharmacol Toxicol* (1992) **32**:329–76. doi: 10.1146/annurev.pa.32.040192.001553
40. Alitalo K, Winqvist R, Lin CC, de la Chapelle A, Schwab M, Bishop JM. Aberrant expression of an amplified c-myb oncogene in two cell lines from a colon carcinoma. *Proc Natl Acad Sci U S A* (1984) **81**:4534–8. doi: 10.1073/pnas.81.14.4534
41. Pagnan G, Stuart DD, Pastorino F, Raffaghello L, Montaldo PG, Allen TM, et al. Delivery of c-myb antisense oligodeoxynucleotides to human neuroblastoma cells via disialoganglioside GD(2)-targeted immunoliposomes: antitumor effects. *J Natl Cancer Inst* (2000) **92**:253–61. doi: 10.1093/jnci/92.3.253
42. Gray MJ, Van Buren G, Dallas NA, Xia L, Wang X, Yang AD, et al. Therapeutic targeting of neuropilin-2 on colorectal carcinoma cells implanted in the murine liver. *J Natl Cancer Inst* (2008) **100**:109–20. doi: 10.1093/jnci/djm279
43. Whitehead KA, Langer R, Anderson DG. Knocking down barriers: advances in siRNA delivery. *Nat Rev Drug Discov* (2009) **8**:29–38. doi: 10.1038/nrd2742
44. Mossé YP, Laudenslager M, Longo L, Cole KA, Wood A, Attiyeh EF, et al. Identification of ALK as a major familial neuroblastoma predisposition gene. *Nature* (2008) **455**:930–5. doi: 10.1038/nature07261
45. Di Paolo D, Brignole C, Pastorino F, Carosio R, Zorzoli A, Rossi M, et al. Neuroblastoma-targeted nanoparticles entrapping siRNA specifically knockdown ALK. *Mol Ther* (2011) **19**:1131–40. doi: 10.1038/mtnano.2011.54
46. Di Paolo D, Ambrogio C, Pastorino F, Brignole C, Martinengo C, Carosio R, et al. Selective therapeutic targeting of the anaplastic lymphoma kinase with liposomal siRNA induces apoptosis and inhibits angiogenesis in neuroblastoma. *Mol Ther* (2011) **19**:2201–12. doi: 10.1038/mt.2011.142
47. Minchinton AI, Tannock IF. Drug penetration in solid tumours. *Nat Rev Cancer* (2006) **6**:583–92. doi: 10.1038/nrc1893
48. Niethammer D, Handgretinger R. Clinical strategies for the treatment of neuroblastoma. *Eur J Cancer* (1995) **31A**:568–71. doi: 10.1016/0959-8049(95)00032-E
49. Corti A, Pastorino F, Curnis F, Arap W, Ponzoni M, Pasqualini R. Targeted drug delivery and penetration into solid tumors. *Med Res Rev* (2012) **32**:1078–91. doi: 10.1002/med.20238
50. Kolonin MG, Sun J, Do KA, Vidal CI, Ji Y, Baggerly KA, et al. Synchronous selection of homing peptides for multiple tissues by *in vivo* phage display. *FASEB J* (2006) **20**:979–81. doi: 10.1096/fj.05-5186fje
51. Folkman J. Angiogenesis in cancer, vascular, rheumatoid and other disease. *Nat Med* (1995) **1**:27–31. doi: 10.1038/nm0195-27
52. Browder T, Butterfield CE, Kräling BM, Shi B, Marshall B, O'Reilly MS, et al. Antiangiogenic scheduling of chemotherapy improves efficacy against experimental drug-resistant cancer. *Cancer Res* (2000) **60**:1878–86.
53. Jain RK. Normalizing tumor vasculature with anti-angiogenic therapy: a new paradigm for combination therapy. *Nat Med* (2001) **7**:987–9. doi: 10.1038/89889
54. Jain RK. The next frontier of molecular medicine: delivery of therapeutics. *Nat Med* (1998) **4**:655–7. doi: 10.1038/nm0698-655
55. Huang X, Molema G, King S, Watkins L, Edgington TS, Thorpe PE. Tumor infarction in mice by antibody-directed targeting of tissue factor to tumor vasculature. *Science* (1997) **275**:547–50. doi: 10.1126/science.275.5299.547
56. Sergeeva A, Kolonin MG, Mollard JJ, Pasqualini R, Arap W. Display technologies: application for the discovery of drug and gene delivery agents. *Adv Drug Deliv Rev* (2006) **58**:1622–54. doi: 10.1016/j.addr.2006.09.018
57. Zurita AJ, Arap W, Pasqualini R. Mapping tumor vascular diversity by screening phage display libraries. *J Control Release* (2003) **91**:183–6. doi: 10.1016/S0168-3659(03)00236-0
58. Pasqualini R, Koivunen E, Kain R, Lahdenranta J, Sakamoto M, Stryhn A, et al. Aminopeptidase N is a receptor for tumor-homing peptides and a target for inhibiting angiogenesis. *Cancer Res* (2000) **60**:722–7.
59. Marchiò S, Lahdenranta J, Schlingemann RO, Valdembri D, Wesseling P, Arap MA, et al. Aminopeptidase A is a functional target in angiogenic blood vessels. *Cancer Cell* (2004) **5**:151–62. doi: 10.1016/S1535-6108(04)00025-X
60. Jain RK. Delivery of molecular medicine to solid tumors. *Science* (1996) **271**:1079–80. doi: 10.1126/science.271.5252.1079
61. Jain RK. Transport of molecules, particles, and cells in solid tumors. *Annu Rev Biomed Eng* (1999) **1**:241–63. doi: 10.1146/annurev.bioeng.1.1.241
62. Heldin CH, Rubin K, Pietras K, Ostman A. High interstitial fluid pressure – an obstacle in cancer therapy. *Nat Rev Cancer* (2004) **4**:806–13. doi: 10.1038/nrc1456
63. Olive KP, Jacobetz MA, Davidson CJ, Gopinathan A, McIntyre D, Honess D, et al. Inhibition of Hedgehog signaling enhances delivery of chemotherapy in a mouse model of pancreatic cancer. *Science* (2009) **324**:1457–61. doi: 10.1126/science.1171362

Conflict of Interest Statement: The authors declare that the research was conducted in the absence of any commercial or financial relationships that could be construed as a potential conflict of interest.

Received: 03 June 2013; accepted: 08 July 2013; published online: 05 August 2013.

Citation: Pastorino F, Brignole C, Loi M, Di Paolo D, Di Fiore A, Perri P, Pagnan G and Ponzoni M (2013) Nanocarrier-mediated targeting of tumor and tumor vascular cells improves uptake and penetration of drugs into neuroblastoma. *Front. Oncol.* **3**:190. doi: 10.3389/fonc.2013.00190

This article was submitted to Frontiers in Pharmacology of Anti-Cancer Drugs, a specialty of Frontiers in Oncology.

Copyright © 2013 Pastorino, Brignole, Loi, Di Paolo, Di Fiore, Perri, Pagnan and Ponzoni. This is an open-access article distributed under the terms of the Creative Commons Attribution License (CC BY). The use, distribution or reproduction in other forums is permitted, provided the original author(s) or licensor are credited and that the original publication in this journal is cited, in accordance with accepted academic practice. No use, distribution or reproduction is permitted which does not comply with these terms.



Positron emission tomography as a method for measuring drug delivery to tumors *in vivo*: the example of [¹¹C]docetaxel

Astrid A. M. van der Veldt^{1,2*}, Egbert F. Smit³ and Adriaan A. Lammertsma²

¹ Department of Internal Medicine, VU University Medical Center, Amsterdam, Netherlands

² Department of Radiology and Nuclear Medicine, VU University Medical Center, Amsterdam, Netherlands

³ Department of Pulmonary Diseases, VU University Medical Center, Amsterdam, Netherlands

Edited by:

Fabrizio Marzocchi, Istituto Superiore di Sanità, Italy

Reviewed by:

Amit K. Tiwari, Tuskegee University, USA

Matteo Bellone, San Raffaele Scientific Institute, Italy

*Correspondence:

Astrid A. M. van der Veldt,
Department of Internal Medicine, VU University Medical Center, P.O. Box 7057, 1007 MB Amsterdam, Netherlands
e-mail: aam.vanderveldt@vumc.nl

Systemic anticancer treatments fail in a substantial number of patients. This may be caused by inadequate uptake and penetration of drugs in malignant tumors. Consequently, improvement of drug delivery to solid tumors may enhance its efficacy. Before evaluating strategies to enhance drug uptake in tumors, better understanding of drug delivery to human tumors is needed. Positron emission tomography (PET) is an imaging technique that can be used to monitor drug pharmacokinetics non-invasively in patients, based on radiolabeling these drugs with short-lived positron emitters. In this mini review, principles and potential applications of PET using radiolabeled anticancer drugs will be discussed with respect to personalized treatment planning in oncology. In particular, it will be discussed how these radiolabeled anticancer drugs could help to develop strategies for improved drug delivery to solid tumors. The development and clinical implementation of PET using radiolabeled anticancer drugs will be illustrated by validation studies of carbon-11 labeled docetaxel (¹¹C]docetaxel) in lung cancer patients.

Keywords: positron emission tomography, radiolabeled anticancer drugs, drug delivery, tumors, [¹¹C]docetaxel, lung cancer

INTRODUCTION

To date, an increasing number of anticancer drugs is available for treating cancer patients. Nevertheless, resistance to anticancer drugs remains a problem in a substantial number of patients and, consequently, these patients may suffer from drug-induced toxicities without any benefit. Tumor response to anticancer drugs is, amongst others, thought to be directly related to drug concentrations in tumor tissue. Strategies that improve drug delivery to tumors may therefore enhance efficacy of anticancer drugs. Prior to the evaluation of these strategies, better understanding of drug delivery to human tumors is needed. Direct assessment of tumor drug concentrations in cancer patients, however, is challenging, as it requires accessibility to tumors that are usually deeply seated within the body. Positron emission tomography (PET) is an imaging technique that can be used to monitor drug pharmacokinetics non-invasively in patients by radiolabeling drugs of interest with short-lived positron emitters. In this mini review, principles and potential applications of PET using radiolabeled anticancer drugs will be discussed for personalized treatment planning in oncology. Furthermore, development and clinical implementation of radiolabeled anticancer drugs will be illustrated by validation studies of carbon-11 labeled docetaxel (¹¹C]docetaxel) in lung cancer patients. Finally, it will be discussed how these radiolabeled anticancer drugs could help to develop strategies for improved drug delivery to tumors.

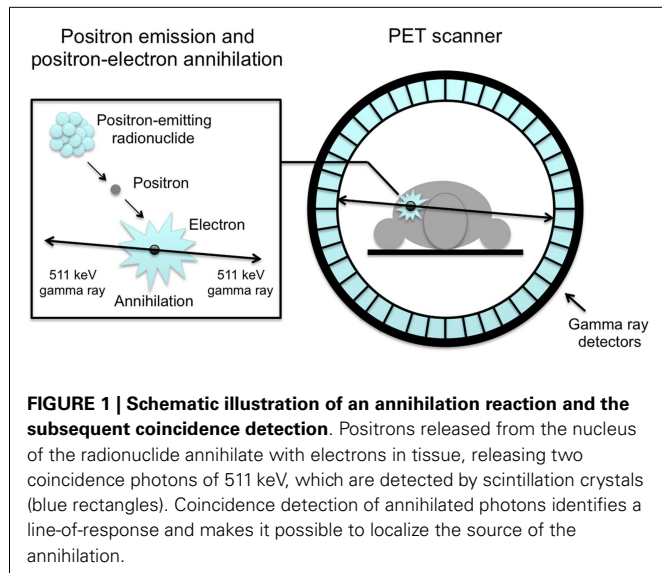
POSITRON EMISSION TOMOGRAPHY

PRINCIPLES OF PET

Positron emission tomography is a highly sensitive nuclear imaging technique that enables non-invasive *in vivo* monitoring of dynamic processes (1). PET tracers are molecules of interest that are labeled with a positron emitting radionuclide. Such a radionuclide decays by emission of a positron from its nucleus, which almost immediately results in the simultaneous emission of two gamma rays in opposite direction. For PET imaging, in general short-lived radionuclides, such as carbon-11 [¹¹C], fluorine-18 [¹⁸F], and oxygen-15 [¹⁵O] are used. A PET scanner usually consists of a ring of detectors and is capable of detecting high-energy gamma rays that are emitted from tissue after intravenous administration of a PET tracer (Figure 1). After reconstruction, data obtained provide information on the 3-dimensional tracer concentration within the body. To date, a PET scanner is combined with an integrated computed tomography (CT) scanner (2), which is used for attenuation correction as well as anatomical localization of tracer uptake.

KINETIC MODELING OF PET DATA

In clinical practice, a PET image can be extremely useful for diagnosis and staging of cancer. However, absolute quantification of tracer kinetics in tissue is necessary for complete characterization of functional processes *in vivo*. For quantification of tracers, their uptake in tissue needs to be measured as function of time.



Therefore, PET data need to be acquired as dynamic rather than static scans. For diagnostic purposes, usually whole body scans are performed, which consist of a series of static scans by moving the scanner bed over multiple bed positions. During a dynamic PET scan, patients are scanned at one bed position and detailed (kinetic) information on a selected part of the body is obtained. As a result, a dynamic scan is limited by the field of view of the PET scanner, which is \sim 15–20 cm. Consequently, the tissue of interest needs to be adequately defined prior to acquisition of the PET data. Net tracer uptake in tissue is determined by its delivery, extraction from blood and washout from tissue as function of time. Each tracer has its own distinct behavior *in vivo*, which can be described by tracer kinetic models (3). Several compartmental models have been developed to describe PET data. In Figure 2, schematic diagrams of standard single tissue and two tissue compartment models are presented. The kinetic rate constants in these models can be estimated from dynamic PET data. To this end, a tissue time-activity curve (TAC; Figure 3) is fitted to the appropriate model equation using the arterial plasma TAC as input function, and the best fit then provides estimates of these kinetic parameters (Figure 4). The arterial input function can be obtained from arterial blood sampling using an on-line detection system (4). Arterial blood sampling, however, is an invasive and cumbersome procedure. In principle, the time course of the tracer in a large arterial blood structure, e.g., the aorta, can also be used to generate a non-invasive image derived input function.

PET IMAGING IN ONCOLOGY

Over the past decade, clinical applications of PET have expanded, particularly in oncology. To date, 2-deoxy-2-[¹⁸F]fluoro-D-glucose ([¹⁸F]FDG) is the most widely used PET tracer for evaluation of cancer. High [¹⁸F]FDG uptake in tumors is based on altered glucose metabolism in most cancer cells (5). As [¹⁸F]FDG uptake in tissue is not specific for malignancy and does not provide information on other biological characteristics of tumors, other PET tracers have been developed. For example, 3-deoxy-3-[¹⁸F]fluorothymidine ([¹⁸F]FLT) has been developed

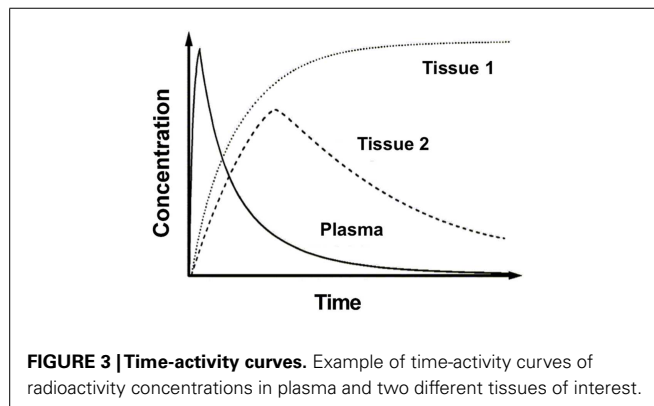
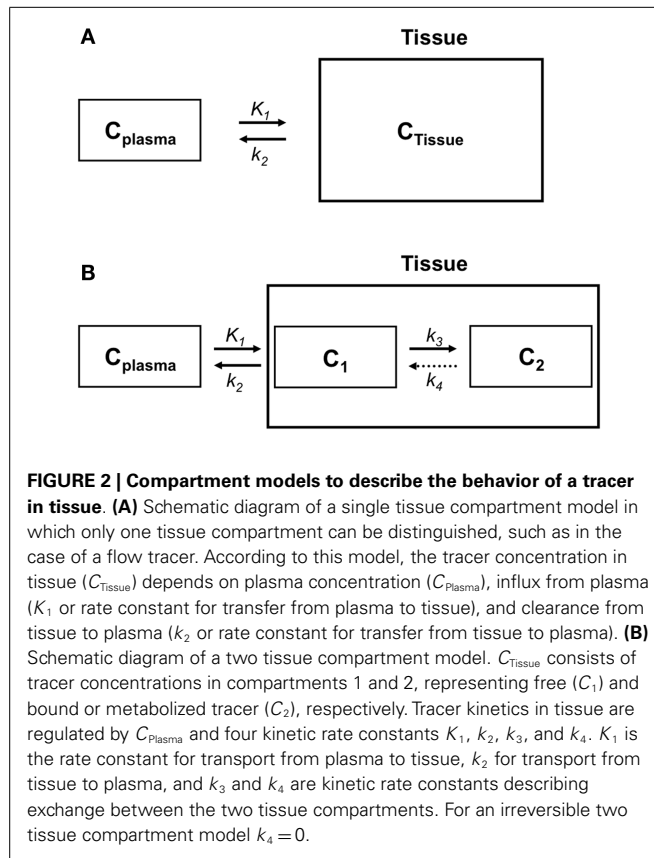


FIGURE 3 | Time-activity curves. Example of time-activity curves of radioactivity concentrations in plasma and two different tissues of interest.

to measure tumor proliferation (6). In addition, radioactive water ($[^{15}\text{O}]\text{H}_2\text{O}$) can be used to measure tumor perfusion (7), whereas hypoxia tracers such as [¹⁸F]fluoroazomycin arabinofuranoside ([¹⁸F]FAZA) and [¹⁸F]fluoromisonidazole ([¹⁸F]FMISO) can be used to determine hypoxic areas in tumors (8). Although these PET tracers may provide additional information on various biological processes in tumors and could be useful for response evaluation, they are not specific enough to predict tumor response to specific anticancer drugs. As an alternative, anticancer drugs can be labeled with positron emitters. Using PET, these radiolabeled drugs can then be used to monitor drug pharmacokinetics in patients non-invasively. As tumor response to

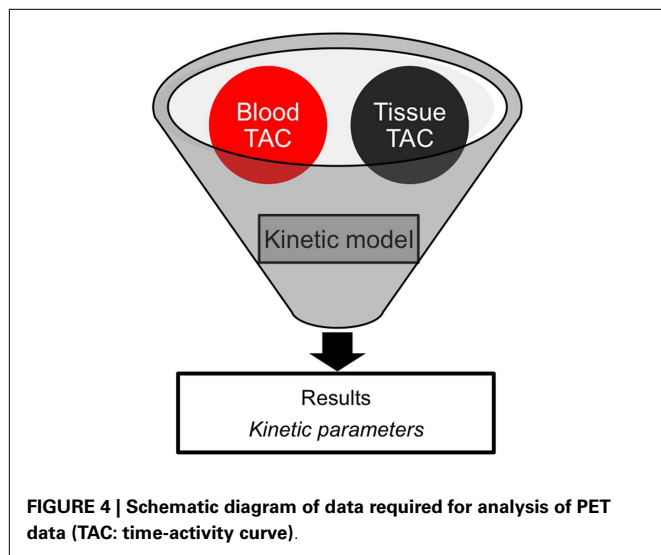


FIGURE 4 | Schematic diagram of data required for analysis of PET data (TAC: time-activity curve).

anticancer drugs is thought to be directly related to drug concentrations in tumor tissue, uptake of radiolabeled anticancer drugs in tumors may predict treatment outcome. Preliminary PET studies using F-18 labeled 5-fluorouracil ($[^{18}\text{F}]5\text{-FU}$; (9, 10)), tamoxifen ($[^{18}\text{F}]$ fluorotamoxifen; (11)), and C-11 labeled docetaxel ($[^{11}\text{C}]$ docetaxel; (12)) showed that high tumor uptake of the radiolabeled anticancer drug was associated with improved tumor response following corresponding therapy. These studies suggest that radiolabeled anticancer drugs may be useful for prediction of outcome prior to start of treatment. Consequently, an increasing number of anticancer drugs has now been radiolabeled including radiolabeled cytotoxic agents (e.g., $[^{11}\text{C}]$ temozolomide, $[^{18}\text{F}]$ 5-fluorouracil, and $[^{11}\text{C}]$ docetaxel), selective hormone receptor modulators (e.g., $[^{18}\text{F}]$ fluorotamoxifen), tyrosine kinase inhibitors (TKIs, e.g., N- $[^{11}\text{C}]$ methylimatinib, $[^{11}\text{C}]$ sorafenib, and $[^{11}\text{C}]$ erlotinib), and monoclonal antibodies [Mabs, e.g., $[^{89}\text{Zr}]$ cetuximab, $[^{89}\text{Zr}]$ trastuzumab, and $[^{89}\text{Zr}]$ bevacizumab; (10, 11, 13–20)].

DEVELOPMENT OF RADIOLABELED ANTICANCER DRUGS

For the development of radiolabeled anticancer drugs, a complex, and expensive research infrastructure is required: a cyclotron for production of positron emitters, an on-site good manufacturing practice laboratory for synthesis of the tracer, a PET/CT scanner for acquisition of images, an on-line blood sampler in case of arterial blood sampling, an on-site laboratory for measurements of radioactivity concentrations and radioactive metabolites in plasma, and dedicated computers and software to analyze and quantify acquired PET data. In addition, these facilities need to be staffed by qualified personnel including a cyclotron operator, a chemist who synthesizes the PET tracer, a radiopharmacist who is responsible for quality control of the tracer production, a technologist for acquiring PET images, a (nuclear medicine) physician who is clinically responsible for the patient as well as for arterial blood sampling, a chemist for analyzing blood samples during PET scanning, and a physicist who is responsible for acquisition protocols and data analyses. The short half-lives of most PET tracers

require that these facilities and personnel are located and working in the same building at very close proximity. Besides these logistic issues, the use of PET and radiolabeled anticancer drugs can be limited by technical issues including complex tracer synthesis and the spatial resolution of the scanner. Before implementation of a new PET tracer in the clinic, technical, and biological validation of the tracer is required. To this end, the optimal patient population should be selected based on patient characteristics and technical issues.

THE EXAMPLE OF $[^{11}\text{C}]$ DOCETAXEL PET IN LUNG CANCER PATIENTS

DOCETAXEL

The cytotoxic agent docetaxel is a taxane, a class of drugs consisting of microtubule stabilizing agents that function primarily by interfering with microtubular dynamics, inducing cell cycle arrest and apoptosis (21). In clinical practice, docetaxel is administered as a 1-h intravenous infusion, usually given at a dose of 75 or 100 mg m^{-2} in a three-weekly regimen. In 1996, docetaxel was first approved for the treatment of anthracycline-refractory metastatic breast cancer. Thereafter, the drug was registered as monotherapy as well as in combination strategies for the treatment of several advanced malignancies including hormone refractory metastatic prostate cancer, gastric adenocarcinoma, head and neck cancer, and non-small cell lung cancer (NSCLC) (21). In these malignancies, docetaxel has shown clinical efficacy, including tumor response and improved survival. Nevertheless, failure of docetaxel therapy occurs and patients are often subjected to docetaxel related toxicities without gaining benefit.

LABELING OF DOCETAXEL

Docetaxel has been radiolabeled with the radionuclide carbon-11 (22, 23). As a stable carbon atom is replaced by carbon-11 (Figure 5), the chemical structure of the tracer $[^{11}\text{C}]$ docetaxel is identical to that of the drug docetaxel. Hence, pharmacokinetics of tracer and drug are identical. As the specific activity of $[^{11}\text{C}]$ docetaxel is approximately $10 \text{ GBq } \mu\text{mol}^{-1}$, which contains $30 \mu\text{g}$ docetaxel for a typical administration of 370 MBq $[^{11}\text{C}]$ docetaxel, only 0.02% of a therapeutic dose of docetaxel is administered for PET. As a result, $[^{11}\text{C}]$ docetaxel microdosing prevents patients from drug-induced toxicities that are associated with therapeutic doses. The following paragraphs describe successive steps in the validation of $[^{11}\text{C}]$ docetaxel for use in lung cancer patients.

BIODISTRIBUTION OF $[^{11}\text{C}]$ DOCETAXEL IN RATS

In preparation of humans studies, the biodistribution of $[^{11}\text{C}]$ docetaxel in healthy rats was investigated (24). This preclinical study was needed to obtain an initial estimate of the expected radiation dose in humans, which in turn was required for obtaining ethics permission to conduct human studies. The biodistribution of $[^{11}\text{C}]$ docetaxel was determined in healthy male rats at 5, 15, 30, and 60 min after injection. This preclinical study showed the highest $[^{11}\text{C}]$ docetaxel uptake in spleen, followed by urine, lung and liver, whereas brain and testes showed the lowest uptake (Figure 6). Within less than 5 min, $[^{11}\text{C}]$ docetaxel essentially had cleared from blood and plasma. As the estimated effective dose in

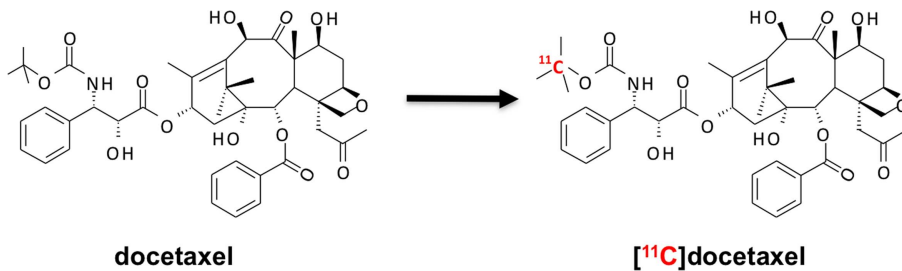


FIGURE 5 | Synthesis of [¹¹C]docetaxel. [¹¹C]docetaxel is synthesized by replacing a stable carbon atom by carbon-11 (22, 23), so that chemical properties of stable and labeled compound are exactly the same.

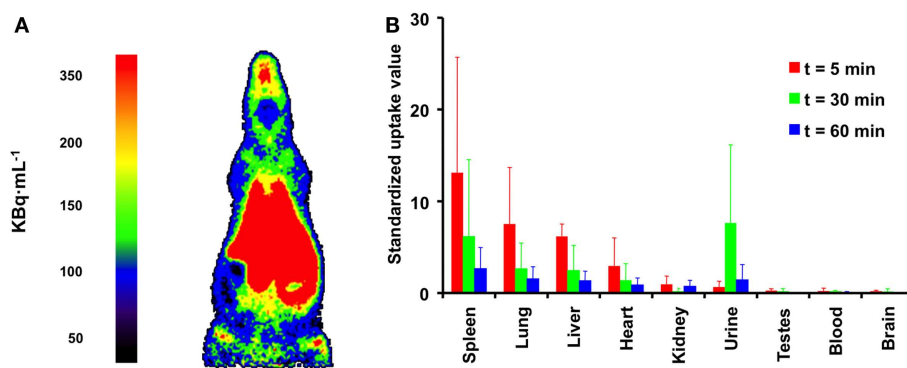


FIGURE 6 | Biodistribution of [¹¹C]docetaxel in healthy male rats. (A) PET image showing the biodistribution of [¹¹C]docetaxel in a male rat. This image was obtained using a high resolution research tomograph (HRRT) with a spatial resolution of about 2.5 mm. Red indicates the highest

[¹¹C]docetaxel uptake. (B) Standardized uptake values of [¹¹C]docetaxel in organs as obtained from dissection studies. Standardized uptake values were calculated as tissue radioactivity concentration normalized for injected dose and body weight.

humans extrapolated from this rat study was $5.4 \mu\text{Sv MBq}^{-1}$, the use of [¹¹C]docetaxel in humans was considered to be safe.

BIODISTRIBUTION OF [¹¹C]DOCETAXEL IN HUMANS

Following the preclinical study in rats, both biodistribution and actual human radiation dosimetry of [¹¹C]docetaxel was determined in seven patients with solid tumors using whole body PET/CT scans (25). Gall bladder and liver showed high [¹¹C]docetaxel uptake, whilst uptake in brain and normal lung was low (Figure 7). In the liver, the percentage injected dose at 1 h was $47 \pm 9\%$. In addition, [¹¹C]docetaxel was rapidly cleared from plasma and no radiolabeled metabolites were detected. The effective dose of [¹¹C]docetaxel was $4.7 \mu\text{Sv MBq}^{-1}$, which was comparable to the estimated effective dose in rats. In contrast to the preclinical study in rats, [¹¹C]docetaxel showed low uptake in human lungs. As a result, [¹¹C]docetaxel could be a useful tracer for tumors in the thoracic region.

QUANTIFICATION OF TUMOR UPTAKE

Although uptake of [¹¹C]docetaxel in normal tissues may be interesting, its uptake in tumor tissue is more important. The feasibility of quantitative [¹¹C]docetaxel PET scans was evaluated in patients with lung cancer (Figure 8). In addition, it was investigated whether [¹¹C]docetaxel kinetics were associated with

tumor perfusion or tumor size. In this study, 34 lung cancer patients underwent dynamic PET/CT scans using [¹¹C]docetaxel and [¹⁵O] H_2O (12). For quantification of [¹¹C]docetaxel kinetics, the optimal tracer kinetic model was determined. Tumor kinetics of [¹¹C]docetaxel were irreversible and could be quantified using Patlak graphical analysis. Furthermore, it was shown that reproducible quantification of [¹¹C]docetaxel kinetics in tumors was possible using a non-invasive image derived input function. In tumors, the net rate of influx (K_i) of [¹¹C]docetaxel was variable and strongly related to tumor perfusion, but not to tumor size. Finally, effects of dexamethasone administration on drug uptake in tumors were investigated, as corticosteroids are potent inducers of the drug efflux transporter ABCB1. Prior to administration of therapeutic doses of docetaxel, all patients are premedicated with corticosteroids, as this reduces incidence and severity of docetaxel induced fluid retention and hypersensitivity reactions significantly (26, 27). In this dynamic PET study, the first 24 patients were premedicated with dexamethasone, whereas the last 10 patients were not. In dexamethasone premedicated patients, uptake of [¹¹C]docetaxel in tumors was significantly lower than in patients without premedication, indicating that co-medication may affect accumulation of drugs in tumor tissue. Finally, in a subgroup of patients who subsequently received docetaxel therapy, high tumor uptake of [¹¹C]docetaxel was related with improved

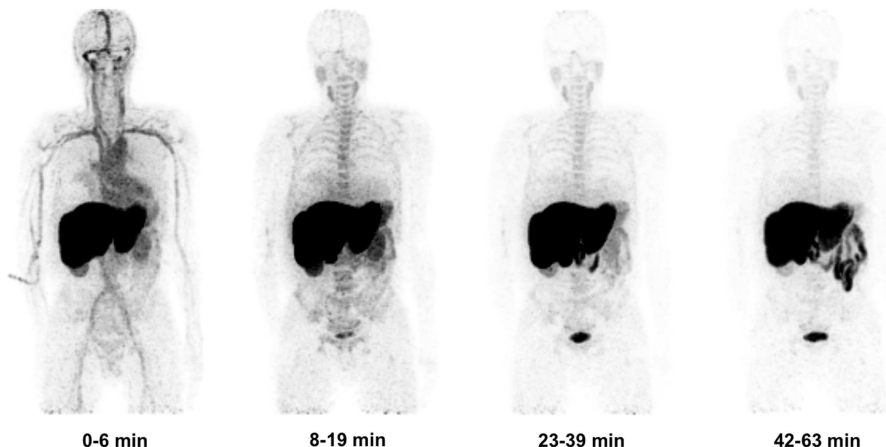


FIGURE 7 | Biodistribution of [¹¹C]docetaxel in patients. Four successive [¹¹C]docetaxel whole body PET scans showing that [¹¹C]docetaxel first accumulates in liver, before being excreted into bile and ultimately into intestine. Because of high [¹¹C]docetaxel uptake in the liver, these projections do not show the high uptake of [¹¹C]docetaxel in the gall bladder (25).

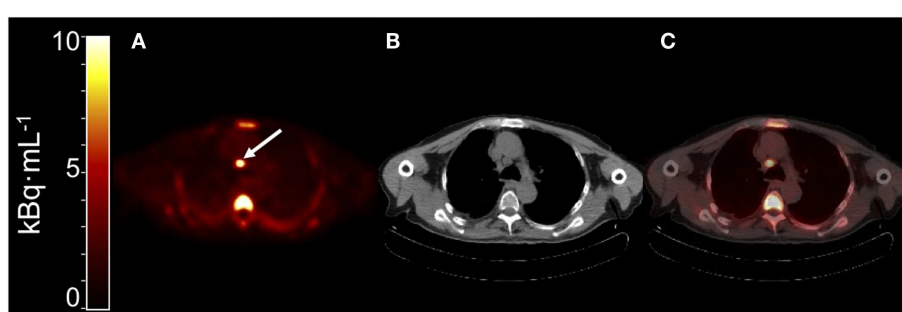


FIGURE 8 | (A) Summed PET image of [¹¹C]docetaxel uptake from 10 to 60 min post injection showing a mediastinal metastasis with increased uptake [arrow; (12)]. **(B)** Corresponding CT image. **(C)** PET-CT fusion image.

tumor response (12, 28), suggesting that the observed variation in [¹¹C]docetaxel kinetics between tumors may reflect differential sensitivity to docetaxel therapy.

VALIDATION OF THE MICRODOSING CONCEPT

[¹¹C]docetaxel microdosing protects patients from toxicities that are associated with therapeutic doses of docetaxel. However, pharmacokinetics of [¹¹C]docetaxel at tracer doses may be different from those at therapeutic doses, as the latter can significantly affect uptake of radiolabeled anticancer drugs in normal organs as well as in tumors (29–32). Therefore, the microdosing concept was validated for [¹¹C]docetaxel in another study (28). The research question to be addressed was whether a PET study using a tracer dose of [¹¹C]docetaxel could predict tumor uptake of unlabeled docetaxel during a therapeutic infusion. For this purpose, docetaxel naïve lung cancer patients underwent two [¹¹C]docetaxel PET scans, one after a bolus injection of a tracer dose [¹¹C]docetaxel and another during a combined infusion of a tracer dose [¹¹C]docetaxel and a therapeutic dose of docetaxel (75 mg m^{-2}). Compartmental and spectral analyses were used to quantify [¹¹C]docetaxel tumor

kinetics. In addition, [¹¹C]docetaxel PET measurements were used to estimate the area under the curve of therapeutic doses of docetaxel in tumors. At 90 min, the accumulated amount of docetaxel in tumors was <1% of the total infused dose of docetaxel, indicating that only a small amount accumulates in tumors. In addition, the uptake of therapeutic doses in tumors was related to the uptake of [¹¹C]docetaxel during the microdosing scan, indicating that [¹¹C]docetaxel PET can be used to predict tumor uptake of docetaxel during chemotherapy.

COMBINATION THERAPY

Within the context of combination therapy, effects of the anti-angiogenic drug bevacizumab on tumor perfusion and [¹¹C]docetaxel uptake in lung tumors were investigated in NSCLC patients (33). Bevacizumab is a humanized monoclonal antibody that targets circulating vascular endothelial growth factor (VEGF) and subsequently prevents binding of VEGF to its receptors. Combined with chemotherapy, bevacizumab has been approved for the treatment of several advanced malignancies including NSCLC (34). It is assumed that anti-angiogenic drugs,

such as bevacizumab, transiently normalize abnormal tumor vasculature and contribute to improved delivery of subsequent chemotherapy (35). To investigate this concept, a study was performed in NSCLC patients using PET and [¹¹C]docetaxel. Within 5 h, a therapeutic dose of bevacizumab reduced both perfusion and [¹¹C]docetaxel uptake in NSCLC. These effects persisted after 4 days and were not associated with significant changes in heterogeneity of [¹¹C]docetaxel uptake in tumors. Reduction in [¹¹C]docetaxel delivery to tumors was accompanied by rapid reduction in circulating levels of VEGF. The clinical relevance of these findings is notable (36–38), as there was no evidence for substantial improvement in drug delivery to tumors after administration of bevacizumab. This study highlights the ability of PET to potentially optimize scheduling of (anti-angiogenic) drugs.

CONCLUSION

PET using radiolabeled anticancer drugs may help to reveal the underlying mechanisms of treatment failure in cancer patients. In particular, this technology enables assessment of accumulation of

drugs in human tumors and, in turn, prediction of treatment outcome. However, development of radiolabeled drugs faces several caveats on the path from development to clinical implementation, as it can be very challenging due to technical, logistical, financial, and/or patient related issues. To facilitate clinical implementation of radiolabeled drugs, a step-wise approach needs to be applied. In this regard, the step-wise validation of [¹¹C]docetaxel in lung cancer patients provides a framework for investigating the PET microdosing concept for other radiolabeled anticancer drugs. The [¹¹C]docetaxel PET studies have shown that only a small amount of docetaxel accumulates in tumor tissue, which is further decreased by co-medication (dexamethasone) and other anticancer drugs (bevacizumab). In addition, it is conceivable that drug delivery to tumors is also dependent on the localization of tumors in the body, as drug delivery may differ between organs (e.g., brain versus liver). In this way, PET using radiolabeled anticancer drugs may provide insight into drug delivery to human tumors and may facilitate rational treatment choices that are tailored to improve drug delivery to tumors.

REFERENCES

- Gambhir SS. Molecular imaging of cancer with positron emission tomography. *Nat Rev Cancer* (2002) **2**:683–93. doi:10.1038/nrc882
- Surti S, Kuhn A, Werner ME, Perkins AE, Kolthammer J, Karp JS. Performance of Philips Gemini TF PET/CT scanner with special consideration for its time-of-flight imaging capabilities. *J Nucl Med* (2007) **48**:471–80.
- Gunn RN, Gunn SR, Cunningham VJ. Positron emission tomography compartmental models. *J Cereb Blood Flow Metab* (2001) **21**:635–52. doi:10.1097/00004647-200106000-00002
- Boellaard R, van Lingen A, van Balen SC, Hoving BG, Lammertsma AA. Characteristics of a new fully programmable blood sampling device for monitoring blood radioactivity during PET. *Eur J Nucl Med* (2001) **28**:81–9. doi:10.1007/s002590000405
- Warburg O. On the origin of cancer cells. *Science* (1956) **123**:309–14. doi:10.1126/science.123.3191.309
- Shields AF, Grierson JR, Dohmen BM, Machulla HJ, Stayanoff JC, Lawhorn-Crews JM, et al. Imaging proliferation in vivo with [F-18]FLT and positron emission tomography. *Nat Med* (1998) **4**:1334–6. doi:10.1038/3337
- van der Veldt AA, Hendrikse NH, Harms H, Comans EF, Posmus PE, Smit EF, et al. Quantitative parametric perfusion images using oxygen-15 labeled water and a clinical PET-CT scanner: test-retest variability in lung cancer. *J Nucl Med* (2010) **51**:1684–90. doi:10.2967/jnumed.110.079137
- Sorger D, Patt M, Kumar P, Wiebe LI, Barthel H, Seese A, et al. [¹⁸F]Fluoroazomycinarabinofuranoside (¹⁸FAZA) and [¹⁸F]Fluoromisonidazole (¹⁸FMISO): a comparative study of their selective uptake in hypoxic cells and PET imaging in experimental rat tumors. *Nucl Med Biol* (2003) **30**:317–26. doi:10.1016/S0969-8051(02)00442-0
- Dimitrakopoulou-Strauss A, Strauss LG, Schlag P, Hohenberger P, Mohler M, Oberdorfer F, et al. Fluorine-18-fluorouracil to predict therapy response in liver metastases from colorectal carcinoma. *J Nucl Med* (1998) **39**:1197–202.
- Moehler M, Dimitrakopoulou-Strauss A, Gutzler F, Raeth U, Strauss LG, Stremmel W. ¹⁸F-labeled fluorouracil positron emission tomography and the prognoses of colorectal carcinoma patients with metastases to the liver treated with 5-fluorouracil. *Cancer* (1998) **83**:245–53. doi:10.1002/(SICI)1097-0142(19980715)83:2<245::AID-CNCR7>3.0.CO;2-P
- Inoue T, Kim EE, Wallace S, Yang DJ, Wong FC, Bassa P, et al. Positron emission tomography using [¹⁸F]fluorotamoxifen to evaluate therapeutic responses in patients with breast cancer: preliminary study. *Cancer Biother Radiopharm* (1996) **11**:235–45. doi:10.1089/cbr.1996.11.235
- van der Veldt AA, Lubberink M, Greuter HN, Comans EF, Herder GJ, Yaquib M, et al. Absolute quantification of [¹¹C]docetaxel kinetics in lung cancer patients using positron emission tomography. *Clin Cancer Res* (2011) **17**:4814–24. doi:10.1158/1078-0432.CCR-10-2933
- Slobbe P, Poot AJ, Windhorst AD, van Dongen GA. PET imaging with small-molecule tyrosine kinase inhibitors: TKI-PET. *Drug Discov Today* (2012) **17**:1175–87. doi:10.1016/j.drudis
- van der Veldt AA, Luurtsema G, Lubberink M, Lammertsma AA, Hendrikse NH. Individualized treatment planning in oncology: role of PET and radiolabelled anticancer drugs in predicting tumour resistance. *Curr Pharm Des* (2008) **14**:2914–31. doi:10.2174/138161208786404344
- Bahce I, Smit EF, Lubberink M, van der Veldt AA, Yaquib M, Windhorst AD, et al. Development of [¹¹C]erlotinib positron emission tomography for in vivo evaluation of EGFR receptor mutational status. *Clin Cancer Res* (2013) **19**:183–93. doi:10.1158/1078-0432.CCR-12-0289
- Kil KE, Ding YS, Lin KS, Alexoff D, Kim SW, Shea C, et al. Synthesis and positron emission tomography studies of carbon-11-labeled imatinib (Gleevec). *Nucl Med Biol* (2007) **34**:153–63. doi:10.1016/j.nucmedbio.2006.11.004
- Saleem A, Brown GD, Brady F, Aboagye EO, Osman S, Luthra SK, et al. Metabolic activation of temozolamide measured in vivo using positron emission tomography. *Cancer Res* (2003) **63**:2409–15.
- Cai W, Chen K, He L, Cao Q, Koong A, Chen X. Quantitative PET of EGFR expression in xenograft-bearing mice using ⁶⁴Cu-labeled cetuximab, a chimeric anti-EGFR monoclonal antibody. *Eur J Nucl Med Mol Imaging* (2007) **34**:850–8. doi:10.1007/s00259-006-0361-6
- Verel I, Visser GW, Boerman OC, van Eerd JE, Finn R, Boellaard R, et al. Long-lived positron emitters zirconium-89 and iodine-124 for scouting of therapeutic radioimmunoconjugates with PET. *Cancer Biother Radiopharm* (2003) **18**:655–61. doi:10.1089/10849780332287745
- Nagengast WB, de Vries EG, Hospers GA, Mulder NH, de Jong JR, Hollema H, et al. In vivo VEGF imaging with radiolabeled bevacizumab in a human ovarian tumor xenograft. *J Nucl Med* (2007) **48**:1313–9. doi:10.2967/jnumed.107.041301
- Montero A, Fossella F, Hortobagyi G, Valero V. Docetaxel for treatment of solid tumours: a systematic review of clinical data. *Lancet Oncol* (2005) **6**:229–39. doi:10.1016/S1470-2045(05)70094-2
- van Tilburg EW, Franssen EJ, van der Hoeven JJ, van der Meij M, Elshove D, Lammertsma AA, et al. Radiosynthesis of [¹¹C]docetaxel. *J Label Compd Radiopharm* (2004) **47**:763–77. doi:10.1002/jlcr.861
- van Tilburg EW, Mooijer MP, Brinkhorst J, van der Meij M, Windhorst AD. Improved and semi-automated GMP-compliant radiosynthesis of [¹¹C]docetaxel. *Appl Radiat Isot* (2008) **66**:1414–8. doi:10.1016/j.apradiso.2008.02.076

24. van der Veldt AA, Lammertsma AA, Hendrikse NH. [11C]docetaxel and positron emission tomography for noninvasive measurements of docetaxel kinetics. *Clin Cancer Res* (2007) **13**:7522–3. doi:10.1158/1078-0432.CCR-07-1626
25. van der Veldt AA, Hendrikse NH, Smit EF, Mooijer PJ, Rynders AY, Gerristen WR, et al. Biodistribution and radiation dosimetry of ¹¹C-labeled docetaxel in cancer patients. *Eur J Nucl Med* (2010) **37**:1950–8. doi:10.1007/s00259-010-1489-y
26. Latreille J, Gelmon KA, Hirsh V, Laberge F, Maksymiuk AW, Shepherd FA, et al. Phase II trial of docetaxel with dexamethasone premedication in patients with advanced non-small cell lung cancer: the Canadian experience. *Invest New Drugs* (1999) **16**:265–70. doi:10.1023/A:1006126505910
27. Piccart MJ, Klijn J, Paridaens R, Nooij M, Mauriac L, Coleman R, et al. Corticosteroids significantly delay the onset of docetaxel-induced fluid retention: final results of a randomized study of the European Organization for Research and Treatment of Cancer Investigational Drug Branch for Breast Cancer. *J Clin Oncol* (1997) **15**:3149–55.
28. van der Veldt AA, Lubberink M, Mathijssen RH, Loos W, Herder GJ, Greuter HN, et al. Toward prediction of efficacy of chemotherapy: a proof of concept study in lung cancer patients using [11C]docetaxel and positron emission tomography. *Clin Cancer Res* (2013) **19**:4163–73. doi:10.1158/1078-0432.CCR-12-3779
29. Harte RJ, Matthews JC, O'Reilly SM, Tilsley DW, Osman S, Brown G, et al. Tumor, normal tissue, and plasma pharmacokinetic studies of fluorouracil biomodulation with N-phosphonacetyl-L-aspartate, folinic acid, and interferon alfa. *J Clin Oncol* (1999) **17**:1580–8.
30. Propper DJ, de Bono J, Saleem A, Ellard S, Flanagan E, Paul J, et al. Use of positron emission tomography in pharmacokinetic studies to investigate therapeutic advantage in a phase I study of 120-hour intravenous infusion XR5000. *J Clin Oncol* (2003) **21**:203–10. doi:10.1200/JCO.2003.02.008
31. Saleem A, Harte RJ, Matthews JC, Osman S, Brady F, Luthra SK, et al. Pharmacokinetic evaluation of N-[2-(dimethylamino)ethyl]acridine-4-carboxamide in patients by positron emission tomography. *J Clin Oncol* (2001) **19**:1421–9.
32. Solbach C, Patt M, Reimold M, Blocher A, Dohmen BM, Bares R, et al. Vinblastine syntheses and preliminary imaging in cancer patients. *J Pharm Pharm Sci* (2007) **10**:266s–76.
33. van der Veldt AA, Lubberink M, Bahce I, Walraven M, de Boer MP, Greuter HN, et al. Rapid decrease in delivery of chemotherapy to tumors after anti-VEGF therapy: implications for scheduling of anti-angiogenic drugs. *Cancer Cell* (2012) **21**:82–91. doi:10.1016/j.ccr.2011.11.023
34. Sandler A, Gray R, Perry MC, Brahmer J, Schiller JH, Dowlati A, et al. Paclitaxel-carboplatin alone or with bevacizumab for non-small cell lung cancer. *N Engl J Med* (2006) **355**:2542–50. doi:10.1056/NEJMoa061884
35. Jain RK. Normalizing tumor vasculature with anti-angiogenic therapy: a new paradigm for combination therapy. *Nat Med* (2001) **7**:987–9. doi:10.1038/89889
36. Casanovas O. Cancer: limitations of therapies exposed. *Nature* (2012) **484**:44–6. doi:10.1038/484044a
37. van der Veldt AA, Lammertsma AA, Smit EF. Scheduling of anticancer drugs: timing may be everything. *Cell Cycle* (2012) **11**:4339–43. doi:10.4161/cc.22187
38. van der Veldt AA, Smit EF. Bevacizumab in neoadjuvant treatment for breast cancer. *N Engl J Med* (2012) **366**:1637–40. doi:10.1056/NEJMcl202229

Conflict of Interest Statement: The authors declare that the research was conducted in the absence of any commercial or financial relationships that could be construed as a potential conflict of interest.

Received: 31 May 2013; paper pending published: 26 June 2013; accepted: 30 July 2013; published online: 13 August 2013.

*Citation: van der Veldt AAM, Smit EF and Lammertsma AA (2013) Positron emission tomography as a method for measuring drug delivery to tumors in vivo: the example of [¹¹C]docetaxel. *Front. Oncol.* **3**:208. doi:10.3389/fonc.2013.00208*

This article was submitted to Frontiers in Pharmacology of Anti-Cancer Drugs, a specialty of Frontiers in Oncology.

Copyright © 2013 van der Veldt, Smit and Lammertsma. This is an open-access article distributed under the terms of the Creative Commons Attribution License (CC BY). The use, distribution or reproduction in other forums is permitted, provided the original author(s) or licensor are credited and that the original publication in this journal is cited, in accordance with accepted academic practice. No use, distribution or reproduction is permitted which does not comply with these terms.



Vascular permeability and drug delivery in cancers

Sandy Azzi^{1,2,3†}, Jagoda K. Hebda^{1,2,3†} and Julie Gavard^{1,2,3*}

¹ CNRS, UMR8104, Paris, France

² INSERM, U1016, Paris, France

³ Sorbonne Paris Cite, Université Paris Descartes, Paris, France

Edited by:

Fabrizio Marcucci, Istituto Superiore di Sanità, Italy

Reviewed by:

Ronald Berenson, Compliment Corporation, USA

Raffaella Giavazzi, Istituto di Ricerche Farmacologiche "Mario Negri" – IRCCS, Italy

***Correspondence:**

Julie Gavard, Institut Cochin, 22 rue Mechain, Room 306, Paris 75014, France

e-mail: julie.gavard@inserm.fr

[†]Sandy Azzi and Jagoda K. Hebda have contributed equally to this work.

The endothelial barrier strictly maintains vascular and tissue homeostasis, and therefore modulates many physiological processes such as angiogenesis, immune responses, and dynamic exchanges throughout organs. Consequently, alteration of this finely tuned function may have devastating consequences for the organism. This is particularly obvious in cancers, where a disorganized and leaky blood vessel network irrigates solid tumors. In this context, vascular permeability drives tumor-induced angiogenesis, blood flow disturbances, inflammatory cell infiltration, and tumor cell extravasation. This can directly restrain the efficacy of conventional therapies by limiting intravenous drug delivery. Indeed, for more effective anti-angiogenic therapies, it is now accepted that not only should excessive angiogenesis be alleviated, but also that the tumor vasculature needs to be normalized. Recovery of normal state vasculature requires diminishing hyperpermeability, increasing pericyte coverage, and restoring the basement membrane, to subsequently reduce hypoxia, and interstitial fluid pressure. In this review, we will introduce how vascular permeability accompanies tumor progression and, as a collateral damage, impacts on efficient drug delivery. The molecular mechanisms involved in tumor-driven vascular permeability will next be detailed, with a particular focus on the main factors produced by tumor cells, especially the emblematic vascular endothelial growth factor. Finally, new perspectives in cancer therapy will be presented, centered on the use of anti-permeability factors and normalization agents.

Keywords: VEGF, permeability, VE-cadherin, endothelial barrier, tumor angiogenesis

VASCULAR PERMEABILITY IN CANCERS

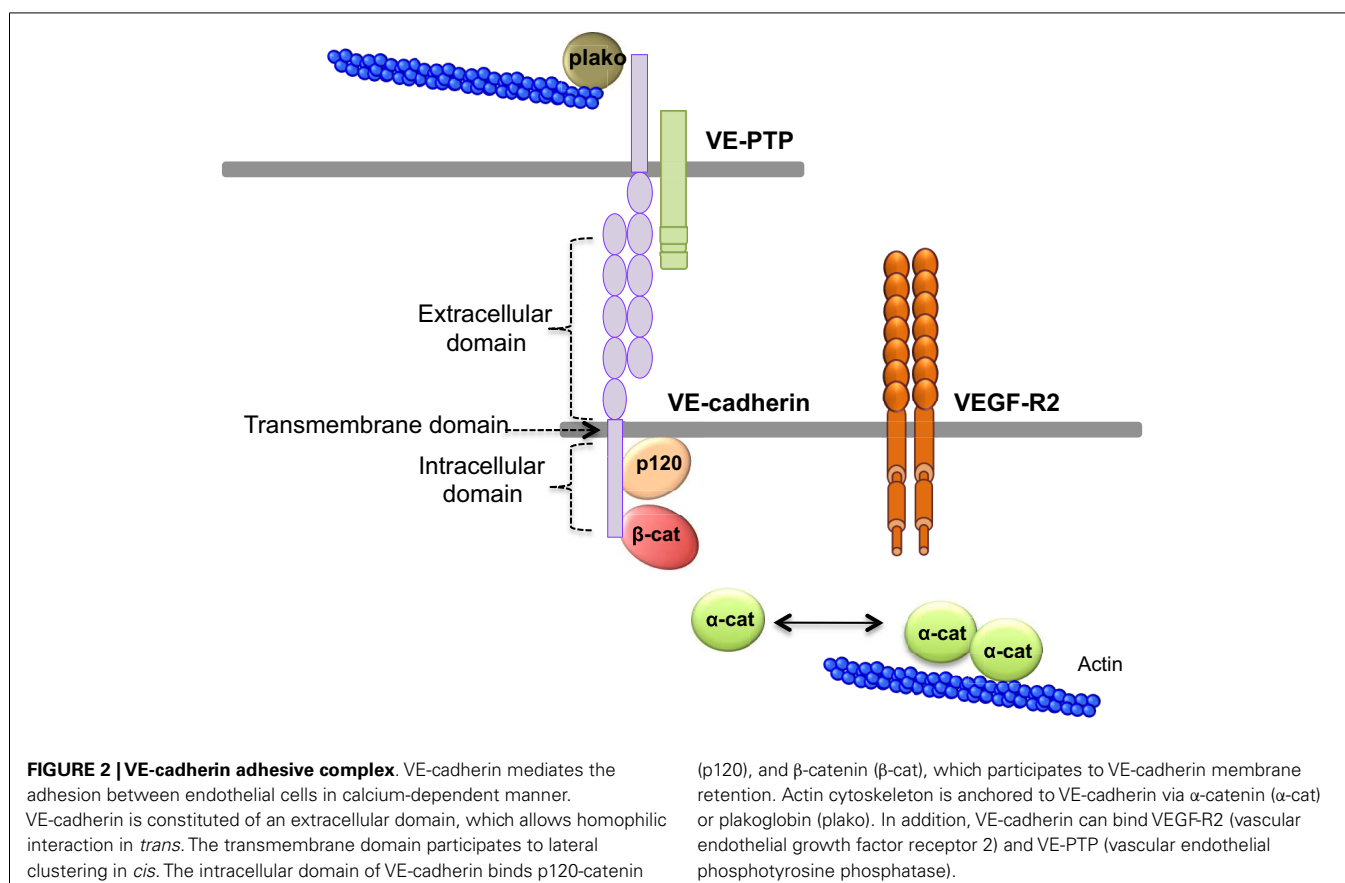
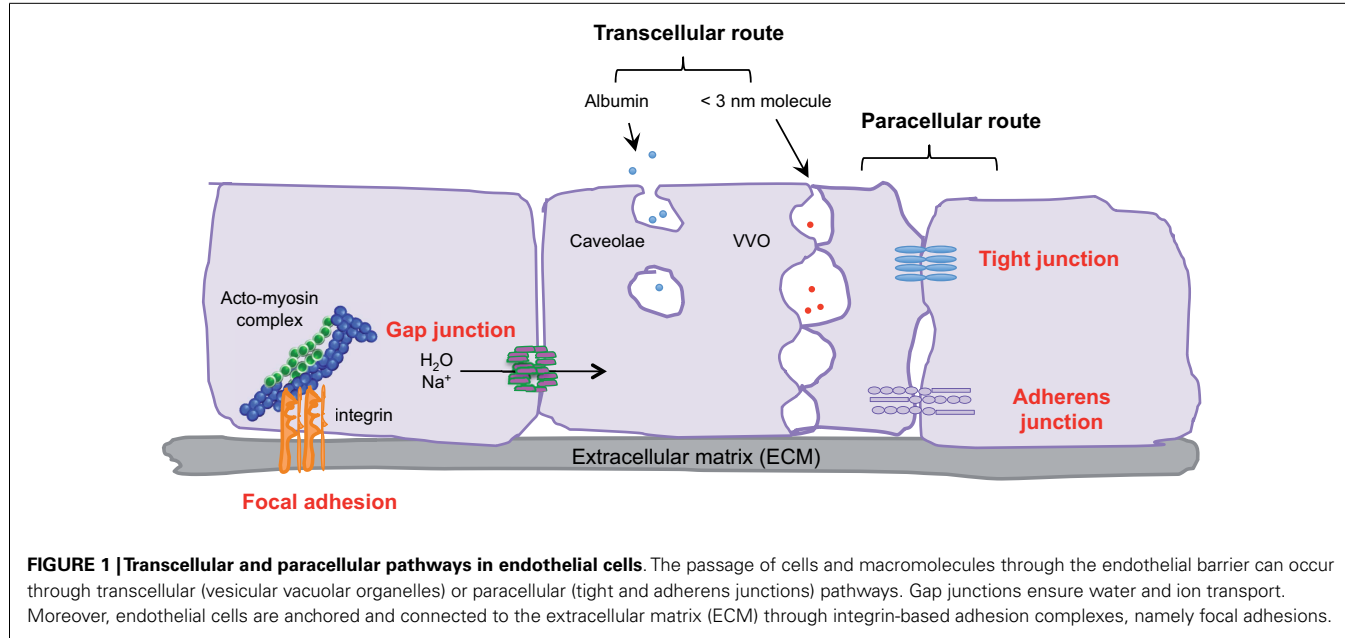
VASCULAR BARRIER ORGANIZATION

Endothelial cells, pericytes, smooth muscle cells, and the basal membrane collectively form the blood vascular wall, which ensures selective exchanges between plasma and irrigated tissues. The passage of macromolecules, fluids, and cells through this endothelial barrier can occur either through (transcellular) or between cells (paracellular) (1). The ability to pass from the interstitial space to the blood compartment, and *vice versa* depends on charge, size, and binding characteristics.

Small molecules (inferior to 3 nm) are commonly transported by the transcellular route, which requires a system of trafficking vesicles, called vesicular vacuolar organelles (VVOs) (Figure 1). Several permeability factors, such as vascular endothelial growth factor (VEGF) and histamine have been demonstrated to activate VVOs and to orchestrate vascular homeostasis (2). These VVOs comprise, among other things, clustered caveolae, and rely on caveolin-1 protein function, that notably guarantees albumin transport. Interestingly, caveolin-1 plays a dual regulatory role in microvascular permeability by stabilizing caveolae structures and allowing caveolar transcytosis, while acting as a negative regulator through endothelial nitric oxide synthase (eNOS) (3, 4).

Cells and macromolecules larger than 3 nm use the paracellular pathway, which is mediated by the coordinated opening and closing of endothelial cell–cell junctions. Adherens (A) and tight (TJ) junctions maintain the restrictiveness of the barrier, while gap junctions connect adjacent endothelial cells. Gap junctions

are responsible for water and ion transport but do not contribute significantly or directly to the establishment of vascular barriers (Figure 1). Among AJ proteins, the most important is vascular endothelial cadherin (VE-cadherin), which is exclusively expressed in vessels (1, 5). In mice, VE-cadherin gene deletion results in early embryonic lethality due to massive vascular defects, while loss of its function provokes a hyperpermeability phenotype in adults (6, 7). VE-cadherin comprises five immunoglobulin-like domain repeats in its extracellular region, one single-pass transmembrane domain and a short cytoplasmic tail. While the extracellular domain confers Ca⁺⁺ dependency and allows homophilic interaction in *trans* (i.e., between cadherins on neighboring cells), the transmembrane domain participates in lateral clustering within the same cell (*cis*) (8). The cytoplasmic part of VE-cadherin binds to proteins from the armadillo-repeat gene family, namely p120-catenin and either β-catenin or plakoglobin (γ-catenin). This complex serves to strengthen adhesion forces and allows dynamic contacts (Figure 2). p120-catenin interacts with the juxtamembrane part of the VE-cadherin cytoplasmic domain and is involved in its retention at the cell surface, while β/γ-catenins, on the other hand, act as constitutive partners of VE-cadherin, bound to its carboxy-terminal part (9, 10). Importantly, VE-cadherin is also connected to the actin cytoskeleton through the actin-binding protein, α-catenin (5). Other adhesive proteins that accumulate in or close to AJ, include N-cadherin, platelet-endothelial cell adhesion molecule (PECAM-1), and junctional adhesion molecules (JAMs).



Tight junctions participate in endothelial cell cohesion and block molecule diffusion along the apical and basolateral poles (11). They rely on transmembrane adhesion proteins (occludin

and claudins), JAM family proteins, and intracellular connectors, including ZO-1, -2, -3 (Zonula Occludens). First, occludin and claudins contain four transmembrane domains with

N- and C-terminal intracellular parts. Second, JAM-A belongs to the immunoglobulin superfamily with one intracellular short domain, one single transmembrane domain, and two extracellular immunoglobulin-like domains. Third, the ZO proteins contain three PDZ (post synaptic density protein PSD95, Drosophila disk large tumor suppressor Dlg1, and zonula occludens-1 protein zo-1), one SH3 (SRC homology 3) and one guanylyl kinase-like domains (11). Contrary to VE-cadherin, deletion of the claudin-5 gene does not impair mouse embryo development, but rather leads to post-natal death caused by a defective blood-brain barrier (12). Thus, VE-cadherin is instrumental in vascular barrier integrity, while claudins may have a more restrictive role (13). Nevertheless AJ and TJ are functionally and structurally linked and can influence each other (14, 15).

Within blood vessels, endothelial cells are interactively anchored to the extracellular matrix (ECM) through integrin-based adhesion complexes, namely focal adhesions (Figure 1). Indeed, integrins bridge the ECM to the acto-myosin contractility apparatus (16), and allow endothelial cells to adapt to extracellular signals and cues (e.g., shear stress and secreted molecules). From a molecular standpoint, Rho-GTPase activation, stress fiber formation, and acto-myosin contraction are finely tuned through integrin adhesion and collectively contribute to the modulation of endothelial junction integrity (17, 18). More recently, it was demonstrated that the integrin-associated focal adhesion tyrosine kinase (FAK) contributes to the impairment of vascular barrier function (19). Indeed, VEGF-induced FAK activation was shown to lead to VE-cadherin/FAK interaction in association with β -catenin phosphorylation on tyrosine Y142, resulting in VE-cadherin/ β -catenin dissociation, junction opening, and endothelial barrier disruption.

Hence, vascular barrier properties depend on both structural (basal membrane, smooth muscle cells, endothelial cells) and functional (VVO, AJ, TJ) features. To endorse this role, endothelial cell adhesion has to be tightly regulated. Indeed, aberrant and uncontrolled increase of vascular permeability can participate in the progression of many pathological states, such as chronic inflammatory diseases, diabetes, and tumor angiogenesis.

VASCULAR LEAKAGE IN THE TUMOR MICROENVIRONMENT

Compared to normal tissues, tumor vasculature is immature and exhibits structural abnormalities, such as dilatation, saccular formation, and a hyper-branched and twisted pattern. Moreover, solid tumors usually present few to none functional lymphatic vessels (20, 21). Many molecular and cellular factors contribute to this morphological and functional failure, in which vascular permeability is central. Rapidly growing tumors secrete an abundance of different factors (VEGF, chemokines, and others) that govern uncontrolled angiogenesis. In such microenvironments, most of the criteria that define the endothelial barrier properties are circumvented.

First, tumor vessels are characterized by extensive angiogenesis, i.e., neovessel formation from pre-existing vascular networks. In this scenario, tumor endothelial cells have a proliferation rate 50–200 times faster than that of normal quiescent endothelial cells (22). They also have to migrate and rearrange into vascular tubules, dedicated to fuel the tumor mass. This high endothelial plasticity in

the constantly remodeled vascular wall is accompanied by elevated permeability. Tumor vessel hyperpermeability correlates with faint VE-cadherin expression, opening of paracellular junctions, and transcellular holes formation (23). In the course of tumor growth, the direct consequence of hyperpermeable vessels is plasma membrane protein extravasation and formation of a provisory matrix to allow endothelial cell sprouting and formation of new vessels (24).

Morphologically, the pericytes surrounding tumor vessels are abnormally shaped and are weakly associated with endothelial cells (25). In addition, tumor blood vessels lack smooth muscles (Figure 3). Similarly, the basal membrane can be either unusually thick or totally absent (26). In these conditions, resistance to blood flow is increased, and thereby the efficacy in tumor blood supply is reduced. As a consequence, despite a high microvessel density, tumors are poorly vascularized with hyperpermeable vasculature. This could lead *in fine* to the accumulation of metabolic products (lactic and carbonic acids) and extracellular pH decrease (27). Tumor vessel defects also quell oxygen supply, frequently causing hypoxia in the tumor microenvironment. Hypoxia, in turn, supports tumor angiogenesis through the hypoxia-inducible transcription factors (HIF), and further elevates the expression of pro-angiogenic molecules, such as VEGF, TNF (tumor necrosis factor), and PDGF (platelet-derived growth factor). Interestingly, because of its involvement in chemo- and radio-resistance, as well as metastasis, hypoxia has been suggested as an adverse prognostic factor (28).

Within the tumor microenvironment, the ECM undergoes significant compositional modifications most notably by increasing the levels of expression of collagen-1, matrix metalloproteases (MMP)-1 and -2, and laminin-5 (29). For instance, collagen-1 deposit increases ECM stiffness, and this is related with poor prognosis and higher metastasis potential (30). In addition, ECM stiffness enhances integrin expression and promotes focal adhesion signaling, and consequently influences tumor cell malignancy (31).

In summary, abnormal blood vessels and lack of lymphatic vessels in tumors, as well as increased ECM stiffness and relatively high interstitial fluid pressure (IFP) collectively contribute to the functional outcome called enhanced permeability and retention (EPR). This phenomenon facilitates both macromolecule extravasation and retention. Whereas normal vessels form a selective barrier, limiting cell and macromolecule passage, the tumor vasculature is extremely leaky and not restrictive. Consequently, although these features could benefit to tumor angiogenesis and growth, anti-tumor drug delivery is rather limited.

IMPACT ON DRUG DELIVERY

To gain in bioavailability and selectivity toward tumor cells, therapeutic molecules must counteract biological and physical barriers, among which are endothelial transport and blood flow. Drug efflux pumps are one of the main obstacles that anti-cancer drugs must overcome. These transporters are highly expressed in a large panel of cancer cells, as well as in the blood-brain barrier, where they ensure drug detoxification (32, 33).

However, tumor vessels cannot ensure correct tumor blood perfusion, since they are structurally aberrant and hyperpermeable

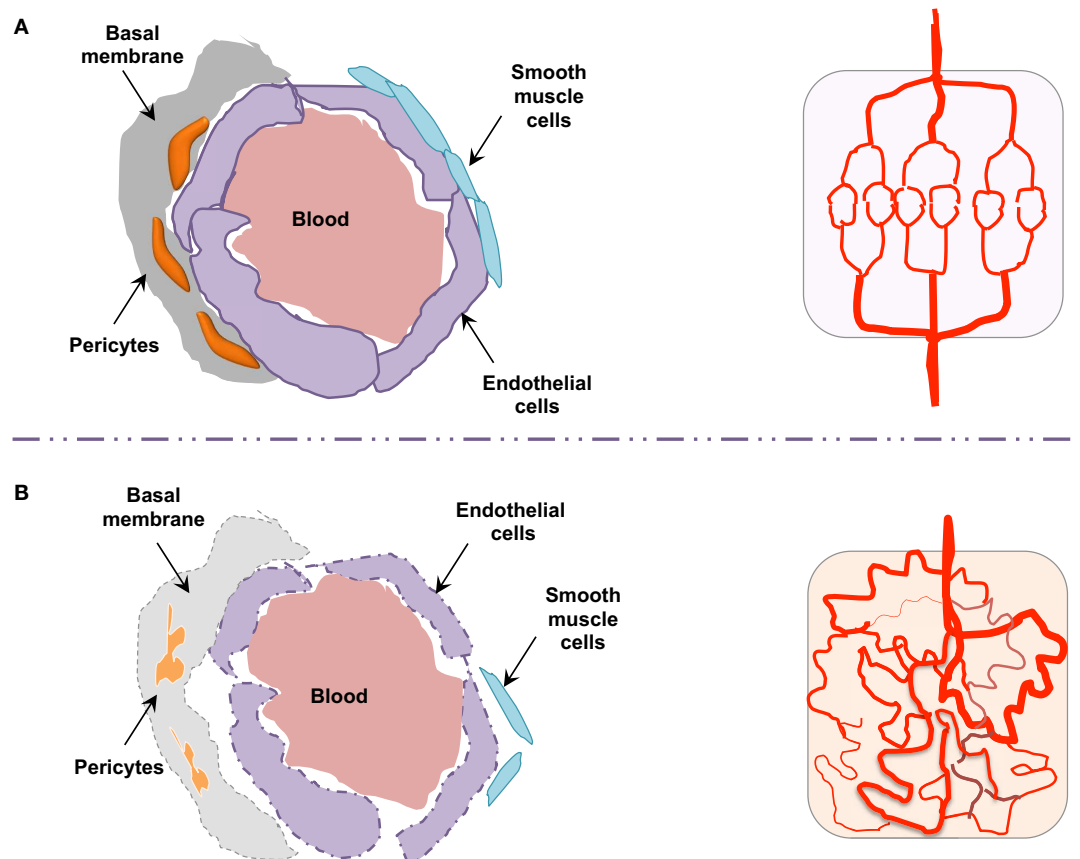


FIGURE 3 | Endothelial barrier in normal and tumor vessels. The endothelial barrier structure differs in normal (A) and tumor (B) blood vessels. Contrary to normal vessels, the tumor vasculature pattern is extremely

disorganized and anarchic, presents morphological and structural difference, i.e., weak association between endothelial cells, abnormal shapes of pericytes, lack of smooth muscles, as well as basal membrane modification.

(24). The pressure difference between vessels and surrounding tissues constitutes also an important physical barrier. Upon vascular leakage, transcapillary interstitial fluid flow decreases and IFP increases resulting in poor drug penetration through tumor vessels (21). In addition to blood vessel leakage, both the absence of a functional lymphatic system and increased ECM-frictional resistance also lead to tumor IFP increase (34). This ultimately provokes disruption in blood flow directions, again limiting drug delivery.

Importantly, tumor drug delivery can be tailored by changing the size and charge of the delivered molecule. Of interest, molecules larger than 40 kDa cannot be passively eliminated through renal clearance and are unable to cross normal blood vessels through endothelial junctions; however, they could easily penetrate tumors through leaky vessels. EPR of tumor vessels permits the passage of molecules ranging from 40 to 70 kDa, thus, in association with other properties such as the ability to traverse relatively long distances, prolonged plasma half-life and slow clearance, these larger molecule have been proposed to be the most appropriate for specific tumor delivery (35, 36). In addition, due to the negative charges of the vessel luminal face, the use of cationic therapeutic molecules may also favor vascular accumulation, which in turn can elevate tumor drug concentration (37).

Thus, although drug delivery is strongly impaired in tumors because of structural and functional vascular defects, some of these constraints, such as vessel leakiness, can be exploited for curative purposes.

MOLECULAR MECHANISMS INVOLVED IN VASCULAR PERMEABILITY

As presented above, endothelial barrier integrity ensures vascular and tissue homeostasis. In cancers, deregulation of this fine-tuned function leads to the formation of a chaotic blood vessel network associated with elevated permeability. We will now detail the molecular mechanisms involved in tumor-driven vascular permeability, focusing on the main factors produced by tumor cells, such as VEGF and chemokines. This knowledge could open new avenues for drug design.

VASCULAR ENDOTHELIAL GROWTH FACTOR

Vascular endothelial growth factor belongs to the family of platelet-derived growth factors and was originally referred to as vascular permeability factor (38). It is a homodimeric glycoprotein of which several forms have been described in mammals, these are: VEGF-A, B, C, D, and the placenta growth factor PIGF. Among these, VEGF-A is the most commonly studied and better described

in literature. Various cell types, such as endothelial cells, smooth muscle cells, fibroblasts, and immune cells (macrophages, lymphocytes, neutrophils, and eosinophils) can produce and release VEGF within the environment. In turn, VEGF can act in both an autocrine and paracrine manner. In cancers, tumor cells constitute an important source of VEGF. VEGF stimulates endothelial cell growth and promotes vasculogenesis and angiogenesis. It also increases vascular permeability, its first described function, in many tissues, and plays a crucial role in tumor vasculature development (22). VEGF intracellular signaling is mediated by three tyrosine kinase-receptors, namely VEGF-R1, -R2, and -R3, as well as co-receptors such as neuropilins. The binding of the ligand to its cognate receptors induces their dimerization, autophosphorylation, and subsequent signal transduction (39). VEGF-A interacts with both VEGF-R1 and -R2, but only VEGF-R2 is directly involved in normal and pathological vascular permeability (40). However, VEGF-R1 is reported to act as a regulator of VEGF-R2 signaling, and thus might indirectly regulate vascular permeability.

VEGF-A promotes vascular permeability by disruption of AJ and TJ, resulting in transient opening of endothelial cell–cell contacts (5, 14) (**Figure 4**). Indeed, VEGF-A promotes tyrosine phosphorylation of VE-cadherin and of its binding partners β -catenin, plakoglobin, and p120, in a Src-dependent mechanism (41). Consistent with this, VE-cadherin phosphorylation is inhibited in Src-deficient mice (41). VE-cadherin can also associate with VEGF-R2 and inhibit its phosphorylation and subsequent internalization (42). This association potentiates the phosphorylation of AJ components by Src, thus impairing endothelial barrier integrity and favoring tumor cell extravasation and dissemination in pathological models (43). The VE-cadherin/VEGF-R2 association also contributes to VE-cadherin-induced contact inhibition of cell growth and requires the β -, but not p120-catenin, binding domain of VE-cadherin (42, 44). In addition, VEGF-A mediates VE-cadherin phosphorylation and internalization via the sequential activation of Src, the guanine nucleotide exchange factor Vav2, the Rho-GTPase Rac, and its downstream effector, the serine-threonine kinase PAK (**Figure 4**). This signaling pathway culminates in the PAK-dependent phosphorylation of VE-cadherin, which directs its internalization (45). Moreover, VEGF signaling decreases VE-cadherin/p120-catenin association promoting clathrin-dependent VE-cadherin endocytosis (46). Indeed, p120 binding to VE-cadherin prevents its internalization, while its silencing by siRNA leads to VE-cadherin degradation, and loss of cell–cell contacts (10, 47). The expression of VE-cadherin mutants that compete with the endogenous molecule for binding with p120, triggers VE-cadherin degradation, suggesting that p120 might act as plasma membrane retention signal. More recently, a motif within VE-cadherin was identified to be responsible for VE-cadherin/p120 coupling and endocytosis sorting (48). In this context, VE-cadherin-mediated cell–cell contacts are stabilized by the small GTPase Rap1 and its effector, the cyclic adenosine monophosphate (cAMP)-activated guanidine exchange factor Epac (49, 50). Small GTPases also regulate myosin light chain (MLC) phosphorylation, acto-myosin contractility, and endothelial permeability (51). Indeed, VEGF induces the phosphorylation of MLC that results in the formation of stress fibers which exert centripetal tension on intercellular junctions (52).

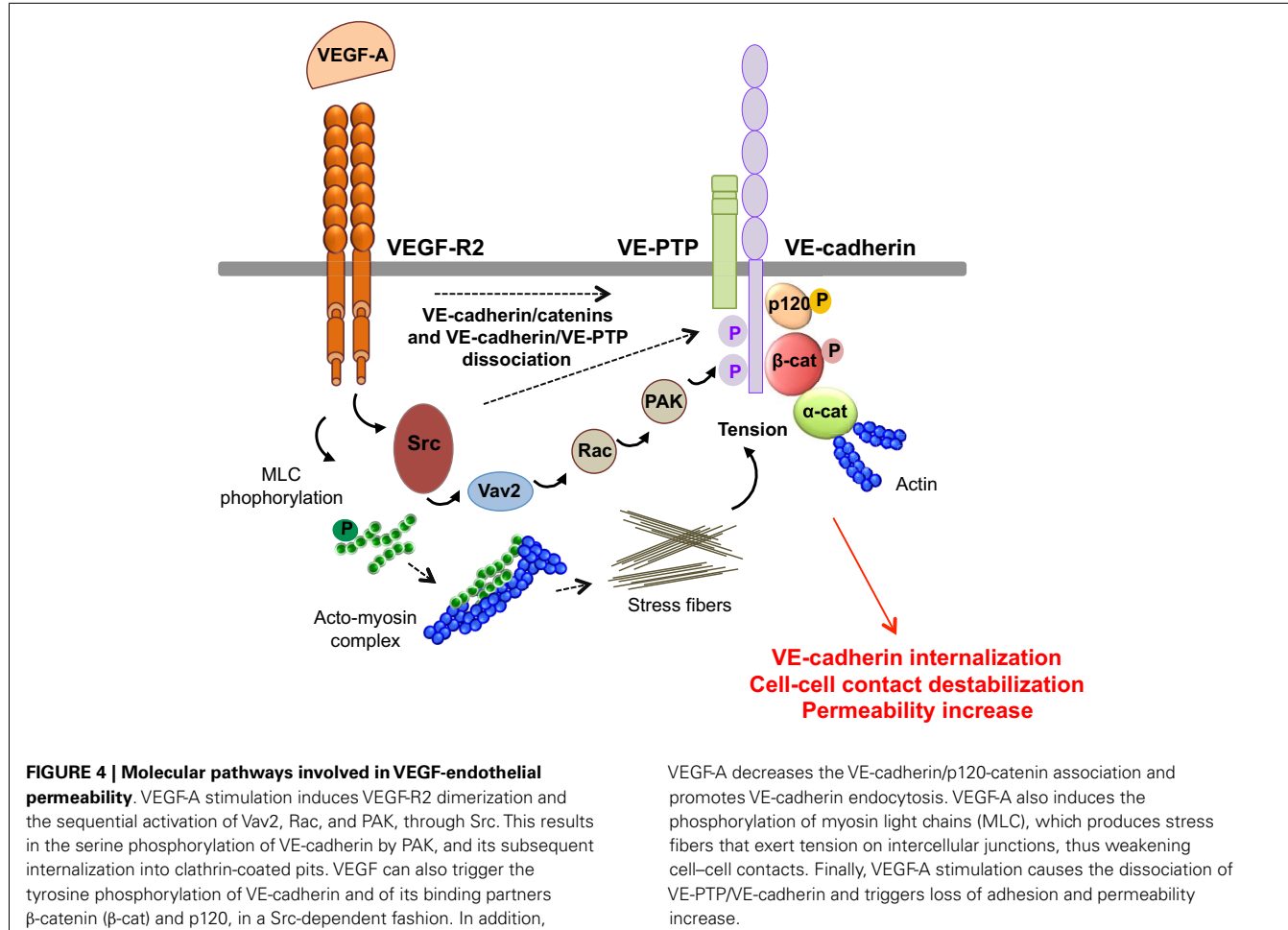
Of note, endothelial permeability can also be regulated through changes in the expression of AJ and TJ components (15, 53). For example, VEGF signaling through VEGF-R2 induces the expression of SRF (serum response factor), which is important for VE-cadherin expression (54). Indeed, SRF knockdown in mice reduces VE-cadherin expression and angiogenesis. Furthermore, claudin-5 expression is regulated by VE-cadherin, confirming that the latter is instrumental in controlling endothelial barrier function (15). Recently, it has been described that VEGF is involved in claudin-5 down-regulation in peritoneal endothelium, inducing ascites in ovarian cancer patients (55).

INTERLEUKIN-8

Cytokines are key drivers of immune responses and play important roles in cancer progression. Among these, the chemokine IL-8 (CXCL8, CXC chemokine ligand 8) is overexpressed and secreted by cancerous cells. Of note, their cognate G-protein-coupled receptors (GPCR), CXCR1 and CXCR2, are expressed on endothelial cells, tumor cells, and neutrophils/tumor-associated-macrophages, indicative of pleiotropic activities of IL-8. Activation of IL-8 endothelial receptors is known to promote angiogenic responses, through enhanced proliferation, survival, and migration (56). Furthermore, intratumoral IL-8 concentration is proposed to chiefly cause neutrophil recruitment into the tumor microenvironment and to promote metastasis (57). Besides its chemotactic role, IL-8 arose as an essential factor of angiogenesis and increased vascular permeability (58). Indeed, IL-8 can provoke VEGF-R2 phosphorylation and transactivation, which in turn result in both Src and RhoA activation, leading to endothelial gap formation, and elevated permeability (59). IL-8 can also increase permeability in mouse and human endothelial cells via a VEGF-R2 independent mechanism (60). IL-8 initiates a signaling route through CXCR2/Rac/PI3K γ that triggers the phosphorylation and subsequent internalization of VE-cadherin, thereby promoting increased permeability. Moreover, blockade of CXCR2 and PI3K γ with pharmacological inhibitors or by RNA interference (RNAi), limits IL-8-induced neovascularization and vessel leakage (60). In glioblastoma, cancer cells were found to secrete high concentrations of IL-8, which was further demonstrated to function as a key factor involved in tumor-induced permeability *in vitro*, and to signal to brain microvascular endothelial cells via CXCR2, promoting VE-cadherin cell–cell junction remodeling, and elevated permeability (61). Similarly, in prostate cancers, IL-8 secretion is associated with increased Akt expression and activation, which impacts on endothelial cell survival, angiogenesis, and cell migration (62).

TRANSFORMING GROWTH FACTOR- β 1

TGF- β 1 is a multifunctional polypeptide member of the transforming growth factor beta superfamily. It regulates the production of cytokines and ECM components, and is involved in diverse biological processes, such as proliferation and differentiation in many cell types (63–65). Within the tumor microenvironment, macrophages, mesenchymal, and cancer cells secrete TGF- β 1 under hypoxic and inflammatory conditions. TGF- β 1 was suggested to act as a potent inducer of angiogenesis, since its increased expression correlates with high microvessel density



and poor prognosis in various types of cancers (66). TGF- β 1 also augments vascular permeability by altering cell-cell contacts. This is thought to involve p38 mitogen-activated protein kinase (MAPK) and RhoA signaling cascades, which in turn modulate ECM adhesion and lead to the loss of endothelial-barrier integrity and function (67). In primary breast tumors, TGF- β 1 activity is associated with an increased risk of lung metastasis. Indeed, angiopoietin-related protein 4 (ANGPTL4), a TGF- β 1 target gene, disrupts endothelial cell-cell junctions, and facilitates the extravasation of breast cancer cells (68). Moreover, TGF- β 1 induces the expression of VEGF in fibroblasts (69), whereas it inhibits angiopoietin-1, an anti-permeability factor, therefore exacerbating tumor-associated vascular leakage (70). In addition, TGF- β 1 potentiates the secretion and activation of MMPs (71).

STROMAL CELL-DERIVED FACTOR 1

Stromal cell-derived factor 1, also known as CXCL12, is a member of the α -chemokine subfamily and the ligand for the GPCR CXCR4. In adulthood, SDF-1 was implicated in angiogenesis by recruiting endothelial progenitor cells from the bone marrow (72). SDF-1 is highly expressed in a number of cancers and is associated with tumor extravasation and increased metastases (73, 74). CXCR4 expression also corroborates with metastatic properties

of breast cancer cells (75). Indeed, CXCR4 levels were found to be higher in malignant breast tumors in comparison to those of normal healthy counterparts. *In vivo*, neutralizing CXCR4/SDF-1 signaling axis significantly impaired breast cancer cell extravasation and propagation (75, 76). SDF-1 can also mediate endothelial permeability via CXCR4, as for instance, SDF-1 stimulation of breast cancer cells *in vitro* increased their passage across the endothelial barrier. This effect is dependent on both PI3K/Akt and calcium signaling in endothelial cells (77). Inhibiting this pathway with anti-CXCR4 antibodies, on the other hand, decreased vascular leakage (77). Moreover, SDF-1 is involved in macrophage recruitment to breast tumors in mice, in response to chemotherapy (78). This action is believed to stimulate tumor blood vessel growth, counteracting the effects of the drug. Finally, it is to be noted that VEGF stimulates SDF-1 secretion and *vice versa* (79, 80). However, VEGF implication in SDF-1-induced permeability remains to be elucidated.

INTERLEUKIN-10

IL-10, also known as human cytokine synthesis inhibitory factor, is an anti-inflammatory cytokine. The role of IL-10 in cancers, though well accepted, is vaguely understood (81). Indeed, IL-10 is suspected to exert both pro- and anti-tumor activities, and

contradictory results have been reported regarding its involvement in tumor angiogenesis. On one hand, IL-10 could hamper angiogenesis and tumor growth in mice bearing VEGF-producing ovarian cancer (82), and suppress tumor growth and metastasis of human melanoma cells (83). On the other hand, other studies have suggested that IL-10 may promote angiogenesis in a melanoma cell model, by inhibiting macrophage functions and inducing tumor and vascular cell proliferation (84).

MATRIX METALLOPROTEINASES

Metalloproteinases are a large family of proteases that include MMP and ADAM (a disintegrin and metalloproteinase). MMPs belong to a family of zinc-containing endopeptidases that degrade various components of the ECM. Their aberrant over-expression correlates with cancer progression, cell invasion, and metastasis (85). Tumor-associated macrophages secrete VEGF and MMP-9, which are directly involved in both breast cancer and colorectal cancer cell invasion and metastasis (86). In addition, MMPs promote tumor progression by rearrangement of the ECM. Indeed, they trim cell adhesion molecules and degrade matrix proteins, favoring cell proliferation, and angiogenesis. MMP-7 can shed VE-cadherin, while MMP-2 and MMP-9 are involved in occludin proteolysis, thus enhancing endothelial permeability (87, 88). MMPs can also potentiate vascular leakage in a more indirect fashion, via cleavage and activation of chemokines such as IL-8, which is processed by MMP-9 (89, 90). Moreover, *in vitro* experiments have demonstrated a role for ADAM10 and ADAM17 in endothelial gap formation in response to cytokines. This is probably mediated by the cleavage of adhesion molecules within cell–cell junctions, including VE-cadherin and JAM-A (91).

SEMAPHORINS

Semaphorins correspond to a family of secreted and membrane-bound proteins that can act as both attractive and repulsive guidance molecules (92, 93). Besides their role in neural development, some of these molecules can modulate endothelial plasticity (94). Indeed, semaphorin 4D plays a positive role in endothelial migration and tumor angiogenesis (95, 96). In contrast, class 3 semaphorins, notably semaphorin 3A (S3A), and semaphorin 3E, are reported to operate as selective inhibitors of VEGF-induced angiogenesis (97–100). However, S3A and VEGF can also cooperate to induce vascular permeability (101). Indeed, S3A induces Akt phosphorylation through PI3K signaling, thus enhancing vascular permeability (101). In glioblastoma, the cancer stem-like cell sub-population expresses and secretes S3A *ex vivo* (102). In this context, S3A mediates endothelial cell–cell junction destabilization and elevates endothelial permeability (102). On a molecular level, S3A disrupts the VE-cadherin/PP2A complex, allowing VE-cadherin serine phosphorylation and subsequent internalization (45, 102). Consistent with this, inhibition of S3A by blocking antibody or by silencing RNAs has been demonstrated to abrogate these effects.

NITRIC OXIDE AND PEROXYNITRITE

Nitric oxide (NO) is a highly reactive free radical, which mediates a myriad of cellular reactions (103). NO is produced from L-arginine and oxygen by NO synthases (NOS). There are three

major NOS isoforms: inducible NO synthase (NOS2/iNOS), eNOS (NOS3/eNOS), and neuronal NO synthase (NOS1/nNOS). NOS3 is constitutively expressed in endothelial cells, cardiac myocytes, and hippocampal pyramidal cells and is involved in suppressing platelet aggregation, maintaining vascular tone, inhibiting smooth muscle cell proliferation, and prompting angiogenesis (104). In cancers, NOS3 generates NO in blood vessels, which can favor endothelial proliferation, migration, and tumor progression (105, 106). Of note, NOS3 can be induced by VEGF in a MAPK/PLC- γ -dependent manner (107). NOS3 may also be involved in modulating vascular leakage. Indeed, it has been reported that eNOS translocation to the cytosol, but not to the Golgi, is associated with hyperpermeability *in vitro* and *in vivo* (108, 109). Stimulation of endothelial cells with platelet-activating factor (PAF) induces S-nitrosylation of β -catenin and p120 and significantly diminishes their association with VE-cadherin (110). Furthermore, VEGF treatment elicited S-nitrosylation of β -catenin at the Cys619 residue, within the VE-cadherin interaction site (111). Inhibition of β -catenin S-nitrosylation prevents NO-dependent dissociation of β -catenin from VE-cadherin and disassembly of AJ complexes, thereby inhibiting VEGF-mediated endothelial permeability (111). Moreover, oxidized products of NO, such as peroxynitrite (ONOO $^-$), activate MMPs, which favor matrix rearrangement and endothelial permeability as discussed above. However, NO can induce cytotoxic effects on cancer cells. The balance between NO-mediated permeability and angiogenesis or apoptosis should thus be considered in tumor-targeted therapy (112).

In conclusion, endothelial permeability-mediated signaling pathways converge at the disruption and destabilization of cell–cell contacts, promoting AJ and TJ restructuration and subsequent opening of endothelial cell–cell junctions. We will now present the anti-permeability factors and normalization agents that may represent new perspectives in cancer therapy.

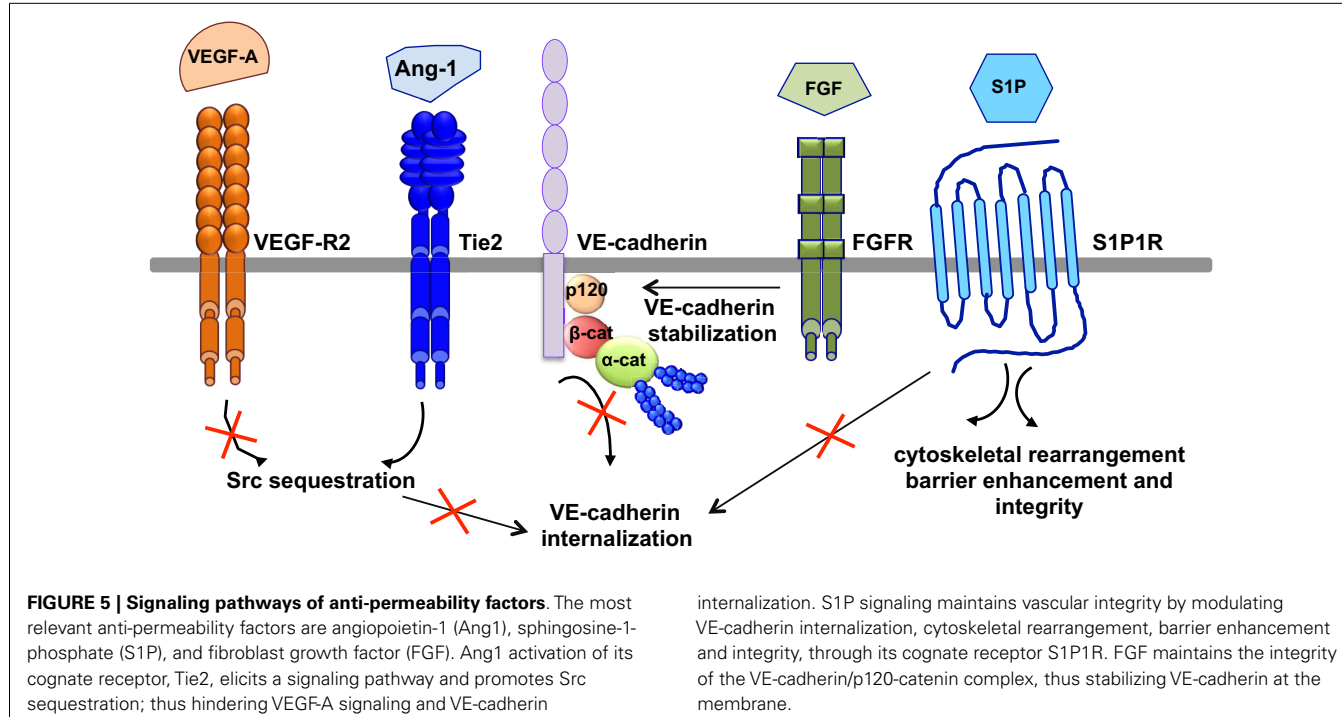
PERSPECTIVES IN CANCER THERAPY

It is now well accepted that vascular permeability limits drug delivery thus restraining the efficacy of conventional therapies. New approaches aim now at diminishing both excessive angiogenesis and hyperpermeability. In this paragraph, perspectives in cancer therapy, such as the use of anti-permeability factors and blood vessel normalization agents will be discussed.

ANTI-PERMEABILITY FACTORS

The most relevant anti-permeability factors are angiopoietin-1 and its cognate receptor Tie2, sphingosine-1-phosphate (S1P), and fibroblast growth factor (FGF) (**Figure 5**).

Angiopoietin-1 is a potent pro-angiogenic factor with the particularity of stabilizing blood vessels and counteracting VEGF-induced vascular permeability (63, 113). As mentioned above, VEGF elevates endothelial permeability via VE-cadherin adhesion destabilization in a Src-dependent mechanism (41, 45). Angiopoietin-1 elicits a signaling pathway through Tie2 that promotes the sequestration of Src though mammalian diaphanous (mDia) (114), thus hindering VEGF signaling and VE-cadherin internalization. In an intact endothelial monolayer, angiopoietin-1 promotes the interaction of Tie2 with the vascular endothelial protein tyrosine phosphatase VE-PTP (115,



116). VE-PTP associates with VE-cadherin and stabilizes it at the plasma membrane by blocking its tyrosine phosphorylation in response to VEGF-R2 activation (117). Angiopoietin-1 also maintains the barrier integrity by increasing the association between VE-cadherin and plakoglobin (118), thus strengthening cell–cell contacts and limiting endothelial permeability. Consistently, VEGF signaling *in vivo* triggers the dissociation of VE-PTP from VE-cadherin, facilitating leukocyte extravasation and vessel leakage (119). Furthermore, angiopoietin-1 balances VEGF pro-permeability actions by controlling NO release from endothelial cells. Indeed, it increases eNOS phosphorylation on Thr497, and subsequently reduces NO release and transendothelial permeability (120).

In addition to angiopoietin-1, S1P, a biologically active phosphorylated lipid growth factor released from activated platelets, has emerged as an endothelial barrier protective agent. In both pulmonary artery and lung microvascular endothelial cells, S1P was able to reverse barrier dysfunctions elicited by thrombin (121). At the molecular level, S1P signaling maintains vascular integrity by cytoskeletal rearrangement and barrier enhancement through Rac activation (121). Moreover, high-density lipoproteins, acting as major plasma carriers for S1P, promote endothelial-barrier integrity via the Akt signaling pathway (122). Plasma-derived S1P also plays an essential role in maintaining vascular integrity. Indeed, mutant mice engineered to selectively lack S1P in plasma show increased vascular leak and impaired survival after administration of permeability inducing factors (123). Elevated leak was associated with interendothelial cell gaps in venules and was reversed by acute treatment with an agonist for the S1P receptor 1 (S1PR1) (123). Furthermore, recent works present S1PR1, as a key component of vascular stability (124, 125). These two studies elegantly showed that S1PR1 inhibits VEGF-induced VE-cadherin

internalization. S1P signaling maintains vascular integrity by modulating VE-cadherin internalization, cytoskeletal rearrangement, barrier enhancement and integrity.

Other factors, such as FGF, can act as VE-cadherin stabilizing agents. Indeed, the inhibition of FGF signaling results in the dissociation of the VE-cadherin/p120-catenin complex, and subsequent VE-cadherin internalization, disassembly of AJ and TJ, and loss of vascular barrier integrity (126).

Thus, since they counteract VEGF-induced permeability and contribute to the maintenance of vascular barrier function, anti-permeability factors appear as potential therapeutic candidates. Another promising approach is the use of anti-VEGF/VEGFR drugs to promote normalization of the vascular wall and its microenvironment.

NORMALIZATION AGENTS

From 1950 to the 2000s, the only existing non-invasive treatment for solid tumors has been chemotherapy, which is mainly based on reducing tumor cell proliferation. Because its lack of selectivity causes a large panel of side effects, new strategies, such as molecular and personalized therapies, attempt to focus on molecules overexpressed in cancers. Unfortunately, the results from clinical trials targeting such molecules in anti-cancer therapy have been quite disappointing with an overall low extension of survival, with the exception of imatinib, a tyrosine kinase inhibitor (TKI) used in chronic myelogenous leukemia treatment (127). In addition, anti-angiogenic molecules have been suggested to improve anti-cancer therapy, not only because they reduce tumor vascularization, but also thanks to their “normalization” action, which improves drug delivery.

Bevacizumab (commercialized as Avastin) was one of the first clinically available anti-angiogenic drugs. This humanized mouse antibody targeting VEGF was FDA-approved about a decade ago

for combination use with standard chemotherapy in colorectal and non-small cell lung cancers. In addition, bevacizumab alone can significantly curb disease progression in patients with metastatic renal cell cancer (128). Recently published data suggest promising clinical efficacy of bevacizumab monotherapy in metastatic melanoma (129). Beside anti-VEGF, broad-spectrum multi-target TKI prolong cancer-free survival by collectively decreasing tumor vessel diameter, density, and permeability, even when administered in the absence of conventional therapies. For instance, sunitinib and sorafenib monotherapies appear particularly efficient in gastrointestinal and renal cancers (130). Nevertheless, both bevacizumab and TKI can cause serious adverse effects, such as gastrointestinal perforations.

The Notch ligand delta-like 4 (Dll4) has recently emerged as a critical regulator of tumor angiogenesis (131). Activation of the Notch pathway in neighboring endothelial cells causes inhibition of tip cell formation, an early event in sprouting angiogenesis. Mechanistically, this is believed to occur through the down-regulation of VEGF-R2/3 pro-angiogenic pathway and the up-regulation of VEGF-R1 anti-angiogenic pathway (132). Interestingly, VEGF can also operate upstream of Dll4 to potentiate its effects (133). However, the exact role of Dll4 in tumor growth and its potential in anti-cancer therapy remain unclear. Indeed, Dll4/Notch activation reduces overall tumor angiogenesis, while tumor vascular function was improved and tumor growth was heightened (134). This supports the notion that further strategy in anti-cancer therapy could be based on Dll4/Notch signaling blockade. On the other hand, Dll4-driven Notch activation might reduce both tumor-induced angiogenesis and endothelial cell responsiveness to VEGF (135), and therefore argue rather for the use of Dll4 as an effective therapeutic approach in cancers.

COMBINATION THERAPY AND FUTURE STRATEGIES

Recently, based on general hallmarks of the tumor vasculature, i.e., poor blood flow, leakage, and reduced drug uptake, a new trend in anti-cancer treatment has emerged, that involves combining vascular normalization agents with traditional therapies to improve treatment response.

To re-establish an efficient tumor vascularization, assistant molecules, namely those bearing anti-angiogenic or anti-permeability properties, have been designed and tested in clinical trials, in parallel with cytotoxic drugs. In this scenario, the use of either the vasoconstrictor Angiotensin II (136) or the vasodilator Bradykinin B2 receptor agonist (137) improves tumor treatment uptake, through an increase in transcapillary pressure. Similarly, to facilitate stromal barrier crossing, the ECM-degrading enzyme collagenase (138) was shown to exert favorable changes in the transcapillary pressure gradient and thereby enhance anti-cancer drug penetration.

Alternatively, bevacizumab, the anti-VEGF drug, impinges on both microvascular density and tumor IFP, and improves drug uptake in colorectal carcinoma patients (139). Moreover, pazopanib, an inhibitor of VEGF and PDGF receptors, induces better tumor liposomal drug delivery (140). Likewise, radiotherapy combined with anti-integrin antibody (intetumumab) reduces

tumor vessel density, while increasing tumor cell apoptosis and hindering metastasis (141). Interestingly, apart from its role in permeability, high levels of VEGF have been reported to promote T-reg proliferation, inhibit antigen-presenting cell maturation and as a consequence, decrease immune responses (142, 143). Therefore, anti-angiogenic drugs, especially those targeting VEGF actions, could improve cancer immunotherapy by stimulating tumor microenvironment immune responses (142). Although significant evidence has demonstrated the benefits of anti-VEGF therapies in cancer treatment, its general use is still controversial. First, significant increase in overall survival is observed only when bevacizumab is combined with standard chemotherapies. In addition, many patients exhibit resistance to anti-VEGF treatments, while timing and doses to be administered, cost and relapse effects raise some major concerns. Finally, vascular regrowth remains highly problematic. Indeed, a second wave of angiogenesis orchestrated by pro-angiogenic ligands of the FGF family could account for the short-term efficacy of VEGF-based anti-angiogenic therapies (144). Unlike bevacizumab, combination of TKI with conventional chemotherapy does not improve the outcome of anti-cancer treatment. In this scenario, use of erlotinib, a potent inhibitor of the epidermal growth factor receptor tyrosine kinase, with standard chemotherapy has failed to enhance tumor response or survival in lung carcinoma (145). Highly efficient TKI monotherapy could be combined with chemotherapy only when tumor cells become resistant to TKIs.

Alternatively, dose, schedule, and decreased toxicity may amend tumor responses. Contrary to standard chemotherapy, i.e., high doses with prolonged drug-free breaks, metronomic chemotherapy refers to chronic and equally spaced administration of low doses of cytotoxic drugs, without pauses. For example, reduced but continuous doses of cyclophosphamide suppressed tumor growth more effectively than canonical chemotherapy scheduling, even in drug-resistant tumors (146). Interestingly, metronomic chemotherapy exerts anti-tumor and anti-metastatic actions by decreasing VEGF serum concentration and increasing apoptosis of cancer cells (147). For those reasons, metronomic chemotherapy could be considered as an anti-angiogenic chemotherapy.

Importantly, the efficacy of anti-angiogenic therapy combined with cytotoxic conventional therapies (chemo- and/or radiotherapies) depends on optimal treatment scheduling. Indeed for each anti-cancer therapy, a “normalization window,” has to be determined to define period and doses necessary for tumor vessel normalization (148).

ACKNOWLEDGMENTS

The authors are thankful to the members from the Julie Gavard laboratory, especially Dr. J. Dwyer for comments on the manuscript. This research was funded by *Ligue nationale contre le cancer comité de Paris*, *Fondation ARC*, *Fondation pour la Recherche Médicale*, and by a Marie Curie International Reintegration Grant within The Seventh Framework Programme. Jagoda K. Hebda is supported by doctoral fellowship from Université Paris Descartes and Sandy Azzi by a post-doctoral fellowship from Fondation ARC.

REFERENCES

- Gavard J. Breaking the VE-cadherin bonds. *FEBS Lett* (2009) **583**:1–6. doi:10.1016/j.febslet.2008.11.032
- Feng D, Nagy JA, Hipp J, Dvorak HF, Dvorak AM. Vesiculo-vacuolar organelles and the regulation of venule permeability to macromolecules by vascular permeability factor, histamine, and serotonin. *J Exp Med* (1996) **183**:1981–6. doi:10.1084/jem.183.5.1981
- Schubert W, Frank PG, Woodman SE, Hyogo H, Cohen DE, Chow CW, et al. Microvascular hyperpermeability in caveolin-1 (−/−) knock-out mice. Treatment with a specific nitric-oxide synthase inhibitor, L-NAMe, restores normal microvascular permeability in Cav-1 null mice. *J Biol Chem* (2002) **277**:40091–8. doi:10.1074/jbc.M205948200
- Minshall RD, Sessa WC, Stan RV, Anderson RG, Malik AB. Caveolin regulation of endothelial function. *Am J Physiol Lung Cell Mol Physiol* (2003) **285**:L1179–83.
- Dejana E. Endothelial cell-cell junctions: happy together. *Nat Rev Mol Cell Biol* (2004) **5**:261–70. doi:10.1038/nrm1357
- Carmeliet P, Lampugnani MG, Moons L, Breviario F, Compernolle V, Bono F, et al. Targeted deficiency or cytosolic truncation of the VE-cadherin gene in mice impairs VEGF-mediated endothelial survival and angiogenesis. *Cell* (1999) **98**:147–57. doi:10.1016/S0092-674(00)81010-7
- Crosby CV, Fleming PA, Argraves WS, Corada M, Zanetta L, Dejana E, et al. VE-cadherin is not required for the formation of nascent blood vessels but acts to prevent their disassembly. *Blood* (2005) **105**:2771–6. doi:10.1182/blood-2004-06-2244
- Koch AW, Bozic D, Pertz O, Engel J. Homophilic adhesion by cadherins. *Curr Opin Struct Biol* (1999) **9**:275–81. doi:10.1016/S0959-440X(99)80038-4
- Huber AH, Stewart DB, Laurens DV, Nelson WJ, Weis WI. The cadherin cytoplasmic domain is unstructured in the absence of beta-catenin. A possible mechanism for regulating cadherin turnover. *J Biol Chem* (2001) **276**:12301–9. doi:10.1074/jbc.M010377200
- Xiao K, Allison DF, Buckley KM, Kottke MD, Vincent PA, Faundez V, et al. Cellular levels of p120 catenin function as a set point for cadherin expression levels in microvascular endothelial cells. *J Cell Biol* (2003) **163**:535–45. doi:10.1083/jcb.200306001
- Tsukita S, Furuse M, Itoh M. Multifunctional strands in tight junctions. *Nat Rev Mol Cell Biol* (2001) **2**:285–93. doi:10.1038/35067088
- Nitta T, Hata M, Gotoh S, Seo Y, Sasaki H, Hashimoto N, et al. Size-selective loosening of the blood-brain barrier in claudin-5-deficient mice. *J Cell Biol* (2003) **161**:653–60. doi:10.1083/jcb.200302070
- Kluger MS, Clark PR, Tellides G, Gerke V, Pober JS. Claudin-5 controls intercellular barriers of human dermal microvascular but not human umbilical vein endothelial cells. *Arterioscler Thromb Vasc Biol* (2013) **33**:489–500. doi:10.1161/ATVBAHA.112.300893
- Gavard J, Gutkind JS. VE-cadherin and claudin-5: it takes two to tango. *Nat Cell Biol* (2008) **10**:883–5. doi:10.1038/ncb0808-883
- Taddei A, Giampietro C, Conti A, Orsenigo F, Breviario F, Pirazzoli V, et al. Endothelial adherens junctions control tight junctions by VE-cadherin-mediated upregulation of claudin-5. *Nat Cell Biol* (2008) **10**:923–34. doi:10.1038/ncb1752
- Geiger B, Spatz JP, Bershadsky AD. Environmental sensing through focal adhesions. *Nat Rev Mol Cell Biol* (2009) **10**:21–33. doi:10.1038/nrm2593
- Schwartz MA, Shattil SJ. Signaling networks linking integrins and rho family GTPases. *Trends Biochem Sci* (2000) **25**:388–91. doi:10.1016/S0968-0004(00)01605-4
- Huvemeers S, Oldenburg J, Spanjaard E, Van Der Krogt G, Grigoriev I, Akhmanova A, et al. Vin-culin associates with endothelial VE-cadherin junctions to control force-dependent remodeling. *J Cell Biol* (2012) **196**:641–52. doi:10.1083/jcb.201108120
- Chen XL, Nam JO, Jean C, Lawson C, Walsh CT, Goka E, et al. VEGF-induced vascular permeability is mediated by FAK. *Dev Cell* (2012) **22**:146–57. doi:10.1016/j.devcel.2011.11.002
- Leu AJ, Berle DA, Lymboussaki A, Alitalo K, Jain RK. Absence of functional lymphatics within a murine sarcoma: a molecular and functional evaluation. *Cancer Res* (2000) **60**:4324–7.
- Wu M, Frieboes HB, McDougall SR, Chaplain MA, Cristini V, Lowengrub J. The effect of interstitial pressure on tumor growth: coupling with the blood and lymphatic vascular systems. *J Theor Biol* (2013) **320**:131–51. doi:10.1016/j.jtbi.2012.11.031
- Folkman J. Angiogenesis. *Annu Rev Med* (2006) **57**:1–18. doi:10.1146/annurev.med.57.121304.131306
- Hashizume H, Baluk P, Morikawa S, McLean JW, Thurston G, Roberge S, et al. Openings between defective endothelial cells explain tumor vessel leakiness. *Am J Pathol* (2000) **156**:1363–80. doi:10.1016/S0002-9440(10)65006-7
- Le Guelte A, Dwyer J, Gavard J. Jumping the barrier: VE-cadherin, VEGF and other angiogenic modifiers in cancer. *Biol Cell* (2011) **103**:593–605. doi:10.1042/BC20110069
- Morikawa S, Baluk P, Kaidoh T, Haskell A, Jain RK, McDonald DM. Abnormalities in pericytes on blood vessels and endothelial sprouts in tumors. *Am J Pathol* (2002) **160**:985–1000. doi:10.1016/S0002-9440(10)64920-6
- Baluk P, Morikawa S, Haskell A, Mancuso M, McDonald DM. Abnormalities of basement membrane on blood vessels and endothelial sprouts in tumors. *Am J Pathol* (2003) **163**:1801–15. doi:10.1016/S0002-9440(10)63540-7
- Tredan O, Galmarini CM, Patel K, Tannock IF. Drug resistance and the solid tumor microenvironment. *J Natl Cancer Inst* (2007) **99**:1441–54. doi:10.1093/jnci/djm135
- Keith B, Johnson RS, Simon MC. HIF1alpha and HIF2alpha: sibling rivalry in hypoxic tumour growth and progression. *Nat Rev Cancer* (2012) **12**:9–22.
- Seftor RE, Seftor EA, Koshikawa N, Meltzer PS, Gardner LM, Bilban M, et al. Cooperative interactions of laminin 5 gamma2 chain, matrix metalloproteinase-2, and membrane type-1-matrix metalloproteinase are required for mimicry of embryonic vasculogenesis by aggressive melanoma. *Cancer Res* (2001) **61**:6322–7.
- Barkan D, Green JE, Chambers AF. Extracellular matrix: a gatekeeper in the transition from dormancy to metastatic growth. *Eur J Cancer* (2010) **46**:1181–8. doi:10.1016/j.ejca.2010.02.027
- Levental KR, Yu H, Kass L, Lakins JN, Egeblad M, Erler JT, et al. Matrix crosslinking forces tumor progression by enhancing integrin signaling. *Cell* (2009) **139**:891–906. doi:10.1016/j.cell.2009.10.027
- Cordon-Cardo C, O'Brien JP, Casals D, Rittman-Grauer L, Biedler JL, Melamed MR, et al. Multidrug-resistance gene (P-glycoprotein) is expressed by endothelial cells at blood-brain barrier sites. *Proc Natl Acad Sci U S A* (1989) **86**:695–8. doi:10.1073/pnas.86.2.695
- Gottesman MM. Mechanisms of cancer drug resistance. *Annu Rev Med* (2002) **53**:615–27. doi:10.1146/annurev.med.53.082901.103929
- Netti PA, Berk DA, Swartz MA, Grodzinsky AJ, Jain RK. Role of extracellular matrix assembly in interstitial transport in solid tumors. *Cancer Res* (2000) **60**:2497–503.
- Seymour LW, Miyamoto Y, Maeda H, Brereton M, Strohalm J, Ulbrich K, et al. Influence of molecular weight on passive tumour accumulation of a soluble macromolecular drug carrier. *Eur J Cancer* (1995) **31A**:766–70. doi:10.1016/0959-8049(94)00514-6
- Fang J, Nakamura H, Maeda H. The EPR effect: unique features of tumor blood vessels for drug delivery, factors involved, and limitations and augmentation of the effect. *Adv Drug Deliv Rev* (2011) **63**:136–51. doi:10.1016/j.addr.2010.04.009
- Campbell RB, Fukumura D, Brown EB, Mazzola LM, Izumi Y, Jain RK, et al. Cationic charge determines the distribution of liposomes between the vascular and extravascular compartments of tumors. *Cancer Res* (2002) **62**:6831–6.
- Senger DR, Galli SJ, Dvorak AM, Perruzzi CA, Harvey VS, Dvorak HF. Tumor cells secrete a vascular permeability factor that promotes accumulation of ascites fluid. *Science* (1983) **219**:983–5. doi:10.1126/science.6823562
- Waltenberger J, Claesson-Welsh L, Siegbahn A, Shibuya M, Heldin CH. Different signal transduction properties of KDR and Flt1, two receptors for vascular endothelial growth factor. *J Biol Chem* (1994) **269**:26988–95.
- Olsson AK, Dimberg A, Kreuger J, Claesson-Welsh L. VEGF receptor signalling – in control of vascular function. *Nat Rev Mol Cell Biol* (2006) **7**:359–71. doi:10.1038/nrm1911
- Eliceiri BP, Paul R, Schwartzberg PL, Hood JD, Leng J, Cheresh

- DA. Selective requirement for Src kinases during VEGF-induced angiogenesis and vascular permeability. *Mol Cell* (1999) **4**:915–24. doi:10.1016/S1097-2765(00)80221-X
42. Lampugnani MG, Orsenigo F, Gagliani MC, Tacchetti C, Dejana E. Vascular endothelial cadherin controls VEGFR-2 internalization and signaling from intracellular compartments. *J Cell Biol* (2006) **174**:593–604. doi:10.1083/jcb.200602080
43. Weis S, Cui J, Barnes L, Cheresh D. Endothelial barrier disruption by VEGF-mediated Src activity potentiates tumor cell extravasation and metastasis. *J Cell Biol* (2004) **167**:223–9. doi:10.1083/jcb.200408130
44. Grazia Lampugnani M, Zanetti A, Corada M, Takahashi T, Balconi G, Breviario F, et al. Contact inhibition of VEGF-induced proliferation requires vascular endothelial cadherin, beta-catenin, and the phosphatase DEP-1/CD148. *J Cell Biol* (2003) **161**:793–804. doi:10.1083/jcb.200209019
45. Gavard J, Gutkind JS. VEGF controls endothelial-cell permeability by promoting the beta-arrestin-dependent endocytosis of VE-cadherin. *Nat Cell Biol* (2006) **8**:1223–34. doi:10.1038/ncb1486
46. Xiao K, Garner J, Buckley KM, Vincent PA, Chiasson CM, Dejana E, et al. p120-Catenin regulates clathrin-dependent endocytosis of VE-cadherin. *Mol Biol Cell* (2005) **16**:5141–51. doi:10.1091/mbc.E05-05-0440
47. Davis MA, Ireton RC, Reynolds AB. A core function for p120-catenin in cadherin turnover. *J Cell Biol* (2003) **163**:525–34. doi:10.1083/jcb.200307111
48. Nanes BA, Chiasson-Mackenzie C, Lowery AM, Ishiyama N, Faundez V, Ikura M, et al. p120-catenin binding masks an endocytic signal conserved in classical cadherins. *J Cell Biol* (2012) **199**:365–80. doi:10.1083/jcb.201205029
49. Cullere X, Shaw SK, Andersson L, Hirashiki J, Luscinskas FW, Mayadas TN. Regulation of vascular endothelial barrier function by Epac, a cAMP-activated exchange factor for Rap GTPase. *Blood* (2005) **105**:1950–5. doi:10.1182/blood-2004-05-1987
50. Fukuhara S, Sakurai A, Sano H, Yamagishi A, Somekawa S, Takakura N, et al. Cyclic AMP potentiates vascular endothelial cadherin-mediated cell-cell contact to enhance endothelial barrier function through an Epac-Rap1 signaling pathway. *Mol Cell Biol* (2005) **25**:136–46. doi:10.1128/MCB.25.1.136-146.2005
51. Stockton RA, Schaefer E, Schwartz MA. p21-activated kinase regulates endothelial permeability through modulation of contractility. *J Biol Chem* (2004) **279**:46621–30. doi:10.1074/jbc.M408877200
52. Wojciak-Stothard B, Ridley AJ. Rho GTPases and the regulation of endothelial permeability. *Vasc Pharmacol* (2002) **39**:187–99. doi:10.1016/S1537-1891(03)00008-9
53. Hebda JK, Leclair HM, Azzi S, Roussel C, Scott MG, Bidere N, et al. The C-terminus region of beta-arrestin1 modulates VE-cadherin expression and endothelial cell permeability. *Cell Commun Signal* (2013) **11**:37. doi:10.1186/1478-811X-11-37
54. Franco CA, Merickay M, Parlakian A, Gary-Bobo G, Gao-Li J, Paulin D, et al. Serum response factor is required for sprouting angiogenesis and vascular integrity. *Dev Cell* (2008) **15**:448–61. doi:10.1016/j.devcel.2008.07.019
55. Herr D, Sallmann A, Bekes I, Konrad R, Holzheu I, Kreienberg R, et al. VEGF induces ascites in ovarian cancer patients via increasing peritoneal permeability by down-regulation of Claudin 5. *Gynecol Oncol* (2012) **127**:210–6. doi:10.1016/j.ygyno.2012.05.002
56. Li A, Dubey S, Varney ML, Dave BJ, Singh RK. IL-8 directly enhanced endothelial cell survival, proliferation, and matrix metalloproteinases production and regulated angiogenesis. *J Immunol* (2003) **170**:3369–76.
57. De Larco JE, Wuertz BR, Furcht LT. The potential role of neutrophils in promoting the metastatic phenotype of tumors releasing interleukin-8. *Clin Cancer Res* (2004) **10**:4895–900. doi:10.1158/1078-0432.CCR-03-0760
58. Schraufstatter IU, Chung J, Burger M. IL-8 activates endothelial cell CXCR1 and CXCR2 through Rho and Rac signaling pathways. *Am J Physiol Lung Cell Mol Physiol* (2001) **280**:L1094–103.
59. Petreaca ML, Yao M, Liu Y, Defea K, Martins-Green M. Transactivation of vascular endothelial growth factor receptor-2 by interleukin-8 (IL-8/CXCL8) is required for IL-8/CXCL8-induced endothelial permeability. *Mol Biol Cell* (2007) **18**:5014–23. doi:10.1091/mbc.E07-01-0004
60. Gavard J, Hou X, Qu Y, Masedunskas A, Martin D, Weigert R, et al. A role for a CXCR2/phosphatidylinositol 3-kinase gamma signaling axis in acute and chronic vascular permeability. *Mol Cell Biol* (2009) **29**:2469–80. doi:10.1128/MCB.01304-08
61. Dwyer J, Hebda JK, Le Guellec A, Galan-Moya EM, Smith SS, Azzi S, et al. Glioblastoma cell-secreted interleukin-8 induces brain endothelial cell permeability via CXCR2. *PLoS One* (2012) **7**:e45562. doi:10.1371/journal.pone.0045562
62. MacManus CF, Pettigrew J, Seaton A, Wilson C, Maxwell PJ, Berlingeri S, et al. Interleukin-8 signaling promotes translational regulation of cyclin D in androgen-independent prostate cancer cells. *Mol Cancer Res* (2007) **5**:737–48. doi:10.1158/1541-7786.MCR-07-0032
63. Dumont N, Arteaga CL. A kinase-inactive type II TGFbeta receptor impairs BMP signaling in human breast cancer cells. *Biochem Biophys Res Commun* (2003) **301**:108–12. doi:10.1016/S0006-291X(02)02977-7
64. Siegel PM, Massague J. Cytostatic and apoptotic actions of TGF-beta in homeostasis and cancer. *Nat Rev Cancer* (2003) **3**:807–21. doi:10.1038/nrc1208
65. Bierie B, Moses HL. Tumour microenvironment: TGFbeta: the molecular Jekyll and Hyde of cancer. *Nat Rev Cancer* (2006) **6**:506–20. doi:10.1038/nrc1926
66. Hasegawa Y, Takanashi S, Kanehira Y, Tsushima T, Imai T, Okumura K. Transforming growth factor-beta1 level correlates with angiogenesis, tumor progression, and prognosis in patients with nonsmall cell lung carcinoma. *Cancer* (2001) **91**:964–71. doi:10.1002/1097-0142(20010301)91:5<964::AID-CNCR1086>3.3.CO;2-F
67. Goldberg PL, Macnaughton DE, Clements RT, Minnear FL, Vincent PA. p38 MAPK activation by TGF-beta1 increases MLC phosphorylation and endothelial monolayer permeability. *Am J Physiol Lung Cell Mol Physiol* (2002) **282**:L146–54.
68. Padua D, Zhang XH, Wang Q, Nadal C, Gerald WL, Gomis RR, et al. TGFbeta primes breast tumors for lung metastasis seeding through angiopoietin-like 4. *Cell* (2008) **133**:66–77. doi:10.1016/j.cell.2008.01.046
69. Pertovaara L, Kaipainen A, Mustonen T, Orpana A, Ferrara N, Saksela O, et al. Vascular endothelial growth factor is induced in response to transforming growth factor-beta in fibroblastic and epithelial cells. *J Biol Chem* (1994) **269**:6271–4.
70. Enholt B, Paavonen K, Ristimaki A, Kumar V, Gunji Y, Klefstrom J, et al. Comparison of VEGF, VEGF-B, VEGF-C and Ang-1 mRNA regulation by serum, growth factors, oncoproteins and hypoxia. *Oncogene* (1997) **14**:2475–83. doi:10.1038/sj.onc.1201090
71. Hagedorn HG, Bachmeier BE, Nierlich AG. Synthesis and degradation of basement membranes and extracellular matrix and their regulation by TGF-beta in invasive carcinomas (Review). *Int J Oncol* (2001) **18**:669–81.
72. Salcedo R, Oppenheim JJ. Role of chemokines in angiogenesis: CXCL12/SDF-1 and CXCR4 interaction, a key regulator of endothelial cell responses. *Microcirculation* (2003) **10**:359–70. doi:10.1080/mic.10.3-4.359.370
73. Dewan MZ, Ahmed S, Iwasaki Y, Ohba K, Toi M, Yamamoto N. Stromal cell-derived factor-1 and CXCR4 receptor interaction in tumor growth and metastasis of breast cancer. *Biomed Pharmacother* (2006) **60**:273–6. doi:10.1016/j.bioph.2006.06.004
74. Gassmann P, Haier J, Schluter K, Domikowsky B, Wendel C, Wiesner U, et al. CXCR4 regulates the early extravasation of metastatic tumor cells in vivo. *Neoplasia* (2009) **11**:651–61.
75. Muller A, Homey B, Soto H, Ge N, Catron D, Buchanan ME, et al. Involvement of chemokine receptors in breast cancer metastasis. *Nature* (2001) **410**:50–6. doi:10.1038/35065016
76. Yagi H, Tan W, Dillenburg-Pilla P, Armando S, Amornphimoltham P, Simaan M, et al. A synthetic biology approach reveals a CXCR4-G13-Rho signaling axis driving transendothelial migration of metastatic breast cancer cells. *Sci Signal* (2011) **4**:r460. doi:10.1126/scisignal.2002221
77. Lee BC, Lee TH, Avraham S, Avraham HK. Involvement of the chemokine receptor CXCR4 and its ligand stromal cell-derived factor 1alpha in breast cancer cell migration through human brain microvascular endothelial

- cells. *Mol Cancer Res* (2004) **2**: 327–38. doi:10.1172/JCI44562
78. Welford AF, Biziato D, Coffelt SB, Nucera S, Fisher M, Pucci F, et al. TIE2-expressing macrophages limit the therapeutic efficacy of the vascular-disrupting agent combretastatin A4 phosphate in mice. *J Clin Invest* (2011) **121**:1969–73. doi:10.1172/JCI44562
79. Kijowski J, Baj-Krzyworzeka M, Majka M, Reca R, Marquez LA, Christofidou-Solomidou M, et al. The SDF-1-CXCR4 axis stimulates VEGF secretion and activates integrins but does not affect proliferation and survival in lymphohematopoietic cells. *Stem Cells* (2001) **19**:453–66. doi:10.1634/stemcells.19-5-453
80. Salvucci O, Yao L, Villalba S, Sajewicz A, Pittaluga S, Tosato G. Regulation of endothelial cell branching morphogenesis by endogenous chemokine stromal-derived factor-1. *Blood* (2002) **99**:2703–11. doi:10.1182/blood.V99.8.2703
81. Hamidullah, Changkija B, Konwar R. Role of interleukin-10 in breast cancer. *Breast Cancer Res Treat* (2012) **133**:11–21. doi:10.1007/s10549-011-1855-x
82. Kohno T, Mizukami H, Suzuki M, Saga Y, Takei Y, Shimpo M, et al. Interleukin-10-mediated inhibition of angiogenesis and tumor growth in mice bearing VEGF-producing ovarian cancer. *Cancer Res* (2003) **63**:5091–4.
83. Huang S, Xie K, Bucana CD, Ullrich SE, Bar-Eli M. Interleukin 10 suppresses tumor growth and metastasis of human melanoma cells: potential inhibition of angiogenesis. *Clin Cancer Res* (1996) **2**:1969–79.
84. Garcia-Hernandez ML, Hernandez-Pando R, Gariglio P, Berumen J. Interleukin-10 promotes B16-melanoma growth by inhibition of macrophage functions and induction of tumour and vascular cell proliferation. *Immunology* (2002) **105**:231–43. doi:10.1046/j.1365-2567.2002.01363.x
85. Rundhaug JE. Matrix metalloproteinases, angiogenesis, and cancer: commentary re: A. C. Lockhart et al., Reduction of wound angiogenesis in patients treated with BMS-275291, a broad spectrum matrix metalloproteinase inhibitor. *Clin. Cancer Res.*, **9**: 00–00, 2003. *Clin Cancer Res* (2003) **9**:551–4.
86. Pollard JW. Tumour-educated macrophages promote tumour progression and metastasis. *Nat Rev Cancer* (2004) **4**:71–8. doi:10.1038/nrc1256
87. Ichikawa Y, Ishikawa T, Momiyama N, Kamiyama M, Sakurada H, Matsuyama R, et al. Matrilysin (MMP-7) degrades VE-cadherin and accelerates accumulation of beta-catenin in the nucleus of human umbilical vein endothelial cells. *Oncol Rep* (2006) **15**:311–5.
88. Reijerkerk A, Kooij G, Van Der Pol SM, Khazan S, Dijkstra CD, De Vries HE. Diapedesis of monocytes is associated with MMP-mediated occludin disappearance in brain endothelial cells. *FASEB J* (2006) **20**:2550–2. doi:10.1096/fj.06-6099fje
89. Van den Steen PE, Proost P, Wuyts A, Van Damme J, Opdenakker G. Neutrophil gelatinase B potentiates interleukin-8 ten-fold by aminoterminal processing, whereas it degrades CTAP-III, PF-4, and GRO-alpha and leaves RANTES and MCP-2 intact. *Blood* (2000) **96**:2673–81.
90. Van Den Steen PE, Wuyts A, Husson SJ, Proost P, Van Damme J, Opdenakker G. Gelatinase B/MMP-9 and neutrophil collagenase/MMP-8 process the chemokines human GCP-2/CXCL6, ENA-78/CXCL5 and mouse GCP-2/LIX and modulate their physiological activities. *Eur J Biochem* (2003) **270**:3739–49. doi:10.1046/j.1432-1033.2003.03760.x
91. Koenen RR, Pruessmeyer J, Soehnlein O, Fraemohs L, Zernecke A, Schwarz N, et al. Regulated release and functional modulation of junctional adhesion molecule A by disintegrin metalloproteinases. *Blood* (2009) **113**:4799–809. doi:10.1182/blood-2008-04-152330
92. Kolodkin AL, Matthes DJ, O'Connor TP, Patel NH, Admon A, Bentley D, et al. Fasciclin IV: sequence, expression, and function during growth cone guidance in the grasshopper embryo. *Neuron* (1992) **9**:831–45. doi:10.1016/0896-6273(92)90237-8
93. Kolodkin AL, Matthes DJ, Goodman CS. The semaphorin genes encode a family of transmembrane and secreted growth cone guidance molecules. *Cell* (1993) **75**:1389–99. doi:10.1016/0092-8674(93)90625-Z
94. Treps L, Le Guelte A, Gavard J. Emerging roles of semaphorins in the regulation of epithelial and endothelial junctions. *Tissue Barriers* (2013) **1**:e23272. doi:10.4161/tisb.23272
95. Basile JR, Holmbeck K, Bugge TH, Gutkind JS. MT1-MMP controls tumor-induced angiogenesis through the release of semaphorin 4D. *J Biol Chem* (2007) **282**: 6899–905. doi:10.1074/jbc.M609570200
96. Sierra JR, Corso S, Caione L, Cepero V, Conrotto P, Cignetti A, et al. Tumor angiogenesis and progression are enhanced by Sema4D produced by tumor-associated macrophages. *J Exp Med* (2008) **205**:1673–85. doi:10.1084/jem.20072602
97. Kessler O, Shraga-Heled N, Lange T, Gutmann-Raviv N, Sabo E, Baruch L, et al. Semaphorin-3F is an inhibitor of tumor angiogenesis. *Cancer Res* (2004) **64**:1008–15. doi:10.1158/0008-5472.CAN-03-3090
98. Varshavsky A, Kessler O, Abramovitch S, Kigel B, Zaffyayar S, Akiri G, et al. Semaphorin-3B is an angiogenesis inhibitor that is inactivated by furin-like proprotein convertases. *Cancer Res* (2008) **68**:6922–31. doi:10.1158/0008-5472.CAN-07-5408
99. Sakurai A, Gavard J, Annas-Linhabes Y, Basile JR, Amornphimoltham P, Palmby TR, et al. Semaphorin 3E initiates antiangiogenic signaling through plexin D1 by regulating Arf6 and R-Ras. *Mol Cell Biol* (2010) **30**:3086–98. doi:10.1128/MCB.01652-09
100. Wu F, Zhou Q, Yang J, Duan GJ, Ou JJ, Zhang R, et al. Endogenous axon guiding chemorepulsive semaphorin-3F inhibits the growth and metastasis of colorectal carcinoma. *Clin Cancer Res* (2011) **17**:2702–11. doi:10.1158/1078-0432.CCR-10-0839
101. Acevedo LM, Barillas S, Weis SM, Gothert JR, Chervosh DA. Semaphorin 3A suppresses VEGF-mediated angiogenesis yet acts as a vascular permeability factor. *Blood* (2008) **111**:2674–80. doi:10.1182/blood-2007-08-110205
102. Le Guelte A, Galan-Moya EM, Dwyer J, Treps L, Kettler G, Hebd JK, et al. Semaphorin 3A elevates endothelial cell permeability through PP2A inactivation. *J Cell Sci* (2012) **125**:4137–46. doi:10.1242/jcs.108282
103. Blaise GA, Gauvin D, Gangal M, Authier S. Nitric oxide, cell signaling and cell death. *Toxicology* (2005) **208**:177–92. doi:10.1016/j.tox.2004.11.032
104. Crowell JA, Steele VE, Sigman CC, Fay JR. Is inducible nitric oxide synthase a target for chemoprevention? *Mol Cancer Ther* (2003) **2**:815–23.
105. Jenkins DC, Charles IG, Thomsen LL, Moss DW, Holmes LS, Baylis SA, et al. Roles of nitric oxide in tumor growth. *Proc Natl Acad Sci U S A* (1995) **92**:4392–6. doi:10.1073/pnas.92.10.4392
106. Ambs S, Merriam WG, Bennett WP, Felley-Bosco E, Ogunfusika MO, Oser SM, et al. Frequent nitric oxide synthase-2 expression in human colon adenomas: implication for tumor angiogenesis and colon cancer progression. *Cancer Res* (1998) **58**:334–41.
107. Lala PK, Chakraborty C. Role of nitric oxide in carcinogenesis and tumour progression. *Lancet Oncol* (2001) **2**:149–56. doi:10.1016/S1470-2045(00)00256-4
108. Figueroa XF, Gonzalez DR, Martinez AD, Duran WN, Boric MP. ACh-induced endothelial NO synthase translocation, NO release and vasodilatation in the hamster microcirculation in vivo. *J Physiol* (2002) **544**:883–96. doi:10.1113/jphysiol.2002.021972
109. Sanchez FA, Savalia NB, Duran RG, Lal BK, Boric MP, Duran WN. Functional significance of differential eNOS translocation. *Am J Physiol Heart Circ Physiol* (2006) **291**:H1058–64. doi:10.1152/ajpheart.00370.2006
110. Marin N, Zamorano P, Carrasco R, Mujica P, Gonzalez FG, Quezada C, et al. S-Nitrosation of beta-catenin and p120 catenin: a novel regulatory mechanism in endothelial hyperpermeability. *Circ Res* (2012) **111**:553–63. doi:10.1161/CIRCRESAHA.112.274548
111. Thibeault S, Rautureau Y, Oubaha M, Faubert D, Wilkes BC, Delisle C, et al. S-nitrosylation of beta-catenin by eNOS-derived NO promotes VEGF-induced endothelial cell permeability. *Mol Cell* (2010) **39**:468–76. doi:10.1016/j.molcel.2010.07.013
112. Hussain SP, Hofseth LJ, Harris CC. Radical causes of cancer. *Nat Rev Cancer* (2003) **3**:276–85. doi:10.1038/nrc1046
113. Thurston G, Suri C, Smith K, McClain J, Sato TN, Yancopoulos GD, et al. Leakage-resistant blood vessels in mice transgenically over-expressing angiopoietin-1. *Science* (1999) **286**:2511–4. doi:10.1126/science.286.5449.2511
114. Gavard J, Patel V, Gutkind JS. Angiopoietin-1 prevents VEGF-induced endothelial permeability by sequestering Src through mDia.

- Dev Cell* (2008) **14**:25–36. doi:10.1016/j.devcel.2007.10.019
115. Fukuhara S, Sako K, Minami T, Noda K, Kim HZ, Kodama T, et al. Differential function of Tie2 at cell-cell contacts and cell-substratum contacts regulated by angiopoietin-1. *Nat Cell Biol* (2008) **10**:513–26. doi:10.1038/ncb1714
116. Saharinen P, Eklund L, Miettinen J, Wirkkala R, Anisimov A, Winderlich M, et al. Angiopoietins assemble distinct Tie2 signalling complexes in endothelial cell-cell and cell-matrix contacts. *Nat Cell Biol* (2008) **10**:527–37. doi:10.1038/ncb1715
117. Nawroth R, Poell G, Ranft A, Kloep S, Samulowitz U, Fachinger G, et al. VE-PTP and VE-cadherin ectodomains interact to facilitate regulation of phosphorylation and cell contacts. *EMBO J* (2002) **21**:4885–95. doi:10.1093/emboj/cdf497
118. Nottebaum AF, Cagna G, Winderlich M, Gamp AC, Linnepe R, Polaschegg C, et al. VE-PTP maintains the endothelial barrier via plakoglobin and becomes dissociated from VE-cadherin by leukocytes and by VEGF. *J Exp Med* (2008) **205**:2929–45. doi:10.1084/jem.20080406
119. Broermann A, Winderlich M, Block H, Frye M, Rossant J, Zarbock A, et al. Dissociation of VE-PTP from VE-cadherin is required for leukocyte extravasation and for VEGF-induced vascular permeability in vivo. *J Exp Med* (2011) **208**:2393–401. doi:10.1084/jem.20101525
120. Oubaha M, Gratton JP. Phosphorylation of endothelial nitric oxide synthase by atypical PKC zeta contributes to angiopoietin-1-dependent inhibition of VEGF-induced endothelial permeability in vitro. *Blood* (2009) **114**:3343–51. doi:10.1182/blood-2008-12-196584
121. Garcia JG, Liu F, Verin AD, Birukova A, Dechert MA, Gerthoffer WT, et al. Sphingosine 1-phosphate promotes endothelial cell barrier integrity by Edg-dependent cytoskeletal rearrangement. *J Clin Invest* (2001) **108**:689–701. doi:10.1172/JCI2001112450
122. Argraves KM, Gazzolo PJ, Groh EM, Wilkerson BA, Matsuura BS, Twal WO, et al. High density lipoprotein-associated sphingosine 1-phosphate promotes endothelial barrier function. *J Biol Chem* (2008) **283**:25074–81. doi:10.1074/jbc.M801214200
123. Camerer E, Regard JB, Cornelissen I, Srinivasan Y, Duong DN, Palmer D, et al. Sphingosine-1-phosphate in the plasma compartment regulates basal and inflammation-induced vascular leak in mice. *J Clin Invest* (2009) **119**:1871–9.
124. Gaengel K, Niaudet C, Hagikura K, Lavina B, Muhl L, Hofmann JJ, et al. The sphingosine-1-phosphate receptor S1PR1 restricts sprouting angiogenesis by regulating the interplay between VE-cadherin and VEGFR2. *Dev Cell* (2012) **23**:587–99. doi:10.1016/j.devcel.2012.08.005
125. Jung B, Obinata H, Galvani S, Mendelson K, Ding BS, Skoura A, et al. Flow-regulated endothelial S1P receptor-1 signaling sustains vascular development. *Dev Cell* (2012) **23**:600–10. doi:10.1016/j.devcel.2012.07.015
126. Murakami M, Nguyen LT, Zhuang ZW, Moodie KL, Carmeliet P, Stan RV, et al. The FGF system has a key role in regulating vascular integrity. *J Clin Invest* (2008) **118**:3355–66. doi:10.1172/JCI35298
127. Kieran MW, Kalluri R, Cho YJ. The VEGF pathway in cancer and disease: responses, resistance, and the path forward. *Cold Spring Harb Perspect Med* (2012) **2**:a006593. doi:10.1101/cshperspect.a006593
128. Yang JC, Haworth L, Sherry RM, Hwu P, Schwartzentruber DJ, Topalian SL, et al. A randomized trial of bevacizumab, an anti-vascular endothelial growth factor antibody, for metastatic renal cancer. *N Engl J Med* (2003) **349**:427–34. doi:10.1056/NEJMoa021491
129. Schuster C, Eikesdal HP, Puntervoll H, Geisler J, Geisler S, Heinrich D, et al. Clinical efficacy and safety of bevacizumab monotherapy in patients with metastatic melanoma: predictive importance of induced early hypertension. *PLoS ONE* (2012) **7**:e38364. doi:10.1371/journal.pone.0038364
130. Jain RK, Duda DG, Clark JW, Loefler JS. Lessons from phase III clinical trials on anti-VEGF therapy for cancer. *Nat Clin Pract Oncol* (2006) **3**:24–40. doi:10.1038/ncponc0403
131. Hellstrom M, Phng LK, Hofmann JJ, Wallgard E, Coultais L, Lindblom P, et al. Dll4 signalling through Notch1 regulates formation of tip cells during angiogenesis. *Nature* (2007) **445**:776–80. doi:10.1038/nature05571
132. Phng LK, Potente M, Leslie JD, Babbage J, Nyqvist D, Lobov I, et al. Nrarp coordinates endothelial Notch and Wnt signalling to control vessel density in angiogenesis. *Dev Cell* (2009) **16**:70–82. doi:10.1016/j.devcel.2008.12.009
133. Patel NS, Li JL, Generali D, Poulsom R, Cranston DW, Harris AL. Up-regulation of delta-like 4 ligand in human tumor vasculature and the role of basal expression in endothelial cell function. *Cancer Res* (2005) **65**:8690–7. doi:10.1158/0008-5472.CAN-05-1208
134. Li JL, Sainson RC, Shi W, Leek R, Harrington LS, Preusser M, et al. Delta-like 4 Notch ligand regulates tumor angiogenesis, improves tumor vascular function, and promotes tumor growth in vivo. *Cancer Res* (2007) **67**:11244–53. doi:10.1158/0008-5472.CAN-12-4354
135. Segarra M, Williams CK, Sierra Mde L, Bernardo M, McCormick PJ, Maric D, et al. Dll4 activation of Notch signaling reduces tumor vascularity and inhibits tumor growth. *Blood* (2008) **112**:1904–11. doi:10.1182/blood-2007-11-26045
136. Nagamitsu A, Greish K, Maeda H. Elevating blood pressure as a strategy to increase tumor-targeted delivery of macromolecular drug SMANCS: cases of advanced solid tumors. *Jpn J Clin Oncol* (2009) **39**:756–66. doi:10.1093/jjco/hyp074
137. Sarin H, Kanevsky AS, Fung SH, Butman JA, Cox RW, Glen D, et al. Metabolically stable bradykinin B2 receptor agonists enhance transvascular drug delivery into malignant brain tumors by increasing drug half-life. *J Transl Med* (2009) **7**:33. doi:10.1186/1479-5876-7-33
138. Eikenes L, Bruland OS, Brekke C, Davies Cde L. Collagenase increases the transcapillary pressure gradient and improves the uptake and distribution of monoclonal antibodies in human osteosarcoma xenografts. *Cancer Res* (2004) **64**:4768–73. doi:10.1158/0008-5472.CAN-03-1472
139. Willett CG, Boucher Y, Di Tomaso E, Duda DG, Munn LL, Tong RT, et al. Direct evidence that the VEGF-specific antibody bevacizumab has antivascular effects in human rectal cancer. *Nat Med* (2004) **10**:145–7. doi:10.1038/nm988
140. Tailor TD, Hanna G, Yarmolenko PS, Dreher MR, Betof AS, Nixon AB, et al. Effect of pazopanib on tumor microenvironment and liposome delivery. *Mol Cancer Ther* (2010) **9**:1798–808. doi:10.1158/1535-7163.MCT-09-0856
141. Ning S, Tian J, Marshall DJ, Knox SJ. Anti-alpha_v integrin monoclonal antibody intetumumab enhances the efficacy of radiation therapy and reduces metastasis of human cancer xenografts in nude rats. *Cancer Res* (2010) **70**:7591–9. doi:10.1158/0008-5472.CAN-10-1639
142. Huang Y, Goel S, Duda DG, Fukumura D, Jain RK. Vascular normalization as an emerging strategy to enhance cancer immunotherapy. *Cancer Res* (2013) **73**:2943–8. doi:10.1158/0008-5472.CAN-12-4354
143. Terme M, Pernot S, Marcheteau E, Sandoval F, Benhamouda N, Colussi O, et al. VEGFA-VEGFR pathway blockade inhibits tumor-induced regulatory T-cell proliferation in colorectal cancer. *Cancer Res* (2013) **73**:539–49. doi:10.1158/0008-5472.CAN-12-2325
144. Casanovas O, Hicklin DJ, Bergers G, Hanahan D. Drug resistance by evasion of antiangiogenic targeting of VEGF signaling in late-stage pancreatic islet tumors. *Cancer Cell* (2005) **8**:299–309. doi:10.1016/j.ccr.2005.09.005
145. Gatzemeier U, Pluzanska A, Szczesna A, Kaukel E, Roubec J, De Rosa F, et al. Phase III study of erlotinib in combination with cisplatin and gemcitabine in advanced non-small-cell lung cancer: the Tarceva Lung Cancer Investigation Trial. *J Clin Oncol* (2007) **25**:1545–52. doi:10.1200/JCO.2005.05.1474
146. Browder T, Butterfield CE, Kraling BM, Shi B, Marshall B, O'Reilly MS, et al. Antiangiogenic scheduling of chemotherapy improves efficacy against experimental drug-resistant cancer. *Cancer Res* (2000) **60**:1878–86.
147. Mainetti LE, Rico MJ, Fernandez-Zenobi MV, Perroud HA, Roggero EA, Rozados VR, et al. Therapeutic efficacy of metronomic chemotherapy with cyclophosphamide and doxorubicin on murine mammary adenocarcinomas. *Ann Oncol* (2013). doi:10.1093/annonc/mdt164. [Epub ahead of print].
148. Jain RK. Normalization of tumor vasculature: an emerging concept

in antiangiogenic therapy. *Science* (2005) 307:58–62. doi:10.1126/science.1104819

Conflict of Interest Statement: The authors declare that the research was conducted in the absence of any commercial or financial relationships

that could be construed as a potential conflict of interest.

Received: 29 May 2013; paper pending published: 23 June 2013; accepted: 01 August 2013; published online: 15 August 2013.

Citation: Azzi S, Hebda JK and Gavard J (2013) Vascular permeability and drug

delivery in cancers. *Front. Oncol.* 3:211. doi: 10.3389/fonc.2013.00211

This article was submitted to Frontiers in Pharmacology of Anti-Cancer Drugs, a specialty of Frontiers in Oncology.

Copyright © 2013 Azzi, Hebda and Gavard. This is an open-access article distributed under the terms of the Creative Commons Attribution License (CC BY).

The use, distribution or reproduction in other forums is permitted, provided the original author(s) or licensor are credited and that the original publication in this journal is cited, in accordance with accepted academic practice. No use, distribution or reproduction is permitted which does not comply with these terms.



Ultrasonic enhancement of drug penetration in solid tumors

Chun-Yen Lai[†], Brett Z. Fite[†] and Katherine W. Ferrara*

Department of Biomedical Engineering, University of California Davis, Davis, CA, USA

Edited by:

Ronald Berenson, Compliment Corporation, USA

Reviewed by:

Hervé Emonard, Centre National de la Recherche Scientifique, France

Jacques Barbet, Arronax GIP, France

***Correspondence:**

Katherine W. Ferrara, Department of Biomedical Engineering, University of California Davis, 451 East Health Sciences Drive, Davis, CA 95616, USA

e-mail: kwferrara@ucdavis.edu

[†]Chun-Yen Lai and Brett Z. Fite have contributed equally to this work.

Increasing the penetration of drugs within solid tumors can be accomplished through multiple ultrasound-mediated mechanisms. The application of ultrasound can directly change the structure or physiology of tissues or can induce changes in a drug or vehicle in order to enhance delivery and efficacy. With each ultrasonic pulse, a fraction of the energy in the propagating wave is absorbed by tissue and results in local heating. When ultrasound is applied to achieve mild hyperthermia, the thermal effects are associated with an increase in perfusion or the release of a drug from a temperature-sensitive vehicle. Higher ultrasound intensities locally ablate tissue and result in increased drug accumulation surrounding the ablated region of interest. Further, the mechanical displacement induced by the ultrasound pulse can result in the nucleation, growth and collapse of gas bubbles. As a result of such cavitation, the permeability of a vessel wall or cell membrane can be increased. Finally, the radiation pressure of the propagating pulse can translate particles or tissues. In this perspective, we will review recent progress in ultrasound-mediated tumor delivery and the opportunities for clinical translation.

Keywords: ultrasound, sonoporation, vascular permeability, tumor penetration, enhanced drug delivery

THE PROBLEM

The goal of this Frontiers issue is to explore methods to enhance the penetration of drugs within solid tumors. Combining ultrasound with a drug does indeed have the potential to enhance delivery; however, due to the requirement to guide the beam to the tumor such treatment will be a possibility only for localized primary tumors and well-characterized metastases that are accessible to sound waves. Ultrasound is easily directed to superficial organs such as the breast and prostate, as well as most abdominal organs, and has also been applied in the treatment of brain tumors. The effects of high intensity ultrasound on biological tissue, and particularly on the central nervous system, have been recognized for more than 70 years; the ability to heat and ablate tissue was described initially (1–5). Within studies in the 1940s and 1950s, ultrasound was also determined to have non-thermal effects on tissue, typically characterized as mechanical effects (6). The mechanical effects of ultrasound can act directly upon the tumor tissue or on injected microbubbles whose oscillations enhance vascular or cell membrane permeability. Although early studies were not geared toward drug delivery, these same mechanisms of high temperature ablation or mild hyperthermia can increase drug accumulation within a lesion and lesion boundary. In recent strategies, the increased temperature is applied to influence both the tissue and the drug capsule.

ENHANCED EXTRAVASATION OF NANOTHERAPEUTICS THROUGH MECHANICAL AND THERMAL EFFECTS ON TISSUE

The direct effects of ultrasound on tissue and vasculature have been reported to enhance the extravasation of antibodies and nanotherapeutics (7–9). In some cases, the mechanical effects of ultrasound have been shown to enhance therapeutic penetration.

With a center frequency of 1 MHz ultrasound at a peak negative pressure (PNP) of 8.95 MPa, antibody penetration has been shown to be enhanced at the tumor periphery, presumably through mechanical effects (8). The compression and rarefaction resulting from the ultrasound wave can produce the nucleation, growth, and collapse of gas bubbles within tissues. Such cavitation is assumed to facilitate transport within tumor tissue.

The thermal dose delivered by ultrasound is typically measured in cumulative equivalent minutes at 43°C (CEM 43) which is defined as $tR^{(43-T)}$, with t being the time of treatment, T the average temperature during treatment, and R a constant that equals 0.25 for temperatures between 37 and 43°C and 0.5 above 43°C (10, 11). Hyperthermia has been demonstrated to increase tumor blood flow and microvascular permeability (12). While it has long been recognized that heat increases the accumulation of small particles in the heated region of interest, the typical protocol has involved 1 h or more of heating. However, by combining the mechanical and thermal effects of ultrasound, enhanced delivery has been achieved with a shorter treatment (13). In such studies, the temperature goal is ~41–42°C and insonation continued for ~5–20 min. As a result of hyperthermia and the mechanical effects of ultrasound, we have observed that the accumulation of liposomes in an insonified tumor can be increased up to threefold to as much as 22%ID/g. While ultrasound was shown to enhance accumulation in syngeneic murine tumors, the ultrasound parameters that were required to enhance nanoparticle accumulation were shown to differ between epithelial and epithelial-mesenchymal transition (EMT) tumor phenotypes (7). While mild hyperthermia enhanced accumulation in the epithelial tumors, likely through decreased intratumoral pressure and enhanced apparent permeability, higher ultrasound pressure was

required to enhance delivery in the poorly vascularized EMT phenotype. Further, excessive temperature or thermal dose can result in vascular stasis, particularly in highly vascular epithelial tumors. The requirement to personalize the ultrasound parameters to the tumor biology will likely require image guidance to insure clinical success.

In part due to the differing effects of mild hyperthermia with tumor biology, the use of high temperature ablation to enhance delivery has been explored as a methodology that is likely to be generally effective in increasing delivery. While it seems counterintuitive that tissue ablation can greatly enhance accumulation, edema, enhanced blood flow, and increased transport in the region surrounding the ablated site can successfully improve delivery. In our experience, the peak delivery in regions surrounding ablation can exceed 30%ID/g. Also of clinical interest, the hyperthermia surrounding radiofrequency (rf) ablation lesions has been used to enhance local delivery; however, the temperature obtained with such devices ranges from 50 to 90°C (14). Rf ablation has been applied in previous studies to achieve a similar enhanced delivery, and such techniques are now in clinical trials (15, 16). High intensity focused ultrasound similarly enhances delivery surrounding the site of ablation, although combinations of ablation and drug delivery remain primarily under pre-clinical investigation.

RELEASE OF DRUG FROM NANOPARTICLES WITHIN THE VASCULATURE

Nanoparticles that can be triggered to release a small molecule cargo within a tumor have shown the potential to increase both the local concentration of the drug and tumor penetration. Yet, the challenge of developing particles that are stable in circulation and release their cargo upon activation has long been recognized as a major challenge in pharmaceutical development. While many activatable particles are under development (11, 17–23), thermally sensitive liposomes have been frequently combined with ultrasound in recent pre-clinical and clinical studies and will be considered here. In studies of thermally sensitive liposomes, imaging has been used to verify that amphipathic cargo released within the tumor vasculature remains concentrated within the tumor in the region of release (18). We have found that release of drug from such temperature-sensitive vehicles can be highly effective, resulting in a complete response in aggressive murine tumors (unpublished data).

Temperature-sensitive liposomes were initially proposed containing 1,2-dipalmitoyl-*sn*-glycero-3-phosphocholine (DPPC) with a phase transition of $T_m = \sim 41^\circ\text{C}$ and multiple formulations containing DPPC have been proposed (24, 25). The incorporation of lyso-phospholipids in DPPC-based liposomes decreases the phase transition temperature and speeds the release of the cargo, likely due to the creation of local defects within the lipid bilayer (26). The Thermodox™ formulation, with the incorporation of a lyso-phospholipid, releases at a clinically desirable temperature of $\sim 39^\circ\text{C}$. The incorporation of the lyso-phospholipids also enhances the ion permeability and drug release rates at the membrane phase transition (27). Unfortunately, using the conventional ammonium sulfate loading, liposomes containing lyso-phospholipids also rapidly release their cargo within the blood pool. As a result, while local delivery can be achieved within tens

of minutes after injection, the dose limiting toxicities of such formulations have typically limited their application to single dose administration. Although the pre-clinical data using Thermodox has been very exciting, this activatable doxorubicin formulation reportedly failed to meet its primary endpoint in the Phase III HEAT Study in patients with hepatocellular carcinoma (HCC). Yet, in spite of this setback, the potential for temperature-sensitive vehicles to have a significant impact on the concentration and penetration of drugs within solid tumors is substantial. Although early clinical studies have typically been limited to one-time treatment, with new formulations repeated treatment should be feasible and the resulting clinical impact enhanced. Multiple alternative formulations have been proposed and compared and have been shown to enhance circulation time (25, 28–30). Alternative strategies using metal-drug complexes, a Brij surfactant and phosphatidylglycerol have been reported to enhance the stability of temperature-sensitive liposomes and are promising alternatives for future investigation. The ultrasound parameters used to enhance delivery with temperature-sensitive liposomes have also varied widely with the center frequency typically ranging from 1 to 3 MHz and duty cycle ranging from ~10 to 100% (20, 31, 32).

MICROBUBBLES

Micron-scale gas bubbles with a stabilizing shell are used in ultrasound imaging to improve imaging of the blood pool and have been widely applied in pre-clinical studies of enhanced drug delivery. The microbubble shell can be coupled to nanotherapeutics, such as liposomes, or coated with a drug (33, 34). The gas core can transport oxygen or other useful gas cargo, although for imaging the gas core is selected to reduce diffusion through the shell material (35). Alternative formulations in which liquid perfluorocarbon particles are injected and change to a gaseous phase *in vivo* have also been shown to have efficacy in the delivery of drugs to solid tumors (36).

Reflections of ultrasound waves from tissue increase in proportion to variations in density and compressibility of the medium and therefore highly compressible gas bubbles produce strong ultrasound echoes. These small bubbles expand and contract in response to ultrasound waves. When driven at a frequency near the resonance frequency that is determined by the size and physical composition of the microbubble, a multi-fold expansion can result. During the subsequent collapse, the velocity of the microbubble wall can reach hundreds of meters per second (37, 38), and the gas core can fragment into a set of small gas particles (39). Also, during microbubble collapse, small jets can impact nearby cell membranes and result in enhanced transport of materials into the cell. *In vitro* studies in phantom materials and *ex vivo* studies within tissues have confirmed that the oscillating microbubble can travel through the vessel wall or can affect the mechanical integrity of the vessel (40–42). Still, such jets affect cells only within a distance on the order of tens of microns. Therefore, the application of microbubbles to alter vascular, rather than tumor cell, permeability is attractive since the vascular concentration is initially high and large numbers of microbubbles are required to effectively change the membrane permeability of a large fraction of cells within a tissue. Within the vasculature, catheters have also been applied to direct streams of bubbles to a

region of interest (43). Also, microbubble-enhanced gene delivery has been widely studied since the biological amplification resulting from transfection is expected to increase the impact of treatment although the protocols have varied (44–48). Within such studies, microbubbles and DNA have been co-injected or combined into a single vehicle and the administration has been intratumoral or intravascular. Typical ultrasound parameters for enhanced tumor gene delivery have included a center frequency on the order of 1 MHz and a low pulse repetition frequency; however, the peak negative ultrasound pressure has varied significantly and successful transfection at higher ultrasound frequencies has also been reported.

The ultrasound parameters used to increase vascular permeability must be chosen carefully as insonation of microbubbles with low ultrasound frequencies has been shown to reduce blood flow (49). A parameter space for safe and effective use of microbubbles for enhancing vascular permeability has been established (41, 50–52). Many parameters, including microbubble dosage and size, the ultrasound center frequency, pulse duration, pulse repetition frequency, and the PNP determine the effect of the oscillating microbubble on the surrounding tissue.

In addition to the formation of jets, physical mechanisms exploited in microbubble-enhanced delivery include radiation forces and microstreaming of fluid (53, 54). Radiation force refers to a mechanism by which oscillating microbubbles or other particles are displaced, most typically in the direction of wave propagation (55–57). This displacement can be used to enhance vascular targeting of a microbubble or microbubble-drug conjugate. Further, local motion of fluid surrounding the oscillating bubble is known as microstreaming and has been shown to increase cellular uptake of therapeutics (53, 54).

One of the most important applications for the use of microbubbles to enhance delivery has been the enhancement of blood brain barrier (BBB) permeability (58–65). In general, the technique consists of systemically injecting microbubbles and insonifying the region of the brain where enhanced permeability is desired. Here again, a parameter space has been established within which enhanced BBB transport is achieved with minimal hemorrhage and cell death. Still, the extension of these techniques into the clinic is expected to require the use of real-time cavitation detection, as individual variations in the skull penetration of the ultrasound wave are significant and the therapeutic window for effective and safe therapy is relatively small (66). As noted above, pre-clinical-application of microbubble-enhanced delivery is widespread. In addition, the authors are aware of yet unreported small clinical studies of microbubble-enhanced delivery to solid tumors.

APPLICATION OF IMAGING TECHNOLOGY

A major reason for the expansion of the application of therapeutic ultrasound is the development of methods to monitor the treated location and the temperature using MRI (67) or ultrasound (68). While mild hyperthermia ($CEM 43 < 0.5$) is associated with increased metabolism, blood flow, and tissue repair, higher thermal doses are associated with enhanced cell death and therefore the methods to carefully control and monitor the delivered temperature are critically important (69). Image guidance using nuclear

medicine techniques is also attractive due to their high sensitivity and the opportunity for quantitation of delivery (70, 71). By radiolabeling nanoparticles, the rate and magnitude of extravasation can be directly estimated from PET data (71). Even with the relatively low spatial resolution of PET (~ 1 mm), the penetration of nanoparticle-based therapeutics has been assessed and shown to differ from small molecular weight agents (72).

In order to fully evaluate the enhanced penetration of a drug resulting from ultrasound, multiple imaging labels can be incorporated with drug accumulation and penetration assessed at the whole body, organ, and cellular scales (8, 9, 70, 73, 74). Multiple MRI protocols can be proposed for the guidance of ultrasound therapies including diffusion-weighted (75, 76), T2-weighted (77, 78), and contrast enhanced T1-weighted imaging (79–81), fluid attenuated inversion recovery (FLAIR) (82), heteronuclear (^{23}Na) (83), spectroscopy (84), and displacement sensitive sequences via MR elastography (85). Following HIFU ablation of the prostate, gadolinium enhanced MRI is often used to evaluate the extent of tissue damage. Although contrast enhanced T1-weighted MRI can detect tissue damage following HIFU ablation (86, 87), it does not correlate to histological results (intensity of necrosis, presence of foci of viable cancer) immediately following HIFU (87). However, for follow-up examinations, DCE MRI has demonstrated good sensitivity and diffusion MRI has shown specificity in identifying tumor progression after HIFU ablation (75, 88).

In addition to endogenous contrast mechanisms that can be used to guide and assess ultrasound therapies, exogenous agents can be used to report on specific changes. For example, co-administration of two paramagnetic contrast agents (gadolinium and thulium) within liposomal drug carriers has been previously utilized to follow internalization and cellular trafficking of the vehicle (89). Similarly, multi modal liposomal agents spanning CT and MRI have been used to assess the penetration of liposomes within tumors and have been proposed for cross modality registration and as a means to guide imaging-based interventions (73, 74). Many physiological parameters can also be assessed by MRI and coupled with the soft tissue anatomical information motivate MRI as an excellent tool for guiding thermal therapies (90, 91).

In addition to the role of MRI in the assessment of drug penetration and distribution, MR thermometry can be applied to monitor the temperature of a region during an intervention (92–100). The proton resonance frequency (PRF) of water is frequently used to detect changes in temperature (101) both because it has a thermal coefficient that is linear over a wide temperature range and, excepting adipose tissue, the PRF shift has little dependence on tissue type even following coagulation (99, 102). The PRF shift can be measured rapidly with gradient echo sequences, which is advantageous during thermal therapies where high temporal resolution is desirable, especially during ablative processes, to avoid damage to surrounding tissue. Further increases in temporal resolution can be gained via partial parallel imaging techniques using phased arrays (103–105) utilizing various algorithms (105).

Neither clinical focused ultrasound (FUS) systems, which typically operate around 1 MHz (106, 107), nor clinical MR scanners (e.g., 1.5, or 3 T) are ideal for small animal imaging. In the former,

the focal spot depth may encompass an appreciable portion of the animal, while the latter may have insufficient signal-to-noise ratio (SNR) to easily obtain detailed images of murine tumors. The smaller focal depth at higher FUS frequencies makes them more suitable for pre-clinical imaging of small animals (108). High field scanners are especially useful for small animal thermal imaging because in addition to providing higher SNR, which can be used for higher spatial resolutions, they also improve the sensitivity of thermal measurements made with the PRF shift method, which itself has a first order dependence on magnetic field strength.

FUTURE APPLICATIONS

The use of the thermal and mechanical effects of ultrasound to enhance delivery to solid tumors is expanding. With the increasing availability of MRI-guided high intensity focused ultrasound, well-controlled and calibrated clinical studies are feasible. Both the use of ultrasound to alter tissue properties and to release a drug from a carrier are in widespread pre-clinical evaluation. With the addition of microbubbles, drug penetration through the endothelium can also be increased, although the protocols are currently more complex due to the need to co-inject the therapeutic and microbubbles.

REFERENCES

- Wall PD, Fry WJ, Stephens R, Tucker D, Lettvín JY. Changes produced in the central nervous system by ultrasound. *Science* (1951) **114**:686–7. doi:10.1126/science.114.2974.686
- Fry WJ, Dunn F. Ultrasonic irradiation of the central nervous system at high sound levels. *J Acoust Soc Am* (1956) **28**:129–31. doi:10.1121/1.1908200
- Fry FJ, Ades HW, Fry WJ. Production of reversible changes in the central nervous system by ultrasound. *Science* (1958) **127**:83–4. doi:10.1126/science.127.3289.83
- Lynn JG, Zwemer RL, Chick AJ, Miller AE. A new method for the generation and use of focused ultrasound in experimental biology. *J Gen Physiol* (1942) **26**:179–93. doi:10.1085/jgp.26.2.179
- Lynn J, Zwemer RL, Chick AJ. The biological application of focused ultrasound waves. *Science* (1942) **96**:119–20. doi:10.1126/science.96.2483.119
- Fry WJ, Wulff VJ, Tucker D, Fry FJ. Physical factors involved in ultrasonically induced changes in living systems: Identification of non-temperature effects. *J Acoust Soc Am* (1950) **22**:867–76. doi:10.1121/1.1906707
- Watson K, Lai CY, Qin S, Kruse DE, Lin YC, Seo JW, et al. Ultrasound increases nanoparticle delivery by reducing intratumoral pressure and increasing transport in epithelial and epithelial-mesenchymal transition tumors. *Cancer Res* (2012) **72**:1485–93. doi:10.1158/0008-5472.CAN-11-3232
- Wang S, Shin IS, Hancock H, Jang B-S, Kim H-S, Lee SM, et al. Pulsed high intensity focused ultrasound increases penetration and therapeutic efficacy of monoclonal antibodies in murine xenograft tumors. *J Control Release* (2012) **162**:218–24. doi:10.1016/j.jconrel.2012.06.025
- Frenkel V. Ultrasound mediated delivery of drugs and genes to solid tumors. *Adv Drug Deliv Rev* (2008) **60**:1193–208. doi:10.1016/j.addr.2008.03.007
- Dewhirst MW, Vujaskovic Z, Jones E, Thrall D. Re-setting the biologic rationale for thermal therapy. *Int J Hyperthermia* (2005) **21**:779–90. doi:10.1080/02656730500271668
- Jones EL, Oleson JR, Prosnitz LR, Samulski TV, Vujaskovic Z, Yu DH, et al. Randomized trial of hyperthermia and radiation for superficial tumors. *J Clin Oncol* (2005) **23**:3079–85. doi:10.1200/JCO.2005.05.520
- Gaber MH, Wu NZ, Hong K, Huang SK, Dewhirst MW, Papahadjopoulos D. Thermosensitive liposomes: extravasation and release of contents in tumor microvascular networks. *Int J Radiat Oncol Biol Phys* (1996) **36**:1177–87. doi:10.1016/S0360-3016(96)00389-6
- Yuh EL, Shulman SG, Mehta SA, Xie J, Chen L, Frenkel V, et al. Delivery of systemic chemotherapeutic agent to tumors by using focused ultrasound: study in a murine model. *Radiology* (2005) **234**(2):431–7. doi:10.1148/radiol.2342030889
- Ahmed M, Monsky WE, Girnun G, Lukyanov A, D’Ippolito G, Kruskal JB, et al. Radiofrequency thermal ablation sharply increases intratumoral liposomal doxorubicin accumulation and tumor coagulation. *Cancer Res* (2003) **63**:6327–33.
- Goldberg SN, Ahmed M. Minimally invasive image-guided therapies for hepatocellular carcinoma. *J Clin Gastroenterol* (2002) **35**:S115–29. doi:10.1097/00004836-200211002-00008
- Wood BJ, Poon RT, Locklin JK, Dreher MR, Ng KK, Eugeni M, et al. Phase I study of heat-deployed liposomal doxorubicin during radiofrequency ablation for hepatic malignancies. *J Vasc Interv Radiol* (2012) **23**:248–55. doi:10.1016/j.jvir.2011.10.018
- Viglianti BL, Abraham SA, Michelich CR, Yarmolenko PS, MacFall JR, Bally MB, et al. In vivo monitoring of tissue pharmacokinetics of liposome/drug using MRI: illustration of targeted delivery. *Magn Reson Med* (2004) **51**:1153–62. doi:10.1002/mrm.20074
- Ponce AM, Viglianti BL, Yu DH, Yarmolenko PS, Michelich CR, Woo J, et al. Magnetic resonance imaging of temperature-sensitive liposome release: drug dose painting and antitumor effects. *J Natl Cancer Inst* (2007) **99**:53–63. doi:10.1093/jnci/djk005
- Kong G, Anyarambhatla G, Petros WP, Braun RD, Colvin OM, Needham D, et al. Efficacy of liposomes and hyperthermia in a human tumor xenograft model: importance of triggered drug release. *Cancer Res* (2000) **60**:6950–7.
- Dromi S, Frenkel V, Luk A, Traughber B, Angstadt M, Bur M, et al. Pulsed-high intensity focused ultrasound and low temperature sensitive liposomes for enhanced targeted drug delivery and antitumor effect. *Clin Cancer Res* (2007) **13**:2722–7. doi:10.1158/1078-0432.CCR-06-2443
- Loo C, Lowery A, Halas N, West J, Drezek R. Immunotargeted nanoshells for integrated cancer imaging and therapy. *Nano Lett* (2005) **5**:709–11. doi:10.1021/nl050127s
- Derfus AM, von Maltzahn G, Harris TJ, Duza T, Vecchio KS, Ruoslahti E, et al. Remotely triggered release from magnetic nanoparticles. *Adv Mater* (2007) **19**:3932–6. doi:10.1002/adma.200700091

In the future, the effects of ultrasound may transcend the local effect through enhanced immune response. The addition of immunotherapy to standard-of-care cancer therapies has shown evidence of efficacy in the pre-clinical and clinical settings (109–115). The immune system is often tolerant to antigens presented by the tumor and therefore strategies to induce tumor-specific immunity must overcome obstacles including: insufficient and dysfunctional populations of antigen-presenting cells and lymphocytes, the difficulty of inducing potent immunity without inducing unacceptable autoimmune toxicities, the low immunogenicity of antigens expressed by tumor cells, and immunoregulatory pathways that dampen the tumor-specific immune response (116). The use of ultrasound ablation to generate an immune response has been shown to be a promising technique for immune activation (110–112, 114, 115, 117–121). Ultrasound ablation is thought to act through dendritic cell maturation and T-cell immunity (122), and is particularly advantageous because it is completely non-invasive, can be controlled with high spatial precision and uses no harmful ionizing radiation (123, 124).

ACKNOWLEDGMENTS

The authors acknowledge the support of NIHCA103828, NIHCA134659 and NIHCA112356

23. Gannon CJ, Patra CR, Bhattacharya R, Mukherjee P, Curley SA. Intracellular gold nanoparticles enhance non-invasive radiofrequency thermal destruction of human gastrointestinal cancer cells. *J Nanobiotechnol* (2008) **6**:2. doi:10.1186/1477-3155-6-2
24. Yatvin MB, Weinstein JN, Dennis WH, Blumenthal R. Design of liposomes for enhanced local release of drugs by hyperthermia. *Science* (1978) **202**:1290–3. doi:10.1126/science.364652
25. Paoli EE, Kruse DE, Seo JW, Zhang H, Kheiroloomoo A, Watson KD, et al. An optical and microPET assessment of thermally-sensitive liposome biodistribution in the Met-1 tumor model: Importance of formulation. *J Control Release* (2010) **143**:13–22. doi:10.1016/j.jconrel.2009.12.010
26. Needham D, Anyarambhatla G, Kong G, Dewhirst MW. A new temperature-sensitive liposome for use with mild hyperthermia: characterization and testing in a human tumor xenograft model. *Cancer Res* (2000) **60**:1197–201.
27. Mills JK, Needham D. Lysolipid incorporation in dipalmitoylphosphatidylcholine bilayer membranes enhances the ion permeability and drug release rates at the membrane phase transition. *Biochim Biophys Acta* (2005) **1716**:77–96. doi:10.1016/j.bbamem.2005.08.007
28. Tagami T, Ernsting MJ, Li S-D. Optimization of a novel and improved thermosensitive liposome formulated with DPPC and a Brij surfactant using a robust in vitro system. *J Control Release* (2011) **154**:290–7. doi:10.1016/j.jconrel.2011.05.020
29. Lindner LH, Eichhorn ME, Eibl H, Teichert N, Schmitt-Sody M, Issels RD, et al. Novel temperature-sensitive liposomes with prolonged circulation time. *Clin Cancer Res* (2004) **10**:2168–78. doi:10.1158/1078-0432.CCR-03-0035
30. Kheiroloomoo A, Mahakian LM, Lai C-Y, Lindfors HA, Seo JW, Paoli EE, et al. Copper-doxorubicin as a nanoparticle cargo retains efficacy with minimal toxicity. *Mol Pharm* (2010) **7**:1948–58. doi:10.1021/mp100245u
31. Partanen A, Yarmolenko PS, Viitala A, Appanaboyina S, Haemmerich D, Ranjan A, et al. Mild hyperthermia with magnetic resonance-guided high-intensity focused ultrasound for applications in drug delivery. *Int J Hyperthermia* (2012) **28**:320–36. doi:10.3109/02656736.2012.680173
32. Staruch RM, Ganguly M, Tancock IF, Hynnen K, Chopra R. Enhanced drug delivery in rabbit VX2 tumours using thermosensitive liposomes and MRI-controlled focused ultrasound hyperthermia. *Int J Hyperthermia* (2012) **28**:776–87. doi:10.3109/02656736.2012.736670
33. Lum AFH, Borden MA, Dayton PA, Kruse DE, Simon SI, Ferrara KW. Ultrasound radiation force enables targeted deposition of model drug carriers loaded on microbubbles. *J Control Release* (2006) **111**:128–34. doi:10.1016/j.jconrel.2005.11.006
34. Kheiroloomoo A, Dayton PA, Lum AFH, Little E, Paoli EE, Zheng H, et al. Acoustically-active microbubbles conjugated to liposomes: characterization of a proposed drug delivery vehicle. *J Control Release* (2007) **118**:275–84. doi:10.1016/j.jconrel.2006.12.015
35. Kwan JJ, Kaya M, Borden MA, Dayton PA. Theranostic oxygen delivery using ultrasound and microbubbles. *Theranostics* (2012) **2**:1174–84. doi:10.7150/thno.4410
36. Rapoport N. Phase-shift, stimuli-responsive perfluorocarbon nanodroplets for drug delivery to cancer. *Wiley Interdiscip Rev Nanomed Nanobiotechnol* (2012) **4**:492–510. doi:10.1002/wnn.1176
37. Chomas JE, Dayton PA, May D, Allen J, Klibanov A, Ferrara K. Optical observation of contrast agent destruction. *Appl Phys Lett* (2000) **77**:1056–8. doi:10.1063/1.1287519
38. Chomas JE, Dayton P, May D, Ferrara K. Threshold of fragmentation for ultrasonic contrast agents. *J Biomed Opt* (2001) **6**:141–50. doi:10.1117/1.1352752
39. Chomas JE, Dayton P, Allen J, Morgan K, Ferrara KW. Mechanisms of contrast agent destruction. *IEEE Trans Ultrason Ferroelectr Freq Control* (2001) **48**:232–48. doi:10.1109/58.896136
40. Qin S, Caskey CF, Ferrara KW. Ultrasound contrast microbubbles in imaging and therapy: physical principles and engineering. *Phys Med Biol* (2009) **54**:R27–57. doi:10.1088/0031-9155/54/6/R01
41. Caskey CF, Steiger SM, Qin S, Dayton PA, Ferrara KW. Direct observations of ultrasound microbubble contrast agent interaction with the microvessel wall. *J Acoust Soc Am* (2007) **122**:1191–200. doi:10.1121/1.2747204
42. Caskey CF, Qin S, Dayton PA, Ferrara KW. Microbubble tunneling in gel phantoms. *J Acoust Soc Am* (2009) **125**:EL183–9. doi:10.1121/1.3097679
43. Kilroy JP, Klibanov AL, Wamhoff BR, Hossack JA. Intravascular ultrasound catheter to enhance microbubble-based drug delivery via acoustic radiation force. *IEEE Trans Ultrason Ferroelectr Freq Control* (2012) **59**:2156–66. doi:10.1109/TUFFC.2012.2442
44. Miller DL, Song J. Lithotripter shock waves with cavitation nucleation agents produce tumor growth reduction and gene transfer in vivo. *Ultrasound Med Biol* (2002) **28**:1343–8. doi:10.1016/S0301-5629(02)00572-0
45. Miller DL, Song J. Tumor growth reduction and DNA transfer by cavitation-enhanced high-intensity focused ultrasound in vivo. *Ultrasound Med Biol* (2003) **29**:887–93. doi:10.1016/S0301-5629(03)00031-0
46. Hauff P, Seemann S, Reszka R, Schultze-Mosgau M, Reinhardt M, Buzasi T, et al. Evaluation of gas-filled microparticles and sonoporation as gene delivery system: feasibility study in rodent tumor models. *Radiology* (2005) **236**:572–8. doi:10.1148/radiol.2362040870
47. Howard CM, Forsberg F, Minimo C, Liu JB, Merton DA, Claudio PP. Ultrasound guided site specific gene delivery system using adenoviral vectors and commercial ultrasound contrast agents. *J Cell Physiol* (2006) **209**:413–21. doi:10.1002/jcp.20736
48. Sonoda S, Tachibana K, Uchino E, Yamashita T, Sakoda K, Sonoda KH, et al. Inhibition of melanoma by ultrasound-microbubble-aided drug delivery suggests membrane permeabilization. *Cancer Biol Ther* (2007) **6**:1276–83.
49. Burke CW, Klibanov AL, Sheehan JP, Price RJ. Inhibition of glioma growth by microbubble activation in a subcutaneous model using low duty cycle ultrasound without significant heating. *J Neurosurg* (2011) **114**:1654–61. doi:10.3171/2010.11.JNS101201
50. McDannold N, Vykhodtseva N, Hynnen K. Effects of acoustic parameters and ultrasound contrast agent dose on focused-ultrasound induced blood-brain barrier disruption. *Ultrasound Med Biol* (2008) **34**:1016–20. doi:10.1016/j.ultrasmedbio.2007.11.009
51. Choi JJ, Feshitan JA, Baseri B, Shougang W, Yao-Sheng T, Borden MA, et al. Microbubble-size dependence of focused ultrasound-induced blood-brain barrier opening in mice in vivo. *IEEE Trans Biomed Eng* (2010) **57**:145–54. doi:10.1109/TBME.2009.2034533
52. Steiger SM, Caskey CF, Adamson RH, Qin S, Curry FR, Wisner ER, et al. Enhancement of vascular permeability with low-frequency contrast-enhanced ultrasound in the chorioallantoic membrane model. *Radiology* (2007) **243**:112–21. doi:10.1148/radiol.2431060167
53. Delalande A, Kotopoulos S, Postema M, Midoux P, Pichon C. Sonoporation: mechanistic insights and ongoing challenges for gene transfer. *Gene* (2013) **525**(2):191–9. doi:10.1016/j.gene.2013.03.095
54. Sirsi SR, Borden MA. Advances in ultrasound mediated gene therapy using microbubble contrast agents. *Theranostics* (2012) **2**:1208–22. doi:10.7150/thno.4306
55. Dayton PA, Zhao S, Bloch SH, Schumann P, Penrose K, Matsunaga TO, et al. Application of ultrasound to selectively localize nanodroplets for targeted imaging and therapy. *Mol Imaging* (2006) **5**:160–74.
56. Dayton PA, Morgan KE, Klibanov ALS, Brandenburger G, Nightingale KR, Ferrara KW. A preliminary evaluation of the effects of primary and secondary radiation forces on acoustic contrast agents. *IEEE Trans Ultrason Ferroelectr Freq Control* (1997) **44**:1264–77. doi:10.1109/58.656630
57. Dayton P, Klibanov A, Brandenburger G, Ferrara K. Acoustic radiation force in vivo: a mechanism to assist targeting of microbubbles. *Ultrasound Med Biol* (1999) **25**:1195–201. doi:10.1016/S0301-5629(99)00062-9
58. O'Reilly MA, Hynnen K. Ultrasound enhanced drug delivery to the brain and central nervous system. *Int J Hyperthermia* (2012) **28**:386–96. doi:10.3109/02656736.2012.666709
59. Hynnen K, McDannold N, Martin H, Jolesz FA, Vykhodtseva N. The threshold for brain damage in rabbits induced by bursts of ultrasound in the presence of an ultrasound contrast agent (optison). *Ultrasound Med Biol*

- (2003) **29**:473–81. doi:10.1016/S0301-5629(02)00741-X
60. Baseri B, Choi JJ, Deffieux T, Samiotaki G, Tung Y-S, Olumolade O, et al. Activation of signaling pathways following localized delivery of systemically administered neurotrophic factors across the blood-brain barrier using focused ultrasound and microbubbles. *Phys Med Biol* (2012) **57**:N65–81. doi:10.1088/0031-9155/57/7/N65
61. Choi JJ, Feshitan JA, Shougang W, Yao-Sheng T, Baseri B, Borden MA, et al. The dependence of the ultrasound-induced blood-brain barrier opening characteristics on microbubble size in vivo. *AIP Conf Proc* (2009) **1113**:58–62. doi:10.1063/1.3131471
62. Choi JJ, Small SA, and Konofagou EE. Optimization of blood-brain barrier opening in mice using focused ultrasound. *IEEE Ultrasonics Symposium (IEEE Cat. No.06CH37777)*; 2006 Oct 3–6; Vancouver, Canada (2006). p. 540–3.
63. Konofagou EE, Choi J, Baseri B, Lee A. Characterization and optimization of trans-blood-brain barrier diffusion in vivo. *AIP Conf Proc* (2009) **1113**:418–22. doi:10.1063/1.3131462
64. Konofagou EE, Choi J, Lee A, Baseri B. Molecular imaging through the blood-brain barrier: safety assessment and parameter dependence. *Proc IEEE Int Symp Biomed Imaging*; 2009 Jun 28 to Jul 1; Boston, MA (2009). p. 771–4. doi:10.1109/ISBI.2009.5193163
65. Konofagou EE, Tung Y-S, Choi J, Deffieux T, Baseri B, Vlachos F. Ultrasound-induced blood-brain barrier opening. *Curr Pharm Biotechnol* (2012) **13**:1332–45. doi:10.2174/138920112800624364
66. Tung YS, Marquet F, Teichert T, Ferrera V, Konofagou EE. Feasibility of noninvasive cavitation-guided blood-brain barrier opening using focused ultrasound and microbubbles in nonhuman primates. *Appl Phys Lett* (2011) **98**:163704-1–163704-3. doi:10.1063/1.3580763
67. Fite BZ, Liu Y, Kruse DE, Caskey CF, Walton JH, Lai CY, et al. Magnetic resonance thermometry at 7T for real-time monitoring and correction of ultrasound induced mild hyperthermia. *PLoS ONE* (2012) **7**:e35509. doi:10.1371/journal.pone.0035509
68. Lai C, Kruse DE, Caskey CF, Stephens DN, Sutcliffe PL, Ferrara KW. Noninvasive thermometry assisted by a dual-function ultrasound transducer for mild hyperthermia. *IEEE Trans Ultrason Ferroelectr Freq Control* (2010) **57**:2671–84. doi:10.1109/TUFFC.2010.1741
69. Roemer RB. Engineering aspects of hyperthermia therapy. *Annu Rev Biomed Eng* (1999) **1**:347–76. doi:10.1146/annurev.bioeng.1.1.347
70. Rygh CB, Qin SP, Seo JW, Mahakian LM, Zhang H, Adamson R, et al. Longitudinal investigation of permeability and distribution of macromolecules in mouse malignant transformation using PET. *Clin Cancer Res* (2011) **17**:550–9. doi:10.1158/1078-0432.CCR-10-2049
71. Qin S, Seo JW, Zhang H, Qi J, Curry F-RE, Ferrara KW. An imaging-driven model for liposomal stability and circulation. *Mol Pharm* (2009) **7**:12–21. doi:10.1021/mp0900122j
72. Wong AW, Ormsby E, Zhang H, Seo JW, Mahakian LM, Caskey CF, et al. A comparison of image contrast with (64)Cu-labeled long circulating liposomes and (18)F-FDG in a murine model of mammary carcinoma. *Am J Nucl Med Mol Imaging* (2013) **3**:32–43.
73. Zheng J, Liu J, Dunne M, Jaffray D, Allen C. In vivo performance of a liposomal vascular contrast agent for CT and MR-based image guidance applications. *Pharm Res* (2007) **24**:1193–201. doi:10.1007/s11095-006-9220-1
74. Huang H, Dunne M, Lo J, Jaffray DA, Allen C. Comparison of computed tomography- and optical image-based assessment of liposome distribution. *Mol Imaging* (2013) **12**:148–60.
75. Kim CK, Park BK, Lee HM, Kim SS, Kim E. MRI techniques for prediction of local tumor progression after high-intensity focused ultrasonic ablation of prostate cancer. *AJR Am J Roentgenol* (2008) **190**:1180–6. doi:10.2214/AJR.07.2924
76. Kim CK, Park BK, Kim B. Diffusion-weighted MRI at 3 T for the evaluation of prostate cancer. *AJR Am J Roentgenol* (2010) **194**:1461–9. doi:10.2214/AJR.09.3654
77. Hyynen K, Damianou C, Darkazanli A, Unger E, Schenck JF. The feasibility of using MRI to monitor and guide noninvasive ultrasound surgery. *Ultrasound Med Biol* (1993) **19**:91–2. doi:10.1016/0301-5629(93)90022-G
78. Funaki K, Fukunishi H, Funaki T, Sawada K, Kaji Y, Maruo T. Magnetic resonance-guided focused ultrasound surgery for uterine fibroids: relationship between the therapeutic effects and signal intensity of preexisting T2-weighted magnetic resonance images. *Am J Obstet Gynecol* (2007) **196**:e1–6. doi:10.1016/j.ajog.2006.08.030
79. McDannold NJ, Hyynen K, Wolf D, Wolf G, Jolesz FA. MRI evaluation of thermal ablation of tumors with focused ultrasound. *J Magn Reson Imaging* (1998) **8**:91–100. doi:10.1002/jmri.1880080119
80. Punwani S, Emberton M, Walkden M, Sohaib A, Freeman A, Ahmed H, et al. Prostatic cancer surveillance following whole-gland high-intensity focused ultrasound: comparison of MRI and prostate-specific antigen for detection of residual or recurrent disease. *Br J Radiol* (2012) **85**:720–8. doi:10.1259/bjr/61380797
81. Tempany CM, Stewart EA, McDannold N, Quade BJ, Jolesz FA, Hyynen K. MR imaging-guided focused ultrasound surgery of uterine leiomyomas: a feasibility study. *Radiology* (2003) **226**:897–905. doi:10.1148/radiol.2271020395
82. Chen L, Bouley D, Yuh E, D'Arceuil H, Butts K. Study of focused ultrasound tissue damage using MRI and histology. *J Magn Reson Imaging* (1999) **10**:146–53. doi:10.1002/(SICI)1522-2586(199908)10:2<146::AID-JMRI6>3.0.CO;2-3
83. Jacobs MA, Ouwerkerk R, Kamel I, Bottomley PA, Bluemke DA, Kim HS. Proton, diffusion-weighted imaging, and sodium (23Na) MRI of uterine leiomyomata after MR-guided high-intensity focused ultrasound: a preliminary study. *J Magn Reson Imaging* (2009) **29**:649–56. doi:10.1002/jmri.21677
84. Cirillo S, Petrachini M, D'Urso L, Dellamonica P, Illing R, Regge D, et al. Endorectal magnetic resonance imaging and magnetic resonance spectroscopy to monitor the prostate for residual disease or local cancer recurrence after transrectal high-intensity focused ultrasound. *BJU Int* (2008) **102**:452–8. doi:10.1111/j.1464-410X.2008.07633.x
85. Wu T, Felmlee JP, Greenleaf JE, Riederer SJ, Ehman RL. Assessment of thermal tissue ablation with MR elastography. *Magn Reson Med* (2001) **45**:80–7. doi:10.1002/1522-2594(200101)45:1<80::AID-MRM1012>3.0.CO;2-Y
86. Kirkham AP, Emberton M, Hoh IM, Illing RO, Freeman AA, Allen C. MR imaging of prostate after treatment with high-intensity focused ultrasound. *Radiology* (2008) **246**:833–44. doi:10.1148/radiol.2463062080
87. Rouviere O, Lyonnet D, Raudrant A, Colin-Pangaud C, Chapelon JY, Bouvier R, et al. MRI appearance of prostate following transrectal HIFU ablation of localized cancer. *Eur Urol* (2001) **40**:265–74. doi:10.1159/000049786
88. Ben Cheikh A, Girouin N, Ryon-Taponnier P, Mege-Lechevallier F, Gelet A, Chapelon JY, et al. MR detection of local prostate cancer recurrence after transrectal high-intensity focused US treatment: preliminary results. *J Radiol* (2008) **89**:571–7. doi:10.1016/S0221-0363(08)71483-5
89. Delli Castelli D, Dastru W, Terreno E, Cittadino E, Mainini F, Torres E, et al. In vivo MRI multicontrast kinetic analysis of the uptake and intracellular trafficking of paramagnetically labeled liposomes. *J Control Release* (2010) **144**:271–9. doi:10.1016/j.jconrel.2010.03.005
90. Howseman AM, Bowtell RW. Functional magnetic resonance imaging: imaging techniques and contrast mechanisms. *Philos Trans R Soc Lond B Biol Sci* (1999) **354**:1179–94. doi:10.1098/rstb.1999.0473
91. Gore JC, Manning HC, Quarles CC, Waddell KW, Yankelev TE. Magnetic resonance in the era of molecular imaging of cancer. *Magn Reson Imaging* (2011) **29**:587–600. doi:10.1016/j.mri.2011.02.003
92. Parker DL. Applications of NMR imaging in hyperthermia – an evaluation of the potential for localized tissue heating and noninvasive temperature monitoring. *IEEE Trans Biomed Eng* (1984) **31**:161–7. doi:10.1109/TBME.1984.325382
93. Rieke V, Butts Pauly K. MR thermometry. *J Magn Reson Imaging* (2008) **27**:376–90. doi:10.1002/jmri.21265
94. Parker DL, Smith V, Sheldon P, Crooks LE, Fussell L. Temperature distribution measurements in two-dimensional NMR imaging. *Med Phys* (1983) **10**:321–5. doi:10.1118/1.595307

95. Le Bihan D, Delannoy J, Levin RL. Temperature mapping with MR imaging of molecular diffusion: application to hyperthermia. *Radiology* (1989) **171**:853–7.
96. Young IR, Hand JW, Oatridge A, Prior MV, Forse GR. Further observations on the measurement of tissue T1 to monitor temperature in vivo by MRI. *Magn Reson Med* (1994) **31**: 342–5. doi:10.1002/mrm.1910310317
97. Graham SJ, Stanisz GJ, Kecovjevic A, Bronskill MJ, Henkelman RM. Analysis of changes in MR properties of tissues after heat treatment. *Magn Reson Med* (1999) **42**:1061–71. doi:10.1002/(SICI)1522-2594(199912)42:6<1061::AID-MRM1>3.0.CO;2-T
98. Chen J, Daniel BL, Pauly KB. Investigation of proton density for measuring tissue temperature. *J Magn Reson Imaging* (2006) **23**:430–7. doi:10.1002/jmri.20516
99. Ishihara Y, Calderon A, Watanabe H, Okamoto K, Suzuki Y, Kuroda K, et al. Precise and fast temperature mapping using water proton chemical-shift. *Magn Reson Med* (1995) **34**:814–23. doi:10.1002/mrm.1910340606
100. Galiana G, Branca RT, Jenista ER, Warren WS. Accurate temperature imaging based on intermolecular coherences in magnetic resonance. *Science* (2008) **322**:421–4. doi:10.1126/science.1163242
101. Quesson B, de Zwart JA, Moonen CTW. Magnetic resonance temperature imaging for guidance of thermotherapy. *J Magn Reson Imaging* (2000) **12**:525–33. doi:10.1002/1522-2586(200010)12:4<525::AID-JMRI3>3.0.CO;2-V
102. Peters RD, Hinks RS, Henkelman RM. Ex vivo tissue-type independence in proton-resonance frequency shift MR thermometry. *Magn Reson Med* (1998) **40**:454–9. doi:10.1002/mrm.1910400316
103. Weidensteiner C, Keriou N, Quesson B, de Senneville BD, Trillaud H, Moonen CT. Stability of real-time MR temperature mapping in healthy and diseased human liver. *J Magn Reson Imaging* (2004) **19**:438–46. doi:10.1002/jmri.20019
104. Bankson JA, Stafford RJ, Hazle JD. Partially parallel imaging with phase-sensitive data: increased temporal resolution for magnetic resonance temperature imaging. *Magn Reson Med* (2005) **53**:658–65. doi:10.1002/mrm.20378
105. Guo JY, Kholmovski EG, Zhang L, Jeong EK, Parker DL. k-Space inherited parallel acquisition (KIPA): application on dynamic magnetic resonance imaging thermometry. *Magn Reson Imaging* (2006) **24**:903–15. doi:10.1016/j.mri.2006.03.001
106. Kohler MO, Mougenot C, Quesson B, Enholm J, Le Bail B, Laurent C, et al. Volumetric HIFU ablation under 3D guidance of rapid MRI thermometry. *Med Phys* (2009) **36**:3521–35. doi:10.1111/j.1352-3151.2009.012112
107. Enholm JK, Kohler MO, Quesson B, Mougenot C, Moonen CTW, Sokka SD. Improved volumetric MR-HIFU ablation by robust binary feedback control. *IEEE Trans Biomed Eng* (2010) **57**:103–13. doi:10.1109/TBME.2009.2034636
108. Ergun AS. Analytical and numerical calculations of optimum design frequency for focused ultrasound therapy and acoustic radiation force. *Ultrasound* (2011) **51**:786–94. doi:10.1016/j.ultras.2011.03.006
109. Wu F, Wang Z-B, Cao Y-D, Zhou Q, Zhang Y, Xu Z-L, et al. Expression of tumor antigens and heat-shock protein 70 in breast cancer cells after high-intensity focused ultrasound ablation. *Ann Surg Oncol* (2007) **14**:1237–42. doi:10.1245/s10434-006-9275-6
110. Wu F, Zhou L, Chen WR. Host antitumor immune responses to HIFU ablation. *Int J Hyperthermia* (2007) **23**:165–71. doi:10.1080/02656730701206638
111. Zhou Q, Zhu X-Q, Zhang J, Xu Z-L, Lu P, Wu F. Changes in circulating immunosuppressive cytokine levels of cancer patients after high intensity focused ultrasound treatment. *Ultrasound Med Biol* (2008) **34**:81–7. doi:10.1016/j.ultrasmedbio.2007.07.013
112. Lu P, Zhu X-Q, Xu Z-L, Zhou Q, Zhang J, Wu F. Increased infiltration of activated tumor-infiltrating lymphocytes after high intensity focused ultrasound ablation of human breast cancer. *Surgery* (2009) **145**:286–93. doi:10.1016/j.surg.2008.10.010
113. Xu Z-L, Zhu X-Q, Lu P, Zhou Q, Zhang J, Wu F. Activation of tumor-infiltrating antigen presenting cells by high intensity focused ultrasound ablation of human breast cancer. *Ultrasound Med Biol* (2009) **35**: 50–7. doi:10.1016/j.ultrasmedbio.2008.08.005
114. Zhang Y, Deng J, Feng J, Wu F. Enhancement of antitumor vaccine in ablated hepatocellular carcinoma by high-intensity focused ultrasound. *World J Gastroenterol* (2010) **16**:3584–91. doi:10.3748/wjg.v16.i28.3584
115. Deng J, Zhang Y, Feng J, Wu F. Dendritic cells loaded with ultrasound-ablated tumor induce in vivo specific antitumor responses. *Ultrasound Med Biol* (2010) **36**:441–8. doi:10.1016/j.ultrasmedbio.2009.12.004
116. Higgins JP, Bernstein MB, Hodge JW. Enhancing immune responses to tumor-associated antigens. *Cancer Biol Ther* (2009) **8**:1440–9. doi:10.4161/cbt.8.15.9133
117. Liu F, Hu Z, Qiu L, Hui C, Li C, Zhong P, et al. Boosting high-intensity focused ultrasound-induced anti-tumor immunity using a sparse-scan strategy that can more effectively promote dendritic cell maturation. *J Transl Med* (2010) **8**:7. doi:10.1186/1479-5876-8-7
118. Dalfior D, Delahunt B, Brunelli M, Parisi A, Ficarra V, Novara G, et al. Utility of racemase and other immunomarkers in the detection of adenocarcinoma in prostatic tissue damaged by high intensity focused ultrasound therapy. *Pathology* (2010) **42**:1–5. doi:10.3109/00313020903434447
119. Zhong-Lin X, Xue-Qiang Z, Pei L, Qiang Z, Jun Z, Feng W. Activation of tumor-infiltrating antigen presenting cells by high intensity focused ultrasound ablation of human breast cancer. *Ultrasound Med Biol* (2009) **35**(1):50–7. doi:10.1016/j.ultrasmedbio.2008.08.005
120. Zhang H, Liu L, Sharma R, Alfieri A, Saha S, Garg M, et al. High intensity focused ultrasound (HIFU)-enhanced autologous in situ vaccination for prostate cancer. *Int J Radiat Oncol Biol Phys* (2008) **72**:S165–6. doi:10.1016/j.ijrobp.2008.06.516
121. Hu Z, Yang XY, Liu Y, Sankin GN, Pua EC, Morse MA, et al. Investigation of HIFU-induced anti-tumor immunity in a murine tumor model. *J Transl Med* (2007) **5**:34. doi:10.1186/1479-5876-5-34
122. Zerbini A, Pilli M, Fagnoni F, Pelosi G, Pizzi MG, Schivazappa S, et al. Increased immunostimulatory activity conferred to antigen-presenting cells by exposure to antigen extract from hepatocellular carcinoma after radiofrequency thermal ablation. *J Immunother* (2008) **31**:271–82. doi:10.1097/CJI.0b013e318160ff1c
123. ter Haar G, Rivens I, Chen L, Riddler S. High intensity focused ultrasound for the treatment of rat tumours. *Phys Med Biol* (1991) **36**:1495–501. doi:10.1088/0031-9155/36/11/009
124. Chen L, ter Haar G, Hill CR, Eccles SA, Box G. Treatment of implanted liver tumors with focused ultrasound. *Ultrasound Med Biol* (1998) **24**:1475–88. doi:10.1016/S0301-5629(98)00134-3

Conflict of Interest Statement: The authors declare that the research was conducted in the absence of any commercial or financial relationships that could be construed as a potential conflict of interest.

Received: 28 June 2013; accepted: 25 July 2013; published online: 19 August 2013.
Citation: Lai C-Y, Fite BZ and Ferrara KW (2013) Ultrasonic enhancement of drug penetration in solid tumors. Front. Oncol. 3:204. doi:10.3389/fonc.2013.00204

This article was submitted to Frontiers in Pharmacology of Anti-Cancer Drugs, a specialty of Frontiers in Oncology.

Copyright © 2013 Lai, Fite and Ferrara. This is an open-access article distributed under the terms of the Creative Commons Attribution License (CC BY). The use, distribution or reproduction in other forums is permitted, provided the original author(s) or licensor are credited and that the original publication in this journal is cited, in accordance with accepted academic practice. No use, distribution or reproduction is permitted which does not comply with these terms.



Tumor-penetrating peptides

Tambet Teesalu^{1,2}, Kazuki N. Sugahara^{1,3} and Erkki Ruoslahti^{1,4*}

¹ Cancer Research Center, Sanford-Burnham Medical Research Institute, La Jolla, CA, USA

² Laboratory of Cancer Biology, Centre of Excellence for Translational Medicine, Institute of Biomedicine and Translational Medicine, University of Tartu, Tartu, Estonia

³ Department of Surgery, College of Physicians and Surgeons, Columbia University, New York, NY, USA

⁴ Department of Cell, Molecular and Developmental Biology, University of California Santa Barbara, Santa Barbara, CA, USA

Edited by:

Angelo Corti, San Raffaele Scientific Institute, Italy

Reviewed by:

Angelo Corti, San Raffaele Scientific Institute, Italy

Fabrizio Marzocchi, Istituto Superiore di Sanità, Italy

***Correspondence:**

Erkki Ruoslahti, Cancer Research Center, Sanford-Burnham Medical Research Institute, 10901 North Torrey Pines Road, La Jolla, CA 92037, USA
e-mail: ruoslahti@sanfordburnham.org

Tumor-homing peptides can be used to deliver drugs into tumors. Phage library screening in live mice has recently identified homing peptides that specifically recognize the endothelium of tumor vessels, extravasate, and penetrate deep into the extravascular tumor tissue. The prototypic peptide of this class, iRGD (CRGDKGPD), contains the integrin-binding RGD motif. RGD mediates tumor-homing through binding to $\alpha\beta$ integrins, which are selectively expressed on various cells in tumors, including tumor endothelial cells. The tumor-penetrating properties of iRGD are mediated by a second sequence motif, R/KXXR/K. This C-end Rule (or CendR) motif is active only when the second basic residue is exposed at the C-terminus of the peptide. Proteolytic processing of iRGD in tumors activates the cryptic CendR motif, which then binds to neuropilin-1 activating an endocytic bulk transport pathway through tumor tissue. Phage screening has also yielded tumor-penetrating peptides that function like iRGD in activating the CendR pathway, but bind to a different primary receptor. Moreover, novel tumor-homing peptides can be constructed from tumor-homing motifs, CendR elements and protease cleavage sites. Pathologies other than tumors can be targeted with tissue-penetrating peptides, and the primary receptor can also be a vascular “zip code” of a normal tissue. The CendR technology provides a solution to a major problem in tumor therapy, poor penetration of drugs into tumors. The tumor-penetrating peptides are capable of taking a payload deep into tumor tissue in mice, and they also penetrate into human tumors *ex vivo*. Targeting with these peptides specifically increases the accumulation in tumors of a variety of drugs and contrast agents, such as doxorubicin, antibodies, and nanoparticle-based compounds. Remarkably the drug to be targeted does not have to be coupled to the peptide; the bulk transport system activated by the peptide sweeps along any compound that is present in the blood.

Keywords: synapic targeting, homing peptide, tumor-penetrating peptide, neuropilin-1, $\alpha\beta$ integrins, C-end Rule

INTRODUCTION

A major problem in systemic therapy is that only a small proportion of administered drug reaches its intended target site(s). Selective delivery of the drug to the target tissue can alleviate this problem. Affinity-based physical targeting (synapic, pathotropic, or active targeting) makes use of molecular markers that are specifically expressed at the target, and not elsewhere in the body, to accomplish selective targeting of systemically administered drugs (1). The desired outcome of the synapic targeting is similar to topical application: increased local accumulation and lower systemic concentration of the therapeutic payload.

Synapic targeting efforts have led to improved cancer drug delivery, but this approach only partially solves the selective delivery problem. Delivering a payload to a molecule specifically expressed on the surface of vascular cells in the target tissue can be effective because the vasculature is readily available for blood-borne probes. Thus, anti-angiogenic and vascular disrupting compounds can benefit from this approach. In fact, many of these compounds inherently target the vascular endothelium. An obvious example is antibodies that block the vascular

endothelial growth factor receptors [VEGF-Rs, (2)]. These receptors are generally expressed at elevated levels in tumor vasculature. Hence the antibody (or other VEGFR ligand) has more binding sites in tumor vessels than elsewhere and could selectively carry a payload there. Less well known is that many of the natural and designed anti-angiogenic proteins highjack integrin-binding plasma proteins (fibronectin, vitronectin, fibrinogen) to selectively target the angiogenic tumor vessels. The anti-angiogenic proteins for which this has been shown include angiostatin, endostatin, anginex, and anastellin (3). However, besides tumor vessels, it is desirable to also target the tumor cells (and stromal cells) within the tumor. While delivering a drug to tumor vessels can improve the efficacy of the drug, the drug still has to extravasate and penetrate into the extravascular tumor tissue to reach the tumor cells. The technology we review in this article provides a solution to the tumor penetration problem. It can also help to deal with another, less appreciated problem of synapic delivery: that the number of available receptors in a tumor is likely to be too low for the delivery of sufficient quantities of a payload drug.

VASCULAR ZIP CODES IN DRUG DELIVERY

The endothelia of vessels in different organs, even when morphologically indistinguishable, are molecularly (and as a result, likely functionally) different [“vascular zip codes,” (4)]. Moreover, specific response patterns are activated in vascular cells during processes such as tumor growth, inflammation, tissue repair, and atherosclerosis. Many of the zip codes elicited by these processes are secondary to angiogenesis, the sprouting of new blood vessels from existing vessels. A common denominator is endothelial cell (and pericyte) activation, but each condition can also put an individual signature of the vasculature. One set of activation-related cell surface molecules, comprised of P-selectin, E-selectin, ICAM-1, and VCAM-1, is turned on by inflammation in venular endothelial cells and mediates leukocyte rolling and adhesion/emigration in response to inflammation (5, 6). Another signature set of cell surface molecules, comprising certain integrins, growth factor receptors, extracellular proteases, and extracellular matrix proteins, is expressed during angiogenesis, which is the main factor making tumor vasculature distinguishable from normal vasculature in the adult organism. Lymphangiogenesis and macrophage infiltration also contribute to tumor-related marker molecules (7).

In vivo phage display has been instrumental in establishing the extent of the molecular specialization in the vasculature and has contributed a number of new markers of tumor vasculature (4, 8). Bacteriophage can be genetically modified to incorporate random peptide sequences as fusions with the coat proteins at a diversity of about one billion variants per library, which is close to the total number of possible permutations of a random 7-amino acid sequence (1.28E9). For *in vivo* selection, a library of phage displaying random peptides is injected systemically into the animals, followed by removal of target organs, amplification of the bound phage, and subjecting the amplified pool to another round of selection. *In vivo* peptide phage screening combines subtractive elements (removal of phage displaying pan-specific peptides) with positive selection at the target tissue (9). This technology has yielded peptides with unique tumor-penetrating properties as discussed below.

TUMOR-PENETRATING PEPTIDES

MODULAR STRUCTURE OF TUMOR-PENETRATING PEPTIDES

About 10 years ago, our laboratory identified a peptide, LyP-1 (CGNKRTRGC), with the ability to take the phage expressing it to the lymphatic vessels and hypoxic areas in tumors (10, 11). Surprisingly, the LyP-1 phage reached its targets in tumors within minutes of intravenous injection. Given that the phage is a nanoparticle and consequently diffuses slowly, diffusion did not seem to account for the rapid spreading within the tumor. It took the discovery of the CendR system, and the realization that it was responsible for the spreading within tumors of a more recently identified tumor-homing peptide, iRGD, to understand how these peptides penetrate into tumors (12, 13).

Tumor-penetrating peptides like iRGD and LyP-1 contain three independent modules: a vascular homing motif, an R/KXXR/K tissue penetration motif, and a protease recognition site. These modules cooperate to ensure a multistep, highly specific process of tumor-homing and penetration. The sequence of the prototypic tumor-penetrating peptide, iRGD, is CRGDR/KGPDC. We mostly

use the K-variant, CRGDKGPDC, because it appears to provide stronger tumor-homing than the R-variant. Following systemic administration, the iRGD peptide is first recruited through its RGD motif to αv integrins, which are overexpressed on tumor endothelial cells. After the initial binding, proteolytic processing exposes the internal R/KXXR/K motif at the C-terminus of the truncated peptide. We have termed the R/KXXR/K motif the C-end Rule or CendR motif (pronounced sender) because of the requirement of C-terminal exposure for activity. The C-terminal CendR motif interacts with neuropilin-1 (NRP-1), and the NRP-1 interaction triggers the activation of a transport pathway (CendR pathway) through the vascular wall and through extravascular tumor tissue (12, 13). These peptides can take along both conjugated and co-administered payloads into the tumor parenchyma.

We came across the CendR phenomenon while screening phage libraries for peptides that would bind to and internalize into cells isolated from tumors grown in mice. We were initially disappointed to find that, independent of the starting library configuration (we used cysteine-flanked cyclic and linear random heptapeptide libraries), the selected peptides all looked similar; they all had a C-terminal arginine or lysine residues with another basic amino acid at the -3 position. However, we soon realized that the consensus motif, R/KXXR/K, had to be some kind of a master cell internalization signal and set out to study it. It is worth noting that, while our laboratory used the filamentous phage display system introduced by Smith (14, 15) in our early studies (8, 16), we later switched to the T7 phage. The important distinction is that in T7, the exogenous peptide is expressed at the C-terminus of the phage coat protein, whereas it is at the N-terminal end in the filamentous phage. Thus, the C-terminal truncations producing the CendR motif could only be selected for in the T7 system.

The binding and internalization of R/KXXR/K-displaying phage or synthetic nanoparticles required the presence of free C-terminal arginine or lysine residues as addition of additional amino acid residues to the motif or amidation of the carboxyl terminus resulted in loss of activity (12). In addition to the prostate cancer cell lines, the active CendR motif triggered binding, and internalization in many cultured tumor cell lines and in cells in suspensions prepared from normal mouse tissues. Studies on the prototypic active CendR peptide, RPAPPAR, showed that the binding only takes place for the peptide made of L-amino acids and that the binding can be inhibited by excess of free peptide, suggesting the existence of a saturable receptor with a chiral recognition specificity. In contrast, cell-penetrating peptides, widely used for intracellular delivery of payloads *in vitro* are independent of position and chirality, and no specific receptors for them have been identified.

Affinity chromatography with RPAPPAR identified NRP-1 as the main binding molecule for RPAPPAR. NRP-1 is a transmembrane receptor with major roles in cell migration and endothelial cell sprouting in blood vessels, while NRP-2 with a similar, but not identical binding specificity is abundant and plays an important role in lymphatic vessels (17, 18). NRP-1 is best known for its role as a co-receptor for certain members of the vascular endothelial growth factor (VEGF) and semaphorin families (19, 20). The NRP-1-binding VEGFs and semaphorins, and TGF β ,

all have C-terminal CendR motifs. Tuftsin is an immonomodulatory peptide that has been shown to bind to NRP-1 [it has a C-terminal arginine residue, but lacks the complete CendR motif; (21)]. It induces vascular permeability (22), but no evidence on tissue penetration has been presented.

The b1b2 domain of NRP-1 that contains the binding pocket for the CendR motif has been crystallized together with tuftsin (23). Molecular modeling studies show that peptides with a C-terminal CendR motif, such as RPAPAR fit well to the binding pocket, but do not provide an explanation for the role of the penultimate arginine residue, which remains outside the binding pocket [Figure 1; (24, 25)]. Perhaps this arginine could be engaging an as-yet unknown molecule in a three-way interaction with NRP-1.

Based on molecular simulations and phage binding to purified NRP-1 protein it appears that formation of a stable complex between a CendR peptide and NRP-1 requires interaction of the -2 and -3 residues with loop III of the b1 domain of the NRP-1, as in the case of RPAR, RRAR, RDAR, RPDR, RPRR, and RPPR (25). For a stable interaction to occur, loop III must be engaged in a pairwise interaction that stabilizes the interaction of the C-terminal carboxylic group with the CendR binding pocket in the b1 domain of NRP-1.

Interestingly, the D-conformer of RPAPAR is a poor fit with the binding pocket, suggesting that the D-Tat, even with a C-terminal arginine would not bind to NRP-1. The modeling studies also indicate that under some circumstances a cyclic peptide could fit into the binding pocket (24). Indeed, peptides built on a thermostable, protease-resistant cyclotide kalata B1 scaffold have been described that are thought to interact with NRP-1 as intact cyclic peptides (26). These modeling studies provide a basis for *in silico* screening of CendR analogs and evaluation of low molecular

weight compounds resulting from high throughput screening. The molecules that bind to the CendR binding pocket on b1b2 domain of NRP-1 will be either acting as agonists or antagonists with potential applications in cancer drug delivery, and in diseases associated with elevated vascular permeability and pathogen spreading in tissues (see below).

A wide range of other receptors have been reported to use NRP-1 as a co-receptor, earning NRP-1 designation as a “hub” receptor (27), but it is not clear whether the ligands of these receptors use the CendR motif binding site for docking to NRP-1. Whereas NRP-1 can signal independently of other signal-transducing receptors, the primary role of NRP-1 is believed to be acting as a co-receptor that ensures the recruitment and presentation of various ligands to the effector receptors. NRP-1 is overexpressed in many cancer cell lines, where it is implicated in migration, proliferation, and survival. NRP-1 is overexpressed in tumors, both in cancer cells and in stromal cells, and is implicated in development and maintenance of the tumor vessels and in tumor growth and progression (28, 29). NRP-1 is a target of anti-cancer therapy with antibodies and peptide-bound therapeutic agents (30–34). However, as the NRPs are also widely expressed in normal vessels, the overexpression in tumors will only afford a degree of tumor specificity. Another aspect is that in bloodstream, plasma proteases carboxypeptidases [e.g., carboxypeptidase M and N; (35)] rapidly remove C-terminal arginine residues, thus limiting the efficacy of systemic active CendR peptides in tumor drug delivery. In contrast, the localized tumor-specific proteolytic activation of the cryptic CendR motif of our tumor-penetrating peptides results in tumor-specific activation of a cell and tissue penetration pathway.

THE CendR PATHWAY

The ability of VEGF and semaphorins to increase vascular permeability has been recognized for some time. Dvorak and Feng (36) showed that VEGF induces the formation of a network of tubular vesicles in endothelial cells they named the “Vesiculo-vacuolar organelle,” and presented morphological evidence that these interconnected vesicles could form a pathway through cells. The complicating factor in interpreting these results is the activity of the main signaling receptors for VEGF (VEGF-Rs) and for the semaphorins (plexins). CendR peptides allow one to study the NRP binding in isolation of other receptors and have made it possible to show that NRP-1 [and NRP-2, (37)] activate a trans-tissue transport pathway.

The uptake of the payload of CendR peptides into intracellular vesicles shows that the entry into cells is through an endosomal route. Moreover, the rapid penetration of the payloads of tumor-homing CendR peptides into tumors *in vivo* and *ex vivo*, and its energy dependence (13, 37, 38) shows that this is an active transport pathway, not one dependent on diffusion. The CendR pathway may be distinct from the known endosomal pathways, but at this point the evidence to that effect is limited to the use of various pharmaceutical inhibitors of the known pathways (12). The extravasation and tumor-penetration activities of iRGD suggest that the payload of the CendR endocytic vesicles is also at least partially released from cells by fusion of the endosomes with the plasma membrane. We have not yet observed the exocytosis phase of this presumed transcellular pathway, but the rapid tissue

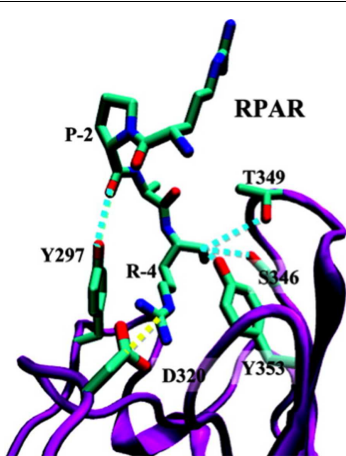


FIGURE 1 | Ribbon representation of the NRP-1-RPAR complex showing the most notable interactions found between the peptide and the binding pocket of NRP-1. The ligand and the interacting side chains of the receptor are depicted as solid lines. NRP-1 backbone is shown in purple and RPAR backbone in green. Hydrogen bonds are shown as blue discontinuous lines while salt bridges are marked by yellow discontinuous lines. Reprinted with permission from Haspel et al. (24). Copyright 2011 American Chemical Society.

penetration of the CendR payloads support of this possibility. However, we cannot exclude that an alternative pathway such as propelling cell surface-bound payload forward by the cell membrane or membrane projections. Genetic and proteomics studies are underway to elucidate the cellular molecular basis of the CendR pathway.

Our discovery of the CendR tissue transport pathway raises the fascinating question of the physiological function of this pathway. While the focus so far has been on how this pathway might be used in drug delivery, it obviously does not exist for this purpose. One possibility is that it facilitates the transfer of nutrients to cells that are far from blood vessels or otherwise under duress. The overexpression of NRP-1 in tumors suggests that supplying nutrient deficient/hypoxic areas in tumors may be yet another way tumors make use of a physiological pathway to foster their own growth. The CendR pathway may have been hijacked by viruses and microbial toxins for cell entry and tissue spreading. Cleavage of a viral surface proteins and pro-toxins by host proteases (most commonly furins and related enzymes) at sites that create an active CendR motif is a recurrent theme seen in many pathogens. Examples include the Human T-lymphotropic virus-2, Crimean–Congo hemorrhagic fever virus, tick-born encephalitis virus, and Ebola viruses, as well as anthrax toxin (39–43). CendR sequences are also present in snake and bee venoms (e.g., mellitin), and may contribute to the spreading of these toxins in tissues.

Vascular edema is associated with many diseases (hemorrhagic virus infections, sepsis, and vascular leak syndromes). Several proinflammatory vasoactive (poly)peptides capable of increasing vascular permeability display a functionally important arginine residue at their C-terminus. Examples include complement C3a and C5a anaphylatoxins (C-terminal sequences ASHLGLAR and KDMQLGR, respectively) as well as kinins (bradykinin and kallidin, which have an identical C-terminal sequence, RPPGF-SPFR). Intriguingly, we have observed that phage that display peptides corresponding to the C-terminal amino acids of C5/3a and bradykinin bind to the recombinant b1b2 domain of NRP (in preparation) and that the binding is reversed by an excess of the free peptide. It remains to be seen whether the NRP/CendR axis plays a role in the activity of C3/5a, bradykinin, and/or other vasoactive peptides.

DESIGNER PEPTIDES FOR CendR PATHWAY ACTIVATION

Having worked out the two-motif requirement for a tumor-homing peptide to have CendR activity, we tested the universality of the concept by designing a new peptide with such activities. We used as the starting point the NGR tumor-homing motif previously identified by our laboratory (44, 45), which recognizes a form of aminopeptidase N in angiogenic tumor vessels (46, 47). We added a second arginine to the NGR motif to convert it into the CendR motif, RNGR and embedded that motif in the iRGD framework by replacing RGDK with RNGR. The resulting peptide, iNGR (CRNGRGPDC) has all the properties of iRGD, except that its tumor recruitment is not mediated by integrin but another receptor, presumably aminopeptidase N (48). We have also designed tumor-homing CendR peptides by arranging in tandem a CendR motif, a proteolytic cleavage site for a tumor-associated protease that cleaves after a basic residue, and a tumor-homing motif (Teesalu et al., in preparation). These peptides also home to and

penetrate into tumors. A construct created to deliver a non-specific cell-penetrating peptide, appears to serendipitously follow this design (49). Whether these tandem tumor-penetrating peptides are as effective as the peptides in which the homing motif and CendR motif overlap remains to be seen. The iRGD and LyP-1 peptides lose their affinity for the primary receptor [αv integrins for iRGD and a mitochondrial/cell surface protein p32 for LyP-1 (7) after the proteolytic cleavage that activates the CendR motif has taken place (13, 37)]. The resulting release of the peptide from the primary receptor may facilitate subsequent binding to NRP-1 and make the primary receptor available for binding of another intact peptide. Peptides with tandem motifs would lack this latter feature. Another possible design for CendR activation would be blocking the C-terminus with a chemical group other than an amino acid or peptide. One can envision peptides, the CendR activity of which is triggered by a phosphatase, demethylase, sulfatase, etc. To the extent such an enzyme is specific for the target tissue, new useful probes could be created.

DRUG DELIVERY WITH TUMOR-PENETRATING PEPTIDES

THE DRUG PENETRATION PROBLEM

To reach tumor cells and tumor-associated parenchymal cells (e.g., tumor-associated fibroblasts, macrophages), drugs must cross the vascular barrier and penetrate into the extravascular stroma. Cancerous tissue is heterogeneous, with striking regional differences in tumor structure (leaky vasculature and defective lymphatics, which causes buildup of interstitial fluid pressure in the tumor), and physiology (e.g., inflammation, fibrosis, hypoxia, acidity). These features translate into steep drug gradients and variability in the uptake and distribution of anti-cancer drugs within tumor parenchyma (50). For example, evaluation of doxorubicin distribution in tumors after systemic administration showed that the concentration of this drug decreases exponentially with distance from tumor blood vessels, reaching half of its perivascular concentration at a distance of about 40 μm (51). The distribution of trastuzumab (Herceptin) in breast tumor xenografts is also highly heterogeneous with many tumor cells exposed to no detectable drug (52). To some extent, the tumor drug delivery challenges are alleviated by the Enhanced Permeability and Retention (EPR) effect – accumulation of compounds (typically liposomes, nanoparticles, and macromolecular drugs) in tumor tissue more than they do in normal tissues. The underlying causes of the EPR effect are abnormal structure and function of tumor vessels: poorly aligned endothelial cells with fenestrations, deficient pericyte coverage, and lack of lymphatic drainage. However, EPR is highly variable as it is influenced by differences between tumor types and heterogeneity within individual tumor. Tumor interstitial pressure (IFP) depends on integrity of blood and lymphatic vessels, tumor cell proliferation, deposition of matrix molecules, and interaction of cells with the matrix molecules. The difference between tumor microvascular fluid pressure and IFP determines intratumoral convection fluxes that have a major influence on the vascular exit of the compounds over 10 kDa. Intratumoral fluid pressure gradients can be in some cases favorably influenced by vasodilatory compounds such as bradykinin, endothelin, and calcium channel antagonists, to allow better tumor perfusion and increased drug delivery (53). Other approaches include dissolving extracellular matrix with enzymes such as collagenase or hyaluronidase (54),

or killing or inhibiting the activity of tumor-associated fibroblasts (55). Obviously, the delivery of enzymes and drugs aimed at lowering the IFP to the tumor parenchyma faces the similar tumor penetration challenges seen for the cancer drugs.

CendR-ENHANCED DRUG DELIVERY

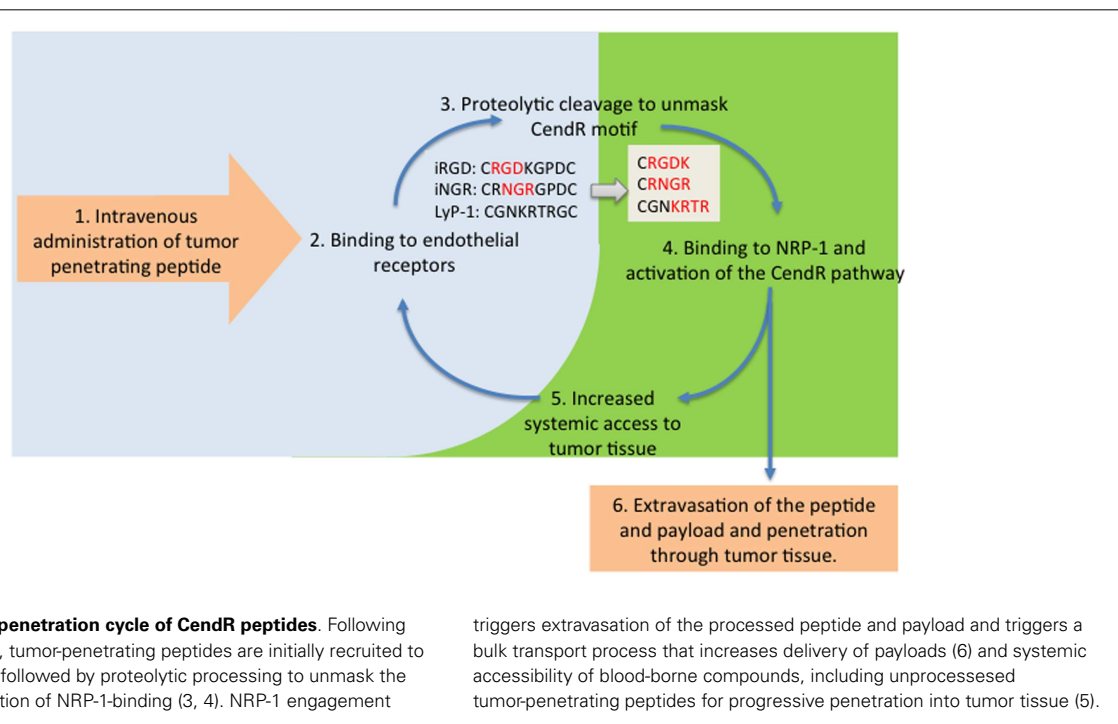
The tumor-homing CendR peptides provide a solution to the drug penetration problem. A probe or drug attached to iRGD or LyP-1 is delivered to extracellular tumor tissue more effectively than the drug alone. We have extensively demonstrated the tumor penetration with fluorescein (FAM)-labeled peptides. Intravenously injected FAM-iRGD, LyP-1, and iNGR are found dispersed in tumor parenchyma minutes after administered, whereas FAM-labeled inactive control peptides do not appear in the tumors at all. FAM-labeled homing peptides that lack a CendR motif bind to the blood vessels, but do not penetrate into the rest of the tumor (10, 11, 13, 48). Remarkably, iRGD and LyP-1 have quite different distributions within tumors, presumably reflecting the expression of their primary receptors in different tumor compartments (7, 10, 13). The effect of the cryptic CendR motif is vividly illustrated by the differences between iRGD and conventional RGD peptides, such as CRGDC and cycloRGDFK. While iRGD payload, even a poorly diffusing nanoparticle, readily enters tumor parenchyma, the conventional RGD peptides only take their payload to the tumor vessels (13, 38). LyP-1 and CGKRK, a peptide we have recently shown to also use p32 as its receptor but lack the CendR activity (56) show a similar difference (11, 57).

The observations with the fluorescent probe described above prompted us to study the ability of iRGD and the other CendR peptides to enhance the delivery of actual anti-cancer drugs to tumors. We have shown that therapeutics as diverse as a small molecular weight drug (doxorubicin), trastuzumab (anti-Her2 antibody), and the nanoparticle drugs Abraxane and Doxil can

benefit from iRGD-enhanced delivery (13, 38). In showing this, we mostly made use of a unique property of iRGD and other similar peptides; they can enhance tumor penetration of payloads that are not attached to the peptide, just administered at the same time. The reason is that iRGD activates a bulk transport pathway that moves along any compound present in the blood when the system is active. The scheme in **Figure 2** illustrates this principle.

Timing measurements have shown that the CendR pathway is active for about 1 h, with peak activity about 30 min after the administration of the peptide (38). The timing agrees with the half-life of the peptide in the blood, which for a peptide of this size can be expected to be about 10 min (58). The main reason for the short half-life is elimination of the peptide through filtration into the urine. It remains to be determined whether prolonging the half-life of the peptide would further enhance drug delivery into tumors. We compared the efficacy of directly conjugating the drug to iRGD and the co-administration with Abraxane as the drug. Both methods gave significantly higher anti-tumor activity than the drug alone, and seemed equally effective in this regard in the tumor system we studied (38). However, it should be noted that the number of receptors at the target limits the efficacy of the conjugated delivery. Calculations show that a gram of tumor tissue is not likely to have more than a few picomoles of any given receptor available for targeting of drugs with probes coupled to the drug (1). Most drugs to be effective require greater concentrations than could be delivered to this small amount of receptor. The co-administration mode does not have this limitation, as only the triggering of the trans-tissue transport pathway is needed. Another major advantage is that it is not necessary to conjugate the drug to the homing peptide, which would create a new chemical entity with the attendant regulatory hurdles.

LyP-1 coupled to Abraxane nanoparticles also increased the efficacy of the drug (59) and iNGR promoted the activity of



doxorubicin in a mouse tumor model in a way similar to iRGD (48), by a factor of about 3. Importantly, the iRGD work with doxorubicin showed that there was no change in the main side effect of this drug, cardiotoxicity. This side effect was nearly eliminated by a threefold reduction of the drug dose. Thus, the tumor-penetrating peptides can be used both to enhance the activity of anti-cancer drugs, or lowering the side effect with the same anti-cancer activity, or some of both.

The tumor-penetrating peptides can also enhance tumor imaging, as demonstrated by coating iron oxide nanoparticles with iRGD for MRI imaging. iRGD gave stronger images than a conventional RGD peptide, CRGDC; the main difference was that iRGD spread into the whole tumor, whereas only highlighted the tumor vessels (13). LyP-1 has been used in optical imaging of tumors (11, 61) and atherosclerotic plaques (60), as well as in MRI and PET imaging of plaques (61). LyP-1 homes to and penetrates into activated macrophages in tumors and atherosclerotic plaques (60, 61) revealing a similarity between the macrophages in tumors and the plaques (61). LyP-1 has also been shown to selectively accumulate in tumor-draining lymph nodes prior to the arrival of tumor cells, defining a premalignant niche in tumors (62).

CONCLUSION AND FUTURE PROSPECTS

The discovery of tumor-penetrating peptides has led to the identification of a new trans-tissue transport pathway, the C-end Rule or CendR pathway. The physiological function of the CendR pathway and its molecular workings are obviously important questions

to be answered in future studies. Activating the pathway in a tumor-specific manner, which is accomplished with peptides the CendR motif of which is activated in tumors, provides a way of increasing the activity of anti-cancer drugs and enhancing tumor imaging. Thus, the tumor-penetrating CendR peptides represent a potentially significant advance in cancer treatment.

ACKNOWLEDGMENTS

The authors' original work reviewed in this article is supported by Cancer Center Support Grant CA30199 to SBMRI, Innovator Awards W81XWH-08-1-0727, W81XWH-09-0698 from the Department of Defense, and grant CA CA152327 from the National Cancer Institute. Tambet Teesalu is supported by European Research Council starting grant (GliomaDDS) and the Wellcome Trust Award 095077/Z/10/Z.

NIH AUTHOR DISCLAIMER

The views and opinions of authors expressed on OER websites do not necessarily state or reflect those of the U.S. Government, and they may not be used for advertising or product endorsement purposes.

DOD AUTHOR DISCLAIMER

The opinions expressed herein are those of the author(s) and are not necessarily representative of those of the Uniformed Services University of the Health Sciences (USUHS), the Department of Defense (DOD); or, the United States Army, Navy, or Air Force.

REFERENCES

- Ruosahti E, Bhatia SN, Sailor MJ. Targeting of drugs and nanoparticles to tumors. *J Cell Biol* (2010) **188**:759–68. doi:10.1083/jcb.200910104
- Ferrara N, Alitalo K. Clinical applications of angiogenic growth factors and their inhibitors. *Nat Med* (1999) **5**:1359–64. doi:10.1038/9467
- Akerman ME, Pilch J, Peters D, Ruosahti E. Angiostatic peptides use plasma fibronectin to home to angiogenic vasculature. *Proc Natl Acad Sci U S A* (2005) **102**:2040–5. doi:10.1073/pnas.0409844102
- Ruosahti E. Peptides as targeting elements and tissue penetration devices for nanoparticles. *Adv Mater* (2012) **24**:3747–56. doi:10.1002/adma.201200454
- Girard JP, Springer TA. High endothelial venules (HEVs), specialized endothelium for lymphocyte migration. *Immunol Today* (1995) **16**:449–57. doi:10.1016/0167-5699(95)80023-9
- Libby P, DiCarli M, Weissleder R. The vascular biology of atherosclerosis and imaging targets. *J Nucl Med* (2010) **51**(Suppl 1):33S–7. doi:10.2967/jnumed.109.069633
- Fogal V, Zhang L, Krajewski S, Ruosahti E. Mitochondrial/cell-surface protein p32/gC1qR as a molecular target in tumor cells and tumor stroma. *Cancer Res* (2008) **68**:7210–8. doi:10.1158/0008-5472.CAN-07-6752
- Pasqualini R, Ruosahti E. Tissue targeting with phage peptide libraries. *Mol Psychiatry* (1996) **1**:423.
- Teesalu T, Sugahara KN, Ruosahti E. Mapping of vascular ZIP codes by phage display. *Methods Enzymol* (2012) **503**:35–56. doi:10.1016/B978-0-12-396962-0.00002-1
- Laakkonen P, Porkka K, Hoffman JA, Ruosahti E. A tumor-homing peptide with a targeting specificity related to lymphatic vessels. *Nat Med* (2002) **8**:751–5.
- Laakkonen P, Akerman ME, Biliran H, Yang M, Ferrer F, Karpanen T, et al. Antitumor activity of a homing peptide that targets tumor lymphatics and tumor cells. *Proc Natl Acad Sci U S A* (2004) **101**:9381–6. doi:10.1073/pnas.0403317101
- Teesalu T, Sugahara KN, Kotamraju VR, Ruosahti E. C-end rule peptides mediate neuropilin-1-dependent cell, vascular, and tissue penetration. *Proc Natl Acad Sci USA* (2009) **106**:16157–62. doi:10.1073/pnas.0908201106
- Sugahara KN, Teesalu T, Karmali PP, Kotamraju VR, Agemy L, Girard OM, et al. Tissue-penetrating delivery of compounds and nanoparticles into tumors. *Cancer Cell* (2009) **16**:510–20. doi:10.1016/j.ccr.2009.10.013
- Scott JK, Smith GP. Searching for peptide ligands with an epitope library. *Science* (1990) **249**:386–90. doi:10.1126/science.1696028
- Smith GP. Filamentous fusion phage, novel expression vectors that display cloned antigens on the virion surface. *Science* (1985) **228**:1315–7. doi:10.1126/science.4001944
- Koivunen E, Gay DA, Ruosahti E. Selection of peptides binding to the alpha 5 beta 1 integrin from phage display library. *J Biol Chem* (1993) **268**:20205–10.
- Yuan L, Moyon D, Pardanaud L, Breant C, Karkkainen MJ, Alitalo K, et al. Abnormal lymphatic vessel development in neuropilin 2 mutant mice. *Development* (2002) **129**:4797–806.
- Xu Y, Yuan L, Mak J, Pardanaud L, Caunt M, Kasman I, et al. Neuropilin-2 mediates VEGF-C-induced sprouting together with VEGFR3. *J Cell Biol* (2010) **188**:115–30. doi:10.1083/jcb.200903137
- He Z, Tessier-Lavigne M. Neuropilin is a receptor for the axonal chemorepellent semaphorin III. *Cell* (1997) **90**:739–51. doi:10.1016/S0092-8674(00)80534-6
- Soker S, Takashima S, Miao HQ, Neufeld G, Klagsbrun M. Neuropilin-1 is expressed by endothelial and tumor cells as an isoform-specific receptor for vascular endothelial growth factor. *Cell* (1998) **92**:735–45. doi:10.1016/S0092-8674(00)81402-6
- von Wronski MA, Raju N, Pillai R, Bogdan NJ, Marinelli ER, Nanjappan P, et al. Tuftsin binds neuropilin-1 through a sequence similar to that encoded by exon 8 of vascular endothelial growth factor. *J Biol Chem* (2006) **281**:5702–10. doi:10.1074/jbc.M511941200
- Gerdin B, Lindeberg G, Ragnarsdóttir U, Saldeen T, Wallin R. Structural requirements for microvascular permeability-increasing ability of peptides. Studies on analogues of a fibrinogen pentapeptide fragment. *Biochim Biophys Acta* (1983) **757**:366–70. doi:10.1016/0304-4165(83)90063-6

23. Vander Kooi CW, Jusino MA, Perman B, Neau DB, Bellamy HD, Leahy DJ. Structural basis for ligand and heparin binding to neuropilin B domains. *Proc Natl Acad Sci U S A* (2007) **104**:6152–7. doi:10.1073/pnas.0700043104
24. Haspel N, Zanuy D, Nussinov R, Teesalu T, Ruoslahti E, Aleman C. Binding of a C-end rule peptide to the neuropilin-1 receptor, a molecular modeling approach. *Biochemistry* (2011) **50**:1755–62. doi:10.1021/bi101662j
25. Zanuy D, Kotla R, Nussinov R, Teesalu T, Sugahara KN, Aleman C, et al. Sequence dependence of C-end rule peptides in binding and activation of neuropilin-1 receptor. *J Struct Biol* (2013) **182**:78–86. doi:10.1016/j.jsb.2013.02.006
26. Getz JA, Cheneval O, Craik DJ, Daugherty PS. Design of a Cyclotide antagonist of neuropilin-1 and -2 that potently inhibits endothelial cell migration. *ACS Chem Biol* (2013) **8**:1147–54. doi:10.1021/cb4000585
27. Uwienicz KA, Fernig DG. Neuropilins, a versatile partner of extracellular molecules that regulate development and disease. *Front Biosci* (2008) **13**:4339–60. doi:10.2741/3008
28. Bagri A, Tessier-Lavigne M, Watts RJ. Neuropilins in tumor biology. *Clin Cancer Res* (2009) **15**:1860–4. doi:10.1158/1078-0432.CCR-08-0563
29. Pellet-Many C, Frankel P, Jia H, Zachary I. Neuropilins, structure, function and role in disease. *Biochem J* (2008) **411**:211–26. doi:10.1042/BJ20071639
30. Jia H, Bagherzadeh A, Hartzoulakis B, Jarvis A, Lohr M, Shaikh S, et al. Characterization of a bicyclic peptide neuropilin-1 (NP-1) antagonist (EG3287) reveals importance of vascular endothelial growth factor exon 8 for NP-1 binding and role of NP-1 in KDR signaling. *J Biol Chem* (2006) **281**:13493–502. doi:10.1074/jbc.M512121200
31. Hong TM, Chen YL, Wu YY, Yuan A, Chao YC, Chung YC, et al. Targeting neuropilin 1 as an antitumor strategy in lung cancer. *Clin Cancer Res* (2007) **13**:4759–68. doi:10.1158/1078-0432.CCR-07-0001
32. Liang WC, Dennis MS, Stawicki S, Chanthery Y, Pan Q, Chen Y, et al. Function blocking antibodies to neuropilin-1 generated from a designed human synthetic antibody phage library. *J Mol Biol* (2007) **366**:815–29. doi:10.1016/j.jmb.2006.11.021
33. Karjalainen K, Jaalouk DE, Bueso-Ramos CE, Zurita AJ, Kuniyasu A, Eckhardt BL, et al. Targeting neuropilin-1 in human leukemia and lymphoma. *Blood* (2011) **117**:920–7. doi:10.1182/blood-2010-05-282921
34. Nasarre C, Roth M, Jacob L, Roth L, Koncina E, Thien A, et al. Peptide-based interference of the transmembrane domain of neuropilin-1 inhibits glioma growth in vivo. *Oncogene* (2010) **29**:2381–92. doi:10.1038/onc.2010.9
35. Skidgel RA. Bradykinin-degrading enzymes, structure, function, distribution, and potential roles in cardiovascular pharmacology. *J Cardiovasc Pharmacol* (1992) **20**(Suppl 9):S4–9. doi:10.1097/00005344-199206209-00002
36. Dvorak AM, Feng D. The vesiculo-vacuolar organelle (VVO). A new endothelial cell permeability organelle. *J Histochem Cytochem* (2001) **49**:419–32. doi:10.1177/002215540104900401
37. Roth L, Agemy L, Kotamraju VR, Braun G, Teesalu T, Sugahara KN, et al. Transtumoral targeting enabled by a novel neuropilin-binding peptide. *Oncogene* (2012) **31**:3754–63. doi:10.1038/onc.2011.537
38. Sugahara KN, Teesalu T, Karmali PP, Kotamraju VR, Agemy L, Greenwald DR, et al. Coadministration of a tumor-penetrating peptide enhances the efficacy of cancer drugs. *Science* (2010) **328**:1031–5. doi:10.1126/science.1183057
39. Chambers TJ, Weir RC, Grakoui A, McCourt DW, Bazan JF, Fletterick RJ, et al. Evidence that the N-terminal domain of nonstructural protein NS3 from yellow fever virus is a serine protease responsible for site-specific cleavages in the viral polyprotein. *Proc Natl Acad Sci U S A* (1990) **87**:8898–902. doi:10.1073/pnas.87.22.8898
40. Wool-Lewis RJ, Bates P. Endoproteolytic processing of the ebola virus envelope glycoprotein, cleavage is not required for function. *J Virol* (1999) **73**:1419–26.
41. Sjöberg M, Wallin M, Lindqvist B, Garoff H. Furin cleavage potentiates the membrane fusion-controlling intersubunit disulfide bond isomerization activity of leukemia virus Env. *J Virol* (2006) **80**:5540–51. doi:10.1128/JVI.01851-05
42. Sanchez AJ, Vincent MJ, Erickson BR, Nichol ST. Crimean-congo hemorrhagic fever virus glycoprotein precursor is cleaved by furin-like and SKI-1 proteases to generate a novel 38-kilodalton glycoprotein. *J Virol* (2006) **80**:514–25. doi:10.1128/JVI.80.1.514-525.2006
43. Molloy SS, Bresnahan PA, Leppala SH, Klimpel KR, Thomas G. Human furin is a calcium-dependent serine endoprotease that recognizes the sequence arg-X-X-arg and efficiently cleaves anthrax toxin protective antigen. *J Biol Chem* (1992) **267**:16396–402.
44. Arap W, Pasqualini R, Ruoslahti E. Cancer treatment by targeted drug delivery to tumor vasculature in a mouse model. *Science* (1998) **279**:377–80. doi:10.1126/science.279.5349.377
45. Koivunen E, Wang B, Ruoslahti E. Phage libraries displaying cyclic peptides with different ring sizes, ligand specificities of the RGD-directed integrins. *Biotechnology (N Y)* (1995) **13**:265–70. doi:10.1038/nbt0395-265
46. Pasqualini R, Koivunen E, Kain R, Lahdenranta J, Sakamoto M, Stryhn A, et al. Aminopeptidase N is a receptor for tumor-homing peptides and a target for inhibiting angiogenesis. *Cancer Res* (2000) **60**:722–7.
47. Corti A, Curnis F, Arap W, Pasqualini R. The neovasculature homing motif NGR, more than meets the eye. *Blood* (2008) **112**:2628–35. doi:10.1182/blood-2008-04-150862
48. Alberici L, Roth L, Sugahara KN, Agemy L, Kotamraju VR, Teesalu T, et al. De novo design of a tumor-penetrating peptide. *Cancer Res* (2013) **73**:804–12. doi:10.1158/0008-5472.CAN-12-1668
49. Myrberg H, Zhang L, Mae M, Langell U. Design of a tumor-homing cell-penetrating peptide. *Bioconjug Chem* (2008) **19**(1):70–5. doi:10.1021/bc0701139
50. Tredan O, Galmarini CM, Patel K, Tannock IF. Drug resistance and the solid tumor microenvironment. *J Natl Cancer Inst* (2007) **99**:1441–54. doi:10.1093/jnci/djm135
51. Primeau AJ, Rendon A, Hedley D, Lilge L, Tannock IF. The distribution of the anticancer drug doxorubicin in relation to blood vessels in solid tumors. *Clin Cancer Res* (2005) **11**:8782–8. doi:10.1158/1078-0432.CCR-05-1664
52. Baker JH, Lindquist KE, Huxham LA, Kyle AH, Sy JT, Minchinton AI. Direct visualization of heterogeneous extravascular distribution of trastuzumab in human epidermal growth factor receptor type 2 over-expressing xenografts. *Clin Cancer Res* (2008) **14**:2171–9. doi:10.1158/1078-0432.CCR-07-4465
53. Feron O. Targeting the tumor vascular compartment to improve conventional cancer therapy. *Trends Pharmacol Sci* (2004) **25**:536–42. doi:10.1016/j.tips.2004.08.008
54. Tufto I, Hansen R, Ryberg D, Nygaard KHH, Tufto J, Davies CDL. The effect of collagenase and hyaluronidase on transient perfusion in human osteosarcoma xenografts grown orthotopically and in dorsal skinfold chambers. *Anticancer Res* (2007) **27**:1475–81.
55. Xing F, Saidou J, Watabe K. Cancer associated fibroblasts (CAFs) in tumor microenvironment. *Front Biosci* (2010) **15**:166–79. doi:10.2741/3613
56. Agemy L, Kotamraju VR, Friedmann-Morvinski D, Sharma S, Sugahara KN, Ruoslahti E. Proapoptotic peptide-mediated cancer therapy targeted to cell surface p32. *Mol Ther* (Forthcoming 2013).
57. Agemy L, Friedmann-Morvinski D, Kotamraju VR, Roth L, Sugahara KN, Girard OM, et al. Targeted nanoparticle enhanced proapoptotic peptide as potential therapy for glioblastoma. *Proc Natl Acad Sci U S A* (2011) **108**:17450–5. doi:10.1073/pnas.1114518108
58. Werle M, Bernkop-Schnurch A. Strategies to improve plasma half life time of peptide and protein drugs. *Amino Acids* (2006) **30**:351–67. doi:10.1007/s00726-005-0289-3
59. Karmali PP, Kotamraju VR, Kastanin M, Black M, Missirlis D, Tirrell M, et al. Targeting of albumin-embedded paclitaxel nanoparticles to tumors. *Nanomedicine* (2009) **5**:73–82. doi:10.1016/j.nano.2008.07.007
60. Uchida M, Kosuge H, Terashima M, Willits DA, Liepold LO, Young MJ, et al. Protein cage nanoparticles bearing the LyP-1 peptide for enhanced imaging of macrophage-rich vascular lesions. *ACS Nano* (2011) **5**:2493–502. doi:10.1021/nn102863y
61. Hamzah J, Kotamraju VR, Seo JW, Agemy L, Fogal V, Mahakian LM, et al. Specific penetration and accumulation of a homing peptide within atherosclerotic plaques

- of apolipoprotein E-deficient mice. *Proc Natl Acad Sci U S A* (2011) **108**:7154–9. doi:10.1073/pnas.1104540108
62. Zhang F, Niu G, Lin X, Jacobson O, Ma Y, Eden HS, et al. Imaging tumor-induced sentinel lymph node lymphangiogenesis with LyP-1 peptide. *Amino Acids* (2012) **42**:2343–51. doi:10.1007/s00726-011-0976-1

Conflict of Interest Statement: Tambet Teesalu, Kazuki N. Sugahara, and Erkki Ruoslahti are shareholders in CendR Therapeutics Inc., and Erkki Ruoslahti is a shareholder in EnduRx Pharmaceuticals. The companies have rights to some of the technology described in the paper.

Received: 18 June 2013; paper pending published: 27 June 2013; accepted: 06

August 2013; published online: 27 August 2013.

Citation: Teesalu T, Sugahara KN and Ruoslahti E (2013) Tumor-penetrating peptides. *Front. Oncol.* **3**:216. doi:10.3389/fonc.2013.00216

This article was submitted to Pharmacology of Anti-Cancer Drugs, a section of the journal *Frontiers in Oncology*.

Copyright © 2013 Teesalu, Sugahara and Ruoslahti. This is an open-access

article distributed under the terms of the Creative Commons Attribution License (CC BY). The use, distribution or reproduction in other forums is permitted, provided the original author(s) or licensor are credited and that the original publication in this journal is cited, in accordance with accepted academic practice. No use, distribution or reproduction is permitted which does not comply with these terms.



Tumor targeting via integrin ligands

Udaya Kiran Marelli¹, Florian Rechenmacher¹, Tariq Rashad Ali Sobahi², Carlos Mas-Moruno³ and Horst Kessler^{1,2*}

¹ Institute for Advanced Study (IAS) and Center for Integrated Protein Science (CIPSM), Department Chemie, Technische Universität München, Garching, Germany

² Department of Chemistry, Faculty of Science, King Abdulaziz University, Jeddah, Saudi Arabia

³ Biomaterials, Biomechanics and Tissue Engineering Group, Department of Materials Science and Metallurgical Engineering, Technical University of Catalonia (UPC), Barcelona, Spain

Edited by:

Angelo Corti, San Raffaele Scientific Institute, Italy

Reviewed by:

Angelo Corti, San Raffaele Scientific Institute, Italy

Fabrizio Marucci, Istituto Superiore di Sanità, Italy

***Correspondence:**

Horst Kessler, Institute for Advanced Study (IAS) and Center for Integrated Protein Science (CIPSM), Department Chemie, Technische Universität München, Lichtenbergstrasse 4, 85747 Garching, Germany
e-mail: kessler@tum.de

Selective and targeted delivery of drugs to tumors is a major challenge for an effective cancer therapy and also to overcome the side-effects associated with current treatments. Overexpression of various receptors on tumor cells is a characteristic structural and biochemical aspect of tumors and distinguishes them from physiologically normal cells. This abnormal feature is therefore suitable for selectively directing anticancer molecules to tumors by using ligands that can preferentially recognize such receptors. Several subtypes of integrin receptors that are crucial for cell adhesion, cell signaling, cell viability, and motility have been shown to have an upregulated expression on cancer cells. Thus, ligands that recognize specific integrin subtypes represent excellent candidates to be conjugated to drugs or drug carrier systems and be targeted to tumors. In this regard, integrins recognizing the RGD cell adhesive sequence have been extensively targeted for tumor-specific drug delivery. Here we review key recent examples on the presentation of RGD-based integrin ligands by means of distinct drug-delivery systems, and discuss the prospects of such therapies to specifically target tumor cells.

Keywords: integrins, RGD, tumor, targeted delivery, $\alpha v \beta 3$, $\alpha v \beta 5$, $\alpha 5 \beta 1$ and $\alpha v \beta 6$

INTRODUCTION

Cancer diagnosis, therapy, and monitoring represent fundamental topics of research in medicine and are of utmost importance in healthcare of today's society. An efficient cancer therapy should possess exceptional abilities not only to ensure a complete removal

of the tumor but also to prevent its spreading and invasion to other tissues by metastasis. Current clinical approaches to treat cancer include, and often combine, surgery, chemotherapy, radiation therapy as well as immunotherapy. However, these methods in general still fail to treat highly aggressive metastatic cancers, and present some serious limitations. For instance, irradiation of tumors may damage adjacent healthy tissues, and chemotherapy, which is based on a non-specific systemic distribution regime, requires high drug dosage and promotes severe adverse side effects. For example, the administration of Paclitaxel (PTX), a drug used for the treatment of lung, ovarian, and breast cancers, has been associated with unwanted effects such as hypersensitivity reactions, myelosuppression, and neurotoxicity (1, 2), among others. Doxorubicin (DOX), another drug used in cancer chemotherapy, has also been described to have cardiotoxic side effects (3, 4). Moreover, chemotherapy might turn inefficient due to acquired chemoresistance as exemplified in the case of Gemcitabine – prime therapeutic used to treat pancreatic cancers (5), for DOX (3) and also for PTX (6, 7).

Tumor targeted drug-delivery (**Figure 1**) represents a promising approach to overcome some of the above mentioned limitations (8). This strategy aims to specifically guide and direct anticancer therapeutics (or imaging agents) to tumor cells without interfering with normal tissues. Such targeted approach relies on the fact that tumor vasculature and tumor cells display a well-differentiated pattern of (over-)expression of specific receptors (i.e., receptors required for tumor angiogenesis), which is consistent with the concept of "Vascular Zip Codes" (9, 10). Targeted drug-delivery methods hence employ small molecules or

Abbreviations: A549, human non-small cell lung carcinoma; ATCC, CCL-185 cells; ATCC, HTB-65 cells; bFGF, basic fibroblast growth factor; BMEC, brain microvascular endothelial cells; Cap-RGD, Ac-CCVVVTGRGDSPSSK-COOH; DCP-TEPA, dicetylphosphate-tetraethylenepentamine; DOPE, dioleoylphosphatidylethanolamine; DPPC, 1,2-dipalmitoyl-sn-glycero-3-phosphocholine; DSPC, distearoylphosphatidylcholine; DSPE, distearoylphosphatidylethanolamine; DTPA, diethylenetriameneacetate; FDG, fluoro-2-deoxy-D-glucose; HEK, human embryonic kidney; HeLa, human cervical carcinoma cells; HPAE-co-PLA/DPPE, poly[(amine-ester)-co-(D,L-lactide)]/1,2-dipalmitoyl-sn-glycero-3-phosphoethanolamine copolymer; HPMA, N-(2-hydroxypropyl)methacrylamide; HAS, human serum albumin; HUVEC, human umbilical vein endothelial cells; IV, intravenous; Luc-pDNA, luciferase pDNA; Mal-PEG-PCL, maleimide-poly(ethylene glycol)-block-poly(ϵ -caprolactone); MDR, multi-drug resistance; MeWo, human malignant skin melanoma; MMAE, monomethyl-auristatin-E; MRI, magnetic resonance imaging; NSCLC, non-small cell lung cancer; PCL-PEEP, poly(ϵ -caprolactone)-block-poly-(ethyl ethylene phosphate); pCMVLuc, *Photinus pyralis* luciferase under control of the CMV enhancer/promoter; PEG, polyethylene glycol; PEI, polyethylenimine; PEO-b-PCL, poly(ethylene oxide)-block-poly(ϵ -caprolactone); PET, positron emission tomography; PGA, poly-glutamic acid; PLA, poly(lactic acid); PLG, poly-L-glutamic acid; PLGA, poly(D,L-lactide-co-glycolide); PLL, poly(L-lysine); PLys, polylysine; pORF-hTRAIL, plasmid expressing the tumor necrosis factor-related apoptosis-inducing ligand (TRAIL); P(PEGMEMA), poly[poly(ethylene glycol) methyl ether methacrylate]; sFlt-1, soluble fms-like tyrosine kinase-1 (pDNA encoding the soluble form of VEGF receptor-1); SPECT, single-photon emission computed tomography; TAT peptide, CGRKKRRQRRR; Tf, transferrin; TfR, transferrin receptor; TLT, transplantable liver tumors; VEGF, vascular endothelial growth factors.

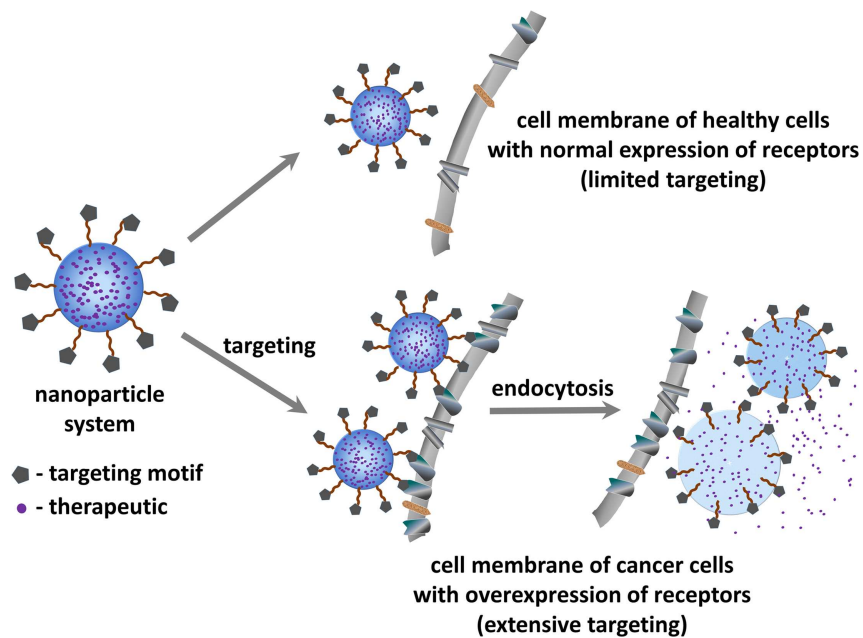


FIGURE 1 | Schematic representation of the principle of tumor targeted drug delivery for treating cancer.

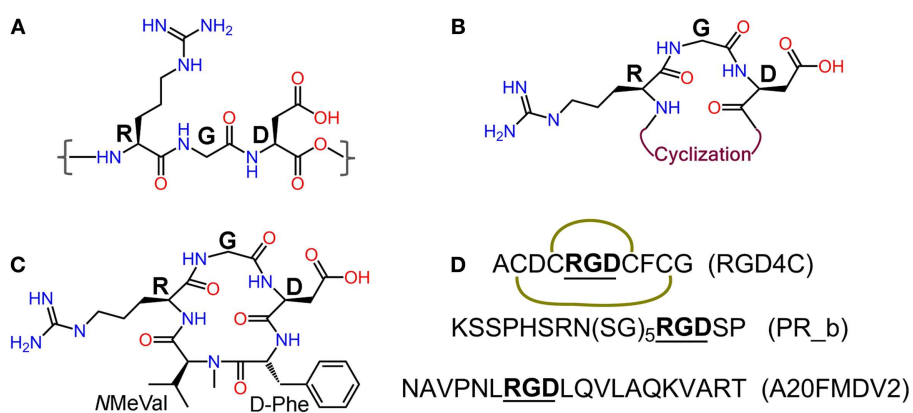


FIGURE 2 | (A) Integrin recognition motif RGD; **(B)** schematic representation of cyclic RGD (cRGD); **(C)** Cilengitide – c(RGDf-NMeVal); **(D)** peptide sequences of RGD4C (the green curves indicate disulfide bridges), $\alpha 5\beta 1$ ligand PR_b, and $\alpha v\beta 6$ ligand A20FMDV2.

monoclonal antibodies selective to receptors that are proven to be abnormally expressed on tumors. The conjugation of anticancer drugs to these selective ligands will allow a preferential or selective delivery of the drug to the tumor.

As a result, this technique benefits from several advantages: (i) non-specific interactions with normal tissues are reduced, and thus the adverse side-effects associated to conventional chemotherapy can be minimized. (ii) Site-directed drug release leads to higher local concentrations at the diseased tissue and thus allows dosage reduction. (iii) Acquired chemoresistance can potentially be reduced by co-delivering other therapeutics capable of regulating cancer multi-drug resistance (MDR). To avail these advantages, well accessible cell surface receptors are preferred over intracellular targets where (complex) drug internalization mechanisms need

to be taken into consideration. In this regard, one of the most intensely referred class of proteins for targeted therapy is the integrin family (11).

Integrins are heterodimeric transmembrane glycoproteins consisting of an α and a β subunit. In total, 24 different subtypes of integrins that are constituted from 18 α and 8 β subunits have been discovered to date (12). Almost half of them bind to various extra cellular matrix (ECM) proteins such as fibronectin, vitronectin, and collagen through the tripeptide motif Arg-Gly-Asp = RGD [(13), Figure 2], and are vital in the adhesion, signaling, migration, and survival of most cells (14). Integrins have also very important roles in cancer progression and some subtypes have been described to be highly over-expressed on many cancer cells. This is the case of integrins $\alpha v\beta 3$, $\alpha v\beta 5$, and $\alpha 5\beta 1$, which are crucial mediators

of angiogenesis in cancer (8, 15–17). Underlying cause for this is the elevated demand by the enlarging tumor for adequate supply of necessary nutrients and oxygen. In order to meet these demands through blood supply, tumor tissue with a rapidly overgrowing number of cells, signals [via growth factors like vascular endothelial growth factor (VEGF) or basic fibroblast growth factor (bFGF)] for increased angiogenesis, a state known as “angiogenic switch.” Sprouting of new blood vessels and overexpression of integrins in tumor tissues and vasculature are thus key features in the pathophysiology of cancer. Other integrins such as $\alpha v\beta 6$ and $\alpha 6\beta 4$ are also observed to be expressed on tumor cells (8). Another pivotal function of integrins is the promotion of cell migration by virtue of their binding to ECM components. This phenomenon is responsible for the process of tumor proliferation, migration, invasion, and metastasis (18). These functional aspects together with the high expression levels found on tumor cells have converted integrins into very interesting proteins for targeted cancer diagnosis and therapy studies.

Our review shortly recapitulates recent developments in integrin targeted cancer therapy, with special focus on targeted delivery of chemotherapy or gene therapy via non-viral vectors like nanoparticles (NPs), micelles, vesicles, or other systems grafted with RGD-based integrin ligands. Considering the vastness of the topic, we have only cited a limited amount of recent works. For previous studies and developments in this field other detailed reviews are available (19–22). Applications based on integrin targeting antibodies and therapies involving the blocking of integrin functions with antagonists and other ligands are not subject of this review.

INTEGRIN LIGANDS AND INTEGRIN TARGETING

Since the discovery of the integrin recognizing RGD motif by Ruoslahti et al. (13, 23), extensive research has been carried out to develop RGD-based peptide and peptidomimetic integrin ligands (24). Various synthetic strategies have been applied to develop RGD peptide analogs with enhanced biological properties and pharmacokinetics like affinity and selectivity for different integrin subtypes, metabolic stability, and biodistribution. These strategies include the introduction of amino acids flanking the tripeptidic RGD sequence, cyclization, and variation of stereochemical configuration of the constituent amino acids (25), and N-methylation (26, 27) (Figure 2). Cilengitide – c(RGDF-NMeVal) (Figure 2), a very potent antagonist of $\alpha v\beta 3$, was developed by using some of these approaches and has been clinically tested by Merck primarily for treatment of glioblastoma multiforme (28, 29). Despite promising preliminary data, its use as anticancer therapeutic has been discontinued due to failure in phase-III clinical trials (Merck press release on Cilengitide studies: <http://www.merck.de/de/presse/extNewsDetail.html?newsId=C47977D13865FCB9C1257B1D001EF9CA&newsType=1>). Other well-known RGD peptides are cRGDFV (25) – the parent peptide for Cilengitide, cRGDFK (30), and RGD4C (ACDCRGDCFCG) (31). RGD4C is susceptible to be expressed by recombinant methods into proteins and viruses for their targeted delivery. Targeting integrins using cRGDFX, cRGDeV, cRGDyV, and other peptides or peptidomimetics (Figure 2) has also been reported in the literature.

TARGETED DRUG DELIVERY

Targeted delivery can be accomplished by two approaches: the direct conjugation of the targeting motif to the drug or the use of drug vehicular systems grafted with the targeting motif. Of these, the use of carrier systems offers several advantages compared to direct conjugation methods:

1. Carrier systems have the capacity to present multiple ligands on each particle. This facilitates effective targeting via multiple and simultaneous interactions between the ligands and the receptors, exploiting the concept of multivalency.
2. Vehicular systems may keep the drug unexposed to physiological systems, thereby protecting it from degradation or alteration, and more importantly, minimizing undesirable non-specific interactions of the drug with normal tissues. Therefore, these systems may remarkably reduce the side effects of the drug.
3. Targeted carrier systems usually are internalized via receptor-mediated endocytosis and the drug is directly released within cell. This is more effective to attain higher in-cell drug concentrations for amplified therapeutic activity.
4. Being larger in size ($\sim >100$ nm) than classical drugs, carrier systems are not filtered off by renal pathways (size limit for renal filtration ~ 5 nm). This enables a prolonged half-life time of carrier particles in the blood stream and allows for a gradual release of the drug over longer periods of time. Such release kinetics avoid high systemic concentrations of the drug and improves the effectiveness of the administered dose.
5. The abnormal architecture and permeability of tumor vasculature promotes extravasation of the particles that are in blood circulation. This phenomenon is called enhanced permeability and retention (EPR) effect. Facilitated by this passive transport mechanism, the nano-sized vehicular systems enter into tumor tissues. However, the quick clearance of these NPs from the tissue is prevented by their large size and lead to prolonged retention times in tumor. Hence, the double targeting – passive and active receptor-mediated targeting, enhances therapeutic efficacy.

Among the carrier systems, viral vectors such as retroviruses and adenoviruses have been successfully developed and found to be efficient in targeted gene therapy (32). However, their use is associated with several disadvantages that have precluded their clinical application. In the first place, they can produce unwanted immune responses (33). Also, it is not easy to express viruses composed with targeting moieties that contain unnatural amino acids or chemically modified scaffolds. Moreover, viral vectors can only be used for gene therapy and are not suitable for delivery of chemotherapeutics. Last but not least, they also carry a negative public perception concerning safety (33, 34). Therefore, development of non-viral targeting vectors is a preferred alternative in targeted therapy. In this regard, various kinds of polymer-based nanocarriers have been developed for tumor targeting using integrin ligands including the use of RGD coated virus like particles (VLPs) which use only the capsid of the viruses (35). In the following sections, some representative examples are discussed according to the targeted integrin subtype.

TARGETING $\alpha v\beta 3$ AND $\alpha v\beta 5$ INTEGRINS

As previously introduced, the $\alpha v\beta 3$ integrin subtype plays a major role in angiogenesis, tumor neovascularization, and tumor metastasis (8). The angiogenic pathways dependent on $\alpha v\beta 3$ have been described to be induced by bFGF or tumor necrosis factor α (TNF- α). Its expression is upregulated on angiogenic endothelial cells (36–38) and on various tumor cell lines (39, 40). Antagonistic inhibition of $\alpha v\beta 3$ integrin has been shown to suppress angiogenesis (41) and to induce apoptosis (42). The well-established biological roles, high expression on tumor tissues, and the availability of ligands with high affinity, have set $\alpha v\beta 3$ the most extensively studied integrin for tumor targeting. The integrin $\alpha v\beta 5$ is also involved in angiogenesis but through a distinct pathway stimulated by VEGF or transforming growth factor α (TGF- α) (16). Since most RGD-containing peptidic $\alpha v\beta 3$ antagonists also recognize $\alpha v\beta 5$, although usually with a lower affinity, these two integrin subtypes are discussed together.

TARGETED DELIVERY OF CHEMOTHERAPY USING POLYMERIC VEHICLES

Encapsulation of drugs in polymer-based carrier systems is a practical approach to protect them from degradation in biological system. Furthermore, these systems may reduce the systemic toxicity of the drug and also enhance their safe elimination from the physiological system. In addition, these vehicles often ameliorate the drug's pharmacokinetic profile and biological distribution within the organism. Phospholipid or polypeptide-based polymers are commonly employed to prepare drug-delivery vehicles as they are akin to biological molecular components and thus display low toxicity and are easily biodegradable. Since the physicochemical properties of these polymers can be easily tuned to produce liposomes, micelles, or NPs, via well-established protocols, these materials are frequently used to construct drug-delivery vehicles. In fact, liposomes have already been used for the formulation and delivery of DOX (4). These vehicles may additionally be PEGylated to improve their aqueous solubility and to reduce non-specific interactions with plasma proteins and membranes. Besides encapsulation, drugs can as well be bound to these systems by chemical methods. This enables drug stability and also secured pH-sensitive release of drugs *in situ*. These sorts of carrier systems have been equipped with integrin targeting ligands and experimented for their capabilities as targeted drug-delivery systems in cancer treatment. Some illustrative recent works are listed in Table 1.

TARGETED DELIVERY OF CHEMOTHERAPY USING PROTEIN-BASED NPs

Although polymer-based vehicle systems are a common choice for drug delivery, their long-term biological toxicity might be an issue and needs to be carefully assessed. For this reason, protein-based NPs are considered an attractive alternative for targeted therapy due to their high biocompatibility, biodegradable properties, and water solubility. With regard to this, albumin is one of the proteins that has been most majorly explored for drug delivery. For example, linking *c*(RGDyK)C to albumin NPs loaded with Gemcitabine showed an increased *in vitro* and *in vivo* anti-tumor efficacy in BxPC-3 pancreatic cancer cell lines compared to NPs without the targeting sequence (43). The conjugation of cyclic RGD to albumin not only lead to successful targeting but

also increased the intracellular uptake of NPs and Gemcitabine as monitored by fluorescence studies. The $\alpha v\beta 3$ -mediated uptake of the RGD-conjugated components into pancreatic cells was further confirmed by competitive inhibition studies using soluble RGD ligands. In another study (44), Fluorouracil-bearing *c*RGDFK-albumin nanospheres have shown significant improvement in binding to $\alpha v\beta 3$ -expressing HUVEC cells *in vitro*. A considerable improvement in prevention of lung metastasis and angiogenesis, and in tumor regression was observed *in vivo* in B16F10 tumor-bearing mice as compared with the activity of the free drug. The binding of nanospheres conjugated with RGD to endothelial cells was eightfold higher than that of nanospheres without RGD or conjugated with the RAD sequence (which does not bind to integrins). Similarly, enhanced homing to tumors and endothelial cell binding were reported for *c*RGDFK-PEG-albumin NPs that were linked to the antimitotic agent monomethyl-auristatin-E (MMAE) (45). These studies were carried out on HUVECs and C26 carcinoma-bearing mice. Two kinds of target systems were prepared with an RGD peptide linked to albumin either by a PEG chain (RGD-PEG-MMAE-HSA) or a short alkyl chain (RGD-MMAE-HSA). After IV administration in mice, fluorescent studies showed colocalization of both carrier systems with the tumor vasculature and tumor cells.

Besides the use of albumin as drug-delivery system, spider silk is a protein that holds great promise for application in targeted therapies. Due to its water solubility, excellent biocompatibility, and unique mechanical properties, spider silk has attracted growing interest in a number of biomedical areas. Spider silks are currently under investigation for the encapsulation and controlled release of drugs and growth factors, with so far optimistic outcomes (46). Scheibel's group has prepared spider silks containing the integrin recognition motifs GRGDSP or *c*RGDFK by either recombinant expression or chemical methods, respectively (47). These RGD functionalized proteins have been used to generate spider silk films that retain the biophysical properties observed for silks prepared using the native proteins. Significant improvements in the attachment and proliferation of BALB/3T3 mouse fibroblasts were observed on films containing the RGD sequence but not on unmodified or RGE-containing silk. These results encourage further exploration of spider silk protein as a prospective carrier system for targeted drug delivery in cancer.

TARGETED DELIVERY OF CHEMOTHERAPY USING METALLIC NPs

Gold and other metallic NPs can be used for the polyvalent display of targeting scaffolds (48). Ease of preparation and functionalization as well as unique physicochemical properties make gold NPs very attractive systems for use in cancer diagnosis and therapy. For instance, PEGylated gold NPs coupled to a *c*RGD peptidomimetic via thiol chemistry showed good affinity and binding to $\alpha v\beta 3$ -positive PC-3 prostate cancer cells *in vitro* (49). In another study, Yang et al. have examined the utility of multifunctional PEGylated superparamagnetic iron oxide (SPIO) NPs in targeted drug delivery and PET/Magnetic Resonance Imaging (MRI) (50). To this end, *c*RGDFc and a common ^{64}Cu chelator were bound to the distal ends of the PEG chains, whereas the drug, DOX, was conjugated to the SPIO particles via pH-sensitive hydrazone bonds.

Table 1 | Outline of representative recent examples of polymer-based targeted delivery studies using $\alpha v\beta 3$ and/or $\alpha v\beta 5$ integrin ligands.

Carrier system	Targeting motif	Drug	Cellular system	Results and characteristics (reference)
Cholesterol/DOPE/DSPC/DSPE-(PEO)4-cRGDfK/DSPE-mPEG2000	cRGDfK	DOX	R40P murine pancreatic and SN12C renal carcinoma cells	Fifteen fold increase in drug efficacy relative to animals treated with free drug (95)
PLG-PEG micelles	cRGDfC	DOX	U87MG human glioblastoma cells	pH-sensitive drug release, higher cellular uptake, higher accumulation at tumor sites as monitored by positron emission tomography (PET) and <i>ex vivo</i> fluorescence experiments (96)
PLGA-4-arm-PEG branched NPs	cRGDfC	–	Pancreatic tumor in mice and U87MG glioma cells	Efficient uptake by U87MG glioma cells over-expressing $\alpha v\beta 3$. Highest accumulation at tumor site as monitored by whole body imaging. Low <i>in vivo</i> inherent physiological toxicity for the NPs (97)
PGA-PTX-E-[c(RGDfK)]2 conjugate NPs	cRGDfK	PTX	4T1 murine breast cancer tumors	Augmented antitumor activity and reduced systemic toxicity for PTX, blockade of endothelial cell migration to VEGF and adhesion to fibrinogen. Lysosomal enzyme assisted release of PTX is observed (98)
PLGA-PEG NPs	GRGDS and RGD peptidomimetic	PTX and DOX	HUVECs and syngenic TLT cells	High cellular uptake <i>in vitro</i> , improved anticancer efficacy and higher survival rate of mice (99)
cRGDyK-PEG-PLA-PTX micelle	cRGDyK	PTX	Intracranial glioblastoma model	2.5-Fold increase in antiglioblastoma cell cytotoxicity effect over non-targeted system, improved drug accumulation, increase in life time of diseased mice (100)
FOR OTHER STUDIES USING PLGA-PLL NPs PLEASE SEE REF. (101, 102)				
HPMA copolymers	cRGDfK	Geldanamycin	PC-3 and DU145 prostate cancer cell lines	Tumor growth inhibition activity as efficient as free drug, decrease in IC ₅₀ values for targeted conjugates. Improvements in biodistribution profile, both <i>in vitro</i> and <i>in vivo</i> antiangiogenic, and antitumor activities for targeted systems (103–105)
HPMA copolymers	cRGDfK	Docetaxel	PC-3 and DU145 prostate cancer cell lines	Inhibition of PC3, DU145 cell growth and also of HUVECs <i>in vitro</i> . <i>In vivo</i> tumor regression is also observed (106)
PCL-PEEP and Mal-PEG-PCL micelles	Tf and cRGDfK	PTX	BMEC and U87MG glioma cells	Double targeting by Tf and RGD ligand. Uptake of micelles increased 2.4 times for BMEC compared to micelles lacking Tf. High drug accumulation in brain upon IV injection (107)
HPAE-co-PLA/DPPE polymer NPs	Tf and cRGDfK	PTX	HUVECs and HeLa cells	<i>In vitro</i> cytotoxicity for NPs coated with cRGD is increased 10 times in $\alpha v\beta 3$ -expressing HUVECs while Tf targeting to Tf receptor over-expressed HeLa cells lead to twofold increase. pH-sensitive intracellular drug release (108)
PFC (perfluorocarbon) NPs	Non-peptidic $\alpha v\beta 3$ antagonist	Fumagillin	Vx-2 adenocarcinoma tumor	Diminished development of tumor neovasculature and reduced tumor growth are observed at much lower drug concentrations compared to the previous concentration used in rodent and human clinical trials (109)
P(PEGMEMA) based micelles	RGD	Albendazole	OVCAR-3 ovarian cancer cells	Improved cellular uptake of polymeric micelles and 80% cell deaths at a micelle concentration of 10 $\mu\text{g mL}^{-1}$ (110)

The cRGD-conjugated SPIO nanocarriers exhibited higher cellular uptake and cytotoxicity in U87MG cells compared to cRGD-free systems. Also, *in vivo* PET imaging of U87MG tumor-bearing mice revealed increased tumor accumulation of cRGD-SPIO NPs compared to cRGD-free counterparts. Intracellular specific drug

release by SPIOs was facilitated by pH-selective cleavage of the SPIO-DOX hydrazone linkage. Such multifunctional systems that are able to simultaneously target a cell or tissue, deliver a drug, and provide a diagnosis are known as theranostics, which constitute an upcoming area of research.

TARGETED DELIVERY OF GENE THERAPY

Delivery of gene therapy using targeted non-viral vehicles has been widely studied (20). A directed delivery of DNA or RNA fragments is required to prevent from using high doses, which otherwise can lead to off-target gene silencing effects. Using carrier systems for gene therapy is advantageous as it reduces the problems of

biodegradability, nucleosomal cleavage, and size and charge limited membrane impermeability associated with the delivery of nucleic acids. As mentioned earlier, non-viral vectors are also helpful to overcome complications and safety issues described for viral vectors. Here, we briefly tabulate some recent targeted gene therapy studies (**Table 2**).

Table 2 | Outline of recent targeted gene delivery studies using $\alpha v\beta 3$ and/or $\alpha v\beta 5$ integrin ligands.

Carrier system	Targeting motif	Gene	Cellular system	Results and Characteristics (reference)
PEG-PLys polyplex micelle	cRGDfK	Luc-pDNA	HeLa cells and 293T cells	Enhanced transfection efficiency (TE) and perinuclear accumulation of pDNA within 3 h of incubation (111)
PEG-PLys polyplex micelle: cross-linked by thiolation	cRGDfK	Luc-pDNA	HeLa cells and 293T cells	Improvements in TE, selection of endocytic pathways and regulation of intracellular trafficking by cRGD. Preferential caveolae mediated endocytosis is observed. Thiol cross-linking helped polyplex stabilization and pDNA protection (112)
PEG-PLys polyplex micelle: cross-linked by thiolation	cRGDfK	sFlt-1	BxPC-3 pancreatic adenocarcinoma tumors	Upon IV injection, significant tumor-specific TE and gene expression is observed which lead to a decrease in tumor vasculature. Thiol cross-linking has to be optimized to improve results (113, 114)
PEG-PEI polyplex micelles	B6 peptide and RGD bicyclo peptide	pCMVLuc	DU145 and PC3 prostate cancer cells	Significant improvement in TE via targeting. RGD helped in initial association of polyplexes to cells whereas the internalization is observed to be mediated by TfR endocytosis (115)
PEG-PEI polyplex micelles	Non-cyclic RGD-peptidomimetic		MeWo and A549 cells	Increased binding, uptake, and luciferase transgene expression in model cells (116)
PEG-PEI polyplex micelles	cRGDyK	pORF-hTRAIL	Intracranial U87 glioblastoma tumor xenografts	Higher gene transfection and increased therapeutic efficiency of TRAIL are observed and is reflected in improved longevities of mice (117)
DNA/PEI-Au-RGD nanoclusters	Cap-RGD	pEGFP-Luc	HeLa cells	A 5.4- to 35-fold increase in TE corresponding to a low or high density of $\alpha v\beta 3$ on HeLa cells. Observed TEs are far higher than that for targeted or untargeted commercial transfection vector – JetPEI. Higher concentration of gold NPs is found to be toxic (118)
PEG–oligo(ethane amino) amide polymers	B6 peptide or cRGDfK	pEGFP-Luc	Mouse N2A neuroblastoma and DU145 human prostate adenocarcinoma cells	Selective binding and transfection efficiency are observed which are mediated by the targeting ligands. The carrier systems however required use of endosomolytic agents for release of polyplexes from endosomes (119)
DCP-TEPA polycation liposomes	cRGDfK	siLuc2	B16F10-luc2 murine melanoma cells	Successful targeting, transfection, and knockdown of luc2 expression <i>in vitro</i> in B16F10-luc2 cells and also <i>in vivo</i> as monitored by imaging in mice with tumor-bearing lungs, is observed (120)
PEO- <i>b</i> -PCL micelles	RGD4C	mdr1 siRNA and DOX	MDA435/LCC6 cells resistant to DOX	The system is decorated with cell penetrating peptide (TAT) as well. Dual functional micelles showed improved cellular uptake and mdr1 activity leading to lowered P-gp expression both at the mRNA and protein levels. These effects caused reversal of MDR for DOX, which increased DOX accumulation in cytoplasm and nucleus, and enhanced DOX cytotoxicity (121)

PHOTOTHERAPY USING TARGETED SYSTEMS

Gormley et al. have tested the use of targeted gold nanorods (GNRs) for plasmonic photothermal therapy (PPTT) aiming at reducing the amount of heat required in thermal therapy (51). To this end, PEGylated GNRs were prepared and functionalized with cRGDfK via thiol chemistry. Studies on HUVEC and DU145 prostate cancer cells showed effective *in vitro* selective targeting of RGD-GNRs to both these cell types but not *in vivo* in a DU145 mice model. The absence of *in vivo* effects was attributed to faster clearance of GNRs from physiological system due to the presence of negative charges in cRGDfK-functionalized GNRs. On similar lines, for PPTT, Akhavan et al. have projected reduced single layer graphene oxide nanorods (GONRs) functionalized by amphiphilic PEG polymers containing RGD-based peptides (52). RGD-presenting GONRs showed increased radiation absorption compared to non-functionalized GONRs and also improved destruction of U87MG human glioblastoma cells at reduced doses as low as $1\text{ }\mu\text{g mL}^{-1}$. Irradiation for 8 min with near-infrared radiation at this concentration resulted in remarkable values of cell destruction ($\geq 97\%$). On the contrary, $<11\%$ of cell destruction and 7% of DNA fragmentation were observed for non-targeted nanorods using the same concentration.

TARGETING THE $\alpha v \beta 1$ INTEGRIN

In addition to $\alpha v \beta 3$ and $\alpha v \beta 5$, an upregulated expression of $\alpha v \beta 1$ in tumor vasculature and other cancer cells has also been described (36, 53–57). $\alpha v \beta 1$ primarily recognizes fibronectin through the RGD binding motif. Kim et al. have reported that $\alpha v \beta 1$ inhibition induces cell apoptosis in endothelial cells (58) and also showed that this integrin mediates the migration of endothelial cells. Noteworthy, it has been shown that $\alpha 5$ might substitute the activity of αv during vasculature remodeling (59). For these reasons, targeting of this integrin has also been approached in cancer therapy.

Kokkoli and co-workers have explored $\alpha v \beta 1$ integrin for targeting cancer cells by using a fibronectin mimetic $\alpha v \beta 1$ -selective RGD-containing peptide, named PR_b (60) (Figure 2). This group produced DPPC-based liposomal NPs covered by PEG and further decorated with PR_b peptide, and studied their targeting capacity in a CT26.WT mouse colon carcinoma experimental model. The quantities of PEG and peptide were fine-tuned in order to optimize the delivery of the nanovector. By increasing the quantity of conjugated peptide, an enhancement in binding of liposomes to cells was observed, whereas the opposite effect was found when the concentration of PEG was augmented. The cytotoxicity of 5-Fluorouracil carried by these PR_b targeted liposomes was found to be comparable to that of the free drug and better than that of the particles containing only the control GRGDSP sequence, confirming the importance of targeting $\alpha v \beta 1$ on this cancer model. Similar results were obtained in studies using HCT116 and RKO human colon cancer cells (60). This liposomal system has been further investigated for the delivery and cytotoxicity of DOX to MDA-MB 231 breast cancer cells (61). Confocal microscopy experiments showed that these targeted liposomes were internalized in breast cancer cells via an endocytic pathway, and transferred within the first minutes into early endosomes, and after prolonged times into late endosomes and lysosomes. Particularly at high concentrations, the

therapeutic effect of encapsulated DOX in MDA-MB 231 cells was comparable to that of the free DOX.

In a recent approach, PR_b targeted polymersomes have also been explored for siRNA delivery (62). T47D breast cancer cells were studied to check the expression of Orai3. The downregulation of Orai3 levels results in cell apoptosis. The delivery of Orai3 by PR_b-conjugated polymersomes decreased the viability of cancer cells but did not affect non-cancerous MCF10A breast cells. When compared to a commercial transfection agent (Lipofectamine RNAiMAX), the observed therapeutic effect of the polymerome formulation is still moderate. However, this method has not shown any systemic toxicity unlike other transfection reagents.

TARGETING THE $\alpha v \beta 6$ INTEGRIN

The integrin subtype $\alpha v \beta 6$ is expressed at low or undetectable levels in most adult epithelia, but may be upregulated during inflammation and wound healing (8). $\alpha v \beta 6$ preferentially binds to TGF- $\beta 1$ latency associated peptide (LAP) (63), but can also recognize the ECM proteins tenascin and fibronectin (64). In this regard, $\alpha v \beta 6$ is biologically important for the activation of TGF- $\beta 1$ and has been shown to control TGF- β activity or signaling in fibrosis and to play a crucial role in TGF- β -integrin crosstalk in carcinomas (65). Furthermore, $\alpha v \beta 6$ was found to be significantly upregulated in tumor tissues (8) and in certain cancer types including colon (66), ovarian carcinoma (67), and in early stage of non-small cell lung cancer (NSCLC), which is associated with poor patient survival (68, 69). Other studies have shown that $\alpha v \beta 6$ expression is correlated with the development of metastasis in gastric cancer and the enhanced survival and invasive potential of carcinoma cells (70, 71). This pathological relevance has turned $\alpha v \beta 6$ into a promising target for tumor diagnostics and antitumor therapy.

To date, several linear and cyclic peptides as well as peptidomimetics have been developed to target specifically the $\alpha v \beta 6$ integrin subtype (68, 70, 72–74). For instance, the high affinity $\alpha v \beta 6$ -specific 20-mer peptide H2009.1 (75) was conjugated as a tetramer to a poly-glutamic acid polymer carrying DOX, and was shown to specifically target $\alpha v \beta 6$ -expressing cells *in vitro* (76). In another work, the selectivity of this peptide toward $\alpha v \beta 6$ was exploited to guide fluorescent quantum dots to lung adenocarcinoma cell line H2009 *in vitro* (68). Recently, this peptide has also been conjugated to a water soluble PTX conjugate resulting in selective cytotoxicity for the $\alpha v \beta 6$ -expressing NSCLC cell line (77). The conjugate was able to reduce the rate of tumor growth *in vivo*, however without an increased benefit over the use of free PTX. Furthermore, the same peptide was used to investigate the multimeric effect on functionalized liposomes (78). In this study, liposomes displaying tetramers of the H2009.1 peptide demonstrated higher drug delivery and toxicity toward $\alpha v \beta 6$ -expressing cells than liposomes displaying single copies of H2009.1, even if the total number of peptides bound to each liposome was identical. In another approach, H2009.1 was used to functionalize the surface of multifunctional micelles encapsulated with SPIO and DOX for MRI and drug-delivery applications, respectively (79). The functionalized micelles significantly increased cell targeting and uptake in $\alpha v \beta 6$ -expressing H2009 cells, as verified by MRI and confocal imaging.

A20FMDV2 (80, 81) is another $\alpha\beta 6$ -selective 20-mer peptide (**Figure 2**) that can be used for targeted therapies. As an example, this peptide was radiolabeled on solid phase using 4-[¹⁸F]fluorobenzoic acid and the conjugate was selectively taken up by $\alpha\beta 6$ -positive tumors but not by $\alpha\beta 6$ -negative tumors, as monitored in mice by PET (70). In a similar approach, A20FMDV2 was conjugated to 5-[¹⁸F]fluoro-1-pentyne via an azide-based 1,3-dipolar cycloaddition (click chemistry). However, no difference in tumor targeting *in vivo* was observed for such strategy compared to the previous labeling method (82). ¹⁸F-labeled derivatives of the same peptide were described to improve tumor uptake capacity in BxPC-3 (pancreatic cancer) xenograft-bearing mice over [¹⁸F]-FDG (83). Recently, A20FMDV2 was conjugated to an ¹⁸F-based tracer by copper-free, strain promoted click chemistry. However, the resulting derivative did not show a remarkable *in vivo* tumor uptake by mouse with mouse model DX3puro $\beta 6$ -tumor (84). Furthermore, A20FMDV2 was conjugated to DTPA and labeled with ¹¹¹In for SPECT imaging. In this study, the conjugate showed specific localization in $\alpha\beta 6$ -tissues, and displayed increased uptake in an $\alpha\beta 6$ -positive tumor and in a mouse xenograft model bearing breast tumors that express $\alpha\beta 6$ endogenously (85). Additionally, A20FMDV2 was incorporated into a recombinant adenovirus type 5 (Ad5) leading to increased cytotoxicity on a panel of $\alpha\beta 6$ -positive human carcinoma cell lines *in vitro* and enhancement in tumor uptake and improved tumor transduction in an $\alpha\beta 6$ -positive xenograft model *in vivo* over the Ad5 wild type (86).

In another approach pursued by the Gambhir research group, cystine knot peptides showing high affinity for $\alpha\beta 6$ but none for the related subtypes $\alpha\beta 3$, $\alpha\beta 5$, and $\alpha 5\beta 1$ were developed and conjugated to ⁶⁴Cu-DOTA for PET-based tumor imaging (87). Injection of these conjugates into mice bearing either $\alpha\beta 6$ -positive BxPC-3 xenografts or $\alpha\beta 6$ -negative tumors, and monitoring by PET imaging, showed $\alpha\beta 6$ -selective targeting for the tumors expressing $\alpha\beta 6$. In a recent study (88), two cystine knot peptides were labeled with ¹⁸F-fluorobenzoate and their capacity to be taken up by tumor cells assessed *in vivo*. PET imaging revealed for both peptides specific targeting of $\alpha\beta 6$ -positive BxPC-3 xenografted tumors over $\alpha\beta 6$ -negative HEK 293 tumors. These results illustrate the potential of the described strategies to be clinically used in PET imaging of $\alpha\beta 6$ -over-expressing tumors.

CONCLUDING REMARKS

A wide variety of carrier systems have been described to achieve tumor-specific therapeutic effects via integrin targeting. The principal success of this strategy is evidenced by two main observations – the dosage of drug has been usually reduced and an enhanced (and often selective) activity against tumors is achieved. The data obtained from independent studies using different carrier systems are promising and there is therefore hope to bring the targeted delivery methods into practice. However, a number of aspects related to the use of these drug-delivery systems in cancer therapy should be carefully considered.

In the first place, comparative studies between distinct carrier systems are missing. Such studies could provide useful insights on their relative advantages and disadvantages, and help in their

further development and optimization. Detailed studies concerning the systemic toxicity and long-term side effects of the drug-delivery vectors in physiological systems are also essential. Another important aspect to optimize the concentration of drugs in cancer therapy would be to evaluate the efficiency of drug uptake with regard to the overall administered dose, but most studies have only rated the efficiency of the targeted systems in comparison to untargeted systems, without mentioning about the concentrations of the drug used. The investigation of the metabolic stability of these systems in gut and liver as well as their bioavailability profile would also be crucial to improve the efficacy of the therapy. Further optimization of such drug formulations could be directed toward new routes of administration, including, though certainly difficult, orally available conjugates.

It should be mentioned that most studies in this field rank the antitumor potency of the targeted systems based on the reduction in tumor volume and size, parameters that will however not entirely assure the success of the therapy. More satisfactory would be to carry out longer experiments to ensure the complete removal of tumors and arrest of resurrections. In this regard, recent findings have suggested that antiangiogenic therapeutics that aim at treating cancer primarily through reduction and control of tumor growth, may, in some cases, indirectly promote cancer invasiveness and metastasis (89, 90). This ultimately alarms development of targeted therapies which can inhibit multiple cellular functions and affecting not only cell survival *in situ* but also mechanisms involved in the promotion and progression of metastasis. Further investigations on this matter should include the study of targeted therapy on early stage and late stage tumors, and the effect (if any) of these strategies in the development of drug resistance mechanisms by some tumors. Additionally, treatment of cancer often necessitates a combination therapy (combination of different therapeutics or therapies). In this respect, it is demanding to study the usage of targeted approaches for delivering multiple drugs or therapies either by a single carrier system or multiple carrier systems. These studies are further pending in literature. Most of the studies on targeted gene delivery have used luciferase model system. Though it is a good analogous system for understanding gene delivery, proper experimental gene therapy studies aimed to treat cancers are to be extensively studied.

The choice of an optimal integrin ligand is another aspect of paramount importance in the design of integrin-based targeted therapies in cancer. This will depend on the differential pattern of integrin expression in cancer cell types and the biological activity and selectivity profiles of the targeting ligands. Many applications have used linear or cyclic RGD peptides to deliver drugs or nucleotides to tumors. Most of these peptides are active for $\alpha\beta 3$; however, it is often ignored that these ligands may target other integrin subtypes as well. This might not be relevant as long as simplified cellular or experimental animal models are investigated. However, it may raise safety concerns if clinical applications in humans are to be envisaged. E.g., the habitually used peptide – *c*(RGDFX), developed in our group long ago (25, 30), has about 1 nM affinity for $\alpha\beta 3$ and is certainly selective against $\alpha IIb\beta 3$ (low affinity for the platelet receptor).

Nonetheless, the compound also has affinity in the low nanomolar range for $\alpha v\beta 5$ (7.6 nM) and $\alpha 5\beta 1$ (15 nM) (73). Thus, the use of c(RGDFX) might not always provide enough selectivity to distinguish between distinct cell types. In this regard, our group has recently developed (91, 92) and functionalized (93, 94) peptidomimetics which can clearly discriminate between $\alpha v\beta 3$ and $\alpha 5\beta 1$. Application of such single integrin subtype selective ligands

will enable a selective and controlled delivery of drugs to tumors, taking advantage of the distinct patterns of integrin expression found for each cancer type.

It is on the basis of these considerations that targeted therapy with integrin ligands be translated into clinical studies, and be demonstrated whether such strategy will result in a clear benefit for cancer patients.

REFERENCES

- Kumar S, Mahdi H, Bryant C, Shah JP, Garg G, Munkarah A. Clinical trials and progress with paclitaxel in ovarian cancer. *Int J Womens Health* (2010) **2**:411–27. doi: 10.2147/IJWH.S7012
- Weiss RB, Donehower RC, Wiernik PH, Ohnuma T, Gralla RJ, Trump DL, et al. Hypersensitivity reactions from taxol. *J Clin Oncol* (1990) **8**:1263–8.
- Prados J, Melguizo C, Ortiz R, Vélez C, Alvarez PJ, Arias JL, et al. Doxorubicin-loaded nanoparticles: new advances in breast cancer therapy. *Anti-cancer Agents Med Chem* (2012) **12**:1058–70. doi: 10.2174/187152012803529646
- Lao J, Madani J, Puertolas T, Álvarez M, Hernández A, Pazocid R, et al. Liposomal doxorubicin in the treatment of breast cancer patients: a review. *J Drug Deliv* (2013) **456409**:1–12. doi: 10.1155/2013/456409
- Bergman AM, Pinedo HM, Peters GJ. Determinants of resistance to 2',2'-difluorodeoxycytidine (gemcitabine). *Drug Resist Updat* (2002) **5**:19–33. doi: 10.1016/S1368-7646(02)00002-X
- Yusuf RZ, Duan Z, Lamendola DE, Penson RT, Seiden MV. Paclitaxel resistance: molecular mechanisms and pharmacologic manipulation. *Curr Cancer Drug Targets* (2003) **3**:1–19. doi: 10.2174/156800903333754
- Galletti E, Magnani M, Renzulli MI, Botti M. Paclitaxel and docetaxel resistance: molecular mechanisms and development of new generation taxanes. *ChemMed-Chem* (2007) **2**:920–42. doi: 10.1002/cmde.200600308
- Desgrosellier JS, Cheresh DA. Integrins in cancer: biological implications and therapeutic opportunities. *Nat Rev Cancer* (2010) **10**:9–22. doi: 10.1038/nrc2748
- Ruoslahti E. Specialization of tumour vasculature. *Nat Rev Cancer* (2002) **2**:83–90. doi: 10.1038/nrc724
- Teesalu T, Sugahara KN, Ruoslahti E. Mapping of vascular ZIP codes by phage display. *Methods Enzymol* (2012) **503**:35–56. doi: 10.1016/B978-0-12-396962-0.00002-1
- Goodman SL, Picard M. Integrins as therapeutic targets. *Trends Pharmacol Sci* (2012) **33**:405–12. doi: 10.1016/j.tips.2012.04.002
- Barczyk M, Carracedo S, Gullberg D. Integrins. *Cell Tissue Res* (2010) **339**:269–80. doi: 10.1007/s00441-009-0834-6
- Pierschbacher MD, Ruoslahti E. Cell attachment activity of fibronectin can be duplicated by small synthetic fragments of the molecule. *Nature* (1984) **309**:30–3. doi: 10.1038/309030a0
- Cabodi S, Di Stefano P, Leal Mdel P, Tinnirello A, Bisaro B, Morello V, et al. Integrins and signal transduction. *Adv Exp Med Biol* (2010) **674**:43–54. doi: 10.1007/978-1-4419-6066-5_5
- Cox D, Brennan M, Moran N. Integrins as therapeutic targets: lessons and opportunities. *Nat Rev Drug Discov* (2010) **9**:804–20. doi: 10.1038/nrd3266
- Weis SM, Cheresh DA. αV integrins in angiogenesis and cancer. *Cold Spring Harb Perspect Med* (2011) **1**:a006478. doi: 10.1101/cshperspect.a006478
- Rathinam R, Alahari SK. Important role of integrins in the cancer biology. *Cancer Metastasis Rev* (2010) **29**:223–37. doi: 10.1007/s10555-010-9211-x
- Moschos SJ, Drogowski LM, Reppert SL, Kirkwood JM. Integrins and cancer. *Oncology (Williston Park, NY)* (2007) **21**:13–20.
- Temming K, Schiffelers RM, Molema G, Kok RJ. RGD-based strategies for selective delivery of therapeutics and imaging agents to the tumour vasculature. *Drug Resist Updat* (2005) **8**:381–402. doi: 10.1016/j.drup.2005.10.002
- Park J, Singha K, Son S, Kim J, Namgung R, Yun CO, et al. A review of RGD-functionalized nonviral gene delivery vectors for cancer therapy. *Cancer Gene Ther* (2012) **19**:741–8. doi: 10.1038/cgt.2012.64
- Danhier F, Le Breton A, Préat V. RGD-based strategies to target $\alpha v\beta 3$ integrin in cancer therapy and diagnosis. *Mol Pharm* (2012) **9**:2961–73. doi: 10.1021/mp3002733
- Chen K, Chen X. Integrin targeted delivery of chemotherapeutics. *Theranostics* (2011) **1**:189–200. doi: 10.7150/thno/v01p0189
- Ruoslahti E. The RGD story: a personal account. *Matrix Biol* (2003) **22**:459–65. doi: 10.1016/S0945-053X(03)00083-0
- Meyer A, Auernheimer J, Modlinger A, Kessler H. Targeting RGD recognizing integrins: drug development, biomaterial research, tumor imaging and targeting. *Curr Pharm Des* (2006) **12**:2723–47. doi: 10.2174/13816120677947740
- Aumailley M, Gurrath M, Müller G, Calvete J, Timpl R, Kessler H. Arg-Gly-Asp constrained within cyclic pentapeptides. Strong and selective inhibitors of cell adhesion to vitronectin and laminin fragment P1. *FEBS Lett* (1991) **291**:50–4. doi: 10.1016/0014-5793(91)81101-D
- Chatterjee J, Gilon C, Hoffman A, Kessler H. N-methylation of peptides: a new perspective in medicinal chemistry. *Acc Chem Res* (2008) **41**:1331–42. doi: 10.1021/ar8000603
- Chatterjee J, Rechenmacher F, Kessler H. N-methylation of peptides and proteins: an important element for modulating biological functions. *Angew Chem Int Ed Engl* (2013) **52**:254–69. doi: 10.1002/anie.201205674
- Dechantsreiter MA, Planker E, Mathä B, Lohof E, Hölzemann G, Jonczyk A, et al. N-methylated cyclic RGD peptides as highly active and selective $\alpha v\beta 3$ integrin antagonists. *J Med Chem* (1999) **42**:3033–40. doi: 10.1021/jm970832g
- Mas-Moruno C, Rechenmacher F, Kessler H. Cilengitide: the first anti-angiogenic small molecule drug candidate design, synthesis and clinical evaluation. *Anticancer Agents Med Chem* (2010) **10**:753–68. doi: 10.2174/187152010794728639
- Haubner R, Gratias R, Diefenbach B, Goodman SL, Jonczyk A, Kessler H. Structural and functional aspects of RGD-containing cyclic pentapeptides as highly potent and selective integrin $\alpha v\beta 3$ antagonists. *J Am Chem Soc* (1996) **118**:7461–72. doi: 10.1021/ja9603721
- Koivunen E, Wang B, Ruoslahti E. Phage libraries displaying cyclic peptides with different ring sizes: ligand specificities of the RGD-directed integrins. *Nat Biotechnol* (1995) **13**:265–70. doi: 10.1038/nbt0395-265
- Hajitou A. Targeted systemic gene therapy and molecular imaging of cancer contribution of the vascular-targeted AAVP vector. *Adv Genet* (2010) **69**:65–82. doi: 10.1016/S0065-2660(10)69008-6
- Smaglik P. Merck blocks “safer” gene therapy trials. *Nature* (2000) **403**:817. doi: 10.1038/35002743
- Edelstein ML, Abedi MR, Wixon J. Gene therapy clinical trials worldwide to 2007 – an update. *J Gene Med* (2007) **9**:833–42. doi: 10.1002/jgm.1100
- Hovlid ML, Steinmetz NF, Laufer B, Lau JL, Kuzelka J, Wang Q, et al. Guiding plant virus particles to integrin-displaying cells. *Nanoscale* (2012) **4**:3698–705. doi: 10.1039/c2nr30571b
- Avraamides CJ, Garmy-Susini B, Varner JA. Integrins in angiogenesis and lymphangiogenesis. *Nat Rev Cancer* (2008) **8**:604–17. doi: 10.1038/nrc2353
- Brooks PC, Clark RA, Cheresh DA. Requirement of vascular integrin $\alpha v\beta 3$ for angiogenesis. *Science* (1994) **264**:569–71. doi: 10.1126/science.7512751
- Sipkins DA, Cheresh DA, Kazemi MR, Nevin LM, Bednarski MD, Li KC. Detection of tumor angiogenesis *in vivo* by $\alpha v\beta 3$ -targeted magnetic resonance imaging. *Nat Med* (1998) **4**:623–6. doi: 10.1038/nm0598-623
- Beck V, Herold H, Benge A, Luber B, Hutzler P, Tschesche H, et al. ADAM15 decreases integrin $\alpha v\beta 3$ /vitronectin-mediated ovarian cancer cell adhesion and motility in an RGD-dependent fashion. *Int J Biochem Cell Biol* (2005) **37**:590–603. doi: 10.1016/j.biocel.2004.08.005

40. Chen X, Park R, Tohme M, Shahinian AH, Bading JR, Conti PS. MicroPET and autoradiographic imaging of breast cancer αv -integrin expression using ^{18}F - and ^{64}Cu -labeled RGD peptide. *Bioconjug Chem* (2004) **15**:41–9. doi:10.1021/bc0300403
41. Brooks PC, Strömbäck S, Klemke R, Visscher D, Sarkar FH, Cheresh DA. Antiantigenic $\alpha v\beta 3$ blocks human breast cancer growth and angiogenesis in human skin. *J Clin Invest* (1995) **96**:1815–22. doi:10.1172/JCI118227
42. Meerovitch K, Bergeron F, Leblond L, Groulx B, Poirier C, Bubenik M, et al. A novel RGD antagonist that targets both $\alpha v\beta 3$ and $\alpha 5\beta 1$ induces apoptosis of angiogenic endothelial cells on type I collagen. *Vascul Pharmacol* (2003) **40**:77–89. doi:10.1016/j.vpharmacol.2003.02.003
43. Ji S, Xu J, Zhang B, Yao W, Xu W, Wu W, et al. RGD-conjugated albumin nanoparticles as a novel delivery vehicle in pancreatic cancer therapy. *Cancer Biol Ther* (2012) **13**:206–15. doi:10.4161/cbt.13.4.18692
44. Dubey PK, Singodaria D, Verma RK, Vyas SP. RGD modified albumin nanospheres for tumour vasculature targeting. *J Pharm Pharmacol* (2011) **63**:33–40. doi:10.1111/j.2042-7158.2010.01180.x
45. Temming K, Meyer DL, Zabinski R, Dijkers EC, Poelstra K, Molema G, et al. Evaluation of RGD-targeted albumin carriers for specific delivery of auristatin E to tumor blood vessels. *Bioconjug Chem* (2006) **17**:1385–94. doi:10.1021/bc060087z
46. Wenk E, Wandrey AJ, Merkle HP, Meinel L. Silk fibroin spheres as a platform for controlled drug delivery. *J Control Release* (2008) **132**:26–34. doi:10.1016/j.jconrel.2008.08.005
47. Wohlrab S, Müller S, Schmidt A, Neubauer S, Kessler H, Leal-Egaña A, et al. Cell adhesion and proliferation on RGD-modified recombinant spider silk proteins. *Biomaterials* (2012) **33**:6650–9. doi:10.1016/j.biomaterials.2012.05.069
48. Arnold M, Cavalcanti-Adam EA, Glass R, Blümmel J, Eck W, Kantlehner M, et al. Activation of integrin function by nanopatterned adhesive interfaces. *Chemphyschem* (2004) **5**:383–8. doi:10.1002/cphc.200301014
49. Arosio D, Manzoni L, Araldi EM, Scolastico C. Cyclic RGD functionalized gold nanoparticles for tumor targeting. *Bioconjug Chem* (2011) **22**:664–72. doi:10.1021/bc100448r
50. Yang X, Hong H, Grailer JJ, Rowland IJ, Javadi A, Hurley SA, et al. cRGD-functionalized, DOX-conjugated, and ^{64}Cu -labeled superparamagnetic iron oxide nanoparticles for targeted anticancer drug delivery and PET/MR imaging. *Biomaterials* (2011) **32**:4151–60. doi:10.1016/j.biomaterials.2011.02.006
51. Gormley AJ, Malugin A, Ray A, Robinson R, Ghandehari H. Biological evaluation of RGDFK-gold nanorod conjugates for prostate cancer treatment. *J Drug Target* (2011) **19**:915–24. doi:10.3109/1061186X.2011.623701
52. Akhavan O, Ghaderi E, Emamy H. Nontoxic concentrations of PEGylated graphene nanoribbons for selective cancer cell imaging and photothermal therapy. *J Mater Chem* (2012) **22**:20626–33. doi:10.1039/c2jm34330d
53. Kim S, Bell K, Mousa SA, Varner JA. Regulation of angiogenesis *in vivo* by ligation of integrin $\alpha 5\beta 1$ with the central cell-binding domain of fibronectin. *Am J Pathol* (2000) **156**:1345–62. doi:10.1016/S0002-9440(10)65005-5
54. Kim S, Harris M, Varner JA. Regulation of integrin $\alpha v\beta 3$ -mediated endothelial cell migration and angiogenesis by integrin $\alpha 5\beta 1$ and protein kinase A. *J Biol Chem* (2000) **275**:33920–8. doi:10.1074/jbc.M003668200
55. Jayne DG, Heath RM, Dewhurst O, Scott N, Guillou PJ. Extracellular matrix proteins and chemoradiotherapy: $\alpha 5\beta 1$ integrin as a predictive marker in rectal cancer. *Eur J Surg Oncol* (2002) **28**:30–6. doi:10.1053/ejso.2001.1182
56. Jia Y, Zeng ZZ, Markwart SM, Rockwood KE, Ignatowski KM, Ethier SP, et al. Integrin fibronectin receptors in matrix metalloproteinase-1-dependent invasion by breast cancer and mammary epithelial cells. *Cancer Res* (2004) **64**:8674–81. doi:10.1158/0008-5472.CAN-04-0069
57. Chen J, De S, Brainard J, Byzova TV. Metastatic properties of prostate cancer cells are controlled by VEGF. *Cell Commun Adhes* (2004) **11**:1–11. doi:10.1080/15419060490471739
58. Kim S, Bakre M, Yin H, Varner JA. Inhibition of endothelial cell survival and angiogenesis by protein kinase A. *J Clin Invest* (2002) **110**:933–41. doi:10.1172/JCI0214268
59. van der Flier A, Badu-Nkansah K, Whittaker CA, Crowley D, Bronson RT, Lacy-Hulbert A, et al. Endothelial $\alpha 5$ and αv integrins cooperate in remodeling of the vasculature during development. *Development* (2010) **137**:2439–49. doi:10.1242/dev.049551
60. Garg A, Tisdale AW, Haidari E, Kokkoli E. Targeting colon cancer cells using PEGylated liposomes modified with a fibronectin-mimetic peptide. *Int J Pharm* (2009) **366**:201–10. doi:10.1016/j.ijpharm.2008.09.016
61. Shroff K, Kokkoli E. PEGylated liposomal doxorubicin targeted to $\alpha 5\beta 1$ -expressing MDA-MB-231 breast cancer cells. *Langmuir* (2012) **28**:4729–36. doi:10.1021/la204466g
62. Pangburn TO, Georgiou K, Bates FS, Kokkoli E. Targeted polymersome delivery of siRNA induces cell death of breast cancer cells dependent upon Orai3 protein expression. *Langmuir* (2012) **28**:12816–30. doi:10.1021/la300874z
63. Munger JS, Huang X, Kawakatsu H, Griffiths MJ, Dalton SL, Wu J, et al. The integrin $\alpha v\beta 6$ binds and activates latent TGF beta 1: a mechanism for regulating pulmonary inflammation and fibrosis. *Cell* (1999) **96**:319–28. doi:10.1016/S0092-8674(00)80545-0
64. Plow EF, Haas TA, Zhang L, Loftus J, Smith JW. Ligand binding to integrins. *J Biol Chem* (2000) **275**:21785–8. doi:10.1074/jbc.R000003200
65. Margadant C, Sonnenberg A. Integrin-TGF-beta crosstalk in fibrosis, cancer and wound healing. *EMBO Rep* (2010) **11**:97–105. doi:10.1038/embor.2009.276
66. Bates RC, Bellovin DI, Brown C, Maynard E, Wu B, Kawakatsu H, et al. Transcriptional activation of integrin $\beta 6$ during the epithelial-mesenchymal transition defines a novel prognostic indicator of aggressive colon carcinoma. *J Clin Invest* (2005) **115**:339–47. doi:10.1172/JCI23183
67. Ahmed N, Pansino F, Baker M, Rice G, Quinn M. Association between $\alpha v\beta 6$ integrin expression, elevated p42/44 kDa MAPK, and plasminogen-dependent matrix degradation in ovarian cancer. *J Cell Biochem* (2002) **84**:675–86. doi:10.1002/jcb.10080
68. Elayadi AN, Samli KN, Prudkin L, Liu YH, Bian A, Xie XJ, et al. A peptide selected by biopanning identifies the integrin $\alpha v\beta 6$ as a prognostic biomarker for nonsmall cell lung cancer. *Cancer Res* (2007) **67**:5889–95. doi:10.1158/0008-5472.CAN-07-0245
69. Prudkin L, Liu DD, Ozburn NC, Sun MH, Behrens C, Tang X, et al. Epithelial-to-mesenchymal transition in the development and progression of adenocarcinoma and squamous cell carcinoma of the lung. *Mod Pathol* (2009) **22**:668–78. doi:10.1038/modpathol.2009.19
70. Hausner SH, DiCaro D, Marik J, Marshall JF, Sutcliffe JL. Use of a peptide derived from foot-and-mouth disease virus for the non-invasive imaging of human cancer: generation and evaluation of 4-[^{18}F]fluorobenzoyl A20FMDV2 for *in vivo* imaging of integrin $\alpha v\beta 6$ expression with positron emission tomography. *Cancer Res* (2007) **67**:7833–40. doi:10.1158/0008-5472.CAN-07-1026
71. Kawashima A, Tsugawa S, Boku A, Kobayashi M, Minamoto T, Nakanishi I, et al. Expression of αv integrin family in gastric carcinomas: increased $\alpha v\beta 6$ is associated with lymph node metastasis. *Pathol Res Pract* (2003) **199**:57–64. doi:10.1078/0344-0338-00355
72. Goodman SL, Hölzemann G, Sulyok GAG, Kessler H. Nanomolar small molecule inhibitors for $\alpha v\beta 6$, $\alpha v\beta 5$, and $\alpha v\beta 3$ integrins. *J Med Chem* (2002) **45**:1045–51. doi:10.1021/jm0102598
73. Bochen A, Marelli UK, Otto E, Pallarola D, Mas-Moruno C, Di Leva FS, et al. Bispecificity of isoDGR peptides for fibronectin binding integrin subtypes $\alpha 5\beta 1$ and $\alpha v\beta 6$: conformational control through flanking amino acids. *J Med Chem* (2013) **56**:1509–19. doi:10.1021/jm301221x
74. Hsiao JR, Chang Y, Chen YL, Hsieh SH, Hsu KF, Wang CF, et al. Cyclic $\alpha v\beta 6$ -targeting peptide selected from biopanning with clinical potential for head and neck squamous cell carcinoma. *Head Neck* (2010) **32**:160–72. doi:10.1002/hed.21166
75. Oyama T, Sykes KF, Samli KN, Minna JD, Johnston SA, Brown KC. Isolation of lung tumor specific peptides from a random peptide library: generation of diagnostic and cell-targeting reagents. *Cancer Lett* (2003) **202**:219–30. doi:10.1016/j.canlet.2003.08.011
76. Guan H, McGuire MJ, Li S, Brown KC. Peptide-targeted

- polyglutamic acid doxorubicin conjugates for the treatment of $\alpha\beta 6$ -positive cancers. *Bioconjug Chem* (2008) **19**:1813–21. doi:10.1021/bc800154f
77. Li S, Gray BP, McGuire MJ, Brown KC. Synthesis and biological evaluation of a peptide-paclitaxel conjugate which targets the integrin $\alpha\beta 6$. *Bioorg Med Chem* (2011) **19**:5480–9. doi:10.1016/j.bmc.2011.07.046
78. Gray BP, Li SZ, Brown KC. From phage display to nanoparticle delivery: functionalizing liposomes with multivalent peptides improves targeting to a cancer biomarker. *Bioconjug Chem* (2013) **24**:85–96. doi:10.1021/bc300498d
79. Guthi JS, Yang SG, Huang G, Li SZ, Khemtong C, Kessinger CW, et al. MRI-visible micellar nanomedicine for targeted drug delivery to lung cancer cells. *Mol Pharm* (2007) **7**:32–40. doi:10.1021/mp0001393
80. DiCara D, Rapisarda C, Sutcliffe JL, Violette SM, Weinreb PH, Hart IR, et al. Structure-function analysis of Arg-Gly-Asp helix motifs in $\alpha\beta 6$ integrin ligands. *J Biol Chem* (2007) **282**:9657–65. doi:10.1074/jbc.M610461200
81. Logan D, Abughazaleh R, Blakemore W, Curry S, Jackson T, King A, et al. Structure of a major immunogenic site on foot-and-mouth disease virus. *Nature* (1993) **362**:566–8. doi:10.1038/362566a0
82. Hausner SH, Marik J, Gagnon MK, Sutcliffe JL. *In vivo* positron emission tomography (PET) imaging with an $\alpha\beta 6$ specific peptide radiolabeled using ^{18}F -“click” chemistry: evaluation and comparison with the corresponding 4-[^{18}F]fluorobenzoyl- and 2-[^{18}F]fluoropropionyl-peptides. *J Med Chem* (2008) **51**:5901–4. doi:10.1021/jm800608s
83. Hausner SH, Abbey CK, Bold RJ, Gagnon MK, Marik J, Marshall JE, et al. Targeted *in vivo* imaging of integrin $\alpha\beta 6$ with an improved radiotracer and its relevance in a pancreatic tumor model. *Cancer Res* (2009) **69**:5843–50. doi:10.1158/0008-5472.CAN-08-4410
84. Hausner SH, Carpenter RD, Bauer N, Sutcliffe JL. Evaluation of an integrin $\alpha\beta 6$ -specific peptide labeled with [^{18}F]fluorine by copper-free, strain-promoted click chemistry. *Nucl Med Biol* (2013) **40**:233–9. doi:10.1016/j.nucmedbio.2012.10.007
85. Saha A, Ellison D, Thomas GJ, Vallath S, Mather SJ, Hart IR, et al. High-resolution *in vivo* imaging of breast cancer by targeting the pro-invasive integrin $\alpha\beta 6$. *J Pathol* (2010) **222**:52–63. doi:10.1002/path.2745
86. Coughlan L, Vallath S, Saha A, Flak M, McNeish IA, Vassaux G, et al. *In vivo* retargeting of adenovirus type 5 to $\alpha\beta 6$ integrin results in reduced hepatotoxicity and improved tumor uptake following systemic delivery. *J Virol* (2009) **83**:6416–28. doi:10.1128/JVI.00445-09
87. Kimura RH, Teed R, Hackel BJ, Pysz MA, Chuang CZ, Sathirachinda A, et al. Pharmacokinetically stabilized cystine knot peptides that bind $\alpha\beta 6$ integrin with single-digit nanomolar affinities for detection of pancreatic cancer. *Clin Cancer Res* (2012) **18**:839–49. doi:10.1158/1078-0432.CCR-11-1116
88. Hackel BJ, Kimura RH, Miao Z, Liu H, Sathirachinda A, Cheng Z, et al. ^{18}F -fluorobenzoate-labeled cystine knot peptides for PET imaging of integrin $\alpha\beta 6$. *J Nucl Med* (2013) **54**(7):1101–5. doi:10.2967/jnmed.112.110759
89. Loges S, Mazzone M, Hohensinner P, Carmeliet P. Silencing or fueling metastasis with VEGF inhibitors: antiangiogenesis revisited. *Cancer Cell* (2009) **15**:167–70. doi:10.1016/j.ccr.2009.02.007
90. Shojai F. Anti-angiogenesis therapy in cancer: current challenges and future perspectives. *Cancer Lett* (2012) **320**:130–7. doi:10.1016/j.canlet.2012.03.008
91. Heckmann D, Meyer A, Marinelli L, Zahn G, Stragies R, Kessler H. Probing integrin selectivity: rational design of highly active and selective ligands for the $\alpha 5\beta 1$ and $\alpha 6\beta 4$ integrin receptor. *Angew Chem Int Ed Engl* (2007) **46**:3571–4. doi:10.1002/anie.200700008
92. Heckmann D, Meyer A, Laufer B, Zahn G, Stragies R, Kessler H. Rational design of highly active and selective ligands for the $\alpha 5\beta 1$ integrin receptor. *ChemBioChem* (2008) **9**:1397–407. doi:10.1002/cbic.200800032
93. Rechenmacher F, Neubauer S, Polleux J, Mas-Moruno C, De Simone M, Cavalcanti-Adam EA, et al. Functionalizing $\alpha\beta 3$ - or $\alpha\beta 1$ -selective integrin antagonists for surface coating: a method to discriminate integrin subtypes *in vitro*. *Angew Chem Int Ed Engl* (2013) **52**:1572–5. doi:10.1002/anie.201206370
94. Rechenmacher F, Neubauer S, Mas-Moruno C, Dorfner PM, Polleux J, Guasch J, et al. A Molecular toolkit for the functionalization of titanium-based biomaterials that selectively control integrin-mediated cell adhesion. *Chem Eur J* (2013) **19**(28):9218–23. doi:10.1002/chem.201301478
95. Murphy EA, Majeti BK, Barnes LA, Makale M, Weis SM, Lutu-Fuga K, et al. Nanoparticle-mediated drug delivery to tumor vasculature suppresses metastasis. *Proc Natl Acad Sci U S A* (2008) **105**:9343–8. doi:10.1073/pnas.0803728105
96. Xiao Y, Hong H, Javadi A, Engle JW, Xu W, Yang Y, et al. Multifunctional unimolecular micelles for cancer-targeted drug delivery and positron emission tomography imaging. *Biomaterials* (2012) **33**:3071–82. doi:10.1016/j.biomaterials.2011.12.030
97. Ding H, Yong KT, Roy I, Hu R, Wu F, Zhao L, et al. Bioconjugated PLGA-4-arm-PEG branched polymeric nanoparticles as novel tumor targeting carriers. *Nanotechnology* (2011) **22**:165101. doi:10.1088/0957-4484/22/16/165101
98. Eldar-Bocck A, Miller K, Sanchis J, Lupu R, Vicent MJ, Satchi-Fainaro R. Integrin-assisted drug delivery of nano-scaled polymer therapeutics bearing paclitaxel. *Biomaterials* (2011) **32**:3862–74. doi:10.1016/j.biomaterials.2011.01.073
99. Danhier F, Vroman B, Lecouterier N, Crokart N, Pourcelle V, Freichels H, et al. Targeting of tumor endothelium by RGD-grafted PLGA-nanoparticles loaded with paclitaxel. *J Control Release* (2009) **140**:166–73. doi:10.1016/j.jconrel.2009.08.011
100. Zhan C, Gu B, Xie C, Li J, Liu Y, Lu W. Cyclic RGD conjugated poly(ethylene glycol)-co-poly(lactic acid) micelle enhances paclitaxel anti-glioblastoma effect. *J Control Release* (2010) **143**:136–42. doi:10.1016/j.jconrel.2009.12.020
101. Liu P, Qin L, Wang Q, Sun Y, Zhu M, Shen M, et al. cRGD-functionalized mPEG-PLGA-PLL nanoparticles for imaging and therapy of breast cancer. *Biomaterials* (2012) **33**:6739–47. doi:10.1016/j.biomaterials.2012.06.008
102. Yin P, Wang Y, Qiu Y, Hou L, Liu X, Qin J, et al. Bufalin-loaded mPEG-PLGA-PLL-cRGD nanoparticles: preparation, cellular uptake, tissue distribution, and anticancer activity. *Int J Nanomedicine* (2012) **7**:3961–9. doi:10.2147/IJN.S32063
103. Borgman MP, Ray A, Kolhatkar RB, Sausville EA, Burger AM, Ghandehari H. Targetable HPMA copolymer-aminohexylgeldanamycin conjugates for prostate cancer therapy. *Pharm Res* (2009) **26**:1407–18. doi:10.1007/s11095-009-9851-0
104. Borgman MP, Aras O, Geyser-Stoops S, Sausville EA, Ghandehari H. Biodistribution of HPMA copolymer-aminohexylgeldanamycin-RGDFK conjugates for prostate cancer drug delivery. *Mol Pharm* (2009) **6**:1836–47. doi:10.1021/mp900134c
105. Greish K, Ray A, Bauer H, Larson N, Malugin A, Pike D, et al. Anticancer and antiangiogenic activity of HPMA copolymer-aminohexylgeldanamycin-RGDFK conjugates for prostate cancer therapy. *J Control Release* (2011) **151**:263–70. doi:10.1016/j.jconrel.2010.12.015
106. Ray A, Larson N, Pike DB, Grüner M, Naik S, Bauer H, et al. Comparison of active and passive targeting of docetaxel for prostate cancer therapy by HPMA copolymer-RGDFK conjugates. *Mol Pharm* (2011) **8**:1090–9. doi:10.1021/mp100402n
107. Zhang P, Hu L, Yin Q, Feng L, Li Y. Transferrin-modified c[RGDFK]-paclitaxel loaded hybrid micelle for sequential blood-brain barrier penetration and glioma targeting therapy. *Mol Pharm* (2012) **9**:1590–8. doi:10.1021/mp200600t
108. Xu Q, Liu Y, Su S, Li W, Chen C, Wu Y. Anti-tumor activity of paclitaxel through dual-targeting carrier of cyclic RGD and transferrin conjugated hyperbranched copolymer nanoparticles. *Biomaterials* (2012) **33**:1627–39. doi:10.1016/j.biomaterials.2011.11.012
109. Winter PM, Schmieder AH, Caruthers SD, Keene JL, Zhang H, Wickline SA, et al. Minute dosages of $\alpha\beta 3$ -targeted fumagillin nanoparticles impair Vx-2 tumor angiogenesis and development in rabbits. *FASEB J* (2008) **22**:2758–67. doi:10.1096/fj.07-103929
110. Kim Y, Pourgholami MH, Morris DL, Stenzel MH. An optimized RGD-decorated micellar drug delivery system for albendazole for the treatment of ovarian cancer: from RAFT polymer synthesis to cellular uptake. *Macromol Biosci* (2011) **11**:219–33. doi:10.1002/mabi.201000293

111. Oba M, Fukushima S, Kanayama N, Aoyagi K, Nishiyama N, Koyama H, et al. Cyclic RGD peptide-conjugated polyplex micelles as a targetable gene delivery system directed to cells possessing $\alpha\beta 3$ and $\alpha\beta 5$ integrins. *Bioconjug Chem* (2007) **18**:1145–1123. doi:10.1021/bc0700133
112. Oba M, Aoyagi K, Miyata K, Matsumoto Y, Itaka K, Nishiyama N, et al. Polyplex micelles with cyclic RGD peptide ligands and disulfide cross-links directing to the enhanced transfection via controlled intracellular trafficking. *Mol Pharm* (2008) **5**:1080–92. doi:10.1021/mp000070s
113. Oba M, Vachutinsky Y, Miyata K, Kano MR, Ikeda S, Nishiyama N, et al. Antiangiogenic gene therapy of solid tumor by systemic injection of polyplex micelles loading plasmid DNA encoding soluble flt-1. *Mol Pharm* (2010) **7**:501–9. doi:10.1021/mp9002317
114. Vachutinsky Y, Oba M, Miyata K, Hiki S, Kano MR, Nishiyama N, et al. Antiangiogenic gene therapy of experimental pancreatic tumor by sFlt-1 plasmid DNA carried by RGD-modified crosslinked polyplex micelles. *J Control Release* (2011) **149**:51–7. doi:10.1016/j.jconrel.2010.02.002
115. Nie Y, Schaffert D, Rödl W, Ogris M, Wagner E, Günther M. Dual-targeted polyplexes: one step towards a synthetic virus for cancer gene therapy. *J Control Release* (2011) **152**:127–34. doi:10.1016/j.jconrel.2011.02.028
116. Merkel OM, Germershausen O, Wada CK, Tarcha PJ, Merdan T, Kissel T. Integrin $\alpha\beta 3$ targeted gene delivery using RGD peptidomimetic conjugates with copolymers of PEGylated poly(ethylene imine). *Bioconjug Chem* (2009) **20**:1270–80. doi:10.1021/bc9001695
117. Zhan C, Meng Q, Li Q, Feng L, Zhu J, Lu W. Cyclic RGD-polyethylene glycol-polyethylenimine for intracranial glioblastoma-targeted gene delivery. *Chem Asian J* (2012) **7**:91–6. doi:10.1002/asia.201100570
118. Ng QK, Sutton MK, Soonsawad P, Xing L, Cheng H, Segura T. Engineering clustered ligand binding into nonviral vectors: $\alpha\beta 3$ targeting as an example. *Mol Ther* (2009) **17**:828–36. doi:10.1038/mt.2009.11
119. Martin I, Dohmen C, Mas-Moruno C, Troiber C, Kos P, Schaffert D, et al. Solid-phase-assisted synthesis of targeting peptide-PEG-oligo(ethane amino)amides for receptor-mediated gene delivery. *Org Biomol Chem* (2012) **10**:3258–68. doi:10.1039/c2ob06907e
120. Yonenaga N, Kenjo E, Asai T, Tsuruta A, Shimizu K, Dewa T, et al. RGD-based active targeting of novel polycation liposomes bearing siRNA for cancer treatment. *J Control Release* (2012) **160**:177–81. doi:10.1016/j.jconrel.2011.10.004
121. Xiong XB, Uludag H, Lavasanifar A. Virus-mimetic polymeric micelles for targeted siRNA delivery. *Biomaterials* (2010) **31**:5886–93. doi:10.1016/j.biomaterials.2010.03.075

Conflict of Interest Statement: The authors declare that the research was

conducted in the absence of any commercial or financial relationships that could be construed as a potential conflict of interest.

Received: 15 July 2013; paper pending published: 25 July 2013; accepted: 13 August 2013; published online: 30 August 2013.

Citation: Marelli UK, Rechenmacher F, Sobahi TRA, Mas-Moruno C and Kessler H (2013) Tumor targeting via integrin ligands. *Front. Oncol.* **3**:222. doi:10.3389/fonc.2013.00222

This article was submitted to Pharmacology of Anti-Cancer Drugs, a section of the journal *Frontiers in Oncology*.

Copyright © 2013 Marelli, Rechenmacher, Sobahi, Mas-Moruno and Kessler. This is an open-access article distributed under the terms of the Creative Commons Attribution License (CC BY). The use, distribution or reproduction in other forums is permitted, provided the original author(s) or licensor are credited and that the original publication in this journal is cited, in accordance with accepted academic practice. No use, distribution or reproduction is permitted which does not comply with these terms.



Ways to enhance lymphocyte trafficking into tumors and fitness of tumor infiltrating lymphocytes

Matteo Bellone^{1*} and Arianna Calcinotto^{1,2}

¹ Cellular Immunology Unit, Department of Immunology, Infectious Diseases and Transplantation, San Raffaele Scientific Institute, Milan, Italy

² Università Vita Salute San Raffaele, Milan, Italy

Edited by:

Ronald Berenson, Compliment Corporation, USA

Reviewed by:

Carine Michiels, University of Namur, Belgium

Marc Poirot, Institut National de la Santé et de la Recherche Médicale, France

***Correspondence:**

Matteo Bellone, Cellular Immunology Unit, San Raffaele Scientific Institute, Via Olgettina 58, Milan 20132, Italy
e-mail: bellone.matteo@hsr.it

The tumor is a hostile microenvironment for T lymphocytes. Indeed, irregular blood flow, and endothelial cell (EC) anergy that characterize most solid tumors hamper leukocyte adhesion, extravasation, and infiltration. In addition, hypoxia and reprogramming of energy metabolism within cancer cells transform the tumor mass in a harsh environment that limits survival and effector functions of T cells, regardless of being induced *in vivo* by vaccination or adoptively transferred. In this review, we will summarize on recent advances in our understanding of the characteristics of tumor-associated neo-angiogenic vessels as well as of the tumor metabolism that may impact on T cell trafficking and fitness of tumor infiltrating lymphocytes. In particular, we will focus on how advances in knowledge of the characteristics of tumor ECs have enabled identifying strategies to normalize the tumor vasculature and/or overcome EC anergy, thus increasing leukocyte-vessel wall interactions and lymphocyte infiltration in tumors. We will also focus on drugs acting on cells and their released molecules to transiently render the tumor microenvironment more suitable for tumor infiltrating T lymphocytes, thus increasing the therapeutic effectiveness of both active and adoptive immunotherapies.

Keywords: cytotoxic T lymphocyte, vaccine, adoptive T cell therapy, pH, redox, proton pump inhibitor, NGR-TNF, combination therapy

INTRODUCTION

Active and adoptive cancer immunotherapies have breached the wall between bench and bedside at last, and have just entered a new golden age. This is the result of several concomitant technological advancements and breakthrough discoveries. On the one hand, powerful technical tools (e.g., tetramers and live imaging) have been made available to more deeply investigate the interactions between the growing tumor and the host, and especially the immune system. Thus, sophisticated genetically engineered animal models have allowed building new theories on the process of cancer immune surveillance (1). Furthermore, high-throughput technologies are making possible investigating the tumor microenvironment as a whole (2), and genomic landscaping, proteomic profiling, and more recently metabolomics and algorithms applied to cancer histochemistry (3–8) are drawing an entirely new picture of the tumor mass. On the other hand, strong efforts from hundreds of laboratories around the world in the last 20 years have defined tumor-associated antigens (TAAs) and adjuvants to such an high degree of knowledge [e.g.,(9)] that active immunotherapy has eventually reached the bedside with the first FDA approved cancer vaccine for metastatic prostate cancer patients (10). Even more importantly, clinical grade *in vitro* expanded tumor infiltrating lymphocytes (TILs) and genetically engineered T cells have demonstrated the full potential of adoptive immunotherapy (11, 12).

Yet, several hurdles still need to be overcome (Figure 1) to extend such treatments to the majority of cancer patients. Firstly, the tumor mass is characterized by abnormal tumor vessels and

interstitium that limit leukocyte adhesion, extravasation, and infiltration (13), and favors hypoxia and reprogramming of energy metabolism within cancer cells (14). Metabolic alterations within the tumor mass also limit T cell functions, and the tumor microenvironment eventually becomes a site of immune privilege where several cancer cell intrinsic and extrinsic mechanisms suppress the tumor-specific T cell response (15).

Here, we will summarize on recent advances in our understanding of the characteristics of tumor-associated neo-angiogenic vessels as well as of the tumor metabolism that may impact on T cell trafficking and fitness of TILs. We will also report on drugs acting on cells and their released molecules to transiently render the tumor microenvironment more suitable for tumor TILs (Figure 1), thus increasing T cell trafficking into tumors and the therapeutic effectiveness of both active and adoptive immunotherapies.

T CELL ADHESION TO THE ENDOTHELIUM, EXTRAVASATION, AND INFILTRATION WITHIN INFLAMED TISSUES

Once a T cell has been activated in secondary lymphoid organs, it reaches the blood flow and navigates within vessels to the site of extravasation, which usually coincides with a site of inflammation. Activated T cells prefer to exit the blood stream at the level of post-capillary venules, where the hemodynamic shear stress is lower than in arteries and capillaries and the endothelium is more prone to extravasation. Activated T cells travel more efficiently than naïve T cells to inflamed tissues because they upregulate adhesion molecules and chemoattractant receptors for inflammation

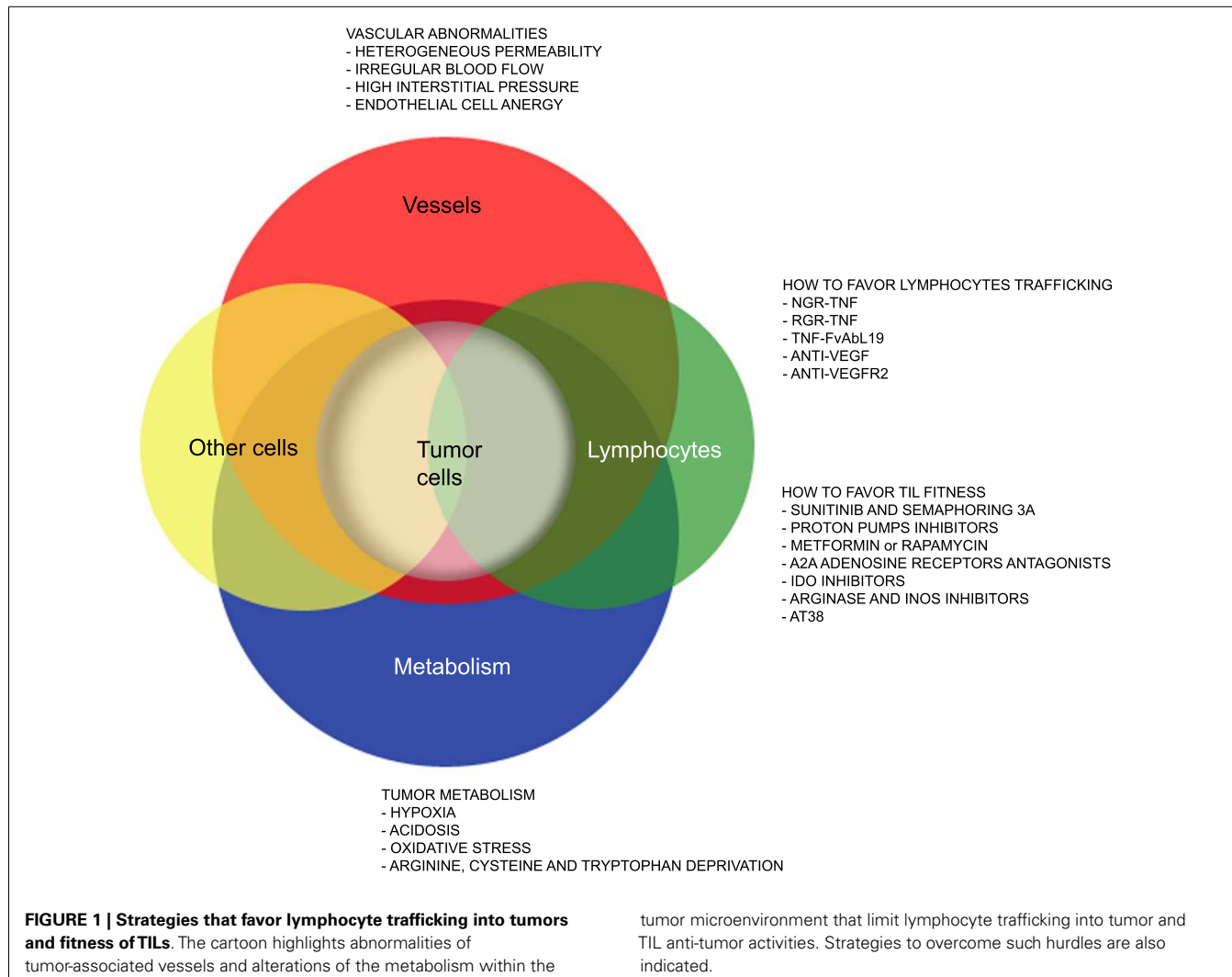


FIGURE 1 | Strategies that favor lymphocyte trafficking into tumors and fitness of TILs. The cartoon highlights abnormalities of tumor-associated vessels and alterations of the metabolism within the

tumor microenvironment that limit lymphocyte trafficking into tumor and TIL anti-tumor activities. Strategies to overcome such hurdles are also indicated.

induced ligands. Transendothelial migration involves specific adhesive interactions between T cells and endothelial cells (ECs) that guide the lymphocytes from the vascular compartment to the extravascular tissue. We refer the interested reader to excellent reviews on this topic (16–20). In brief, T cells undergo four distinct adhesion steps during their migration through blood vessels. These include tethering, rolling, activation, and arrest. Tethering and rolling of leukocytes are mediated by interactions between selectins and specific carbohydrate moieties bound to a protein backbone (21), which allow rapid engagement with high tensile strength. The selectins are a family of three C-type lectins expressed by bone marrow-derived cells and ECs. L-selectin (CD62L) is expressed by all myeloid cells, naïve T cells, and some activated and memory cells. P-selectin (CD62P) is found in secretory granules of platelets and ECs and is expressed on the cell surface after activation by inflammatory stimuli. E-selectin (CD62E) is expressed by acutely inflamed ECs in most organs and by non-inflamed skin microvessels. Thus, P-selectin glycoprotein ligand 1 (PSGL-1) and CD43 on activated T cells engage CD62P and CD62E on activated ECs, respectively. Rolling T cells

receive signals from chemokines on ECs, which induce modulation of integrins to acquire high avidity for their ligands. Integrins may participate to the rolling phase but are essential for the firm adhesion of leukocytes. In particular, activated T cells depend on lymphocyte function-associated antigen 1 (LFA-1), very late antigen-4 (VLA-4; α 4 β 1), and α 4 β 7 for their interactions with activated ECs that express intracellular adhesion molecule 1 (ICAM-1), intracellular adhesion molecule 2 (ICAM-2), VCAM-1, and mucosal addressin-cell adhesion molecule type 1 (MAdCAM-1), respectively (22).

Quiescent ECs poorly interact with circulating leukocytes. Autacoid mediators released by mast cells and other cells of the innate immunity, upon stimulation by inflammatory signals (e.g., infection and tissue damage), cause rapid enhancement of venular permeability, translocation of integrins, and chemokines from intracellular stores to the cell surface and formation of a provisional matrix (23), all processes that favor T cell-EC interactions.

A very different scenario may characterize T cell-EC interactions in tumor-associated vessels.

TUMOR-ASSOCIATED MODIFICATIONS OF THE ENDOTHELIUM HAMPER T CELL ADHESION, EXTRAVASATION, AND TUMOR INFILTRATION

While acute inflammation is an efficacious means by which the organism repairs a tissue that has been damaged by a physical insult or infection, chronic inflammation has emerged as indispensable requisite for chronic diseases including cancer (24). Indeed, tumor-promoting inflammation has been recently recognized as an enabling characteristic that allows cancer cells to acquire multiple hallmark capabilities including sustaining proliferative signaling, resisting cell death, avoiding immune destruction, activating invasion, and metastasis and inducing angiogenesis (25). Virtually any neoplastic lesion contains immune inflammatory cells although with variable densities (26). Yet, gene expression profiling of the total cellular composition of tumors has evidenced at least two subsets of tumors. The first “inflamed” subset is characterized by transcripts encoding innate immune cell molecules, chemokines that can contribute to effector T cell recruitment, various T lineage-specific markers, and, paradoxically, immune inhibitory mechanisms. Conversely, the “not-inflamed” phenotype is distinguished for high expression of angiogenesis-associated factors as well as macrophages and fibroblasts (2). Thus, it has been hypothesized that TILs effectively extravasate in inflamed tumors but are inhibited by immunosuppressive mechanisms, including indoleamine-2,3-dioxygenase (IDO), programmed cell death 1 ligand 1 (PD-L1), and forkhead box P3 (FoxP3)⁺ regulatory T cells (Tregs), whereas, T cell migration is defective in not-inflamed tumors (2).

More in general, vessels are irregularly distributed within the tumor mass that, when reaches 1–2 mm in diameter, presents a patchy distribution of less-perfused and hypoxic areas (27). Hypoxia is one of the strongest stimulators of angiogenesis, largely through the expression of hypoxia inducible transcription factors [HIFs; (28)]. Tumor vessels that sprout from existing ones are disorganized, tortuous, dilated, saccular, and leakier than the normal ones. Also the composition of the vessel is abnormal, and ECs may acquire aberrant morphology, pericytes may be absent or loosely attached, and the vessel may lack basement membrane or have it unusually thick (13, 29). In addition, tumor cells may mimic ECs and generate vascular conduits, which however, are even more abnormal (30). All together, these vascular abnormalities render tumor vessels leakier than normal ones, may increase the interstitial pressure, cause heterogeneous permeability, and promote irregular blood flow, therefore making leukocyte trafficking within the tumor mass difficult. Interstitial pressure is also increased by the extrinsic compression of tumor vessels by proliferating cancer cells. In addition, angiogenic factors such as vascular EC growth factors (VEGFs) and fibroblast growth factors (FGFs) cause down-regulation of ICAM-1/2, VCAM-1, and CD34 on ECs, a phenomenon defined as “EC anergy” (31–33). Thus, the few effector T cells that circulate in tumor vessels, regardless of being induced *in vivo* by vaccination or adoptively transferred (34, 35), can hardly interact with ECs and begin their migration through blood vessels (Figure 2A). In line with this view, gene expression profiling and *in situ* immunohistochemical staining of large cohorts of cancer patients have shown that more aggressive tumors are characterized by peritumoral immune infiltrates (36), whereas a strong *in situ*

accumulation of T cells both in the center of the tumor and the invading margin correlates with a favorable prognosis regardless of the local extent of the tumor and of metastasis (37).

WAYS TO FAVOR T CELL ADHESION TO TUMOR-ASSOCIATED ENDOTHELIAL CELLS, EXTRAVASATION, AND TUMOR INFILTRATION

Crossing the abnormal tumor vessel barrier and interstitium is one major hurdle for tumor-specific T cells that have reached the tumor mass (Figure 1). Few years ago, we proposed that delivery of vasoactive inflammatory cytokines like tumor necrosis factor α (TNF) to neo-angiogenic vessels might represent a good strategy to induce selective activation of ECs in tumor tissues, thereby enhancing T cell extravasation and tumor infiltration (38). TNF is produced in the tumor microenvironment mainly by macrophages, but also by smooth muscle cells, ECs and tumor cells (39), and it affects primarily the tumor-associated vasculature (40). Indeed, most tumor cells and vessels of normal tissues are resistant to TNF (41). Depending on the amount of TNF that reaches the tumor mass, its effects range from EC activation, to increased vessel permeability, EC damage, and massive hemorrhagic necrosis (42). The *in vivo* effects of TNF have been well characterized both in pre-clinical models and in humans undergoing isolated limb perfusion, a regional cancer therapy used to deliver high doses of a drug into the bloodstream of a limb avoiding severe systemic side effects (42). An alternative strategy to avoid TNF-induced systemic toxicity is indeed to selectively target minute amounts of the cytokine to the tumor vessels. Selective delivery of TNF to tumor vessels has been achieved by fusing this cytokine with a tumor-vasculature-homing peptide that contains the Cys-Asn-Gly-Arg-Cys (NGR) sequence, a ligand of a CD13 isoform expressed by neo-angiogenic vessels (43, 44). The new moiety called NGR-TNF was shown to transiently enhance tumor vessel permeability (45), thus increasing the penetration of chemotherapy agents in murine models of lymphoma, melanoma, and spontaneous prostate cancer without TNF-related systemic toxicity (46, 47). NGR-TNF is currently under clinical investigation in various clinical studies in cancer patients (48).

In accordance with our original hypothesis (38), we have recently shown that extremely low doses of NGR-TNF (5 ng/Kg) are sufficient to induce the up-regulation of VCAM-1 and ICAM-2 on the endothelial lining of tumor vessels as well as the release, in the tumor microenvironment, of chemokines that favor T-cell trafficking (Figure 2B). Rapid and transient modification of the tumor microenvironment can enhance the infiltration of either fully activated endogenous or adoptively transferred T cells in transplantable melanoma and autochthonous prostate cancer (49). Additionally, we have demonstrated that NGR-TNF can increase the therapeutic efficacy of tumor vaccines and adoptive immunotherapy with no evidence of toxic reactions (49). The effects of NGR-TNF on tumor infiltration by leukocytes go beyond the transient activation of tumor-associated ECs (50). Indeed, NGR-TNF transiently modifies the endothelial barrier function by loosening VE-cadherin dependent adherence junctions (51), thus favoring T cell extravasation (Figure 2B). It can also transiently reduce hypoxic areas of the tumor (52) and favor TIL proliferation and survival (50).

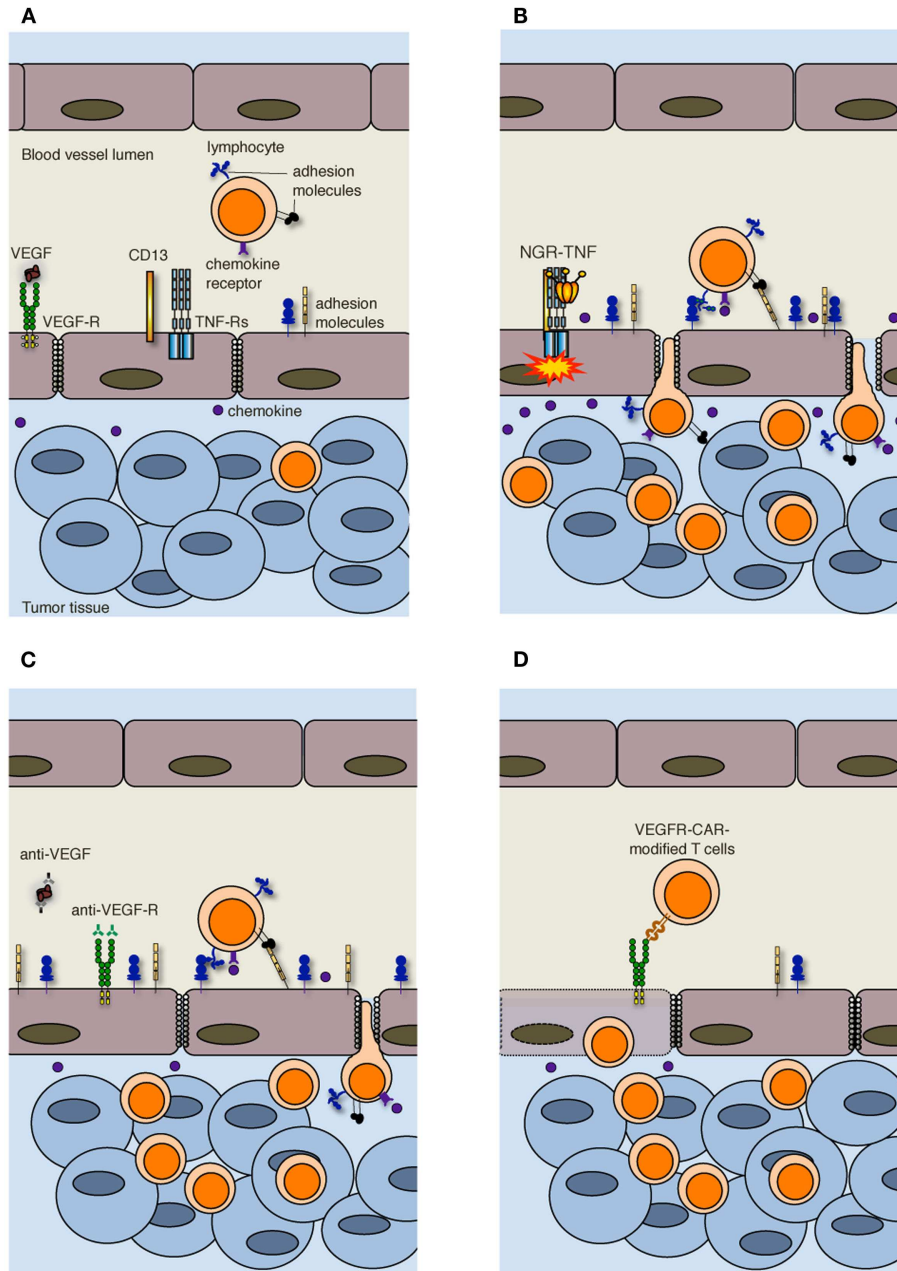


FIGURE 2 | Strategies to increase T cell infiltration into tumors. **(A)** Increased interstitial pressure, heterogeneous permeability and irregular blood flow, together with reduced expression of adhesion molecules on ECs, limit lymphocyte penetration in tumors. **(B)** NGR-TNF, which selectively binds CD13 expressed in ECs of neo-angiogenic vessels and favors the interaction of TNF with TNF receptors (TNF-Rs), alters tumor vessel permeability by loosening VE-cadherin dependent adherence junctions, induces up-regulation of adhesion molecules in ECs, and elicits the release of pro-inflammatory cytokines and chemokines, thereby

favoring the recruitment and extravasation of T lymphocytes. **(C)** Anti-VEGF and anti-VEGFR antibodies both transiently normalize the tumor-vasculature and overcome EC anergy, thus favoring T cell trafficking within tumors. **(D)** Also immunization against VEGF-R2 or the adoptive transfer of autologous T cells genetically engineered to express chimeric antigen receptor targeted against VEGF-R2 (VEGFR-CAR) favor tumor infiltration by T cells, although the mechanism has not yet been clarified. It has been proposed that VEGF-R-specific T cells kill both ECs and MDSCs and Tregs (not shown) that express VEGF-R.

A similar compound, consisting of TNF fused to another tumor-vasculature-homing peptide (RGR) has been recently shown to stabilize tumor vessels and to enhance active immunotherapy in experimental pancreatic neuroendocrine

tumors (52). Notably, a recent phase II study of NGR-TNF (0.8 µg/m²) in combination with doxorubicin in relapsed ovarian cancer patients showed that patients with baseline peripheral blood lymphocyte count higher than the first quartile had

improved progression-free survival and overall survival (53), therefore suggesting that a similar effect may occur in humans.

Other strategies have been pursued to target TNF to the tumor. As an example, TNF has been fused with the single chain Fv Ab L19, which is specific for the extradomain B of fibronectin expressed by the tumor neovasculature (54). However, the location of the target molecules in tumor vessels and their level of expression are different from that of CD13, and additional studies are necessary to investigate whether this compound acts in synergy with active or adoptive immunotherapy.

Leukocyte infiltration in tumors can also be favored by the use of classic anti-angiogenic drugs. VEGF is the focus of most of these approaches (55). The importance of VEGF-mediated mechanisms in cancer is underlined by clinical data showing that the expression of VEGF in tumor tissue is negatively correlated with the presence of TILs. This was reported to be one of the strongest prognostic factors in ovarian carcinoma (56). In addition, VEGF negatively regulates functional maturation of and antigen presentation by dendritic cells (DCs), favors the accrual and activity of cell populations with immunosuppressive functions including myeloid derived suppressor cells [MDSCs; (57)] and regulatory T cells [Tregs; (58)], and induces T cell apoptosis, therefore contributing to the immunosuppressive tumor microenvironment (59). Over the last decades several therapeutic approaches have been proposed to counteract VEGF and neoangiogenesis, such as anti-VEGF antibodies and tyrosine kinase inhibitors of multiple pro-angiogenic growth factor receptors (13). Inhibition of VEGF interaction with its receptors has been also reported to be at the basis of vessel “normalization” (29). Anti-angiogenic drugs transiently normalize the tumor-vasculature, pruning away immature and leaky vessels and remodeling the remaining vasculature. As a result, the enhanced oncotic pressure gradient together with decreased interstitial fluid pressure and hydrostatic pressure gradient facilitate delivery of oxygen, nutrients, and also chemotherapeutic agents into the tumor microenvironment (13). Some of these strategies can also overcome EC anergy and promote leukocyte infiltration in tumors [**Figure 2C**; (60–62)]. In addition, it has been reported that lower-dose of anti-VEGF (DC101; 10 mg/Kg), when compared with the standard high dose (40 mg/Kg), normalizes the tumor-vasculature, favors extravasation of T cells, reduces the fraction of MDSCs, and polarizes macrophages toward an M1 phenotype within the tumor mass (63). Thus, anti-angiogenic drugs and TNF targeting are conceptually different approaches, as the former aims at vessel normalization, whereas the latter exploits the cytokine as an inflammatory agent that induces vascular activation.

Alternative approaches to target the VEGF-VEGF receptor (VEGFR) pathway are immunization against VEGFR-2 (64) or the adoptive transfer of autologous T cells genetically engineered to express a chimeric antigen receptor targeted against VEGFR-2 [**Figure 2D**; (65)]. The simultaneous targeting of VEGFR-2 and TAAs by a mixture of genetically engineered T cells expressing a chimeric antigen receptor targeting VEGFR-2 and T cells expressing a TCR specific for a melanoma-associated TAA synergistically eradicated established melanoma tumors in mice and prolonged their tumor free survival (66). The mechanism behind this synergy is still under investigation, and the transduction of anti-VEGFR-2

CAR into TCR transgenic T cells did not enhance the therapeutic efficacy of adoptively transferred cells (66). Because of the extensive tumor necrosis induced by the adoptive transfer of T cells, vessels could not be investigated in these tumors (66). The authors favor the hypothesis that anti-VEGFR-2 T cells not only target ECs but also suppressor cell populations including MDSCs and Tregs that express VEGFR-2 (67, 68).

In general, anti-VEGF-mediated transient normalization of tumor vessels lasts between few days to a month (29). Unfortunately, the anti-angiogenic drugs available to date are not sufficiently selective in damaging only neo-angiogenic vessels. Risks of sustained and/or aggressive anti-angiogenic therapies are the unselected recruitment of pro-angiogenic inflammatory cells, and excessive trimming of vessels with inadequate delivery of oxygen and drugs. The latter effect may be dangerous also for highly vascularized tissues, including the cardiovascular, endocrine, and nervous systems (69).

As mentioned before, targeting TNF to the tumor vessels enhances tumor permeability to chemotherapeutic agents (48). We have recently reported that the combination of active or adoptive immunotherapy, vascular targeting, and chemotherapy act in synergy against melanoma (49). Our preliminary results also suggest that in the context of adoptive T cell therapy after hematopoietic stem cell transplantation (70, 71), NGR-TNF dramatically increases the infiltration of TILs into the prostate of mice affected by autochthonous prostate cancer (49) and contributes to tumor debulking (Mondino A. Personal communication).

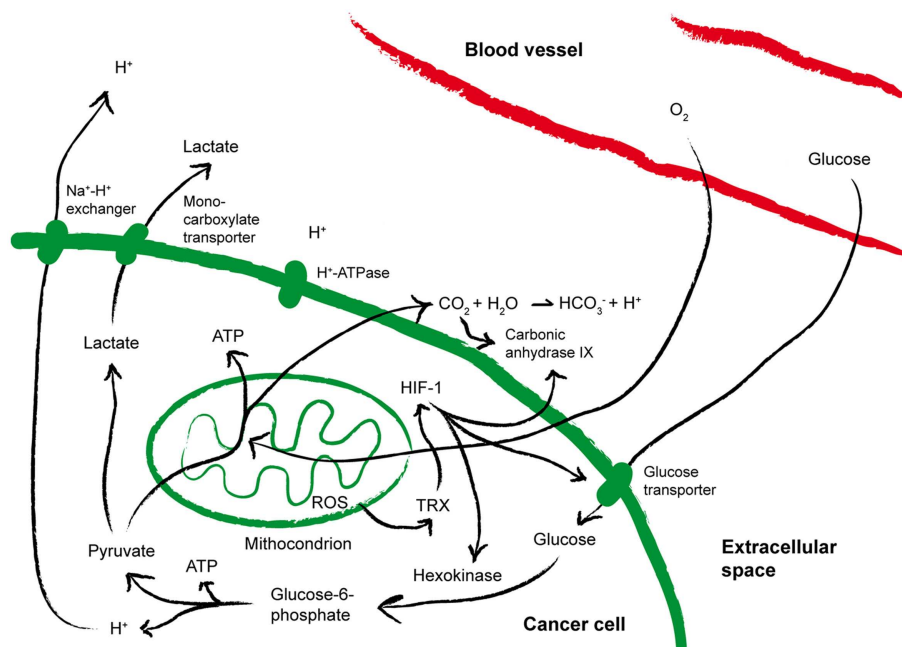
Interestingly, chemotherapeutic agents, beside their effects in promoting anti-tumor immunity by inducing a more immunogenic death of cancer cells, increasing their sensitivity to immune effectors or depleting the tumor microenvironment of Treg cells and MDSCs (72, 73) have been shown to promote intratumor expression of chemokines attracting T cells (74).

Taken together, these findings support the concept that increasing T-cell traffic to the tumor, possibly in association with immunogenic chemotherapy, may be a valid strategy to enhance response to immunotherapy in cancer patients.

REPROGRAMMING ENERGY METABOLISM IN CANCER

Reprogramming energy metabolism is an emerging hallmark of cancer closely linked to hypoxia and neoangiogenesis (25). Indeed, uncontrolled cell proliferation requires a continuous adjustment of energy metabolism in order to fuel cell growth and division also in the absence of adequate tumor perfusion (14). As early as in 1930, Otto Warburg showed that cancer cells craving for energy take up much more glucose than normal cells and mainly process it through aerobic glycolysis, the so-called “Warburg effect” (75). Curiously enough, also T cells that differentiate from the naïve to the effector state upregulate genes encoding glycolytic enzymes (76), but tumor cells incorporate 10- to 100-fold greater glucose than T cells over a fixed time period (77), thus suggesting a biased competition for glucose between cancer cells and activated T cells within the same microenvironment.

As summarized in **Figure 3**, a direct consequence of aerobic glycolysis is the production of lactate from pyruvate, and acidic metabolites that cause drop in extracellular pH (78), which may select for more aggressive acid-resistant clones and favor

**FIGURE 3 | Metabolic alterations within the tumor**

microenvironment. The cartoon summarizes the metabolic alterations often found within the tumor microenvironment that may impact on T cell

fitness. See the text for more details. ATP, Adenosine-5'-triphosphate; HIF-1, hypoxia inducible factor 1; ROS, reactive oxygen species; TRX, thioredoxin.

tumor invasion (14). Pyruvate decarboxylation within mitochondria causes the generation and subsequent release of CO_2 , which favors increased expression of carbonic anhydrase IX (CA-IX), a cancer-associated membrane bound isoform of the enzyme carbonic anhydrase that catalyzes the hydration of CO_2 to bicarbonate and H^+ , thus contributing to acidify the extracellular microenvironment of tumors (79, 80). A low extracellular pH triggers the activation on tumor cell membranes of transporters that protect the cytosol from acidosis. In addition, hypoxia stabilizes the heterodimer HIF-1, which in turn induces the up-regulation of glucose transporters and CA-IX, thereby increasing acidity within the tumor microenvironment (80). As a result, while in normal tissues the extracellular pH is maintained around 7.4, in malignant tumors the pH can drop to values of 6.0 and less, with averages of 0.2–0.6 units lower than in normal tissues (81). The tumor-supporting role of low pH has been recently corroborated by the observation that pharmacologic inhibition of CA-IX or of the vacuolar H^+ -ATPases display antineoplastic effects (79, 82).

Hypoxia and pH are also strongly tangled with reduction-oxidation (redox) reactions (Figure 3). Already at the earliest stages of tumor development, free radicals, HIF-1-induced gene expression and hypoxia are strictly interconnected (83). Indeed, reactive oxygen species (ROS) are generated in mitochondria of cells exposed to low oxygen (84), and the phenomenon is further amplified by cyclic reoxygenation. Also the anti-oxidant systems upregulated by tumor cells to counterbalance oxidative stress contribute to the altered redox of the tumor microenvironment and to tumor progression. Overexpression of reducing enzymes such as thioredoxin (TRX) has been found in many tumors and correlated

to poor prognosis (85, 86). TRX induces and stabilizes HIF-1 α (87), and co-localizes with both HIF-1 α and CA-IX in hypoxic areas of the tumors (79). In addition, proton pumps have been proposed to de-toxify tumor cells from microenvironmental ROS (88). Thus, hypoxia, acidosis, redox-remodeling can cooperate to establish a more aggressive malignant phenotype, and possibly to promote the derangement of immune functions (77).

ALTERATIONS OF THE TUMOR METABOLISM THAT IMPACT ON T CELL FITNESS

The immune system has been proposed as sensor of the metabolic state (89). Bidirectional communication and coordination between metabolism and immunity, while effective in maintaining and defending the internal environment from the environment around us, may result in inhibition of immune functions and may favor chronic inflammation and cancer. A well-known example of metabolism-mediated limitation of the function and survival of TILs is tryptophan consumption by tumor cells and antigen presenting cells (APCs) producing IDO (90). This mechanism can also restrain the therapeutic efficacy of checkpoint blockade strategies such as targeting of cytotoxic T lymphocyte antigen-4 (CTLA-4), glucocorticoid-induced TNFR family related gene (GITR), and the PD-1/PD-L1 axis (91).

More specifically, hypoxia, acidosis, and redox-remodeling are all perceived as sensors by the immune system. Thus, as summarized in Table 1, hypoxia inhibits TCR-triggered signaling, proliferation and cytokine production by T cells (92, 93). Intracellular HIF-1 α appears to have a direct role in T cell inhibition, since HIF-1 α is induced upon TCR triggering (94, 95), it is further

Table 1 | Effects of the tumor metabolism on TILs.

Metabolic alteration	Species	Inhibition	Promotion	Reference
Hypoxia	<i>Mus musculus</i>	Expansion of CD8 ⁺ T cells IL2 and IFN γ production by CD8 ⁺ and CD4 ⁺ T cells	Development of more lytic CTLs VEGF production Expression of TCR and LFA-1 on CD8 ⁺ T cells	Caldwell et al. (92)
	Human	Voltage-dependent K ⁺ channels		Conforti et al. (93)
	<i>Mus musculus</i>		HIF-1 α expression	Lukashev et al. (94)
	<i>Mus musculus</i>		Accumulation of extracellular adenosine	Sitkovsky et al. (96)
	Human and <i>Mus musculus</i>		Treg recruitment	Facciabene et al. (97)
	<i>Mus musculus</i>	Treg differentiation	Th17 differentiation	Dang et al. (98)
	Human		Th17 survival	Kryczek et al. (100)
	<i>Mus musculus</i>	T cell-mediated cytotoxicity		MacDonald (105)
	Human and <i>Mus musculus</i>		Lymphocyte apoptosis	Lugini et al. (108), Calcinotto et al. (113)
	<i>Mus musculus</i>	CTL response <i>in vivo</i>	CTL activation <i>in vitro</i>	Droge et al. (109)
Low intratumor pH	<i>Mus musculus</i>	IL2-mediated T cell proliferation		Ratner (110)
	<i>Mus musculus</i>	CTL-mediated cytotoxicity		Redegeld et al. (111)
	Human	Proliferation and effector function of T cells		Fischer et al. (112)
	Human and <i>Mus musculus</i>	CTL proliferation, cytolytic activity and IL2, TNF α and IFN γ production		Calcinotto et al. (49)
	Human and <i>Mus musculus</i>		Down-modulation of TCR CD3 ζ chain	Rodriguez et al. (122), Rodriguez et al. (123)
	<i>Mus musculus</i>	Activation of JAK, STAT, ERK and AKT		Bingisser et al. (125), Mazzoni et al. (126)
	<i>Mus musculus</i>	Conformational flexibility of TCR and CD8 molecules		Nagaraj et al. (134)
Oxidative stress	Human and <i>Mus musculus</i>	Intratumor infiltration of T cells		Molon et al. (135)
	Human		Release of cysteine and TRX by DCs	Angelini et al. (137)

increased in hypoxic conditions, and knocking down HIF-1 α in T cells increases their cytokine production potential both *in vitro* and *in vivo* (94). T cells are also inhibited by hypoxia-driven accumulation of extracellular adenosine (96).

More recently it has been reported that hypoxia within the tumor microenvironment promotes Treg recruitment through the induction of CC-chemokine ligand 28 (97). Conversely, up-regulation of HIF-1 α under hypoxic conditions inhibits Treg differentiation through FoxP3 degradation, and favors the differentiation of Th17 cells by directly inducing RAR-related orphan receptor gamma t (ROR γ t) transcription (98) and glycolytic genes (99). HIF-1 α also induces several survival promoting genes in Th17 cells, thus preventing their apoptosis (100). Th17 cells are a subpopulation of T helper cells producing IL17, IL17F, and IL22, which play a critical role in immunity to certain pathogens and autoimmune inflammation (101). The role of Th17 cells in cancer is more debated. Indeed, Th17 exert anti-tumorigenic activities, likely by facilitating the recruitment of other effector immune cells (102), and pro-tumorigenic activities by inducing tumor

vascularization and the release of tumor-promoting factors by tumor and stromal cells (103). Thus, the effects of hypoxia on the tumor microenvironment are rather complex, and the use of HIF inhibitors for therapeutic purposes should be carefully balanced to avoid the dominance of pro-tumorigenic over anti-tumorigenic mechanisms.

Hypoxia may also render the tumor cells more resistant to cytotoxic T lymphocyte (CTL)-mediated lysis through HIF-1 α -dependent induction in cancer cells of miR-210, which downregulates the expression of *PTPN1*, *HOXA1*, and *TP53I11* genes (104). It remains to be defined how coordinated silencing of these three genes affects cancer cell susceptibility to CTL lysis. The effect of hypoxia on CTLs is still debated (77). Interestingly, simultaneous glucose deprivation and hypoxia block T cell-mediated cytotoxicity *in vitro* (105), therefore suggesting an additional mechanism of immunosuppression within the tumor microenvironment.

There are relatively few reports on the impact of low intratumor pH on T cells (106). Clinical evidence suggests that metabolic acidosis is often associated with immunodeficiency (107). Indeed,

both leukocyte activation and the bactericidal capacity of leukocytes are generally impaired at reduced pH (106) suggesting that T cells could be extremely sensitive to pH variations. Lymphocytes also die at the same acidic pH malignant tumor cells perfectly remain alive (108). Droege et al. (109) studied the effect of lactate on murine T-cell populations and found that lactate is able to suppress the CTL response *in vivo*, whereas activation of CTLs *in vitro* is increased. Few years later, it was reported that the proliferation of IL-2-stimulated T cells is inhibited at pH 6.7 (110), and the cytolytic activity against cancer cells of CTLs is markedly reduced when T cells are exposed to acidic pH (111). More recently, Fischer and colleagues demonstrated that high lactic acid concentrations, as the ones found in the tumor environment, block lactic acid export in human T cells, thereby disturbing proliferation and effector functions (112).

We have found that lowering the pH *in vitro* to values most frequently detected within tumors (pH 6–6.5) induces hyporesponsiveness in both human and mouse tumor-specific CTLs, which is characterized by impaired proliferation, cytolytic activity, and cytokine secretion (113). Interestingly, buffering of culture pH to physiologic values associates with the complete recovery of T cell functions, although longer exposure or lower pH values causes permanent damage and T cell death (113), arguing that a portion of T cell immunity might be lost at tumor site when extreme metabolic alterations are present. From a molecular standpoint, TCR triggering at low pH associates with reduced expression of IL-2R α (CD25) and TCR, and diminished activation of signal transducer and activator of transcription 5 (STAT5) and extracellular signal-regulated kinase (ERK) (113), signaling alterations frequently found in anergic T cells (114, 115). Interestingly, similar characteristics were found in tumor-specific CTLs infiltrating melanoma lesions, whose pH was 6.5 (113). Thus, acidity *per se* is a novel tumor cell extrinsic mechanism of immune escape (116).

Whereas redox-activated signaling events are physiologically needed both as antimicrobial defense and to guarantee the correct spatial and temporal extension of the immune reaction, redox-remodeling within the tumor microenvironment negatively affects immune surveillance. Indeed, oxygen ions and peroxides are potent antibacterial agents produced by phagocytic cells including macrophages and neutrophils (117). ROS are also implicated in NLRP3 inflammasome activation in myeloid cells (118). It has also been increasingly appreciated that endogenous ROS are required for optimal T cell activation (119). Yet, exogenous oxidative stress may dramatically suppress T cell activation and effector functions. As an example, macrophages within the tumor microenvironment express inducible nitric oxide synthase (iNOS) and can induce tumor killing by generating large amounts of nitric oxide (NO). However, iNOS is also expressed by MDSCs, a heterogeneous population of cells of myeloid origin that include immature macrophages, granulocytes, DCs and other myeloid cells (57). MDSCs also express arginase 1 (Arg1) that together with iNOS metabolizes the essential aminoacid arginine to either L-ornithine and urea, or to L-citrulline and NO (120, 121). Depletion of arginine from the microenvironment induces T cell dysfunction because of loss of CD3 ζ chain expression (122, 123), and prevents the up-regulation of cell cycle regulators by these cells (124), thus

blocking their proliferation. In addition, NO blocks the activation of Janus-activated kinase 1 (JAK1), JAK3, STAT5, ERK, and AKT (125, 126), thus suppressing several T cell functions (125–129).

Depletion of L-arginine may also trigger superoxide (O_2^-) generation from iNOS (130, 131), which is eventually converted to hydrogen peroxide. ROS contribute to the MDSC-mediated suppression of tumor-specific T cell responses in tumor-bearing mice (57, 132).

Finally, the reaction between NO and O_2^- generates reactive nitrogen-oxide species (RNOS), among which peroxynitrite ($ONOO^-$) (133). $ONOO^-$ mediated nitration of tyrosine residues in the TCR and CD8 co-receptor causes a decreased conformational flexibility of these molecules and failure in proper T cell activation (134). Nitration of chemokines also prevents intratumoral infiltration of antigen-specific T cells (135).

Also Tregs modulate the redox of the microenvironment by subtracting cysteine necessary to effector T cell function (136). Indeed, DCs within the tumor microenvironment may have additional nutritional and redox-remodeling roles, since they reduce the extracellular microenvironment required for T cell activation by releasing cysteine and TRX (137). In the same vein, Tregs diminish glutathione synthesis in DCs and consume extracellular cysteine (138), thus remodeling extracellular redox.

Additional hypoxia-driven metabolic dysfunctions, leading to the accumulation of extracellular adenosine, further increased by Tregs (139, 140), could act in synergy with acidic pH in dampening T cell function through A2A adenosine receptor-driven cAMP intracellular accumulation (96).

All together these findings sustain the concept that hypoxia, nutrient deprivation, abnormal glycolysis, and low pH act in synergy crippling immune surveillance (Figure 1).

Also alterations of the lipid metabolism that occur in the tumor microenvironment might affect T cell functions [e.g., (141)], but direct *in vivo* evidences of this phenomenon are poor.

STRATEGIES THAT IMPACT ON TUMOR METABOLISM AND PROMOTE FITNESS OF TUMOR INFILTRATING LYMPHOCYTES

Different therapeutic approaches have been proposed to modulate hypoxia, tumor acidity or redox, which directly or indirectly affect TIL viability and effector functions (Figure 1). Being the tumor microenvironment so complex and redundant, the risk remains that interfering with one metabolic pathway, thus inhibiting one pro-tumoral mechanism, may favor another. For the sake of brevity, we will touch upon some clarifying examples.

It has been reported that the anti-VEGF monoclonal antibody bevacizumab induces intratumoral hypoxia, likely through excessive vessel remodeling (142), thus increasing the population of cancer stem cells (CSCs) in human breast cancer xenografts (143), and promoting epithelial to mesenchymal transition (EMT) in a murine model of bevacizumab-resistant pancreatic cancer (144). Angiogenesis inhibitors targeting the VEGF pathway may also elicit tumor adaptation and progression to stages of greater malignancy, with heightened invasiveness and in some cases increased lymphatic and distant metastasis (145). Bevacizumab has also been shown to induce malignant traits through induction of paracrine factors, which recruited pro-angiogenic myeloid cells

(146), whose phenotype is reminiscent of MDSCs. Thus, anti-angiogenic compounds while cutting nutritional support to tumor cells, may favor local hypoxia and MDSC accumulation.

Also sunitinib, a receptor tyrosine kinase inhibitor with anti-angiogenic properties (147), which has been recently approved for the treatment of metastatic renal cell carcinoma (148), induces hypoxia, through a yet undefined mechanism, and increase in CSCs (143). Interestingly, semaphoring 3A (Sema3A), an endogenous anti-angiogenic agent, counteracts sunitinib-induced tumor hypoxia, and Sema3A and sunitinib synergize to enhance survival of tumor-bearing mice (149). In addition, one cycle of treatment with sunitinib is sufficient to increase the proportion of type 1 T cells (150), likely by reducing MDSCs (151). These findings have been confirmed in mouse models of cancer, in which sunitinib reduced viability and proliferation of MDSCs (152) and their accumulation in tumors (153).

Several drugs have been identified that target HIF-1 α , thus inhibiting angiogenesis (154). However, HIF-1 inhibitors may impact on balance between Treg and Th17 cells favoring the former (99, 155). Thus, further investigation is needed to fully elucidate the therapeutic potential of HIF-1 inhibitors in cancer patients.

Conversely, hypoxia can be skillfully utilized to selectively target TILs. Indeed, hypoxia induces expression of CD137 (4-1BB) on TILs, and low-dose intratumoral injections of agonist anti-CD137 monoclonal antibodies avoid systemic toxicity while achieving anti-tumor systemic effects (156). In addition, intratumoral anti-CD137 antibodies synergized with systemic blockade of PD-L1 (156).

Several strategies have been proposed to neutralize intratumor acidity and therefore affect TILs. Robey et al. (157) reported that oral treatment with NaHCO₃ increased the extracellular pH of spontaneous metastases, inhibited cancer cell extravasation and colonization in mouse models of breast and prostate cancer. However, no information is available on the effects of systemic administration of bicarbonate on T cells and there is some concern related to the risk of metabolic alkalosis.

We obtained evidence that systemic administration of the PPI esomeprazole (12.5 mg/Kg) to tumor-bearing mice caused a rapid (within 60 min) increase in tumor pH, which associated with enhanced IFN γ production by TILs (113). Indeed, on a per cell basis, TILs in the tumor of PPI-treated mice produced more IFN γ than TILs from mice treated with vehicle (113). PPI treatment also increased phosphorylated ERK in TILs, thus giving molecular support to the PPI-mediated effect. As expected for a drug that is administered as a pro-drug and requires protonation at low pH (158), IFN γ production by T cells isolated from the spleen, lung, and kidney of mice treated either with PPIs or vehicle did not differ (113), thus suggesting that also the effects of PPIs on T cells are restricted to area of acidosis. PPIs also affected adoptively transferred T cells that reached the tumor, and PPI treatment increased the therapeutic potential of both active and adoptive immunotherapies (113). Because of the high selectivity for an acidic milieu and instability, PPIs can be safely used at high doses (158) as the one tested by us (113), which also affect tumor cells *in vivo* (159). Thus, PPI treatment may represent a promising strategy for recovering specific immunity and improving the efficacy of T cell-based cancer treatments.

PPIs are also known for their anti-oxidant and anti-inflammatory activities (160). Vacuolar proton pumps are expressed in the membrane of phagolysosomes of neutrophils, and lysosomal acidification is relevant for neutrophil oxidative burst. Thus, PPIs reduce release of ROS by neutrophils further impacting on the tumor microenvironment. While the mechanism of action of PPIs on leukocytes is still under investigation (160), our data suggest that *in vivo* PPIs enhance anti-tumor activities of TILs (113, 116).

Cancer cells promote chronic autophagy as survival adaptation to the acidic microenvironment (161). Because at least *in vitro* autophagy can also be induced in tumor cells by PPIs (162), strategies might be devised to inhibit autophagy during PPI treatment, yet taking into account the potentially negative effects of autophagy inhibitors on TILs (163).

Regarding redox, it has been reported that the anti-diabetic drug metformin or the mTOR inhibitor rapamycin, restore catabolic mitochondrial fatty acid oxidation and favor the induction of memory T cells, thus increasing the therapeutic efficacy of cancer vaccines (141, 164, 165).

Several pre-clinical studies also support the use of A2A adenosine receptors (A2ARs) antagonists to increase T cell activity within the tumor microenvironment (166). As an example, the compounds ZM241385 or 1,3,7-trimethylxanthine (caffeine) showed to increase the anti-tumor activity of adoptively transferred T cells in mice bearing large tumors (167). Curiously, drinking coffee was found to correlate with significant decreased risk of cutaneous malignant melanoma only in women (167, 168), suggesting that caffeine may also impact on cancer immune surveillance.

Finally, therapeutic strategies targeting either Tregs (169, 170) or MDSCs (171, 172); (173, 174), collaborate in making the tumor microenvironment more permissive for TIL survival and anti-tumor activities. Interestingly, MDSCs impair T cell trafficking through down-regulation of CD62L on CD4 and CD8 T cells (175) and chemokine nitration (135). Thus, therapeutic strategies that block MDSCs accrual at the tumor site and their immuno-suppressive function, and more specifically drugs interfering with chemokine nitration, are expected to significantly improve the efficacy of both active and adoptive immunotherapies.

CONCLUSION AND PERSPECTIVES

Despite considerable progress over the last decade, the tumor microenvironment is an area of research that remains ripe for further investigation, especially with regard to the relentless and dynamic modifications in its cellular composition and metabolism.

Accumulating experimental evidence lends weight to the concept that the most effective therapeutic strategies against cancer will be the ones that consider the tumor and its microenvironment as a whole, and yet simultaneously and coordinately address several individual aspects of this complex system. So far, either chemotherapy, surgery or radiotherapy have been combined with either one of active immunotherapy and/or adoptive T cell therapy, checkpoint blockade strategies or drugs that modify the vascularization and metabolism of the tumor (38, 50, 116, 176–178), thus improving distribution and synergistic anti-cancer activity of drugs and T cells. A step forward will be to carefully devise

multiple targeted therapies that simultaneously or subsequently attack tumor cells and the diverse aspects of the tumor microenvironment, and yet preserve the function of organs not involved by the neoplasm. Thus, it can be anticipated that adoptive and active immunotherapy given together with treatments that transiently normalize and/or activate tumor-associated ECs and drugs that impact on tumor metabolism and reduce the local immunosuppressive environment would greatly benefit cancer patients without causing relevant systemic toxic effects. As an example, in TRAMP mice affected by advanced prostate cancer, the combination of non-myeloablative total body irradiation, hematopoietic stem cell transplantation, infusion of donor mature lymphocytes, and tumor-specific vaccination overcomes tumor-specific T cell tolerance, prompts tumor debulking, and induces long-lasting tumor-specific memory response that protects mice from tumor recurrence (70). Interestingly, the addition of NGR-TNF at the peak of the vaccination-induced immune response favors penetration of activated T cells within the transformed prostate epithelium (49) and guarantees an even stronger anti-tumor activity (Mondino A. Personal communication). We are investigating the possibility to add PPIs to this already complex combined therapy to favor the anti-tumor activity of adoptively transferred and vaccine-induced T cells that have reached the prostate.

Given the outstanding results obtained with immune checkpoint blockers in cancer patients (179), it will be particularly interesting to investigate the therapeutic efficacy of their combination with metabolism and vessel modulators.

It is also important to underline that more is not always better (180). One example is the recent failure of a well-designed and carefully analyzed multi-institutional clinical trial in which

732 patients with previously untreated metastatic colorectal cancer were randomly assigned to receive the combination of capecitabine, oxaliplatin, and bevacizumab (i.e., a monoclonal antibody against VEGF) or the same three drugs with cetuximab (i.e., a monoclonal antibody directed against the epidermal growth factor receptor; EGFR) (181). The four-drug combination resulted in significantly shorter progression-free survival and inferior quality of life. A similarly negative effect was obtained when another anti-EGFR monoclonal antibody (i.e., panitumumab) was added to the combination of folinic acid, fluorouracil, oxaliplatin, and bevacizumab in previously untreated metastatic colorectal cancer patients (182).

Thus, additional investigation is needed to define the best settings for each combination approach. In this perspective, reliable animal models of human diseases remain instrumental.

ACKNOWLEDGMENTS

We thank Catia Traversari (MolMed, Milan, Italy), and Angelo Corti and Vincenzo Russo (San Raffaele Scientific Institute, Milan, Italy) for comments on the manuscript. Funding: This work was supported by grants from the Associazione Italiana per la Ricerca sul Cancro (AIRC; AIRC 5 × 1000) and the Ministero della Salute. Author contributions: Matteo Bellone and Arianna Calcinotto were both responsible for all aspects of the manuscript – from conception to approval of the final manuscript. We apologize to any investigators whose work has not been underlined in this review due to oversight or space limitations. Arianna Calcinotto conducted this study as partial fulfillment of her PhD in Molecular Medicine, Program in Molecular Oncology, Università Vita-Salute San Raffaele, Milan, Italy.

REFERENCES

- Dunn GP, Old LJ, Schreiber RD. The three Es of cancer immunoediting. *Annu Rev Immunol* (2004) **22**:329–60. doi:10.1146/annurev.immunol.22.012703.104803
- Gajewski TF, Fuertes M, Spaapen R, Zheng Y, Kline J. Molecular profiling to identify relevant immune resistance mechanisms in the tumor microenvironment. *Curr Opin Immunol* (2011) **23**:286–92. doi:10.1016/j.coim.2010.11.013
- Ogino S, Galon J, Fuchs CS, Dranoff G. Cancer immunology – analysis of host and tumor factors for personalized medicine. *Nat Rev Clin Oncol* (2011) **8**:711–9. doi:10.1038/nrclinonc.2011.122
- Benjamin DI, Cravatt BF, Nomura DK. Global profiling strategies for mapping dysregulated metabolic pathways in cancer. *Cell Metab* (2012) **16**:565–77. doi:10.1016/j.cmet.2012.09.013
- Charoentong P, Angelova M, Efremova M, Gallasch R, Hackl H, Galon J, et al. Bioinformatics for cancer immunology and immunotherapy. *Cancer Immunol Immunother* (2012) **61**:1885–903. doi:10.1007/s00262-012-1354-x
- Galon J, Pages F, Marincola FM, Thurin M, Trinchieri G, Fox BA, et al. The immune score as a new possible approach for the classification of cancer. *J Transl Med* (2012) **10**:1. doi:10.1186/1479-5876-10-1
- Klinke DJ II. An evolutionary perspective on anti-tumor immunity. *Front Oncol* (2012) **2**:202. doi:10.3389/fonc.2012.00202
- Vogelstein B, Papadopoulos N, Velculescu VE, Zhou S, Diaz LA Jr, Kinzler KW. Cancer genome landscapes. *Science* (2013) **339**:1546–58. doi:10.1126/science.1235122
- Robbins PF, Lu YC, El-Gamil M, Li YF, Gross C, Gartner J, et al. Mining exomic sequencing data to identify mutated antigens recognized by adoptively transferred tumor-reactive T cells. *Nat Med* (2013) **19**:747–52. doi:10.1038/nm.3161
- Kantoff PW, Higano CS, Shore ND, Berger ER, Small EJ, Penson DF, et al. Sipuleucel-T immunotherapy for castration-resistant prostate cancer. *N Engl J Med* (2010) **363**:411–22. doi:10.1056/NEJMoa1001294
- Restifo NP, Dudley ME, Rosenberg SA. Adoptive immunotherapy for cancer: harnessing the T cell response. *Nat Rev Immunol* (2012) **12**:269–81. doi:10.1038/nri3191
- Scholler J, Brady TL, Binder-Scholl G, Hwang WT, Plesa G, Hege KM, et al. Decade-long safety and function of retroviral-modified chimeric antigen receptor T cells. *Sci Transl Med* (2012) **4**:132ra153. doi:10.1126/scitranslmed.3003761
- Chung AS, Lee J, Ferrara N. Targeting the tumour vasculature: insights from physiological angiogenesis. *Nat Rev Cancer* (2010) **10**:505–14. doi:10.1038/nrc2868
- Cairns RA, Harris IS, Mak TW. Regulation of cancer cell metabolism. *Nat Rev Cancer* (2011) **11**:85–95. doi:10.1038/nrc2981
- Mellor AL, Munn DH. Creating immune privilege: active local suppression that benefits friends, but protects foes. *Nat Rev Immunol* (2008) **8**:74–80. doi:10.1038/nri2233
- von Andrian UH, Mackay CR. T-cell function and migration. Two sides of the same coin. *N Engl J Med* (2000) **343**:1020–34.
- Ley K, Kansas GS. Selectins in T-cell recruitment to non-lymphoid tissues and sites of inflammation. *Nat Rev Immunol* (2004) **4**:325–35. doi:10.1038/nri1351
- Luster AD, Tager AM. T-cell trafficking in asthma: lipid mediators grease the way. *Nat Rev Immunol* (2004) **4**:711–24. doi:10.1038/nri1438
- Alon R, Dustin ML. Force as a facilitator of integrin conformational changes during leukocyte arrest on blood vessels and antigen-presenting cells. *Immunity* (2007) **26**:17–27. doi:10.1016/j.immuni.2007.01.002
- Masopust D, Schenkel JM. The integration of T cell migration, differentiation and function. *Nat Rev Immunol* (2013) **13**:309–20. doi:10.1038/nri3442

21. Lasky LA, Singer MS, Dowbenko D, Imai Y, Henzel WJ, Grimley C, et al. An endothelial ligand for L-selectin is a novel mucin-like molecule. *Cell* (1992) **69**:927–38. doi:10.1016/0092-8674(92)90612-G
22. Bevilacqua MP. Endothelial-leukocyte adhesion molecules. *Annu Rev Immunol* (1993) **11**:767–804. doi:10.1146/annurev.ij.11.040193.004003
23. Pober JS, Kluger MS, Schechner JS. Human endothelial cell presentation of antigen and the homing of memory/effector T cells to skin. *Ann NY Acad Sci* (2001) **941**:12–25. doi:10.1111/j.1749-6632.2001.tb03706.x
24. Medzhitov R. Origin and physiological roles of inflammation. *Nature* (2008) **454**:428–35. doi:10.1038/nature07201
25. Hanahan D, Weinberg RA. Hallmarks of cancer: the next generation. *Cell* (2011) **144**:646–74. doi:10.1016/j.cell.2011.02.013
26. Pages F, Galon J, Dieu-Nosjean MC, Tartour E, Sautes-Fridman C, Fridman WH. Immune infiltration in human tumors: a prognostic factor that should not be ignored. *Oncogene* (2010) **29**:1093–102. doi:10.1038/onc.2009.416
27. Huang H, Bhat A, Woodnutt G, Lappe R. Targeting the ANGPTLIE2 pathway in malignancy. *Nat Rev Cancer* (2010) **10**:575–85. doi:10.1038/nrc2894
28. Dayan F, Mazure NM, Brahimi-Horn MC, Pouyssegur J. A dialogue between the hypoxia-inducible factor and the tumor microenvironment. *Cancer Microenviron* (2008) **1**:53–68. doi:10.1007/s12307-008-0006-3
29. Jain RK. Normalization of tumor vasculature: an emerging concept in antiangiogenic therapy. *Science* (2005) **307**:58–62. doi:10.1126/science.1104819
30. Hendrix MJ, Seftor EA, Hess AR, Seftor RE. Vasculogenic mimicry and tumour-cell plasticity: lessons from melanoma. *Nat Rev Cancer* (2003) **3**:411–21. doi:10.1038/nrc1092
31. Piali L, Fichtel A, Terpe HJ, Imhof BA, Gisler RH. Endothelial vascular cell adhesion molecule 1 expression is suppressed by melanoma and carcinoma. *J Exp Med* (1995) **181**:811–6. doi:10.1084/jem.181.2.811
32. Griffioen AW, Damen CA, Martinotti S, Blijham GH, Groenewegen G. Endothelial intercellular adhesion molecule-1 expression is suppressed in human malignancies: the role of angiogenic factors. *Cancer Res* (1996) **56**:1111–7.
33. Hellwig SM, Damen CA, Van Adrichem NP, Blijham GH, Groenewegen G, Griffioen AW. Endothelial CD34 is suppressed in human malignancies: role of angiogenic factors. *Cancer Lett* (1997) **120**:203–11. doi:10.1016/S0304-3835(97)00310-8
34. Rosenberg SA, Restifo NP, Yang JC, Morgan RA, Dudley ME. Adoptive cell transfer: a clinical path to effective cancer immunotherapy. *Nat Rev Cancer* (2008) **8**:299–308. doi:10.1038/nrc2355
35. Dougan M, Dranoff G. Immune therapy for cancer. *Annu Rev Immunol* (2009) **27**:83–117. doi:10.1146/annurev.immunol.021908.132544
36. Fridman WH, Galon J, Pages F, Tarbour E, Sautes-Fridman C, Kroemer G. Prognostic and predictive impact of intra- and peritumoral immune infiltrates. *Cancer Res* (2011) **71**:5601–5. doi:10.1158/0008-5472.CAN-11-1316
37. Galon J, Costes A, Sanchez-Cabo F, Kirilovsky A, Mlecnik B, Lagorce-Pages C, et al. Type, density, and location of immune cells within human colorectal tumors predict clinical outcome. *Science* (2006) **313**:1960–4. doi:10.1126/science.1129139
38. Bellone M, Mondino A, Corti A. Vascular targeting, chemotherapy and active immunotherapy: teaming up to attack cancer. *Trends Immunol* (2008) **29**:235–41. doi:10.1016/j.it.2008.02.003
39. Bemelmans MH, Van Tits LJ, Buurman WA. Tumor necrosis factor: function, release and clearance. *Crit Rev Immunol* (1996) **16**:1–11. doi:10.1615/CritRevImmunol.v16.i1.10
40. Manda T, Shimomura K, Mukamoto S, Kobayashi K, Mizota T, Hirai O, et al. Recombinant human tumor necrosis factor-alpha: evidence of an indirect mode of anti-tumor activity. *Cancer Res* (1987) **47**:3707–11.
41. McIntosh JK, Mule JJ, Travis WD, Rosenberg SA. Studies of effects of recombinant human tumor necrosis factor on autochthonous tumor and transplanted normal tissue in mice. *Cancer Res* (1990) **50**:2463–9.
42. ten Hagen TLM, Seynhaeve ALB, Eggertmann AMM. Tumor necrosis factor-mediated interactions between inflammatory response and tumor vascular bed. *Immunol Rev* (2008) **222**:299–315. doi:10.1111/j.1600-065X.2008.00619.x
43. Pasqualini R, Koivunen E, Kain R, Lahdenranta J, Sakamoto M, Stryhn A, et al. Aminopeptidase N is a receptor for tumor-homing peptides and a target for inhibiting angiogenesis. *Cancer Res* (2000) **60**:722–7.
44. Curnis F, Arrigoni G, Sacchi A, Fischetti L, Arap W, Pasqualini R, et al. Differential binding of drugs containing the NGR motif to CD13 isoforms in tumor vessels, epithelia, and myeloid cells. *Cancer Res* (2002) **62**:867–74.
45. Curnis F, Sacchi A, Borgna L, Magni F, Gasparri A, Corti A. Enhancement of tumor necrosis factor alpha antitumor immunotherapeutic properties by targeted delivery to aminopeptidase N (CD13). *Nat Biotechnol* (2000) **18**:1185–90. doi:10.1038/81183
46. Curnis F, Sacchi A, Corti A. Improving chemotherapeutic drug penetration in tumors by vascular targeting and barrier alteration. *J Clin Invest* (2002) **110**:475–82. doi:10.1172/JCI200215223
47. Bertilaccio MT, Grioni M, Sutherland BW, Degl'Innocenti E, Freschi M, Jachetti E, et al. Vascular-targeted tumor necrosis factor-alpha increases the therapeutic index of doxorubicin against prostate cancer. *Prostate* (2008) **68**:1105–15. doi:10.1002/pros.20775
48. Marcucci F, Bellone M, Rumio C, Corti A. Approaches to improve tumor accumulation and interactions between monoclonal antibodies and immune cells. *Mabs* (2013) **5**:34–46. doi:10.4161/mabs.22775
49. Calcinotto A, Grioni M, Jachetti E, Curnis F, Mondino A, Parmiani G, et al. Targeting TNF-alpha to neoangiogenic vessels enhances lymphocyte infiltration in tumors and increases the therapeutic potential of immunotherapy. *J Immunol* (2012) **188**:2687–94. doi:10.4049/jimmunol.1101877
50. Bellone M, Calcinotto A, Corti A. Won't you come on in? How to favor lymphocyte infiltration in tumors. *Oncobiology* (2012) **1**:986–8. doi:10.4161/onci.20213
51. Dondossola E, Gasparri AM, Colombo B, Sacchi A, Curnis F, Corti A. Chromogranin A restricts drug penetration and limits the ability of NGR-TNF to enhance chemotherapeutic efficacy. *Cancer Res* (2011) **71**:5881–90. doi:10.1158/0008-5472.CAN-11-1273
52. van Laarhoven HW, Gambarota G, Heerschap A, Lok J, Verhagen I, Corti A, et al. Effects of the tumor vasculature targeting agent NGR-TNF on the tumor microenvironment in murine lymphomas. *Invest New Drugs* (2006) **24**:27–36. doi:10.1007/s10637-005-4540-2
53. Lorusso D, Scambia G, Amadio G, Di Legge A, Pietragalla A, De Vincenzo R, et al. Phase II study of NGR-hTNF in combination with doxorubicin in relapsed ovarian cancer patients. *Br J Cancer* (2012) **107**:37–42. doi:10.1038/bjc.2012.233
54. Borsig L, Balza E, Carnemolla B, Sassi F, Castellani P, Berndt A, et al. Selective targeted delivery of TNFalpha to tumor blood vessels. *Blood* (2003) **102**:4384–92. doi:10.1182/blood-2003-04-1039
55. Ferrara N, Hillan KJ, Gerber HP, Novotny W. Discovery and development of bevacizumab, an anti-VEGF antibody for treating cancer. *Nat Rev Drug Discov* (2004) **3**:391–400. doi:10.1038/nrd1381
56. Zhang L, Conejo-Garcia JR, Kartasios D, Gimotty PA, Massobrio M, Regnani G, et al. Intratumor T cells, recurrence, and survival in epithelial ovarian cancer. *N Engl J Med* (2003) **348**:203–13. doi:10.1056/NEJMoa020177
57. Gabrilovich DI, Ostrand-Rosenberg S, Bronte V. Coordinated regulation of myeloid cells by tumours. *Nat Rev Immunol* (2012) **12**:253–68. doi:10.1038/nri3175
58. Zou W. Regulatory T cells, tumour immunity and immunotherapy. *Nat Rev Immunol* (2006) **6**:295–307. doi:10.1038/nri1806
59. Rabinovich GA, Gabrilovich D, Sotomayor EM. Immunosuppressive strategies that are mediated by tumor cells. *Annu Rev Immunol* (2007) **25**:267–96. doi:10.1146/annurev.immunol.25.022106.141609
60. Dirkx AEM, Oude Egbrink MGA, Castermans K, Van Der Schaft DWJ, Thijssen VLJL, Dings RPM, et al. Anti-angiogenesis therapy can overcome endothelial cell anergy and promote leukocyte-endothelium interactions and infiltration in tumors. *FASEB J* (2006) **20**:621–30. doi:10.1096/fj.05-4493com
61. Li B, Lalani AS, Harding TC, Luan B, Koprivnikar K, Huan Tu G, et al. Vascular endothelial growth factor blockade reduces intratumoral

- regulatory T cells and enhances the efficacy of a GM-CSF-secreting cancer immunotherapy. *Clin Cancer Res* (2006) **12**:6808–16. doi:10.1158/1078-0432.CCR-06-1558
62. Shrimali RK, Yu Z, Theoret MR, Chinnasamy D, Restifo NP, Rosenberg SA. Antiangiogenic agents can increase lymphocyte infiltration into tumor and enhance the effectiveness of adoptive immunotherapy of cancer. *Cancer Res* (2010) **70**:6171–80. doi:10.1158/0008-5472.CAN-10-0153
63. Huang Y, Yuan J, Righi E, Kamoun WS, Ancukiewicz M, Nezivar J, et al. Vascular normalizing doses of antiangiogenic treatment reprogram the immunosuppressive tumor microenvironment and enhance immunotherapy. *Proc Natl Acad Sci U S A* (2012) **109**:17561–6. doi:10.1073/pnas.1215397109
64. Wei YQ, Wang QR, Zhao X, Yang L, Tian L, Lu Y, et al. Immunotherapy of tumors with xenogeneic endothelial cells as a vaccine. *Nat Med* (2000) **6**:1160–6. doi:10.1038/80506
65. Chinnasamy D, Yu Z, Theoret MR, Zhao Y, Shrimali RK, Morgan RA, et al. Gene therapy using genetically modified lymphocytes targeting VEGFR-2 inhibits the growth of vascularized syngeneic tumors in mice. *J Clin Invest* (2010) **120**:3953–68. doi:10.1172/JCI43490
66. Chinnasamy D, Tran E, Yu Z, Morgan RA, Restifo NP, Rosenberg SA. Simultaneous targeting of tumor antigens and the tumor vasculature using T lymphocyte transfer synergize to induce regression of established tumors in mice. *Cancer Res* (2013) **73**:3371–80. doi:10.1158/0008-5472.CAN-12-3913
67. Yang L, Debusk LM, Fukuda K, Fingleton B, Green-Jarvis B, Shyr Y, et al. Expansion of myeloid immune suppressor Gr+CD11b+ cells in tumor-bearing host directly promotes tumor angiogenesis. *Cancer Cell* (2004) **6**:409–21. doi:10.1016/j.ccr.2004.08.031
68. Suzuki H, Onishi H, Wada J, Yamasaki A, Tanaka H, Nakano K, et al. VEGFR2 is selectively expressed by FOXP3high CD4+ Treg. *Eur J Immunol* (2010) **40**:197–203. doi:10.1002/eji.200939887
69. Choueiri TK, Schutz FA, Je Y, Rosenberg JE, Bellmunt J. Risk of arterial thromboembolic events with sunitinib and sorafenib: a systematic review and meta-analysis of clinical trials. *J Clin Oncol* (2010) **28**:2280–5. doi:10.1200/JCO.2009.27.2757
70. Hess Michelini R, Freschi M, Manzo T, Jachetti E, Degl'Innocenti E, Grioni M, et al. Concomitant tumor and minor histocompatibility antigen-specific immunity initiate rejection and maintain remission from established spontaneous solid tumors. *Cancer Res* (2010) **70**:3505–14. doi:10.1158/0008-5472.CAN-09-4253
71. Hess Michelini R, Manzo T, Sturmheit T, Bassi V, Rocchi M, Freschi M, et al. Vaccine-instructed intratumoral IFN-gamma enables regression of autochthonous mouse prostate cancer in allogeneic T cell transplantation. *Cancer Res* (2013) **73**(15):4641–52. doi:10.1158/0008-5472.CAN-12-3464
72. Lake RA, Robinson BW. Immunotherapy and chemotherapy – a practical partnership. *Nat Rev Cancer* (2005) **5**:397–405. doi:10.1038/nrc1613
73. Zitvogel L, Apetoh L, Ghiringhelli F, Kroemer G. Immunological aspects of cancer chemotherapy. *Nat Rev Immunol* (2008) **8**:59–73. doi:10.1038/nri2216
74. Abastado JP. The next challenge in cancer immunotherapy: controlling T-cell traffic to the tumor. *Cancer Res* (2012) **72**:2159–61. doi:10.1158/0008-5472.CAN-11-3538
75. Warburg O, Wind F, Negelein E. The metabolism of tumors in the body. *J Gen Physiol* (1927) **8**:519–30. doi:10.1085/jgp.8.6.519
76. Cham CM, Xu H, O'Keefe JP, Rivas FV, Zagouras P, Gajewski TF. Gene array and protein expression profiles suggest post-transcriptional regulation during CD8+ T cell differentiation. *J Biol Chem* (2003) **278**:17044–52. doi:10.1074/jbc.M212741200
77. Cham CM, Gajewski TF. Metabolic mechanisms of tumor resistance to T cell effector function. *Immunol Res* (2005) **31**:107–18. doi:10.1385/IR:31:2:107
78. Gatenby RA, Gillies RJ. Why do cancers have high aerobic glycolysis? *Nat Rev Cancer* (2004) **4**:891–9. doi:10.1038/nrc1478
79. Supuran CT. Carbonic anhydrases: novel therapeutic applications for inhibitors and activators. *Nat Rev Drug Discov* (2008) **7**:168–81. doi:10.1038/nrd2467
80. Chiche J, Ilc K, Laferriere J, Trottier E, Dayan F, Mazure NM, et al. Hypoxia-inducible carbonic anhydrase IX and XII promote tumor cell growth by counteracting acidosis through the regulation of the intracellular pH. *Cancer Res* (2009) **69**:358–68. doi:10.1158/0008-5472.CAN-08-2470
81. Helmlinger G, Yuan F, Dellian M, Jain RK. Interstitial pH and pO₂ gradients in solid tumors in vivo: high-resolution measurements reveal a lack of correlation. *Nat Med* (1997) **3**:177–82. doi:10.1038/nm0297-177
82. Fais S, De Milito A, You H, Qin W. Targeting vacuolar H+-ATPases as a new strategy against cancer. *Cancer Res* (2007) **67**:10627–30. doi:10.1158/0008-5472.CAN-07-1805
83. Dewhirst MW, Cao Y, Moeller B. Cycling hypoxia and free radicals regulate angiogenesis and radiotherapy response. *Nat Rev Cancer* (2008) **8**:425–37. doi:10.1038/nrc2397
84. Pani G, Giannoni E, Galeotti T, Chiarugi P. Redox-based escape mechanism from death: the cancer lesson. *Antioxid Redox Signal* (2009) **11**:2791–806. doi:10.1089/ars.2009.2739
85. Arner ES, Holmgren A. The thioredoxin system in cancer. *Semin Cancer Biol* (2006) **16**:420–6. doi:10.1016/j.semcancer.2006.10.009
86. Ceccarelli J, Delfino L, Zappia E, Castellani P, Borghi M, Ferrini S, et al. The redox state of the lung cancer microenvironment depends on the levels of thioredoxin expressed by tumor cells and affects tumor progression and response to prooxidants. *Int J Cancer* (2008) **123**:1770–8. doi:10.1002/ijc.23709
87. Csiki I, Yanagisawa K, Haruki N, Nadaf S, Morrow JD, Johnson DH, et al. Thioredoxin-1 modulates transcription of cyclooxygenase-2 via hypoxia-inducible factor-1alpha in non-small cell lung cancer. *Cancer Res* (2006) **66**:143–50. doi:10.1158/0008-5472.CAN-05-1357
88. De Milito A, Iessi E, Logozzi M, Lozupone F, Spada M, Marino ML, et al. Proton pump inhibitors induce apoptosis of human B-cell tumors through a caspase-independent mechanism involving reactive oxygen species. *Cancer Res* (2007) **67**:5408–17. doi:10.1158/0008-5472.CAN-06-4095
89. Odegaard JJ, Chawla A. The immune system as a sensor of the metabolic state. *Immunity* (2013) **38**:644–54. doi:10.1016/j.jimmuni.2013.04.001
90. Munn DH, Mellor AL. Indoleamine 2,3-dioxygenase and metabolic control of immune responses. *Trends Immunol* (2013) **34**:137–43. doi:10.1016/j.it.2012.10.001
91. Holmgard RB, Zamarin D, Munn DH, Wolchok JD, Allison JP. Indoleamine 2,3-dioxygenase is a critical resistance mechanism in antitumor T cell immunotherapy targeting CTLA-4. *J Exp Med* (2013) **210**:1389–402. doi:10.1084/jem.20130066
92. Caldwell CC, Kojima H, Lukashev D, Armstrong J, Farber M, Apasov SG, et al. Differential effects of physiologically relevant hypoxic conditions on T lymphocyte development and effector functions. *J Immunol* (2001) **167**:6140–9.
93. Conforti L, Petrovic M, Mohammad D, Lee S, Ma Q, Barone S, et al. Hypoxia regulates expression and activity of Kv1.3 channels in T lymphocytes: a possible role in T cell proliferation. *J Immunol* (2003) **170**:695–702.
94. Lukashev D, Klebanov B, Kojima H, Grinberg A, Ohta A, Berenfeld L, et al. Cutting edge: hypoxia-inducible factor 1alpha and its activation-inducible short isoform I.1 negatively regulate functions of CD4+ and CD8+ T lymphocytes. *J Immunol* (2006) **177**:4962–5.
95. Thiel M, Caldwell CC, Kreth S, Kuboki S, Chen P, Smith P, et al. Targeted deletion of HIF-1alpha gene in T cells prevents their inhibition in hypoxic inflamed tissues and improves septic mice survival. *PLoS ONE* (2007) **2**:e853. doi:10.1371/journal.pone.0000853
96. Sitkovsky MV, Kjaergaard J, Lukashev D, Ohta A. Hypoxia-adenosinergic immunosuppression: tumor protection by T regulatory cells and cancerous tissue hypoxia. *Clin Cancer Res* (2008) **14**:5947–52. doi:10.1158/1078-0432.CCR-08-0229
97. Facciabene A, Peng X, Hagemann IS, Balint K, Barchetti A, Wang LP, et al. Tumour hypoxia promotes tolerance and angiogenesis via CCL28 and T(reg) cells. *Nature* (2011) **475**:226–30. doi:10.1038/nature10169
98. Dang EV, Barbi J, Yang HY, Jinaseuna D, Yu H, Zheng Y, et al. Control of T(H)17/T(reg) balance by hypoxia-inducible factor 1. *Cell* (2011) **146**:772–84. doi:10.1016/j.cell.2011.07.033

99. Shi LZ, Wang R, Huang G, Vogel P, Neale G, Green DR, et al. HIF1alpha-dependent glycolytic pathway orchestrates a metabolic checkpoint for the differentiation of TH17 and Treg cells. *J Exp Med* (2011) **208**:1367–76. doi:10.1084/jem.20110278
100. Kryczek I, Wu K, Zhao E, Wei S, Vatan L, Szeliga W, et al. IL-17+ regulatory T cells in the microenvironments of chronic inflammation and cancer. *J Immunol* (2011) **186**:4388–95. doi:10.4049/jimmunol.1003251
101. Weaver CT, Elson CO, Fouser LA, Kolls JK. The Th17 pathway and inflammatory diseases of the intestines, lungs, and skin. *Annu Rev Pathol* (2013) **8**:477–512. doi:10.1146/annurev-pathol-011110-130318
102. Martin-Orozco N, Muranski P, Chung Y, Yang XO, Yamazaki T, Lu S, et al. T helper 17 cells promote cytotoxic T cell activation in tumor immunity. *Immunity* (2009) **31**:787–98. doi:10.1016/j.immuni.2009.09.014
103. Zou W, Restifo NP. T(H)17 cells in tumour immunity and immunotherapy. *Nat Rev Immunol* (2010) **10**:248–56. doi:10.1038/nri2742
104. Norman MZ, Buart S, Romero P, Ketari S, Janji B, Mari B, et al. Hypoxia-inducible miR-210 regulates the susceptibility of tumor cells to lysis by cytotoxic T cells. *Cancer Res* (2012) **72**:4629–41. doi:10.1158/0008-5472.CAN-12-1383
105. MacDonald HR. Energy metabolism and T-cell-mediated cytolysis. II. Selective inhibition of cytolysis by 2-deoxy-D-glucose. *J Exp Med* (1977) **146**:710–9. doi:10.1084/jem.146.3.710
106. Lardner A. The effects of extracellular pH on immune function. *J Leukoc Biol* (2001) **69**:522–30.
107. Kellum JA. Metabolic acidosis in patients with sepsis: epiphénoménon or part of the pathophysiology? *Crit Care Resusc* (2004) **6**:197–203.
108. Lugini L, Matarrese P, Tinari A, Lozupone F, Federici C, Iessi E, et al. Cannibalism of live lymphocytes by human metastatic but not primary melanoma cells. *Cancer Res* (2006) **66**:3629–38. doi:10.1158/0008-5472.CAN-05-3204
109. Droege W, Roth S, Altmann A, Mihm S. Regulation of T-cell functions by L-lactate. *Cell Immunol* (1987) **108**:405–16. doi:10.1016/0008-8749(87)90223-1
110. Ratner S. Lymphocytes stimulated with recombinant human interleukin-2: relationship between motility into protein matrix and in vivo localization in normal and neoplastic tissues of mice. *J Natl Cancer Inst* (1990) **82**:612–6. doi:10.1093/jnci/82.7.612
111. Redegeld F, Filippini A, Sitkovsky M. Comparative studies of the cytotoxic T lymphocyte-mediated cytotoxicity and of extracellular ATP-induced cell lysis. Different requirements in extracellular Mg²⁺ and pH. *J Immunol* (1991) **147**:3638–45.
112. Fischer K, Hoffmann P, Voelkl S, Meidenbauer N, Ammer J, Edinger M, et al. Inhibitory effect of tumor cell-derived lactic acid on human T cells. *Blood* (2007) **109**:3812–9. doi:10.1182/blood-2006-07-035972
113. Calcinotto A, Filippini P, Grioni M, Iero M, De Milito A, Riccupito A, et al. Modulation of microenvironment acidity reverses anergy in human and murine tumor-infiltrating T lymphocytes. *Cancer Res* (2012) **72**:2746–56. doi:10.1158/0008-5472.CAN-11-1272
114. Grundstrom S, Dohlsten M, Sundstedt A. IL-2 unresponsiveness in anergic CD4+ T cells is due to defective signaling through the common gamma-chain of the IL-2 receptor. *J Immunol* (2000) **164**:1175–84.
115. Wells AD, Walsh MC, Sankaran D, Turka LA. T cell effector function and anergy avoidance are quantitatively linked to cell division. *J Immunol* (2000) **165**:2432–43.
116. Bellone M, Calcinotto A, Filippini P, De Milito A, Fais S, Rivoltini L. The acidity of the tumor microenvironment is a mechanism of immune escape that can be overcome by proton pump inhibitors. *Oncimmunology* (2013) **2**:e22058. doi:10.4161/onci.22058
117. Babior BM, Kipnes RS, Curnutte JT. Biological defense mechanisms. The production by leukocytes of superoxide, a potential bactericidal agent. *J Clin Invest* (1973) **52**:741–4. doi:10.1172/JCI107236
118. Rubartelli A. Redox control of NLRP3 inflammasome activation in health and disease. *J Leukoc Biol* (2012) **92**:951–8. doi:10.1189/jlb.0512265
119. Williams MS, Kwon J. T cell receptor stimulation, reactive oxygen species, and cell signaling. *Free Radic Biol Med* (2004) **37**:1144–51. doi:10.1016/j.freeradbiomed.2004.05.029
120. Wu G, Morris SM Jr. Arginine metabolism: nitric oxide and beyond. *Biochem J* (1998) **336**(Pt 1):1–17.
121. Bogdan C. Nitric oxide and the immune response. *Nat Immunol* (2001) **2**:907–16. doi:10.1038/35098532
122. Rodriguez PC, Zea AH, Culotta KS, Zabaleta J, Ochoa JB, Ochoa AC. Regulation of T cell receptor CD3zeta chain expression by L-arginine. *J Biol Chem* (2002) **277**:21123–9. doi:10.1074/jbc.M110675200
123. Rodriguez PC, Quiceno DG, Zabaleta J, Ortiz B, Zea AH, Piazuelo MB, et al. Arginase I production in the tumor microenvironment by mature myeloid cells inhibits T-cell receptor expression and antigen-specific T-cell responses. *Cancer Res* (2004) **64**:5839–49. doi:10.1158/0008-5472.CAN-04-0465
124. Rodriguez PC, Quiceno DG, Ochoa AC. L-arginine availability regulates T-lymphocyte cell-cycle progression. *Blood* (2007) **109**:1568–73. doi:10.1182/blood-2006-06-031856
125. Bingisser RM, Tilbrook PA, Holt PG, Kees UR. Macrophage-derived nitric oxide regulates T cell activation via reversible disruption of the Jak3/STAT5 signaling pathway. *J Immunol* (1998) **160**:5729–34.
126. Mazzoni A, Bronte V, Visintin A, Spitzer JH, Apolloni E, Serafini P, et al. Myeloid suppressor lines inhibit T cell responses by an NO-dependent mechanism. *J Immunol* (2002) **168**:689–95.
127. Lejeune P, Lagadec P, Onier N, Pinard D, Ohshima H, Jeannin JE. Nitric oxide involvement in tumor-induced immunosuppression. *J Immunol* (1994) **152**:5077–83.
128. Bobe P, Benihoud K, Grandjond D, Opolon P, Pritchard LL, Huchet R. Nitric oxide mediation of active immunosuppression associated with graft-versus-host reaction. *Blood* (1999) **94**:1028–37.
129. Sato K, Ozaki K, Oh I, Meguro A, Hatanaka K, Nagai T, et al. Nitric oxide plays a critical role in suppression of T-cell proliferation by mesenchymal stem cells. *Blood* (2007) **109**:228–34. doi:10.1182/blood-2006-02-002246
130. Xia Y, Tsai AL, Berka V, Zweier JL. Superoxide generation from endothelial nitric-oxide synthase. A Ca²⁺/calmodulin-dependent and tetrahydrobiopterin regulatory process. *J Biol Chem* (1998) **273**:25804–8. doi:10.1074/jbc.273.40.25804
131. Bronte V, Serafini P, De Santo C, Marigo I, Tosello V, Mazzoni A, et al. IL-4-induced arginase 1 suppresses alloreactive T cells in tumor-bearing mice. *J Immunol* (2003) **170**:270–8.
132. Kusmartsev S, Gabrilovich DI. Role of immature myeloid cells in mechanisms of immune evasion in cancer. *Cancer Immunol Immunother* (2006) **55**:237–45. doi:10.1007/s00262-005-0048-z
133. Squadrito GL, Pryor WA. The formation of peroxynitrite in vivo from nitric oxide and superoxide. *Chem Biol Interact* (1995) **96**:203–6. doi:10.1016/0009-2797(94)03591-U
134. Nagaraj S, Gupta K, Pisarev V, Kinarsky L, Sherman S, Kang L, et al. Altered recognition of antigen is a mechanism of CD8+ T cell tolerance in cancer. *Nat Med* (2007) **13**:828–35. doi:10.1038/nm1609
135. Molon B, Ugel S, Del Pozzo F, Soldani C, Zilio S, Avella D, et al. Chemokine nitration prevents intratumoral infiltration of antigen-specific T cells. *J Exp Med* (2011) **208**:1949–62. doi:10.1084/jem.20101956
136. Yan Z, Garg SK, Kipnis J, Banerjee R. Extracellular redox modulation by regulatory T cells. *Nat Chem Biol* (2009) **5**:721–3. doi:10.1038/nchembio.212
137. Angelini G, Gardella S, Ardy M, Ciriolo MR, Filomeni G, Di Trapani G, et al. Antigen-presenting dendritic cells provide the reducing extracellular microenvironment required for T lymphocyte activation. *Proc Natl Acad Sci U S A* (2002) **99**:1491–6. doi:10.1073/pnas.022630299
138. Yan Z, Garg SK, Banerjee R. Regulatory T cells interfere with glutathione metabolism in dendritic cells and T cells. *J Biol Chem* (2010) **285**:41525–32. doi:10.1074/jbc.M110.189944
139. Kobie JJ, Shah PR, Yang L, Rebhahn JA, Fowell DJ, Mosmann TR. T regulatory and primed uncommitted CD4 T cells express CD73, which suppresses effector CD4 T cells by converting 5'-adenosine monophosphate to adenosine. *J Immunol* (2006) **177**:6780–6.
140. Deaglio S, Dwyer KM, Gao W, Friedman D, Usheva A, Erat A, et al.

- al. Adenosine generation catalyzed by CD39 and CD73 expressed on regulatory T cells mediates immune suppression. *J Exp Med* (2007) **204**:1257–65. doi:10.1084/jem.20062512
141. Pearce EL, Walsh MC, Cejas PJ, Harms GM, Shen H, Wang LS, et al. Enhancing CD8 T-cell memory by modulating fatty acid metabolism. *Nature* (2009) **460**:103–7. doi:10.1038/nature08097
142. Keunen O, Johansson M, Oudin A, Sanzey M, Rahim SA, Fack F, et al. Anti-VEGF treatment reduces blood supply and increases tumor cell invasion in glioblastoma. *Proc Natl Acad Sci U S A* (2011) **108**:3749–54. doi:10.1073/pnas.1014480108
143. Conley SJ, Gheorghenescu E, Kakarala P, Newman B, Korkaya H, Heath AN, et al. Antiangiogenic agents increase breast cancer stem cells via the generation of tumor hypoxia. *Proc Natl Acad Sci U S A* (2012) **109**:2784–9. doi:10.1073/pnas.1018866109
144. Carbone C, Moccia T, Zhu C, Paradiso G, Budillon A, Chiao PJ, et al. Anti-VEGF treatment-resistant pancreatic cancers secrete proinflammatory factors that contribute to malignant progression by inducing an EMT cell phenotype. *Clin Cancer Res* (2011) **17**:5822–32. doi:10.1158/1078-0432.CCR-11-1185
145. Paez-Ribes M, Allen E, Hudock J, Takeda T, Okuyama H, Vinals F, et al. Antiangiogenic therapy elicits malignant progression of tumors to increased local invasion and distant metastasis. *Cancer Cell* (2009) **15**:220–31. doi:10.1016/j.ccr.2009.01.027
146. Shojaei F, Wu X, Malik AK, Zhong C, Baldwin ME, Schanz S, et al. Tumor refractoriness to anti-VEGF treatment is mediated by CD11b+Gr1+ myeloid cells. *Nat Biotechnol* (2007) **25**:911–20. doi:10.1038/nbt1323
147. Christensen JG. A preclinical review of sunitinib, a multitargeted receptor tyrosine kinase inhibitor with anti-angiogenic and antitumour activities. *Ann Oncol* (2007) **18**(Suppl 10):x3–10. doi:10.1093/annonc/mdm408
148. Motzer RJ, Hutson TE, Tomczak P, Michaelson MD, Bukowski RM, Oudard S, et al. Overall survival and updated results for sunitinib compared with interferon alfa in patients with metastatic renal cell carcinoma. *J Clin Oncol* (2009) **27**:3584–90. doi:10.1200/JCO.2008.20.1293
149. Maione F, Capano S, Regano D, Zentilin L, Giacca M, Casanovas O, et al. Semaphorin 3A overcomes cancer hypoxia and metastatic dissemination induced by antiangiogenic treatment in mice. *J Clin Invest* (2012) **122**:1832–48. doi:10.1172/JCI58976
150. Finke JH, Rini B, Ireland J, Rayman P, Richmond A, Golshayan A, et al. Sunitinib reverses type-1 immune suppression and decreases T-regulatory cells in renal cell carcinoma patients. *Clin Cancer Res* (2008) **14**:6674–82. doi:10.1158/1078-0432.CCR-07-5212
151. van Cruyssen H, Van Der Veldt AA, Vroeling L, Oosterhoff D, Broxterman HJ, Schepers RJ, et al. Sunitinib-induced myeloid lineage redistribution in renal cell cancer patients: CD1c+ dendritic cell frequency predicts progression-free survival. *Clin Cancer Res* (2008) **14**:5884–92. doi:10.1158/1078-0432.CCR-08-0656
152. Ko JS, Zea AH, Rini BI, Ireland JL, Elson P, Cohen P, et al. Sunitinib mediates reversal of myeloid-derived suppressor cell accumulation in renal cell carcinoma patients. *Clin Cancer Res* (2009) **15**:2148–57. doi:10.1158/1078-0432.CCR-08-1332
153. Bose A, Taylor JL, Alber S, Watkins SC, Garcia JA, Rini BI, et al. Sunitinib facilitates the activation and recruitment of therapeutic anti-tumor immunity in concert with specific vaccination. *Int J Cancer* (2011) **129**:2158–70. doi:10.1002/ijc.25863
154. Pan F, Barbi J, Pardoll DM. Hypoxia-inducible factor 1: A link between metabolism and T cell differentiation and a potential therapeutic target. *Oncogene* (2012) **1**:510–5. doi:10.1461/onci.19457
155. Kryczek I, Zhao E, Liu Y, Wang Y, Vatan L, Szeliga W, et al. Human TH17 cells are long-lived effector memory cells. *Sci Transl Med* (2011) **3**:104ra100. doi:10.1126/scitranslmed.3002949
156. Palazon A, Martinez-Forero I, Teijeira A, Morales-Kastresana A, Alfaro C, Sanmamed MF, et al. The HIF-1alpha hypoxia response in tumor-infiltrating T lymphocytes induces functional CD137 (4-1BB) for immunotherapy. *Cancer Discov* (2012) **2**:608–23. doi:10.1158/2159-8290.CD-11-0314
157. Robey IF, Baggett BK, Kirkpatrick ND, Roe DJ, Dosescu J, Sloane BF, et al. Bicarbonate increases tumor pH and inhibits spontaneous metastases. *Cancer Res* (2009) **69**:2260–8. doi:10.1158/0008-5472.CAN-07-5575
158. Mullin JM, Gabello M, Murray LJ, Farrell CP, Bellows J, Wolov KR, et al. Proton pump inhibitors: actions and reactions. *Drug Discov Today* (2009) **14**:647–60. doi:10.1016/j.drudis.2009.03.014
159. De Milito A, Canese R, Marino ML, Borghi M, Iero M, Villa A, et al. pH-dependent antitumor activity of proton pump inhibitors against human melanoma is mediated by inhibition of tumor acidity. *Int J Cancer* (2010) **127**:207–19. doi:10.1002/ijc.25009
160. Kedika RR, Souza RF, Speicher SJ. Potential anti-inflammatory effects of proton pump inhibitors: a review and discussion of the clinical implications. *Dig Dis Sci* (2009) **54**:2312–7. doi:10.1007/s10620-009-0951-9
161. Wojtkowiak JW, Rothberg JM, Kumar V, Schramm KJ, Haller E, Proemsey JB, et al. Chronic autophagy is a cellular adaptation to tumor acidic pH microenvironments. *Cancer Res* (2012) **72**:3938–47. doi:10.1158/0008-5472.CAN-11-3881
162. Marino ML, Fais S, Djavaheri-Mergny M, Villa A, Meschini S, Lozupone F, et al. Proton pump inhibition induces autophagy as a survival mechanism following oxidative stress in human melanoma cells. *Cell Death Dis* (2010) **1**:e87. doi:10.1038/cddis.2010.67
163. Townsend KN, Hughson LR, Schlie K, Poon VI, Westerback A, Lum JJ. Autophagy inhibition in cancer therapy: metabolic considerations for antitumor immunity. *Immunol Rev* (2012) **249**:176–94. doi:10.1111/j.1600-065X.2012.01141.x
164. Li Q, Rao RR, Araki K, Pollicino K, Odunsi K, Powell JD, et al. A central role for mTOR kinase in homeostatic proliferation induced CD8+ T cell memory and tumor immunity. *Immunity* (2011) **34**:541–53. doi:10.1016/j.immuni.2011.04.006
165. Li Q, Rao R, Vazzana J, Goedegebuure P, Odunsi K, Gillanders W, et al. Regulating mammalian target of rapamycin to tune vaccination-induced CD8(+) T cell responses for tumor immunity. *J Immunol* (2012) **188**:3080–7. doi:10.4049/jimmunol.1103365
166. Ohta A, Gorelik E, Prasad SJ, Ronchese F, Lukashev D, Wong MK, et al. A2A adenosine receptor protects tumors from antitumor T cells. *Proc Natl Acad Sci U S A* (2006) **103**:13132–7. doi:10.1073/pnas.0605251103
167. Stensvold I, Jacobsen BK. Coffee and cancer: a prospective study of 43,000 Norwegian men and women. *Cancer Causes Control* (1994) **5**:401–8. doi:10.1007/BF01694753
168. Veierod MB, Thelle DS, Laake P. Diet and risk of cutaneous malignant melanoma: a prospective study of 50,757 Norwegian men and women. *Int J Cancer* (1997) **71**:600–4. doi:10.1002/(SICI)1097-0215(19970516)71:4<600::AID-IJC15>3.3.CO;2-C
169. Colombo MP, Piconese S. Regulatory-T-cell inhibition versus depletion: the right choice in cancer immunotherapy. *Nat Rev Cancer* (2007) **7**:880–7. doi:10.1038/nrc2250
170. Chaudhry A, Rudensky AY. Control of inflammation by integration of environmental cues by regulatory T cells. *J Clin Invest* (2013) **123**:939–44. doi:10.1172/JCI57175
171. Ugel S, Delpozzo F, Desantis G, Papalini F, Simonato F, Sonda N, et al. Therapeutic targeting of myeloid-derived suppressor cells. *Curr Opin Pharmacol* (2009) **9**:470–81. doi:10.1016/j.coph.2009.06.014
172. Filipazzi P, Huber V, Rivoltini L. Phenotype, function and clinical implications of myeloid-derived suppressor cells in cancer patients. *Cancer Immunol Immunother* (2012) **61**:255–63. doi:10.1007/s00262-011-1161-9
173. Rodriguez PC, Ochoa AC. Arginine regulation by myeloid derived suppressor cells and tolerance in cancer: mechanisms and therapeutic perspectives. *Immunol Rev* (2008) **222**:180–91. doi:10.1111/j.1600-065X.2008.00608.x
174. Nagaraj S, Gabrilovich DI. Myeloid-derived suppressor cells in human cancer. *Cancer J* (2010) **16**:348–53. doi:10.1097/PPO.0b013e3181eb3358
175. Hanson EM, Clements VK, Sinha P, Ilkovich D, Ostrand-Rosenberg S. Myeloid-derived suppressor cells down-regulate L-selectin expression on CD4+ and CD8+ T cells. *J Immunol* (2009) **183**:937–44. doi:10.4049/jimmunol.0804253
176. Terme M, Ullrich E, Delahaye NF, Chaput N, Zitvogel L. Natural killer cell-directed therapies: moving from unexpected results to successful strategies. *Nat*

- Immunol* (2008) **9**:486–94. doi:10.1038/ni1580
177. Rigamonti N, Bellone M. Prostate cancer, tumor immunity and a renewed sense of optimism in immunotherapy. *Cancer Immunol Immunother* (2012) **61**:453–68. doi:10.1007/s00262-012-1216-6
178. Saggar JK, Yu M, Tan Q, Tan-noek IF. The tumor microenvironment and strategies to improve drug distribution. *Front Oncol* (2013) **3**:154. doi:10.3389/fonc.2013.00154
179. Lipson EJ. Re-orienting the immune system: durable tumor regression and successful re-induction therapy using anti-PD1 antibodies. *Oncoimmunology* (2013) **2**:e23661. doi:10.4161/onci.23661
180. Mayer RJ. Targeted therapy for advanced colorectal cancer – more is not always better. *N Engl J Med* (2009) **360**:623–5. doi:10.1056/NEJMMe0809343
181. Tol J, Koopman M, Cats A, Rodenburg CJ, Creemers GJ, Schrama JG, et al. Chemotherapy, bevacizumab, and cetuximab in metastatic colorectal cancer. *N Engl J Med* (2009) **360**:563–72. doi:10.1056/NEJMoa0808268
182. Hecht JR, Mitchell E, Chidac T, Scroggin C, Hagenstad C, Spigel D, et al. A randomized phase IIIB trial of chemotherapy, bevacizumab, and panitumumab compared with chemotherapy and bevacizumab alone for metastatic colorectal cancer. *J Clin Oncol* (2009) **27**:672–80. doi:10.1200/JCO.2008.19.8135
- Conflict of Interest Statement:** The authors declare that the research was conducted in the absence of any commercial or financial relationships that could be construed as a potential conflict of interest.
- Received: 27 June 2013; paper pending published: 12 July 2013; accepted: 23 August 2013; published online: 11 September 2013.*
- Citation: Bellone M and Calcinotto A (2013) Ways to enhance lymphocyte trafficking into tumors and fitness of tumor infiltrating lymphocytes. *Front. Oncol.* **3**:231. doi:10.3389/fonc.2013.00231*
- This article was submitted to Pharmacology of Anti-Cancer Drugs, a section of the journal *Frontiers in Oncology*.
- Copyright © 2013 Bellone and Calcinotto. This is an open-access article distributed under the terms of the Creative Commons Attribution License (CC BY). The use, distribution or reproduction in other forums is permitted, provided the original author(s) or licensor are credited and that the original publication in this journal is cited, in accordance with accepted academic practice. No use, distribution or reproduction is permitted which does not comply with these terms.



Tumor delivery of chemotherapy combined with inhibitors of angiogenesis and vascular targeting agents

Marta Cesca¹, Francesca Bizzaro¹, Massimo Zucchetti² and Raffaella Giavazzi^{1*}

¹ Laboratory of Biology and Treatment of Metastases, Department of Oncology, IRCCS-Istituto di Ricerche Farmacologiche "Mario Negri," Milan, Italy

² Laboratory of Cancer Pharmacology, Department of Oncology, IRCCS-Istituto di Ricerche Farmacologiche "Mario Negri," Milan, Italy

Edited by:

Angelo Corti, San Raffaele Scientific Institute, Italy

Reviewed by:

Ronald Berenson, Compliment Corporation, USA

Matteo Bellone, San Raffaele Scientific Institute, Italy

***Correspondence:**

Raffaella Giavazzi, Laboratory of Biology and Treatment of Metastases, Department of Oncology, IRCCS-Istituto di Ricerche

Farmacologiche "Mario Negri," Via La Masa 19, 20156 Milan, Italy

e-mail: raffaella.giavazzi@marionegri.it

Numerous angiogenesis-vascular targeting agents have been admitted to the ranks of cancer therapeutics; most are used in polytherapy regimens. This review looks at recent progress and our own preclinical experience in combining angiogenesis inhibitors, mainly acting on VEGF/VEGFR pathways, and vascular targeting agents with conventional chemotherapy, discussing the factors that determine the outcome of these treatments. Molecular and morphological modifications of the tumor microenvironment associated with drug distribution and activity are reviewed. Modalities to improve drug delivery and strategies for optimizing combination therapy are examined.

Keywords: combination therapies, angiogenesis inhibitors, tyrosine kinase receptor inhibitors, vascular disrupting agents, drug delivery, paclitaxel, tumor microenvironment

INTRODUCTION

Recognition of the multi-compartment nature of the tumor microenvironment has challenged the conventions of anticancer therapy, giving rise to a radically different approach toward the discovery of new treatments. Historically aimed at killing tumor cells (cytotoxic agents), the search now seeks to identify novel "biologics," that selectively target not only the cancer cell, but also the tumor stroma.

Angiogenesis – the development of new vasculature – is required for tumor growth, invasion, and metastatic dissemination, hence the rationale for anti-angiogenic therapy (1). Numerous angiogenesis-targeting agents have been admitted to the ranks of cancer therapeutics (2). Drugs targeting the tumor vasculature have been developed and have shown efficacy in preclinical models and in some clinical trials (1–3).

The most validated anti-angiogenic strategy to prevent tumor vessel formation targets the vascular endothelial growth factor (VEGF) axis. VEGF can be blocked directly, with the antibody bevacizumab (Avastin®), or, among others, with the VEGF-trap (Aflibercept®), an engineered soluble VEGF receptor able to bind VEGF as well as platelet growth factor (PLGF) (4), or indirectly by inhibiting receptor activity with antibodies or small-molecule tyrosine kinase receptor inhibitors (RTKIs). Sunitinib (Sutent®), sorafenib (Nexavar®), and pazopanib (Votrient®) have been approved for different tumor types (5). An alternative strategy is to selectively destroy the existing vasculature with vascular disrupting agents (VDA) (6–8). VDA cause a pronounced and rapid shutdown of blood flow to solid tumors, leading to tumor necrosis and death. Small molecules, flavonoids (DMXAA), and tubulin-binding agents (Ca4P, ZD6126, Ave8062, Oxi4503), have entered into Phase II–III studies.

Inhibition of a single target or pathway is of limited benefit for cancer patients (9). The primary clinical use of bevacizumab is combined with chemotherapy, as only the combination significantly prolonged overall survival in patients with metastatic colorectal cancer (CRC) (10) and recurrent/advanced non-small cell lung cancer (NSCLC) (11), or extended progression-free survival in patients with advanced ovarian cancer (12–14) and renal cell cancer (15). Unlike bevacizumab, the multitargeted profile of RTKIs makes them active as single agents, and any clear advantage in combination with chemotherapy has yet to be demonstrated (16).

The mechanism by which anti-angiogenic agents increase the efficacy of chemotherapy is not yet clear. An angiogenesis inhibitor combined with chemotherapy affects multiple compartments, depriving the tumors of nutrients and oxygen (i.e., anti-vascular and anti-angiogenic effect), and killing highly proliferative tumor cells (i.e., cytotoxic effect) (17). In terms of drug delivery this sounds paradoxical since the anti-angiogenic therapy, by modifying the tumor vasculature, potentially impairs the delivery of cytotoxic drugs (18).

The tumor microenvironment has an abnormal vasculature, structurally and functionally (increased vessel permeability, dilatation and tortuosity, reduced pericyte coverage, and abnormal basement membranes), mainly because of an imbalance between pro- and anti-angiogenic factors (19, 20). As a consequence, tumor blood flow is impaired and this, together with compression of the blood vessel by the growing cancer, results in high interstitial fluid pressure (IFP), hypoxic regions within the tumor, and ultimately reduced drug delivery (21, 22).

Anti-VEGF, and more in general anti-angiogenesis agents, modify the tumor microenvironment; abnormal microvessels are destroyed and the remaining vessels are remodeled (2). These

changes, that led Jain and coworkers to formulate the hypothesis of “vascular normalization,” should lead to a transient increase in vascular patency, a drop in IFP and alleviation of hypoxia, providing a “window of opportunity” for the delivery of drugs, with better therapeutic outcome. For reviews on tumor microenvironment normalization see Jain (23, 24). The normalization hypothesis offers a solution to the paradox that some angiogenesis inhibitors are efficacious when combined with chemotherapy.

Whether these morphological changes are accompanied by functional modifications, such as improved drug delivery, is still debated (25–27). Current attempts at combination treatments are often empirical, though rational protocols are needed that take account of drug pharmacokinetics, and their metabolic interactions and mechanism of action, as well as the biological characteristics of the tumor microenvironment (28). Careful dosing, scheduling, and sequencing of treatments, to avoid possible negative interactions and side effects, become essential to optimize the efficacy of combinations (7, 29). Optimization requires reliable, robust end points to monitor the activity of the combination.

This review focuses on recent progress, and our own preclinical experience in combining angiogenesis inhibitors/vascular targeting agents with conventional chemotherapy. Molecular, morphological and functional modifications of the tumor microenvironment related to drug distribution and activity are reviewed and, we examine some modalities to improve drug delivery and strategies for the optimization of combination therapy.

COMBINATION WITH BEVACIZUMAB

Bevacizumab is a humanized monoclonal antibody that targets VEGF (30). It has been approved, in combination with chemotherapy, for a number of malignancies, including colon, lung, and ovarian (in Europe) cancer (10–12), and for kidney cancer combined with interferon-gamma.

According to the hypothesis of vessel “normalization,” Jain and coworkers showed in a number of tumor models transplanted in the cranial window or in the dorsal skinfold chamber of mice, that vessels began to function better when treated with a neutralizing antibody anti-VEGF, possibly enhancing delivery of chemotherapy (31). Next, the duration of the “normalization window” was associated with alleviation of hypoxia, which plays a role in drug resistance and tumor progression. Radiotherapy was also more effective when administered during the normalization window (32). However, while preclinical studies have reported morphological and functional changes in the tumor vasculature after blocking VEGF, studies on drug delivery after anti-angiogenesis treatment are scanty. A tendency to a higher CPT11 concentration, that paralleled increased tumor perfusion, was observed in a colon carcinoma growing in nude mice after VEGF-blocking therapy. This suggested an increase in transport capability by vessels surviving anti-angiogenic treatment that compensated the reduction in the number of patent blood vessels (33).

The main concern about the “normalization window” is the limited time in which it occurs. As an example, orthotopic neuroblastoma xenografts treated with bevacizumab were evaluated at serial time points for treatment-associated changes in intra-tumoral vascular physiology, penetration of chemotherapy, and efficacy of combination therapy. After bevacizumab, there was a

progressive decrease in tumor microvessel density, with a rapid, sustained fall in tumor vessel permeability and tumor IFP, while tumor perfusion (mirrored by drug delivery) improved. Unfortunately these changes were short-lasting; the improvement in drug delivery was observed only for a few days after bevacizumab, but not when both drugs were given concomitantly. Although the combination was always superior to single-agent treatment, sequential treatment within the “normalization window” gave no significant advantage over concomitant treatment (34).

Our laboratory found that bevacizumab in combination with chemotherapy delayed tumor progression in mice bearing ovarian carcinoma xenografts, significantly prolonging survival (35). We observed a clear effect of bevacizumab on vessel morphology toward a “normalization” phenotype (e.g., decrease in vessel number, increase in pericyte coverage), but this was not related to increased drug uptake into tumor. While these findings do not explain the better outcome with the combination, we hypothesize that after bevacizumab, distribution of the cytotoxic drug might be better in more vital and actively proliferating areas of the tumor. Studies are in progress using Imaging Mass Spectrometry to clarify the spatial distribution of drugs into the tumor tissue after angiogenesis inhibitors (36).

Similar considerations can be extended to the combination of bevacizumab with large molecules, such as antibodies. For example reduced uptake of trastuzumab (a monoclonal antibody directed against HER-2/neu) after bevacizumab was observed in HER-2 expressing breast cancer xenografts. This was presumably due to tumor blood flow and vascular permeability reduction which contribute to the changes of trastuzumab pharmacokinetics (37). However the combination of bevacizumab with trastuzumab has given promising results in breast cancer patients (38).

Few clinical studies report the effects of anti-angiogenic therapy on drug uptake. One of the first pointers to the anti-vascular effect of bevacizumab in a clinical setting, came from a phase I study, in which patients with non-metastatic CRC were given a single infusion of bevacizumab, concomitantly with neo-adjuvant chemotherapy with 5-fluorouracil. Twelve days after its infusion, bevacizumab reduced tumor blood perfusion and vascular volume, accompanied by decreases in microvessel density, lower IFP, and increased pericyte coverage, confirming the drug’s anti-vascular and normalizing effects in human tumors (39). Vessel permeability, assessed as computed tomography (CT) contrast agent extravasation, and fluorodeoxyglucose (FDG) uptake into the tumor during positron emission tomography (PET) scans, did not change, indirectly showing cytotoxic drug uptake was not affected. PET scan 6 weeks after the bevacizumab and chemotherapy showed reduced FDG uptake than in previous scans, in accordance with the “temporary” duration of the normalization window (39).

To elucidate the effects of angiogenesis inhibitors on drug delivery, a recent study used PET to investigate bevacizumab combined with (¹¹C)docetaxel in NSCLC patients. Bevacizumab reduced perfusion and the net influx rate of docetaxel, shortly after its administration, and for several days afterward, showing no substantial improvement in drug delivery into tumors. Interestingly, bevacizumab prolonged systemic drug exposure, reducing plasma clearance, and causing more homogeneous intratumoral

distribution, as a result of some normalization of tumor vasculature (40). These findings indicate that anti-VEGF therapy not only does not improve tumor drug delivery, but rather has an opposite effect. The authors also suggested that the anti-angiogenic drug might be given after the anticancer agent, as the immediate decrease in tumor perfusion should reduce the clearance of drugs from tumors.

Thus, there is currently a large body of evidence indicating that agents such as bevacizumab cause vascular normalization, but whether this phenomenon favors or not drug penetration into tumors remains unclear. Studies in humans highlight the importance of drug scheduling and call for further studies to optimize combination modalities (41).

COMBINATION WITH RECEPTOR TYROSINE KINASE INHIBITORS

A large number of small molecules that are multi-receptor RTKIs, have progressed through clinical development (5). Unlike bevacizumab, the RTKIs have antitumor activity in monotherapy, and are rarely used in combination with chemotherapy in clinical practice, as no clear benefit has been reported (16). Clinical data on chemotherapy uptake after RTKIs are lacking.

The partial advantage we have observed, in preclinical models combining sunitinib (VEGFRs, PDGFRs, and c-Kit inhibitor) with chemotherapy (42) raises the question whether these molecules differ from bevacizumab in their anti-angiogenic actions and herein in their ability to facilitate drug distribution and activity.

Several preclinical studies have exploited RTKIs in combination with chemotherapy aimed to study drug interaction and modification of the tumor/stroma compartment which can ultimately affect drug distribution. RTKIs often give rise to increased hypoxia and decreased drug uptake [for review see Ref. (43)].

For example, the small-molecule axitinib (VEGFRs, PDGFR, and c-KIT inhibitor) affected tumor vasculature as the number of blood vessels decreased, and hypoxia increased (44, 45). In combination with cyclophosphamide, this led to decreased delivery of its metabolite (4-OH-CPA) into the tumor, with the consequence of limited antitumor activity, and no tumor regressions (44). Interestingly, the anti-vascular activity of axitinib, could be turned to a therapeutic advantage if cyclophosphamide was injected intratumor: axitinib slowed leakage of 4-OH-CPA, increasing its retention (46). Thus drug retention, as consequence of anti-angiogenic therapy, can be exploited for combination with drugs injected intra-tumor or for systemic delivery of pro-drugs directly activated in the tumor (46). (See also combination with VDA below).

Some years ago we studied the combination of SU6668 (a first-generation VEGFR-2, FGFR, and PDGFR β inhibitor) with paclitaxel on ovarian cancer xenograft models (47, 48). The combination affected tumor burden and prolonged overall survival, depending on the tumor's sensitivity to paclitaxel (less efficient on the resistant tumor), the treatment regimen (less active, though less toxic at a metronomic schedule) and the tumor burden at the beginning of treatment (less active on large tumors). Though SU6668 alone and in combination affected tumor vascular density (48), there was no improvement in paclitaxel uptake. The limited advantage given by SU6668 added to paclitaxel on the resistant tumor compared to the sensitive one indicated that angiogenesis

inhibitors and cytotoxic agents act on the tumor and host compartments independently, with some combined effects on the same compartment (the host), as paclitaxel is a strong vascular targeting drug (49).

These initial findings prompted us to investigate morphological and functional changes of the tumor vasculature induced by the RTKI vandetanib (VEGFR2, EGFR, and RET inhibitor), and its effect on intratumoral delivery and the antitumor activity of paclitaxel (27). In line with previous observations, the combination of vandetanib plus paclitaxel had greater antitumor activity than the single agent treatments (50). However, changes in vascular morphology and function (normalization) induced by vandetanib were not associated with any increase in paclitaxel delivery into the tumor. In fact, our results showed that the antitumor activity of vandetanib combined with paclitaxel is at least partly dependent on the drug sequence. In mice pretreated with vandetanib, paclitaxel delivery decreased, reflecting a decrease in tumor perfusion, assessed as Hoechst 33342 levels, an indicator of vascular perfusion (27). The decrease in uptake of paclitaxel after vandetanib was particularly evident at an early time point (1 h after paclitaxel) as levels were similar later (24 h after paclitaxel). As plasma data excluded reduced drug availability, this might have been due to less efficient paclitaxel penetration in the more poorly perfused vandetanib-treated tumor, followed by longer retention for the same reason. Vandetanib impaired paclitaxel uptake already after 1 day of treatment, with maximum effect after 5 days. On stopping vandetanib, paclitaxel uptake by the tumor was restored, indicating that vandetanib's effect on drug distribution in tumors is reversible as it is the "normalization" phenomenon (27).

We have observed reduced paclitaxel delivery into the tumor with no change in systemic pharmacokinetics, in combination experiments with different RTKIs (sunitinib and the dual inhibitors of VEGFR2 and FGFR2, brivanib and E-3810), despite the improved antitumor activity. E-3810 reduced vessel number, and induced tumor microenvironment modifications which ultimately lead to remodeling of the extracellular matrix (51).

At variance, inhibition of PDGFR signaling with an increase in taxol uptake into the tumor and greater therapeutic effect have been described (52). Imatinib, beside its original selectivity for Bcr-Abl tyrosine kinase, affects PDGFR β , lowers IFP and microvessel density, and improves tumor oxygenation, consequently increasing the tumor concentration of small molecules such as docetaxel, or bigger ones such as liposomal doxorubicin (53).

One possible explanation for these controversial findings could be the different inhibitors of angiogenesis used in those study. Also the dose of the anti-angiogenic drug, might play an important role, as a too high dose can cause too rapid vessel pruning and not favor drug delivery and anticancer effects (24). The effect of different doses of RTKI on vessel morphology and functionality was not explored in the above study.

In the light of these considerations, we suggest that the combination of RTKI with chemotherapy is feasible. A better use of pharmacodynamics and pharmacokinetics, might help to maximize the effect and avoid negative interactions of RTKI combined with chemotherapy. Recently we have shown that the addition of certain chemotherapeutics to sunitinib is able to counteract the unwanted negative effect on tumor metastasization (42).

COMBINATIONS WITH OTHER ANGIOGENESIS INHIBITORS

The first combination modalities based on anti-angiogenic compounds used TNP-470, an inhibitor of methionine aminopeptidase, an essential enzyme for endothelial cell proliferation. TNP-470 potentiated the antitumor activity of cytotoxic therapeutics, increasing their biodistribution into tumor tissue, an effect that was sufficient *per se* to account for the greater delay in tumor growth (54).

A number of molecular targets, alternatives to VEGF/VEGFR and related growth factors, implicated in vascular remodeling, are worth considering for the development of novel therapeutic modalities.

Semaphorin 3A (Sema3A) is expressed in endothelial cells, where it serves as an endogenous inhibitor of angiogenesis, and is lost during tumor progression. Its long-term re-expression at a later stage of carcinogenesis stably normalized the tumor vasculature in transgenic mouse tumor models and impaired tumor growth (55). In an accompanying study the authors showed there were larger amounts of doxorubicin in Sema3A-treated tumors, than controls, so Sema3A re-expression substantially extends the normalization window of tumor blood vessels and improves the delivery efficiency of chemotherapeutic drugs (56).

Selective killing of tumor neovasculature with an antibody directed against tumor vascular endothelial VE-cadherin, conjugated with an α -particle-emitting isotope generator, caused vascular remodeling, increased tumor delivery of chemotherapy, and reduced tumor growth. Interestingly, the effect was seen when chemotherapy was scheduled several days after the anti-vascular therapy. The authors pointed out that after depletion of the majority of vessels, the remaining ones appear more mature, so small-molecule drugs more homogeneously distribute and accumulate better, as reflected in the improvement of antitumor activity (57).

COMBINATION WITH VASCULAR TARGETING AGENTS

Therapeutic vascular targeting agents comprise small molecules, mainly tubulin-binding agents, flavonoids, antagonists of junctional proteins intended to selectively target the tumor vasculature (VDA), and compounds that target proteins expressed selectively on tumor vasculature used to deliver bioactive molecules (6, 58, 59). VDA induce morphologic changes in endothelial cells, triggering a cascade of events that results in rapid reduction of blood flow, and vessel occlusion, with subsequent tumor cell death. The hallmark of VDA action is the induction of massive central necrosis of tumor tissues, leaving a rim of viable, actively proliferating cells at the periphery of the lesion. The ability of these proliferating cells to repopulate the tumor explains the limited activity of these agents as monotherapy, but also justifies their use in combination with cytotoxic drugs. IFP levels dropped rapidly after VDA (60) suggesting that if they are used appropriately in conjunction with other drugs the efficacy of treatment may be enhanced. The benefit from such combinations should be complementary, with the VDA acting primarily on the tumor vasculature, and the chemotherapy mainly affecting proliferating tumor cells.

A number of VDA have reached the clinical stage (61). Their effects on tumor vasculature have obvious implications in the design of combination treatments given their possible interference with distribution of the cytotoxic drug (62). The sequence

of administration has to take into account that the vessel shutdown induced by the VDA given after the cytotoxic compound would trap it within the tumor, at the same time preventing the possible VDA-induced impairment of drug distribution in the tumor. Conversely, the opposite schedule, i.e., the VDA before the cytotoxic drug, might generate favorable conditions for its activity because the highly proliferating cells at the periphery of VDA-treated tumors are an ideal target for cytotoxic drugs (7).

We administered the VDA ZD6126 followed by paclitaxel 24–72 h later; this combination had greater antineoplastic activity than each single agent, leading to complete tumor remissions (63). That study showed a significant increase in proliferative activity at the tumor periphery after ZD6126, concomitant with the induction of massive necrosis. It is therefore conceivable that pretreatment with ZD6126 affects the inner part of the tumor, while chemotherapy targets the actively proliferating cells in the viable peripheral rim. The pharmacokinetics of paclitaxel in the ZD6126-treated tumor indicated greater accumulation in the peripheral rim of the tumor than the interior part.

The actual target in the tumor periphery might include endothelial cells, thus providing a rationale for combining a VDA with an anti-angiogenic agent (64). Rapid mobilization of circulating progenitor endothelial cells which home into the viable rim surrounding the necrotic area was reported in a tumor model of mice treated with the VDA OXi-4053, which was associated with the tumor vasculature (65).

THE DUAL FACE OF PACLITAXEL

Paclitaxel is one of the most widely used cytotoxic drugs, employed in the treatments of several neoplasms. This tubulin-binding agent promotes microtubule polymerization (at high concentrations) and impairs microtubule dynamics (at low concentrations), ultimately affecting mitosis, as well as other microtubule-dependent cell functions (66). The anticancer activity of paclitaxel extends beyond its cytotoxicity against tumor cells, since paclitaxel, and the tubulin-binding agents in general, also targets tumor stroma and vasculature inhibiting endothelial cell functions related to angiogenesis, at lower concentrations than those required for the cytotoxic activity (7, 49).

We have shown by *in vivo* optical, and dynamic contrast enhanced (DCE)-MRI imaging that paclitaxel can modify certain tumor vessel functions related to vascular perfusion and permeability (fractional plasma volume, fPV, and volume transfer coefficient, k_{Trans}) (67). This was associated with increased tumor uptake of the antibody F8 (which selectively recognize perivascular EDA-fibronectin) conjugated to interleukin 2 (F8-IL2) (68). The use of antibody-based delivery of therapeutic agents in cancer therapy is beyond our scope and is covered by excellent reviews (59, 69).

Herein paclitaxel given before, but not after, F8-IL2 potentiated the latter's antitumor activity on EDA-Fn expressing human melanoma xenografts. We attributed this to increased vascular permeability and perfusion at the tumor site, as the area perfused by Hoechst 33342 was larger in paclitaxel treated tumors than controls.

Although the mechanism of this effect of paclitaxel is far from clear, our findings are in line with other reports. Jain and coworkers

proposed that taxane-induced tumor cell apoptosis reduced the IFP generated by neoplastic cell proliferation (solid stress) and decompressed tumor blood vessels. The increase in vessel diameter suggests that taxanes might improve tumor response by increasing the vascular surface area for the delivery of therapeutics (70). Paclitaxel and docetaxel lowered IFP and significantly increased albumin extravasation regardless of their cytotoxic activity, suggesting that these effects might be taxane-specific and related to the drugs' pharmacodynamics (71).

The translational potential of these findings is substantiated by clinical studies. In breast cancer patients treated with neo-adjuvant chemotherapy, paclitaxel lowered IFP, and increased oxygenation (72); this suggests that at least these tumors would be best treated first with paclitaxel to reduce IFP and increase pO_2 in order to improve the delivery of subsequent therapy, particularly of large molecules such as antibodies. However, the theory of solid stress in tumors only partially explains the biologic mechanisms by which taxanes boost the activity of combination therapy.

Two mechanisms have been proposed to explain the activity of co-administration of albumin-bound paclitaxel (Abraxane®, nab-paclitaxel) and gemcitabine in patients with pancreatic cancer (73). In a first study nab-paclitaxel increased the intratumoral concentration of gemcitabine in a mouse model of pancreatic ductal adenocarcinoma (PDA) (74). In a second study the nab-paclitaxel co-administered with gemcitabine caused tumor regression, due to a different mechanism, as gemcitabine was stabilized in the tumor by paclitaxel's reduction in the levels of cytidine deaminase, the enzyme primarily responsible for gemcitabine metabolism, with no changes in overall drug delivery (75).

CONCLUSION

The inhibition of tumor growth by drugs affecting the tumor vasculature has been achieved in preclinical and clinical studies. The combination of an angiogenesis inhibitor, namely bevacizumab, with chemotherapy, showed a benefit in patients with advanced disease, leading to increased interest in developing more effective ways to combine anti-angiogenic/vascular targeting agents with conventional chemotherapy. Morphological changes in the

tumor microenvironment and vasculature are widely observed after angiogenesis inhibitors. However, the balance between lowering tumor microvessel density, impairing their function, and reducing/increasing drug uptake needs to be carefully considered in choosing the doses and schedule for combination settings.

Some preclinical studies have reported functional improvement in tumor blood perfusion after angiogenesis inhibitors, with increased tumor exposure to cytotoxic drugs. However, in other studies tumor vascular patency decreased, and hypoxia increased, with impaired cytotoxic drug uptake. The causal relationships between the effect on the microvasculature, the IFP reduction, and the improved trans-vascular transport are still not completely clear.

Nevertheless the combination of angiogenesis inhibitors with chemotherapy is almost always superior to single-drug treatment, indicating the beneficial effect of tumor cell starvation induced by angiogenesis inhibition. The order of administration of the two types of agents – anti-vascular and antitumor – is critical for a successful outcome and has far-reaching impact on the design of combination therapy. Careful optimization of drug scheduling and dosage is essential to maximize tumor response. Robust tumor pharmacodynamics and pharmacokinetics could help in fine-tuning drug timing and sequences so as ultimately to achieve a better outcome.

Monitoring the activity of angiogenesis inhibitors/vascular targeting agents is a significant practical challenge in the clinical setting, where non-invasive procedures such as imaging analysis and the detection of soluble biomarkers can be used to optimize the administration and determine the efficacy of combination regimens in patients.

ACKNOWLEDGMENTS

We are grateful to the Italian Association for Cancer Research (AIRC IG No. 10424, and AIRC 5 per mille No. 12182) for backing to Raffaella Giavazzi, and to Fondazione CARIPLO (No. 2011-0617), for support to Marta Cesca. The authors thank J. D. Baggott for editing assistance.

REFERENCES

- Folkman J. Angiogenesis: an organizing principle for drug discovery? *Nat Rev Drug Discov* (2007) **6**:273–86. doi:10.1038/nrd2115
- Carmeliet P, Jain RK. Molecular mechanisms and clinical applications of angiogenesis. *Nature* (2011) **473**:298–307. doi:10.1038/nature10144
- Ferrara N, Kerbel RS. Angiogenesis as a therapeutic target. *Nature* (2005) **438**:967–74. doi:10.1038/nature04483
- Heath VL, Bicknell R. Anticancer strategies involving the vasculature. *Nat Rev Clin Oncol* (2009) **6**:395–404. doi:10.1038/nrclinonc.2009.52
- Matrana MR, Atkinson B, Jonasch E, Tannir NM. Emerging targeted therapies in metastatic renal cell carcinoma. *Curr Clin Pharmacol* (2011) **6**:189–98. doi:10.2174/157488411797189398
- Tozer GM, Kanthou C, Baguley BC. Disrupting tumour blood vessels. *Nat Rev Cancer* (2005) **5**:423–35. doi:10.1038/nrc1628
- Giavazzi R, Bani MR, Taraboletti G. Tumor-host interaction in the optimization of paclitaxel-based combination therapies with vascular targeting compounds. *Cancer Metastasis Rev* (2007) **26**:481–8. doi:10.1007/s10555-007-9074-y
- Spear MA, Lorusso P, Mita A, Mita M. Vascular disrupting agents (VDA) in oncology: advancing towards new therapeutic paradigms in the clinic. *Curr Drug Targets* (2011) **12**:2009–15. doi:10.2174/138945011798829366
- Gasparini G, Longo R, Fanelli M, Teicher BA. Combination of antiangiogenic therapy with other anticancer therapies: results, challenges, and open questions. *J Clin Oncol* (2005) **23**:1295–311. doi:10.1200/JCO.2005.10.022
- Hurwitz H, Fehrenbacher L, Novotny W, Cartwright T, Hainsworth J, Heim W, et al. Bevacizumab plus irinotecan, fluorouracil, and leucovorin for metastatic colorectal cancer. *N Engl J Med* (2004) **350**:2335–42. doi:10.1056/NEJMoa032691
- Sandler A, Gray R, Perry MC, Brahmer J, Schiller JH, Dowlati A, et al. Paclitaxel-carboplatin alone or with bevacizumab for non-small-cell lung cancer. *N Engl J Med* (2006) **355**:2542–50. doi:10.1056/NEJMoa061884
- Burger RA, Brady MF, Bookman MA, Fleming GF, Monk BJ, Huang H, et al. Incorporation of bevacizumab in the primary treatment of ovarian cancer. *N Engl J Med* (2011) **365**:2473–83. doi:10.1056/NEJMoa1104390
- Perren TJ, Swart AM, Pfisterer J, Ledermann JA, Pujade-Lauraine E, Kristensen G, et al. A phase 3 trial of bevacizumab in ovarian cancer. *N Engl J Med* (2011) **365**:2484–96. doi:10.1056/NEJMoa1103799
- Stark D, Nankivell M, Pujade-Lauraine E, Kristensen G, Elit L, Stockler M, et al. Standard chemotherapy with or without bevacizumab in advanced ovarian cancer: quality-of-life outcomes from the International Collaboration on Ovarian Neoplasms (ICON7) phase 3 randomised trial. *Lancet Oncol* (2013) **14**:236–43. doi:10.1016/S1470-2045(12)70567-3

15. Jonasch E, Tannir NM. Adjuvant and neoadjuvant therapy in renal cell carcinoma. *Cancer J* (2008) **14**:315–9. doi:10.1097/PPO.0b013e31818675d4
16. Scagliotti G, Novello S, Von Pawel J, Reck M, Pereira JR, Thomas M, et al. Phase III study of carboplatin and paclitaxel alone or with sorafenib in advanced non-small-cell lung cancer. *J Clin Oncol* (2010) **28**:1835–42. doi:10.1200/JCO.2009.26.1321
17. Teicher BA. A systems approach to cancer therapy (antioncogenics + standard cytotoxics → mechanism(s) of interaction). *Cancer Metastasis Rev* (1996) **15**:247–72. doi:10.1007/BF00437479
18. Minchinton AI, Tannock IF. Drug penetration in solid tumours. *Nat Rev Cancer* (2006) **6**:583–92. doi:10.1038/nrc1893
19. Baluk P, Hashizume H, McDonald DM. Cellular abnormalities of blood vessels as targets in cancer. *Curr Opin Genet Dev* (2005) **15**:102–11. doi:10.1016/j.gde.2004.12.005
20. McDonald DM, Choyke PL. Imaging of angiogenesis: from microscope to clinic. *Nat Med* (2003) **9**:713–25. doi:10.1038/nm0603-713
21. Jain RK. Normalizing tumor vasculature with anti-angiogenic therapy: a new paradigm for combination therapy. *Nat Med* (2001) **7**:987–9. doi:10.1038/89889
22. Hagendoorn J, Tong R, Fukumura D, Lin Q, Lobo J, Padera TP, et al. Onset of abnormal blood and lymphatic vessel function and interstitial hypertension in early stages of carcinogenesis. *Cancer Res* (2006) **66**:3360–4. doi:10.1158/0008-5472.CAN-05-2655
23. Goel S, Duda DG, Xu L, Munn LL, Boucher Y, Fukumura D, et al. Normalization of the vasculature for treatment of cancer and other diseases. *Physiol Rev* (2011) **91**:1071–121. doi:10.1152/physrev.00038.2010
24. Jain RK. Normalizing tumor microenvironment to treat cancer: bench to bedside to biomarkers. *J Clin Oncol* (2013) **31**:2205–18. doi:10.1200/JCO.2012.46.3653
25. Franco M, Man S, Chen L, Emmenegger U, Shaked Y, Cheung AM, et al. Targeted anti-vascular endothelial growth factor receptor-2 therapy leads to short-term and long-term impairment of vascular function and increase in tumor hypoxia. *Cancer Res* (2006) **66**:3639–48. doi:10.1158/0008-5472.CAN-05-3295
26. Ellis LM, Hicklin DJ. VEGF-targeted therapy: mechanisms of anti-tumour activity. *Nat Rev Cancer* (2008) **8**:579–91. doi:10.1038/nrc2403
27. Cesca M, Frapolli R, Berndt A, Scarlato V, Richter P, Kosmehl H, et al. The effects of vandetanib on paclitaxel tumor distribution and antitumor activity in a xenograft model of human ovarian carcinoma. *Neoplasia* (2009) **11**:1155–64.
28. Marcucci F, Corti A. How to improve exposure of tumor cells to drugs: promoter drugs increase tumor uptake and penetration of effector drugs. *Adv Drug Deliv Rev* (2012) **64**:53–68. doi:10.1016/j.addr.2011.09.007
29. Moschetta M, Cesca M, Pretto F, Giavazzi R. Angiogenesis inhibitors: implications for combination with conventional therapies. *Curr Pharm Des* (2010) **16**:3921–31. doi:10.2174/138161210794455021
30. Ferrara N, Hillan KJ, Gerber HP, Novotny W. Discovery and development of bevacizumab, an anti-VEGF antibody for treating cancer. *Nat Rev Drug Discov* (2004) **3**:391–400. doi:10.1038/nrd1381
31. Yuan F, Chen Y, Dellian M, Safabakhsh N, Ferrara N, Jain RK. Time-dependent vascular regression and permeability changes in established human tumor xenografts induced by an anti-vascular endothelial growth factor/vascular permeability factor antibody. *Proc Natl Acad Sci U S A* (1996) **93**:14765–70. doi:10.1073/pnas.93.25.14765
32. Winkler F, Kozin SV, Tong RT, Chae SS, Booth MF, Garkavtsev I, et al. Kinetics of vascular normalization by VEGFR2 blockade governs brain tumor response to radiation: role of oxygenation, angiopoietin-1, and matrix metalloproteinases. *Cancer Cell* (2004) **6**:553–63. doi:10.1016/j.ccr.2004.10.011
33. Wildiers H, Guetens G, De Boeck G, Verbeken E, Landuyt B, Landuyt W, et al. Effect of antivascular endothelial growth factor treatment on the intratumoral uptake of CPT-11. *Br J Cancer* (2003) **88**:1979–86. doi:10.1038/sj.bjc.6601005
34. Dickson PV, Hamner JB, Sims TL, Fraga CH, Ng CY, Rajasekaran S, et al. Bevacizumab-induced transient remodeling of the vasculature in neuroblastoma xenografts results in improved delivery and efficacy of systemically administered chemotherapy. *Clin Cancer Res* (2007) **13**:3942–50. doi:10.1158/0008-4322.CCR-07-0278
35. Oliva P, Decio A, Castiglioni V, Bassi A, Pesenti E, Cesca M, et al. Cisplatin plus paclitaxel and maintenance of bevacizumab on tumour progression, dissemination, and survival of ovarian carcinoma xenograft models. *Br J Cancer* (2012) **107**:360–9. doi:10.1038/bjc.2012.261
36. Morosi L, Spinelli P, Zucchetti M, Pretto F, Carra A, D'Incalci M, et al. Determination of Paclitaxel distribution in solid tumors by nano-particle assisted laser desorption ionization mass spectrometry imaging. *PLoS ONE* (2013) **8**:e72532. doi:10.1371/journal.pone.0072532
37. Pastuskovas CV, Mundo EE, Williams SP, Nayak TK, Ho J, Ulu-fatu S, et al. Effects of anti-VEGF on pharmacokinetics, biodistribution, and tumor penetration of trastuzumab in a preclinical breast cancer model. *Mol Cancer Ther* (2012) **11**:752–62. doi:10.1158/1535-7163.MCT-11-0742-T
38. Hurvitz S, Pegram M, Lin L, Chan D, Allen H, Dichmann R, et al. Final results of a phase II trial evaluating trastuzumab and bevacizumab as first line treatment of HER2-amplified advanced breast cancer. *Cancer Res* (2009) **69**(Suppl.):6094. doi:10.1158/0008-5472.SABCS-09-6094
39. Willett CG, Boucher Y, Di Tomaso E, Duda DG, Munn LL, Tong RT, et al. Direct evidence that the VEGF-specific antibody bevacizumab has antivascular effects in human rectal cancer. *Nat Med* (2004) **10**:145–7. doi:10.1038/nm988
40. Van der Veldt AA, Lubberink M, Bahce I, Walraven M, De Boer MP, Greuter HN, et al. Rapid decrease in delivery of chemotherapy to tumors after anti-VEGF therapy: implications for scheduling of anti-angiogenic drugs. *Cancer Cell* (2012) **21**:82–91. doi:10.1016/j.ccr.2011.11.023
41. Van der Veldt AA, Lammertsma AA, Smit EF. Scheduling of anticancer drugs: timing may be everything. *Cell Cycle* (2012) **11**:4339–43. doi:10.4161/cc.22187
42. Rovida A, Castiglioni V, Decio A, Scarlato V, Scanziani E, Giavazzi R, et al. Chemotherapy counteracts metastatic dissemination induced by antiangiogenic treatment in mice. *Mol Cancer Ther* (2013). doi:10.1158/1535-7163.MCT-13-0244. [Epub ahead of print].
43. Ma J, Waxman DJ. Combination of antiangiogenesis with chemotherapy for more effective cancer treatment. *Mol Cancer Ther* (2008) **7**:3670–84. doi:10.1158/1535-7163.MCT-08-0715
44. Ma J, Waxman DJ. Modulation of the antitumor activity of metronomic cyclophosphamide by the angiogenesis inhibitor axitinib. *Mol Cancer Ther* (2008) **7**:79–89. doi:10.1158/1535-7163.MCT-07-0584
45. Fenton BM, Paoni SF. The addition of AG-013736 to fractionated radiation improves tumor response without functionally normalizing the tumor vasculature. *Cancer Res* (2007) **67**:9921–8. doi:10.1158/0008-5472.CAN-07-1066
46. Ma J, Chen CS, Blute T, Waxman DJ. Antiangiogenesis enhances intratumoral drug retention. *Cancer Res* (2011) **71**:2675–85. doi:10.1158/0008-5472.CAN-10-3242
47. Garofalo A, Naumova E, Manenti L, Ghilardi C, Ghisleni G, Camatti M, et al. The combination of the tyrosine kinase receptor inhibitor SU6668 with paclitaxel affects ascites formation and tumor spread in ovarian carcinoma xenografts growing orthotopically. *Clin Cancer Res* (2003) **9**:3476–85.
48. Naumova E, Ubezio P, Garofalo A, Borsotti P, Cassis L, Riccardi E, et al. The vascular targeting property of paclitaxel is enhanced by SU6668, a receptor tyrosine kinase inhibitor, causing apoptosis of endothelial cells and inhibition of angiogenesis. *Clin Cancer Res* (2006) **12**:1839–49. doi:10.1158/1078-0432.CCR-05-1615
49. Belotti D, Vergani V, Drudis T, Borsotti P, Pitelli MR, Viale G, et al. The microtubule-affecting drug paclitaxel has antiangiogenic activity. *Clin Cancer Res* (1996) **2**:1843–9.
50. Troiani T, Serkova NJ, Gustafson DL, Henthorn TK, Lockerbie O, Merz A, et al. Investigation of two dosing schedules of vandetanib (ZD6474), an inhibitor of vascular endothelial growth factor receptor and epidermal growth factor receptor signaling, in combination with irinotecan in a human colon cancer xenograft model. *Clin Cancer Res* (2007) **13**:6450–8. doi:10.1158/1078-0432.CCR-07-1094
51. Bello E, Taraboletti G, Colella G, Zucchetti M, Forestieri D, Licandro SA, et al. The tyrosine kinase inhibitor E-3810 combined with paclitaxel inhibits the growth of advanced-stage triple-negative breast cancer xenografts. *Mol Cancer Ther* (2013) **12**:131–40. doi:10.1158/1535-7163.MCT-12-0275-T
52. Pietras K, Rubin K, Sjöblom T, Buchdunger E, Sjoquist M, Heldin CH, et al. Inhibition of

- PDGF receptor signaling in tumor stroma enhances antitumor effect of chemotherapy. *Cancer Res* (2002) **62**:5476–84.
53. Vlahovic G, Ponce AM, Rabbani Z, Salahuddin FK, Zgonjanin L, Spasojevic I, et al. Treatment with imatinib improves drug delivery and efficacy in NSCLC xenografts. *Br J Cancer* (2007) **97**:735–40. doi:10.1038/sj.bjc.6603941
54. Teicher BA, Dupuis NP, Robinson MF, Emi Y, Goff DA. Antiangiogenic treatment (TNP-470/minocycline) increases tissue levels of anti-cancer drugs in mice bearing Lewis lung carcinoma. *Oncol Res* (1995) **7**:237–43.
55. Maiione F, Molla F, Meda C, Latini R, Zentilin L, Giacca M, et al. Semaphorin 3A is an endogenous angiogenesis inhibitor that blocks tumor growth and normalizes tumor vasculature in transgenic mouse models. *J Clin Invest* (2009) **119**:3356–72. doi:10.1172/JCI36308
56. Maiione F, Capano S, Regano D, Zentilin L, Giacca M, Casanovas O, et al. Semaphorin 3A overcomes cancer hypoxia and metastatic dissemination induced by antiangiogenic treatment in mice. *J Clin Invest* (2012) **122**:1832–48. doi:10.1172/JCI58976
57. Escoria FE, Henke E, McDermott MR, Villa CH, Smith-Jones P, Blasberg RG, et al. Selective killing of tumor neovasculature paradoxically improves chemotherapy delivery to tumors. *Cancer Res* (2010) **70**:9277–86. doi:10.1158/0008-5472.CAN-10-2029
58. Thorpe PE. Vascular targeting agents as cancer therapeutics. *Clin Cancer Res* (2004) **10**:415–27. doi:10.1158/1078-0432.CCR-0642-03
59. Neri D, Bicknell R. Tumour vascular targeting. *Nat Rev Cancer* (2005) **5**:436–46. doi:10.1038/nrc1627
60. Skliarenko JV, Lunt SJ, Gordon ML, Vitkin A, Milosevic M, Hill RP. Effects of the vascular disrupting agent ZD6126 on interstitial fluid pressure and cell survival in tumors. *Cancer Res* (2006) **66**:2074–80. doi:10.1158/0008-5472.CAN-05-2046
61. Patterson DM, Rustin GJ. Vascular damaging agents. *Clin Oncol (R Coll Radiol)* (2007) **19**:443–56. doi:10.1016/j.clon.2007.03.014
62. Chaplin DJ, Horsman MR, Siemann DW. Current development status of small-molecule vascular disrupting agents. *Curr Opin Investig Drugs* (2006) **7**:522–8.
63. Martinelli M, Bonezzi K, Riccardi E, Kuhn E, Frapolli R, Zucchetti M, et al. Sequence dependent antitumor efficacy of the vascular disrupting agent ZD6126 in combination with paclitaxel. *Br J Cancer* (2007) **97**:888–94.
64. Goto H, Yano S, Matsumori Y, Ogawa H, Blakey DC, Sone S. Sensitization of tumor-associated endothelial cell apoptosis by the novel vascular-targeting agent ZD6126 in combination with cisplatin. *Clin Cancer Res* (2004) **10**:7671–6. doi:10.1158/1078-0432.CCR-04-1171
65. Shaked Y, Henke E, Roodhart JM, Mancuso P, Langenberg MH, Colleoni M, et al. Rapid chemotherapy-induced acute endothelial progenitor cell mobilization: implications for antiangiogenic drugs as chemosensitizing agents. *Cancer Cell* (2008) **14**:263–73. doi:10.1016/j.ccr.2008.08.001
66. Jordan MA, Wilson L. Microtubules as a target for anticancer drugs. *Nat Rev Cancer* (2004) **4**:253–65. doi:10.1038/nrc1317
67. Moschetta M, Pretto F, Berndt A, Galler K, Richter P, Bassi A, et al. Paclitaxel enhances therapeutic efficacy of the F8-IL2 immunocytokine to EDA-fibronectin-positive metastatic human melanoma xenografts. *Cancer Res* (2012) **72**:1814–24. doi:10.1158/0008-5472.CAN-11-1919
68. Frey K, Schliemann C, Schwager K, Giavazzi R, Johannsen M, Neri D. The immunocytokine F8-IL2 improves the therapeutic performance of sunitinib in a mouse model of renal cell carcinoma. *J Urol* (2010) **184**:2540–8. doi:10.1016/j.juro.2010.07.030
69. Sievers EL, Senter PD. Antibody-drug conjugates in cancer therapy. *Annu Rev Med* (2013) **64**:15–29. doi:10.1146/annurev-med-050311-201823
70. Griffon-Etienne G, Boucher Y, Brekken C, Suit HD, Jain RK. Taxane-induced apoptosis decompresses blood vessels and lowers interstitial fluid pressure in solid tumors: clinical implications. *Cancer Res* (1999) **59**:3776–82.
71. Bronstad A, Berg A, Reed RK. Effects of the taxanes paclitaxel and docetaxel on edema formation and interstitial fluid pressure. *Am J Physiol Heart Circ Physiol* (2004) **287**:H963–8. doi:10.1152/ajpheart.01052.2003
72. Taghian AG, Abi-Raad R, Assaad SI, Casty A, Ancukiewicz M, Yeh E, et al. Paclitaxel decreases the interstitial fluid pressure and improves oxygenation in breast cancers in patients treated with neoadjuvant chemotherapy: clinical implications. *J Clin Oncol* (2005) **23**:1951–61. doi:10.1200/JCO.2005.08.119
73. Zhang DS, Wang DS, Wang ZQ, Wang FH, Luo HY, Qiu MZ, et al. Phase I/II study of albumin-bound nab-paclitaxel plus gemcitabine administered to Chinese patients with advanced pancreatic cancer. *Cancer Chemother Pharmacol* (2013) **71**:1065–72. doi:10.1007/s00280-013-2102-4
74. Von Hoff DD, Ramanathan RK, Borad MJ, Laheru DA, Smith LS, Wood TE, et al. Gemcitabine plus nab-paclitaxel is an active regimen in patients with advanced pancreatic cancer: a phase I/II trial. *J Clin Oncol* (2011) **29**:4548–54. doi:10.1200/JCO.2011.36.5742
75. Frese KK, Neesse A, Cook N, Bapiro TE, Lolkema MP, Jodrell DI, et al. nab-Paclitaxel potentiates gemcitabine activity by reducing cytidine deaminase levels in a mouse model of pancreatic cancer. *Cancer Discov* (2012) **2**:260–9. doi:10.1158/2159-8290.CD-11-0242

Conflict of Interest Statement: The authors declare that the research was conducted in the absence of any commercial or financial relationships that could be construed as a potential conflict of interest.

Received: 17 July 2013; accepted: 15 September 2013; published online: 01 October 2013.

Citation: Cesca M, Bizzaro F, Zucchetti M and Giavazzi R (2013) Tumor delivery of chemotherapy combined with inhibitors of angiogenesis and vascular targeting agents. *Front. Oncol.* **3**:259. doi:10.3389/fonc.2013.00259

This article was submitted to Pharmacology of Anti-Cancer Drugs, a section of the journal *Frontiers in Oncology*.

Copyright © 2013 Cesca, Bizzaro, Zucchetti and Giavazzi. This is an open-access article distributed under the terms of the Creative Commons Attribution License (CC BY). The use, distribution or reproduction in other forums is permitted, provided the original author(s) or licensor are credited and that the original publication in this journal is cited, in accordance with accepted academic practice. No use, distribution or reproduction is permitted which does not comply with these terms.



Current advances in mathematical modeling of anti-cancer drug penetration into tumor tissues

MunJu Kim¹, Robert J. Gillies² and Katarzyna A. Rejniak^{1,3*}

¹ Integrated Mathematical Oncology, H. Lee Moffitt Cancer Center and Research Institute, Tampa, FL, USA

² Department of Cancer Imaging and Metabolism, H. Lee Moffitt Cancer Center and Research Institute, Tampa, FL, USA

³ Department of Oncologic Sciences, College of Medicine, University of South Florida, Tampa, FL, USA

Edited by:

Angelo Corti, San Raffaele Scientific Institute, Italy

Reviewed by:

Timothy W. Secomb, University of Arizona, USA

Philippe Martinive, University of Liège, Belgium

Hermann Frieboes, University of Louisville, USA

***Correspondence:**

Katarzyna A. Rejniak, Integrated Mathematical Oncology, H. Lee Moffitt Cancer Center and Research Institute, 12902 Magnolia Drive, SRB-4 24000G, Tampa, FL 33612, USA

e-mail: kasia.rejniak@moffitt.org

Delivery of anti-cancer drugs to tumor tissues, including their interstitial transport and cellular uptake, is a complex process involving various biochemical, mechanical, and biophysical factors. Mathematical modeling provides a means through which to understand this complexity better, as well as to examine interactions between contributing components in a systematic way via computational simulations and quantitative analyses. In this review, we present the current state of mathematical modeling approaches that address phenomena related to drug delivery. We describe how various types of models were used to predict spatio-temporal distributions of drugs within the tumor tissue, to simulate different ways to overcome barriers to drug transport, or to optimize treatment schedules. Finally, we discuss how integration of mathematical modeling with experimental or clinical data can provide better tools to understand the drug delivery process, in particular to examine the specific tissue- or compound-related factors that limit drug penetration through tumors. Such tools will be important in designing new chemotherapy targets and optimal treatment strategies, as well as in developing non-invasive diagnosis to monitor treatment response and detect tumor recurrence.

Keywords: drug penetration, drug distribution, drug pharmacodynamics, tumor microenvironment, solid tumor, mathematical modeling

INTRODUCTION

Systemic chemotherapy is one of the most widely used treatments in all kinds of cancers and at every stage of tumor progression. However, success of the systemic treatment depends not only on the efficacy of chemical compounds, but also on whether these compounds can reach all tumor cells in concentrations sufficient to exert therapeutic effect. Most clinically used anti-cancer drugs, however, lead to the emergence of anti-drug resistance, and to overcome this therapeutic limitation, the chemotherapeutic agents are often used in combination with other drugs of different pharmacokinetic properties or in combination with other anti-cancer treatments.

The process of drug delivery is complex and embraces different temporal and spatial scales, including the organism level (where drug absorption, distribution, metabolism, excretion, and toxicity are studied in various organs and are known together under the acronym ADME-T), tissue and cell scales (where the main processes include drug extravasation into the tumor tissue, its penetration via interstitial transport, and cellular uptake), and intracellular level (where drug internalization, intracellular pharmacokinetics, accumulation, and efflux are investigated). In this review, we will focus on these mathematical models that act on the tissue scale. We refer the reader to the following research papers and review articles that address the other modeling scales (1–11).

Transport of drug particles at the tissue level encounters several physiological and physical barriers. The architecture of tumor vasculature is leaky and tortuous when compared to the vasculature of normal tissues. As a result, the blood flow is chaotic and the supply of nutrients and drugs irregular. This, in turn, leads to the emergence of regions of transient or permanent hypoxia. The cellular and stromal architecture of tumor tissue is far from being as well organized as that of normal tissues, and it is characterized by increased cell packing density, high variability in tumor cell sizes, and their locations. Together, these result in a non-uniform exposure of tumor cells to metabolites and drugs. Elevated interstitial fluid pressure (IFP), which is a consequence of the lack of functional lymphatic vessels, and vascular hyperpermeability, reduce extravasation of both fluid, and drug molecules from the vascular system, hindering advective transport through the tumor tissue. A dense extracellular matrix (ECM) with irregular alignment of ECM fibers and with increased fiber cross-linking, also hinders the diffusion process. In general, it is difficult to predict the extent of drug penetration into the tumor tissue and to determine the influence of various microenvironmental factors on drug interstitial transport. The former issue can be addressed by developing imaging techniques to visualize either the drug uptake or its lethal effects. The latter can be tested using systematical computational simulations of properly formulated mathematical models.

Several imaging approaches have been used to visualize the effects of drug penetration into the tumor tissue, including naturally fluorescent drugs showing their spatial distribution (12–14), specific imaging biomarkers showing the effects of anti-cancer drugs, such as cell DNA damage (15, 16), intravital microscopic imaging for real-time *in vivo* drug distribution (17), or molecular photoacoustic tomography (18). Numerous imaging techniques and their use in oncology have been reviewed in Weissleder and Pittet (19), Gillies et al. (20), and Morse and Gillies (21).

Mathematical modeling provides tools for examining which of the various biophysical features of the tumor tissue and/or stroma and biochemical properties of drug compounds contribute significantly to limited drug penetration. *In silico* simulations are well-suited for testing combinations of multiple parameters that can be varied simultaneously in a controlled manner and over a wide range of values. Such a broad screening of drug or tissue conditions is rarely possible in laboratory experiments, but it is relatively easy and cheap in computer simulations. These theoretical screenings can help to determine the properties of therapeutic compounds optimal for their efficient interstitial transport (designing *in silico* drugs) or make decisions regarding the most effective drug combinations and scheduling protocols (designing *in silico* trials). Moreover, mathematical modeling allows for bridging laboratory experiments with clinical applications by providing the means to extrapolate the *in vivo* results from mouse models to humans. Recently, several review papers discussing the power of mathematical and biophysical modeling have been published (22–29).

In this review, we will focus on the most recent research articles that use mathematical and computational models of anti-cancer drugs acting on the cell and tissue scales. In the most general description, changes in the amount of drug present in the tissue depend on three values: the amount of drug entering the tissue (drug production), how the drug moves within the tissue (drug transport), and the amount leaving the tissue (drug elimination). However, various phenomena can contribute to each of these three processes. For example, a drug can be supplied from the preexisting vascular system or can be released within the tissue from a moving drug carrier (such as a nanoparticle), or it can be activated due to specific environmental conditions (for example, low oxygen level or high acidity). Drugs can be carried through the tissue with the interstitial fluid flow (advective transport) or move randomly due to the Brownian motion of drug molecules (diffusive transport). Drug elimination from the tissue can take place due to its natural half-life (decay), binding to the ECM (degradation or deactivation), or cellular uptake. Mathematically the simplest equation describing the kinetics of drug concentration $c(x,t)$ at location x and at time t may be written as follows:

$$\underbrace{\frac{\partial c(x,t)}{\partial t}}_{\text{change in drug concentration}} = \underbrace{\kappa|_{\text{at region}}}_{\substack{\text{supply, release, activation} \\ \text{DRUG PRODUCTION}}} + \underbrace{D\Delta c(x,t) - u(x,t) \cdot \nabla c(x,t)}_{\substack{\text{diffusion} \\ \text{advection} \\ \text{DRUG TRANSPORT}}} - \underbrace{\alpha c(x,t)}_{\substack{\text{decay, deactivation} \\ \text{DRUG ELIMINATION}}} - \underbrace{\beta c(x,t)|_{\text{at cell}}}_{\text{cellular uptake}}$$

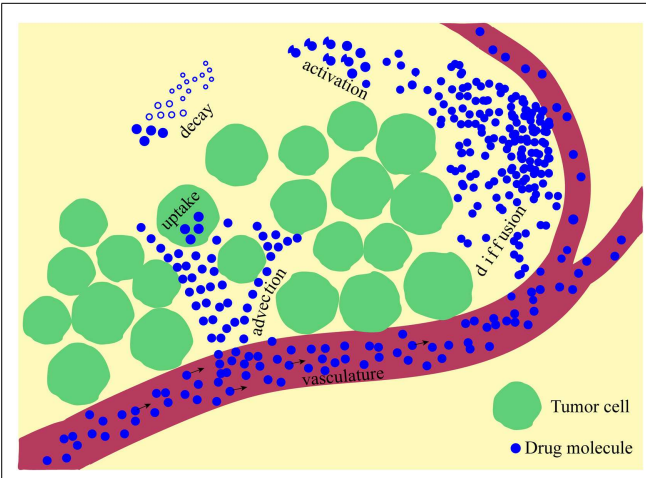
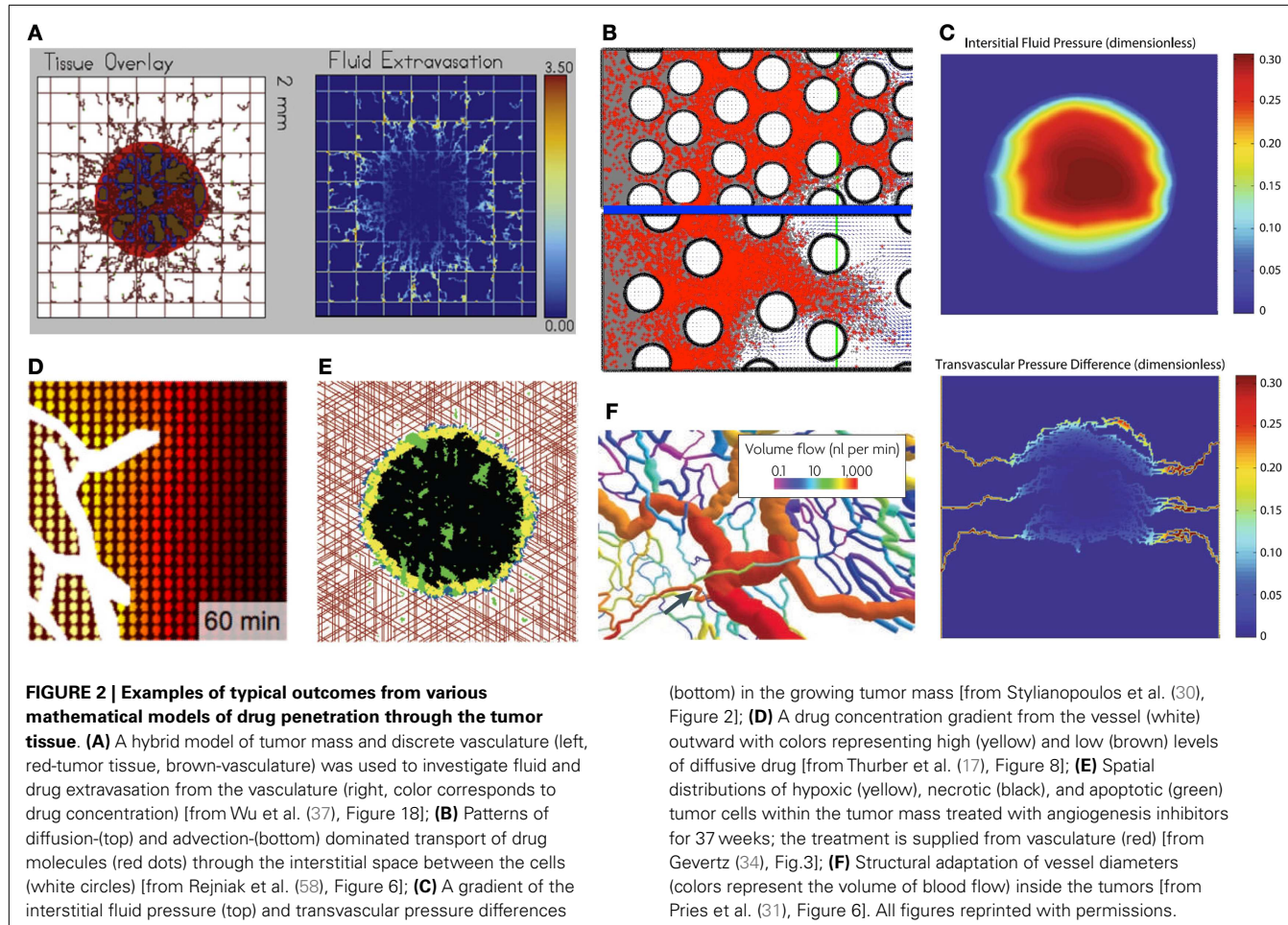


FIGURE 1 | A schematic representation of multiple physical processes involved in drug penetration into the tumor tissue. Drug molecules are supplied from the vasculature and move through the interstitial space via diffusive and advective transports, can be activated and are subject to natural decay before they are taken up by the cells.

Here, κ is a constant rate of drug supply, release, or activation that takes place in a part of the domain (region), which may be a blood vessel (supply), nanoparticle (release), or low oxygen area (activation); D is a constant diffusion coefficient; $u(x,t)$ is the velocity of the interstitial fluid; α is a decay or deactivation rate constant; and β is a rate constant of drug uptake by the cell. Schematically, all processes involved in the drug kinetics are shown in Figure 1. Notably, each of these factors may take a more complex form. A more detailed discussion regarding these processes follows below, and we give examples of how they have been addressed in the mathematical modeling literature and applied to anti-cancer drug kinetics.

MODELS ADDRESSING DRUG VASCULAR SUPPLY

After intravenous infusion, drug molecules circulate in the vascular system before they extravasate into the surrounding tissue. The drug influx rate κ is assumed constant in the equation listed above; however, more complex cases can be modeled wherein the vascular supply process depends not only on the molecule's size, but also on the physical properties of the vasculature and the target tissue. In general, small drug or metabolite molecules can cross the vascular wall more easily than larger molecules can, and they can extravasate into both healthy and tumorous tissues. Larger molecules, such as nanoparticles, require vascular fenestration with larger pores to be able to leave the blood circulation system. Additional factors, such as electrostatic interactions between the particles and the negatively charged pores of



the vessel wall, have been studied by Stylianopoulos et al. (30). The mathematical model predictions suggested that electrostatic repulsion has a minor effect on the transvascular transport of nanoparticles, but electrostatic attraction, caused even by small cationic charges, can lead to a significant increase in the transvascular flux of nanoparticles into the tumor interstitial space (**Figure 2C**).

The blood microcirculation within solid tumors is dysfunctional due to highly irregular vasculature (**Figure 2F**) that hinders delivery of both nutrients and drugs (31, 32). To investigate the distribution processes of small molecule drugs to cancer cells, a computational model based on fluorescent images of tumor functional vasculature was designed by Thurber et al. (17). The model was calibrated with experimental data and used to predict temporal changes in drug distribution profile around vessels with intermittent blood flow for a typical drug administration schedule (**Figure 2D**). Vascular images were also used by Baish et al. (33) to design a mathematical model that analyses drug diffusion in irregularly shaped domains based on two simple measures of vascular geometry. These include the maximum distance in the tissue from the nearest blood vessel and a measure of the shape of the spaces between vessels. This model can also predict how new therapeutic agents that inhibit or stimulate vascular

growth alter the functional efficiency of the vasculature within the tumor tissue. Computational simulations of vasculature-targeting agents and their influence on tumor growth have been also performed by Gevertz (34, 35). These biophysical models (**Figure 2E**) were used to explore the therapeutic effectiveness of two drugs that target the tumor vasculature, angiogenesis inhibitors (such as *avastin*) and vascular disrupting agents (such as *combretastatin*). The simulation results suggested that vasculature-targeting agents, as currently administered, cannot lead to cancer eradication, although a highly efficacious agent may lead to long-term cancer control. The models, however, identified a treatment regimen that can successfully halt simulated tumor growth, even after the cessation of therapy.

Another computational study has been performed to test the effects that different drugs exert on the same mass of tumor tissue. Sinek et al. (36) compared the effectiveness of *doxorubicin* and *cisplatin* in vascularized tumors taking into account vascular and morphological heterogeneity. The simulation results showed that lesion-scale drug and nutrient distribution may significantly impact therapeutic efficacy. It has been also shown how the therapeutic effectiveness of *doxorubicin* penetration depends upon other determinants affecting drug distribution, such as cellular efflux and density, offering some insight into the conditions under

which otherwise promising therapies may fail and, more importantly, when they will succeed. These simulations indicated that macroscopic environmental conditions, notably drug and nutrient distributions, give rise to considerable variation in lesion response, hence clinical resistance. Moreover, the synergy or antagonism of combined therapeutic strategies depends heavily upon this environment.

The elevated IFP and high hydraulic conductivity can act like microenvironmental barriers for transvascular transport to both anti-cancer drugs and nutrients, as have been investigated by Wu et al. (37). It has been shown computationally that small blood vessel resistance and collapse may contribute to lower transcapillary flux of oxygen. Moreover, the higher IFP distribution in the simulated tumors affected oxygen extravasation negatively, which, in turn, hindered tumor growth by decreasing the oxygen transfer to the tissue (**Figure 2A**). In another study Pozrikidis (38) has investigated the overall hydrodynamics of the leakage problem through a permeable capillary, taking into account hydraulic conductivity of arterial, venous, and extravasation flow rates. This showed that interstitium dilation promoted the rate of extravasation.

MODELS ADDRESSING DRUG RELEASE AND ACTIVATION

To increase efficacy of therapeutic compounds and increase the time of drug survival inside the tumor tissue beyond its half-life, various methods of drug release and activation have been proposed. In our simple equation listed above, the release/activation rate κ is defined as a constant, and the release/activation region is hypothetical. However, more complex mechanisms can be incorporated in the models. The release region can represent a nanoparticle and can be varied in both space and time according to the changes in carrier locations; the activation rate may depend on local drug concentration or distribution of metabolites and may take place in hypoxic/acidic tumor areas, respectively, or may be stimulated by external factors, such as temperature or magnetic fields.

Nanoparticles have gained much interest as potential carriers of therapeutic agents due to their size, which enable them to extravasate in the leaky tumor vasculature preferentially, and due to their modular functionality, which allows for release of the drug by controlled diffusion from the core across the polymeric membrane to the matrix. A mathematical model taking into consideration avascular tumor growth followed by angiogenesis and nanoparticle-based drug delivery has been applied by van de Ven et al. (39) to design optimal therapeutic protocols. In particular, the effects of nanoparticles carrying *doxorubicin* were simulated for various parameter values to determine how much drug per particle and how many particles need to be released within the vasculature to achieve remission of the tumor. Moreover, it has been shown that cell death on a population level is non-linear with respect to the drug concentration. The same team has simulated vascular accumulation of blood-borne nanoparticles to analyze how nanoparticle vascular affinity depends on its size and ligand density, as well as vascular receptor expression (40). It has been shown that for high vascular affinities, nanoparticles tend to accumulate mostly at the inlet tumor vessels, leaving the inner and outer vasculature depleted of nanoparticles. For low vascular affinities, nanoparticles distribute quite uniformly in the intratumoral

vasculature, but they exhibit low accumulation doses. It has been shown that an optimal vascular affinity can be identified by providing the proper balance between accumulation dose and uniform spatial distribution of the nanoparticles. This balance depends on the stage of tumor development (vascularity and endothelial receptor expression) and the nanoparticle properties (size, ligand density, and ligand-receptor molecular affinity). The timing and the location of drug release from nanoparticles have been investigated by Kim et al. (41) in a combination of *in vitro* experiments and mathematical modeling. It has been shown that gold nanoparticles carrying either *fluorescein* or *doxorubicin* molecules move and localize differently in an *in vitro* three-dimensional (3D) model of tumor tissue, depending on whether the nanoparticles are positively or negatively charged. Fluorescence microscopy and mathematical modeling show that uptake, not diffusion, is the dominant mechanism in particle delivery. These results indicate that positive particles may be more effective for drug delivery because they are taken up to a greater extent by proliferating cells. Negative particles, which diffuse more quickly, may perform better when delivering drugs deep into tissues.

Another drug carrier, engineered macrophages, that are capable of delivering pro-drugs to hypoxic areas within the tumor have been modeled by Webb et al. (42) and Owen et al. (43). In the former paper, two modes of action in the multicellular spheroids were investigated: either the macrophages delivered an enzyme that activated an externally applied pro-drug (bystander model), or they delivered cytotoxic factors directly (local model). The bystander model was comparable to traditional chemotherapy, with poor targeting of tumor cells in the center of the spheroid that are assumed hypoxic; on the other hand, the local model was more selective for the hypoxic regions. This work suggested that effective targeting of hypoxic tumor cells may require the use of drugs with limited mobility or whose action does not depend on cell proliferation. The latter article addressed a case where therapeutic macrophages were preloaded with nanomagnets and a magnetic field was applied to the tumor site. Both the conventional chemotherapy and chemotherapy with macrophages delivering hypoxia-inducible drugs were compared, and model simulations predicted that combining conventional and macrophage-based therapies would be synergistic, producing greater antitumor effects than the additive effects of each form of therapy. The model also revealed that timing is crucial in this combined approach with efficacy being greatest when the macrophage-based, hypoxia-targeted therapy is administered shortly before or concurrently with chemotherapy.

The effects of applying heat to tumors treated with *cisplatin* have been investigated by El-Kareh and Secomb (44). A theoretical model for the intraperitoneal delivery of *cisplatin* and heat to tumor metastases in tissues adjacent to the peritoneal cavity has shown increased cell uptake of drug, increased cell kill at a given level of intracellular drug, and decreased microvascular density. The model suggested that the experimental finding of elevated intracellular *platinum* levels up to a distance of 5 mm when the drug is delivered by a heated infusion solution is due to penetration of heat, which causes increased cell uptake of the drug. The effects of hyperthermia on chemotherapy were also investigated by Gasselhuber et al. (45) by developing a spatio-temporal

model of the release of *doxorubicin* from low temperature sensitive liposomes. This model showed that this treatment combined with thermal ablation allowed for localized drug delivery with higher concentrations in the tumor tissue than conventional chemotherapy.

MODELS ADDRESSING DRUG DIFFUSIVE TRANSPORT

In the model equation listed above, we used a constant diffusion rate D that leads to homogeneous diffusive transport. However, the diffusion may depend on the structure and other physical properties of the tissue in which this process occurs. One extension of the above equation has been widely used in modeling the spread of gliomas in the brain where the diffusion in the white matter and gray matter was characterized by different diffusion coefficients (46, 47).

In the context of drug penetration into the tumor tissue, Venkatasubramanian et al. (48) have created a mathematical model integrating intracellular metabolism, nutrient and drug diffusion, cell-cycle progression, and drug pharmacokinetics. Results indicated the existence of an optimum drug diffusion coefficient. A low diffusivity prevents effective penetration before the drug is cleared from the blood, and a high diffusivity limits drug retention. This result suggests that increasing the molecular weight of the anti-cancer drug by nanoparticle conjugation would improve its efficacy. The simulations also showed that tumors that grow fast are less responsive to therapy than are tumors growing more slowly with greater numbers of quiescent cells, demonstrating the competing effects of regrowth and cytotoxicity.

The complex interactions of drug particles and the ECM fibers that may hinder the drug molecule diffusion process have been modeled by Stylianopoulos et al. (49, 50). In this 3D model, stochastic fiber networks with varying degrees of alignment were considered. Quantitative analysis of four different structures, ranging from nearly isotropic to perfectly aligned, were performed. The results indicated that the overall diffusion coefficient is not affected by the orientation of the network. However, structural anisotropy results in diffusion anisotropy, which becomes more significant with an increase in the degree of alignment, the size of the diffusing particles, and the fiber volume fraction. These model predictions were validated experimentally, showing for the first time in tumors that the structure and orientation of collagen fibers in the extracellular space leads to diffusion anisotropy. The authors also investigated the effects of charge on the diffusive transport of macromolecules and nanoparticles in the ECM, taking into account steric, hydrodynamic, and electrostatic interactions. The model showed that electrostatic forces between the fibers and the particles result in slowed diffusion. However, the repulsive forces become less important as the fiber diameter increases. These results suggest that optimal particles for delivery to tumors should be initially cationic to target the tumor vessels and then change to neutral charge after exiting the blood vessels.

Since the ECM is composed of multiple cross-linked fibers, the drug particle diffusion in the interstitial space may rather resemble random movement through small nanochannels than diffusion through the open homogeneous space. A computational model that accounts for interface effects on diffusivity has been developed and validated by predicting experimental glucose diffusion

through a nanofluidic membrane (51–53). Moreover, the passive transport of nanoparticles from bulk into a nanochannel has been modeled, showing that subtle changes in nanochannel dimensions may alter the energy barrier. This results in different nanoparticle penetration depths and diffusion mechanisms.

More detailed models of ECM structure, including fiber orientation, cross-link, and remodeling by the embedded cells have been developed by Bauer et al. (54, 55), Dallon and Sherratt (56) and Dallon et al. (57) in the context of vessel sprout and wound healing, respectively. These models have not yet been applied to model the role of ECM structure on drug molecule penetration. However, cellular heterogeneity of the stroma and its influence on both diffusive and advective forms of transport have been modeled by our group using idealized tissue morphologies of various porosity and cellularity values (58). Our simulations revealed that irregularities in the cell spatial configurations can solely result in the formation of interstitial corridors that are followed by drug or imaging agent molecules, leading to the emergence of tissue zones with less exposure to the drugs. Moreover, we showed that the relation between tissue porosity (defined as the extent of void space in the tissue), cellular density (defined as the number of cells per tissue area), and permeability (defined as time needed for a certain number of particles to traverse a predefined distance) is non-linear; thus it is also non-intuitive.

MODELS ADDRESSING DRUG ADVECTIVE TRANSPORT

During advective transport, drug molecules are carried with the flow of the interstitial fluid. This flow can arise from pressure differences within the tissue or from drainage of the fluid into the lymphatic circulation system. Wu et al. (37) investigated the role of the IFP, interstitial fluid flow, and the lymphatic drainage system on the transport of metabolites in developing tumors. The model simulations showed that elevated interstitial hydraulic conductivity combined with poor lymphatic function is the root cause of the development of plateau profiles of the IFP in the tumor, which have been observed in experiments.

At the macroscopic scale, where the individual cells are modeled as surrounded by the ECM space that is interpenetrated by the interstitial fluid, our group investigated the role of both advection and diffusion of drug molecules movement through the stroma (58). Simulation results collected from more than 100 different tissue morphologies showed that tissue cellular porosity and density influence the depth of drug penetration in a non-linear fashion. It has also been shown that for small diffusion coefficients, drug transport is advection dominated independently of tissue structure. Similarly, for all tissue structures considered in our simulations, drug molecule transport was diffusion dominated for large diffusion coefficients. However, for the intermediate values of fluid flow velocity and diffusion coefficients, the nature of interstitial transport depends strongly on the tissue morphology (Figure 2B). This indicates that sole knowledge of drug and tumor biophysical properties without knowledge of tumor tissue histology may lead to false predictions regarding the extent of drug penetration into the tumor tissue.

The significant role of the advective fluid flow in brain tumors has been investigated by Arifin et al. (59, 60). In this work, a computational model was employed to simulate 3D patient-specific

distribution of *carmustine*. This model showed that a quasi-steady transport process is established within 1 day following treatment, and the drug is eliminated rapidly by transcapillary exchange, while its penetration into the tumor is mainly by diffusion. Convection appears to be crucial in influencing the drug distribution in the tumor resulting in non-homogeneous exposure to the drug; the remnant tumor near the ventricle is, by one to two orders of magnitude, less exposed to the drug than is the distal remnant tumor. In addition, local convective flow within the cavity appears to be a crucial factor in distributing the drug so that the tumor domain near the ventricle is prone to minimal drug exposure. The authors also simulated four chemotherapeutic agents (*carmustine*, *paclitaxel*, *fluorouracil*, and *methotrexate*) in a realistic 3D tissue geometry extracted from magnetic resonance images of a brain tumor. The simulation analysis showed that only *paclitaxel* exhibited minimal degradation within the cavity, as well as the best penetration of the remnant tumor.

A mixture of computational modeling and laboratory experiments on gels and tumors reported in Ramanujan et al. (61) showed that the diffusive transport of drug particles might be obstructed more significantly by collagen fiber alignment than particle movement due to fluid advection.

MODELS ADDRESSING DRUG DECAY, DEACTIVATION, AND CELLULAR UPTAKE

In our simple equation above, the rate of drug decay, deactivation, and cellular uptake were defined as proportional to the local drug concentration. In the case of drug decay this is a typical way of incorporating drug half-life. In the case of drug deactivation or degradation, these processes may also depend on environmental factors, such as binding to ECM fibers or interacting with other microenvironmental factors. This aspect of drug pharmacodynamics has usually been neglected in mathematical models due to insufficient experimental data to inform or validate the models. However, with the recent advances in visualizing and experimentally quantifying ECM fibril structure, this process should be easier to incorporate in future mathematical models. Additionally, the process of cellular uptake can depend on various factors. Certain drug molecules may bind to specific cell membrane receptors, and the efficacy of this process will then depend on the number of available receptors. Others may diffuse through the cell membrane, and this diffusion process will depend on both extracellular and intracellular drug concentrations.

The complex interplay between molecular size, affinity, and tumor uptake has been investigated by Schmidt and Wittrup (62) using a mechanistic model that takes into account drug molecular radius, interstitial diffusivity, available volume fraction, and plasma clearance. This model allowed for predicting the magnitude, specificity, time dependence, and affinity dependence of tumor uptake across a broad size spectrum of therapeutic agents. The authors concluded that the intermediate-size targeting agents (~25 kDa) have the lowest levels of tumor uptake, when compared to tumor uptake levels achieved by smaller and larger agents. In Thurber and Wittrup (63), this model was extended to create a mechanistic description of total antibody uptake in a tumor, taking into account both free (unbound) antibody in the interstitium and antibody bound to its target. This allowed for an estimation

of the time course of antibody uptake in solid tumors and its clearance from the blood plasma.

The cellular pharmacodynamics of various anti-cancer drugs was investigated by a mathematical model that takes into account cellular uptake of the drug and both intracellular and extracellular cytotoxicities. In El-Kareh and Secomb (64), the damage induced by *doxorubicin* was expressed as the sum of two terms, representing the peak values over time of intracellular and extracellular drug concentrations. Drug uptake by cells was assumed to include both saturable and unsaturable components, which provided better fits to *in vitro* cytotoxicity data. Model simulations suggested also a mechanism for the emergence of plateaus in the dose-response curve at high concentrations and short exposure time, as observed experimentally in some cases. Similar models were used to investigate the pharmacodynamics of *cisplatin* (65) and *paclitaxel* (66).

TOWARD CLINICAL APPLICATIONS OF MATHEMATICAL MODELS

Mathematical models can also provide the means to scale experimental results from animal to human body size and metabolism, and can be used to test various drug administration procedures and schedules (bolus injections, dose-dense therapies, continuous infusions, and adaptive therapies) in virtual human body. El-Kareh and Secomb (67) used mathematical modeling to determine the optimal mode of delivery for *doxorubicin* by comparing three intravenous administration methods: bolus injection, continuous infusion, and liposomal delivery. The model took into account the relatively slow rate and saturability of *doxorubicin* uptake by cells and predicted peak concentrations of drug attained in tumor cells, as well as peak concentration of free *doxorubicin* in blood plasma. The model simulations suggested that continuous infusion for optimal durations is superior to the other delivery methods. A similar model, but using the tumor cord geometry, was used by Eikenberry (68) to test *doxorubicin* dose optimization. Model simulations showed that extending drug infusion time up to 2 h and fractionating large doses are two strategies that may preserve or increase anti-tumor activity, as well as reduce cardiotoxicity, by decreasing peak plasma concentration. Traina et al. (69) used the Norton-Simon tumor volume growth kinetic model (70) to predict a tolerable dose of *capecitabine* (7 days treatment followed by a 7-day rest) for advanced-stage breast cancer patients and this prediction was confirmed in phase I study. Traina et al. (71) continued to use the Norton-Simon model to optimize chemotherapeutic dosages and schedules in mouse xenograft models. Similar mathematical models have been used to study dose-dense chemotherapies (72) and to evaluate both the limitations of current schedules in breast cancer treatment and therapeutic advantages of novel dose-dense chemotherapies (73). Gatenby et al. (74) examined a novel approach in which cancer therapy was adapted to the evolving temporal and spatial variability of the tumor microenvironment, cellular phenotypes, and therapy-induced perturbations instead of using a typical linear protocol of drug administration. The developed mathematical model suggested that if resistant populations are present before administration of therapy, the total elimination of the drug-sensitive subpopulation will lead to the faster growth of a drug-resistant population. As an alternative,

the simulated treatment was continuously modulated to control the size of tumor cell population that resulted in prolonged survival. The authors went a step further and, actually, tested their predictions experimentally. In subsequent work, Silva et al. (3) parameterized the adaptive therapy model using *in vitro* experiments and showed that this treatment strategy delays tumor burden and increases time to progression in tumor models.

The computational models are also well-suited to simulate treatments based on patient-specific parameters and tissue characteristics leading to personalized medicine. Our group investigates interstitial transport of drug and imaging agents using digitized samples of patients' tumor histology (58). Frieboes et al. (75) implemented a mathematical model of tumor drug-response that integrates simulations with biological data and includes the experimentally observed resistant phenotypes of individual cells. This integrative method could be used to predict resistance based on specific tumor properties, potentially improving treatment outcome. Kim et al. (76) uses a combination of micro- and macroscopic imaging data and computational modeling to investigate blood flow in the heterogeneous tumor tissues. Venkatasubramanian et al. (77) uses breast cancer patients' DCE-MRI (dynamic contrast-enhanced magnetic resonance imaging) data to predict their responsiveness to therapeutic treatment. Their model simulations showed that transvascular transport was correlated with tumor aggressiveness because of the formation of new vessels, and that increased transport heterogeneity led to increased tumor growth and poor drug-response.

Clinically used imaging techniques will be crucial in integrating mathematical models with clinical data in order to make patient-specific predictions. For example, DCE-MRI technique allows for collecting time-activity curves with high spatial and temporal resolution following a bolus injection of a Gadolinium-containing contrast agent, CA. The resulting data can be analyzed to generate spatially explicit (2D and 3D) maps of flow, perfusion, extracellular/extravascular volume fraction and, in some cases, water permeability (78, 79). In general, the delivery and extravasation of CA is modeled with standard 2- or 3-compartment PK models (80) and, as mentioned above, these maps can be used to infer drug distribution in human tumors (77, 81). While many investigators use ROI (region of interest) analyses to derive a single perfusion value to describe a tumor, it is becoming increasingly appreciated that enhancement is heterogeneous and that quantitative descriptors of this heterogeneity improve the precision for diagnosis and monitoring of therapy response (82–86). We contend that perfusion heterogeneity is a key factor in the response of tumors to therapy, both in terms of drug delivery and in the establishment of specific habitats that select for cells with specific phenotypes and hence, therapy responses (87).

CONCLUSION AND FUTURE DIRECTIONS

In this review, we discussed various mathematical models that were used to address different aspects of drug penetration through tumor tissue. All major stages of the penetration process have been investigated computationally: flow to different regions of tumors via blood vessels, crossing the vessel wall by drug molecules, their penetration through the interstitial tumor space, and cellular uptake. Mathematical models are well-suited to address such

complex phenomena since by their nature they are able to handle multiple variables with numerous parameters. It is relatively easy and inexpensive to simulate tumor growth and treatment *in silico* and to compare differences in simulation outcomes when such parameters are changed simultaneously and over a wide range of values. In fact, this area of mathematical research is dynamically expanding. Especially novel are models that account for spatial aspects of drug transport. Half of the papers described in this review and all of the images collected in Figure 2 come from manuscripts that were published in the last 3 years, showing that this field is highly active and productive.

Typically in mathematical models, the drugs are defined as concentrations, as we did in the equation above. This is motivated by the fact that the number of drug molecules considered in the model might be a couple of orders of magnitude larger than the number of cells that form the tissue. However, in this description, only average behavior of drug molecules is captured. When more detailed drug kinetics need to be considered, such as molecule binding to cell receptors, intracellular trafficking, or mechanisms of drug extravasation from a vessel, drugs may be modeled as collections of individual molecules and can be traced individually in the model. Several novel models of this kind have been recently developed. Among models discussed in this review, the work of Ziemys et al. (51, 52), Mahadevan et al. (53), Frieboes et al. (40), and Rejniak et al. (58) traces the behavior of individual drug molecules and their interactions with the cells and/or vessels. In the first two papers the authors also discuss how to scale between the description of the kinetics of individual drug molecules and more general description of drug concentration.

Similarly, the more classical modeling approaches consider tumors as large populations of cells and represent them as cell densities (25, 36, 37, 40, 59, 64, 67, 68, 71, 73, 74, 81). These models can handle multiple cell subpopulations, but the number of different cell types has to be defined *a priori*, and new subpopulations cannot be dynamically created during the simulation. However, under specific conditions cells can be moved from one subpopulation to another. The predefined cell types may include a specific phase of the cell-cycle (a population of cells in G1, G0, S, or G2 phase), a particular cell phenotype (a population of proliferating, quiescent, hypoxic, or necrotic cells), or a particular cell response to the treatment (a population of drug-resistant or drug-sensitive cells). The advantage of continuous models is that they can handle large populations of cells, but the significant disadvantage is that all cell properties in these models must be averaged, since no individual cells are considered. In view of the growing evidence of heterogeneity of tumor cells on the genetic, phenotypic, and drug-response levels, the averaged cell properties and the averaged cell responses to anti-cancer treatments may not be sufficient to make predictions for individual patients.

In contrast, in the individual-cell-based models (called also the single-cell-based models, or the agent-based models) each cell is represented as a separate entity that acts as an independent agent according to some predefined rules (cell phenotype), but cell behavior can also be modulated by interactions with other cells and with the immediate cell microenvironment (selection forces). In this class of models cells may differ from each other significantly (cells may have distinct phenotypes, independently

regulated cell-cycles, different levels of receptors, or different accumulations of mutations). Several models discussed in this review are single-cell-based (34, 35, 43, 52, 53, 58). The main advantage of these models is their natural cellular heterogeneity that better represents tumor multicellular composition than the continuous models. It is, of course, possible to analyze results of individual-cell-based models on a cell population level (in terms of average values and standard deviations, distributions, or correlations), similarly as this is done with experimental measurements. Moreover, these analyses can be compared to results from continuous models. The inverse process, that is extracting detailed information on individual cells from continuous models, is impossible. The main disadvantage of agent-based models is in their limitations to handle large number of cells. Typically, this limit is in thousands of cells, but with constantly increasing speed of computers and with development of novel faster computational techniques (parallel, GPU, or cloud computing) the number of cells that the model can handle in a reasonable time may not be a limitation anymore.

It is worth noting that every mathematical model is by its nature a simplification of the biological system it is assumed to represent, so we do not expect that one model will incorporate all processes involved in drug penetration through the tumor tissue. And we also do not expect that the unified modeling framework addressing all aspects of drug transport through tumor tissue will emerge in the near future. *In silico* models need to be designed to investigate a specific research question similarly to how biological experiments focus on the selected aspects of tumor treatment and do not address in a single experiment all possible combinations of involved factors. Computational models should not be too complex to allow for quantitative analysis of the relative importance of all features and parameters included in the model. However, in contrast to experiments, model parameters (e.g., drug molecular mass or charge, timing and dosing of drugs, and their activation or uptake properties) can be varied over a wide range of values and can be changed simultaneously in a controlled way, giving investigators insight into a full spectrum of drug properties that lead to the desired (or undesired) effects. These model outcomes will then provide guidance for further laboratory experimentation, and both results, positive and negative, will be informative for biologists. The positive results will suggest the environmental conditions or drug concentrations that are worth pursuing experimentally; the negative results will advise the drug concentrations or their properties that do not lead to a desired effect and can be omitted, reducing experimental costs and time. In fact, close collaboration between mathematical modelers, biologists, and clinicians is crucial, in our opinion, for making progress in improving anti-cancer treatments.

In our opinion the computational models of tumor development and treatment that will be successfully applied in personalized medicine need to be single-cell-based to be able to account for differences between tumors in individual patients (inter-tumor heterogeneity) and between distinct regions within the same tumor tissue (intra-tumor heterogeneity). Such models will be able to address phenotypic, genetic, and drug-response heterogeneity observable in patient tumors. The future models need to be temporal to capture the dynamics of tumor growth, cell–cell interactions,

and response to therapy. These models will allow for temporal analysis of model results in order to identify more effective drug administration schedules with potentially variable schedules and dosages that cannot be intuitively inferred from analyzing drug properties in laboratory experiments. The future models should also be spatially explicit and three-dimensional, since both cell growth dynamics and drug transport dynamics are significantly different between the one-, two-, and three-dimensional spaces. *In vivo* tumors have complex geometries, variable cellular densities, irregular vasculature that cannot be captured by simple non-spatial, population-based models. And over all the future models need to be quantitative, based on quantitative experimental data (to inform and parameterize the model), and producing quantitative results, that can be compared to experimental measurements or clinical data.

Given the complexity of processes taking place during tumor development and its treatment, as well as significant inter-patient and intra-tumor variability, the cross-disciplinary approaches that integrate data and methods from various scientific disciplines have a better chance to delineate the mechanisms of tumor resistance to treatment and the way to overcome drug delivery barriers. The mathematical models that are properly integrated with experimental data, such that both *in silico* models and laboratory experiments inform each other, can provide tools for interpreting data, evaluating the most important parameters for designing new experiments, and developing strategies to improve tumor treatment.

ACKNOWLEDGMENTS

This work was supported partially by the Miles for Moffitt Milestones Award and partially by the Physical Sciences-Oncology Program at the National Institute of Health via the Moffitt-PSOC Center grant U54-CA-143970.

REFERENCES

1. Mould DR, Upton RN. Basic concepts in population modeling, simulation, and model-based drug development. *CPT Pharmacometr Syst Pharmacol* (2012) 1:e6. doi:10.1038/psp.2012.4. Epub 2012/01/01
2. Mould DR, Upton RN. Basic concepts in population modeling, simulation, and model-based drug development-part 2: introduction to pharmacokinetic modeling methods. *CPT Pharmacometr Syst Pharmacol* (2013) 2:e38. doi:10.1038/psp.2013.14. Epub 2013/07/28
3. Silva AS, Kam Y, Khin ZP, Minton SE, Gillies RJ, Gatenby RA. Evolutionary approaches to prolong progression-free survival in breast cancer. *Cancer Res* (2012) 72(24):6362–70. doi:10.1158/0008-5472.CAN-12-2235. Epub 2012/10/16
4. Song B, Yuan H, Pham SV, Jameson CJ, Murad S. Nanoparticle permeation induces water penetration, ion transport, and lipid flip-flop. *Langmuir* (2012) 28(49):16989–7000. doi:10.1021/la302879r. Epub 2012/11/23
5. Thurber GM, Weissleder R. A systems approach for tumor pharmacokinetics. *PLoS One* (2011) 6(9):e24696. doi:10.1371/journal.pone.0024696. Epub 2011/09/22
6. Huynh L, Masereeuw R, Friedberg T, Ingelman-Sundberg M, Manivet P. In silico platform for xenobiotics ADME-T pharmacological properties modeling and prediction. Part I: beyond the reduction of animal model use. *Drug Discov Today* (2009) 14(7–8):401–5. doi:10.1016/j.drudis.2009.01.009. Epub 2009/04/03
7. Kerns EH, Di L. *Drug-Like Properties: Concepts, Structure Design and Methods: From ADME to Toxicity Optimization*. Amsterdam: Academic Press (2008). 526 p.
8. Butcher EC, Berg EL, Kunkel EJ. Systems biology in drug discovery. *Nat Biotechnol* (2004) 22(10):1253–9. doi:10.1038/nbt1017. Epub 2004/10/08

9. Beresford AP, Selick HE, Tarbit MH. The emerging importance of predictive ADME simulation in drug discovery. *Drug Discov Today* (2002) **7**(2):109–16. doi:10.1016/S1359-6446(01)02100-6. Epub 2002/01/16
10. Kuh HJ, Jang SH, Wientjes MG, Au JL. Computational model of intracellular pharmacokinetics of paclitaxel. *J Pharmacol Exp Ther* (2000) **293**(3):761–70. Epub 2000/06/28
11. Rippley RK, Stokes CL. Effects of cellular pharmacology on drug distribution in tissues. *Biophys J* (1995) **69**(3):825–39. doi:10.1016/S0006-3495(95)79956-8. Epub 1995/09/01
12. Au JL, Jang SH, Zheng J, Chen CT, Song S, Hu L, et al. Determinants of drug delivery and transport to solid tumors. *J Control Release* (2001) **74**(1-3):31–46. doi:10.1016/S0168-3659(01)00308-X. Epub 2001/08/08
13. Primeau AJ, Rendon A, Hedley D, Lilge L, Tannock IF. The distribution of the anticancer drug doxorubicin in relation to blood vessels in solid tumors. *Clin Cancer Res* (2005) **11**(24):8782–8. doi:10.1158/1078-0432.CCR-05-1664
14. Minchinton AI, Tannock IF. Drug penetration in solid tumours. *Nat Rev Cancer* (2006) **6**(8):583–92. doi:10.1038/nrc1893. Epub 2006/07/25
15. Cardenas-Rodriguez J, Li Y, Galons JP, Cornell H, Gillies RJ, Pagel MD, et al. Imaging biomarkers to monitor response to the hypoxia-activated prodrug TH-302 in the MiaPaCa2 flank xenograft model. *Magn Reson Imaging* (2012) **30**(7):1002–9. doi:10.1016/j.mri.2012.02.015. Epub 2012/05/05
16. Saggar JK, Fung AS, Patel KJ, Tannock IF. Use of molecular biomarkers to quantify the spatial distribution of effects of anticancer drugs in solid tumors. *Mol Cancer Ther* (2013) **12**(4):542–52. doi:10.1158/1535-7163.MCT-12-0967
17. Thurber GM, Yang KS, Reiner T, Kohler RH, Sorger P, Mitchison T, et al. Single-cell and subcellular pharmacokinetic imaging allows insight into drug action in vivo. *Nat Commun* (2013) **4**:1504. doi:10.1038/ncomms2506. Epub 2013/02/21
18. Xi L, Grobmyer SR, Zhou G, Qian W, Yang L, Jiang H. Molecular photoacoustic tomography of breast cancer using receptor targeted magnetic iron oxide nanoparticles as contrast agents. *J Biophotonics* (2012). doi:10.1002/jbio.201200155
19. Weissleder R, Pittet MJ. Imaging in the era of molecular oncology. *Nature* (2008) **452**(7187):580–9. doi:10.1038/nature06917
20. Gillies RJ, Anderson AR, Gatenby RA, Morse DL. The biology underlying molecular imaging in oncology: from genome to anatome and back again. *Clin Radiol* (2010) **65**(7):517–21. doi:10.1016/j.crad.2010.04.005. Epub 2010/06/15
21. Morse DL, Gillies RJ. Molecular imaging and targeted therapies. *Biochem Pharmacol* (2010) **80**(5):731–8. doi:10.1016/j.bcp.2010.04.011. Epub 2010/04/20
22. McGuire MF, Enderling H, Wallace DI, Batra JS, Jordan M, Kumar S, et al. Formalizing an integrative multidisciplinary cancer therapy discovery workflow. *Cancer Res* (2013) **73**(2):6111–7. doi:10.1158/0008-5472.CAN-13-0310
23. Enderling H, Rejniak KA. Simulating cancer: computational models in oncology. *Front Oncol* (2013) **3**:233. doi:10.3389/fonc.2013.00233
24. Choe SC, Zhao G, Zhao Z, Rosenblatt JD, Cho HM, Shin SU, et al. Model for in vivo progression of tumors based on co-evolving cell population and vasculature. *Sci Rep* (2011) **1**:31. doi:10.1038/srep00031. Epub 2012/02/23
25. Frieboes HB, Chaplain MA, Thompson AM, Bearer EL, Lowengrub JS, Cristini V. Physical oncology: a bench-to-bedside quantitative and predictive approach. *Cancer Res* (2011) **71**(2):298–302. doi:10.1158/0008-5472.CAN-10-2676. Epub 2011/01/13
26. Liu C, Krishnan J, Stebbing J, Xu XY. Use of mathematical models to understand anticancer drug delivery and its effect on solid tumors. *Pharmacogenomics* (2011) **12**(9):1337–48. doi:10.2217/pgs.11.71. Epub 2011/09/17
27. Michor F, Liphardt J, Ferrari M, Widom J. What does physics have to do with cancer? *Nat Rev Cancer* (2011) **11**(9):657–70. doi:10.1038/nrc3092. Epub 2011/08/19
28. Byrne HM. Dissecting cancer through mathematics: from the cell to the animal model. *Nat Rev Cancer* (2010) **10**(3):221–30. doi:10.1038/nrc2808. Epub 2010/02/25
29. Swierniak A, Kimmel M, Smieja J. Mathematical modeling as a tool for planning anticancer therapy. *Eur J Pharmacol* (2009) **625**(1-3):108–21. doi:10.1016/j.ejphar.2009.08.041
30. Stylianopoulos T, Soteriou K, Fukumura D, Jain RK. Cationic nanoparticles have superior transvascular flux into solid tumors: insights from a mathematical model. *Ann Biomed Eng* (2013) **41**(1):68–77. doi:10.1007/s10439-012-0630-4
31. Pries AR, Hopfner M, le Noble F, Dewhirst MW, Secomb TW. The shunt problem: control of functional shunting in normal and tumor vasculature. *Nat Rev Cancer* (2010) **10**(8):587–93. doi:10.1038/nrc2895
32. Pries A, Secomb T. Modeling structural adaptation of microcirculation. *Microcirculation* (2008) **15**(8):753–64. doi:10.1080/10739680802229076
33. Baish JW, Stylianopoulos T, Lanning RM, Kamoun WS, Fukumura D, Munn LL, et al. Scaling rules for diffusive drug delivery in tumor and normal tissues. *Proc Natl Acad Sci U S A* (2011) **108**(5):1799–803. doi:10.1073/pnas.1018154108. Epub 2011/01/13
34. Gevertz JL. Computational modeling of tumor response to vascular-targeting therapies – part I: validation. *Comput Math Methods Med* (2011) **2011**:830515. doi:10.1155/2011/830515. Epub 2011/04/05
35. Gevertz J. Optimization of vascular-targeting drugs in a computational model of tumor growth. *Phys Rev E Stat Nonlin Soft Matter Phys* (2012) **85**(4 Pt 1):041914. doi:10.1103/PhysRevE.85.041914. Epub 2012/06/12
36. Sinek JP, Sanga S, Zheng X, Frieboes HB, Ferrari M, Cristini V. Predicting drug pharmacokinetics and effect in vascularized tumors using computer simulation. *J Math Biol* (2009) **58**(4-5):485–510. doi:10.1007/s00285-008-0214-y. Epub 2008/09/11
37. Wu M, Frieboes HB, McDougall SR, Chaplain MAJ, Cristini V, Lowengrub J. The effect of interstitial pressure on tumor growth: coupling with the blood and lymphatic vascular systems. *J Theor Biol* (2013) **320**:131–51. doi:10.1016/j.jtbi.2012.11.031
38. Pozrikidis C. Leakage through a permeable capillary tube into a poroelastic tumor interstitium. *Eng Anal Bound Elem* (2013) **37**(4):728–37. doi:10.1016/j.enganabound.2013.01.011
39. van de Ven AL, Wu M, Lowengrub J, McDougall SR, Chaplain MA, Cristini V, et al. Integrated intravital microscopy and mathematical modeling to optimize nanotherapeutics delivery to tumors. *AIP Adv* (2012) **2**(1):11208. doi:10.1063/1.3699060. Epub 2012/04/11
40. Frieboes HB, Wu M, Lowengrub J, Decuzzi P, Cristini V. A computational model for predicting nanoparticle accumulation in tumor vasculature. *PLoS One* (2013) **8**(2):e56876. doi:10.1371/journal.pone.0056876. Epub 2013/03/08
41. Kim B, Han G, Toley BJ, Kim CK, Rotello VM, Forbes NS. Tuning payload delivery in tumour cylindroids using gold nanoparticles. *Nat Nanotechnol* (2010) **5**(6):465–72. doi:10.1038/nnano.2010.58. Epub 2010/04/13
42. Webb SD, Owen MR, Byrne HM, Murdoch C, Lewis CE. Macrophage-based anti-cancer therapy: modelling different modes of tumour targeting. *Bull Math Biol* (2007) **69**(5):1747–76. doi:10.1007/s11538-006-9189-2
43. Owen MR, Stamper IJ, Muthana M, Richardson GW, Dobson J, Lewis CE, et al. Mathematical modeling predicts synergistic antitumor effects of combining a macrophage-based, hypoxia-targeted gene therapy with chemotherapy. *Cancer Res* (2011) **71**(8):2826–37. doi:10.1158/0008-5472.CAN-10-2834. Epub 2011/03/03
44. El-Kareh AW, Secomb TW. A theoretical model for intraperitoneal delivery of cisplatin and the effect of hyperthermia on drug penetration distance. *Neoplasia* (2004) **6**(2):117–27. doi:10.1593/neo.03205. Epub 2004/05/14
45. Gasselhuber A, Dreher MR, Negussie A, Wood BJ, Rattay F, Haemmerich D. Mathematical spatio-temporal model of drug delivery from low temperature sensitive liposomes during radiofrequency tumour ablation. *Int J Hyperthermia* (2010) **26**(5):499–513. doi:10.3109/02656731003623590. Epub 2010/04/10
46. Rockne R, Rockhill JK, Mrugala M, Spence AM, Kalet I, Hendrickson K, et al. Predicting the efficacy of radiotherapy in individual glioblastoma patients in vivo: a mathematical modeling approach. *Phys Med Biol* (2010) **55**(12):3271–85. doi:10.1088/0031-9155/55/12/001. Epub 2010/05/21
47. Neal ML, Trister AD, Ahn S, Baldock A, Bridge CA, Guyman L, et al. Response classification based on a minimal model of glioblastoma growth is prognostic for clinical outcomes and distinguishes progression from pseudoprogression. *Cancer Res* (2013) **73**(10):2976–86. doi:10.1158/0008-5472.CAN-12-3588. Epub 2013/02/13
48. Venkatasubramanian R, Henson MA, Forbes NS. Integrating cell-cycle progression, drug penetration and energy metabolism to identify improved cancer therapeutic strategies. *J Theor Biol* (2008) **253**(1):98–117. doi:10.1016/j.jtbi.2008.02.016. Epub 2008/04/12
49. Stylianopoulos T, Diop-Frimpong B, Munn LL, Jain RK. Diffusion anisotropy in collagen gels and tumors: the effect of fiber network orientation. *Biophys J* (2010) **99**(10):3119–28. doi:10.1016/j.bpj.2010.08.065. Epub 2010/11/18
50. Stylianopoulos T, Poh MZ, Insin N, Bawendi MG, Fukumura D, Munn LL, et al. Diffusion of particles in the extracellular matrix: the effect of repulsive electrostatic interactions. *Biophys J* (2010) **99**(5):1342–9. doi:10.1016/j.bpj.2010.06.016. Epub 2010/09/08

51. Ziemys A, Kojic M, Milosevic M, Kojic N, Hussain F, Ferrari M, et al. Hierarchical modeling of diffusive transport through nanochannels by coupling molecular dynamics with finite element method. *J Comput Phys* (2011) **230**(14):5722–31. doi:10.1016/j.jcp.2011.03.054
52. Ziemys A, Kojic M, Milosevic M, Ferrari M. Interfacial effects on nanoconfined diffusive mass transport regimes. *Phys Rev Lett* (2012) **108**(23):236102. doi:10.1103/PhysRevLett.108.236102
53. Mahadevan TS, Milosevic M, Kojic M, Hussain F, Kojic N, Serda R, et al. Diffusion transport of nanoparticles at nanochannel boundaries. *J Nanopart Res* (2013) **15**(3):1477. doi:10.1007/s11051-013-1477-9
54. Bauer AL, Jackson TL, Jiang Y. A cell-based model exhibiting branching and anastomosis during tumor-induced angiogenesis. *Biophys J* (2007) **92**(9):3105–21. doi:10.1529/biophysj.106.101501. Epub 2007/02/06
55. Bauer AL, Jackson TL, Jiang Y. Topography of extracellular matrix mediates vascular morphogenesis and migration speeds in angiogenesis. *PLoS Comput Biol* (2009) **5**(7):e1000445. doi:10.1371/journal.pcbi.1000445. Epub 2009/07/25
56. Dallon JC, Sherratt JA. A mathematical model for fibroblast and collagen orientation. *Bull Math Biol* (1998) **60**(1):101–29. doi:10.1006/bulm.1997.0027. Epub 1998/05/09
57. Dallon JC, Sherratt JA, Maini PK. Mathematical modelling of extracellular matrix dynamics using discrete cells: fiber orientation and tissue regeneration. *J Theor Biol* (1999) **199**(4):449–71. doi:10.1006/jtbi.1999.0971. Epub 1999/08/12
58. Rejniak KA, Estrella V, Chen T, Cohen AS, Lloyd MC, Morse DL. The role of tumor tissue architecture in treatment penetration and efficacy: an integrative study. *Front Oncol* (2013) **3**:111. doi:10.3389/fonc.2013.00111. Epub 2013/05/30
59. Arifin DY, Lee KY, Wang CH. Chemotherapeutic drug transport to brain tumor. *J Control Release* (2009) **137**(3):203–10. doi:10.1016/j.jconrel.2009.04.013. Epub 2009/04/21
60. Arifin DY, Lee KY, Wang CH, Smith KA. Role of convective flow in carbustine delivery to a brain tumor. *Pharm Res* (2009) **26**(10):2289–302. doi:10.1007/s11095-009-9945-8. Epub 2009/07/30
61. Ramanujan S, Pluen A, McKee TD, Brown EB, Boucher Y, Jain RK. Diffusion and convection in collagen gels: implications for transport in the tumor interstitium. *Biophys J* (2002) **83**(3):1650–60. doi:10.1016/S0006-3495(02)73933-7
62. Schmidt MM, Wittrup KD. A modeling analysis of the effects of molecular size and binding affinity on tumor targeting. *Mol Cancer Ther* (2009) **8**(10):2861–71. doi:10.1158/1535-7163.MCT-09-0195. Epub 2009/10/15
63. Thurber GM, Wittrup DK. A mechanistic compartmental model for total antibody uptake in tumors. *J Theor Biol* (2012) **314**:57–68. doi:10.1016/j.jtbi.2012.08.034. Epub 2012/09/15
64. El-Kareh AW, Secomb TW. Two-mechanism peak concentration model for cellular pharmacodynamics of Doxorubicin. *Neoplasia* (2005) **7**(7):705–13. doi:10.1593/neo.05118
65. El-Kareh AW, Secomb TW. A mathematical model for cisplatin cellular pharmacodynamics. *Neoplasia* (2003) **5**(2):161–9.
66. El-Kareh AW, Labes RE, Secomb TW. Cell cycle checkpoint models for cellular pharmacology of paclitaxel and platinum drugs. *AAPS J* (2008) **10**(1):15–34. doi:10.1208/s12248-007-9003-6. Epub 2008/05/01
67. El-Kareh AW, Secomb TW. A mathematical model for comparison of bolus injection, continuous infusion, and liposomal delivery of doxorubicin to tumor cells. *Neoplasia* (2000) **2**(4):325–38. doi:10.1038/sj.neo.7900096
68. Eikenberry S. A tumor cord model for doxorubicin delivery and dose optimization in solid tumors. *Theor Biol Med Model* (2009) **6**:16. doi:10.1186/1742-4682-6-16. Epub 2009/08/12
69. Traina TA, Theodoulou M, Feigin K, Patil S, Tan KL, Edwards C, et al. Phase I study of a novel capecitabine schedule based on the Norton–Simon mathematical model in patients with metastatic breast cancer. *J Clin Oncol* (2008) **26**(11):1797–802. doi:10.1200/JCO.2007.13.8388. Epub 2008/04/10
70. Norton L, Simon R. Growth curve of an experimental solid tumor following radiotherapy. *J Natl Cancer Inst* (1977) **58**(6):1735–41. Epub 1977/06/01
71. Traina TA, Dugan U, Higgins B, Kolinsky K, Theodoulou M, Hudis CA, et al. Optimizing chemotherapy dose and schedule by Norton–Simon mathematical modeling. *Breast Dis* (2010) **31**(1):7–18. doi:10.3233/BD-2009-0290. Epub 2010/06/04
72. Morris PG, McArthur HL, Hudis C, Norton L. Dose-dense chemotherapy for breast cancer: what does the future hold? *Future Oncol* (2010) **6**(6):951–65. doi:10.2217/fon.10.59. Epub 2010/06/10
73. Comen E, Morris PG, Norton L. Translating mathematical modeling of tumor growth patterns into novel therapeutic approaches for breast cancer. *J Mammary Gland Biol* (2012) **17**(3–4):241–9. doi:10.1007/s10911-012-9267-z
74. Gatenby RA, Silva AS, Gillies RJ, Frieden BR. Adaptive therapy. *Cancer Res* (2009) **69**(11):4894–903. doi:10.1158/0008-5472.CAN-08-3658. Epub 2009/06/03
75. Friebes HB, Edgerton ME, Fruehauf JP, Rose FR, Worrall LK, Gatenby RA, et al. Prediction of drug response in breast cancer using integrative experimental/computational modeling. *Cancer Res* (2009) **69**(10):4484–92. doi:10.1158/0008-5472.CAN-08-3740. Epub 2009/04/16
76. Kim E, Stamatelos S, Cebulla J, Bhuiwalla ZM, Popel AS, Pathak AP. Multiscale imaging and computational modeling of blood flow in the tumor vasculature. *Ann Biomed Eng* (2012) **40**(11):2425–41. doi:10.1007/s10439-012-0585-5. Epub 2012/05/09
77. Venkatasubramanian R, Arenas RB, Henson MA, Forbes NS. Mechanistic modelling of dynamic MRI data predicts that tumour heterogeneity decreases therapeutic response. *Brit J Cancer* (2010) **103**(4):486–97. doi:10.1038/sj.bjc.6605773
78. Jackson A. Analysis of dynamic contrast enhanced MRI. *Br J Radiol* (2004) **77**(Suppl 2):S154–66. doi:10.1259/bjr/16652509
79. Li X, Huang W, Morris EA, Tudorica LA, Seshan VE, Rooney WD, et al. Dynamic NMR effects in breast cancer dynamic-contrast-enhanced MRI. *Proc Natl Acad Sci USA* (2008) **105**(46):17937–42. doi:10.1073/pnas.0804224105. Epub 2008/11/15
80. Ingrisch M, Sourbron S. Tracer-kinetic modeling of dynamic contrast-enhanced MRI and CT: a primer. *J Pharmacokinet Pharmacodyn* (2013) **40**(3):281–300. doi:10.1007/s10928-013-9315-3. Epub 2013/04/09
81. Weis JA, Miga MI, Arlinghaus LR, Li X, Chakravarthy AB, Abramson V, et al. A mechanically coupled reaction-diffusion model for predicting the response of breast tumors to neoadjuvant chemotherapy. *Phys Med Biol* (2013) **58**(17):5851–66. doi:10.1088/0031-9155/58/17/5851. Epub 2013/08/08
82. Buonaccorsi GA, Rose CJ, O’Connor JP, Roberts C, Watson Y, Jackson A, et al. Cross-visit tumor sub-segmentation and registration with outlier rejection for dynamic contrast-enhanced MRI time series data. *Med Image Comput Comput Assist Interv* (2010) **13**(Pt 3):121–8. doi:10.1007/978-3-642-15711-0_16
83. Canuto HC, McLachlan C, Kettunen MI, Velic M, Krishnan AS, Neves AA, et al. Characterization of image heterogeneity using 2D Minkowski functionals increases the sensitivity of detection of a targeted MRI contrast agent. *Magn Reson Med* (2009) **61**(5):1218–24. doi:10.1002/mrm.21946
84. Karahaliou A, Vassiliou K, Arikidis NS, Skiadopoulos S, Kanavou T, Costaridou L. Assessing heterogeneity of lesion enhancement kinetics in dynamic contrast-enhanced MRI for breast cancer diagnosis. *Brit J Radiol* (2010) **83**(988):296–306. doi:10.1259/bjr/50743919
85. Lee SH, Kim JH, Kim KG, Park JS, Park SJ, Moon WK. Optimal clustering of kinetic patterns on malignant breast lesions: comparison between K-means clustering and three-time-points method in dynamic contrast-enhanced MRI. *Conf Proc IEEE Eng Med Biol Soc* (2007) **2007**:2089–93. doi:10.1109/IEMBS.2007.4352733
86. Turnbull LW. Dynamic contrast-enhanced MRI in the diagnosis and management of breast cancer. *NMR Biomed* (2009) **22**(1):28–39. doi:10.1002/nbm.1273. Epub 2008/07/26
87. Gatenby RA, Grove O, Gillies RJ. Quantitative imaging in cancer evolution and ecology. *Radiology* (2013) **269**(1):8–14. doi:10.1148/radiol.13122697

Conflict of Interest Statement: The authors declare that the research was conducted in the absence of any commercial or financial relationships that could be construed as a potential conflict of interest.

Received: 15 July 2013; accepted: 29 October 2013; published online: 18 November 2013.

Citation: Kim M, Gillies RJ and Rejniak KA (2013) Current advances in mathematical modeling of anti-cancer drug penetration into tumor tissues. *Front. Oncol.* **3**:278. doi:10.3389/fonc.2013.00278

This article was submitted to Pharmacology of Anti-Cancer Drugs, a section of the journal *Frontiers in Oncology*.

Copyright © 2013 Kim, Gillies and Rejniak. This is an open-access article distributed under the terms of the Creative Commons Attribution License (CC BY). The use, distribution or reproduction in other forums is permitted, provided the original author(s) or licensor are credited and that the original publication in this journal is cited, in accordance with accepted academic practice. No use, distribution or reproduction is permitted which does not comply with these terms.